

Lower Columbia River Ecosystem Monitoring Program

Annual Report for Year 16

BPA Project Number: 2003-007-00

Report covers work performed under BPA contract # 86282

Report was completed under BPA contract # 88795

Report covers work performed from: October 2020 – September 2021

Technical Contacts: Sarah Kidd & Ian Edgar

Lower Columbia Estuary Partnership

400 NE 11th Ave

Portland, OR 97232

Phone: (503) 226-1565 x 239

skidd@estuarypartnership.org

iedgar@estuarypartnership.org

BPA Project Manager: Anne M. Creason

Fish & Wildlife Project Manager

Bonneville Power Administration

905 NE 11th Avenue

Portland, Oregon – 97208

Phone: (503) 230-3635

amcreason@bpa.gov

Report Completed: July 2022

This report was funded by the Bonneville Power Administration (BPA), U.S. Department of Energy, as part of BPA's program to protect, mitigate, and enhance fish and wildlife affected by the development and operation of hydroelectric facilities on the Columbia River and its tributaries. The views in this report are the author's and do not necessarily represent the views of BPA.

**Lower Columbia River Ecosystem Monitoring Program
Annual Report for Year 16 (October 1, 2020 to September 30, 2021)**

Sarah A. Kidd¹
Ian Edgar¹
Sneha Rao¹
Roger N. Fuller²
Regan A. McNatt³
Katrina Poppe²
Tawnya D. Peterson⁴
Joseph A. Needoba⁴
Lyle P. Cook⁴
Jeff Cordell⁵
Jason D. Toft⁵
Kerry Accola⁵
Amanda C. Hanson¹
Amy B. Borde⁶
Shon A. Zimmerman⁶
Susan A. Hinton³
Jeffery Grote⁷
Paul M. Chittaro³
David Kuligowski³
Gina M. Ylitalo³
Daniel Lomax³
Valerie I. Cullinan⁶
Lyndal L. Johnson³
Catherine A. Corbett¹

Prepared by the Lower Columbia Estuary Partnership
with funding from the Bonneville Power Administration

Lower Columbia Estuary Partnership
811 SW Naito Parkway, Suite 410
Portland, OR 97204

Suggested Citation:

Kidd, S.A., Edgar, I., Rao S., R.N. Fuller, R. McNatt, K. Poppe, T.D. Peterson, J.A. Needoba, L. Cook, J. Cordell, J.D. Toft, K. Accola, A.C. Hanson, A.B. Borde, S.A. Zimmerman, S. Hinton, J. Grote, P.M. Chittaro, D. Kuligowski, G.M. Ylitalo, D. Lomax, V.I. Cullinan, L.L. Johnson, H.L., and C.A. Corbett. 2022. Lower Columbia River Ecosystem Monitoring Program Annual Report for Year 16 (October 1, 2020 to September 30, 2021). Prepared by the Lower Columbia Estuary Partnership for the Bonneville Power Administration. Available from the Lower Columbia Estuary Partnership, Portland, OR.

¹ Lower Columbia Estuary Partnership

² Estuary Technical Group, Institute for Applied Ecology

³ Northwest Fisheries Science Center, NOAA-National Marine Fisheries Service

⁴ Oregon Health & Science University

⁵ University of Washington

⁶ Pacific Northwest National Laboratory

⁷ Ocean Associates, Inc

Executive Summary

The Ecosystem Monitoring Program (EMP) is managed by the Lower Columbia Estuary Partnership and is an integrated status and trends program for the lower Columbia River. Under the EMP, researchers collect key information on ecological conditions for a range of habitats throughout the lower river characteristic of those used by migrating juvenile salmon and provide information to aid the recovery of threatened and endangered salmonids. The program inventories the different types of habitats within the lower river, tracks trends in the overall condition of these habitats over time, provides a suite of reference sites for use as end points in regional habitat restoration actions, and places findings from management actions into context with the larger ecosystem. The EMP is implemented through a multi-agency collaboration, focusing sampling efforts on examining temporal trends within a study area that extends from the mouth of the river to Bonneville Dam. The goal of this executive summary is to provide a brief synopsis of the ecological conditions observed in the trend sites in 2020 and 2021. The full report following this executive summary should be consulted for detailed scientific methods and findings.

In both 2020 and 2021, data were collected on fish and fish prey, habitat, hydrology, food web, abiotic site conditions, and mainstem river conditions at Ilwaco Slough (river kilometer; rkm 6), Welch Island (rkm 53), Whites Island (rkm 72), Campbell Slough (rkm 149), and Franz Lake (rkm 221). Habitat and hydrology data were also collected at Cunningham Lake (rkm 145) along with with primary production and hydrology data collected at Steamboat Slough (rkm 57, a restoration site included in our longterm biomass study). The trends sampling sites are minimally disturbed, tidally influenced freshwater emergent wetlands with backwater sloughs that represent a subset of the eight hydrogeomorphic reaches across the lower river. In addition to tracking ecological changes in the lower Columbia River, this year a collaborative effort has been made to study the effect of varying flow regimes over the monitoring period, of the mainstem on site-specific biotic and abiotic conditions as well as answering specific longterm questions about the lower Columbia river. Based on the size of the freshet between 2010 – 2021, an NMDS plot of differences in river discharge and river temp between years, hydrologic conditions or cumulative discharge of the mainstem since 2010 were classified into four categories (Table 3). 2021 was classified as dry year, due to low flows before and after the spring freshet and 2020 was classified as an average freshet year. It should be noted, however, that 2020 also retained higher than normal wetland water level conditions across the upper river sites into August, impacting plant community growth similar to a high water year (Figure 10, Figure 38). The primary research questions we have attempted to answer with this report are “*What are the longterm status and trend conditions we see across the estuary and how can we use these data to address identified critical uncertainties about restoring sustainable habitat conditions in the estuary?*” We believe that exploring this question provides crucial information to restoration planning in the face of rising water levels and shifting climate patterns.

This report is a collaborative effort by many researchers. Habitat structure research leads from Lower Columbia Estuary Partnership are Dr. Sarah Kidd, Ian Edgar, and Sneha Rao. Water quality and food web dynamics research leads from Oregon Health and Science University are Dr. Joseph A. Needoba and Dr. Tawnya D. Peterson. Salmon prey and diet research leads from University of Washington are Dr. Jeff Cordell, Dr. Jason Toft, and Kerry Accola. Fish community and genetic composition research leads from NOAA – Fisheries are Regan McNatt and Susan A Hinton. Dr. Sarah Kidd, Ian Edgar, and Sneha Rao, are the lead report editors.

Mainstem Conditions of the Lower Columbia River

Mainstem conditions are evaluated through measures of river discharge at Bonneville Dam and at Beaver Army Terminal (river mile; RM 53). In addition, temperature data and other variables are provided through *in situ* sensor measurements at the Port of Camas (RM 122) and at Beaver Army Terminal (BAT).

River Discharge

Compared to the previous decade, discharge at Bonneville Dam during the freshet in 2020 was approximately average, with a nearly Gaussian shape peaking in late May; however, discharge was very low during the period leading up to the freshet, similar to the case in 2019. The freshet was of similar magnitude as 2019, but was delayed by over a month. In contrast, the freshet was negligible in 2021, and discharge volumes between March and September 2021 were among the lowest observed during the 2010-2021 period.

The Columbia River accounts for the largest proportion of flow throughout the year; however, during the winter months, flows from the Willamette River increase in relative importance, as do flows from other tributaries. Similar to 2019, river discharge associated with the Willamette River and other tributaries contributed a small proportion of total flows in both 2020 and 2021, with the exception of a few periods in the winter months prior to March characterized by significant, distinct peaks.

Water Quality

Water quality parameters measured at RM-122 and RM-53 include temperature, conductivity, turbidity, nitrate, colored dissolved organic matter, dissolved oxygen, and chlorophyll *a* concentration. Temperature is an important variable that influences organismal physiology and particularly the performance and survival of salmonids. We compared the number of days in 2020 and 2021 where temperatures exceeded thresholds associated with reduced performance or physiological stress with the years 2013, 2014, 2015, and 2016. The most conservative threshold (19 °C) was exceeded on 50 days in 2020 and 73 days in 2021. The latter was second only to 2015 in terms of the number of days with average temperature exceeding the 19°C threshold (n = 84 in 2015). The number of days exceeding this threshold in 2021 was almost 2 standard deviations higher than the mean for the years 1995-2021.

Peaks in tributary flow are associated with peaks in colored dissolved organic matter (CDOM), turbidity, and nitrate, underscoring the influence of water source on water quality parameters. Dissolved oxygen saturation exceeded 100% for nearly the entire year, with greater day-to-day variability observed during the summer months, particularly in 2021.

Tidal Wetland Habitat Conditions of the Lower Columbia River

Native and non-native Plant Communities

Overall, 2021 total plant cover was relatively stable across Ilwaco Slough, Welch Island, Whites Island, and Franz Lake compared to historic, longterm averages. Cunningham Lake total cover has continued to increase through 2021, beginning to rebound from the heavy cattle grazing observed in 2017. Campbell Slough has exhibited a small increase in total cover levels in 2021, however the overall cover at Campbell is still low compared to non-grazed conditions. Cattle grazing has continued at Campbell Slough since 2017, with fencing efforts failing to keep the cattle out of the wetland.

Between 2012-2021 the six most common plant species identified throughout the lower river (across the 6 trend sites) in order of overall abundance are *Phalaris arundinacea* (PHAR, non-native), reed canarygrass, *Carex lyngbyei* (CALY, native), Lyngby sedge, *Eleocharis palustris* (ELPA, native), common spikerush, *Sagittaria latifolia* (SALA, native), Wapato, *Leersia oryzoides* (LEOR, native), rice cut grass, and *Ludwigia palustris* (LUPA, native), water purslane (Table 28, Figure 57-Figure 63). While these species are the most common and abundant across all sites over the years, they are not necessarily present at all sites every year.

In 2021, *P. arundinacea* cover levels stayed relatively consistent to those observed in 2020 and previous years, however, at Cunningham, there was a significant increase in *P. arundinacea* levels from 20% in

2018 to 63% in 2021. Franz Lake also experienced a small increase from 13% in 2018 to 27% in 2021. This shift in *P. arundinacea* levels observed at Cunningham and Franz Lake is likely a product of both very low freshet flooding conditions in 2021 and, at Cunningham Lake, a break from grazing pressure. In 2021, data continued to support our findings that annual shifts in *P. arundinacea* cover are strongly correlated with Columbia River discharge levels and site water levels during the growing season, with lower water levels (and lower discharge levels) favoring *P. arundinacea* growth and observed abundance. These findings indicate that annual flooding conditions within sites and across the river (freshet accumulated discharge) are important mechanisms driving much of the observed annual variability in *P. arundinacea* dominance across the estuary. The longterm trends in the abundance of native species *Carex lyngbyei*, *Sagittaria latifolia*, and *Polygonum amphibium* have also been found to be strongly (and significantly) linked to annual river discharge conditions. Generally, *C. lyngbeyi* abundance has been found to increase in years of greater freshet and discharge levels, especially in Ilwaco Slough, where salinity levels are reduced during large discharge years, making growing conditions more favorable for *C. lyngbeyi*. *S. latifolia* has been found to have a delayed reaction to freshet and river discharge conditions, with lower discharge years resulting in an increase in *S. latifolia* abundance the following year. Additionally, *P. amphibium* levels at Franz Lake have also been found to follow a similar trend to *S. latifolia* with a one-year delayed reaction (increase in abundance) to decreased river discharge conditions. For both species, this might be a result of increased rhizome stores from positive growing conditions (low water levels), providing for more robust growth in the following growing season.

Water Quality

Water quality parameters determined at the five fixed trends sites revealed similar patterns to previous years (Sagar et al. 2016, Hansen et al. 2017). Ilwaco stands out for the low dissolved oxygen saturation values, which dipped below 100% (relative to equilibrium with the atmosphere) throughout the spring and summer; the range of hourly values was very large, particularly in 2021, where highs greater than 200% saturation and lows approaching 0% saturation were observed. Similarly, in 2021 the percent saturation of dissolved oxygen exceeded 20% in late July and August at Welch Island and in May at Campbell Slough. Hourly values exceeded 8.5 at Franz Lake Slough in July-August. When looking at the percentage of data points falling below physiological thresholds relevant to the salmonid condition, 2021 was similar to – but not as severe as – 2019, with the greatest percentage of data points falling below a threshold of 6 mg L⁻¹ at Franz Lake Slough in both 2019 and 2021.

With a few exceptions, daily average pH levels were within the range for acceptable water quality as defined by the Washington Department of Ecology (7 -8.5) at all sites in 2021. Daily average pH exceeded 8.5 at Welch Island in late April and hourly data exceeded 8.5 in April and in the summer months (June through August). Similarly, hourly data exceeded a pH of 8.5 in March-April and between June and August at both Campbell Slough and Whites Island. Levels that exceed 9 led to a shift in the speciation of ammonium, from its ionic form to the toxic gas, ammonia.

Concentrations of dissolved nitrate were generally lower in 2020 and 2021 than in previous years such as 2018 and 2019. Soluble reactive phosphate was slightly higher in 2021 than in previous years, likely reflecting lower water levels during this year.

Phytoplankton and Zooplankton

Total algal biomass, as estimated by concentrations of chlorophyll *a*, tends to be highest in March or April, prior to the spring freshet, at Welch Island and Whites Island; in contrast, the highest algal biomass at Campbell Slough and Franz Lake Slough is usually observed in July-August. Similar to previous years, the highest chlorophyll concentrations observed in 2020-21 were found at Campbell Slough and Franz Lake Slough. These sites are prone to the development of algal blooms in the summer months, which often discolor the water. No chlorophyll measurements in 2020 or 2021 exceeded 25 µg L⁻¹, a level above which is associated with poor water quality. If a benchmark of 15 µg L⁻¹ is used, four observations were

above the recommended threshold over the 2020-21 time period, suggesting poor water quality (Oregon State Water Quality Standards). However, since a body of water is only considered impaired when the threshold is exceeded in observations from three consecutive months, no site met this criterion.

Typically, observations show that chlorophyll concentrations are highest in March at Welch Island and Whites Island, while at Campbell Slough and Franz Lake Slough the highest algal biomass is observed in July-August. In 2020 and in 2021, peak chlorophyll concentrations were observed in March or April at Campbell Slough. Similar to previous years, the relative proportion of diatoms at the EMP trends sites was higher in the spring compared to summer, when chlorophytes and cyanobacteria made significant contributions to the total assemblages.

Often, cyanobacteria can account for a large proportion of the phytoplankton assemblage in the summer; in 2020, relatively high densities of cyanobacteria were also observed in February and March at Campbell Slough, and in June at Franz Lake Slough. Data for 2021 are not yet available for comparison. The lack of temporal data makes it difficult to discern patterns related to the season or to the hydrograph. Cell densities were higher in March compared to August, at the sites where data are available, and this is consistent with observations from previous years.

Similar to previous years, analysis of relationships between environmental variables and phytoplankton assemblages revealed that high relative proportions of diatoms are associated with high concentrations of dissolved oxygen. Diatom growth is also associated with a reduction in nutrient concentrations and is indicative of good water quality. Diatoms tend to dominate in the spring months, where populations can get quite large. Most of the annual growth of phytoplankton occurs in the spring and is accomplished by diatoms.

Zooplankton assemblages differ along the spatial gradient from Ilwaco Slough to Franz Lake Slough and over time from early spring to summer. Ilwaco Slough is consistently dominated by copepods, with inputs from rotifers, but very few cladoceran taxa. At the other sites, copepods generally dominated the zooplankton assemblages. At Welch Island and Whites Island, there was an increase in the proportional contribution by cladocerans from spring to summer in each of 2017, 2018, and 2019. At Campbell Slough and Franz Lake Slough, an increase in the proportional contribution of cladocerans was observed from March to June; however, by July, the relative proportions of cladocerans decreased at both sites in 2017 and 2018 and 2019.

Stable isotope ratios of Carbon and Nitrogen

Stable Isotope Ratios (SIR) are used to determine the relative importance of food sources including algae and wetland plants to the food web supporting juvenile salmonids at trends sites. Carbon and nitrogen isotope ratios yield different information: $\delta^{13}\text{C}$ ($^{13}\text{C}/^{12}\text{C}$) ratio is used to identify the primary source of organic matter (i.e., primary producers). In contrast, $\delta^{15}\text{N}$ ($^{15}\text{N}/^{14}\text{N}$) values are useful in determining trophic position. The SIR of C and N were measured in juvenile Chinook salmon muscle tissues and several potential food sources to provide information on the food web supporting juvenile salmonids. These were studied for the influence of cumulative mainstem discharge.

Isotopic values of carbon in particulate organic matter ($\delta^{13}\text{C}$ -POM) collected onto filters revealed $\delta^{13}\text{C}$ signatures in the range of freshwater phytoplankton most of the time, with values closer to terrestrial vascular plants in May and June at Campbell Slough and Franz Lake Slough. $\delta^{13}\text{C}$ -POM at Ilwaco was closer to marine values.

When stable isotope signatures for carbon and nitrogen associated with all primary producers is combined, two broad patterns emerge. The average $\delta^{13}\text{C}$ for all primary producers is slightly higher in very dry years (e.g., 2015) as well as very wet years (e.g., 2017), and lower for more moderate years. In

the case of nitrogen, this effect is more pronounced. Heavier carbon isotope signatures in particulate organic matter (POM) were associated with dry years. In contrast, there were no significant differences in the stable isotope signatures of nitrogen in POM. The stable isotope signatures of periphyton collected across the trend sites between 2011 and 2019 varied widely across the data set. Average values of $\delta^{13}\text{C}$ for periphyton were higher during moderately wet and wet years. There was an increase in the average $\delta^{15}\text{N}$ for periphyton over a gradient of dry to wet years, with the largest spread in data observed for wet years. When the samples from EMP trend sites were grouped according to whether they came from years with low, moderate, or high cumulative discharge (very dry, dry, moderate, wet), there were significant differences in average $\delta^{13}\text{C}$, but not in $\delta^{15}\text{N}$.

According to a Bayesian Inference stable isotope mixing model, phytoplankton carbon contributes to the juvenile salmonid food web as part of the diet of chironomid prey, based on stable isotope signatures of carbon. This carbon is incorporated as POM and as periphyton. Models looking at how different sources of primary production contribute to additional prey sources are being investigated as more data are gathered, but analysis thus far suggests that periphyton constitutes an important source of organic matter for the preferred prey of juvenile salmonids (i.e., amphipods and chironomids). Estimates of dietary contributions from different prey items inferred from stable isotope mixing models suggest that juvenile salmonid growth is supported by amphipods, chironomids, and other crustacean prey, which is consistent with observations derived from stomach analysis.

Macroinvertebrates

This report presents juvenile salmon prey data from 2020 salmon diet sampling, which took place from February – March. Two orders of juvenile salmon prey, Amphipoda and Diptera, had a small, yet consistent presence in benthic data, with amphipods contributing mostly at Ilwaco Slough and Whites Island, and dipterans contributing at all sites. Neuston samples were diverse, consisting predominantly of insects, copepods, collembolans, and cladocerans. Juvenile Chinook salmon diets followed interannual geographic trends consisting of primarily dipterans and other wetland insects at Franz Lake and Campbell Slough, primarily dipterans and amphipods at Whites Island and Welch Island, and primarily amphipods at Ilwaco Slough near the estuary mouth. Prey with highest percent Index of Relative Importance (IRI) for fish in all size classes have been amphipods, dipterans, and cladocerans. Amphipods and dipterans were predominantly comprised of *Americorophium* spp. (amphipods) and Chironomidae (dipterans).

Fish Communities

Examinations of fish communities for all years of sampling show that all five trend sites are different from each other. The one exception is that Welch and Whites, when compared directly to each other, are similar. Thirteen major families of fish have been consistently present at the trend sites. Within those families, the fish species range from native marine species at Ilwaco Slough, to freshwater native and non-native species at the remaining EMP trend sites sampled through 2021. Chinook salmon are captured at all five trend sites and are often the numerically dominant salmonid species. Chum salmon (primarily at Ilwaco Slough) and coho salmon (primarily at Franz Lake) have also been captured at the five sites in low numbers.

Ilwaco Slough, sampled for fish since 2011, is the only trend site that is influenced by marine waters due to its proximity to the mouth of the Columbia River (rkm 6). The species most consistently captured (eight or more of the last 10 years of sampling) are the native threespine stickleback, staghorn sculpin and shiner perch and the non-native banded killifish. Two salmon species, chum and Chinook, are regularly captured at this site. Chum salmon was the dominant species ($\geq 90\%$ of the total salmon numbers) except during 2012 and 2015, when few salmon were captured. Through 2021, six or less individual Chinook salmon were captured during eight of the eleven years of sampling. Most were unmarked salmon (presumed wild); however, marked salmon (presumed hatchery reared) were captured in 2017 and 2018. The majority of Chinook salmon captured at Ilwaco Slough were subyearlings (fork length $<60\text{mm}$,

weight < 2 grams). Genetic analysis of unmarked and marked Chinook salmon captured at Ilwaco Slough has identified two stocks, Spring Creek group-fall and West Cascade-fall.

Welch Island, sampled for fish since 2012, is a tidally influenced, freshwater marsh habitat in the lower Columbia River (rkm 53). The species most consistently captured (10 out of the 10 years of sampling) are the native Chinook salmon, threespine stickleback, and the non-native banded killifish. Chinook salmon comprised 96% or greater of the total numbers of salmon captured within a year and were captured each year. Chum were the second most frequently seen salmon, making up 4% or less of all salmon in a given year, and have been captured in seven of ten years of sampling. Each year 70–100% of the Chinook salmon captured at Welch Island were unmarked (presumably wild) juveniles. Genetic composition of unmarked Chinook salmon captured at Welch Island has been dominated by West Cascade-fall followed by upper Columbia River-summer/fall. There have been minimal instances of Snake River-fall, Spring Creek-fall, and Rogue River. Genetic composition of marked Chinook salmon at Welch Island had been comprised primarily of two genetic stock groups, West Cascade-fall and Spring Creek Group-fall.

Whites Island, sampled for fish since 2009, is a freshwater, tidally influenced marsh, located on the north side of Puget Island in the Columbia River (rkm 72). The species most consistently captured in all years are the native Chinook salmon and threespine stickleback and the non-native banded killifish. Five different species in the Salmonidae family have been identified at Whites Island since 2009. The site has been dominated by juvenile Chinook, followed by chum salmon. Coho, sockeye and mountain whitefish are other species of the Salmonidae family caught at the site. The majority of Chinook salmon captured were unmarked, making up 70–100% of the yearly total. For eight of the sampling years, unmarked juvenile Chinook fry have made up over half of all Chinook catches. Marked Chinook (presumed hatchery origin) were primarily fingerlings with the occasional yearling seen in 2009, 2010 and 2019. From the genetic stock analysis of unmarked Chinook salmon, seven different stocks have been identified since 2009. West Cascade-fall stock is the predominant group, comprising 80% or more of the fish analyzed. For marked Chinook, four genetic stocks have been identified at Whites Island since 2009. The two major groups are West Cascade-fall and Spring Creek Group fall.

Campbell Slough (rkm 149), sampled for fish since 2008, is a freshwater area that is highly influenced by Bonneville Dam discharge, and minimally influenced by standard tidal fluctuations. The species most consistently captured in all years are the native Chinook salmon, threespine stickleback, and the non-native banded killifish. Six species of the family Salmonidae have been observed in Campbell Slough since 2008. The most common species is Chinook salmon followed by chum salmon. Coho, cutthroat trout, sockeye salmon, and mountain whitefish are the remaining species in the Salmonidae family. Fry and fingerling unmarked juvenile Chinook make up most of the salmon catches at the site. No marked juvenile fry chinook have been captured at the site. Marked juvenile Chinook are primarily fingerlings. Seven distinct genetic stocks of marked and unmarked Chinook salmon have been found in Campbell Slough. The most consistent stocks for both marked and unmarked Chinook are Spring Creek Group-fall, followed by West Cascade-fall, although percentage contribution in catches vary extensively over the monitoring years.

Franz Lake, sampled since 2008, is a freshwater site located at the confluence of the Franz Lake outlet channel and the Columbia River (rkm 221). The water levels at this site are almost exclusively controlled by discharge from the nearby Bonneville Dam. High water levels in the spring and warm water temperatures in the early summer regularly prevent monthly fish sampling. The most consistently captured fish species (9 out of 11 years of sampling) are the native threespine stickleback, largescale sucker, northern pikeminnow, and the non-native banded killifish. Nine species of Salmonidae have been captured at this site in the past years, contributing to less than 5% of total catches per year at this site. This could be an outcome of lack of optimal conditions for sampling at this site, among other environmental factors. Salmon catches predominantly consisted of juvenile Chinook and coho. Juvenile

Chinook at Franz Lake are primarily unmarked, and Chinook catches were strong in 2021. The unmarked category of Chinook was predominantly fry (<60 mm fork length) making up more than 70% of those captured followed by fingerlings (60-100 mm fork length). Marked (presumed hatchery origin) Chinook have only been captured in 2008 and 2009. Genetics analysis of Chinook salmon over the course of the 14 years of sampling has been conducted on very few unmarked (23) and marked (41) individuals. No one group is dominant, and no discernable pattern can be seen among the stock groups identified. For unmarked Chinook salmon, stock groups include Spring Creek Group-fall, upper Columbia River-fall, Snake River-fall, West Cascade-fall, mid and upper Columbia-spring, and Willamette River-spring. For marked Chinook salmon, Spring Creek Group-fall are the most common, and West Cascade-fall and Willamette River-spring have also been present.

Closing Summary

The EMP is the only study in the lower Columbia River that monitors fish use and conditions in the lower Columbia River as juvenile salmon outmigrate. The EMP collects longterm habitat data from relatively undisturbed tidal freshwater marshes representing the estuarine-tidal freshwater gradient to allow researchers and restoration practitioners to differentiate between variability associated with natural conditions and variability resulting from human influence. The EMP provides critical information for our understanding of how these wetlands support the life cycle and recovery of endangered and threatened salmonids. In both 2020 and 2021, we monitored water quality, habitat structure, food web dynamics, and fish use at five trend sites from the mouth of the Columbia River to the Bonneville dam to assess habitat function at these sites. We also began a focused effort to evaluate the influence of river discharge on wetland habitat conditions. Results from our collective analyses indicate that differences in annual Columbia River discharge and climate conditions are correlated with significant shifts in wetland food web and habitat conditions including plant community, plankton, and zooplankton abundance, as well as composition, food web nitrogen, and carbon dynamics. These findings are critical for evaluating how future environmental fluctuations predicted with climate change may impact salmonid habitat and food web dynamics. Future EMP research will focus on synthesizing these environmental observations and identifying how shifting climatic, and habitat conditions will impact the salmonid food web.

Management Implications

There are a number of questions that emerge based on several years of observations in the lower Columbia. Some of these include:

- ***How important are biogeochemical processes upstream of Bonneville Dam for the tidal freshwater estuary?*** It is unclear how conditions above Bonneville Dam influence water chemistry and plankton stocks observed downstream. Measurements of water quality and food web components from above the dam would help to determine the degree to which advection is important versus in situ processes such as growth and gas equilibration with the atmosphere.
- ***What is the importance of decomposition of organic matter by microbial organisms in determining its quality for salmon prey?*** Microbial decomposition often results in “trophic upgrading”, whereby less labile compounds are transformed through microbial metabolism to compounds that are more easily assimilated. How are these processes influenced by water chemistry, temperature, and nature of the organic matter (e.g., non-native vs. native plant species)?
- ***What factors contribute to cyanobacteria blooms in Franz Lake Slough? Do these blooms pose a problem for wildlife, and if so, what is the extent of the problem?*** Over the last few years, elevated phosphorus concentrations have been observed at Franz Lake Slough in advance of cyanobacteria blooms, although the source is unknown.

- ***How do pulses in primary production from different sources vary in space and time, and how does this influence secondary production and salmon food webs?*** The timing of availability of different sources of organic matter produced through primary production varies between pelagic phytoplankton and marsh vegetation. It would be helpful to compare the magnitude of these stocks to identify patterns that could inform food web models. In addition, pulse events, such as the production and deposition of pollen, could produce reservoirs of organic matter originating from vascular plants in the water column that is independent of detritus transport.
- ***How does prey quality and quantity vary spatially and temporally across the estuary?*** While studies have shown that emergent wetlands are important for prey production and export, accurate assessments of information on prey sources in the mainstem and floodplain habitats are yet to be made in the lower Columbia River. The spatial and temporal variation of energy densities of chironomids and amphipods in these undisturbed sites of the lower Columbia River would provide an important functional tool for restoration design. Maintenance metabolism and energy ration calculations from juvenile salmon diet data, or future calculations of modeled growth, may address questions about habitat quality for juvenile Chinook salmon. High prey quality and quantity may help mitigate the effects of suboptimal temperatures and hydrological conditions.
- ***How does mainstem cumulative discharge affect prey availability and juvenile salmon health and habitat use?*** Additional information is needed to explore the effect of different mainstem hydrologic conditions on the food web and habitat structure for the EMP. Since many EMP sites serve as reference sites for restoration projects, additional information about changes in habitat use and structure under various freshet conditions would help determine crucial actions in restoration design and mitigate the effects of climate change.
- ***How much do specific environmental factors impact growth, fish condition, residence time, age at maturation, and survival of anadromous salmonids in the estuary?*** Habitat use in the lower Columbia depends on a myriad of abiotic conditions, and a closer look into specific characteristics such as temperature, DO, discharge, etc. would provide critical information about juvenile salmonid behavior which can be used to inform landscape principles in restoration planning. Bioenergetics analysis of subyearling Chinook could be a useful tool for determining impacts of temperature, flow-based variation in food availability, and habitat availability on subyearling growth and presumed survival. (links with the topic above on discharge and prey availability).
- ***How does sediment carbon interact with Greenhouse gases in EMP Trend Sites?*** In order to understand the effects of climate change on the EMP sites, another aspect that needs to be explored further is the exchanges between carbon and greenhouse gases in emergent wetlands. While some data is available from sediment analysis, further exploration is required in terms of accretion and nutrients, and carbon sequestration.
- ***How does discharge and river flow impact availability of off-channel habitat including restored areas?*** Availability of alternate migration pathways and rearing opportunities is important for building population resiliency. Impacts of climate change may limit access to rearing habitat as flows decrease. Applying habitat connectivity models used in Puget Sound to the lower Columbia River could help identify under what flows habitat connectivity is constrained or maximized throughout the entire lower river or specific reaches.

The Estuary Partnership shares results from the monitoring program with other resource managers in the region and results from this multi-faceted program are applied to resource management decisions. Results from the EMP are presented and discussed at an annual Science Work Group meeting. The Science Work Group is composed of over 60 individuals from the lower Columbia River basin representing multiple regional entities (i.e., government agencies, tribal groups, academia, and private sector scientists) with scientific and technical expertise who provide support and guidance to the Estuary Partnership. In addition, EMP results are also shared with regional partners at various conferences, working groups and

meetings throughout the year. Data are often provided to restoration practitioners for use in restoration project design and project review templates (e.g., ERTG templates). Finally, data from the EMP are used to compare and contextualize results from the Action Effectiveness Monitoring Program (see 2022 AEMR report, [link](#)). Furthermore, the Estuary Partnership is working on shifting all EMP and AEMR data into a regional database to store, share, and conduct additional, largescale synthesis analyses of these data by utilizing Tableau.

Acknowledgments

This study could not have been completed without the help of our partners. We are grateful to the Northwest Power and Conservation Council and the Bonneville Power Administration for funding the Ecosystem Monitoring Program through the Columbia Basin Fish and Wildlife Program. We extend much gratitude to Lyndal Johnson who retired from NOAA Fisheries in 2017. Lyndal was a part of the Ecosystem Monitoring Program from the beginning and contributed to the sampling design and analysis of fish communities and contaminants. We also thank Sean Sol who contributed over ten years of fish sampling effort. Amy Borde, Shon Zimmerman, Ron Thom, and others from the Pacific Northwest National Laboratory (PNNL) were instrumental in setting up the overall sampling design. They also collected vegetation composition, elevation, sediment accretion, and surface water elevation at EMP sites from 2005 through 2016. Jennifer Morace of USGS assisted with sampling design and prior years of data collection of abiotic conditions at four of the trend sites. Both she and Whitney Temple of USGS (with large support from Valerie Brennis (formerly of the Estuary Partnership) assisted with designing and collecting portions of the food web study; we thank them immensely for their collaborative work on this program. We thank the University of Washington Wetland Ecosystem Team of Arielle Tonus Ellis, Julia Kobelt, Bob Oxborrow, Michael Caputo, and Cormac Toler-Scott who greatly assisted in processing invertebrate samples. This effort could not have been completed without the help of numerous field assistants: we would like to thank Cailene Gunn and Ethen Whattam from PNNL; Stuart Dyer, Katherine Pippenger, and Lyle Cook from OHSU; Narayan Elasmr and April Silva from Columbia River Estuary Taskforce (CREST); Krista Jones, Jina Sagar, Tiffany Thio, and Matthew Schwartz all formerly from the Estuary Partnership. We also thank the landowners and managers who have allowed us to conduct research on lands they manage, including Alex Chmielewski (Ridgefield National Wildlife Refuge and Franz Lake National Wildlife Refuge), Paul Meyers (Lewis and Clark National Wildlife Refuge), Ian Sinks (Columbia Land Trust), and Stanley Thacker. USFWS Abernathy Fish Technology Center provided the fish feed samples for the stable isotope study. Finally, the Estuary Partnership's Science Work Group provided valuable input throughout the process and peer review on final drafts. The Science Work Group is composed of over 60 members and is integral in ensuring the Estuary Partnership represents the best available science.

Table of Contents

1	Introduction.....	31
1.1	Background.....	31
1.2	Study Area.....	33
1.3	Characterization of Emergent Wetlands in the Lower Columbia River	34
1.3.1	Sampling Effort, 2005-2021.....	34
1.3.2	Site Descriptions	38
1.3.3	Water Year	41
1.4	Report Organization.....	43
2	Methods.....	44
2.1	Mainstem Conditions	44
2.1.1	Overview.....	44
2.1.2	Operation of RM-122 Platform at Port of Camas-Washougal.....	45
2.1.3	Sensor Configuration	45
2.1.4	Sensor Maintenance	46
2.1.5	Quality Control	46
2.2	Abiotic Site Conditions.....	46
2.2.1	Continuous Water Quality Data (Temperature, DO, pH, Conductivity).....	46
2.2.2	Nutrients (N, P).....	50
2.3	Habitat Structure	50
2.3.1	Habitat Metrics Monitored.....	51
2.3.2	Annual Monitoring.....	51
2.3.3	Analyses	53
2.4	Food Web.....	55
2.4.1	Primary Productivity	55
2.4.2	Secondary Productivity	64
2.4.3	Stable Isotope Ratios.....	65
2.5	Macroinvertebrates.....	66
2.5.1	Salmon Prey Availability Sampling.....	66
2.5.2	Salmon Diet.....	69
2.5.3	Salmon Prey Data Analysis.....	72
2.6	Fish.....	73
2.6.1	Fish Community.....	73
2.6.2	Salmon Metrics	75

3	Results.....	79
3.1	Mainstem Conditions	79
3.1.1	Continuous Data From the Mainstem	79
3.2	Abiotic Site Conditions.....	90
3.2.1	Continuous Water Quality.....	90
3.2.2	Dissolved Oxygen at Trends Sites	102
3.2.3	Nutrients.....	108
3.3	Habitat Structure	112
3.3.1	Hydrology	112
3.3.2	Sediment Accretion Rates	123
3.3.3	Vegetation Species Assemblage	134
3.3.4	Channel Morphology	162
3.4	Food Web.....	164
3.4.1	Primary Production	164
3.4.2	Spring Zooplankton Assemblages.....	219
3.4.3	Stable Isotope Ratios of Carbon and Nitrogen.....	226
3.5	Macroinvertebrates.....	248
3.5.1	Salmon Prey Availability	248
3.5.2	Salmon Diet.....	255
3.6	Fish.....	263
3.6.1	Fish Community Composition	264
3.6.2	Salmon Species Composition.....	274
3.6.3	Salmon Metrics	281
3.6.4	PIT-Tag Array Monitoring of Juvenile Salmon Residence	309
4	Status and Trends Discussion	310
4.1	Mainstem Conditions	310
4.1	Abiotic Site Conditions.....	311
4.2	Habitat Structure	312
4.2.1	Hydrology and Sediment Dynamics	312
4.2.2	Vegetation Community Condition and Dynamics	316
4.3	Food Web.....	318
4.3.1	Primary Production	318
4.3.2	Zooplankton	323
4.4	Macroinvertebrates.....	323
4.5	Fish.....	324
5	Juvenile Chinook Salmon Food Web Synthesis Discussion.....	328

5.1	Introduction.....	328
5.2	Characterization of Salmonids in the lower Columbia River	328
5.2.1	Salmon Tidal Wetlands Use Patterns.....	328
5.2.2	Fish Condition and Growth.....	329
5.3	Characterization of Salmonid Prey Conditions in the lower Columbia River	331
5.3.1	Juvenile Salmon Prey and Diet	331
5.4	Characterization of Food Web Primary Productivity in the lower Columbia River 332	
5.4.1	Marsh Plants Fuel the Salmon Food Web.....	332
5.5	Conclusions.....	337
6	Adaptive Management & Lessons Learned	338
7	References.....	342
8	Appendices.....	355
	Appendix A. Site Maps and Habitat Change Analysis	355
	Appendix B. Annual photo points from EMP trends sites.....	373
	Appendix C. Site Hydrographs	403
	Appendix D. Vegetation Species Cover	413
	Appendix E. Fish catch summaries, 2008–2021	419

Table of Figures

Figure 1. Lower Columbia River and estuary with hydrogeomorphic reaches (A-H) specified by color (Simenstad et al. 2011) and wetland zones (1-5) delineated by white lines (Jay et al. 2016). The 2021 EMP trends sites are shown in orange. 34

Figure 2. Ecosystem Monitoring sites sampled in (photos taken in 2016): (a) Ilwaco Slough; (b) Welch Island; (c) Whites Island; (d) Cunningham Lake; (e) Campbell Slough; (f) Franz Lake Slough. Updated site photos were unavailable at the time this report was compiled, UAV images from 2019-2021 are available upon request and will be added to the online Tableau database in future reporting years. 40

Figure 3. Daily average discharge volume (in $m^3 s^{-1}$) in blue for the years 2010 through 2021. Each panel represents one year (Jan – Dec). Also shown in each plot is the maximum and minimum daily average flows for all years combined. If the blue line matches either the minimum or maximum, those are the values that constitute the lowest or highest, respectively, in the time series. 41

Figure 4. Comparative panels of minimum, maximum, and average river discharge at Bonneville Dam in 2015, 2017, and 2019. Panel 4A represents discharge for 2015 which consisted of warm rainy winter, low snowpack and summer drought. Panel 4B represents discharge for 2017 which consisted of high precipitation and large snowpack. Panel 4C represents discharge for 2019, described as an “dry” year. ... 42

Figure 5. Station locations for the two in-situ water quality monitoring platforms in the mainstem Columbia River that support the Ecosystem Monitoring Program. RM-53 (river mile 53) is Beaver Army Terminal, while RM-122 (river mile 122) is located in Camas, WA..... 45

Figure 6. Images are showing deployment of water quality monitors (YSI sondes) at study sites. 47

Figure 7. Time periods are corresponding to sensor deployments at five trends sites (2008–2021). 49

Figure 8. Image of the new PIT detection system at Campbell Slough, installed February 2018. 78

Figure 9. Daily water discharge ($m^3/s \times 10^{-3}$) at Beaver Army Terminal (RM-53) from 2010-2021. Panels show individual years (blue lines) with the daily maximum and minimum indicated (upper and lower dashed lines) in each panel. The final panel shows the maximum (upper dashed line), minimum (lower dashed line) 80

Figure 10. Daily water discharge ($m^3/s \times 10^{-3}$) at Bonneville Dam from 2010-2021. Panels show individual years (blue lines) with the daily maximum and minimum indicated (upper and lower dashed lines) in each panel..... 81

Figure 11. Daily river discharge (in $m^3 s^{-1} \times 10^{-3}$) of the Willamette River measured near the Morrison Bridge for years 2010–2021. Also shown are the daily maximum and minimum values for the years 2010–2021. Data from USGS 14211720. 82

Figure 12. Discharge volume flux associated with the Columbia River at Bonneville dam (top panels), the Willamette River at downtown Portland (middle panels), and Beaver Army Terminal at river mile 53 (bottom panels). Flows at BAT represent the sum of the Columbia, Willamette, and other smaller tributaries. Left panels show data from 2020, middle panels show data from 2021, and right panels show the maximum daily average flows, minimum daily average flows, and average daily flows (solid lines). Flow data are in $m^3s^{-1} \times 10^{-3}$ 83

Figure 13. Discharge comparison between BAT (RM 53) and Camas (RM 122) October 2019-October 2021. 84

Figure 14. Daily discharge fluxes (m^3/s) associated with Columbia River flow (blue), Willamette River flow (orange), and other tributaries (grey). Discharge from the Willamette was determined at the USGS

stream gage at the Morrison Bridge; the contribution from other tributaries was computed by subtracting flows observed in the Willamette from those in the Columbia..... 85

Figure 15. Proportional discharge partitioned into flows from the Columbia (blue), the Willamette (orange), and other tributaries (grey) for the years 2020 and 2021. A comparison with average values computed for the 2010-2021 time series is shown for reference. 85

Figure 16. Series of graphs showing mainstem Columbia River temperatures at Camas, WA between 1997 and 2021. Upper dashed line shows the average maximum daily temperature; bottom dashed line shows the average minimum daily temperature. Blue line shows the daily average temperature for each year. All temperatures in °C. Averages were computed for each 24 h period. Maximum and minimum daily averages were calculated from the 1997-2021 time period..... 87

Figure 17: Mainstem temperature (as daily averages) determined at the Port of Camas, WA, in terms of the number of days exceeding 19 °C between 1995 and 2021 (top panel) and reported as z scores (bottom panel). Z scores represent the number of standard deviations away from the mean value; thus, high z scores indicate water temperatures that exceeded daily average values by large amounts. Months included in the calculation were May through Aug (4 months). ``2021 was 2nd warmest after 2015..... 88

Figure 18. Time series of hourly water quality parameters measured at River Mile 122 (Camas, WA) in 2020 (left panels) and 2021 (right panels). 89

Figure 19. Water quality data (daily average) collected from Ilwaco Slough in 2021, including temperature, salinity, dissolved oxygen (given as percent saturation relative to air), and pH..... 91

Figure 20: Time series of hourly measurements of water quality parameters made at Ilwaco Slough, 2020 and 2021..... 92

Figure 21. Time series of daily averaged measurements of water quality parameters made at Welch Island, 2021. Note that the water quality sonde at Welch Island includes phycocyanin fluorescence, in addition to chlorophyll fluorescence; these data are shown in the panel in the upper right as a green line. 94

Figure 22: Time series of hourly water quality data collected at Welch Island in 2021..... 95

Figure 23. Daily average water quality data collected in 2020 by a water quality sonde at Whites Island in Reach C..... 96

Figure 24: Time series of daily averaged measurements of water quality parameters made at Whites Island, 2021..... 97

Figure 25. Time series of daily averaged measurements of water quality parameters made at Campbell Slough, 2021. 98

Figure 26: Hourly water quality data collected at Campbell Slough in 2020 and 2021, including temperature (oC), chlorophyll *a* fluorescence (in Relative Fluorescence Units, RFU), depth (m), conductivity ($\mu\text{S cm}^{-1}$), pH, and dissolved oxygen (DO) percent saturation relative to the atmosphere (% Sat)..... 99

Figure 27. Time series of daily averaged measurements of water quality parameters made at Franz Lake Slough, 2021. 101

Figure 28. Hourly water quality data collected at Franz Lake Slough in 2020 and 2021, including temperature (oC), chlorophyll *a* fluorescence (in Relative Fluorescence Units, RFU), depth (m), conductivity ($\mu\text{S cm}^{-1}$), pH, and dissolved oxygen (DO) percent saturation relative to the atmosphere (% Sat)..... 102

Figure 29. Water temperatures at EMP sites (Campbell Slough, Franz Lake Slough, Whites Island, Welch Island, and Ilwaco) shown alongside mainstem temperatures determined at the Port of Camas, WA.....	107
Figure 30. Time series are showing concentrations of dissolved nitrate at the five trends sites in 2019..	109
Figure 31. Time series showing concentrations of dissolved phosphate (ortho-phosphate) at the five trends sites in 2019.	110
Figure 32. Time series showing concentrations of dissolved ammonium at the five trends sites in 2019.	111
Figure 33: Ilwaco Slough: Percent time inundation for the month of August along the marsh elevation gradient between 2011-2021. Min Elevation = 1.1, mean elevation = 2.0, Max elevation = 2.4.	117
Figure 34: Welch Island: Percent time inundation for the month of August along the marsh elevation gradient between 2013-2021. Min = 1.3, Mean = 2.0, Max = 2.2	118
Figure 35: Whites Island: Percent time inundation for the month of August along the marsh elevation gradient between 2009-2021. Min = 1.2, Mean = 2.0, Max = 2.4	119
Figure 36: Cunningham Lake: Percent time inundation for the month of August along the marsh elevation gradient between 2009-2021. Min = 2.3, Mean = 2.7, Max = 3.0	120
Figure 37: Campbell Slough: Percent time inundation for the month of August along the marsh elevation gradient between 2008-2021. Min = 2.4, Mean = 3.0, Max = 4.0	121
Figure 38: Franz Lake: Percent time inundation for the month of August along the marsh elevation gradient between 2008, 2012-2021. Min = 3.9, Mean = 4.6, Max = 5.0	122
Figure 39: Longterm accretion rate variability across all 6 trend sites for 2010-2021.	125
Figure 40: A box and whisker plot of the net change in height of all low marsh stakes and all high marsh stakes. The low marsh stakes have a median net accretion of 2.95 cm and the high marsh stakes have a median net accretion of 1.85 cm over the lifetime of all stakes.....	126
Figure 41: EMP site sediment bench elevations in CRD, meters vs. the longterm mean sediment accretion/erosion (+/-, cm). Low (circles) and high (squares) relative within marsh elevations highlighted for each site. No longterm data was available for Cunningham Lake high marsh. Linear regression ($y = -3.317x + 8.898$), $R^2 = 0.761$, p-value = 0.002. For full summary of these data see.....	127
Figure 42: Ilwaco Slough net change in height (cm) per year. Overall, Ilwaco slough is fairly variable and is accreting at an average rate of 0.03 cm/year.	128
Figure 43: Welch Island net change in height (cm) per year. Overall, Welch Island is fairly variable in the low marsh with an average erosional rate of 0.17 cm/year. The high marsh is accreting at an average rate of 0.24cm/year.	129
Figure 44: Whites Island net change in height (cm) per year. Overall, Whites Island is accreting in the low marsh with an average rate of 2.18 cm/year. The high marsh is accreting at a slower average rate of 0.50 cm/year.....	130
Figure 45: Cunningham Lake net change in height (cm) per year. Overall, Cunningham Lake is eroding in the low marsh at an average rate of with an rate of 2.47 cm/year. The high marsh is accreting at an average rate of 0.40 cm/year. Note that the low marsh stakes are lacking data due to being lost during 2017 and only reset in 2020.	131
Figure 46: Campbell Slough net change in height (cm) per year. Overall, Campbell Slough is eroding in the low marsh with an average rate of 0.49 cm/year. The high marsh is eroding at a faster average rate at 1.30 cm/year.....	132

Figure 47: Franz Lake net change in height (cm) per year. Overall, Franz Lake is accreting in the low marsh with an average rate of 0.99 cm/year. The high marsh is accreting at a slower average rate of 0.13 cm/year.....	133
Figure 48: Forecasted sea level rise utilizing the Pevey et al. 2020 model by river km and site, plotted with average net accretion for each site.	134
Figure 49. Changes in mean total species richness over time at each trend site.	139
Figure 50. Changes in mean non-native species richness over time at each trend site.	139
Figure 51. Changes in mean native species richness over time at each trend site.	140
Figure 52. Changes in mean Shannon Diversity over time at each trend site.....	140
Figure 53. Changes in mean total cover (%) over time at each trend site.....	142
Figure 54. Average % total cover (not relative cover) of vegetation at each trend site through 2021.....	143
Figure 55. Changes in mean native species relative cover (%) over time at each trend site.....	144
Figure 56: Changes in mean non-native species relative cover (%) over time at each trend site.	144
Figure 57. Annual mean relative % cover, <i>Phalaris arundinacea</i> (PHAR, non-native), reed canarygrass, for all trend sites. Annual cumulative river discharge from May-Aug included for annual water year context (line is in gray, see Section 3.3.1). Relative species cover data can also be found in Table 30... 151	151
Figure 58: Annual mean relative % cover for <i>Carex lyngbyei</i> (CALY, native), lyngby sedge, for all trend sites. Annual cumulative river discharge from May-Aug included for annual water year context (line is in gray, see Section 3.3.1). Relative species cover data can also be found in Table 30.....	151
Figure 59. Annual mean relative % cover for <i>Eleocharis palustris</i> (ELPA, native), common spikerush. Annual cumulative river discharge from May-Aug included for annual water year context (line is in gray, see Section 3.3.1). Relative species cover data can also be found in Table 30.....	152
Figure 60. Annual mean relative % cover for <i>Sagittaria latifolia</i> (SALA, native). Annual cumulative river discharge from May-Aug included for annual water year context (line is in gray, see Section 3.3.1). Relative species cover data can also be found in Table 30.	152
Figure 61. Annual mean relative % cover for <i>Leersia oryzoides</i> (LEOR, native), rice cut grass. Annual cumulative river discharge from May-Aug included for annual water year context (line is in gray, see Section 3.3.1). Relative species cover data can also be found in Table 30.....	153
Figure 62. Annual mean relative % cover for <i>Ludwigia palustris</i> (LUPA, native), water purslane. Annual cumulative river discharge from May-Aug included for annual water year context (line is in gray, see Section 3.3.1). Relative species cover data can also be found in Table 30.....	153
Figure 63. Annual mean relative % cover for <i>Polygonum amphibium</i> (POAM, native), water knotweed. Annual cumulative river discharge from May-Aug included for annual water year context (line is in gray, see Section 3.3.1). Relative species cover data can also be found in Table 30.....	154
Figure 64: Box plot of elevation range of plant species across each site, sites in order from lower river to upper river from left to right. Species codes: <i>Carex lyngbyei</i> (CALY, native), lyngby sedge, <i>Eleocharis palustris</i> (ELPA, native), common spikerush, <i>Phalaris arundinacea</i> (PHAR, non-native), reed canarygrass, <i>Sagittaria latifolia</i> (SALA, native), wapato, and <i>Polygonum amphibium</i> (POAM, native), water knotweed.	158
Figure 65: Box plot of daily mean inundation range (% , August - across all years) of plant species across each site, sites in order from lower river to upper river from left to right. Species codes: <i>Carex lyngbyei</i> (CALY, native), lyngby sedge, <i>Eleocharis palustris</i> (ELPA, native), common spikerush, <i>Phalaris</i>	

<i>arundinacea</i> (PHAR, non-native), reed canarygrass, <i>Sagittaria latifolia</i> (SALA, native), wapato, and <i>Polygonum amphibium</i> (POAM, native), water knotweed.	159
Figure 66: Mean Annual (%) <i>Phalaris arundinacea</i> (PHAR, non-native), reed canarygrass, vs. daily (%) inundation (August –2012-2018) of PHAR plots. Linear regression ($y = -0.8711x + 66.207$), $R^2 = 0.41$, $p < 0.001$	160
Figure 67: Annual Freshet Cumulative River Discharge (Bonneville Dam, May- August) vs. Mean Annual (%) <i>Phalaris arundinacea</i> (PHAR, non-native), reed canarygrass, (2012-2019). Cunningham Lake, linear regression ($y = -3.36x + 50.2$), $R^2 = 0.70$, $p < 0.001$; Campbell Slough linear regression ($y = -5.25x + 66.1$) $R^2 = 0.75$, $p < 0.001$; Franz Lake, linear regression ($y = -1.13x + 17.2$), $R^2 = 0.61$, $p < 0.001$	161
Figure 68: Mean Annual Relative Native Plant Cover vs. Mean (%) <i>Phalaris arundinacea</i> (PHAR, non-native), reed canarygrass cover (August –2012-2019). Linear regression ($y = -1.0443x + 90.774$), $R^2 = 0.83$, $p < 0.001$	162
Figure 69: Average aboveground standing stock biomass (living + dead, dry weight g/m^2) for summer 2021, through winter 2019 for both the high and low marsh strata across sites sampled. Sites shown in order of rkm from mouth of the Columbia River to the Bonneville dam. Note that sampling was reduced from 16 plots per site to 10 plots per site beginning in Summer 2020. Additionally, note that there was reduced sampling for Summer 2020 and Winter 2021 due to the COVID-19 pandemic. See	170
Figure 70: Average detrital biomass (dry weight g/m^2) for summer 2021, winter 2021, summer 2020, and winter 2020 for both the high and low marsh strata across sites sampled. Sites shown in order of rkm from mouth of the Columbia River to the Bonneville dam. Note that sampling was reduced from 16 plots per site to 10 plots per site beginning in Summer 2020. Additionally, note that there was reduced sampling for Summer 2020 and Winter 2021 due to the COVID-19 pandemic. See.....	173
Figure 71: Total summer standing stock biomass (dry weight, g/m^2) data by elevation for all years data was collected at each site. Mean high and mean low marsh sample elevations (averaged across all years) highlighted as vertical lines on graph. A shows HM elevations, B shows LM elevations. HM = High Marsh, LM = Low Marsh.....	181
Figure 72: Total summer standing stock biomass (dry weight, g/m^2) data split by high and low marsh plant community strata by survey year. Freshet magnitude is shown as the right axis for reference (see section 3.3.1. for details). Biomass data and standard deviation is shown in Table 36.	183
Figure 73: Overall annual mean total standing stock biomass (dry weight, $g/m^2/year$) vs. the Freshet cumulative river discharge for the month of August. Second graph has annual labels for emphasis.....	184
Figure 74: Mean % Carbon and Nitrogen content of above ground living biomass, detritus, and soil across sites, samples collected in the Summer of 2018. Data provided in Table 37.....	185
Figure 75: Mean Carbon and Nitrogen ratio of above ground living biomass, detritus, and soil across sites, samples collected in the Summer of 2018. Data provided in Table 37.....	186
Figure 76: Carbon content (%) of above ground living biomass, detritus, and soil (graphs from top to bottom) vs. sample elevations in meters NAVD88. Significant within site correlations shown in each graph, site summary data provided in Table 37.	187
Figure 77: Nitrogen content (%) of above ground living biomass, detritus, and soil (graphs from top to bottom) vs. sample elevations in meters NAVD88. Significant within site correlations shown in each graph, site summary data provided in Table 37.	188
Figure 78: Carbon and Nitrogen ratio of above ground living biomass, detritus, and soil (graphs from top to bottom) vs. sample elevations in meters NAVD88. Significant within site correlations shown in each graph, site summary data provided in Table 37.	189

Figure 79. Soil N content (%) vs. Soil C content (%), a strong correlation was shown across all sites ($r^2 = 0.95$, $p < 0.001$). Summary data provided in Table 37.	190
Figure 80: Detritus N content (%) vs. Detritus C content (%), a strong correlation was shown across all sites ($r^2 = 0.47$, $p < 0.001$). Summary data provided in Table 37.	190
Figure 81: Mean % ADF Lignin content of above ground living biomass, and detritus across sites, samples collected in the Summer of 2018. For summary data see Table 38.	192
Figure 82: Detritus ADF Lignin content (%) vs. Detritus C content (%), a strong correlation was shown across all sites ($r^2 = 0.67$, $p < 0.001$). Summary data provided in Table 38.	192
Figure 83: Detritus ADF Lignin:Nitrogen (L:N) content (%) vs. Detritus C content (%), a strong correlation was shown across all sites ($r^2 = 0.30$, $p < 0.05$). Summary data provided in Table 38.	193
Figure 84. Mean soil texture composition (%) and bulk density (g/cm^3) across sites, samples collected in the Summer of 2018. For summary data see Table 38.	196
Figure 85: Chlorophyll <i>a</i> concentrations ($\mu\text{g L}^{-1}$) at Welch Island (Welch), Campbell Slough (Campbell), and Franz Lake Slough (Franz) in 2020.	198
Figure 86. Chlorophyll <i>a</i> concentrations ($\mu\text{g L}^{-1}$) at Welch Island (Welch), Campbell Slough (CS), and Franz Lake Slough (FR) in 2021.	198
Figure 87. Chlorophyll <i>a</i> concentration in discrete samples collected from Ilwaco (2011–2019).	199
Figure 88. Chlorophyll <i>a</i> concentration at Welch Island (2014–2021).	199
Figure 89. Chlorophyll <i>a</i> concentration in discrete samples collected from Whites Island (2011–2019).	200
Figure 90. Chlorophyll <i>a</i> concentrations at Campbell Slough (2011–2021).	200
Figure 91. Chlorophyll <i>a</i> concentrations at Franz Lake Slough (2011–2021).	201
Figure 92. Violin boxplots showing chlorophyll concentrations determined at the five off-channel trends sites between 2011 and 2021.	201
Figure 93. Phytoplankton data for EMP sites in 2020. Sites include Ilwaco Slough (IL), Welch Island, Whites Island, Campbell Slough (Campbell), Franz Lake Slough (Franz), and samples from the mainstem river at the Port of Camas, Washington (MS).	203
Figure 94. Summary of species composition data collected in 2020 at EMP sites and the mainstem Columbia River at the Port of Camas, Washington (mainstem = MS), including Whites Island (Whites), Welch Island (Welch), Ilwaco (IL), Campbell Slough (CS), and Franz Lake Slough (Franz).	205
Figure 95. Densities (in cells mL^{-1}) of different phytoplankton taxonomic groups at the EMP site, Ilwaco, in 2020.	206
Figure 96. Relative percentages of different phytoplankton classes at Ilwaco observed during the spring and summer months between 2011 and 2019.	207
Figure 97. Absolute abundances of phytoplankton classes at Ilwaco from 2011 to 2019.	208
Figure 98. Relative percentages of different phytoplankton classes at Welch Island from 2011 to 2019.	209
Figure 99. Densities (in cells mL^{-1}) of different phytoplankton taxonomic groups at the EMP site, Whites Island, in 2020. Data for April and May are missing due to travel restrictions associated with the covid-19 pandemic.	210
Figure 100. Absolute abundances of phytoplankton classes at Welch Island from 2011 to 2019.	211

Figure 101. Relative percentages of different phytoplankton classes at Whites Island from 2011 to 2019	212
Figure 102. Abundances of different phytoplankton classes (in cells/mL) at Whites Island from 2011 to 2019.	213
Figure 103. Relative percentages of different phytoplankton classes at Campbell Slough from 2011 to 2019.	214
Figure 104. Abundances of different phytoplankton classes (in cells/mL) at Campbell Slough from 2011 to 2019.	215
Figure 105. Relative percentages of different phytoplankton classes at Franz Lake Slough from 2011 to 2019.	216
Figure 106. Abundances of different phytoplankton classes (in cells/mL) at Franz Lake Slough from 2011 to 2019.	217
Figure 107. Biplot generated from canonical correspondence analysis relating phytoplankton taxonomic groups (labeled according to month sampled) to environmental variables: PO ₄ = phosphate, NO ₃ = nitrate, Temp = river temperature	218
Figure 108. Percentage of total zooplankton community accounted for by different groups (rotifers, copepods, cladocerans, ciliates, and ‘other’, which includes taxa not included in the other groups listed. These include, for example, nematodes, polychaetes, chironomid larvae, ostracods, etc.) at Ilwaco (including Ilwaco Slough and Ilwaco Marina) from 2011 to 2018.....	220
Figure 109. Percentage of total zooplankton community accounted for by different groups (rotifers, copepods, cladocerans, ciliates, annelids, and ‘other’, which includes taxa not included in the other groups listed. These include taxa that are present at low abundance, for example nematodes) at Welch Island from 2011 to 2018.....	221
Figure 110. Percentage of total zooplankton community accounted for by different groups (rotifers, copepods, cladocerans, ciliates, annelids, and ‘other’, which includes taxa not included in the other groups listed. These include taxa that are present at low abundance, for example nematodes) at Whites Island from 2011 to 2019.....	222
Figure 111. Percentage of total zooplankton community accounted for by different groups (rotifers, copepods, cladocerans, ciliates, annelids, and ‘other’, which includes taxa not included in the other groups listed. These include taxa that are present at low abundance, for example nematodes) at Campbell Slough from 2011 to 2019.....	223
Figure 112. Percentage of total zooplankton community accounted for by different groups (rotifers, copepods, cladocerans, ciliates, annelids, and ‘other’, which includes taxa not included in the other groups listed. These include taxa that are present at low abundance, for example nematodes) at Franz Lake Slough from 2011 to 2018.	224
Figure 113. Comparison of zooplankton densities at Whites Island (Reach C) and Campbell Slough (Reach F) in 2019 showing the mean total density and relative contributions to mean total density at the two sites.	225
Figure 114. Plot of particulate organic matter (POM) data from off-channel trends sites (circles) in isospace; typical isotopic signature ranges for different organic matter sources are shown (derived from Cloern, 2002). The contribution of various sources to measured POM in the lower Columbia is evident in the data spread.....	227
Figure 115. Plots showing stable isotope signatures of all primary producers according to the type of water year (Dry, moderate (“mid”), wet-to-moderate (“Mid/wet”), Very dry, and Wet). The data spread	

for $^{13}\text{C}/^{12}\text{C}$ was greatest for moderately wet, wet, and dry years, while for $^{15}\text{N}/^{14}\text{N}$ was greatest for wet and dry years.....	229
Figure 116. Plots showing average stable isotope signatures ($^{13}\text{C}/^{12}\text{C}$, or Delta 13C, and $^{15}\text{N}/^{14}\text{N}$, or Delta ^{15}N) for particulate organic matter (POM) in different water years. (Dry years, n=63; very dry years, n = 63; wet years, n = 51; moderately wet years, n=77).	230
Figure 117. Violin boxplots showing the $\delta^{13}\text{C}$ and $\delta^{15}\text{N}$ signatures of particulate organic matter at Campbell Slough and Whites Island. The data included samples collected between 2011-2019.....	231
Figure 118. Plots showing stable isotope signatures ($^{13}\text{C}/^{12}\text{C}$, or $\delta^{13}\text{C}$, and $^{15}\text{N}/^{14}\text{N}$, or $\delta^{15}\text{N}$) associated with periphyton in different water years. The data from all sites were pooled.....	233
Figure 119. Boxplots showing the distribution of data for stable isotope of carbon ($\delta^{13}\text{C}$) and nitrogen ($\delta^{15}\text{N}$) from vegetation at EMP sites, CS = Campbell Slough, FR = Franz Lake Slough, IL = Ilwaco, WE = Welch Island, WH = Whites Island.	234
Figure 120. Plots showing average stable isotope signatures ($^{13}\text{C}/^{12}\text{C}$, or $\delta^{13}\text{C}$, and $^{15}\text{N}/^{14}\text{N}$, or $\delta^{15}\text{N}$) for vegetation in different water years. Data from all sites were pooled.....	235
Figure 121. Stable isotope ratios of carbon and nitrogen for vegetation tissues at four of the EMP sites: Welch Island, Whites Island, Campbell Slough, and Franz Lake Slough.	236
Figure 122. Stable isotope ratios of carbon ($\delta^{13}\text{C}$) and nitrogen ($\delta^{15}\text{N}$) for prey sources divided according to their typical habitat (benthic, pelagic, terrestrial, or ‘other’ [unknown, or mixed]). The graphs show the data distribution over the range of observed values, with narrow shapes indicating few data points per observed value (relative to the total number of observations), and wider shapes indicating more data points per observed value. For benthic prey, n=60; for pelagic prey (copepods and cladocerans), n = 16; for terrestrial prey, n =100; for ‘Other’, n = 5.....	238
Figure 123. Isospace plot showing stable isotope signature of chironomids (“mixtures”) compared to vascular plant matter with heavier $\delta^{13}\text{C}$ and $\delta^{15}\text{N}$ (Veg A) and those having light $\delta^{13}\text{C}$ and $\delta^{15}\text{N}$ (Veg B) as well as to periphyton (PERI) and particulate organic matter (POM).....	239
Figure 124. Isospace plot showing isotopic signatures for salmon tissue (“Mixtures”) as well as prey sources (AMPH = amphipods, CHIR = chironomids, OLIGO = oligochaetes, POLY = polychaetes, NEMA = nematodes, and ZOOP = copepods and cladocerans).	241
Figure 125. Isotope ratios (delta 13C and delta 15N) of juvenile salmonid tissues pooled according to years categorized by variations in river flow.	243
Figure 126. Violin plots showing (A) delta 13C ($^{13}\text{C}/^{12}\text{C}$) in juvenile salmon tissue collected from Campbell Slough (CS), Franz Lake Slough (FR), Welch Island (WE), and Whites Island (WH).	244
Figure 127. Boxplot showing delta 13C and 15N values for salmon muscle tissue in April 2014 at four EMP sites: CS = Campbell Slough, FR = Franz Lake Slough, WE = Welch Island, and WH = Whites Island. According to a one-way anova with Tukey’s HSD post hoc testing, signatures of tissues at Campbell Slough were significantly different than those at the other sites.	245
Figure 128. Ratios of $^{13}\text{C}/^{12}\text{C}$ in tissues from salmon prey, including amphipods (AMPH), chironomids, copepods and cladocerans (COPE-CLAD), worms, and insects from sites considered ‘Upriver’ (upstream of the Willamette-Columbia confluence) and ‘Downriver’ (downstream of the Willamette-Columbia confluence).....	246
Figure 129. Estimate of the dietary proportion of juvenile salmon accounted for by different prey items based on output from a Bayesian mixing model. AMPH = amphipods; COPE-CLAD = copepods and cladocerans; CHIR = chironomids; INSECTS = a pool of insects of mixed taxonomy; WORMS =	

polychaetes, oligochaetes, and nematodes. Horizontal line represents the median, whiskers show the range of estimated proportional contributions arising from model output..... 247

Figure 130. Two-dimensional NMDS plot based on Bray-Curtis similarities between log transformed numeric abundances of taxa collected in benthic cores between 2015 and 2018. Each point represents the composition of the average monthly abundance of taxa collected between April and July within a site and year. Correlation with taxa (Pearson $R > 0.4$) are represented as gray vectors. 249

Figure 131. Percent numeric (top) and gravimetric composition (bottom) of benthic core samples collected 2015 – 2020. Percent numeric and gravimetric compositions are sorted by site and year. 250

Figure 132. Average density (counts/meter²) of major juvenile salmonid prey taxa in benthic core samples. Major prey taxa include amphipods (blue) and dipterans (green). Densities were sorted by site and year. Uneven year spacing on x-axis reflects sampling events spaced, by month, each year sampled. For example, a year spaced further from the previous year indicates more sampling events in the first year..... 251

Figure 133. Percent numeric (above) and gravimetric (below) composition of neuston samples collected 2016-2020. Samples were collected between February and March (2020), and April-July (2017-2019), sorted by site and year..... 253

Figure 134. Average density (count per meter towed) of Amphipoda by neuston tow. Samples are sorted by strata (top: emergent vegetation; bottom: open water) and color sorted by prey taxa (Amphipoda: blue; Diptera: green). Note that scales differ. 254

Figure 135. Average density (count per meter towed) of Cladocera collected by neuston tow for sampling years 2015 – 2020. All years are plotted regardless of presence on the x-axis. Samples are sorted by sampling strata (left: emergent vegetation; right: open water), site, and year 255

Figure 136: Percent Index of Relative Importance (IRI) by site and year for juvenile salmon 2008-2020. IRIs are calculated for all size classes (top) and in the 30-59 mm size class (bottom). Note: 2020 fish were collected February-March, while the remaining years represent fish collected April – June..... 257

Figure 137: 2020 Percent Index of Relative Importance (IRI), by site, collected February-March. 2020 fish were in the 30-59 mm fork length size class. Sample size ranged from 5-33 individuals. 257

Figure 138: Instantaneous ration (IR) and energy ration (ER) for individual juvenile salmon in 2020. IR (top) and ER (bottom) indices are color sorted by site. Trendline is not calculated for Franz Lake due to small sample sizes..... 259

Figure 139: All year (Feb-March) instantaneous ration (IR) and energy ration (ER) for juvenile salmon. IR (top) and ER (bottom) indices are color sorted by site. Trendlines not calculated for Franz Lake due to infrequent interannual February-March sampling. 260

Figure 140: Instantaneous ration (IR) and energy ration (ER) for all salmon collected 2012 – 2020. IR (left) and ER (right) indices 2012-2013, 2017-2019 (gray) and 2020 (orange) are calculated for February-March. The solid line is the linear trendline. 261

Figure 141: Quadrant charts of juvenile salmon average maintenance metabolism (J_m) and energy ration. Maintenance metabolism is calculated for 2020 (top) and among all years (bottom), and color sorted by site (top) and time (bottom, 2012-2019 – gray; 2020 – orange). 262

Figure 142: Two-dimensional NMDS plot for % IRI for major prey in juvenile Chinook diets. Percent IRIs are square-root transformed percent IRI and sampled between 2008 and 2020. Each point represents fish collected between April and June within the defined size class (fish fork length in mm) (2008-2017) and all fish collected (2020). Black vectors depict significant species loadings ($p = 0.05$), with strongest weights for Cladocera, Amphipoda, and Diptera. 263

Figure 143. Fish community composition at EMP trend sites sampled from 2008-2021, presented by Family. For each year, the total number of sampling months is presented in parentheses. IS = Ilwaco Slough, WEI = Welch Island, WHI = Whites Island, CS = Campbell Slough, FL = Franz Lake. 265

Figure 144. Nonmetric multidimensional scaling (NMDS) plot based on square-root transformed species abundance at five trend sites, 2008-2021. Significant correlation with variables (Pearson $R > 0.5$) are represented as vectors. IS = Ilwaco Slough, WEI = Welch Island, WHI = Whites Island, CS = Campbell Slough, FL = Franz Lake. Note that 2020 data, while limited, is included. 266

Figure 145. Mean species richness with minimum/maximum ranges for EMP trend sites sampled from 2008-2021. For each year, the total number of sampling months is presented in parentheses. IS = Ilwaco Slough, WEI = Welch Island, WHI = Whites Island, CS = Campbell Slough, FL = Franz Lake. 267

Figure 146. Mean Shannon-Weiner diversity index with standard deviation from EMP trend sites sampled from 2008-2021. For each year, the total number of sampling months is presented in parentheses. IS = Ilwaco Slough, WEI = Welch Island, WHI = Whites Island, CS = Campbell Slough, FL = Franz Lake. 268

Figure 147. Shannon-Weiner diversity index (bars) and species richness (closed circles) for EMP trend sites sampled monthly in 2021. IS = Ilwaco Slough, WEI = Welch Island, WHI = Whites Island, CS = Campbell Slough, FL = Franz Lake. 269

Figure 148. Percent of total fish catches per year that are non-native species for EMP trend sites sampled in 2008-2021. For each year the total number of sampling months is presented in parentheses. IS = Ilwaco Slough, WEI = Welch Island, WHI = Whites Island, CS = Campbell Slough, FL = Franz Lake. 271

Figure 149. Total percentage of the yearly (2008-2021) catch of fish species that have mature stages that could be predatory toward juvenile salmon. Species include small and largemouth bass, northern pikeminnow, walleye, warmouth, and yellow perch. For each year the total number of sampling months is presented in parentheses. IS = Ilwaco Slough, WEI = Welch Island, WHI = Whites Island, CS = Campbell Slough, FL = Franz Lake. 273

Figure 150. Percentage of salmonid species collected at EMP trends sites from 2008 - 2021. Total number of salmonids captured at a given site and year are presented in parentheses. WEI = Welch Island, WHI = Whites Island, CS = Campbell Slough, FL = Franz Lake. 275

Figure 151a. Percentage of marked (red) and unmarked (blue) Chinook salmon captured at the EMP sampling sites from 2008- 2021. The vertical axis represents site and year of sampling. Total number of the specified salmon species captured at a given site are presented in parentheses. IS = Ilwaco Slough; WEI = Welch Island, WHI = Whites Island, CS = Campbell Slough, FL = Franz Lake. 276

Figure 152b. Percentage of marked (red) and unmarked (blue) Coho salmon captured at the EMP sampling sites from 2008- 2021. Vertical Axis represents site and year of sampling. Total number of the specified salmon species captured at a given site are presented in parentheses. IS = Ilwaco Slough; WEI = Welch Island, WHI = Whites Island, CS = Campbell Slough, FL = Franz Lake. 277

Figure 153. Monthly Mean (SE) densities (fish per 1000 m²) of a) marked (red bars) and unmarked (blue bars) juvenile Chinook salmon, b) chum salmon in 2021 (all sites combined). Total number of sampling efforts per month are presented in parentheses. Only two coho salmon were captured at all sites in 2021 therefore no monthly density for coho salmon is shown. 279

Figure 154. Marked (red bars) and unmarked (blue bars) juvenile Chinook salmon densities (fish per 1000 m²) by site and year. Welch 2018 , Whites 2020 and 2021 were truncated for ease of viewing. IS = Ilwaco Slough, WEI = Welch Island, WHI = Whites Island, CS = Campbell Slough, FL = Franz Lake. 280

Figure 155. Genetic stock composition of unmarked (left column) and marked (right column) Chinook Salmon at trend sites from 2008–2020. Genetic sample sizes (probability ≥ 0.90) for each site is presented in parentheses. IS = Ilwaco Slough, WEI = Welch Island, WHI = Whites Island, CS = Campbell Slough,

FL = Franz Lake. Chinook salmon stocks: Desch_F = Deschutes River fall, M&UCR_Sp = mid and upper Columbia River spring, Rogue_R = Rogue River, SCG_F = Spring Creek Group fall, Snake_F = Snake River fall, Snake_Sp/Su = Snake River spring/summer, UCR_Su/Fa = Upper Columbia River summer/fall, WC_F = West Cascade fall, WC_Sp = West Cascade spring, WR_Sp = Willamette River Spring..... 283

Figure 156. Seasonal percent stock composition per site for Chinook Salmon collected in a) 2020 and b) 2008–2020. Note that only February and March were sampled in 2020. Plots include both unmarked and marked Chinook Salmon. Genetic sample sizes for each site is presented in parentheses. IS = Ilwaco Slough, WEI = Welch Island, WHI = Whites Island, CS = Campbell Slough, FL = Franz Lake. Chinook salmon stocks: Desch_F = Deschutes River fall, M&UCR_Sp = mid and upper Columbia River spring, Rogue_R = Rogue River, SCG_F = Spring Creek Group fall, Snake_F = Snake River fall, UCR_Su/Fa = Upper Columbia River summer/fall, WC_F = West Cascade fall, WC_Sp = West Cascade spring, WR_Sp = Willamette River Spring. 284

Figure 157. Nonmetric multidimensional scaling (NMDS) plot based on fourth-root transformed genetic stock abundance at five trend sites, 2008-2020. Significant correlation with genetic stock (Pearson $R > 0.5$) are represented as black vectors. IS = Ilwaco Slough, WEI = Welch Island, WHI = Whites Island, CS = Campbell Slough, FL = Franz Lake. SCG_F = Spring Creek Group fall, UCR_Su/Fa = Upper Columbia River summer/fall, WC_F = West Cascade fall..... 285

Figure 158. Mean (SD) length (mm) of unmarked juvenile Chinook salmon at trends sites in 2021 as compared to previous years. Total number of Chinook salmon weighed and/or measured per year at a site are presented in parentheses. IS = Ilwaco Slough; WEI = Welch Island, WHI = Whites Island, CS = Campbell Slough, FL = Franz Lake..... 287

Figure 159: Mean (SD) weight (g) of unmarked juvenile Chinook salmon at trends sites in 2021 as compared to previous years. Total number of Chinook salmon weighed and/or measured per year at a site are presented in parentheses. IS = Ilwaco Slough; WEI = Welch Island, WHI = Whites Island, CS = Campbell Slough, FL = Franz Lake..... 288

Figure 160. Mean (SD) condition factor of unmarked juvenile Chinook salmon at trends sites in 2021 as compared to previous years. Total number of Chinook salmon weighed and/or measured per year at a site are presented in parentheses. IS = Ilwaco Slough; WEI = Welch Island, WHI = Whites Island, CS = Campbell Slough, FL = Franz Lake..... 289

Figure 161. Mean (SD) length (mm) of marked Chinook salmon at trends sites in 2021 as compared to previous years. Total number of Chinook salmon weighed and/or measured per year at a site are presented in parentheses. IS = Ilwaco Slough; WEI = Welch Island, WHI = Whites Island, CS = Campbell Slough, FL = Franz Lake..... 290

Figure 162. Mean (SD) weight (g) of marked Chinook salmon at trends sites in 2021 as compared to previous years. Total number of Chinook salmon weighed and/or measured per year at a site are presented in parentheses. IS = Ilwaco Slough; WEI = Welch Island, WHI = Whites Island, CS = Campbell Slough, FL = Franz Lake..... 291

Figure 163 Mean (SD) condition factor of marked Chinook salmon at trends sites in 2021 as compared to previous years. Total number of Chinook salmon weighed and/or measured per year at a site are presented in parentheses. IS = Ilwaco Slough; WEI = Welch Island, WHI = Whites Island, CS = Campbell Slough, FL = Franz Lake..... 292

Figure 164. Percentages of life history types of unmarked juvenile Chinook salmon captured at trends sites in 2021 and in previous sampling years. Total numbers of Chinook salmon captured per year at a site are presented in parentheses. IS = Ilwaco Slough; WEI = Welch Island, WHI = Whites Island, CS = Campbell Slough, FL = Franz Lake..... 294

Figure 165. Percentages of life history types of marked juvenile Chinook salmon captured at trends sites in 2021 and in previous sampling years. Total numbers of Chinook salmon captured per year at a site are presented in parentheses. IS = Ilwaco Slough; WEI = Welch Island, WHI = Whites Island, CS = Campbell Slough, FL = Franz Lake.....	295
Figure 166. Mean (SD) length (mm) of chum salmon at trends sites in 2021 compared to previous sampling years. Total number of chum salmon weighed and/or measured per year at a site are presented in parentheses. IS = Ilwaco Slough; WEI = Welch Island, WHI = Whites Island, CS = Campbell Slough, FL = Franz Lake.....	297
Figure 167 Mean (SD) weight (g) of chum salmon at trends sites in 2021 compared to previous sampling years Total number of chum salmon weighed and/or measured per year at a site are presented in parentheses. IS = Ilwaco Slough; WEI = Welch Island, WHI = Whites Island, CS = Campbell Slough, FL = Franz Lake.	298
Figure 168. Mean (SD) condition factor (k) of chum salmon at trends sites in 2021 compared to previous sampling years. Total number of chum salmon used per year at a site are presented in parentheses. IS = Ilwaco Slough; WEI = Welch Island, WHI = Whites Island, CS = Campbell Slough, FL = Franz Lake.	299
Figure 169 Mean (SD) a) length (mm), b) weight (g), and c) condition factor of unmarked coho salmon at Franz Lake by sampling year. Total number of coho salmon captured at Franz Lake per year are presented in parentheses.....	300
Figure 170. . Mean (SD) a) length (mm), b) weight (g), and c) condition factor of marked coho salmon at Franz Lake by sampling year. Total number of coho salmon captured at Franz Lake per year are presented in parentheses.....	301
Figure 171. Relationship between growth rate and discharge for juvenile Chinook Salmon collected at mainstem Columbia River sites, 2005, 2008, and 2013.....	302
Figure 172. Relationships between growth rate and a suite of variables for juvenile Chinook Salmon collected at off-channel Columbia River sites, 2007–2014, and 2016–2018.....	303
Figure 173. Relationships between growth rate and a suite of variables for juvenile Chinook Salmon collected at Welch Island, 2012–2014, and 2016–2018.	304
Figure 174. Relationships between growth rate and year and fish length for juvenile Chinook Salmon collected at Whites Island, 2009–2014, and 2016–2018.....	305
Figure 175. Relationships between growth rate and fish length and genetic stock for juvenile Chinook Salmon collected at Campbell Slough, 2007–2014, and 2016–2018.....	306
Figure 176. Percent lipid content (A) and percent total lipids that were triglycerides (B) determined in whole bodies of juvenile Chinook salmon collected from the trend sites in 2018 compared to previous sampling years. Unlike letters indicate 2018 values within each site that differ significantly from those determined in other years (Kruskal-Wallis, Tukey’s post hoc test, $p < 0.05$). Sites are organized in increasing distance from the mouth of the Columbia River. Site abbreviations: IS = Ilwaco Slough, WEI = Welch Island, WHI = Whites Island, CS = Campbell Slough, FL = Franz Lake.	308
Figure 177. Monthly mean (SD) Fulton’s condition factor of unmarked and marked Chinook Salmon, 2008-2017.	330
Figure 178: Conceptual model of food web interactions within Lower Columbia River emergent wetlands.	333
Figure 179. Overall average summer biomass (g dry weight/m ²) from the high marsh (HM) and low marsh (LM) strata.	335

Figure 180. Average annual summer biomass (g dry weight/m²) compared to river km for the high marsh strata. Results are transformed by Log10 for statistical analysis. 335

Table of Tables

Table 1. Summary of sampling effort by site and year(s) conducted at EMP sampling sites. Bold text indicates that data were collected in 2019. 36

Table 2. Coordinates of the trend sites sampled in 2021. 39

Table 3: Classification of Monitoring years according to cumulative river discharge during the spring freshet between 2010-2021 42

Table 4. Description of the components on the LOBO sensor platforms located at RM-53 and RM-122. Note that the LOBO system was deployed from January through June; after this, the system consisted of a YSI sonde equipped with temperature, conductivity, and dissolved oxygen..... 46

Table 5. Comparison of in situ data with laboratory measurements of water samples..... 46

Table 6. Locations of water quality monitors (YSI sondes) at trends sites. Deployment periods for sensors at each of the sites is shown in Figure 7 47

Table 7. Range, resolution, and accuracy of water quality monitors deployed at four trends sites. m, meters; °C, degrees Celsius; µS/cm, microsiemens per centimeter; mg/L, milligrams per liter. 48

Table 8. Detection limits for colorimetric analysis of nitrogen and phosphorus species. TDN = total dissolved nitrogen, TN = total nitrogen, TDP = total dissolved phosphorus, TP = total phosphorus..... 50

Table 9. Site location and sampling dates for each site sampled in 2021. All habitat and hydrology metrics were sampled at these sites except as otherwise noted. 50

Table 10: Seasonal data collection schedule Winter 2018-Summer 2021. Sp= Species. Some data is still under analysis..... 56

Table 11. The number of samples collected in each year and season (S=summer, F=fall, W=winter, Sp=Spring) for all sample sites and vegetation strata. In 2017-2021 we also sampled at Steamboat Slough, a restoration site located near Whites Island..... 58

Table 12. List of samples analyzed (Xs) and data of collection from five trends sites in the Lower Columbia River in 2021..... 63

Table 13. Potential food sources for marked and unmarked juvenile Chinook salmon and invertebrate consumers. 65

Table 14. The number of invertebrate tow samples (OW and EV) collected at each site per sampling event, 2008-2013, and 2015-2018..... 67

Table 15. The number of Chinook salmon diet samples collected at each site per sampling event, 2008-2013, 2015-2018. 70

Table 16. Location of EMP sampling sites in 2020 and 2021 and the number of beach seine sets per month (ns = not sampled). Sampling was stopped in mid-March 2020 through February 2021 due to COVID-19 pandemic safety protocols issued by NOAA. 74

Table 17: Percentage of hourly dissolved oxygen concentration measurements determined from 2018 to 2021 at the EMP sites (Ilwaco, Welch Island, Whites Island, Campbell Slough, and Franz Lake Slough) falling below three thresholds relevant to juvenile salmonids in the Columbia River: < 6mg L ⁻¹ , <4 mg L ⁻¹ , or <2 mg L ⁻¹	104
Table 18: Temperatures exceeding 19°C in the EMP sites from 2015-2021. Data show the percentage of each month that the daily average temperature exceeded 19°C. No calculation was performed if data collection was less than 7 days of a given month.	106
Table 19. Water surface elevation (WSE) metrics calculated at each site for the sensor deployment period from 2016-2021. Campbell Slough from August 2020 through August 2021 data is currently unavailable. All metrics are in meters, relative to the North American Vertical Datum of 1988 (NAVD 88). MWL = mean water level; MLLW = mean lower low water; MHHW = mean higher high water. Full hydrographs and annual summaries for each year are in Appendix C.....	113
Table 20. Site marsh elevation range in meters based on the vegetation plot elevation (with ≥5% absolute living plant cover), relative to the North American Vertical Datum of 1988 (NAVD88). Mean number of plots, mean elevation, standard deviation (SD), minimum elevation (Min), and maximum elevation (Max). Marsh elevation ranges for all years can be found in Appendix D. Note that the 2021 data for Cunningham Lake was unavailable at the time of analysis; we utilized 2020 survey in place of the 2021 survey.....	115
Table 21. Sediment accretion rates at the trends sites between 2008 and 2021. Note that CS1-1 was decommissioned during Summer 2021 and a new stake was deployed nearby. Additionally, CLM-2 was lost in 2017 and redeployed in 2019.	124
Table 22. Overall total species richness, total native and total non-native species richness over time at the six trend sites, longterm mean also shown for each site. In 2021, a second monitoring area was added to Campbell Slough to represent ungrazed conditions.....	136
Table 23. Total number of plots and average species richness, native and non-native species richness over time at the six trend sites, longterm mean also shown for each site. In 2021, a second monitoring area was added to Campbell Slough to represent ungrazed conditions.	137
Table 24: Diversity indices over time at the six trend sites, longterm mean also shown for each site. In 2021, a second monitoring area was added to Campbell Slough to represent ungrazed conditions.....	138
Table 25. Changes in average relative % cover of living native and non-native plant over time at the six trend sites, longterm mean also shown for each site. In 2021, a second monitoring area was added to Campbell Slough to represent ungrazed conditions.....	145
Table 26. Changes in average relative % cover of living plants by wetland indicator status (WIS) over time at the six trend sites, longterm mean also shown for each site. In 2021, a second monitoring area was added to Campbell Slough to represent ungrazed conditions. Wetland indicator status broken down by FAC = Facultative, FACW= Facultative Wet, and OBL= Obligate.....	146
Table 27. Changes in average relative % cover of living plants, dead plants, bare ground, and open water over time at the six trend sites, longterm mean also shown for each site. In 2021, a second monitoring area was added to Campbell Slough to represent ungrazed conditions. It should also be notes that bare ground, open water, and dead plant materials were not consistently recorded until 2011/2010, which is clearly seen in the historic data. Recent years with abnormal occurrences are highlighted in blue, see text summary for analysis.	147
Table 28. The overall longterm mean cover of the 6 most commonly occurring plant species across all six trend sites from 2012-2021. Species are listed in order of overall average relative % cover.	149

Table 29. *Phalaris arundinacea* (reed canarygrass) average relative % cover and frequency (% of sample plots) at the trend sites between 2005 and 2021. Mean relative cover only calculated among plots that contain reed canarygrass, longterm mean also highlighted. ND indicates No Data. 150

Table 30: Overall total cover of dominant and common plant species found across all six trend sites, mean relative cover calculated within plots where each species was identified. *Carex lyngbyei* (CALY, native), lyngby sedge, *Eleocharis palustris* (ELPA, native), common spikerush, *Leersia oryzoides* (LEOR, native), rice cut grass, *Ludwigia palustris* (LUPA, native), water purslane, *Phalaris arundinacea* (PHAR, non-native), reed canarygrass, *Sagittaria latifolia* (SALA, native), wapato, and *Polygonum amphibium* (POAM, native), water knotweed. 155

Table 31. Physical channel metrics measured at each site. The channel mouth (indicated with an *) was measured in 2016; the year of full channel cross section measurement is provided in parentheses after the site code. Channel cross-section and hydrology data collected in 2017 and 2021 are still under analysis and unavailable at the time this report was written, no cross-section data was collected in 2018, 2019, or 2020. The text below is adapted from the 2016 report. 163

Table 32. The overall proportion of biomass density of the dominant species ($\geq 5\%$ of total sample by dry biomass) across high and low marsh strata sampled for Welch Island, Steamboat Slough, Whites Island, and Franz Lake. When evaluating changes note that sampling is grouped by season and year – such as Summer 2019 sample locations are re-sampled in Winter 2020. New sample locations are stratified through the high/low marsh zones each summer. There was reduced sampling for Summer 2020 and Winter 2021 due to the COVID-19 pandemic. See Appendix D for all plant code information. Welch Island low marsh strata and Franz lake (both strata) were not sampled until summer 2018. 166

Table 33. Overall proportion (by dry biomass) of living (live), dead, and detritus across high and low marsh strata sampled between the winter of 2019 and summer 2021. When evaluating changes note that sampling is grouped by season and year – such as Summer 2019 sample locations are re-sampled in Winter 2020. New sample locations are stratified through the high/low marsh zones each summer. Note that there was reduced sampling for Summer 2020 and Winter 2021 due to the COVID-19 pandemic. 169

Table 34: Average aboveground standing stock biomass (living + dead, dry weight g/m^2) and average detrital biomass (dry weight g/m^2) for 2018-2021 for both the high and low marsh strata across sites sampled. Winter 2022 data still under analysis and post-processing. Sites shown in order of rkm from mouth of the Columbia River to the Bonneville dam. Count= number of samples, Elevation = meters NAVD88, all units in g/m^2 . Annual Export is the mean predicted contribution of organic matter (dry weight $\text{g/m}^2/\text{year}$) both including and excluding detrital material. 177

Table 35: Annual Export is the mean predicted contribution of organic matter (dry weight $\text{g/m}^2/\text{year}$) both including and excluding detrital material, the change in the estimated export by incorporating the detritus is highlighted (negative means more material is kept on site than estimated with standing stock change alone, and positive means more material is exported than estimated without including detritus). Winter 2022 data still under analysis and post-processing. Sites shown in order of rkm from mouth of the Columbia River to the Bonneville dam. 179

Table 36: Total mean summer standing stock biomass (dry weight, g/m^2) data split by high and low marsh plant community strata by survey year. Mean elevation of strata, and standard deviation (SD) of standing stock biomass also presented. Data also depicted in Figure 72. 182

Table 37: Mean % Carbon and Nitrogen content of above ground living biomass, detritus, and soil across sites, samples collected in the Summer of 2018. For comparative graphs see Figure 74 and Figure 75. . 186

Table 38: Mean % ADF Lignin content of above ground living biomass, and detritus across sites, samples collected in the Summer of 2018. 191

Table 39: Plant species-specific mean (\pm SD) living above ground biomass elevation (m, NAVD88), ADF Lignin, C:N ratio, %C, %N, and dry biomass (g/m^2) across all sites sorted by mean elevation within each site (low to high marsh). Y = Native, N = Non-native. Data from summer 2018 biomass data collection. 194

Table 40: Overall plant species-specific mean (\pm SD) living above ground biomass elevation (m, NAVD88), Lignin:Nitrogen (L:N) content, C:N ratio, %C, %N, ADF Lignin %, and dry biomass (g/m^2). Y = Native, N = Non-native. Data from summer 2018 biomass data collection. Summary of common plant species combining all EMP site data (Welch Island, Whites Island, and Franz Lake). 195

Table 41: Mean soil texture composition (%) and bulk density (g/cm^3) across sites, samples collected in the Summer of 2018. For comparative graphs see Figure 84. 197

Table 42: Analysis of similarities of juvenile salmon prey composition differences between paired sites. Includes R-value and adjusted p-value for each significant pairwise comparison. Most non-significant comparisons were not listed. Cumulative contribution of influential species include species that contribute 70% or more to the difference in prey composition between sites. 263

Table 43: Average length, weight and Fulton's Index (k) for unmarked and marked chinook in 2019.... 286

1 Introduction

1.1 Background

The Columbia River supported diverse and abundant populations of fish and wildlife and is thought to have been one of the largest producers of Pacific salmonids in the world (Netboy 1980). Anthropogenic changes since the 1860s encompassing dike construction, land use conversion, and the construction of the hydropower system on the Columbia River basin have resulted in alterations to the hydrograph (i.e., timing, magnitude, duration, frequency, and rate of change in river flows); degraded water quality and increased presence of toxic contaminants; introduction of invasive species; and altered food web dynamics. These changes have subsequently significantly reduced the quantity and quality of habitat available for fish and wildlife species. The availability of suitable habitats affects the diversity, productivity, and persistence of salmon populations (Fresh et al. 2005). Degradation and loss of suitable estuarine habitats can threaten salmon population viability, thus highlighting the importance of identifying limiting factors to salmon survival and filling key knowledge gaps across the habitat gradient of the lower Columbia River to promote salmon recovery.

Threatened and endangered salmonids utilize the shallow water wetland habitats of the lower Columbia River for rearing and refugia, with some stocks utilizing these habitats for long time periods before completing their migratory journey to the ocean (Bottom et al. 2005, Fresh et al. 2005, 2006, Roegner et al. 2008, McNatt et al. 2016). Traditionally, fish and fish habitat research and monitoring efforts have been concentrated in the lower reaches of the estuary, particularly near the mouth of the river, leaving knowledge gaps in the basic understanding of fish habitat use and benefits within the upper, freshwater-dominated reaches of the Columbia River.

Tidal emergent wetland vegetation provides rearing and refuge habitat for juvenile fish and a source of organic matter to the mainstem and downstream habitats, while tidal channels provide access to wetlands and to foraging opportunities. Most emergent wetlands in the lower river cover a narrow elevation range of 0.8 to 2.6 m, relative to the Columbia River Datum (CRD). The annual fluctuations in hydrology drive the spatial and temporal variability of wetland vegetation, specifically the cover and species composition, and affect overall wetland inundation (Sagar et al. 2013). The vegetation species composition in the lower river is spatially variable, with the middle reaches generally showing the greatest species diversity; although some areas are dominated by non-native species such as reed canarygrass (*Phalaris arundinacea*), particularly in the river-dominated upper reaches (Sagar et al. 2013). Identification and quantification of vital habitat metrics allow for a greater predictability in biotic responses to changing environmental conditions and improves our overall understanding of the ecological functions in the lower river.

Salmonids occupy the upper trophic levels in the Columbia River system. They spend portions of their life cycle in fresh, estuarine, and oceanic waters. Threats to their survival could arise from a variety of sources or stressors occurring at any one of several life stages or habitat types. Large-scale changes to the ecological characteristics of the lower Columbia River food web as a consequence of wetland habitat loss have resulted in a significant reduction of microdetritus inputs to the system that historically formed the basis of the aquatic food web (Sherwood et al. 1990). Organic matter derived from fluvial phytoplankton (rather than microdetritus) may be a seasonal driver of the salmon food web (Maier and Simenstad 2009). The consequences of the apparent shift in the type of organic matter fueling food web dynamics are uncertain, and the understanding of shifts in the food web requires a detailed examination of the interactions between multiple trophic levels and environmental conditions. Studying the abundance and

assemblage of phytoplankton and zooplankton over space and time provides crucial information on the diets of preferred salmon prey, such as chironomids and benthic amphipods. In turn, characterizing the abiotic conditions within emergent wetlands, and in the river mainstem is essential for elucidating spatial and temporal patterns in the primary and secondary productivity in the lower river.

The Lower Columbia Estuary Partnership (Estuary Partnership), as part of the Environmental Protection Agency (EPA) National Estuary Program, is required to develop and implement a Comprehensive Conservation and Management Plan. This Management Plan specifically calls for sustained longterm monitoring to understand the ecological conditions and functions, to evaluate the impact of management actions over time (e.g., habitat restoration), and to protect the biological integrity in the lower Columbia River. The Estuary Partnership implements longterm monitoring through the Ecosystem Monitoring Program (EMP). Ultimately, the goal of the EMP is to track ecosystem conditions over time and allow researchers and managers the ability to distinguish between the variability associated with natural conditions and variability resulting from human influence. The EMP partnership collects on-the-ground data from relatively undisturbed emergent wetlands to provide crucial information about habitat structure, fish use, abiotic site conditions, salmon food web dynamics, and river mainstem river conditions to assess the biological integrity of the lower river, enhance our understanding of the estuary functions, and ultimately support recovery of threatened and endangered salmonids. The creation and maintenance of longterm datasets are vital for documenting the history of change within important resource populations. Therefore, through the EMP, we aim to assess the status (i.e., spatial variation) and track the trends (i.e., temporal variation) in the overall conditions of the lower Columbia River, to provide a better basic understanding of ecosystem functions, to provide a suite of reference sites for use as end points in regional habitat restoration actions, and to place findings from other research and monitoring efforts, such as the Action Effectiveness Monitoring into context within the larger ecosystem.

Ecosystem-based monitoring of the fish habitat conditions in the lower river is a regional priority intended to aid in the recovery of historical productivity and diversity of fish and wildlife. In addition to tracking ecological changes in the lower Columbia River, we also measure and study the effect of varying flow regimes over the monitoring period, of the mainstem on site-specific biotic and abiotic conditions. This year, we are specifically addressing uncertainties brought forward by the Expert Regional Technical Group (ERTG). The hydrology of the mainstem Columbia is strongly influenced by winter snow melt and precipitation between the months of October and March (Arelia Werner et al., 2007). The resulting cumulative discharge of the spring freshet depends on the magnitude, frequency, and duration of precipitation (Nilsson and Renöfält, 2008). Several studies indicate that river discharge exerts a significant influence on ecosystem processes like nutrient, sediment, and organic matter transport, as well as biotic structures. Moreover, studying these relationships will allow us to inform impacts associated with extreme high and low flow events, informing restorative actions (Bonada et al., 2006; Larned et al., 2007; Leigh et al., 2010; Rolls et al., 2012). The primary research question we have attempted to answer with this report is “*What are the longterm status and trend conditions we see across the estuary and how can we use these data to address the uncertainties brought forth by the ERTG and others about restoring sustainable habitat conditions in the estuary?*” Additionally, this year, in FY22, we transitioned our databases into a new format to allow additional large-scale synthesis analyses for the 2023 report as well as increasing the public accessibility of the EMP project through the use of Tableau Dashboards.

The EMP is funded by the Northwest Power and Conservation Council/Bonneville Power Administration (NPCC/BPA) and a primary goal for the action agencies (i.e., the BPA and US Army Corps of Engineers) is to collect key information on ecological conditions for a range of habitats and whether the habitats in the lower river are meeting the needs of our migrating juvenile salmonids for growth and survival. Such data provide information toward implementation of the 2008 Federal Columbia River Power System (FCRPS) Biological Opinion (BiOp; NMFS 2008). Specifically, NPCC/BPA funding for this program focuses on

addressing BPA’s Columbia Estuary Ecosystem Restoration Program (CEERP) goal of improving habitat opportunity, capacity and realized function for aquatic organisms, specifically salmonids.

The EMP addresses Action 28 of the Estuary Partnership Comprehensive Conservation and Management Plan; Reasonable and Prudent Alternatives (RPAs) 161, 163, and 198 of the 2000 Biological Opinion for the Federal Columbia River Power System; and RPAs 58, 59, 60, and 61 of the 2008 Biological Opinion. The Estuary Partnership implements the EMP by engaging regional experts at Battelle-Pacific Northwest National Laboratory (PNNL), National Oceanic and Atmospheric Administration National Marine Fisheries Service (NOAA-Fisheries), Estuary Technical Group (ETG), University of Washington (UW), and Oregon Health & Science University (OHSU).

1.2 Study Area

The lower Columbia River and estuary is designated as an “Estuary of National Significance” by the Environmental Protection Agency (EPA) and as such, it is part of the National Estuary Program (NEP) established in Section 320 of the Clean Water Act. The EMP study area encompasses that of the NEP (a.k.a., the Estuary Partnership), including all tidally influenced waters, extending from the mouth of the Columbia River at river kilometer (rkm) 0 to Bonneville Dam at rkm 235 (tidal influence is defined as historical tidal influence, relative to dam construction in the 1930s). The Estuary Partnership and monitoring partners collect data for the EMP from habitats supporting juvenile salmonids, in tidally influenced shallow water emergent wetlands connected to the Columbia River.

The Estuary Partnership and monitoring partners use a multi-scaled stratification sampling design for sampling the emergent wetland component of the EMP based on the Columbia River Estuary Ecosystem Classification (Classification). The Classification, a GIS-based data set, is a six-tier hierarchical framework that delineates the diverse ecosystems and component habitats across different scales in the lower river. The primary purpose of the Classification is to enable management planning and systematic monitoring of diverse ecosystem attributes. The Classification also provides a utilitarian framework for understanding the underlying ecosystem processes that create the dynamic structure of the lower river. As such, it aims to provide the broader community of scientists and managers with a larger scale perspective in order to better study, manage, and restore lower river ecosystems. The EMP sampling design has been organized according to Level 3 of the Classification, which divides the lower river into eight major hydrogeomorphic reaches (Figure 1).

More recently, subsequent to the development of the sampling design, data collected as part of the EMP and other studies (Borde et al. 2011; Borde et al. 2012) have been used to define five emergent marsh (EM) zones based on spatial variation of the hydrologic regime and vegetation patterns observed in the lower river (Jay et al. 2016). Vegetation species assemblages vary temporally and spatially and are broadly grouped into categories, or EM zones, based on vegetation cover and species richness. EM zones are used here to evaluate vegetation patterns within the tidal wetlands of the lower river because they are more representative of vegetation patterns than hydrogeomorphic reach. The zone boundaries are meant to be broad, and variation of the zone boundaries is observed between years. The following river kilometers are currently used to delineate the zones:

EM Zone	River Kilometer (rkm)
1	0 – 39
2	39 – 88
3	89 – 136
4	137 – 181

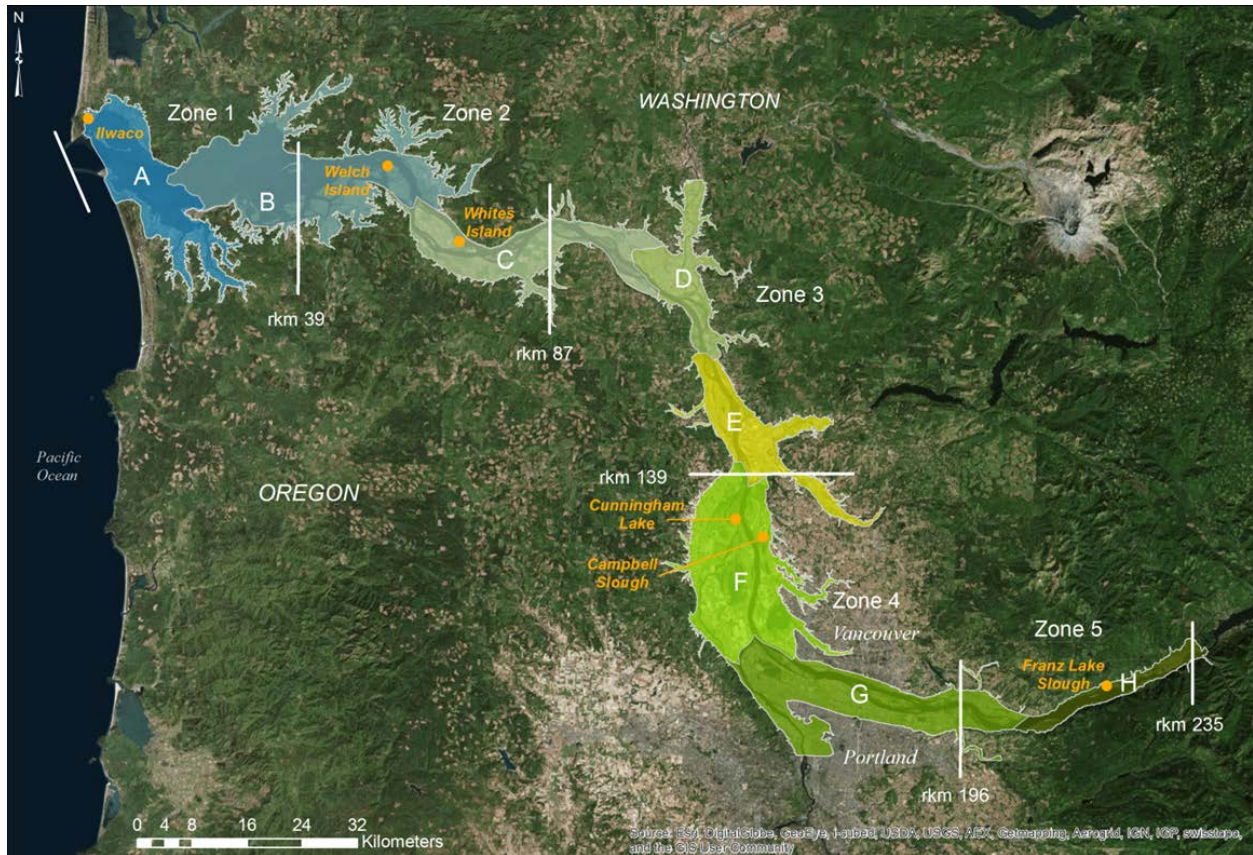


Figure 1. Lower Columbia River and estuary with hydrogeomorphic reaches (A-H) specified by color (Simenstad et al. 2011) and wetland zones (1-5) delineated by white lines (Jay et al. 2016). The 2021 EMP trends sites are shown in orange.

1.3 Characterization of Emergent Wetlands in the Lower Columbia River

1.3.1 Sampling Effort, 2005-2021

The objective of the EMP is to characterize habitat structure and function of estuarine and tidal freshwater habitats within the lower river in order to track ecosystem condition over time, determine ecological variability in these habitats, and provide a better understanding of ecosystem function. The EMP is largely focused on characterizing relatively undisturbed tidally-influenced emergent wetlands that provide important rearing habitat for juvenile salmonids, which also serve as reference sites for restoration actions. The Estuary Partnership and its monitoring partners have focused on providing an inventory of salmon habitats (or “status”) across the lower river and including a growing number of fixed sites for assessing interannual variability (or “trends”). Between 2005 and 2012, three to four status sites in a previously unsampled river reach (as denoted in the Classification described above) were selected for sampling each year, along with ongoing sampling of a growing number of trends sites (Table 1). Since 2007, we have conducted co-located monitoring of habitat structure, fish, fish prey, and basic water quality metrics at multiple emergent wetland sites throughout the lower river. In 2011, the Estuary Partnership added food web and abiotic conditions (i.e., conditions influencing productivity such as

temperature, turbidity, dissolved oxygen, nutrients) sampling and analysis in both the mainstem Columbia River and at the trend sites.

In 2013, the EMP sampling scheme was adjusted to no longer include data collection at status sites and monitoring efforts focused solely on the six trends sites. The six trends sites selected based on EM Zones were Ilwaco Slough (2010-2021), Secret River (2010-2016), Welch Island (2010-2021), Whites Island (2009-2021), Campbell Slough in the Ridgefield National Wildlife Refuge (2005–2021), and Franz Lake (2008-2009, 2011-2021). Habitat and hydrology data were collected at Cunningham Lake (in addition to the trends sites) as a reference site for habitat and hydrology representative of Reach F sites because vegetation has been periodically trampled by livestock at Campbell Slough in past years. Sampling efforts was discontinued in Secret River from 2017. Beginning in 2018, Steamboat Slough, an Action Effectiveness Monitoring and Research site, was included in the habitat biomass data collection efforts to aid in the applied interpretation of these data (Schwartz et al. 2019). Methods from the protocol Lower Columbia River Habitat Status and Trends (v1.0, [ID 85](#)) were used to monitor the status and trends of specified metrics.

Activities Performed, Year 17 Contract (October 1, 2020 – September 30, 2021):

- Salmonid occurrence, community composition, growth, condition, diet, prey availability, and residency
- Habitat structure, including physical, biological and chemical properties of habitats
- Food web characteristics, including the primary and secondary production of shallow water habitats and in the mainstem lower river and,
- Biogeochemistry of tidal freshwater region of the lower river for comparison to the biogeochemistry of the estuary, key for assessing hypoxia, ocean acidification, and climate change impacts.

Table 1. Summary of sampling effort by site and year(s) conducted at EMP sampling sites. Bold text indicates that data were collected in 2019.

Reach	Type of Site	Site Name	Site Code	Vegetation & Habitat¹	Fish & Prey⁵	Abiotic Conditions	Food Web⁴
A	Trend	Ilwaco Slough	BBM	2011-2021	2011-2013, 2015-2021	2011-2013, 2015-2021	2011-2013, 2015-2021
B	Trend	Secret River	SRM	2008 ² , 2012-2016	2012, 2013		2012, 2013
	Tributary	Grays River, lower	-		2015		2015
	Trend	Welch Island	WI2	2012-2021	2012-2021	2014, 2019-2021	2012-2021
C	Status	Ryan Island	RIM	2009	2009		
	Status	Lord-Walker Island 1	LI1	2009	2009		
	Status	Lord-Walker Island 2 ³	LI2	2009			
	Trend	Whites Island	WHC	2009-2021	2009-2021	2009, 2011-2021	2011-2021
	Status	Jackson Island	JIC	2010	2010		
	Status	Wallace Island	WIC	2010	2010		
	Status	Bradwood Landing	BSM		2010		
D	Status	Cottonwood Island small slough	CI2	2005			
	Status	Cottonwood Island large slough	CI1	2005			
	Status	Dibble Slough	DSC	2005		2005	
E	Status	Sandy Island 1, 2	SI1, SI2	2007	2007		
	Status	Deer Island	DIC	2011	2011		
	Status	Martin Island	MIM	2007			
	Status	Goat Island	GIC	2011	2011		
	Status	Burke Island	BIM	2011	2011		
	Tributary	Lower Lewis River	-		2015		
	Status	Lewis River Mouth	NNI	2007			
F	Status	Sauvie Cove	SSC	2005			
	Status	Hogan Ranch	HR	2005			
	Trend	Cunningham Lake	CLM	2005-2021	2007-2009		
	Trend	Campbell Slough	CS1	2005-2021	2007-2021	2008-2021	2010-2021
G	Status	Water Resources Center	WRC	2006			

Reach	Type of Site	Site Name	Site Code	Vegetation & Habitat ¹	Fish & Prey ⁵	Abiotic Conditions	Food Web ⁴
	Status	McGuire Island	MIC	2006			
	Status	Old Channel Sandy River	OSR	2006			2006
	Status	Chattam Island	CIC	2006			
	Status	Government/Lemon Island	GOM	2012	2012	2012	
	Status	Reed Island	RI2	2012	2012	2012	
	Status	Washougal Wetland	OWR	2012	2012	2012	
	Trend	RM122	-			2012-2021	
H	Trend	Franz Lake (slough)	FLM	2008-2009, 2011-2021	2008-2009, 2011-2021	2011-2021	2011-2021
	Status	Sand Island	SIM	2008	2008	2008	
	Status	Beacon Rock		2008	2008		
	Status	Hardy Slough	HC	2008	2008		

¹ Vegetation biomass data were not collected at any EMP sites in 2014. Only the four upstream trends sites were sampled for biomass in 2015.

² Site sampled as part of the Reference Site Study; thus, only vegetation and habitat data were collected.

³ Lord-Walker Island 2 was sampled by the EMP in conjunction with the Reference Site Study; thus, only vegetation and habitat data were collected.

⁴ Phytoplankton and zooplankton only sampled from 2011 – 2019.

⁵ Fish prey data were not collected for juvenile Chinook salmon diet and prey availability analyses in 2014 or 2020.

1.3.2 Site Descriptions

In 2021, the EMP focused primarily on the five trends sites that were monitored over multiple years: Ilwaco Slough, Welch Island, Whites Island, Campbell Slough, and Franz Lake Slough. Habitat and hydrology data were collected at all five trends sites plus Cunningham Lake, which is typically sampled for habitat and hydrology metrics as a control site since livestock grazing activities occasionally occur at Campbell Slough (Table 1). Coordinates for trends sites sampled in 2021 are listed in Table 2. The 2021 trends monitoring sites are described in order below, starting at the mouth of the Columbia River and moving upriver towards Bonneville Dam (Figure 1). Maps of the sites, including vegetation communities, are provided in Appendix A and photo points from all sampling years are provided in Appendix B.

Ilwaco Slough. This site is located in Reach A, EM Zone 1 at river kilometer (rkm) 6, southwest of the entrance of Ilwaco harbor, in Baker Bay, WA. The property is currently owned by Washington Department of Natural Resources. The site has developed in the past century as the bay filled in, likely due to changes in circulation from the construction of the jetties at the mouth of the Columbia River, the placement of dredge material islands at the mouth of the bay, and changes in river flows. Ilwaco Slough marsh is dominated by lush fields of Lyngby's sedge (*Carex lyngbyei*) with higher portions occupied by tufted hairgrass (*Deschampsia cespitosa*) and cattail (*Typha angustifolia*). Being so close to the mouth of the Columbia River, the tidal channel is regularly inundated with brackish water (average salinity < 10 Practical Salinity Units (PSU), however salinity up to 20 PSU occur in the late summer). Selected as a longterm monitoring site in 2011, Ilwaco Slough was sampled for all EMP metrics every year except 2014 when only habitat and hydrology were monitored.

Welch Island. The monitoring site on Welch Island is located in Reach B, EM Zone 2 on the northwest (downstream) corner of the island at rkm 53, which is part of the Lewis and Clark National Wildlife Refuge. The island was present on historical late-1800's maps; however, the island has expanded since then, and wetland vegetation has developed where there was previously open water near the location of the study site. The site is a high marsh dominated by *C. lyngbyei*, but with diverse species assemblage and a scattering of willow trees. Small tidal channels grade up to low marsh depressions within the higher marsh plain. The area was selected as a longterm monitoring site in 2012; two other areas of the island were monitored as part of the Reference Sites Study in 2008 and 2009 (Borde et al. 2011).

Whites Island. The Whites Island site is Reach C, EM Zone 2 located on Cut-Off Slough at the southern (upstream) end of Puget Island, near Cathlamet, Washington at rkm 72. A portion of the island is owned by Washington Department of Fish and Wildlife (WDFW) and is maintained as Columbia white-tailed deer habitat. Whites Island is not present on historical maps from the 1880s and was likely created from dredge material placement. The site is located at the confluence of a large tidal channel and an extensive slough system, approximately 0.2 km from an outlet to Cathlamet Channel; however, according to historic photos, this outlet was not present prior to 2006 and the connection to the river mainstem was approximately 0.7 km from the monitoring site. The site is characterized by high marsh, some willows, scattered large wood, and numerous small tidal channels. This longterm monitoring site has been surveyed annually since 2009.

Cunningham Lake. Cunningham Lake is a floodplain lake located in Reach F, EM Zone 4 at rkm 145 on Sauvie Island in the Oregon DFW Wildlife Area. The site is a fringing emergent marsh at the upper extent of the extremely shallow "lake" (Figure 2f) and at the end of Cunningham Slough, which meanders approximately 8.7 km from Multnomah Channel (a side channel of the Columbia River). The mouth of the Slough is located between rkm 142 and 143 near where Multnomah Channel meets the Columbia River. This longterm monitoring site has been sampled exclusively for habitat and hydrology data

annually since 2005. In some years, the “lake” is covered with Wapato (*Sagittaria latifolia*), however, in all years since 2005, this cover has been sparse or non-existent until 2016 when cover increased once again. In 2017 Cunningham Lake was heavily grazed by cattle. In 2018, greater efforts were made to keep the cattle out; however, some grazing still continued at a lesser extent through 2021 and is expected to continue.

Campbell Slough. The Campbell Slough site is located in Reach F, EM Zone 4 at rkm 149 on the Ridgefield National Wildlife Refuge in Washington. This longterm monitoring site has been surveyed annually since 2005. The monitoring site is an emergent marsh adjacent to the slough, approximately 1.5 km from the mainstem of the Columbia River. The site grades from Wapato up to reed canarygrass. The US Fish and Wildlife Service manages the impact of reed canarygrass within the extensive refuge by allowing cattle grazing in some areas. The site is usually fenced off from cattle except for times during and immediately after high freshets, which can cause holes in the fencing due to high flows and occasional woody debris. Extensive grazing occurred at the site in 2007, but vegetation appeared to recover in subsequent years. In 2010 and 2011, slight evidence of grazing was again observed. Since 2012 the site has been periodically grazed and trampled by cows, affecting primarily the upper marsh portion of the site that is dominated by reed canarygrass. In 2017 this site was heavily impacted by cattle grazing due to the removal of the protective fence in the previous winter (2016). In 2018 an electric fence was installed, however it failed to keep cattle out, and the wetland was grazed during the growing season prior to habitat monitoring. The electric fence was updated in 2019 in an attempt to prevent further grazing, but it failed. Due to COVID-19, no fence was installed in 2020 and grazing has continued to impact the site through 2021 and is expected to continue. In 2021, a secondary area of the site was established in a region of the site where minimal grazing appears to occur. This new monitoring area, named Campbell Slough-Channel, is just across the main slough channel from the historic monitoring area and will be added to this and future reports for comparison.

Franz Lake. The longterm monitoring site located in Reach H, EM Zone 5, the furthest up river site at rkm 221 is Franz Lake, which is part of the Pierce National Wildlife Refuge. The site has an expansive area of emergent marsh extending 2 km from the mouth of the slough to a large, shallow ponded area. Several beaver dams have created a series of ponds along the length of the channel resulting in large areas of shallow-water wetland with fringing banks gradually sloping to an upland ecosystem. The sample site is located approximately 350 m from the channel mouth, spanning an area impacted by a beaver dam. The site is primarily high marsh with scattered willow saplings, fringed by willows, ash, and cottonwood. The beaver dam has come and gone throughout the monitoring years but remained somewhat stable between 2017-2020, and then was breached in 2021 impacting the habitat conditions. The dam was rebuilt by beaver in the fall of 2021 and was observed in place during the winter 2022 field sampling.

Table 2. Coordinates of the trend sites sampled in 2021.

Site Name	Latitude	Longitude
Ilwaco Slough	46°18.035'N	124° 2.784'W
Welch Island	45° 47.032'N	122° 45.291'W
Whites Island	45° 9.561'N	122° 20.408'W
Cunningham Lake	45° 48.448'N	122° 48.285'W
Campbell Slough	45° 47.032'N	122° 45.291'W
Franz Lake	45° 36.035'N	122° 6.184'W



a) Ilwaco Slough



b) Welch Island



c) Whites Island



d) Cunningham Lake



e) Campbell Slough



f) Franz Lake Slough

Figure 2. Ecosystem Monitoring sites sampled in (photos taken in 2016): (a) Ilwaco Slough; (b) Welch Island; (c) Whites Island; (d) Cunningham Lake; (e) Campbell Slough; (f) Franz Lake Slough. Updated site photos were unavailable at the time this report was compiled, UAV images from 2019-2021 are available upon request and will be added to the online Tableau database in future reporting years.

1.3.3 Water Year

River flows in the Columbia and its tributaries are influenced by a combination of winter snowpack and pluvial flows driven by rainfall. High snowpack arises from cold and wet winters, while low snowpack arises from dry conditions throughout the winter, which can be either warm or cold (Figure 4). The timing of precipitation and whether it falls as snow or rain influences the timing and magnitude of the spring freshet. Typically, the freshet begins in late April/early May and persists into June. After that, the summer period tends to be dry and river flows are low between June and October.

Compared to the previous nine years (Figure 3), discharge at Bonneville Dam during the freshet in 2020 was close to average. However, flows were extremely low in 2021, with discharge volumes similar to 2015 (Figure 3). There were periods in 2020 where flows were quite low; river flows from late March until late April were as low as those in 2010, 2013, and 2021; however, the onset of the spring freshet led to flows that were very close to average. In contrast, flows in 2021 were low through the late winter, spring, and summer periods.

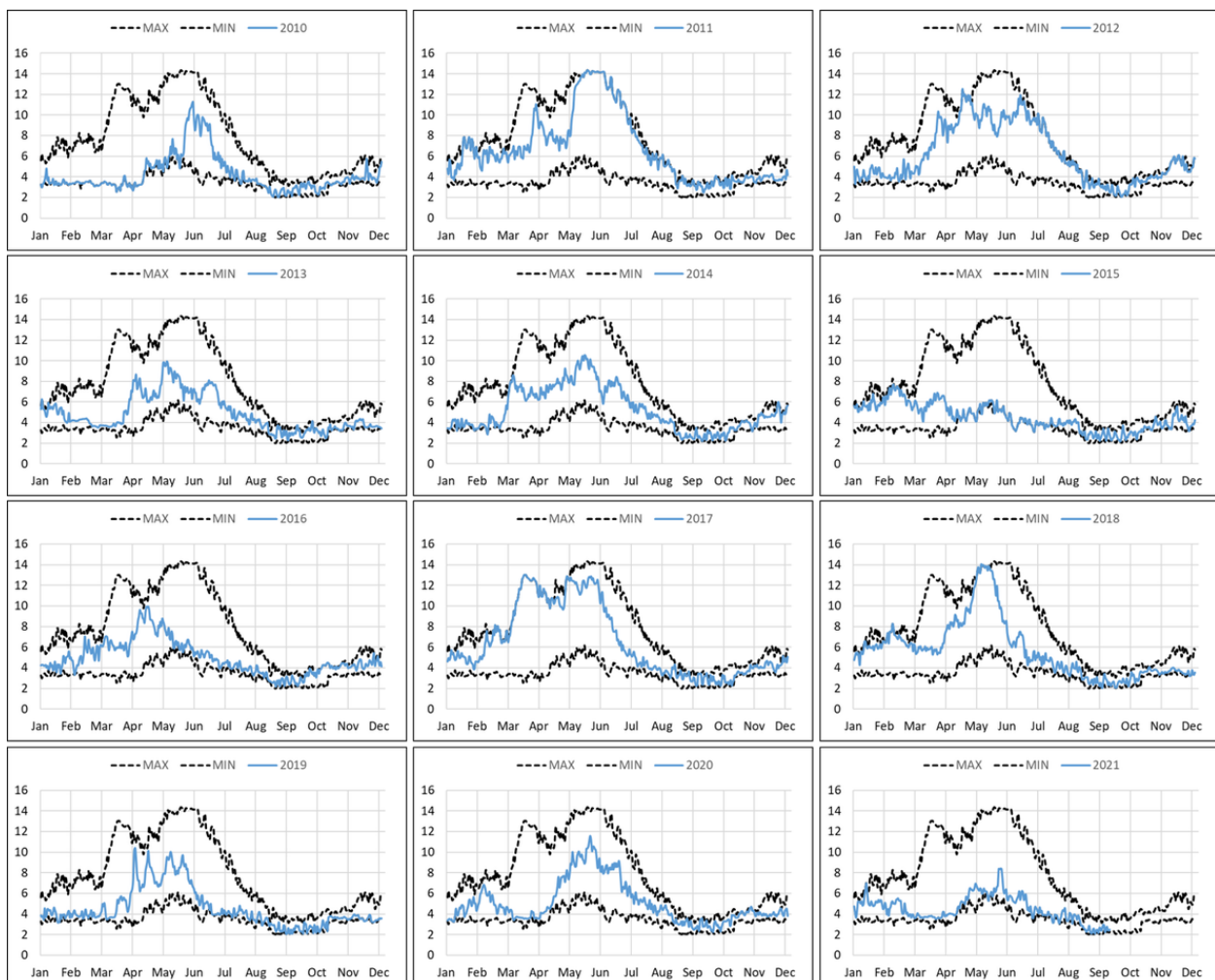


Figure 3. Daily average discharge volume (in $\text{m}^3 \text{s}^{-1}$) in blue for the years 2010 through 2021. Each panel represents one year (Jan – Dec). Also shown in each plot is the maximum and minimum daily average flows for all years combined. If the blue line matches either the minimum or maximum, those are the values that constitute the lowest or highest, respectively, in the time series.

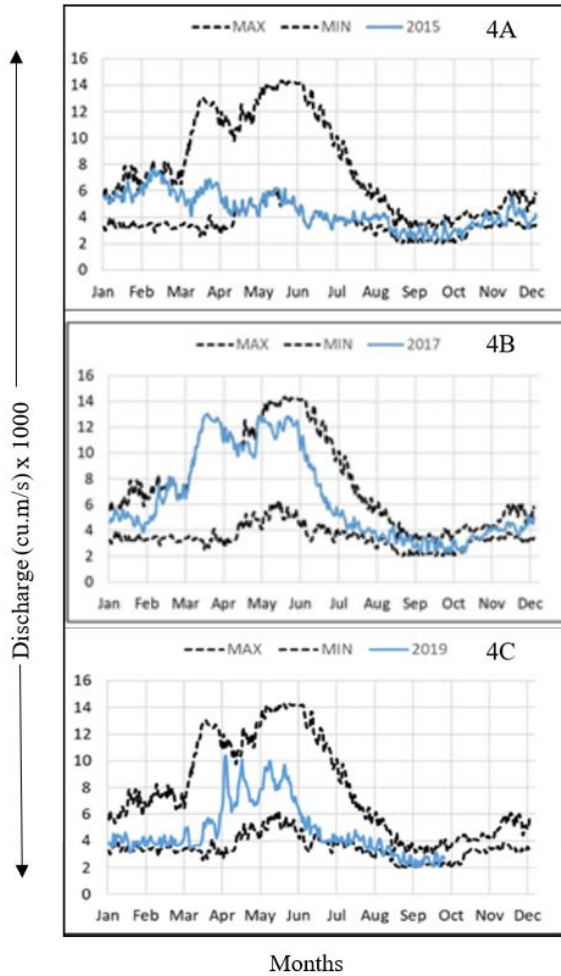


Figure 4. Comparative panels of minimum, maximum, and average river discharge at Bonneville Dam in 2015, 2017, and 2019. Panel 4A represents discharge for 2015 which consisted of warm rainy winter, low snowpack and summer drought. Panel 4B represents discharge for 2017 which consisted of high precipitation and large snowpack. Panel 4C represents discharge for 2019, described as an “dry” year.

Based on Figure 3 an NMDS plot of differences in river discharge and river temp between years, hydrologic conditions or cumulative discharge of the Mainstem since 2010 were classified into four categories (Table 3). The results presented in this report have compared the evolution of abiotic and biotic conditions over the monitoring years and differentiated the results between the tabulated categories. Any additional or modified freshet categories have been included in respective sub-sections.

Table 3: Classification of Monitoring years according to cumulative river discharge during the spring freshet between 2010-2021

Year	Cumulative River Discharge ($m^3 \times 10^{10}$) for May – Aug ²	River Temperature ¹ (days)	Classification
2021	5.4	73	Very dry
2020	7.5	50	Mid
2019	5.9	85	Dry
2018	7.8	79	Mid/wet
2017	8.7	78	Wet

2016	5.5	85	Dry
2015	4.7	102	Very dry
2014	7.3	86	Mid
2013	6.7	84	Mid
2012	9.2	59	Wet
2011	10.4	59	Wet
2010	6.3	47	Mid

¹River temperature: Number of days that the river temp was >19 °C May –Sep

²Freshet: cumulative river discharge (m³ x 10¹⁰) for May – Aug. Also referred to as “Freshet condition” in this report

1.4 Report Organization

We have divided this report into six sections, excluding References and Appendices. In section 2, we describe methods used to collect data from the mainstem and site-specific abiotic and biotic aspects. Methods of analysis are also described in this section. Section 3 presents results of the 2019 monitoring effort. We begin by describing abiotic and nutrient characteristics of the mainstem, and then move onto site-specific abiotic conditions. We then report on site-specific hydrological patterns, sediment dynamics, habitat structure, and channel morphology. We then move on to food web dynamics at the trend sites, reporting on primary and secondary productivities, plankton assemblages, as well as isotope analyses of carbon and nitrogen for vegetation and plankton. Stable isotope ratios for salmon prey and whole body salmon have also been presented in this report. Section 3.5 describes prey availability for 2021 and Section 3.6 reports out on Juvenile Chinook community and genetic stock composition for 2021 at the trend sites. GLM models have been used to study the influences of environmental variables and genetic stocks on growth rates in juvenile salmon. Salmon health were determined by lipid content in body samples. Due to a lack of significant differences between freshet conditions (Table 3) and salmon community composition or influence on growth rates or health, no results have been included for this aspect in this report. Based on the overall results, trends observed over the years have been discussed in Sections 4 and 5. In order to inform restorative actions in the study area, Adaptive Management measures have been provided in Section 6.

2 Methods

2.1 Mainstem Conditions

2.1.1 Overview

There are two in-situ water quality monitoring platforms in the mainstem Columbia River that provide baseline water quality measurements in support of the Ecosystem Monitoring Program. The first platform, funded by the National Science Foundation, was installed in July 2009 at River Mile 53 (in Reach C) and is physically located on a USGS Dolphin piling (46 11.070 N, 123 11.246 W; Figure 5). A second platform, funded by the Ecosystem Monitoring Program, was installed in August 2012 at River Mile 122 (in Reach G) and is physically located on the outer-most floating dock at the Port of Camas-Washougal (45 34.618 N, 122 22.783 W; Figure 5). The monitoring protocol can be found on monitoringmethods.org ([Protocol ID 459](#)). Each instrument platform consists of a physical structure, sensors, sensor control, power supply and distribution, and wireless communication. Data transmitted from the sensors is available within 1–2 hours of collection. Raw data can be downloaded in near-real time from a dedicated webpage (<http://columbia.loboviz.com/>), and data that have been examined for quality assurance is available upon request). In addition to capturing spatial and temporal resolution of basic water quality and biogeochemical observations for the mainstem Columbia River, an outcome of this effort is to provide daily estimates of parameters necessary for the assessment of ecosystem conditions at sites upstream and downstream of the Willamette-Columbia confluence. Knowledge of daily conditions at these sites allows the identification of contributions from lower river tributaries. Availability of these data enables the calculation of fluxes of various inorganic and organic components, such as nitrate concentration or chlorophyll, an estimate of phytoplankton biomass. Knowledge of nutrients and organic matter flux for a large river is important for a variety of applications, including assessment of pollution, an indication of eutrophication, and quantification of material loading to the coastal zone, where many important ecological processes may be affected. Another product is the assessment of Net Ecosystem Metabolism (NEM), which provides a daily measure of the gross primary production and aerobic respiration occurring in the river as measured by hourly changes in dissolved oxygen. NEM is often used by managers to identify changes or impairments to water quality (Caffrey 2004).

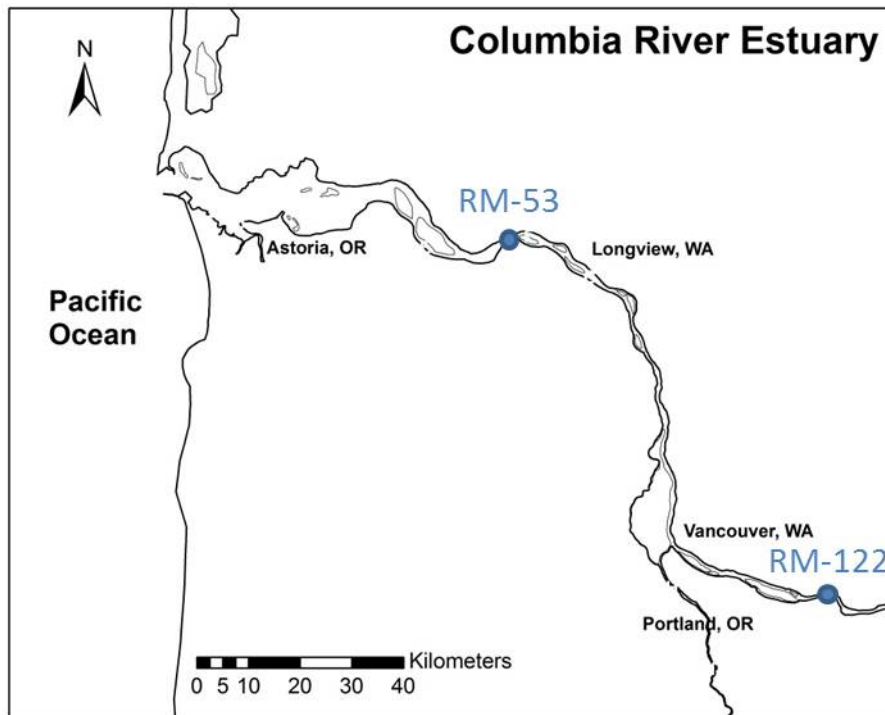


Figure 5. Station locations for the two in-situ water quality monitoring platforms in the mainstem Columbia River that support the Ecosystem Monitoring Program. RM-53 (river mile 53) is Beaver Army Terminal, while RM-122 (river mile 122) is located in Camas, WA.

2.1.2 Operation of RM-122 Platform at Port of Camas-Washougal

In 2020 and 2021, water quality was measured by a YSI sonde equipped with temperature and dissolved oxygen (DO) sensors at the Port of Camas-Washougal (RM-122). At Beaver Army Terminal (RM-53) the platform is a LOBO (Land-Ocean-Biogeochemical-Observatory) equipped with temperature sensors. These data provide information about conditions in the Columbia River mainstem for comparison with the off-channel, EMP sites both upstream (RM-122) and downstream (RM-53) of the Willamette-Columbia confluence. YSI deployed at Camas 3/4/2021.

2.1.3 Sensor Configuration

Instruments and sensors deployed at Camas are described in Table 4. Sensors are configured to collect a sample every hour.

Table 4. Description of the components on the LOBO sensor platforms located at RM-53 and RM-122. Note that the LOBO system was deployed from January through June; after this, the system consisted of a YSI sonde equipped with temperature, conductivity, and dissolved oxygen.

Company	Sensor	Parameters
SeaBird (formerly Satlantic)	LOBO	Power distribution Sensor control Wireless communication Data management
SeaBird (formerly WET Labs)	WQM Water Quality Monitor	Conductivity, Temperature, Dissolved Oxygen, Turbidity, Chlorophyll <i>a</i> Concentration

2.1.4 Sensor Maintenance

The sensors are designed to operate autonomously, at high temporal resolution (hourly), and over long periods between maintenance (estimated at three months, although sensors are typically maintained at shorter intervals). This is achieved through a design that maximizes power usage and minimizes biofouling. Antifouling is achieved through the use of sunlight shielding (to prevent algae growth), window wipers, copper instrument surfaces, and bleach injection of the internal pumping chamber. Maintenance trips include cleaning of all sensors and surfaces and performing any other needed maintenance. Additionally, water samples are collected for laboratory analysis of nutrients and chlorophyll *a*. Maintenance activities took place approximately every three weeks in order to change the batteries, clean and calibrate the instruments, download data, and make any necessary adjustments.

2.1.5 Quality Control

Initial sensor calibration was performed by the manufacturer. Each instrument is supplied with a certificate of calibration, and where appropriate, instructions for recalibration. For example, the Seabird SUNA for nitrate measurements operates with a calibration file determined at the factory under strictly controlled environmental conditions but which can be periodically checked and modified for sensor drift by performing a “blank” measurement at our OHSU laboratory using deionized water. At longer intervals (every 1–2 years) the sensors are returned to the factory for maintenance and recalibration.

During periodic sensor maintenance, samples are collected for additional quality control criteria. At RM-53, nutrients, and chlorophyll *a* samples are returned to the laboratory at OHSU and analyzed using established laboratory techniques. Laboratory-based chlorophyll *a* measurements are used to correct the in situ fluorometer measurements. The discrete samples and the corresponding sensor data for nitrate and chlorophyll *a* are shown in Table 5.

Table 5. Comparison of in situ data with laboratory measurements of water samples.

Location/Parameter/# measurements	Regression equation
RM-122/Nitrate/46	$Y = 0.95x + 1 \quad r^2 = 0.99$
RM-122/Chl/13	$Y = 0.8x + 1 \quad r^2 = 0.93$

2.2 Abiotic Site Conditions

2.2.1 Continuous Water Quality Data (Temperature, DO, pH, Conductivity)

In 2019, water quality was continuously monitored at five trends sites, Ilwaco Slough, Welch Island, Whites Island, Campbell Slough, and Franz Lake (Table 6). The monitoring protocol can be found on

monitoringmethods.org ([Method ID 816](#)). Figure 6 shows how the sensors were deployed to ensure ready access for servicing, and data downloads and Figure 7 shows the periods of deployment of in situ sensors between 2008-2021.

Table 6. Locations of water quality monitors (YSI sondes) at trends sites. Deployment periods for sensors at each of the sites is shown in Figure 7

Site name*	USGS site number	Site name*	Reach	Latitude	Longitude	Monitor deployment date	Monitor retrieval date
Ilwaco Slough			A	46° 18' 19"	-124° 02' 06"	3/13/2021	9/11/21
Welch Island	461518123285700	Unnamed Slough, Welch Island, Columbia River, OR	B	46° 15' 18.4"	-123° 28' 56.8"	3/1/2021	8/9/21
Whites Island	460939123201600	Birnie Slough, White's Island, Columbia River, WA	C	46° 09' 39"	-123° 20' 16"	3/1/2021	8/9/21
Campbell Slough	454705122451400	Ridgefield NWR, Campbell Slough, Roth Unit, WA	F	45° 47' 05"	-122° 45' 15"	3/2/2021	9/21/21
Franz Lake	453604122060000	Franz Lake Slough Entrance, Columbia River, WA	H	45° 36' 04"	-122° 06' 00"	3/4/2021	9/21/21

*Site names used in this report differ from official USGS site names to be consistent with site names used by other EMP partners.



Figure 6. Images are showing deployment of water quality monitors (YSI sondes) at study sites.

The water quality monitors were Yellow Springs Instruments (YSI) models 6600EDS and 6920V2, equipped with water temperature, specific conductance, pH, and dissolved oxygen probes. In addition,

YSI EXO2 units equipped with fluorometer were installed at Campbell Slough and Franz Lake Slough. Addition of a fluorometer provides a capability to detect and monitor chlorophyll and phycocyanin, pigments that approximates the biomass of total phytoplankton and cyanobacteria, respectively. Table 7 provides information on the accuracy and effective ranges for each of the probes. The deployment period for the monitors was set to characterize water quality at the trend sites during the juvenile salmonid migration period. In 2020 and 2021, the monitors were deployed from mid-March through mid-September (Table 7). Data gaps reflect issues in data acquisition, which were unfortunately not caught early due to travel limitations associated with the covid-19 pandemic. In this report, given that the majority of the trends sites are located within Washington State, site-specific water quality data are compared to standards for temperature, pH, and dissolved oxygen set by the Washington Department of Ecology to protect salmonid spawning, rearing, and migration, available at <http://www.ecy.wa.gov/programs/wq/swqs/criteria.html>. Note that water temperature standards set by the Washington Department of Ecology (threshold of 17.5°C) are more conservative than those outlined by the maximum proposed by Bottom et al. (2011) used for comparisons in the mainstem conditions section of this report (Section 2.1).

Table 7. Range, resolution, and accuracy of water quality monitors deployed at four trends sites. m, meters; °C, degrees Celsius; µS/cm, microsiemens per centimeter; mg/L, milligrams per liter.

Monitoring Metric	Range	Resolution	Accuracy
Temperature	-5–70°C	0.01°C	±0.15°C
Specific conductance	0–100,000 µS/cm	1 µS/cm	±1 µS/cm
ROX optical dissolved oxygen	0–50 mg/L	0.01 mg/L	±0–20 mg/L
pH	0–14 units	0.01 units	±0.2 units

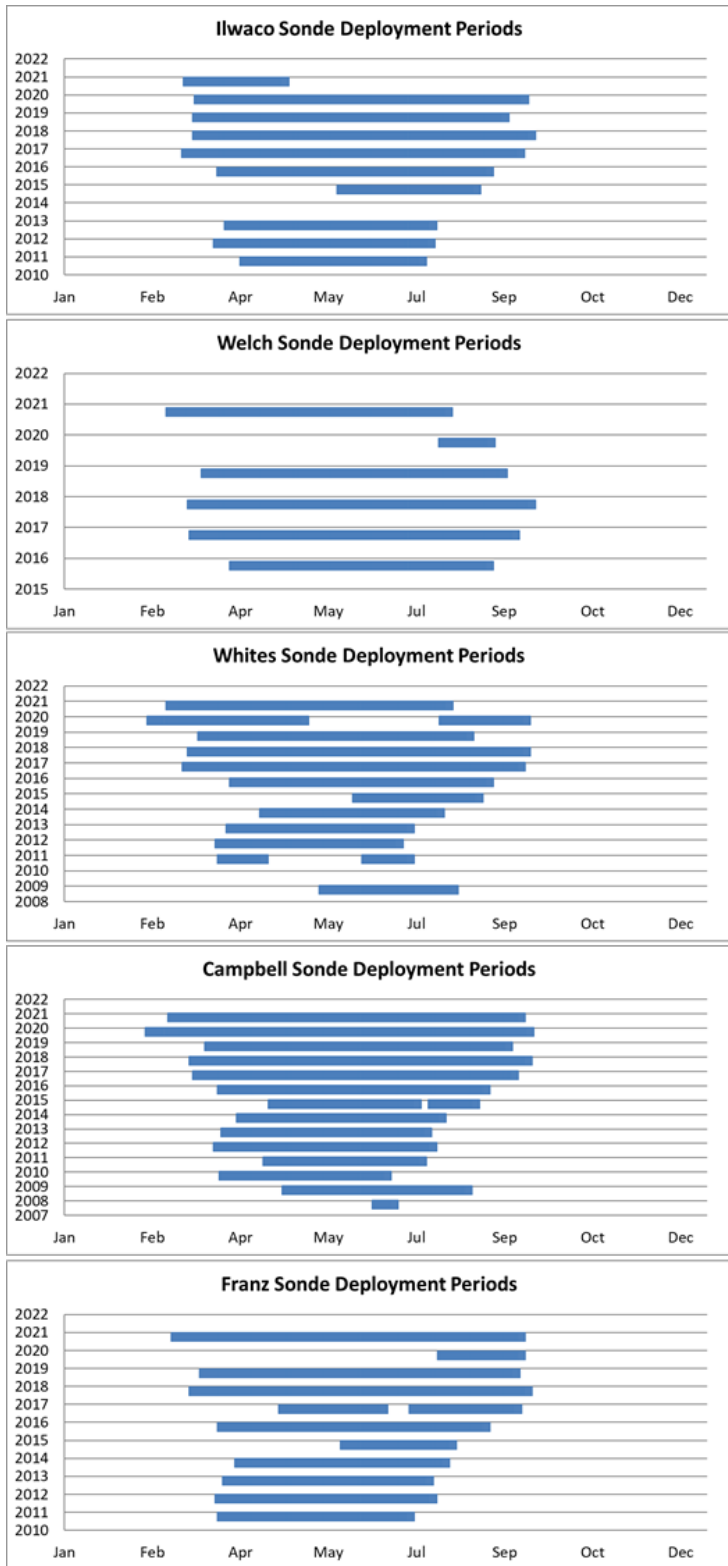


Figure 7. Time periods are corresponding to sensor deployments at five trends sites (2008–2021).

2.2.2 Nutrients (N, P)

Nitrogen and phosphorus are dissolved nutrients that are often present at low enough concentrations to limit plant and phytoplankton growth in aquatic environments relative to other growth requirements. Conversely, in many water bodies, high levels of these nutrients arise from fertilizer and other inputs, which leads to the impairment of water quality following the stimulation of algal and bacterial growth. To analyze water column nutrient concentrations, two 1 L water grab samples were collected from representative open water areas within the sites and subsampled before processing. Three fractions were determined from the subsamples: (1) dissolved inorganic species of nitrogen and phosphorus (nitrate, nitrite, ortho-phosphate, ammonium), (2) total dissolved nitrogen and phosphorus (TDN, TDP), and (3) total nitrogen and phosphorus (TN, TP). Nitrate + nitrite and orthophosphate were determined according to EPA standard methods (EPA 1983a), ammonium was determined colorimetrically (APHA 1998), and total phosphorus were determined according to USGS (1989). Detection limits for each ion or species are given in Table 8. The dates corresponding to sample collection are discussed in Section 2.4.1.2. The monitoring protocol can be found on monitoringmethods.org ([Method ID 1591](#)).

Table 8. Detection limits for colorimetric analysis of nitrogen and phosphorus species. TDN = total dissolved nitrogen, TN = total nitrogen, TDP = total dissolved phosphorus, TP = total phosphorus.

Ion or element	Detection limit (mg/L)
Ammonium	0.00280134
Nitrate + Nitrite	0.00700335
Nitrite	0.00140067
TDN	0.01540737
TN	0.1960938
Phosphate	0.00619476
TDP	0.00619476
TP	0.9601878
Silicic acid	0.0280855

2.3 Habitat Structure

In 2021, LCEP and ETG collected field data on vegetation and habitat conditions at the six trends sites (Figure 1). Monitoring dates are provided in Table 9, and detailed maps of the 2021 monitoring sites are presented in Appendix A.

Table 9. Site location and sampling dates for each site sampled in 2021. All habitat and hydrology metrics were sampled at these sites except as otherwise noted.

Site Name	Site Code	River kilometer (rkm)	Site Type	Sampling Date
Ilwaco Slough (Baker Bay)	BBM	6	Trend	7/26/21
Welch Island	WI2	53	Trend	7/22/21
Whites Island	WHC	72	Trend	7/21/21
Cunningham Lake	CLM	145	Trend	8/17/21
Campbell Slough	CS1	149	Trend	8/16/21
Franz Lake	FLM	221	Trend	8/6/21

2.3.1 Habitat Metrics Monitored

The habitat metrics in this study were monitored using standard monitoring protocols developed for the lower Columbia River (Roegner et al. 2009). In 2020 and 2021, monitoring efforts were focused on vegetation cover, elevation, hydrology, sediment accretion, and the quantification of vegetative biomass production and breakdown. These metrics have been determined to represent important structural components, which can be used to assess habitat function. The rationale for choosing these metrics is discussed below.

Elevation, hydrology, and substrate are the primary factors that control wetland vegetation composition, abundance, and cover. Knowing the elevation, soil, and hydrology required by native tidal wetland vegetation is critical to designing and evaluating the effectiveness of restoration projects (Kentula et al. 1992). In the lowest part of the estuary, salinity is also an important factor determining vegetation composition and distribution. Sediment accretion is important for maintaining wetland elevation. Accretion rates can vary substantially between natural and restored systems (Diefenderfer et al. 2008, Borde et al., 2012); therefore, baseline information on rates is important for understanding the potential evolution of a site. Evaluating vegetative composition and species cover indicates the condition of the site. Vegetation composition is important for the production of organic matter (released to the river in the form of macrodetritus), food web support, habitat for many fish and wildlife species including salmon, and contributions to the biodiversity of the Columbia River estuarine ecosystem. Likewise, vegetative biomass is being collected at the trends sites to begin to quantify the contribution of organic matter from these wetlands to the ecosystem.

Assessment of channel cross sections and channel networks provides information on the potential for many important estuarine functions including fish access (i.e., habitat opportunity; Simenstad and Cordell 2000) and export of prey, organic matter, and nutrients. This information is also necessary to develop the relationship between channel cross-sectional dimensions and marsh size, which aids in understanding the channel dimensions necessary for a self-maintaining restored area (Diefenderfer and Montgomery 2009).

2.3.2 Annual Monitoring

The monitoring frequency for the habitat metrics depends on the variability of the metric between years. The composition, cover, and elevation of vegetation have been monitored annually since 2005. Plant species composition and cover can vary substantially from year to year, depending on climate and related water level differences. Beginning in 2009, we also measured channel cross sections, water surface elevation, and sediment accretion rates. Beginning in 2011 plant biomass was collected at the trend sites, excluding Cunningham Lake annually. In 2015, biomass was collected at the four upstream sites, including Cunningham Lake to maximize collection at sites with reed canarygrass. Sediment samples were collected once from each site to characterize sediment grain size and total organic content but are not repeatedly collected.

Similarly, vegetation community mapping methods were used to characterize the landscape at the site. After repeated mapping at each site, we determined that large-scale changes were not occurring between years; therefore, this effort is no longer repeated during annual monitoring at trends sites unless vegetation changes are observed. Low inter-annual variability of channel morphology at the trends sites has been observed in prior sampling years. Thus only the cross-section at the channel mouth was measured in 2015. Photo points were also designated at each site from which photographs were taken to document the 360-degree view each year. Beginning in 2019, UAV photography began being used, generating high accuracy top-down orthomosaics of each site.

2.3.2.1 *Hydrology*

Continuous water level data is collected annually at all the trends sites. Occasionally sensor failure or loss occurred; however, the sensors have been downloaded and redeployed every year since the initial deployment for the collection of a nearly continuous dataset (Appendix C). The sensors were surveyed for elevation so that depth data could be converted to water surface elevation and evaluated against wetland elevations. The water surface elevation data was used to calculate the following annual hydrologic metrics for each site:

- Mean water level (MWL) – the average water level over the entire year
- Mean lower low water (MLLW) – the average daily lowest water level (*this may shift slightly with different annual deployment elevations of the data logger*)
- Mean higher high water (MHHW) – the average daily highest water level
- Annual water level range – the average difference between the daily high and low water levels
- Annual maximum water level – the maximum water level reached during the year

The monitoring protocol can be found on monitoringmethods.org ([Method ID: 3982](#)).

2.3.2.2 *Sediment Accretion Rate*

At each site beginning in 2008, PVC stakes were placed one meter apart and driven into the sediment and leveled. The distance from the plane at the top of the stakes to the sediment surface is measured as accurately as possible every 10 cm along the one-meter distance. The stakes were measured at deployment then subsequently on an annual basis. Additional stakes were deployed in Whites Island in 2012. New stakes were deployed at four of the five trend sites in 2015 to measure accretion at additional elevations within site. A new set of PVC stakes were installed at Campbell Slough at a lower elevation in 2019 and at Cunningham Lake in 2020 due to previous stakes going missing. The stakes, termed sedimentation stakes or pins, are used to determine gross annual rates of sediment accretion or erosion (Roegner et al. 2009).

The accretion or erosion rate is calculated by averaging the 11 measurements along the one-meter distance from each year and comparing the difference with past year's average. The accretion or erosion rates were plotted against marsh elevation (m, CRD) to test the hypothesis that high accretion is observed at lower marsh elevations. The accretion or erosion rates were also regressed against annual cumulative discharge from the mainstem over the monitoring period. The monitoring protocol can be found on monitoringmethods.org ([Method ID 818](#)).

2.3.2.3 *Salinity*

In order to better assess the influence of salinity on habitat, a conductivity data logger (Onset Computer Corporation) was deployed at the Ilwaco Slough site in August of 2011. The data logger records conductivity and temperature within the slough and derives salinity from those two measurements based on the Practical Salinity Scale of 1978 (see Dauphinee 1980 for the conversion). The monitoring protocol can be found on monitoringmethods.org ([Method ID 816](#)).

2.3.2.4 *Vegetation Species Assemblage*

The vegetation sampling areas at each site were selected to be near a tidal channel and to be representative of the elevations and vegetation communities present at the site. This was easier in the upper portions of the study area, where the sites were generally narrower, and the entire elevation range could be easily covered in the sample area. In the lower estuary, the sites are broad and covered a larger area, so in some cases, multiple sample areas were surveyed if possible, to cover different vegetation communities (e.g., low marsh and high marsh). The monitoring protocol can be found on monitoringmethods.org ([Method ID 822](#)).

Along each transect, vegetative percent cover was evaluated at 2 – 10 m intervals. This interval and the transect lengths were based on the marsh size and/or the homogeneity of vegetation. At each interval on the transect tape, a 1 m² quadrat was placed on the substrate and percent cover was estimated by observers in 5% increments. If two observers were collecting data, they worked together initially to ensure their observations were “calibrated.” Species were recorded by four letter codes (1st two letters of the genus and 1st two letters of species, with a number added if the code had already been used, e.g., LYAM is *Lysichiton americanus*, and LYAM2 is *Lycopus americanus*). In addition to the vegetative cover, features such as bare ground, open water, wood, and drift wrack were also recorded. When plant identification could not be determined in the field, a specimen was collected for later identification using taxonomic keys or manuals at the laboratory. If an accurate identification was not resolved, the plant remained “unidentified” within the database.

2.3.2.5 *Elevation*

Elevation has been measured many times in previous monitoring years at all trend sites at the locations of vegetation quadrats, water level sensor, sediment accretion stakes, and in the channels. While elevations change over time, the change from one year to the next is minimal, so high-resolution elevation measurements are not always collected each year (e.g., elevations were surveyed in 2016 so were not re-surveyed in 2017). The elevation is surveyed using a Trimble or TOPCON real-time kinematic (RTK) GPS with survey-grade accuracy. All surveying was referenced to the NAVD88 vertical datum; the horizontal position was referenced to NAD83. Data collected from the base receiver were processed using the automated Online Positioning User Service (OPUS) provided by the National Geodetic Survey. OPUS provides a Root Mean Squared (RMS) value for each set of static data collected by the base receiver, which is an estimate of error. A local surveyed benchmark was located whenever possible and measured with the RTK to provide a comparison between the local benchmark and OPUS-derived elevations.

Trimble Geomatics Office (TGO) software was used to process the data. Each survey was imported and reviewed. Benchmark information was entered into TGO, and rover antenna heights were corrected for disc sink (measured at each survey point to the nearest centimeter) at each point. The survey was then recomputed within TGO and exported in a GIS shapefile format. Surveys were visually checked within TGO and GIS software for validity. Historically elevations were then converted from NAVD88 to the Columbia River Datum (CRD) based on conversions developed by the USACE (unpublished). Using the CRD alleviates elevation differences associated with the increasing elevation of the riverbed in the landward direction. Sites below rkm 37, the lower limit of the CRD, were converted to mean lower low water (MLLW). Beginning in 2019, NAVD88 elevations were not converted to CRD to aid in the translation of wetland plant community and elevation results to project sponsors implementing restoration projects throughout the river (CRD not being as accessible of a datum as NAVD88).

Quality assurance checks were performed on all data. Elevations from the RTK survey were entered into an Excel spreadsheet and a Tableau Workbook to correspond to the appropriate transect and quadrat location. All elevations in this report are referenced to NAVD88 unless noted otherwise. The monitoring protocol can be found on monitoringmethods.org ([Method ID 818](#)).

2.3.3 *Analyses*

2.3.3.1 *Inundation*

The data from the water level sensors were used to calculate inundation metrics from the marsh and channel elevations collected at the sites. The percent of time each marsh was inundated was calculated daily across each marsh’s elevation gradient. The average inundation daily, as measured by the average numbers of hours a day (converted to a %) the water surface level is above the marsh elevation, is a means of comparing sites to each other and over time. This is similar to the historic sum exceedance value (SEV) analysis; however, it is summarized by day instead of over the entire growing season (Kidd 2017).

The average inundation daily at each site is dependent on the elevation, the position along the tidal and riverine gradient, and the seasonal and annual hydrologic conditions. The average % of the day the mean marsh elevation is inundated for the month of August was calculated for all sites and years. The month of August was chosen because it is a critical time for plant development in the upper river sites, as the freshet draws down and exposes the marsh surface.

Additionally, we have the most consistent amount of data for the month of August all sites and all years monitored. Generally, the trends in % time inundated identified in August correlate well with average % daily inundation for the year. Freshet conditions were also used in the hydrologic analysis; Freshet conditions were defined as the accumulative river discharge at Bonneville Dam from May-August ($m^3 \times 10^{10}$), this metric was developed by J. Needoba at Oregon Health & Science University (OHSU).

In 2021, we performed a combination of the SEV analysis and the average inundation daily analysis by calculating the percent of hours during the month of August that the site was inundated at each elevation band.

The monitoring protocol can be found on monitoringmethods.org ([Method ID 954](#)).

2.3.3.2 *Vegetation Community Change Analysis*

Plant species composition and productivity in tidal wetlands respond to annual variability in key ecological processes such as hydrology, salinity, sediment dynamics, and biological interactions. These processes vary naturally but are also projected to change substantially with climate change. For this reason, understanding how key characteristics and functions of wetlands change in response to these processes is important to longterm salmon recovery.

Processes such as hydrology can vary due to normal inter-annual climate variation that affects the amount and form of precipitation. For example, the phases of ENSO (El Nino/Southern Oscillation) and PDO (Pacific Decadal Oscillation) differ regarding the volume of precipitation received in a year, and the relative ratio of snow to rain which affects the spring freshet. Similarly, sea level and the effects of storm waves can vary from year to year in response to ENSO and other climate patterns. Marsh inundation patterns also vary as a result of the actions of bioengineers such as beavers. Grazing by cattle or other herbivores can affect species composition and wetland biomass productivity. Finally, species interactions such as competition from invasive non-native species can alter vegetation composition and wetland function. The strength of biotic interactions is affected by environmental conditions such as inundation, so the effects of biotic elements like invasive species can also vary from year to year.

Data Classification

To begin to evaluate the spatial and temporal variations in vegetation composition, we calculated changes in species richness, percent cover, and relative % cover within and among trend sites over time. Species richness is simply the total number of plant species. Total richness was calculated for each site and each year, as well as average richness per plot. Percent cover is the % of the soil surface that is covered by a plant species. Total plant cover for a plot may exceed 100% when plants overlap. When recording percent cover, maintaining consistency among observers or between years can be difficult, and for this reason, we use relative percent cover to compare species with each other. The relative cover is the proportion of total vegetative cover represented by a species or guild of species. With relative cover, the sum of all species always adds up to 100. The relative cover is a more reliable method for comparing species with each other or evaluating the change in a species over time. We further segregated plant species by key characteristics including native/non-native provenance and wetland indicator status. Additionally, Shannon diversity (H) and evenness (J) indices were calculated from the relative plant cover data using the standard methods outlined by Magurran (1988).

Most plants were identified to the species level or finer, allowing for clear categorization as native or non-native. However, occasionally at some growth stages, certain plants could not be identified to species level. A few of these taxa contained both native and non-native species or varieties and were classified as “Mixed.” For example, at certain growth stages, several species of *Agrostis* (bentgrass) are difficult to tell apart and were lumped as “*Agrostis* species.” Since this genus includes both native and non-native species, it was classified as “Mixed.” In calculations involving native vs. non-native species, “Mixed” taxa were included with the non-native group.

Most species also have a clear wetland indicator status that has been identified in the literature. Wetland indicator values reflect how dependent on wetland hydrology a species may be (Reed 1988). Obligate wetland species (OBL) are those that appear in wetlands >99% of the time. Facultative-Wet wetland species (FACW) are those that occur in wetlands 67-99% of the time and occasionally are found in non-wetland habitats. Facultative wetland species (FAC) are those that appear in wetlands about half the time (34-66%), and in non-wetland habitats at other times. Facultative upland species (FACU) are those that occur mostly in upland habitats and less than 34% of the time in wetland habitats, and Upland species (UPL) are those that occur in wetlands less than 1% of the time. The relative proportion of species that fall into those categories, and their respective percent cover, change as the environmental conditions and biotic interactions vary. These changes can indicate changes in wetland functions and values with respect to salmon.

Longterm Trends and Drivers Analysis

Longterm plant community change analysis was conducted across all active EMP sites including annual plant community data starting in 2011 through 2021. When applicable plant community metrics were transformed and correlated with hydrologic conditions such as annual freshet conditions and daily inundation, only significant (p-value < 0.05) correlation and regressions were reported. Data analysis was conducted using Microsoft Office Excel (2016), Exploratory (2017), R (2020), and Tableau (2022) software’s.

2.4 Food Web

2.4.1 Primary Productivity

2.4.1.1 *Emergent Wetland Vegetation*

2.4.1.1.1 *Aboveground Vegetation Biomass, Macrodetritus, and Soil*

Starting in the summer of 2017 detritus sampling was included in the biomass sampling and analysis to evaluate detrital production and export. In the winter of 2018 (and all sampling events to follow through 2021) biomass sampling protocols changed slightly to accommodate detrital sampling and streamline data collection (Table 10, Table 11). This included shifting from “strata” mixed species designations to simple high and low marsh strata descriptions across all sites sampled. This change has also included species biomass weights to be recorded individually to assess species-specific contributions to each high and low marsh stratum (in the past mixes of species were assessed together). In general, these changes will allow for a more detailed understanding of species-specific biomass contributions and still allow for longterm comparisons to overall site, high, and low marsh contributions.

Table 10: Seasonal data collection schedule Winter 2018-Summer 2021. Sp= Species. Some data is still under analysis.

Season	Live Sp Cover	Live Sp Weights	Detritus Lignin	Detritus C:N	Live Sp Lignin	Live Sp C:N	Soil C:N	Soil Bulk Density	Soil Grain Size
Winter 2018	X	X	X	X			X		
Spring 2018	X	X	X	X					
Summer 2018	X	X	X	X	X	X	X	X	X
Winter 2019	X	X	X	X					
Summer 2019	X	X	X	X	X	X			
Winter 2020	X	X	X	X	X	X			
Summer 2020	X	X	X	X	X	X			
Winter 2021	X	X	X	X	X	X			
Summer 2021	X	X	X	X	X	X			

Field Methods

From Summer 2011 to Summer 2021, aboveground biomass was sampled to estimate the primary productivity at three trends sites. Samples were collected in the summer (July or August) during the peak biomass period and again during the winter (January, February, or early March) during the winter low biomass period. In 2018, Spring sampling also took place in late March. For the emergent marsh biomass sampling, a 1m² plot was randomly placed along the established vegetation transect, but off-set 2 m from the transect to ensure that the biomass plots did not intersect the vegetation percent cover plots. Biomass was randomly sampled within distinct vegetation strata as determined by plant species dominance, to 1) more clearly associate the samples with vegetation type, and 2) reduce the variability between samples within strata. Within the 1m² biomass plot, a 0.1m² quadrat was placed in a randomly selected corner and all rooted vegetation, live and dead, was removed using shears. Each sample was sorted in the field to separate the primary strata species from other species and to distinguish live from dead plant material. The biomass samples were placed in uniquely numbered bags and held in a cooler until samples were transported to the laboratory. Dominant vegetation species were recorded along with the corresponding biomass sample number. Submerged aquatic vegetation (SAV) plots were sampled in 2011-2013 using similar methods; however, due to the relatively low contribution of this strata to the overall macrodetritus production, the collection did not continue in subsequent years.

Beginning in Summer 2018 at each site, we collected data and samples from at least 18 plots, nine high marshes, and nine low marshes. Plots were located in such a way to sample the dominant plant species present at each site in the high and low marsh and were distributed across the site while avoiding the permanent vegetation transects. During summer 2018, vegetation composition was assessed in a 1m² plot by quantifying % cover for each species that had at least 5% cover and noting any species that was present with less than 5% cover (species denoted as “Other”). If a species had dead biomass present (dead stems or leaves that were still attached to the root system), the % cover of dead biomass was measured separately from the % cover of live biomass. For species with greater than 5% cover, we recorded the average maximum height for both live and dead biomass. The % of the plot that was covered by water was noted, and its depth in cm. The % cover of bare ground and detritus was also noted. Biomass and

detritus collection occurred in a 0.1m² subplot in one of the corners of the larger plot. For this subplot, we noted which of the “Other” species were present since these were collected for biomass analysis. Beginning in winter 2019, the field data methods were changed, and vegetation height, species cover, water, bare ground, and detritus cover data were collected only for the small 0.1m² plot.

Beginning in Summer 2020, due to COVID-19, we reduced the number of plots from 18 plots, 9 high marsh and 9 low marsh plots to 10 plots, 5 high and 5 low marsh plots.

Biomass and Detritus Collection

In a 0.1m², we used clippers to cut all plant biomass at the soil surface. Plant matter was cut around the outer edge of the quadrat frame, and all material that was in or over the subplot was collected, whether or not it was rooted in the subplot. For plants rooted in the plot, only material that was in or over the plot was collected. The material was laid out on a plastic sheet in the field and separated by species and according to whether it was alive or dead. Species with cover >5% in the large plot were separated into separate plastic bags for analysis, while all species that were <5% in the large plot were combined into a single bag. All detritus within each subplot was also collected into a single plastic bag. Detritus was defined as any organic material that was not attached to roots. Samples were stored in coolers on ice until they returned to the lab where they were stored at <5°C until processing.

Beginning in Winter 2020, we began storing samples under 0°C until processing due to issues with samples molding.

Soil Collection

Soils were collected during summer 2018 at five high marsh and five low marsh biomass plots at each site. PVC coring tubes were made with sharpened ends to facilitate soil penetration with minimal effects on soil compaction. Coring tubes had an internal diameter of 5.1cm and were marked around the outside at 10cm from the lip to indicate the depth of the sample to be collected. Spades and sharp knives were used to cut the soil around and beneath the cores. Samples were placed in plastic bags and stored on ice in a cooler until return to the lab.

Beginning Winter 2019, soils were tested at each plot for pH, temperature, salinity, conductivity, and oxidation reduction potential. We used an Extech TE300 ExStik ORP Meter and an Extech EC400 ExStik Waterproof Conductivity, TDS, Salinity, and Temperature Meter to measure the soil properties. The probes were pushed into the soil to a depth of 2cm. They were left to acclimate for 5 minutes before the values were recorded. These data are still under analysis at the time of this report.

Table 11. The number of samples collected in each year and season (S=summer, F=fall, W=winter, Sp=Spring) for all sample sites and vegetation strata. In 2017-2021 we also sampled at Steamboat Slough; a restoration site located near Whites Island.

Site ¹	Strata	2011-12		2012-13			2013-14		2015-16			2016-17		2017-18			2018-19		2019		2020		2021		Total
		S	W	S	F	W	S	W	S	S	W	S	W	S	W	Sp	S	W	S	W	S	W	S	W	
BBM	CALY	3	4	6		6	4	4			6	6													39
BBM	CALY/AGS P	4	3	4		4	6	6			6	6													39
BBM	SAV	4	4	6		6	6																		26
SRM	HM			5		5	9	9			9	9													46
SRM	LM			5		5	9	9			9	9													46
SRM	SAV			6		6	6																		18
WI2	HM			5		9	9	9			1	12	1	1	12	9	9	9	9	9	9	9	5	5	152
WI2	LM			4							2		4	2		9	9	9	9	9	9	9	5	5	72
WI2	SAV			4		4	6																		14
WHC	CALY		1	3		3	3	3	3	3	3	3	3	3	3										31
WHC	HM												1		1	9	9	9	9	9	9	9	5	5	70
WHC	PHAR												1	1	1										2
WHC	PHAR/HM	6	4	5		5	6	6	9	9	9	9	9	8	8										85
WHC	SALA	2	3	3		3	6	6	6	6	6	6	6	6	6										59
WHC	SAV	8	8	6		6	6																		34
WHC	LM															9	9	9	9	9	9	9	5	5	68
CLM	ELPA/SALA								6	6	6		5												23
CLM	PHAR								7	7	7		6												27
CLM	SALA												1												1
CS1	ELPA/SAL A	5	4				6		6	6	7	6													40
CS1	PHAR	3	4				6				6	6													25
CS1	SALA						5		6	6	6	6	6												35
CS1	SAV	8	8				6																		22
FLM	HM															9	9	9	9	9	9	9	6	6	69
FLM	PHAR/HM	4	7	3	2	4	3	5	6	6	6											9	9		46

FLM	PHAR/POA	2	5	2										9
	M													
FLM	POAM	3	2	1	6	4	6	6	6					34
FLM	SAV	5	8	6	6									
FLM	LM									9	9	9	9	9
												9	4	67
													9	

¹BBM – Ilwaco Slough, SRM – Secret River Marsh, WI2 – Welch Island, WHC – Whites Island, CLM – Cunningham Lake, CS1 – Campbell Slough, FLM – Franz Lake.

Laboratory Methods

Biomass and Detritus, dry weight

In the laboratory, live, dead, and detritus samples were stored in a refrigerator prior to processing. Samples were individually rinsed of all non-organic material over a 500 μ m sieve, and any obvious root material was removed. Pre-weighed paper bags or tinfoil were used to secure the individual biomass samples, a wet weight was measured, and the samples were placed in a drying oven set at 90°C for at least four days. When samples were deemed completely dry (checked by reweighing a subset of samples on consecutive days), a dry weight was measured for each sample and its corresponding bag or foil tray. If paper bags were used, they were re-weighed empty to account for any weight loss of the bag. The final sample dry weight was determined by subtracting the dry bag or foil weight from the dry weight of the container with the sample.

Beginning in Summer 2020, wet weight was no longer measured and recorded. Additionally, the drying oven temperature was adjusted to 60°C.

CN Analysis

All detritus samples and a subset of live and dead summer biomass samples were analyzed for carbon and nitrogen content. Live and dead summer biomass samples from each plot were selected for analysis if they covered at least 20% of that plot. Dried samples were pulverized with a small food processor and stored in a desiccator prior to analysis. Carbon and nitrogen content were analyzed with a FlashEA 1112 CN analyzer (Thermo Electron Corp.). Approximately 18-22 mg of each subsample was packaged in a tin capsule. Chemical and soil standards were analyzed approximately every ten samples, and at least 10% of the samples were randomly selected and reanalyzed on a different day. Replicate measurements were averaged for reported results.

Beginning in Winter 2020, all live and dead summer biomass samples with a dry weight greater than 20 mg were analyzed for carbon, and nitrogen content.

ADF Lignin

Dried and ground detritus samples were tested for ADF lignin following Soiltest 2016 Standard Operating Procedures for feed lignin (Section 50.400.600). Soiltest uses an acidified detergent solution with the Ankom digester to dissolve cell solubles, hemicellulose, and soluble minerals leaving a residue of cellulose, lignin, heat-damaged protein, a portion of cell wall protein, and minerals. This residue is then placed in an acid wash, and lignin is determined gravimetrically as the residue remaining after extraction, followed by an ash correction. Reference samples were run with each batch, and a duplicate sample was analyzed every ten samples.

Soil Bulk Density

Soil cores were frozen in the laboratory until processed. Each sample was oven-dried at 60°C for at least four days. The mass of each dried sample was recorded, and bulk density was calculated as the ratio of dry weight to wet volume. Wet volume was assumed to be 204.28 cm³ based on a coring tube internal diameter of 5.1 cm and a coring depth of 10 cm.

Soil TOC/N Analysis

A subsample of each dried soil sample was pulverized and homogenized with a mortar and pestle, and large root fragments were removed. Soil subsamples were tested for the presence of inorganic carbon with a few drops of hydrochloric acid (HCl), which would cause the sample to effervesce with CO₂ bubbles if a significant quantity of carbonate were present. No effervescence was observed; therefore, all soil samples were analyzed for total carbon under the assumption that total carbon measurements were

representative of organic carbon content. Carbon and nitrogen content were analyzed with a FlashEA 1112 CN analyzer (Thermo Electron Corp.). Approximately 100 mg of each subsample was packaged in a tin capsule. Chemical and soil standards were analyzed approximately every ten samples, and at least 10% of the samples were randomly selected and reanalyzed on a different day. Replicate measurements were averaged for reported results.

Soil Texture Analysis

Dried soil samples were sent to Materials Testing & Consulting, Inc. (MTC) in Olympia, Washington for particle size distribution following recommended protocols for measuring conventional sediment variables (PSEP Report TC-3991-04, 1986). Samples were shaken in appropriately sized sieves to separate gravel (>2000 microns), sand (between 62.5 - 2000 microns), and fines (<62.5 microns). The fines were further separated into silt (3.9 – 62.5 microns) and clay (<3.9 microns) using a pipetting technique to measure the differential settling rates of different sized particles. Samples were processed in batches of a maximum of 20 per batch. Each batch included one sample that was analyzed in triplicate.

Analysis

Average dry weight was calculated for various strata and site values. For 2020 to 2021 data (Table 11), the proportion of the dominant species comprising each sample was calculated. Those data were used to identify samples that were primarily a single species. Those samples were then used to make estimates of the aboveground biomass for specific species within the study area. For longterm comparative analysis, all biomass data collected prior to 2021 was assigned wetland elevations based historic RTK survey data collected at plant community plots when elevation could not be determined it was left blank, and the biomass data point was not included in the high vs. low marsh longterm biomass assessment. Starting in 2021 all biomass plots were surveyed in directly with RTK equipment.

When applicable biomass, detritus, and soil metrics were transformed and correlated elevation and with hydrologic conditions such as annual freshet conditions and daily inundation, only significant (p-value < 0.05) correlation and regressions were reported. Data analysis was conducted using Microsoft Office Excel (2016), Exploratory (2017), R (2018), and Tableau (2019-2021) software.

2.4.1.2 *Phytoplankton*

Abundance

Phytoplankton abundance was estimated in two ways: (1) from pigment concentrations, and (2) by direct counts using light microscopy. Phytoplankton abundance can be estimated by measuring the concentration of chlorophyll *a*, a photosynthetic pigment that is common to all types of phytoplankton. Surface water samples were collected into two 1 L brown HDPE bottles and sub-sampled prior to processing. A subsample of water (typically between 60–300 mL) was filtered onto a 25 mL glass-fiber filter (GF/F) for chlorophyll *a* and kept frozen (-80°C) pending analysis. Chlorophyll *a* was determined fluorometrically using a Turner Designs Trilogy fluorometer using the non-acidification method, which is highly selective for chlorophyll *a* even in the presence of chlorophyll *b* (Welschmeyer 1994).

Phytoplankton abundance was also determined by enumeration of individual cells using inverted light microscopy. The dates corresponding to sample collection for determination of nutrient concentrations, zooplankton abundance, and phytoplankton abundance are shown in Table 12. Duplicate 100 mL whole water samples were collected from each of the trends sites. The samples were preserved in 1% Lugol's iodine and examined at 100, 200 and 400x magnification using a Leica DMIL and Zeiss Axiovert 200M inverted light microscopes following concentration achieved through settling 2.5–50 mL of sample in Utermohl chambers (Utermohl 1958) overnight (~24 h). Cell counts were performed at 200 and 400x magnification, with an additional scan done at 100x magnification to capture rare cells in a broader scan

of the slide. The estimated error in abundance measurements was <5% at the class level and ~10% for genus-level counts. The monitoring protocol can be found on monitoringmethods.org ([Method ID 1589](#) and [1590](#)).

Table 12. List of samples analyzed (Xs) and data of collection from five trends sites in the Lower Columbia River in 2021.

Site	Zone	Reach	Date	Nutrients	Zooplankton	Phytoplankton
ILWACO SLOUGH	1	A	3/13/19	X	X	X
			4/8/19	X	X	X
			5/5/21	X	X	X
			6/11/21	X	X	X
			7/9/21	X	X	X
			8/10/21	X	X	X
			9/--/21	X	X	X
WELCH ISLAND	2	B	3/1/21	X	X	X
			4/8/21	X	X	X
			5/7/21	X	X	X
			6/8/21	X	X	X
			7/6/21	X	X	X
			8/9/21	X	X	X
WHITES ISLAND	3	C	3/1/21	X	X	X
			4/9/21	X	X	X
			5/7/21	X	X	X
			6/8/21	X	X	X
			7/6/21	X	X	X
			8/9/21	X	X	X
CAMPBELL SLOUGH	4	F	3/2/21	X	X	X
			4/5/21	X	X	X
			5/3/19	X	X	X
			6/10/21	X	X	X
			7/7/21	X	X	X
			8/10/21	X	X	X
			9/--/21	X	X	X
FRANZ LAKE SLOUGH	5	H	3/4/21	X	X	X
			4/6/21	X	X	X
			5/4/21	X	X	X
			6/10/21	X	X	X
			7/7/21	X	X	X
			8/10/21	X	X	X
			9/--/21	X	X	X

Multivariate Statistical Analyses

Nonmetric Multi-dimensional Scaling (NMDS) and Canonical Analysis of Principal Coordinates (CAP) routines were performed using PRIMER-E v.7 with PERMANOVA+. NMDS is a multivariate technique that identifies the degree of similarity among biological communities within a group of samples in a data set. In NMDS, samples are typically represented in 2-dimensional ordination space using the distance between sample points as a measure of similarity of biological communities; short distances represent the relatively high similarity between samples, while longer distances represent the relatively low similarity between samples.

Major phytoplankton taxa were selected for multivariate analyses if their abundance constituted at least 10% of total phytoplankton abundance in any sample. Taxa that did not meet these criteria were excluded from the analysis. Two NMDS analyses were run for this study that included (i) all major phytoplankton taxa (NMDS_{total}) and (ii) only major diatom taxa (NMDS_{diatom}). Abundances for 25 major phytoplankton

taxa (NMDS_{total}) and ten major diatom taxa (NMDS_{diatom}) were standardized by sample, and the data were square-root transformed in order to achieve a normal distribution of the data prior to analysis.

Canonical Analysis of Principal Coordinates (CAP) is an analytical technique that uses canonical correlation to determine the degree to which environmental factors explain variability among biological communities. A Bray-Curtis resemblance matrix was assembled using the standardized, square-root transformed phytoplankton abundance data and six environmental variables including NO₂⁺, NO₃⁻, NH₄⁺, PO₄³⁻, mean daily water temperature, mean daily dissolved oxygen saturation, and mean daily discharge (at Bonneville Dam). Environmental data were normalized prior to analysis to compare variables on the same scale. Samples with missing environmental data were excluded from multivariate analyses. A total of 70 samples were analyzed in both NMDS analyses, and a total of 38 samples were included for CAP.

2.4.2 Secondary Productivity

2.4.2.1 Zooplankton

Secondary productivity (the rate of growth of consumers of primary production) was not measured directly but was estimated from the abundance of pelagic zooplankton. The samples were collected from near the surface of the water (< 1 m depth) using an 80 µm nylon mesh net with a mouth diameter of 0.5 m and a length of 2 m at five trend sites. A list of the collection dates and sampling sites are given above in Table 12.

Abundance

Zooplankton abundances collected via net tow were determined at each of the five trend sites. The net was fully submerged under the water and was dragged back and forth from a small boat through the water for approximately 3-5 min or over approximately 100 m. The samples were preserved in 1.5% formalin immediately after collection. A flow meter (General Oceanics Inc., Model 2030R) was mounted to the net's bridle to provide an estimate of the volume flowing through the net. The volume of water passing through the net was determined by knowledge of the distance of water passing through the net, the velocity of the water passing through the net, and the volume of water passing through the net, as calculated from both the distance traveled and the net diameter (as described in the flow meter manual). The distance covered (in meters) was determined from:

$$Distance = \frac{Difference\ in\ counts \times Rotor\ Constant}{999999} \quad (1)$$

where the difference in counts refers to the difference between the initial and final counts on the six-digit counter, which registers each revolution of the instrument rotor. The speed is calculated from:

$$Speed = \frac{Distance\ in\ meters \times 100}{Time\ in\ seconds} \quad (2)$$

The volume is determined as:

$$Volume\ in\ m^3 = \frac{3.14 \times net\ diameter^2 \times Distance}{4} \quad (3)$$

For each net tow, the volume of material collected in the cod end of the net was recorded. From this, a concentration factor was calculated, and a final estimate of the volume examined was determined by multiplying the concentration factor by the final volume of the concentrated sample examined under the microscope.

Taxonomy

Zooplankton taxa were broadly categorized into one of the following groupings: rotifers, cladocerans, annelids, ciliates, and copepods, and ‘other.’ Within these groups, individuals were identified to genus or species where possible (rotifers, cladocerans, ciliates, annelids), or to order (copepods). Eggs of rotifers, cladocerans, and copepods were enumerated separately.

2.4.3 Stable Isotope Ratios

The ratios of carbon (C) and nitrogen (N) stable isotopes in tissues of consumers reflect the stable isotope ratios (SIR) of their food sources (Neill and Cornwell 1992, France 1995). Therefore, SIR is useful in the determination of major food sources, as long as the latter have distinct isotopic ratios that allow them to be distinguished. Within the scope of the EMP, SIR analysis is used to estimate the relative importance of food sources including algae and wetland plants to the food web supporting juvenile salmonids at trends sites including Ilwaco Slough, Whites Island, Campbell Slough, and Franz Lake Slough. SIR are suitable for identifying food sources assimilated over a longer time frame compared to point-in-time techniques such as gut content analysis; ideally, a combination of the two approaches provides the best indicator of diet.

C and N isotope ratios yield different information: since the $^{13}\text{C}/^{12}\text{C}$ ($\delta^{13}\text{C}$) ratio varies by only a small amount (<1‰) during the assimilation of organic matter, it is used to identify the primary source of organic matter (i.e., primary producers). In contrast, the ratio of $^{15}\text{N}/^{14}\text{N}$ ($\delta^{15}\text{N}$) changes markedly with trophic level, increasing by 2.2 to 3.4 parts per thousand (per mil, or ‰) with an increase of one trophic level (i.e., from a plant to an herbivore or an herbivore to a carnivore). Thus, $\delta^{15}\text{N}$ values are useful in determining trophic position.

The SIR of C and N were measured in juvenile Chinook salmon muscle tissues and several potential food sources to provide information on the food web supporting juvenile salmonids (Table 13). Juvenile salmon were collected by NOAA Fisheries staff during monthly beach seine sampling and frozen (see Section 2.6). Skinned muscle samples were collected for analysis since SIR signatures are more homogeneous within muscle tissue and since muscle is a good longterm integrator of the food source.

Aquatic invertebrates were collected using a 250 μm mesh net with a rectangular opening in emergent vegetation at the water’s margin. The aquatic midge, Chironomidae, and amphipods were selected because they have been found to be preferred food sources for juvenile salmonids in the lower Columbia River (Maier and Simenstad 2009, Sagar et al. 2013, 2014, 2015). Most invertebrate specimens were found attached to submerged portions of vegetation. Invertebrates were collected by rinsing the exterior of the vegetation with deionized water and removing the invertebrates from the rinse water using clean forceps. Invertebrate samples were then rinsed with deionized water to remove algae or another external particulate matter. Salmon and aquatic invertebrate samples were frozen for later processing.

Table 13. Potential food sources for marked and unmarked juvenile Chinook salmon and invertebrate consumers.

Potential food sources for fish (marked and unmarked)	Potential food sources for invertebrates
Chironomidae	Particulate organic matter
Amphipoda	Periphyton
Oligochaetes	Live vegetation
Nematodes	Dead vegetation
Gastropods	
Zooplankton	

*Only applicable to marked fish

A variety of autotrophs were sampled to characterize the range of potential food sources for invertebrates. Samples of terrestrial and emergent vegetation, aquatic macrophytes, and macroalgae (*Ulva* and miscellaneous seaweeds) were collected from representative areas within each site. Vegetation samples were rinsed at least five times in deionized water to remove external material, such as invertebrates and periphyton, and were kept frozen (-20°C) for later processing. Samples of particulate organic matter (POM) and periphyton were filtered onto combusted 25 mm glass-fiber GF/F filters and frozen (-20°C) for later processing.

Frozen filters, salmon tissue, invertebrate, and plant material were freeze-dried using a Labconco FreezeZone 2.5 L benchtop freeze dry system (Labconco Corp., USA). Plants were categorized as live or dead during field collections based on whether they were attached and by their physical appearance; mixtures of live plants from the same sampling date were composited and ground using a mortar and pestle, as were mixtures of dead vegetation (designated when plant material was detached rather than rooted). Freeze-dried invertebrates of the same taxa from the same collection site and collection date were composited, ground using a clean mortar and pestle, and subsampled when enough material was present. Otherwise, whole bodies of all individuals of the same taxa from the same site were composited into a single sample. Skinned muscle tissue samples from individual juvenile salmonids were analyzed separately by the individual; muscle tissue samples from different bodies were not composited.

SIR of carbon ($\delta^{13}\text{C}$) and nitrogen ($\delta^{15}\text{N}$) were determined at the UC Davis Stable Isotope Facility using a PDZ Europa ANCA-GSL elemental analyzer interfaced to a PDZ Europa 20-20 isotope ratio mass spectrometer (Sercon Ltd., Cheshire, UK). The atomic ratios of the heavy isotope (^{13}C , ^{15}N) to the light isotope (^{12}C , ^{14}N) were compared to universal standards (Vienna PeeDee Belemnite and air for C and N, respectively) and reported in per mil (‰) units.

To estimate the proportional contributions of different food sources for juvenile salmon, the stable isotope mixing model, *simmr* was implemented in R.

2.5 Macroinvertebrates

2.5.1 Salmon Prey Availability Sampling

2.5.1.1 *Open Water and Emergent Vegetation*

To assess the availability of salmon prey at the trends sites, we conducted neuston tows in both open water (OW; in the center of the channel) and emergent vegetation (EV; along the edge of the wetland channel among vegetation). For OW samples, a Neuston net (250 μm mesh) was deployed from a boat for an average distance of 100 m and positioned to sample the top 20 cm of the water column. For EV samples, the Neuston net was pulled through a 10 m transect parallel to the water's edge in the water at least 25 cm deep to enable samples from the top 20 cm of the water column. From 2008 – 2016, neuston tows were taken concurrently with monthly beach seine collections when juvenile Chinook salmon were present at a site (i.e., captured during seine sets). Beginning in 2017, neuston tows were completed during every beach seine collection regardless of whether salmon were captured. Two OW and two EV samples were collected at each site per month; although occasionally one or three tows were performed in each habitat type depending on field conditions (Table 14). Samples were preserved in 95% ethanol. The monitoring protocol can be found on monitoringmethods.org ([Method ID 1622](#)).

Table 14. The number of invertebrate tow samples (OW and EV) collected at each site per sampling event, 2008-2013, and 2015-2018.

		Ilwaco Slough	Secret River	Welch Island	Ryan Island	Bradwood Slough	Jackson Island	Whites Island	Wallace Island	Lord/Walker Island	Burke Island	Goat Island	Deer Island	Campbell Slough	Lemon Island	Washougal	Sand Island	Franz Lake	Hardy Slough	Total Tow Samples
2008	April													3			6	6		15
	May													6				6		12
	June																		4	4
2009	May				3			4		4				5				4		20
	June													4						4
2010	April					4	4	4	4					4						20
	May					4	4	4	4					4						20
	June					4	4	4	4					4						20
	July					4		4	4					2						14
2011	April	2																		2
	May	8						10			4	4	4	4				2		36
	June	4						4												8
2012	February		4																	4
	March			2				2							3					7
	April		4	5				6							4	2				21
	May		1	4				4						4	4	4				21
	June		6	4				4						4	2	4				24
2013	March			4																4
	May		4	4				4						4						16
	June		4	4				3						4						15
	July			4				6												10
2015	April	5												6				6		17
	May			2				4						2				5		13
	June			6				4												10
2016	February			2				6										2		10
	March							2												2
	April			2				4						6				4		16
	May			4				4						4						12
	June			6				4						6						16
	July			4				6												10
	August			4																4
September			4																4	

(Table 13 continued)

		Ilwaco Slough	Secret River	Welch Island	Ryan Island	Bradwood Slough	Jackson Island	Whites Island	Wallace Island	Lord/Walker Island	Burke Island	Goat Island	Deer Island	Campbell Slough	Lemon Island	Washougal	Sand Island	Franz Lake	Hardy Slough	Total Tow Samples	
2017	February	4						4						4							12
	March	4		4				4						4							16
	April	4		4				4						4							16
	May	4		4				4						4							16
	June	4		4				4						4							16
2018	February			4				4						4							16
	March	4		4				4						4				4			20
	April	4		4				4						4							16
	May	4		4				4						4							16
	June/July	4		4				4						4							16
	October	4		4				4						4							16
Total Tow Samples		39	23	81	3	16	12	117	16	4	4	4	4	96	13	10	6	35	4	487	

2.5.1.2 *Benthic Macroinvertebrates*

To characterize the benthic macroinvertebrate assemblage, benthic core sites were selected to correspond to locations directly adjacent those where the fish community, food web metrics, and vegetation were sampled. Benthic cores were collected monthly at the trends sites (n = 5 per site) between April and July. Cores were collected to a depth of 10 cm by driving a 2-inch diameter PVC pipe into the ground at each sampling location. Each core was then placed in a jar and fixed in 10% formalin. Core samples were collected at low tide from exposed sediments and among emergent vegetation. The monitoring protocol can be found on monitoringmethods.org ([Method ID 1593](#)).

2.5.1.3 *Laboratory Methods*

Invertebrate samples collected in neuston tows (n = 36) and benthic cores (n = 77) were identified in the lab using high-resolution optical microscopy and taxonomic references (Mason 1993, Kozloff 1996, Merritt and Cummins 1996, Thorp and Covich 2001, Triplehorn and Johnson 2005). Most individuals were identified to family, although some groups/individuals were identified to coarser (e.g., order) levels. For each sample, the number of individuals in each taxonomic group was counted, then each group was blotted on tissue and weighed to the nearest 0.0001 g. Analysis of neuston tow data included all invertebrates. In benthic core samples, taxa that were not aquatic and/or benthic in their ecology (e.g., adult flies) were considered contaminants and were excluded from analyses of benthic core data.

Samples with an overabundance of taxa were subsampled via volumetric subsampling. The sample was diluted to a particular volume, a portion of the volume was processed, and total counts were calculated as a ratio of the volume sampled. Multiple subsamples were processed to ensure subsample counts were comparable.

2.5.2 *Salmon Diet*

2.5.2.1 *Field Data Collection*

When juvenile Chinook were captured at a site, fish were typically euthanized within an hour of collection. Fish were kept on ice until arrival at the NOAA field station laboratory where they were stored in a -80°F freezer. Chinook salmon bodies were necropsied at the end of the sampling season. Whole stomach samples were preserved in 10% formalin until delivered to the laboratory for processing. The total number of diet samples collected at the EMP sites since 2008 is provided in Table 15. The current report is for sampling in 2020. 2021 diets have not been processed.

2.5.2.2 *Laboratory Methods*

Organisms in the diets were identified in most cases to the family level, although some groups/individuals were identified to coarser (e.g., order) levels, and crustaceans were usually identified to genus or species. Some contents were unidentifiable due to digestion. Each prey taxon was counted, blotted on tissue, and weighed to the nearest 0.0001 g.

Table 15. The number of Chinook salmon diet samples collected at each site per sampling event, 2008-2013, 2015-2018.

		Ilwaco Slough	Secret River	Welch Island	Ryan Island	Bradwood Slough	Jackson Island	Whites Island	Wallace Island	Lord/Walker Island	Burke Island	Goat Island	Deer Island	Campbell Slough	Lemon Island	Washougal	Sand Island	Franz Lake	Pierce Island	Hardy Slough	Total Tow Samples
2008	April													6			13	15	9		43
	May													19				7			26
	June																			13	13
2009	May				9			10		6				10				8			43
	June				10									9							19
2010	April					10	19	16	6					12							63
	May					17	15	14	14					24							84
	June					9	8	18	11					18							64
	July					10		19	11					15							55
	August					8		13													21
2011	May							10			10	13	10	22							65
	June							25													25
	July							2			2										4
2012	February		15	16																	31
	March			14				13							13						40
	April		15	14				10							7	15					61
	May			30				11						18	15	18					92
	June		14	15				15						15	15	36					110
2013	March			9																	9
	May		12	30				15						34							91
	June		1	23				13						9							46
	July		2	25										1							28
2015	April	6																			6
	May			15				15						15				4			49
	June			7				13													20

2016	April			13				13					7					12			45
	May			15				19					13								47
	July			3				8													11
		Ilwaco Slough	Secret River	Welch Island	Ryan Island	Bradwood Slough	Jackson Island	Whites Island	Wallace Island	Lord/Walker Island	Burke Island	Goat Island	Deer Island	Campbell Slough	Lemon Island	Washougal	Sand Island	Franz Lake	Pierce Island	Hardy Slough	Total Tow Samples
2017	February	2						2													4
	March	1						1													2
	April			15				8						1							24
	May			30				30						34							94
	June			32				5						23							60
2018	February			30				4													34
	March			30				30													60
	April			31				30													61
	May			30				30						32							92
	June/July													2							2
	October																				N/A
Total Tow Samples		9	59	427	19	54	42	412	42	6	12	13	30	319	50	69	13	46	9	13	1644

2.5.3 Salmon Prey Data Analysis

Descriptive statistical analysis of the invertebrate community was calculated, in addition to specific analyses of taxa that have been shown to be important prey of juvenile Chinook salmon in the lower Columbia River (Lott 2004, Spilseth and Simenstad 2011). These included Diptera (predominantly comprised of chironomids), Amphipoda (predominantly *Americorophium* spp.), and Cladocera (predominantly *Daphnia* spp.).

Benthic core and neuston tow invertebrate data were quantified by numeric composition (count proportion) and gravimetric composition (weight proportion). For benthic core data, the density and biomass of taxa in each sample were calculated as the total count or weight for a given taxon divided by the core volume (# individuals m⁻³, g m⁻³). For neuston tow data, the density and biomass of taxa in each sample were calculated as the total count or weight for a given taxon divided by the meters towed (# individuals m⁻¹ towed, mg m⁻¹ towed). To compare taxa densities and biomass between study sites, density and biomass data for each taxon were summed across replicate samples taken within a given site each month and then divided by the number of replicates to give an average total density and biomass at each sampling site per month. Averages of predominant juvenile salmonid prey in density/meter² were also included.

Juvenile Chinook diet composition was assessed with three variables, including prey numeric composition (NC), gravimetric composition (GC), and frequency of occurrence (F). These measurements were used to calculate an index of relative importance (IRI) and percent IRI, where IRI is the percentage of the total IRI for each prey taxa, and:

$$IRI = F * (\% NC + \% GC)$$

An IRI has the advantage of accounting for prey weight and numbers, as well as the likelihood of taxa appearing in the diet of individuals (Liao et al. 2001). Because the index incorporates taxa counts, items that were not countable (e.g., plant matter, unidentifiable, highly digested material), were removed from descriptive analyses of diet composition.

Instantaneous and energy ration (IR, ER) measure foraging performance of fish, incorporating prey weight, fish field weight, and energy density in the diet, calculated as:

$$IR = \frac{\text{sum of prey weight}}{\text{fish weight}} \quad ER = \frac{\text{sum of prey energy density}}{\text{fish weight}}$$

Instantaneous ration measures fish fitness and is the ratio of the total prey weight to the total fish mass. Total prey weight was calculated as the sum of the weights of all individual taxa counted in the diet. Energy ration measures energy consumption. For each juvenile Chinook salmon, the sum of individual prey taxon masses was multiplied by the energy density (kJ g⁻¹ wet mass) of each prey taxon and divided by the total fish mass. Thus, energy ration equals kilojoule consumed per gram of fish. Energy densities of prey taxa were compiled and acquired from (David et al., 2016). For descriptive analyses, IR and ER was calculated for each individual salmon diet and averaged across all fish, by fork length, within 2020, by site, overall, among sites for February to March, and overall, by year.

Following methods in Fiechter et al. (2015), maintenance metabolism was calculated for juvenile Chinook salmon used in diet analyses. Because sampling was attenuated in 2020 due to the coronavirus pandemic, direct comparison of 2020 data with other years was only possible for the months of February and March. Maintenance metabolism (J_m) represents the cost of metabolic upkeep where j_m is the mass specific maintenance costs at 0° C (0.003), d is the temperature coefficient for biomass assimilation (0.68), T is water temperature in °C, and W is fish body mass.

$$J_m(\text{maintenance metabolism}) = j_m * e^{dt} * W$$

Maintenance metabolism and energy ration were plotted on a quadrant chart, divided by the 50th percentile, to provide a general assessment of habitat quality and juvenile Chinook salmon growth potential at a given site. For juvenile Chinook salmon, low metabolic cost and high energy assimilation represent relatively positive growing conditions (lower right quadrant), while high metabolic cost and low energy assimilation represent relatively poor growing conditions (upper left quadrant).

Multivariate analyses were used to examine differences in juvenile salmon diet composition among sites. A Bray-Curtis dissimilarity index was calculated on square-root transformed percent IRIs for each fish size class, by site and year. For analysis of community composition, taxa were sorted by Order. A non-metric multidimensional scaling (NMDS) plot was used to graphically represent variation in major prey species composition ($p = 0.05$) among sites in reduced-dimensional space. Points close together represent samples similar in composition and points at a greater distance from each other represent differing composition. Visual variation led to a direct gradient analysis, an analysis of similarities (ANOSIM), to explain statistical differences between groups. ANOSIM p-values and R-statistics showed within group object similarity compared to other groups (1 = all objects in group are more similar than objects from different groups; 0 = there was no difference among groups). Finally, paired sites were compared to identify the species that were contributing to at least 70% of the diet composition differences for each site pair. All multivariate analyses were performed using the Vegan software package in R (Oksanen et al. 2020, R Core Team 2019).

2.6 Fish

2.6.1 Fish Community

In 2021, NOAA Fisheries monitored habitat use by juvenile Chinook salmon and other fishes at five trends sites, Ilwaco Slough in Reach A (sampled in 2011-2021), Welch Island in Reach B (sampled in 2012-2021), Whites Island site in Reach C (sampled in 2009-2021), Campbell Slough in Reach F (sampled in 2007-2021), and Franz Lake in Reach H (sampled in 2008-2016, 2018, 2020-2021), in order to examine year-to-year trends in fish habitat use in the lower river. Coordinates of the sampling sites are shown in Table 16.

The project goal is to collect fish for six months of the year at all sites, March-June and October. Occasionally conditions at a site prohibit sampling, such as extremely high or low water levels, water temperatures become too high for handling fish, or road conditions prevent travelling to launch sites. Fish are collected using a 38 x 3-m variable mesh bag seine (10.0 mm and 6.3 mm wings, 4.8 mm bag). Bag seine sets were deployed using a 17 ft Boston Whaler or 9 ft inflatable raft. Up to three sets were performed per sampling month, as conditions allowed. At each sampling event, the coordinates of the sampling locations, the time of sampling, water temperature, weather, habitat conditions, and tide conditions were recorded. Fish sampling events conducted as part of our regular EMP sampling in 2021 are shown in Table 16. We also list the limited sampling we were able to complete in 2020 before NOAA COVID-19 safety protocols led to a suspension of fieldwork. The monitoring protocol can be found on monitoringmethods.org ([Method ID 826](#)). All non-salmonid fish were identified to the species level and counted. For salmonid species other than Chinook, up to 30 individuals were measured (fork length, nearest mm), weighed (nearest gram), and released. Up to 30 juvenile Chinook salmon were euthanized in the field, measured, weighed, and retained for subsequent laboratory analyses (diet, genetic, lipid, and otolith). If present, an additional 70 Chinook were measured and released. Any additional Chinook were counted and released. All salmonids were checked for adipose fin clips, or other external marks, coded

wire tags, and passive integrated transponder tags to distinguish between marked hatchery fish and unmarked (presumably wild) fish.

Fish bodies retained in the field were frozen and stored at -80°C. At the end of the sampling, season fish were necropsied, and samples were collected for laboratory analyses. Stomach samples for taxonomic analyses were preserved in 10% neutral buffered formalin. Fin clips for genetic analyses were collected and preserved in alcohol, following protocols described in Myers et al. (2006). Otoliths for age and growth determination were also stored dry in a vial. Whole bodies (minus stomachs) for measurements of lipids remained frozen until processed.

Table 16. Location of EMP sampling sites in 2020 and 2021 and the number of beach seine sets per month (ns = not sampled). Sampling was stopped in mid-March 2020 through February 2021 due to COVID-19 pandemic safety protocols issued by NOAA.

Site	2020			2021						
	Feb	Mar	Total	Feb	Mar	Apr	May	Jun	Oct	Total
Ilwaco Slough (Reach A) 46.300530° N, 124.045893° W	3	2	5	ns ¹	3	3	3	3	3	15
Welch Island (Reach B) 46.255011° N, 123.480398° W	1	3	4	ns ¹	3	3	1	2	3	12
Whites Island (Reach C) 46.159350° N, 123.340133° W	2	1	3	ns ¹	1	1	2	2	3	9
Campbell Slough (Reach F) 45.783867° N, 122.754850° W	3	3	6	ns ¹	3	3	2	ns ²	3	11
Franz Lake (Reach H) * 45.600583° N, 122.103067° W	2	ns ¹	2	ns ¹	3	5	1	2	3	14
Total	11	9	20	0	13	15	9	9	15	61

¹ pandemic safety protocols prevented sampling

² water temperature exceeded sampling criteria

Fish species richness (S ; the number of species present) and fish species diversity for each site were calculated by month and year. Fish species diversity was calculated using the Shannon-Weiner diversity index (Shannon and Weaver 1949):

$$H' = -\sum(p_i \ln p_i)$$

Where

p_i = the relative abundance of each species, calculated as the proportion of individuals of a given species to the total number of individuals in the community.

Catch per unit effort (CPUE) and fish density were calculated as described in Roegner et al. (2009), with fish density reported in number per 1000 m².

Multivariate analyses were used to examine differences in the fish community between sites using the Primer-e version 7 (Plymouth Routines In Multivariate Ecological Research) software package (Clarke and Warwick 1994, Clarke and Gorley 2006). A Bray-Curtis index of similarity coefficients was calculated for the square-root transformed species abundance data at each site. A non-metric, multi-dimensional scaling (nMDS) plot was used to graphically examine variation in the fish community between sites. We used a multivariate analog to ANOVA called analysis of similarity (ANOSIM) to quantitatively assess the variation in fish community based on site. The global R-value generated from this analysis indicates the degree of separation, with 0 representing no separation and 1 representing complete separation. ANOSIM also produces pairwise tests which compute an R-value for comparisons of different site locations. Statistical probabilities of both R-values are generated through permutation.

2.6.2 Salmon Metrics

2.6.2.1 Genetic Stock Identification

Genetic stock identification (GSI) techniques were used to investigate the origins of juvenile Chinook salmon captured in habitats of the lower Columbia River and estuary (Manel et al. 2005, Roegner et al. 2010, Teel et al. 2009). From 2008–2013 juvenile Chinook salmon stock composition was estimated by using a regional microsatellite DNA data set (Seeb et al. 2007). Beginning in 2014 stock composition was estimated by using a Single Nucleotide Polymorphism data set that includes baseline data for spawning populations from throughout the Columbia River basin (described in Hess et al. 2014). The overall proportional stock composition of Lower Columbia River samples was estimated with the GSI computer program ONCOR (Kalinowski et al. 2007), which implemented the likelihood model of Rannala and Mountain (1997). Probability of origin was estimated for the following regional genetic stock groups: Deschutes River fall; West Cascades fall; West Cascades spring; Middle and Upper Columbia River spring; Spring Creek Group fall; Snake River fall; Snake River spring; Upper Columbia River summer/fall; Upper Willamette River spring; Rogue River fall; and Coastal OR/WA fall (Seeb et al. 2007, Teel et al. 2009, Roegner et al. 2010). West Cascades and Spring Creek Group Chinook are Lower Columbia River stocks. The monitoring protocols can be found on monitoringmethods.org ([Method ID 948](#))([Method ID 1356](#))([Method 1332](#)) ([Method 5446](#)).

Multivariate analyses were used to examine differences in the genetic stock groups between sites using the PRIMER (Plymouth Routines In Multivariate Ecological Research) software package (Clarke and Warwick 1994, Clarke and Gorley 2006). A Bray-Curtis index of similarity coefficients was calculated for the square-root transformed stock abundance data at each site. A non-metric, multi-dimensional scaling (nMDS) plot was used to graphically examine variation in genetic stock abundance between sites. We used a multivariate analog to ANOVA called analysis of similarity (ANOSIM) to quantitatively assess the variation in salmon stock composition based on site. The global R-value generated from this analysis indicates the degree of separation, with 0 representing no separation and 1 representing complete separation. ANOSIM also produces pairwise tests which compute an R-value for comparisons of different site locations. Statistical probabilities of both R-values are generated through permutation.

2.6.2.2 Lipid Determination and Condition Factor

As part of our study, we determined total, nonvolatile, extractable lipid (reported as percent lipid) and lipid class content in Chinook salmon whole bodies. Lipid content can be a useful indicator of salmon health (Biro et al. 2004) and also affects contaminant uptake and toxicity (Elskus et al. 2005). Studies show that the tissue concentration of a lipophilic chemical that causes a toxic response is directly related to the amount of lipid in an organism (Lassiter and Hallam 1990; van Wezel et al. 1995); in animals with high lipid content, a higher proportion of the hydrophobic compound is associated with the lipid and unavailable to cause toxicity. While lipids may help sequester toxins and protect fish from contaminants, an overabundance of lipids can interfere with buoyancy regulation during early ocean entry and may increase vulnerability to surface predators (Weitkamp 2008).

Prior to analyses, whole body samples from salmon collected in the field were composited by genetic reporting group, date, and site of the collection into a set containing 3-5 fish each. The composited salmon whole body samples (~ 2 g) were homogenized, mixed with drying agents (sodium sulfate and magnesium sulfate), packed into extraction cells, and then extracted with dichloromethane using an accelerated solvent extractor. The sample extracts were collected into pre-cleaned, pre-weighed sample tubes. Approximately 1-2 mL of sample extract was transferred to a pre-weighed sample vial to determine the amount of total, nonvolatile, extractable lipid (reported as percent lipid) by gravimetric analysis as described in Sloan et al. (2014). Another sample extract aliquot (1- 2 mL) was transferred to a second pre-weighed sample vial to measured lipid classes (i.e., sterol esters/wax esters, triglycerides, free fatty acids, cholesterol, phospholipids/polar lipids) using thin-layer chromatography–flame ionization detection (TLC–FID) (Ylitalo et al. 2005; Sloan et al. 2014). In this method, each sample extract was spotted on a silica rod (Chromarod) and developed in a chromatography tank containing 60:10:0.02 hexane: diethyl ether: formic acid (v/v/v). The lipid classes were separated based on polarity and measured using flame ionization detection, using the mean of two measurements. The percent contribution of each lipid class to the total lipid were calculated by dividing the concentration of each lipid class by the total lipid measured.

For all salmonid species, Fulton’s condition factor (K ; Fulton 1902; Ricker 1975) was calculated as an indicator of fish health and fitness, using the formula:

$$K = [\text{weight (g)/fork length (cm)}^3] \times 100$$

The monitoring protocol can be found on monitoringmethods.org ([Method ID 952](#)).

2.6.2.3 *Otoliths (Growth Rates)*

Otoliths from fish ranging in fork length from 35-111 mm (mean = 66 mm, SD = 14.4 mm) were processed for microstructural analysis of recent growth (see Chittaro et al. 2018). Specifically, left sagittal otoliths were embedded in Crystal Bond and polished in a sagittal plane using slurries (Buehler©’s 600 grit silicon carbide, 5.0 alumina oxide, and 1.0 micro polish) and a grinding wheel with Buehler© 1500 micro polishing pads. Polishing ceased when the core of the otolith was exposed, and daily increments (Volk et al. 2010, Chittaro et al. 2015) were visible under a light microscope. We photographed polished otoliths using a digital camera (Leica DFC450) mounted on a compound microscope (Zeiss©). Using Image Pro Plus© (version 7, Mediacybernetics), we took two measurements from each otolith; distance from otolith core to edge (i.e., otolith radius at time of capture, O_c) and distance from otolith core to seven daily increments in from the otolith edge (i.e., otolith radius measured at seven days before capture, O_a). For each individual, fork length at seven days prior to capture (L_a) was estimated using the Fraser-Lee equation:

$$L_a = d + \frac{L_c - d}{O_c} O_a$$

where d is the intercept (3.98mm) of the regression between fish length and otolith radius ($R^2 = 0.81$, $n = 855$) where L_c represents fork length (mm) at capture. Next, the average daily growth rate (mm/day) was calculated for an individuals’ last seven days of life (a),

$$\text{Average daily growth} = \frac{L_c - L_a}{a}$$

Seven days of growth was a reasonable amount of time to estimate growth while in estuarine habitats because, depending on migratory type (i.e., ocean-type versus stream-type) and timing of migration (i.e., sub-yearling versus yearling migrant), Chinook salmon may inhabit estuaries for weeks or months (Healey 1991, Thorpe 1994, Weitkamp et al. 2014).

We used a generalized linear modeling (GLM) approach to investigate the extent to which variability in somatic growth rate (dependent variable) was explained by a suite of independent variables; collection year and day, river discharge, off-channel distance, river kilometer, genetic stock, hatchery or unmarked classification, and fork length. River kilometer and off-channel distance are defined as the distance (km) a site is from the mouth of the Columbia River and the distance (m) between a site and the Columbia River channel respectively. If an individual had a clipped fin or coded wire tag, then it originated from a hatchery and was categorized as “hatchery.” If a fish did not have a mark or tag, then the individual was labeled as “unmarked.” The term “unmarked” is used instead of “naturally produced” or “wild” because some hatcheries do not clip fins nor inject coded wire tags or mark only a fraction of their releases (Sagar et al., 2013).

For all models, we used a gamma family distribution with a log link to account for the normally distributed, but positive, growth rate data. Preliminary analyses indicated a nonlinear relationship between growth rate and day of the year, and therefore, the day of the year was also included in our analyses. In addition, fork length was included in our analyses so as to account for the linear relationship we observed between growth rate and fish size. We ran all possible GLM model combinations of the independent. All model parameters were estimated by maximizing the likelihood function. To compare models, we calculated four values for each model: Akaike’s information criterion (AIC), delta AIC, relative likelihood, and AIC weight. Smaller AIC values indicate “better” models, and when comparing two models, we calculated the difference in AIC values (delta AIC; Akaike, 1973; Burnham & Anderson, 2002). A delta AIC of less than 2 indicates little difference between competing models; a delta AIC of 2–10 indicates moderate support for a difference between the models, and a delta AIC of greater than 10 indicates strong support (Burnham & Anderson, 2002). Relative likelihood represents the likelihood of a model given the data, whereas AIC weight is the discrete probability of each model (Burnham & Anderson, 2002). The best model was defined as having a delta AIC of 0.00, although preference was given to the simplest model if two or more models had a delta AIC of less than 2.

2.6.2.4 *PIT Tag Array*

A passive integrated transponder (PIT) tag detection system has been operating at Campbell Slough since June 2011, with a hiatus in 2012 and 2017. It is located approximately 150 m into the slough channel from the mainstem Columbia River. The system consists of a Destron-Fearing FS1001-MTS multiplexing transceiver, which simultaneously receives, records and stores tag signals from six antennas measuring 4’ by 10’. The system is powered by a 470W solar array with battery backup and is also connected to a wireless modem that allows for daily data downloads. The array is intended to monitor the presence and to estimate residency of PIT tagged fish in Campbell Slough. Unfortunately, due to COVID-19 protocols, we were unable to power up and maintain the site in 2020. Furthermore, once we were able to access the site in October of 2020, we discovered that a large tree and root had disabled some of the antennas and a few electrical components and our solar panels were missing. Plans are currently underway to rebuild the PIT system utilizing updated technology with possible installation in 2022.

The previous detection system at Campbell Slough, consisting of two antennas measuring 4’ by 20’ was in place from 2011-2017. It was not operational in 2017 due to power cables having been severed by rodents and failed structural integrity of one of the antennas. We revamped the PIT detection array at Campbell Slough in 2018 by installing six antennas measuring 4’ x 10’. The antennas were arranged in a vertical “pass-through” configuration (Figure 8) which allowed greater detection capability at a larger range of water levels. An elevated platform was installed to keep the electronic telemetry equipment

above potential water levels. The system continued to run a Destron-Fearing FS1001-MTS multiplexing transceiver and was powered by a 470W solar array with battery backup. A new modem was installed to update the equipment from 3G technology, which is no longer supported by cellular providers, to 4G technology. The location of the interrogation site was moved approximately 90 m further upstream.



Figure 8. Image of the new PIT detection system at Campbell Slough, installed February 2018.

In 2013, a second PIT detection system was installed near the confluence of Horsetail and Oneonta Creeks in the Columbia River Gorge where substantial restoration actions were completed. The Horsetail PIT detection arrays aids in evaluating the effectiveness of the restoration actions by monitoring use of the habitat by fish in the mainstem Columbia River (*Horsetail Restoration Project*). Antennas are located on both sides of the culvert allowing determination of whether salmon pass through the culvert to access the restored floodplain.

The array consists of a Biomark Fish TRACKER IS1001-MTS distributed Multiplexing Transceiver System (MTS), which powers ten antenna units mounted within the culvert system at Horsetail/Oneonta Creek site (Columbia River, OR) beneath Interstate-84. The MTS unit receives, records and stores tag signals from these ten antennas, which all measure approximately 6' by 6' and are mounted on both ends of the 5-barrel culvert system running under the freeway. The system is powered by an 840 watt (W) solar panel array and supported by a 24-volt, 800 amp-hour battery bank back up. The unit is also connected to a fiber optic wireless modem that allows for daily downloads of tag data and system voltage monitoring updates.

3 Results

3.1 Mainstem Conditions

3.1.1 Continuous Data From the Mainstem

Mainstem conditions are evaluated through measures of river discharge at Bonneville Dam, at Beaver Army Terminal (river mile 53), and at the Morrison Bridge site in downtown Portland, operated by the U.S. Geological Survey. In addition, temperature data and other variables are provided through in situ sensor measurements at Camas (river mile 122) and at Beaver Army Terminal (BAT).

3.1.1.1 *Discharge at Beaver Army Terminal (RM-53)*

River discharge at BAT is shown in Figure 9-. BAT discharge includes inputs from tributaries, including the Willamette River, in addition to flows from the Columbia River. In 2020 there were high flows in the early part of the year (winter: January and February), transitioning to low flows in March and April when solar radiance tends to be sufficiently high to promote strong algal growth. After this, flows were moderate (close to average) for the spring freshet period (May-June), subsiding to low levels through the summer and autumn. There were strong peaks in discharge in early November and December, carrying through to January 2021. Aside from the early winter period, flows in 2021 were nearly the lowest in the time series and similar to 2015. The difference between 2021 and 2015 was that the former had no substantially high flows at any time during the year aside from a high peak in January and a moderate peak in February.

Similar to 2019, flows in 2020 could be characterized as having a moderate freshet but low flows otherwise (i.e., low baseline flows), aside from the relatively high flows observed in January. Thus, 2019, 2020, and 2021 had low baseline flows relative to the 2010-2021 average. Cumulative flows for these years consist mainly of winter flows from December-February (mostly characterized as peaks associated with storm events) and the spring freshet, which was nearly absent in 2021.

Discharge fluxes show similar patterns at Beaver Army Terminal (RM-53) and Bonneville Dam (RM-122) (Figure 9).

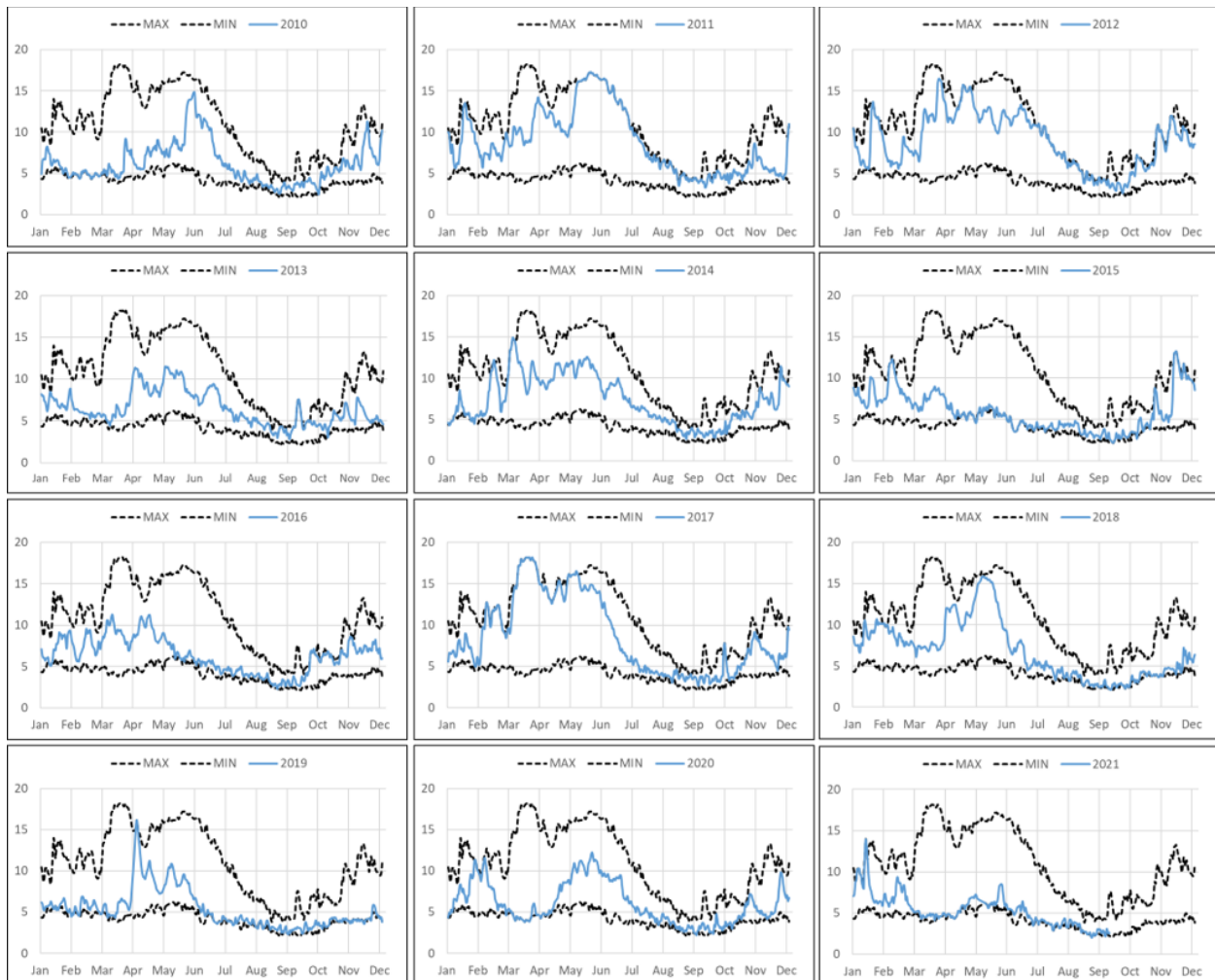


Figure 9. Daily water discharge ($\text{m}^3/\text{s} \times 10^{-3}$) at Beaver Army Terminal (RM-53) from 2010-2021. Panels show individual years (blue lines) with the daily maximum and minimum indicated (upper and lower dashed lines) in each panel. The final panel shows the maximum (upper dashed line), minimum (lower dashed line)

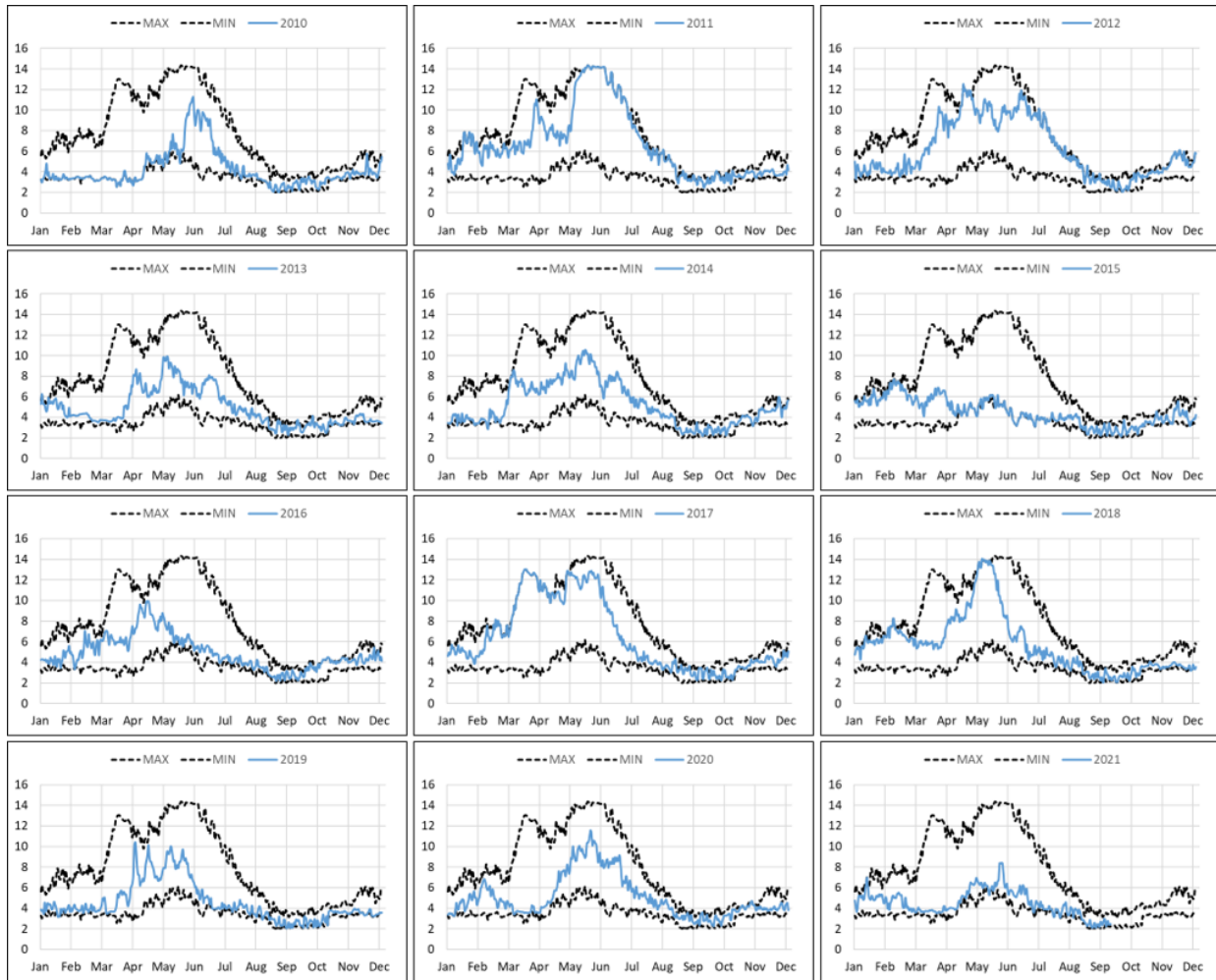


Figure 10. Daily water discharge ($\text{m}^3/\text{s} \times 10^{-3}$) at Bonneville Dam from 2010-2021. Panels show individual years (blue lines) with the daily maximum and minimum indicated (upper and lower dashed lines) in each panel.

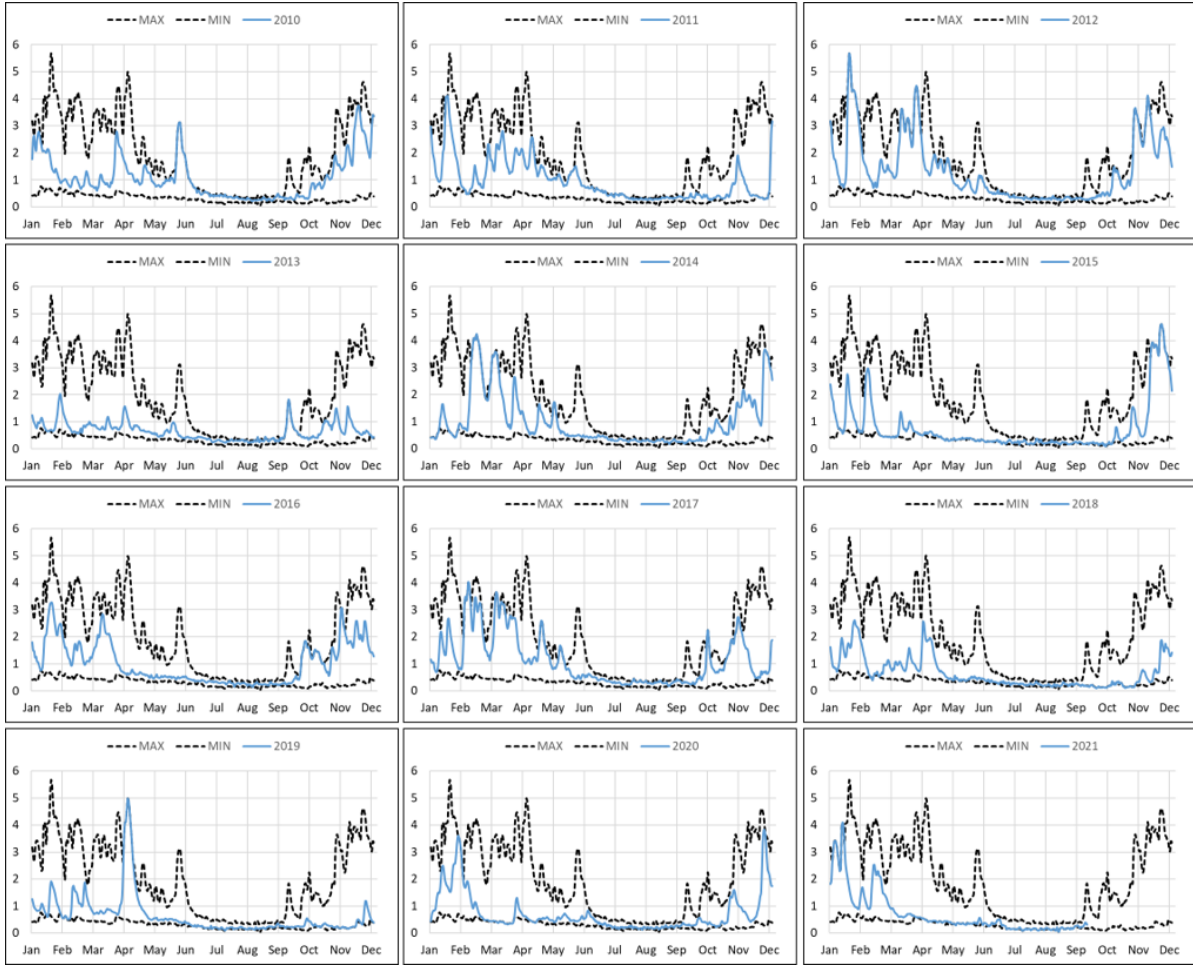


Figure 11. Daily river discharge (in $\text{m}^3 \text{s}^{-1} \times 10^{-3}$) of the Willamette River measured near the Morrison Bridge for years 2010–2021. Also shown are the daily maximum and minimum values for the years 2010–2021. Data from USGS 14211720.

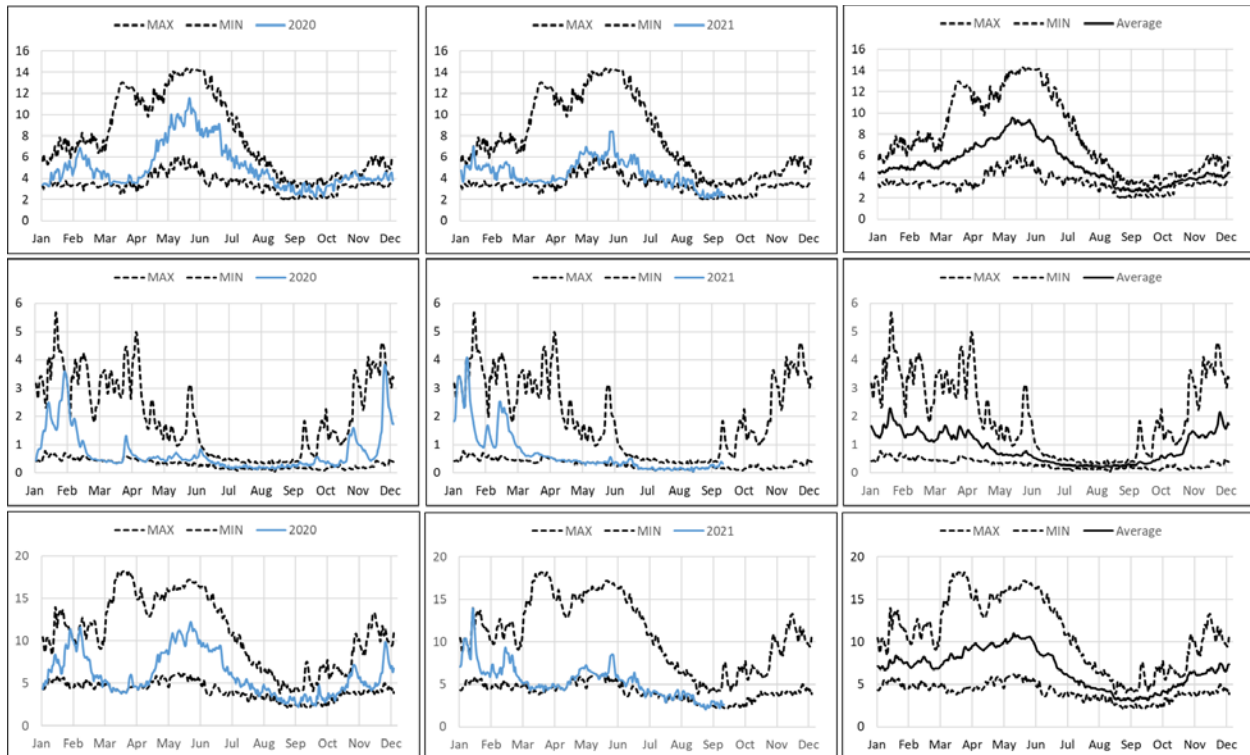


Figure 12. Discharge volume flux associated with the Columbia River at Bonneville dam (top panels), the Willamette River at downtown Portland (middle panels), and Beaver Army Terminal at river mile 53 (bottom panels). Flows at BAT represent the sum of the Columbia, Willamette, and other smaller tributaries. Left panels show data from 2020, middle panels show data from 2021, and right panels show the maximum daily average flows, minimum daily average flows, and average daily flows (solid lines). Flow data are in $m^3s^{-1} \times 10^{-3}$.

The proportion of flow associated with the Columbia River, the Willamette River, and other tributaries at Beaver Army Terminal (RM-53) for years 2010–2021 are shown in Figure 15. The Columbia River (measured at Bonneville dam) accounts for the largest proportion of flow throughout the year; however, during the winter months, flows from the Willamette River increase in relative importance, as do flows from other tributaries (Figure 15). Similar to 2019, river discharge in the early spring of 2020 was lower than average and composed of a relatively small fraction of flow from the Willamette River and tributaries, which influences water quality parameters in the mainstem, including nutrients, turbidity, and colored dissolved organic matter (see later sections). Compared to previous years, the proportional flow from the Willamette and other tributaries was very low and characterized by the absence of distinct peaks during the winter (January through March). The initial phase of the spring freshet had a large contribution from the Willamette and other tributaries; however, by May flows were again strongly dominated by the Columbia. The plots in Figure 15. show more closely how the fractional composition of river discharge varies over the year among the years investigated, highlighting the low contribution from tributaries in 2019 and 2021. The freshet was nearly absent in 2021, much like 2015. In 2020, the freshet was quite distinct from local pluvial flows that typically characterize the time period leading up to the freshet; that is, there was a distinct peak associated with the freshet that is not always seen.

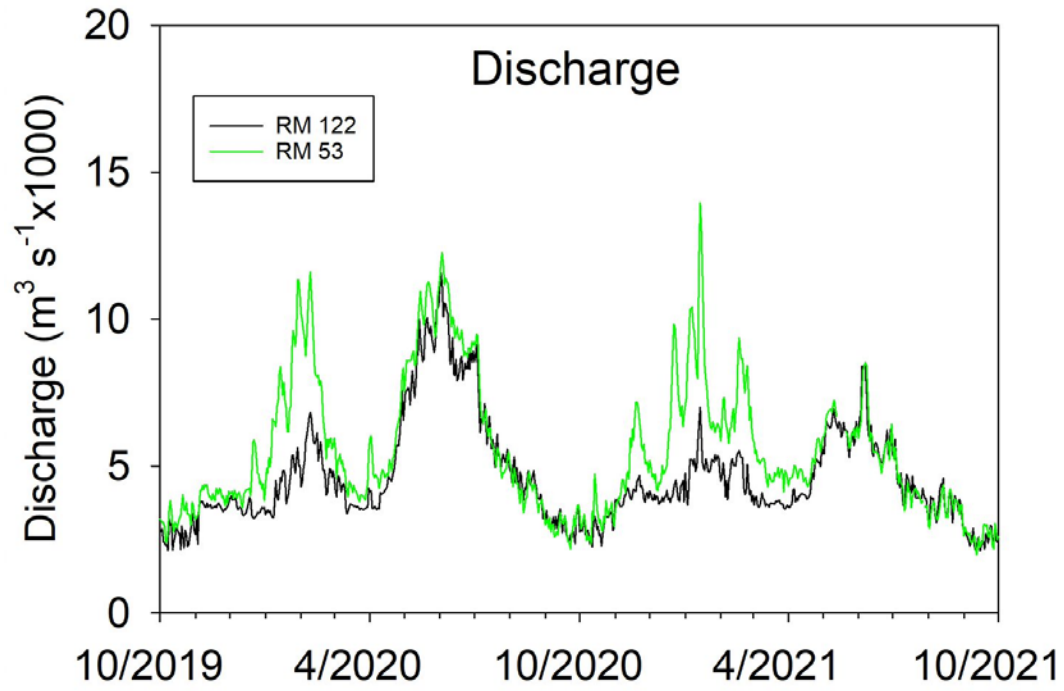


Figure 13. Discharge comparison between BAT (RM 53) and Camas (RM 122) October 2019-October 2021.

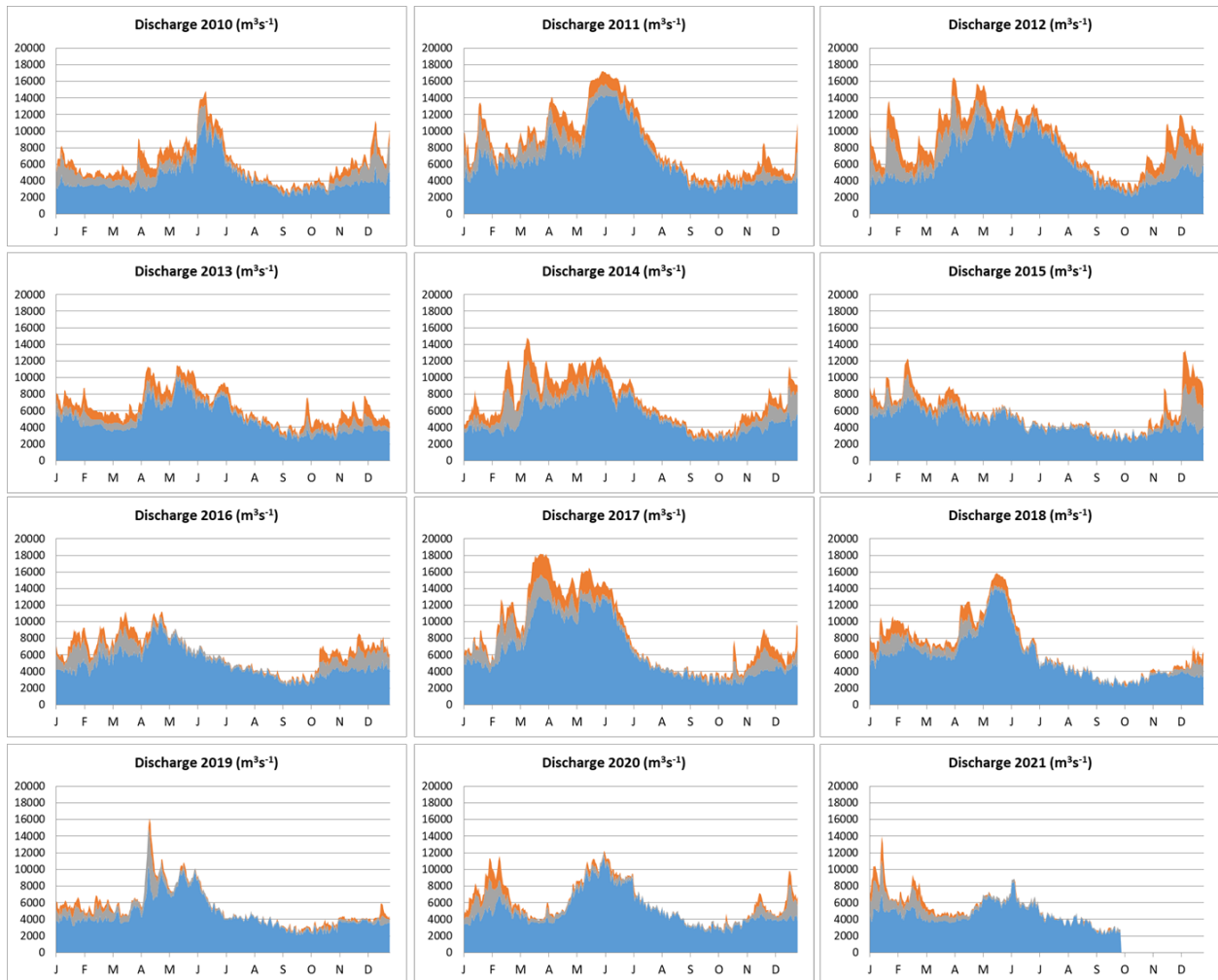


Figure 14. Daily discharge fluxes (m^3/s) associated with Columbia River flow (blue), Willamette River flow (orange), and other tributaries (grey). Discharge from the Willamette was determined at the USGS stream gage at the Morrison Bridge; the contribution from other tributaries was computed by subtracting flows observed in the Willamette from those in the Columbia.

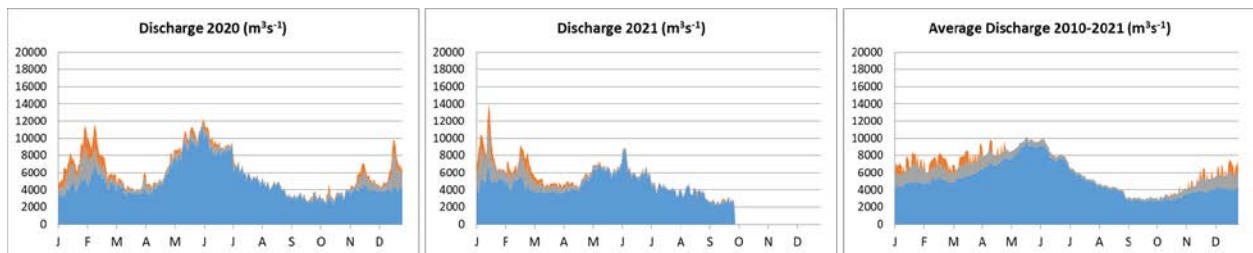


Figure 15. Proportional discharge partitioned into flows from the Columbia (blue), the Willamette (orange), and other tributaries (grey) for the years 2020 and 2021. A comparison with average values computed for the 2010-2021 time series is shown for reference.

Like other years, the contribution of tributaries other than the Willamette to total river discharge in 2020 and 2021, as estimated by difference calculations, was highest in the winter months (Figure 14-Figure 15); notably, the contribution by the Willamette River to the annual freshet was relatively small in 2020, similar to 2019 (Figure 14-Figure 15).

3.1.1.2 *Water Temperature in the Mainstem at Camas (RM-122)*

We showed in previous reports that mainstem hourly temperatures did not vary substantially between Camas (RM-122) and Beaver Army Terminal (RM-53); data from Camas are shown here. Since temperature is an important variable that influences organismal physiology and particularly the performance and survival of salmonids, we compare the number of days in 2020 and 2021 where temperatures exceeded thresholds associated with reduced performance or physiological stress with the years 2013, 2014, 2015, and 2016 (Figure 16-Figure 17). The number of days was computed by summing the number of hours for which a threshold was exceeded and then dividing by 24 to produce a day equivalent. According to Oregon State Water Quality Standards (code 340-041) and Washington State Water Quality Standards (code 173-201A), water temperature should be less than 16°C for optimal performance; rearing and migratory habitats should be less than 18.0°C (Oregon standards) or less than 17.5°C (Washington standards). The Columbia is considered spawning/rearing habitat (Washington State Water Quality Standards) between the mouth and rkm 497 (Oregon–Washington border). Within the migration corridor, temperatures should be less than 20°C (Oregon standards), with a recommendation that water bodies have cold-water refugia having temperatures at least 2°C colder than the daily maximum temperatures of the adjacent water body that are sufficiently distributed to allow salmon/steelhead migration without significant adverse effect. It is recommended that the Columbia River may not exceed a one-day maximum of 20.0 °C (Washington standards). According to recommendations from DEQ/OWEB, year-round temperatures should not exceed 18 °C (Kidd, 2011), with an ideal range of 7.2-15.6 °C for healthy adults and 12.2-13.9 °C for healthy juveniles (Kidd, 2011).

The most conservative threshold (19 °C) was exceeded on 50 days in 2020 and 73 days in 2021, . The latter (2021) had the largest number of days with temperature exceeding 19°C after 2015 (n=84) (Figure 17).

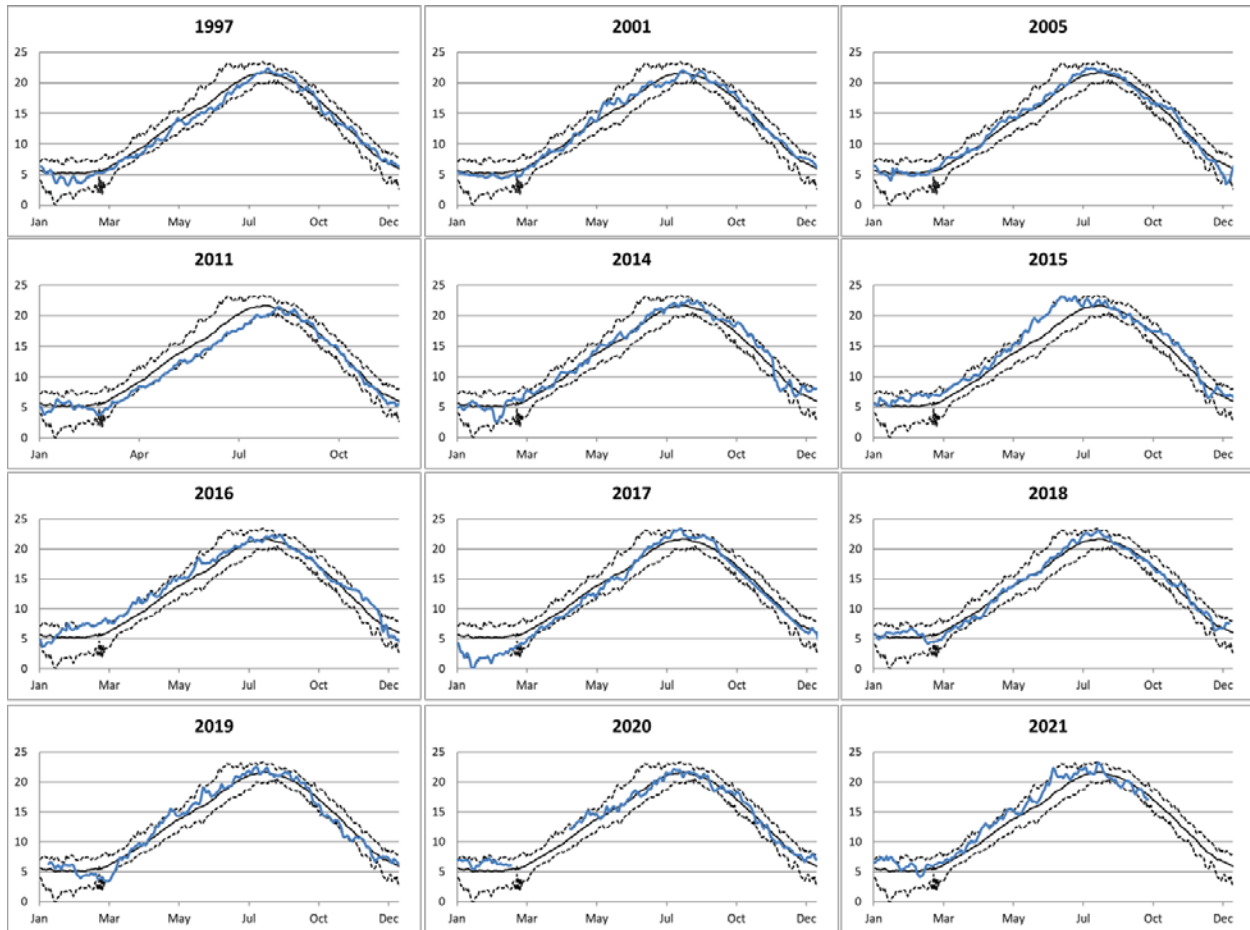


Figure 16. Series of graphs showing mainstem Columbia River temperatures at Camas, WA between 1997 and 2021. Upper dashed line shows the average maximum daily temperature; bottom dashed line shows the average minimum daily temperature. Blue line shows the daily average temperature for each year. All temperatures in °C. Averages were computed for each 24 h period. Maximum and minimum daily averages were calculated from the 1997-2021 time period.

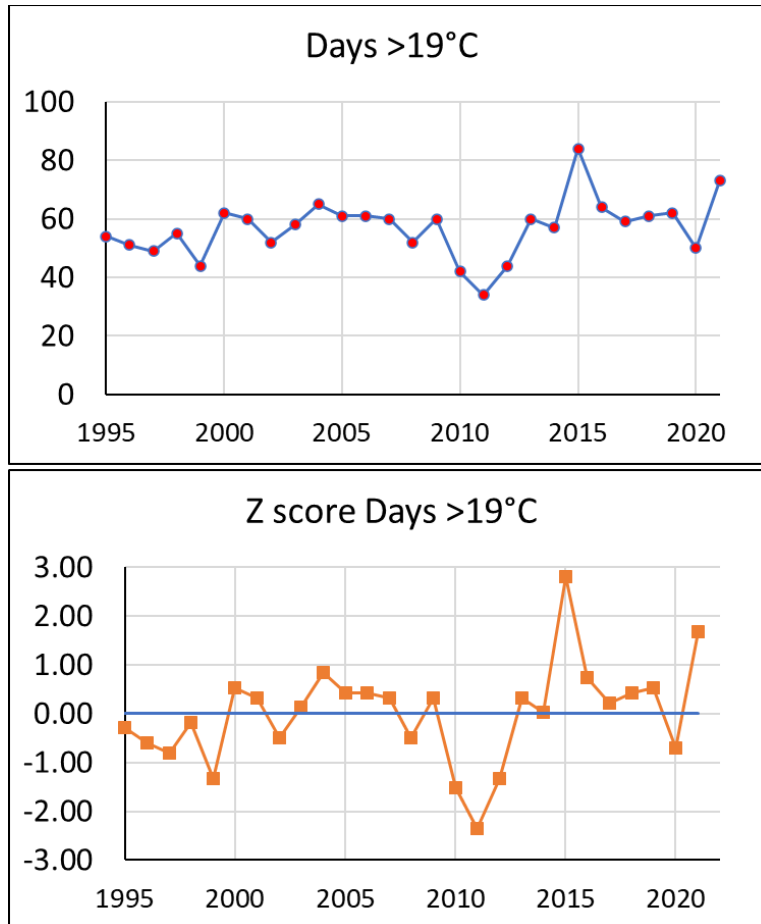


Figure 17: Mainstem temperature (as daily averages) determined at the Port of Camas, WA, in terms of the number of days exceeding 19 °C between 1995 and 2021 (top panel) and reported as z scores (bottom panel). Z scores represent the number of standard deviations away from the mean value; thus, high z scores indicate water temperatures that exceeded daily average values by large amounts. Months included in the calculation were May through Aug (4 months). 2021 was 2nd warmest after 2015.

3.1.1.3 *Water Quality Parameters in the Mainstem*

Time series of water quality parameters measured hourly at RM-122 (Camas) are shown in Figure 18.. The difference in discharge between RM-122 and Beaver Army Terminal (RM-53) is highlighted to show the contribution of tributaries, which is focused on the late-autumn, winter, and spring periods. Similar to 2018, the tributaries had a relatively large contribution to total discharge during the peak in April 2019, as well as during January-February. Peaks in tributary flow are associated with peaks in colored dissolved organic matter (CDOM), turbidity, and nitrate, underscoring the influence of water source on water quality parameters. Chlorophyll *a*, a proxy for the contribution of fluvial phytoplankton to primary production in the river, peaked in April-May as well as in June-July, in association with changes in river discharge.

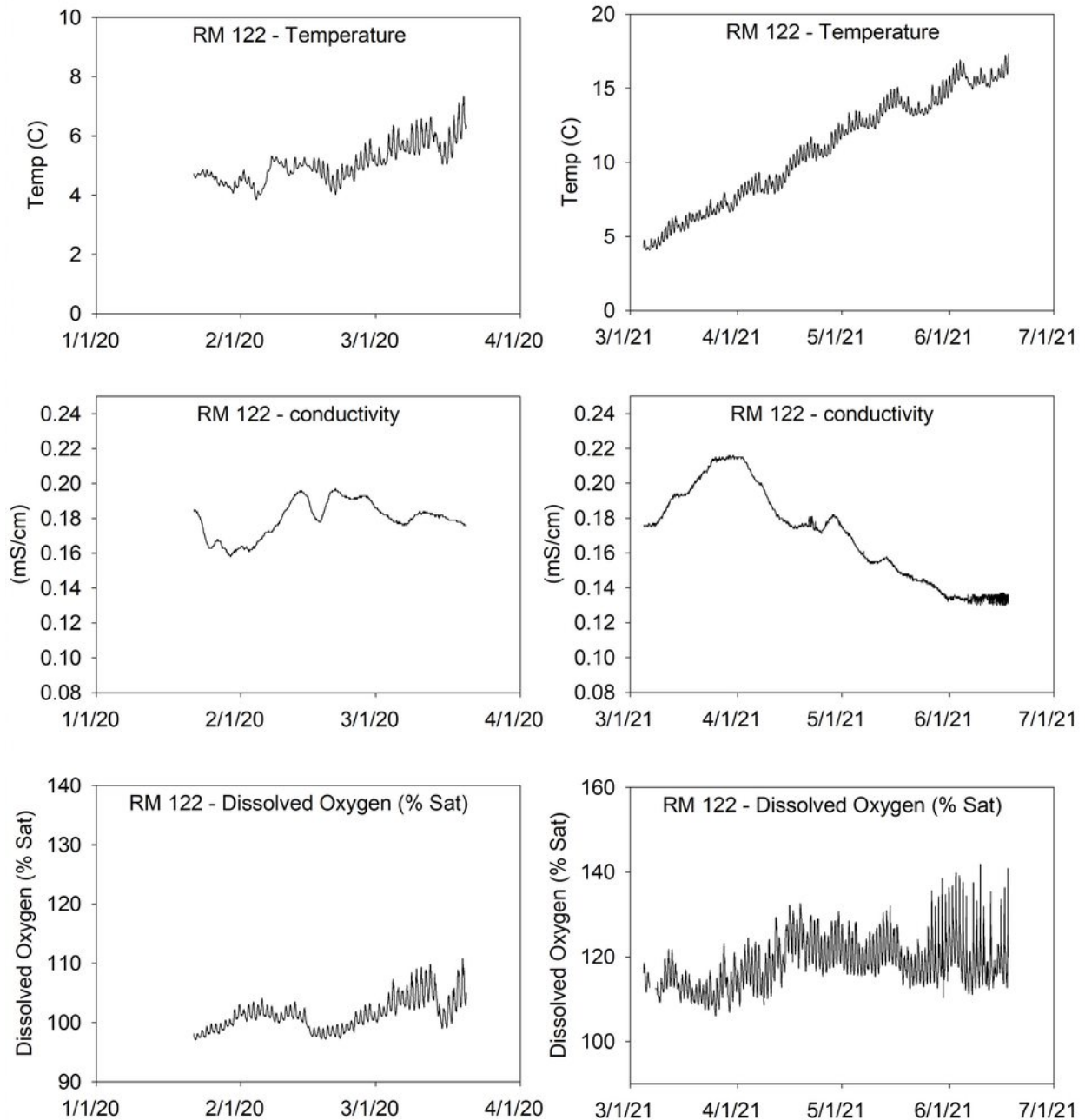


Figure 18. Time series of hourly water quality parameters measured at River Mile 122 (Camas, WA) in 2020 (left panels) and 2021 (right panels).

The percent saturation of dissolved oxygen (i.e., saturation relative to atmospheric equilibrium) reflects the balance between oxygen produced through photosynthesis and oxygen consumed through respiration. Dissolved oxygen saturation exceeded 100% for nearly the entire year, with greater day-to-day variability observed during the summer months (Figure 18.).

Dissolved nitrate concentrations were lower in 2019 compared to previous years during peaks flows; in 2017, nitrate exceeded 50–60 μM in March–April, declining rapidly during the month of April when phytoplankton growth was strong (as evidenced by the increase in chlorophyll *a* during the same period).

In 2018, although nitrate was high in February (~50 μM), concentrations were ~20-40 μM during the period of strong growth of phytoplankton in the spring. The time series of nitrate concentrations closely matches that of dissolved oxygen, partly due to drawdown by primary production and partly due to the contribution of winter sources. Even though nitrate concentrations were lower than in 2017, they were still frequently higher than the recommended benchmark for good water quality (<0.399 mg L^{-1} , or 28.5 μM ; Oregon's National Rivers and Streams Assessment 2008-2009).

3.2 Abiotic Site Conditions

3.2.1 Continuous Water Quality

Measurements of water quality parameters were made every 30 minutes at five trends sites (Ilwaco Slough, Welch Island, Whites Island, Campbell Slough, and Franz Lake Slough) using sensor packages moored at fixed depths. From these data, daily averages were computed to look for seasonal trends. Due to difficulties associated with accessing sites during Covid-19 travel restrictions, the data from 2020 and 2021 have more gaps than in previous years.

3.2.1.1 *Ilwaco Slough*

Water temperature at Ilwaco peaked at just over 20°C in July and August (Figure 19). Ilwaco is strongly influenced by tidal exchange with marine waters from the coastal ocean, particularly in the summer months. Salinity, which is computed from conductivity, is the clearest indicator of this influence: conductivity tends to be highest between late June and mid-September. This is likely true in both 2020 and 2021 as well; however, an issue with the sonde prevented data from being downloaded. At the time of writing, the instrument is under repair at the manufacturer and data collected between June and September should be recovered. Because there was no significant freshet in 2021, the salinity did not dip below 5 PSU at any point during the deployment. DO saturation and pH declined simultaneously from spring to summer, as temperatures increased. In 2019, the daily range in dissolved oxygen saturation was higher prior to and following the spring freshet, likely reflecting the higher levels of primary production associated with the lower river flows; in 2021, the DO saturation declined from March through May and no appreciable freshet was observed that year. Whereas the daily percent saturation of oxygen was between 60 and 80% in June of 2019. In 2021, pH values ranged from 7.5 to 8.2, which does not include data from months when the pH typically is lowest (Figure 19). The range of values observed in 2021 fall within the recommended range for good water quality (6.5–8.5; Washington State Water Quality Standards).

The hourly measurements at Ilwaco are shown in Figure 20. There were data gaps in 2020 that occurred due to a problematic instrument setting that was resolved later in the season. Temperatures exceeded 25 °C late in 2020 but occurred much earlier in 2021 (May/June), coincident with comparatively low flows. Compared to 2020, salinities between March and May were slightly higher in 2021. The hourly data clearly show short-term variations in conditions that reflect tidal influences and variability associated with river flows.

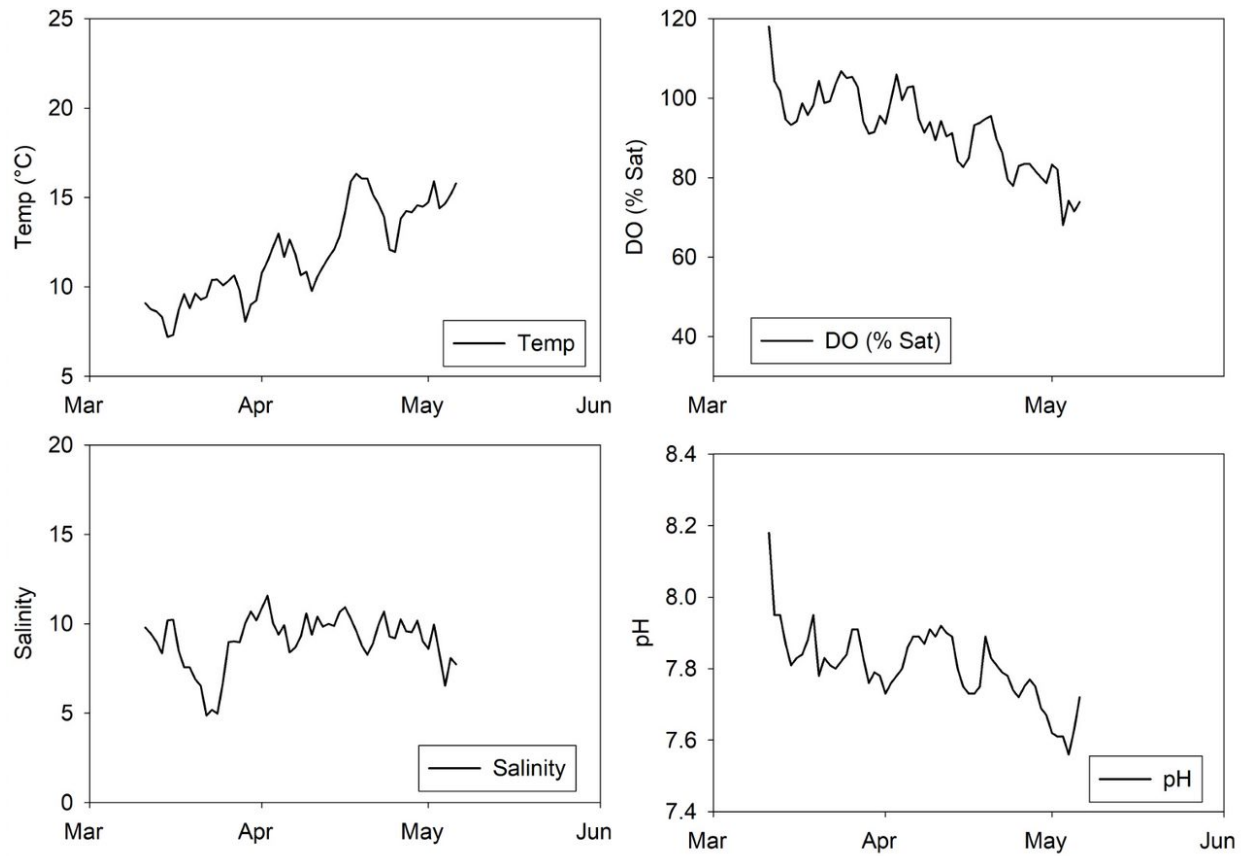


Figure 19. Water quality data (daily average) collected from Ilwaco Slough in 2021, including temperature, salinity, dissolved oxygen (given as percent saturation relative to air), and pH.

Ilwaco 2020 and 2021 Hourly data

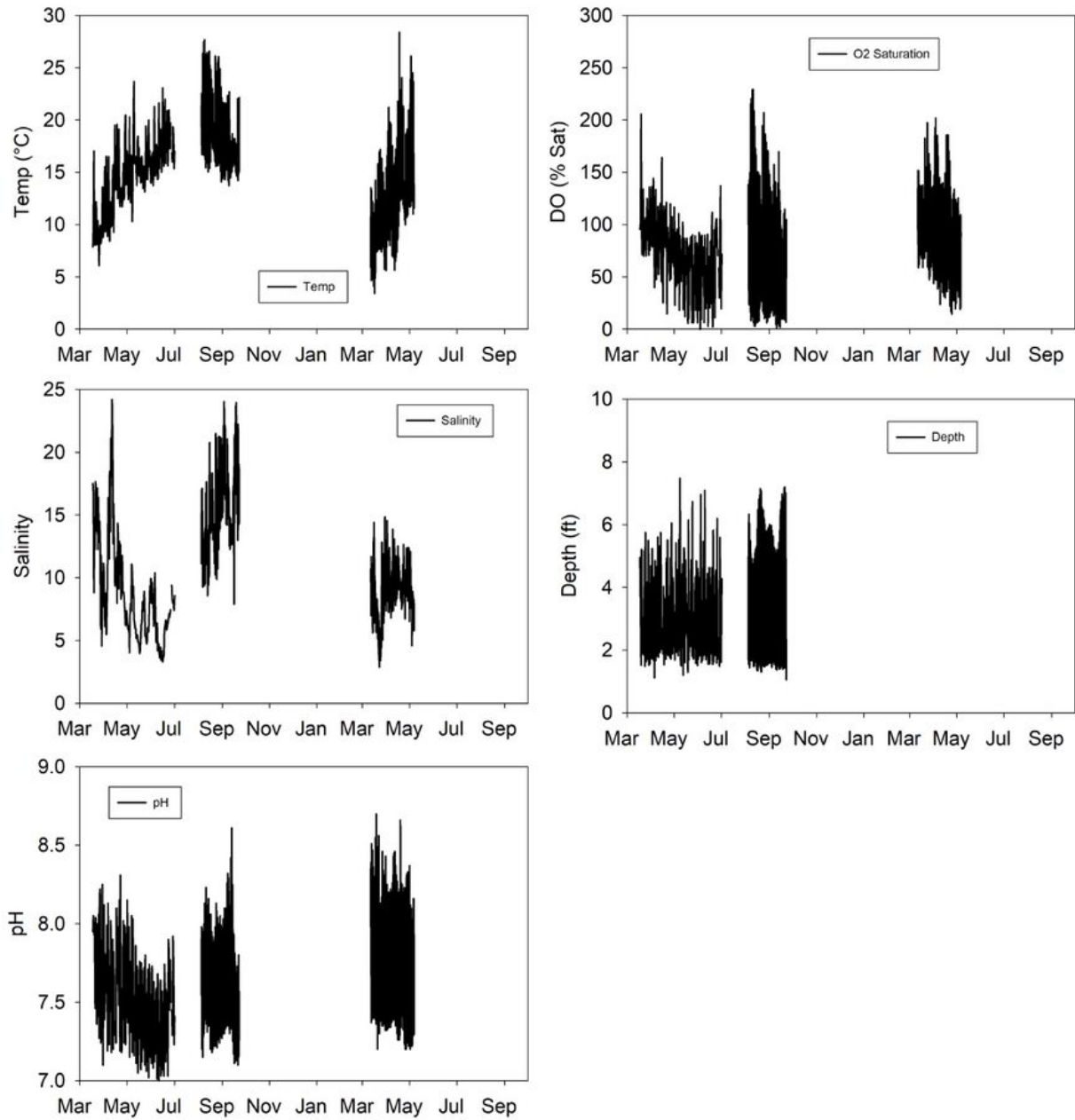


Figure 20: Time series of hourly measurements of water quality parameters made at Ilwaco Slough, 2020 and 2021.

3.2.1.2 *Welch Island*

Maximum summer temperatures at Welch Island reached approximately 23°C in July and August, (Figure 21- Figure 22). Dissolved oxygen saturation was >80% throughout the time series, with values exceeding 120% in April. The lowest values were observed during brief periods in July and August. Although the freshet was very small in 2021, a signal associated with the small peak in flows in early May is discernible in the water quality data. A peak in water depth was associated with a sharp decline in total chlorophyll fluorescence as well as fluorescence associated with phycocyanin, a cyanobacteria pigment. Similarly, a sharp decline in conductivity was observed at the same time, as was a dip in dissolved oxygen saturation and pH. These characteristics are typical of periods of strong river flows. pH

ranged from 7.4 to 8.7 in 2021; aside from a brief period in April, the pH levels observed fell within the recommended range (6.5–8.5; Washington State Water Quality Standards). Chlorophyll *a* was highest prior to the small peak in flow in early May and declined thereafter into the summer months, with the exception of a peak in August that was associated with a large peak in phycocyanin. Phycocyanin fluorescence followed that of total chlorophyll prior to the small peak in flow in May and was negligible in the late spring and summer, with the exception of the August peak.

The hourly data demonstrate diel cycles in dissolved oxygen saturation as well as tidal variations in depth (Figure 19). Daily temperature ranges were largest leading up to the time of peak flow in early May and after peak flows subsided in the summer months. Daily maxima in pH were highest in the summer, coincident with the largest ranges in dissolved oxygen saturation.

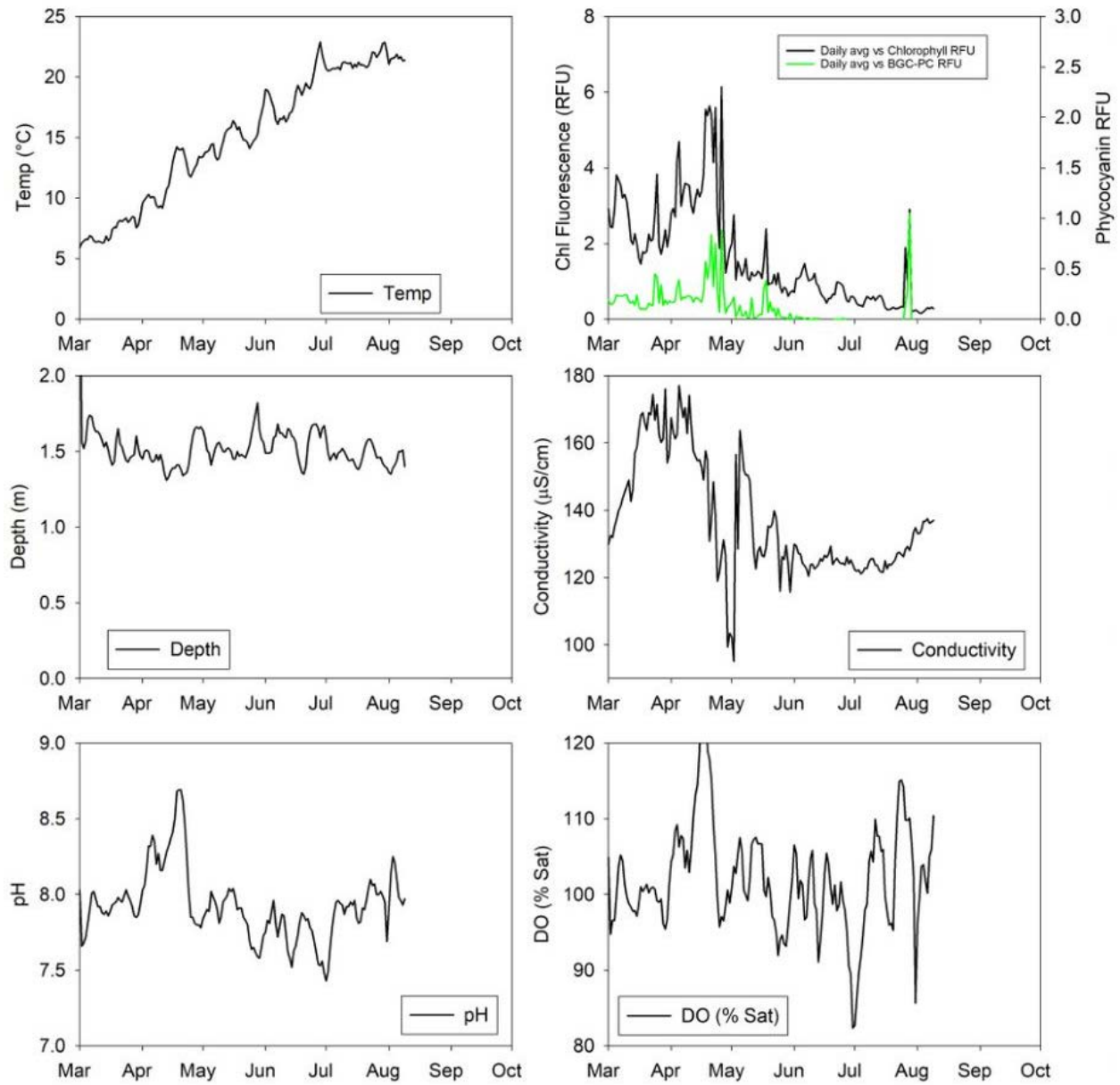


Figure 21. Time series of daily averaged measurements of water quality parameters made at Welch Island, 2021. Note that the water quality sonde at Welch Island includes phycocyanin fluorescence, in addition to chlorophyll fluorescence; these data are shown in the panel in the upper right as a green line.

Welch Is. 2021 - hourly data

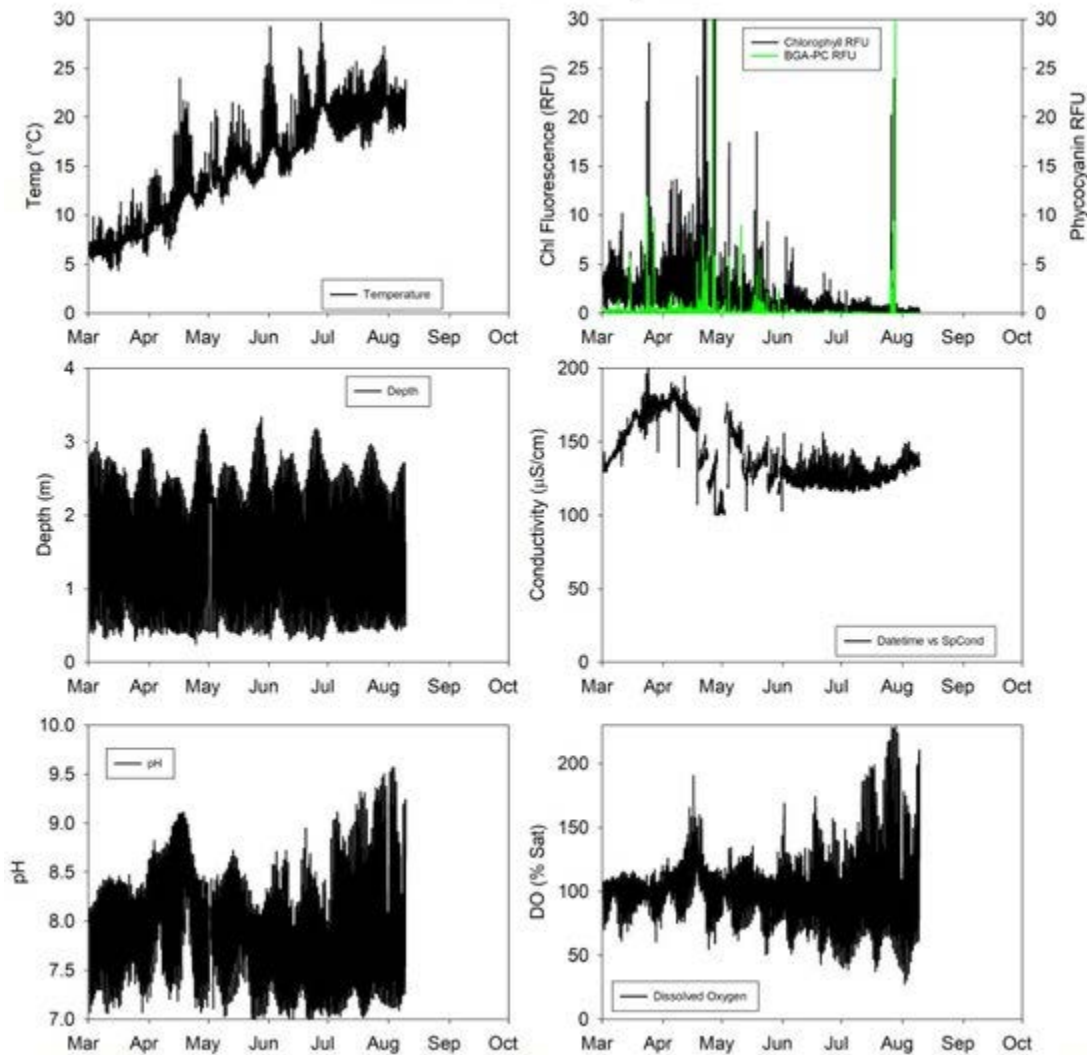


Figure 22: Time series of hourly water quality data collected at Welch Island in 2021.

3.2.1.3 Whites Island

Dissolved oxygen saturation at Whites Island was >90% throughout the time series of observations (Figure 23). The peak in June exceeded 120% dissolved oxygen saturation, indicating strong growth of primary producers. Unfortunately, data gaps between April and June render it impossible to characterize water quality in those months; however, since Whites Island often shares similarities with Welch Island, we can infer that the peak in spring phytoplankton growth likely occurred in April in advance of the peak in river flow in May. Temperatures at Whites Island peaked in the summer during July-August at approximately 22-23 °C, similar to Welch Island. Also similar to Welch Island, conductivity was higher prior to the May peak in flow at Whites Island compared to afterwards. Daily average pH values at Whites Island are not shown in Figure 23, but daily variations are shown in Figure 24, where the data indicate periods where pH is quite low.

Whites 2020 - Daily Average

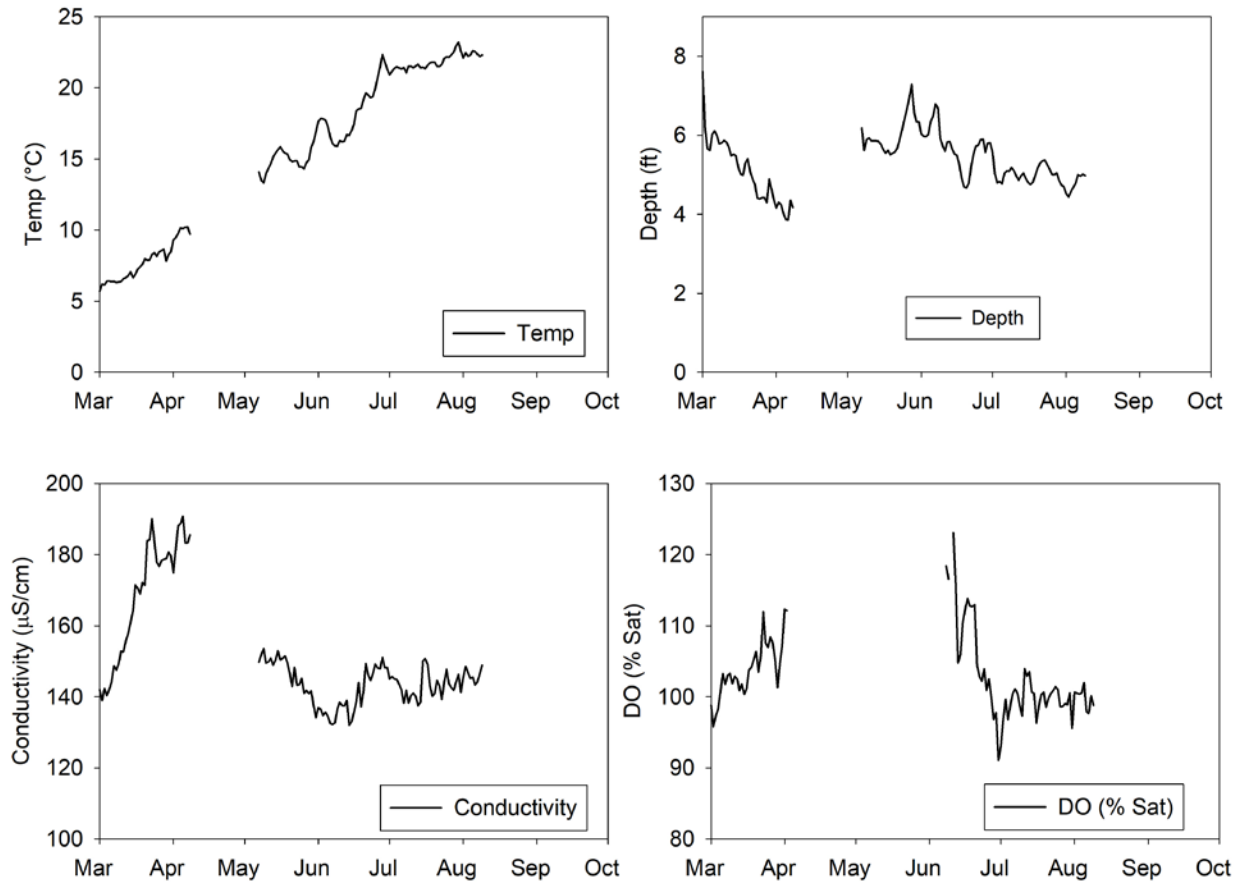


Figure 23. Daily average water quality data collected in 2020 by a water quality sonde at Whites Island in Reach C.

Whites 2021 - hourly data

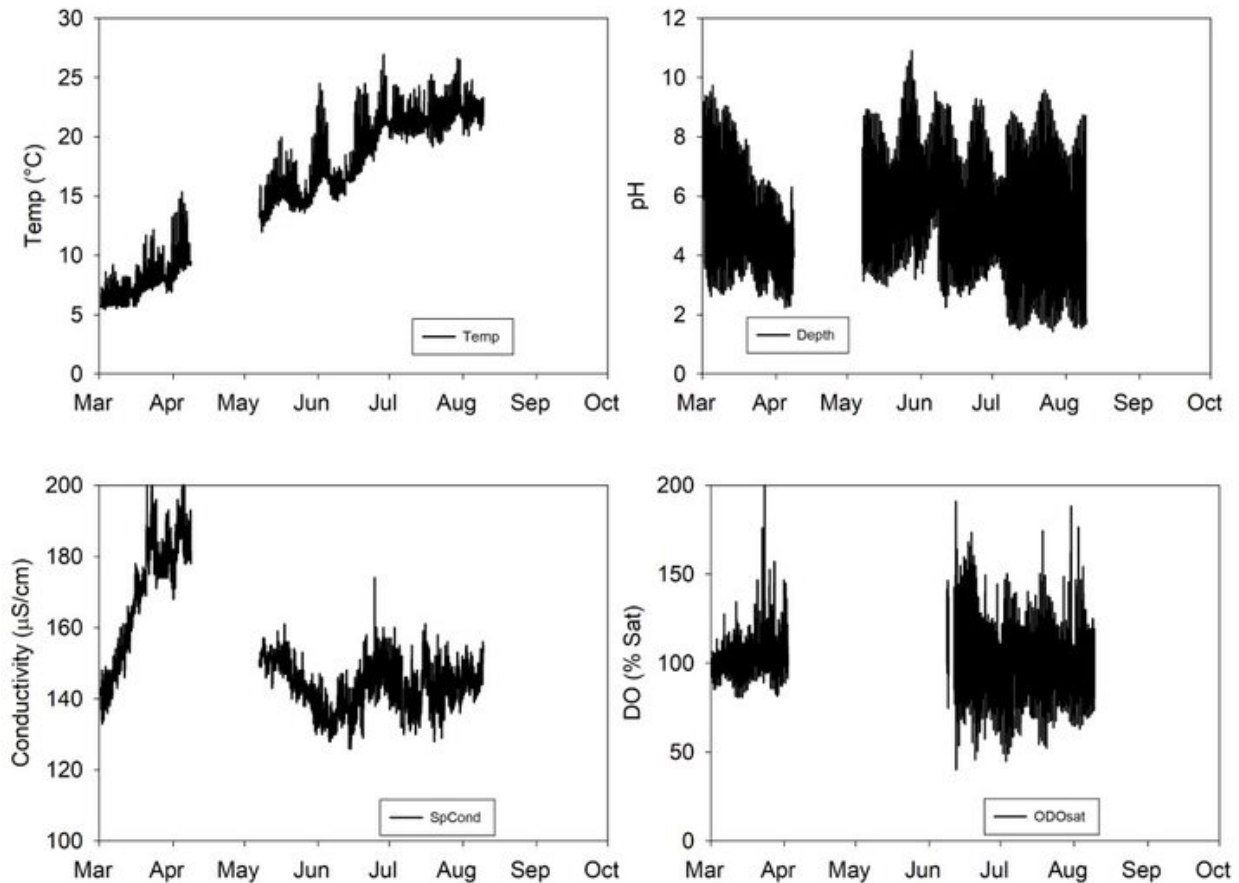


Figure 24: Time series of daily averaged measurements of water quality parameters made at Whites Island, 2021.

3.2.1.4 *Campbell Slough*

Of the five off-channel trends sites, Campbell Slough tends to have the highest summer water temperatures. In 2020 and 2021, daily average water temperatures exceeded 25 °C, with higher values observed in 2021 compared to 2020 (Figure 25); in previous years water temperatures exceeded 25°C from mid-July to mid-August at this site. Water temperatures reached high levels early in 2021 compared to previous years, including 2020. 2021 also had lower water levels throughout the time series, lower water levels (as indicated by the depth sensor), higher conductivity prior to the peak in spring flows in May, lower pH, higher dissolved oxygen saturation in late summer, and higher chlorophyll *a* fluorescence, with a marked peak in both chlorophyll *a* fluorescence and phycocyanin in June. Although the freshet was much reduced in 2021, an increase in sensor depth and a peak in conductivity occurred during peak flows.

In general, biogeochemical properties reflect the influence of the freshet, including a reduction in chlorophyll, dissolved oxygen saturation, conductivity, temperature, and pH. With a reduced freshet in 2021, the signals associated with the small peak in river flow were not as clear as in previous years. Chlorophyll concentrations were lower near the beginning of May relative to the period prior and following the elevated flow (Figure 25). Chlorophyll concentrations observed at Campbell Slough were

below the recommended benchmark of $15 \mu\text{g L}^{-1}$ (based on three samples collected over three consecutive months; Washington State Water Quality Standards).

There were dramatic fluctuations in the percent saturation of dissolved oxygen throughout the year at Campbell Slough, indicating high biological activity at this site. Daily fluctuations were larger in 2021 compared to 2020, with values reaching high values $>200\%$ and low values $<15\%$ (Figure 26).

Campbell 2020 and 2021 Daily Average

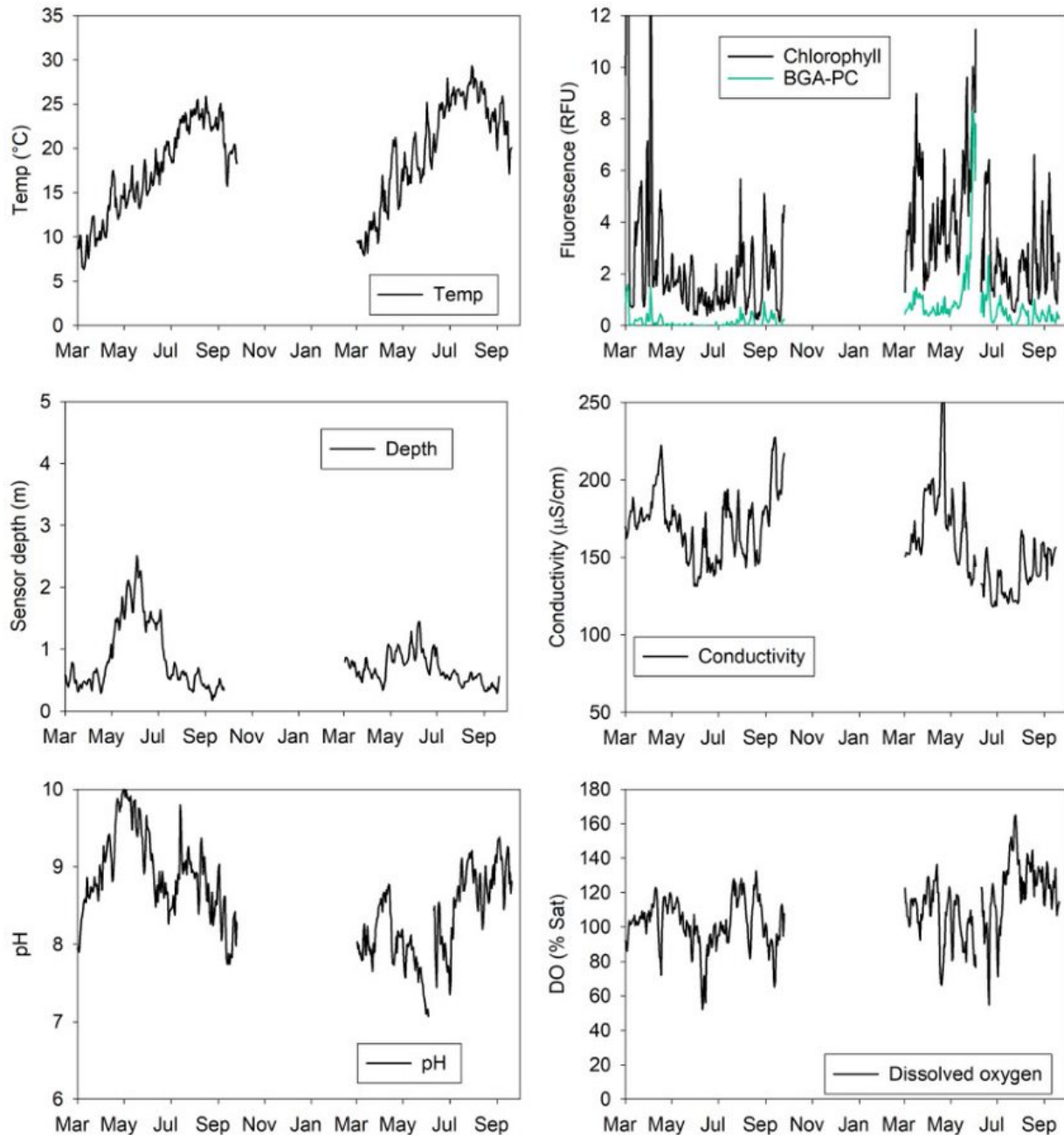


Figure 25. Time series of daily averaged measurements of water quality parameters made at Campbell Slough, 2021.

Campbell 2020 and 2021

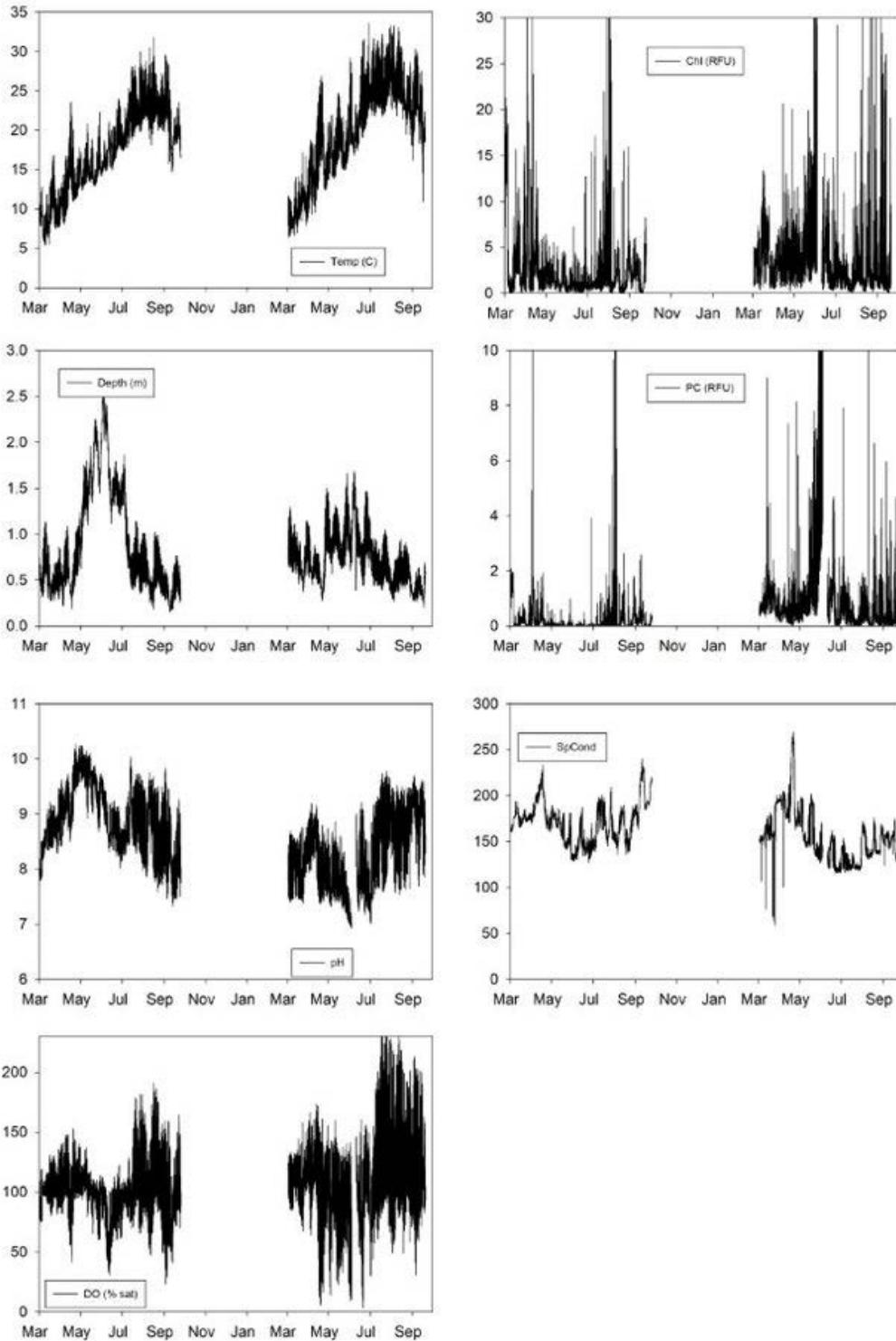


Figure 26: Hourly water quality data collected at Campbell Slough in 2020 and 2021, including temperature (oC), chlorophyll *a* fluorescence (in Relative Fluorescence Units, RFU), depth (m), conductivity ($\mu\text{S cm}^{-1}$), pH, and dissolved oxygen (DO) percent saturation relative to the atmosphere (% Sat).

3.2.1.5 *Franz Lake Slough*

Summer temperatures at Franz exceeded 25°C from late-June through mid-August (Figure 27). Peaks in chlorophyll and phycocyanin fluorescence were observed in mid-May and in early to mid-July; there was a notable peak in phycocyanin in July. The depth sensor showed a peak in early June, which was associated with an influx of water with low conductivity and low chlorophyll. After the first part of July, a beaver dam was constructed, which can be seen by an increase in depth after July (Figure 27). Two peaks in cyanobacteria populations (as inferred by peaks in the pigment, phycocyanin) were observed: one in early July around the time of beaver dam construction and one in late August. Large fluctuations in dissolved oxygen saturation were observed in the summer months between June and September. pH values ranged from ~6.7 to 8.0, with the highest values occurring between June and August when high chlorophyll fluorescence values were observed. Conductivity values were highest following the subsidence of the small peak in river flow that occurred in May.

The hourly data show that the greatest range in daily values of temperature, pH, dissolved oxygen saturation, and chlorophyll are observed during the summer months (Figure 28), when biota are more metabolically active.

Franz - Daily Average 2021

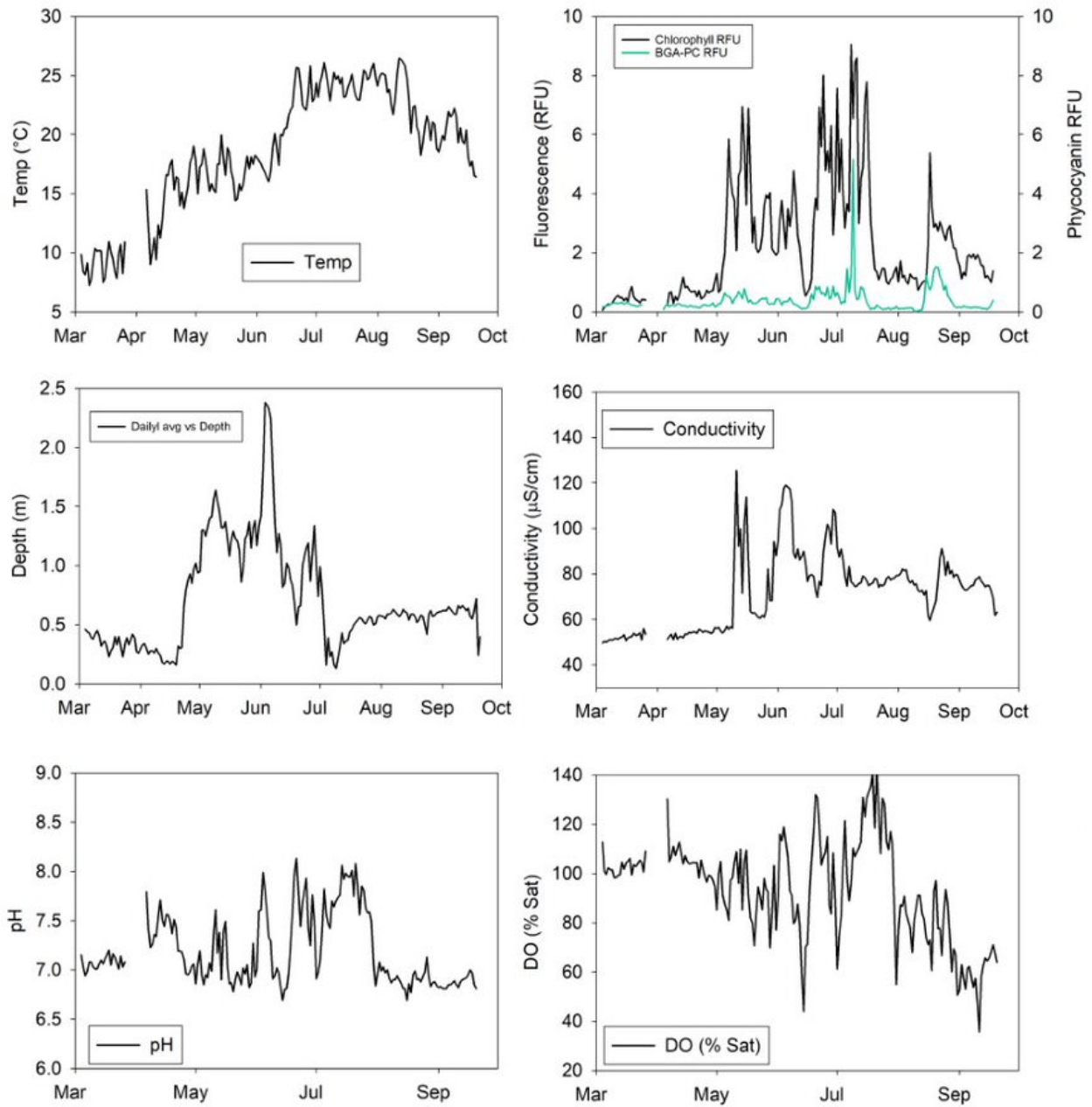


Figure 27. Time series of daily averaged measurements of water quality parameters made at Franz Lake Slough, 2021.

Franz 2020 and 2021 - Hourly Data

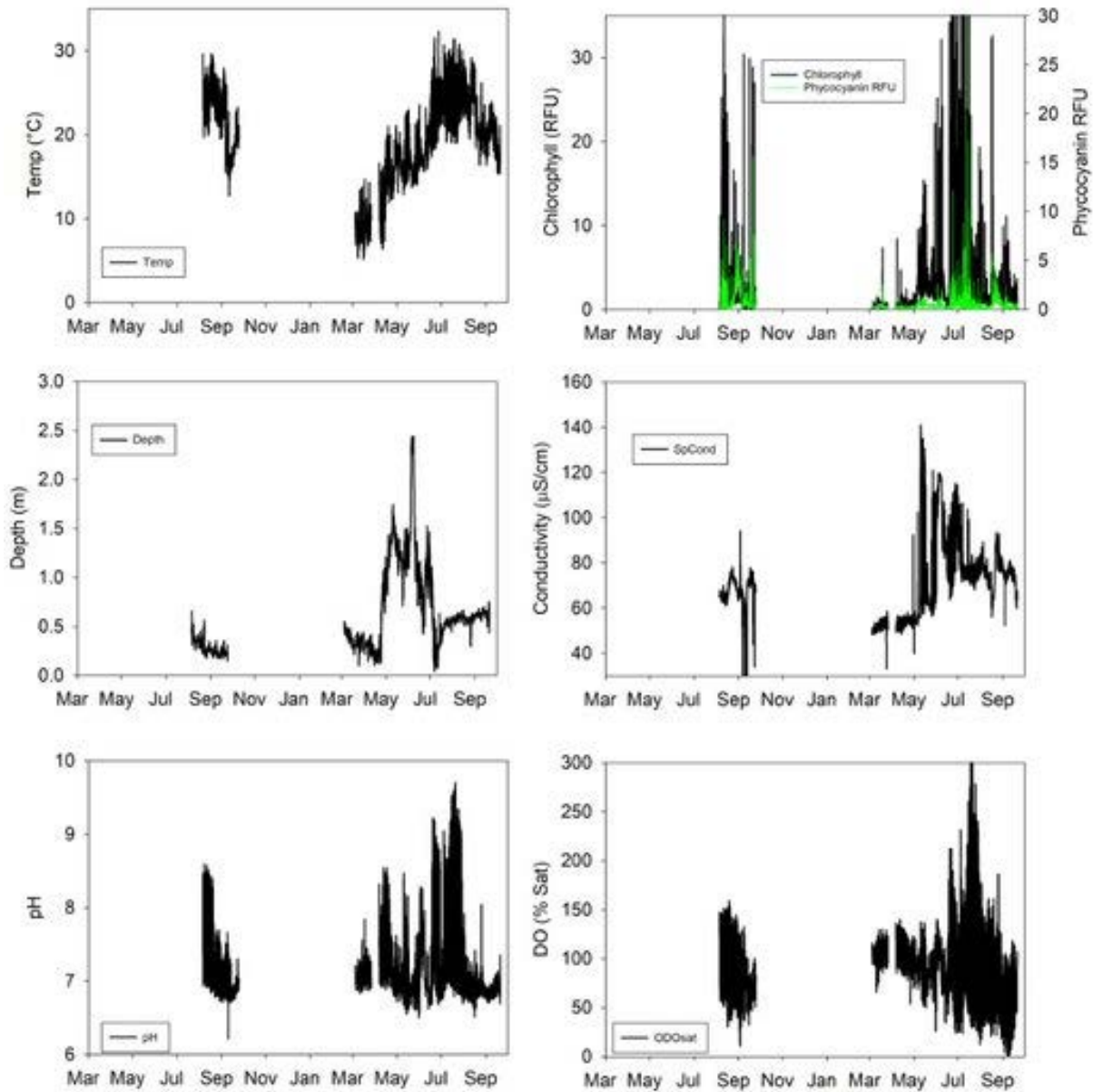


Figure 28. Hourly water quality data collected at Franz Lake Slough in 2020 and 2021, including temperature ($^{\circ}\text{C}$), chlorophyll *a* fluorescence (in Relative Fluorescence Units, RFU), depth (m), conductivity ($\mu\text{S cm}^{-1}$), pH, and dissolved oxygen (DO) percent saturation relative to the atmosphere (% Sat).

3.2.2 Dissolved Oxygen at Trends Sites

There was a wide range of values corresponding to dissolved oxygen saturation relative to the atmosphere at the off-channel trends sites (Ilwaco Slough, Welch Island, Whites Island, Campbell Slough, and Franz Lake Slough). It is recommended that dissolved oxygen should not fall below 6.0 mg L^{-1} for cold-water species, including native salmon (Oregon State Water Quality Standards); lower concentrations (4 and 2 mg L^{-1}) are considered to be increasingly detrimental to aquatic life. Using these thresholds to estimate stress associated with suboptimal levels of dissolved oxygen, we computed the percentage of hourly data

below 6, 4, and 2 mg L⁻¹ for each of the five trend sites (Table 27). In previous years, Ilwaco had the greatest number of hours where dissolved oxygen concentrations were below each of the three threshold levels (e.g., >1400 in 2019); however, problems with sensor performance at Ilwaco in much of 2020 and 2021 resulted in data gaps during months when DO levels are typically low (Table 1). Dissolved oxygen concentrations below the 6 mg L⁻¹ threshold were most prevalent at Franz Lake Slough and Ilwaco.

	Ilwaco			Welch			Whites			Campbell			Franz		
	% of all data collected			% of all data collected			% of all data collected			% of all data collected			% of all data collected		
	<6 mg/l	<4 mg/l	<2 mg/l	<6 mg/l	<4 mg/l	<2 mg/l	<6 mg/l	<4 mg/l	<2 mg/l	<6 mg/l	<4 mg/l	<2 mg/l	<6 mg/l	<4 mg/l	<2 mg/l
4/1/2018	6.3	1.5	0.1	0.0	0.0	0.0	0.0	0.0	0.0	0.0	0.0	0.0	0.0	0.0	0.0
5/1/2018	43.3	31.7	17.1	0.3	0.0	0.0	0.0	0.0	0.0	15.6	5.1	2.2	3.2	0.9	0.0
6/1/2018	51.5	32.5	19.4	3.9	0.1	0.0	1.1	0.0	0.0	12.2	1.8	0.0	7.4	0.0	0.0
7/1/2018	33.6	20.5	11.6	10.9	1.1	0.0	4.4	0.4	0.0	3.9	0.1	0.0	32.3	12.1	0.4
8/1/2018	48.7	28.1	16.0	19.1	4.6	0.0	4.2	0.0	0.0	5.0	0.0	0.0	42.6	21.4	0.0
9/1/2018	44.7	29.5	16.0	17.4	3.1	0.0	1.6	0.0	0.0	0.4	0.0	0.0	44.1	6.7	0.0
4/1/2019	8.9	2.0	0.4	0.0	0.0	0.0	0.0	0.0	0.0	0.0	0.0	0.0	0.0	0.0	0.0
5/1/2019	40.1	23.9	10.8	0.3	0.0	0.0	0.0	0.0	0.0	0.0	0.0	0.0	0.1	0.0	0.0
6/1/2019	46.0	30.6	18.9	10.4	1.9	0.4	1.3	0.0	0.0	1.8	0.4	0.0	32.4	20.1	12.1
7/1/2019	44.1	26.2	14.3	9.9	1.5	0.4	3.5	0.0	0.0	9.9	1.5	0.0	44.2	13.7	0.0
8/1/2019	44.1	27.2	13.8	20.6	4.2	0.0	2.8	0.0	0.0	4.4	0.3	0.0	46.8	19.9	5.0
9/1/2019	45.3	24.2	13.3	26.5	7.7	0.4	#N/A	#N/A	#N/A	16.5	6.9	0.0	66.9	51.6	28.1
4/1/2020	#N/A	#N/A	#N/A	#N/A	#N/A	#N/A	0.1	0.0	0.0	2.4	0.0	0.0	#N/A	#N/A	#N/A
5/1/2020	#N/A	#N/A	#N/A	#N/A	#N/A	#N/A	0.0	0.0	0.0	0.4	0.0	0.0	#N/A	#N/A	#N/A
6/1/2020	#N/A	#N/A	#N/A	#N/A	#N/A	#N/A	#N/A	#N/A	#N/A	15.1	0.7	0.0	#N/A	#N/A	#N/A
7/1/2020	#N/A	#N/A	#N/A	#N/A	#N/A	#N/A	#N/A	#N/A	#N/A	0.0	0.0	0.0	#N/A	#N/A	#N/A
8/1/2020	38.8	23.4	11.5	20.4	2.3	0.0	2.0	0.0	0.0	5.9	0.0	0.0	42.4	4.6	0.0
9/1/2020	43.3	26.0	11.2	23.3	3.5	0.0	1.1	0.0	0.0	15.9	0.7	0.0	43.3	6.6	0.3
4/1/2021	15.6	3.8	0.6	0.0	0.0	0.0	0.0	0.0	0.0	10.7	2.8	0.0	0.0	0.0	0.0
5/1/2021	24.8	8.0	0.0	0.3	0.0	0.0	#N/A	#N/A	#N/A	5.1	0.1	0.0	4.7	0.5	0.0
6/1/2021	#N/A	#N/A	#N/A	6.8	0.0	0.0	2.1	0.0	0.0	13.2	3.4	0.0	17.5	6.5	0.1
7/1/2021	#N/A	#N/A	#N/A	10.6	0.7	0.0	3.4	0.0	0.0	4.6	0.1	0.0	37.4	13.9	0.8
8/1/2021	#N/A	#N/A	#N/A	17.2	3.0	0.0	0.9	0.0	0.0	2.6	0.0	0.0	45.8	17.1	0.1
9/1/2021	#N/A	#N/A	#N/A	16.6	4.2	0.2	#N/A	#N/A	#N/A	0.8	0.0	0.0	56.5	26.8	3.8

Table 17: Percentage of hourly dissolved oxygen concentration measurements determined from 2018 to 2021 at the EMP sites (Ilwaco, Welch Island, Whites Island, Campbell Slough, and Franz Lake Slough) falling below three thresholds relevant to juvenile salmonids in the Columbia River: < 6mg L⁻¹, <4 mg L⁻¹, or <2 mg L⁻¹

3.2.2.1 *Temperature Thresholds at Trends Sites*

Water temperature is an important variable and potential stressor to salmonid populations. Here, we present a time series showing the percentage of days within each month where temperatures corresponded to threshold exceedance of 19°C for five off-channel trends sites (Table 18). According to these criteria, high temperatures posed a potential problem for salmonids during July and August of all years where there are data. It is perhaps more useful to look at June temperature exceedance, since salmonids are typically present in June. With the exception of 2015, the only site where temperature exceedance in June is a persistent problem is Campbell Slough, where >80% of measurements were >19 °C for most years. The exceptions were 2017 and 2020 (Figure 29). Between 2015 and 2021, the percentage of June days where the 19°C threshold was exceeded at Campbell Slough ranged from 33% in 2017 and 2020 to 90% in 2015. Although the number of days with temperatures exceeding 19 °C did not quite reach the levels observed in 2015 (90%), 87% of days in 2021 had water temperatures as high or higher than 19 °C.

Temperatures exceeding 22 °C were observed at Campbell Slough and Franz Lake Slough during the 2009-2021 time series. Temperatures in July and/or August consistently exceeded 22 °C at Campbell Slough. Franz Lake Slough had high temperatures as well, but these were not as consistently high as those observed at Campbell. The only other site having a significant number of days experiencing temperatures exceeding 22 °C was Whites Island in 2015 and 2021.

As has been noted in previous reports, the temperature difference between the Columbia River mainstem and the off-channel EMP sites is larger at Campbell Slough and Franz Lake Slough than it is at Welch Island or Whites Island (Figure 29). As water levels recede, the difference can be on the order of 5 °C; this magnitude of difference was observed in both 2020 and 2021 in July and August at Campbell and Franz, with larger differences observed in 2021 compared to 2020. Negligible differences were observed between the mainstem and the two sites in Reach C (ie, Whites Island) and Reach B (ie, Welch Island). Since Ilwaco is strongly influenced by tidal exchange of marine waters, the temperature difference from the mainstem is strongly seasonal. Temperatures at Ilwaco are similar to or exceed the mainstem during the spring but are cooler than the mainstem during the summer months.

Table 18: Temperatures exceeding 19°C in the EMP sites from 2015-2021. Data show the percentage of each month that the daily average temperature exceeded 19°C. No calculation was performed if data collection was less than 7 days of a given month.

Date	Percentage of Days per Month > 19 deg C					Percentage of Days per Month > 22 deg C				
	Ihwaco	Welch	Whites	Campbell	Franz	Ihwaco	Welch	Whites	Campbell	Franz
Apr-2015	#N/A	#N/A	#N/A	#N/A	#N/A	#N/A	#N/A	#N/A	#N/A	#N/A
May-2015	#N/A	#N/A	#N/A	32	#N/A	#N/A	#N/A	#N/A	0	#N/A
Jun-2015	17	#N/A	100	90	100	0	#N/A	14	83	67
Jul-2015	74	#N/A	100	100	100	0	#N/A	77	100	77
Aug-2015	56	#N/A	100	100	100	0	#N/A	19	96	91
Sep-2015	#N/A	#N/A	#N/A	#N/A	#N/A	#N/A	#N/A	#N/A	#N/A	#N/A
Apr-2016	0	0	0	0	0	0	0	0	0	0
May-2016	0	0	0	19	0	0	0	0	0	0
Jun-2016	10	13	0	87	55	0	0	0	17	14
Jul-2016	55	100	87	100	97	0	0	0	77	48
Aug-2016	23	100	100	100	100	0	13	0	90	33
Sep-2016	#N/A	#N/A	#N/A	#N/A	#N/A	#N/A	#N/A	#N/A	#N/A	#N/A
Apr-2017	0	0	0	0	#N/A	0	0	0	0	#N/A
May-2017	0	0	0	0	0	0	0	0	0	0
Jun-2017	7	0	0	33	13	0	0	0	0	0
Jul-2017	42	87	94	100	93	0	0	6	94	93
Aug-2017	29	100	100	100	100	0	13	48	100	81
Sep-2017	0	82	90	100	78	0	0	15	69	28
Apr-2018	0	0	0	0	0	0	0	0	0	0
May-2018	0	0	0	0	0	0	0	0	0	0
Jun-2018	27	17	3	63	30	0	0	0	20	0
Jul-2018	68	97	100	100	100	0	6	10	97	77
Aug-2018	29	100	100	100	90	0	16	52	90	58
Sep-2018	0	46	57	95	42	0	0	0	47	0
Apr-2019	0	0	0	0	0	0	0	0	0	0
May-2019	3	0	0	16	0	0	0	0	0	0
Jun-2019	27	13	7	83	57	0	0	0	33	10
Jul-2019	71	90	97	100	100	3	10	13	97	81
Aug-2019	81	100	100	100	100	0	19	43	100	42
Sep-2019	18	90	#N/A	100	100	0	0	#N/A	77	53
Apr-2020	3	#N/A	0	0	#N/A	0	#N/A	0	0	#N/A
May-2020	6	#N/A	0	0	#N/A	3	#N/A	0	0	#N/A
Jun-2020	23	#N/A	#N/A	33	#N/A	3	#N/A	#N/A	0	#N/A
Jul-2020	#N/A	#N/A	#N/A	87	#N/A	#N/A	#N/A	#N/A	61	#N/A
Aug-2020	61	100	100	100	100	0	15	15	97	93
Sep-2020	0	#N/A	78	76	45	0	#N/A	0	28	25
Apr-2021	0	0	0	23	4	0	0	0	0	0
May-2021	#N/A	0	0	32	3	#N/A	0	0	0	0
Jun-2021	#N/A	37	37	87	63	#N/A	7	3	60	43
Jul-2021	#N/A	100	100	100	100	#N/A	19	26	100	100
Aug-2021	#N/A	97	100	100	94	#N/A	19	100	94	58
Sep-2021	#N/A	52	#N/A	90	70	#N/A	0	#N/A	55	5

Water Temp 2020 and 2021

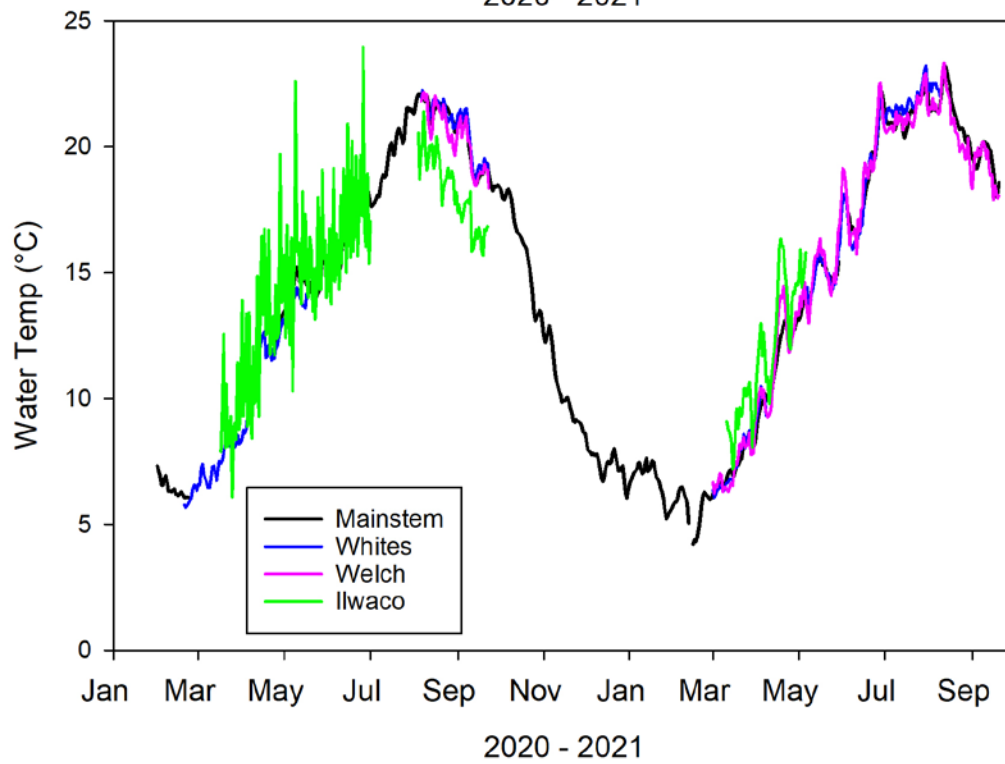
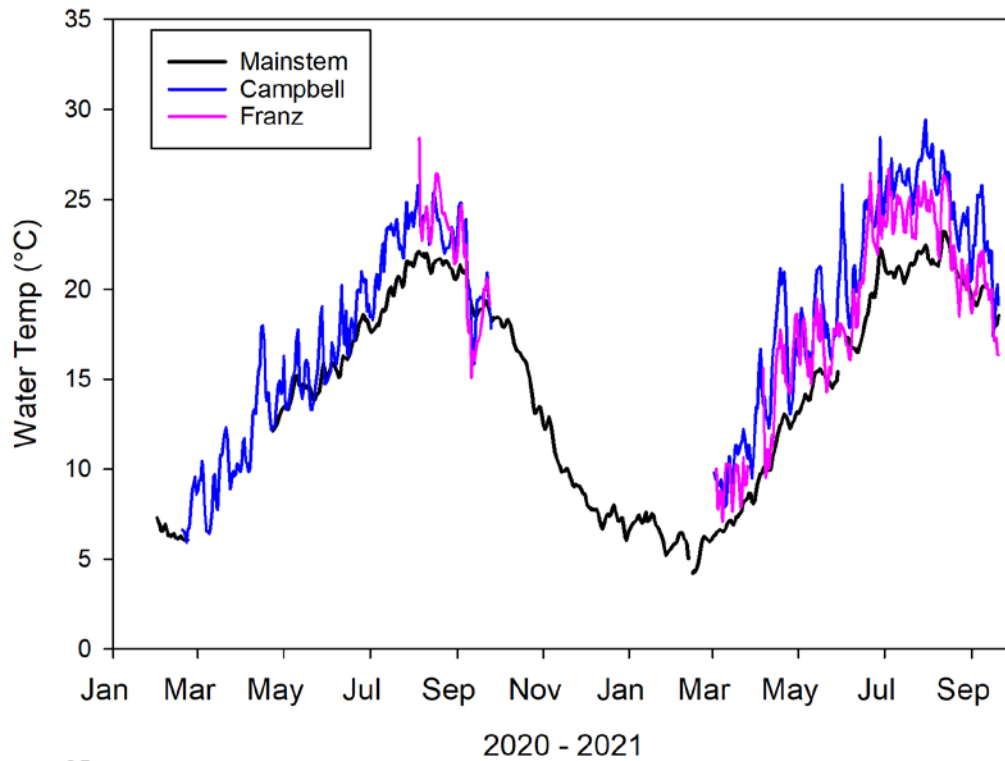


Figure 29. Water temperatures at EMP sites (Campbell Slough, Franz Lake Slough, Whites Island, Welch Island, and Ilwaco) shown alongside mainstem temperatures determined at the Port of Camas, WA.

3.2.3 Nutrients

3.2.3.1 *Dissolved Inorganic Nutrients (nitrate, phosphate)*

Dissolved inorganic nutrients data were collected but not analyzed this year; however, there will be additional analyses conducted for the FY23 report. Dissolved nitrate concentrations reach high levels in the Columbia in the winter. Observations from trends sites in 2019 began in March at the end of winter/early spring when nitrate was nearly 30 μM at three sites most influenced by the Willamette River, the Columbia's largest tributary (Whites Island, Campbell Slough, and Welch Island; Figure 30-Figure 32). Nitrate concentrations at Ilwaco Slough and at Franz Lake Slough were $\sim 20 \mu\text{M}$. Similar to 2018, nitrate concentrations were higher at all sites in March and April compared to May, June, and July. Interestingly, in 2019 we did not observe the decline in nitrate concentration between March and April that was observed in 2018 at both Campbell Slough and Franz Lake Slough, but instead captured a peak in concentrations in April prior to the period of drawdown that accompanies spring primary production. This was not observed at Ilwaco Slough, Welch Island, or Whites (Figure 30-Figure 32). Similar to 2018, there were smaller differences among the monthly observations of nitrate concentration at Ilwaco compared to the other sites due to tidal exchange with the coastal ocean. At the other sites, nitrate concentrations were lowest during the summer months, reaching minimum values in August, with the lowest values observed at Franz Lake Slough. The recommended benchmark for maximum total nitrogen concentration in waters of the Columbia is $<0.255 \text{ mg L}^{-1}$, or $18.2 \mu\text{M}$ according to the Department of Environmental Quality (DEQ; Oregon's National Rivers and Streams Assessment, 2008-2009), with levels exceeding 0.399 mg L^{-1} ($28.5 \mu\text{M}$) considered to be of poor quality. This level was exceeded during the spring at all sites except Ilwaco. The difference in nitrate concentration between the spring and the summer arises in part from dilution by the freshet and drawdown by primary producers. Thus, changes in the annual freshet volume influence the margin of safety for good water quality in waters of the lower Columbia.

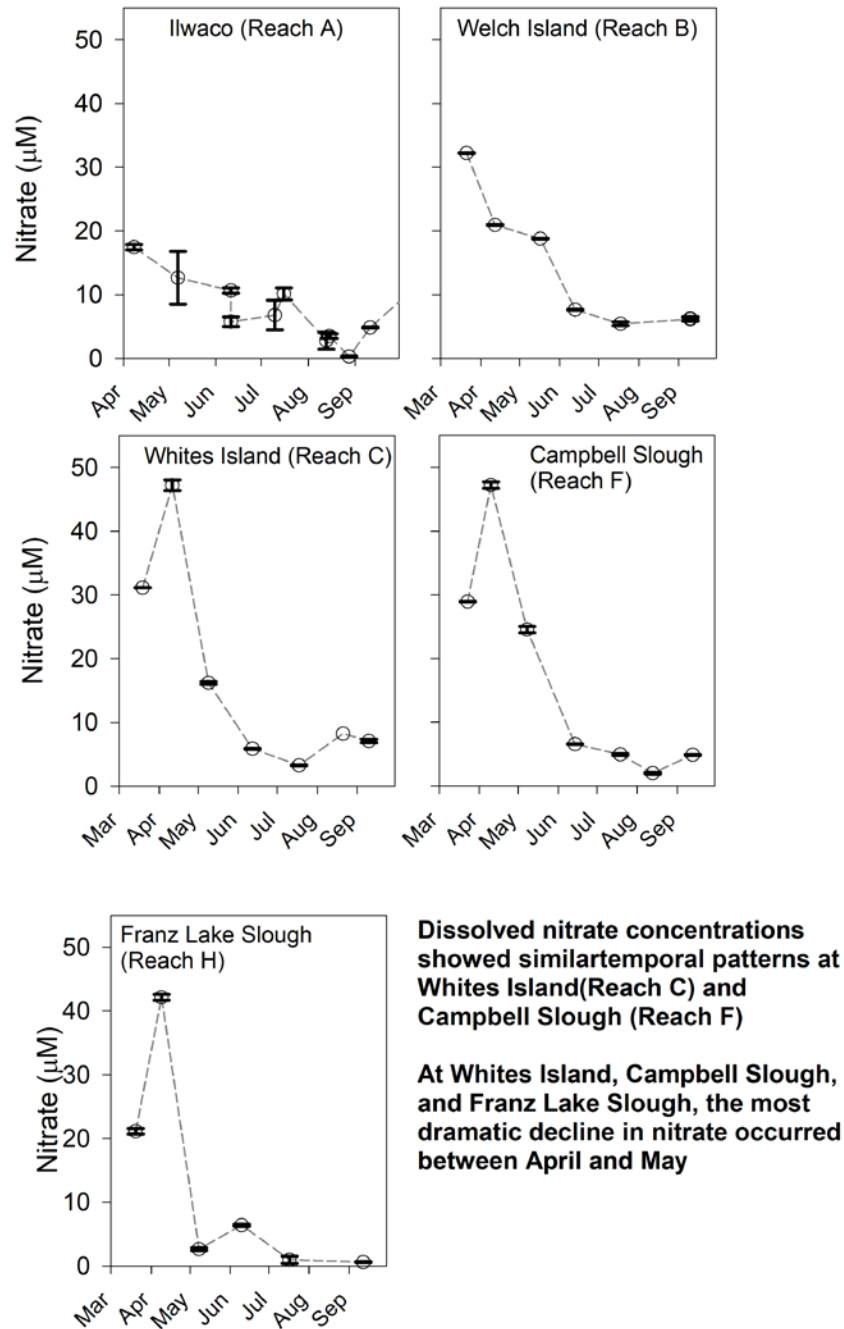


Figure 30. Time series are showing concentrations of dissolved nitrate at the five trends sites in 2019.

Dissolved phosphorus (determined as soluble reactive phosphorus, or ortho-phosphate) were lowest in late June after the freshet subsided (Figure 31-Figure 32), but were otherwise similar before and after than at Welch Island and Whites Island. Phosphate concentrations were more variable at Ilwaco Slough, with higher levels observed during the summer compared to the spring. In contrast, very high phosphate concentrations were observed during the summer in both Campbell Slough and Franz Lake Slough (Figure 30-Figure 32). The DEQ benchmark for total phosphorus is $<0.044 \text{ mg L}^{-1}$ ($1.42 \text{ }\mu\text{M}$) for good water quality and $>0.069 \text{ mg L}^{-1}$ ($2.23 \text{ }\mu\text{M}$) indicating poor water quality. Summer concentrations of phosphate at Campbell Slough and Franz Lake Slough exceeded this level by two-fold.

Ammonium concentrations tend to increase as a result of microbial activity. The highest concentrations were observed at Ilwaco, particularly during the summer (Figure 32). At the other sites, ammonium concentrations tended to decrease in concert with the spring freshet, likely due to dilution and slower microbial growth.

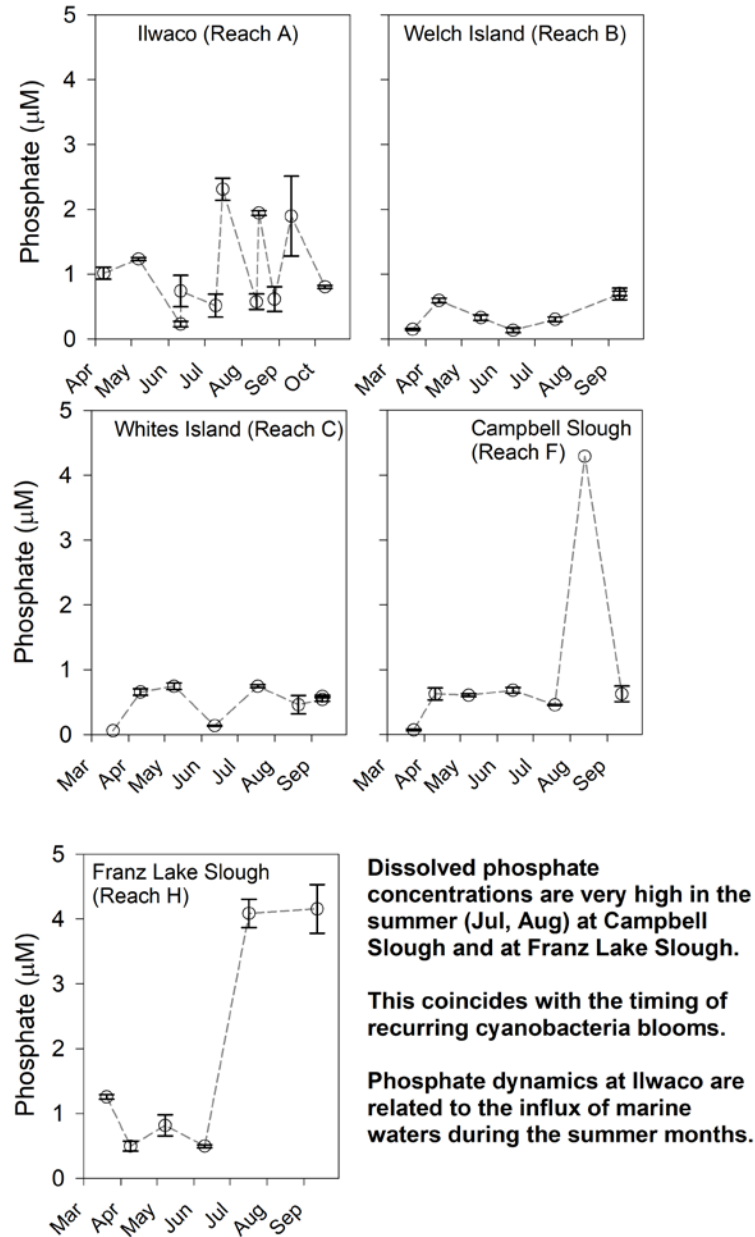


Figure 31. Time series showing concentrations of dissolved phosphate (ortho-phosphate) at the five trends sites in 2019.

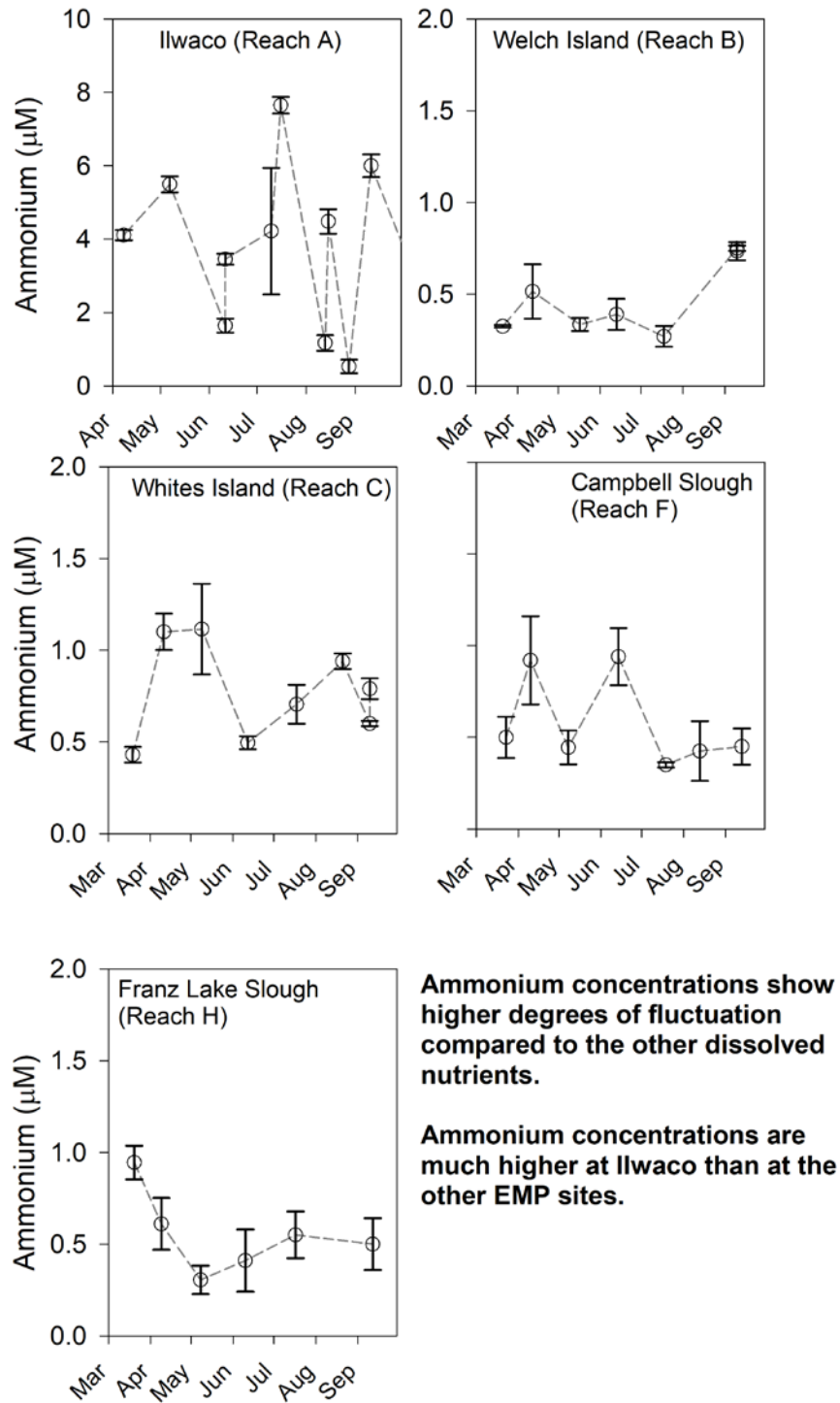


Figure 32. Time series showing concentrations of dissolved ammonium at the five trends sites in 2019.

3.3 Habitat Structure

3.3.1 Hydrology

Hydrologic patterns vary from year to year at all but the most tidal sites. Ilwaco is tidally dominated, while this tidal influence is reduced and traded for greater fluvial influences as you move upriver towards Franz Lake. Hydrographs from all the years in which water surface elevation (WSE) was sampled at the trends sites, including the 2021 water year, are provided in Appendix C. Some data loss occurred during the first half of 2019 at Welch Island and between February and August 2020 at Cunningham Lake. Additionally, due to a sensor failure at Campbell Slough, 2021 data is not yet available. The following observations were made for these sites:

- The WSE at the Ilwaco Slough (rkm 6) is very minimally affected by the spring freshet but is elevated by winter storm events and extreme high tides. Low-water elevation measurements are truncated at the site because the elevation of the tidal channel is above that of extreme low water. The average tidal range across all monitoring years for this site varies between 1.4 m and 1.5 m annually (Table 19). In 2021, the surveyed the wetland plant community range was 1.64 m (Table 20).
- Both Welch Island (rkm 53) and Steamboat (rkm 57) site hydrologies are predominantly tidally driven. Annual maximum WSE in 2021 at this site were observed in January, which coincides with king tide elevations for winter 2021. The average tidal range at this site across all monitoring years is between 2.1 m and 2.2 m (Table 19). Slightly elevated WSE were detectable during the prolonged spring freshet in 2012, 2014, 2017, and 2018. Winter storms also drive higher water levels at this site, particularly elevating the low tide levels. The surveyed wetland plant community range was 0.94 m in 2021 at Welch Island (Table 20).
- The hydrology of Whites Island (rkm 72) is influenced by tidal action as well as periods of prolonged freshets. Annual maximum WSE measurements for 2021 were observed in January with smaller peaks occurring in May and June. These elevations coincide with king tide duration for that month, as well as peak flow durations of the Columbia in 2021. The average tidal range varies between 1.7-1.6 m (Table 19) across monitoring years and the surveyed wetland plant community range was 1.43 m in 2021 (Table 20).
- The Cunningham Lake site (rkm 145) and Campbell Slough site (rkm149), have similar hydrologic patterns. Annual tidal ranges between 2009 and 2021 vary between 0.4 m to 0.6 m at Cunningham Lake, and between 0.3m and 0.4m at Campbell slough. Note that 2021 data for Campbell Slough is not yet available and there is limited data available for Cunningham Slough. This indicates minimal influence of tides at these sites. Historic data indicate that Cunningham Lake has a slightly greater tidal range and slightly lower WSE during flood events compared to Campbell Slough. In most years, the primary hydrologic driver at both sites is the spring freshet, although from 2013 to 2021, winter storms also increased the WSE at these sites. The freshet caused greater flooding at Campbell Slough in both 2020 and 2021 (Table 19). Similar influences were not observed in 2019. The sensor at Cunningham Lake is in the very upper reach of the channel and is therefore elevated above the lowest water levels. The Campbell Slough sensor is in a deeper channel, however, a weir located at the mouth of the slough limits drainage. The topographic range of the wetland monitoring at these sites is slightly different, with Cunningham Lake wetland being more of a shallow gradient the elevation ranging only 1.83 meters on average

from 2019-2021, while the Campbell Slough wetland has a steeper gradient the elevation ranging 2.12 meters on average from 2019-2021 (Table 20). Shallow vs. steep wetland topography can significantly alter the hydrology and plant communities observed between the sites.

- The Franz Lake site (rkm 221) has the smallest tidal signal (in between 0.2-0.3 m, Table 19 and Appendix C) which is difficult to distinguish from diurnal variation from dam operations (Jay et al. 2015). The beaver dam that has been present in most years just below our sample area was gone in 2016 and 2021, resulting in lower water levels in the channel. The beaver dam was present and established during 2017, 2018, 2019, and 2020 elevating the water level in the sampling area above that of the tidal exchange signal in the dry months of August and September (Table 27, Appendix C). In most years, the winter and spring high WSE are both discernable. However, the spring levels are usually considerably higher than those in winter. The elevation range of the wetland at Franz Lake is 1.58 meters on average, and not well predicted by tidal signal (Table 20).

Table 19. Water surface elevation (WSE) metrics calculated at each site for the sensor deployment period from 2016-2021. Campbell Slough from August 2020 through August 2021 data is currently unavailable. All metrics are in meters, relative to the North American Vertical Datum of 1988 (NAVD 88). MWL = mean water level; MLLW = mean lower low water; MHHW = mean higher high water. Full hydrographs and annual summaries for each year are in Appendix C.

2021	Rkm	MWL	MLLW	MHHW	Avg Tidal Range (m)	Maximum WSE	Date of Maximum WSE	Period of Record	Days
Ilwaco	6	1.5	1.0	2.4	1.4	3.5	Jan 12	Jan-Jul	207
Welch	53	1.7	0.7	2.8	2.2	3.8	Jan 12	Jan-Jul	203
Steamboat	57	1.6	0.7	2.6	2.0	3.7	Jan 12	Jan-Jul	204
Whites	72	1.9	1.1	2.9	1.7	3.9	Jan 12	Jan-Dec	202
Cunningham	145	2.8	2.8	3.1	0.2	4.8	Jan 14	Jan-May	146
Campbell	149	NA	NA	NA	NA	NA	NA	NA	0
Franz	221	4.8	4.7	4.9	0.2	6.9	Jan 14	Jan-Aug	217
2020	Rkm	MWL	MLLW	MHHW	Avg Tidal Range (m)	Maximum WSE	Date of Maximum WSE	Period of Record	Days
Ilwaco	6	1.6	1.1	2.5	1.4	3.4	Nov 17	Jan-Dec	366
Welch	53	1.7	0.7	2.8	2.1	3.8	Nov 17	Jan-Dec	366
Steamboat	57	1.6	0.7	2.7	2.0	3.6	Nov 17	Jan-Dec	366
Whites	72	1.9	1.1	2.8	1.7	3.8	Nov 17	Jan-Jul	366
Cunningham	145	2.9	2.9	3.3	0.3	1.2	Feb 8	Jan-Feb; Aug-Dec	184
Campbell	149	3.1	3.0	3.4	0.4	4.7	Jun 3	Jan-Aug	233
Franz	221	5.0	4.9	5.1	0.2	7.9	Jun 3	Jan-Dec	366
2019	Rkm	MWL	MLLW	MHHW	Avg Tidal Range (m)	Maximum WSE	Date of Maximum WSE	Period of Record	Days
Ilwaco	6	NA	NA	NA	NA	NA	NA	NA	NA
Welch	53	1.7	0.6	2.8	2.1	3.3	Dec 12	Sept-Dec	113

Whites	72	1.8	1.1	2.8	1.7	3.7	Jan 20	Jan-Dec	365
Cunningham	145	2.8	2.6	3.1	0.5	5.4	Apr 12	Jan-Aug	223
Campbell	149	2.9	2.7	3.2	0.4	5.6	Apr 12	Jan-Aug	225
Franz	221	5.5	5.4	5.6	0.3	10.3	Apr 11	Jan-Dec	341
2018	Rkm	MWL	MLLW	MHHW	Avg Tidal Range (m)	Maximum WSE	Date of Maximum WSE	Period of Record	Days
Ilwaco	6	1.5	1.0	2.4	1.4	3.1	Mar 02	Jan-Nov	311
Welch	53	1.9	0.9	3.0	2.1	4.0	Jan 30	Jan-Feb, May-July	149
Whites	72	2.2	1.4	3.4	1.7	4.1	May 17	Jan-Dec	365
Cunningham	145	3.3	3.0	3.5	0.5	7.0	May 17	Jan-Dec	365
Campbell	149	3.1	3.0	3.4	0.4	5.9	May 17	Jan-Dec	365
Franz	221	5.6	5.5	5.8	0.3	8.9	May 19	Jan-Jul	218
2017	Rkm	MWL	MLLW	MHHW	Avg Tidal Range (m)	Maximum WSE	Date of Maximum WSE	Period of Record	Days
Ilwaco	6	1.5	1.0	2.4	1.5	3.3	Feb 09	Jan-Feb, Aug-Dec	216
Welch	53	2.0	0.9	3.0	2.1	3.9	Feb 09	Jan-Dec	365
Whites	72	2.2	1.5	3.1	1.6	4.0	Dec 03	Jan-Dec	365
Cunningham	145	2.7	2.4	3.0	0.6	4.2	Dec 30	Jan, Aug-Dec	193
Campbell	149	3.6	3.4	3.8	0.4	6.3	Mar 30	Jan-Dec	365
Franz	221	5.2	5.1	5.3	0.2	8.2	Mar 25	Jan-Dec	365
2016	Rkm	MWL	MLLW	MHHW	Avg Tidal Range (m)	Maximum WSE	Date of Maximum WSE	Period of Record	Days
Ilwaco	6	1.4	0.9	2.4	1.5	3.2	Oct 15	Aug-Dec	147
Welch	53	1.7	0.6	2.8	2.2	3.9	Jan 02	Jan-Dec	366
Whites	72	1.9	1.1	2.8	1.7	4.7	May 10	Aug-Dec	153
Cunningham	145	2.7	2.5	2.9	0.4	3.6	Nov 26	Aug-Dec	152
Campbell	149	3.0	2.8	3.2	0.4	4.5	Mar 12	Jan-Dec	362
Franz	221	3.8	3.7	3.9	0.2	4.6	Dec 23	Aug-Dec	152

Table 20. Site marsh elevation range in meters based on the vegetation plot elevation (with $\geq 5\%$ absolute living plant cover), relative to the North American Vertical Datum of 1988 (NAVD88). Mean number of plots, mean elevation, standard deviation (SD), minimum elevation (Min), and maximum elevation (Max). Marsh elevation ranges for all years can be found in Appendix D. Note that the 2021 data for Cunningham Lake was unavailable at the time of analysis; we utilized 2020 survey in place of the 2021 survey.

Longterm Elevation, m, NAVD88		Mean (SD)	2021	2020	2019
Ilwaco Slough	Plots (n)	40 (0)	40	40	40
	Mean	1.96 (0.05)	2.03	1.95	1.91
	SD	0.22 (0.04)	0.26	0.16	0.23
	Min	1.1 (0.32)	0.81	1.55	0.94
	Max	2.36 (0.07)	2.45	2.31	2.31
	Range	1.26 (0.37)	1.64	0.76	1.38
Welch Island	Plots (n)	41 (0)	41	41	41
	Mean	2.07 (0.01)	2.09	2.06	2.06
	SD	0.16 (0)	0.16	0.16	0.16
	Min	1.34 (0)	1.34	1.34	1.34
	Max	2.24 (0.03)	2.28	2.25	2.20
	Range	0.9 (0.03)	0.94	0.91	0.86
Whites Island	Plots (n)	43 (0.82)	44	43	42
	Mean	2.13 (0.03)	2.14	2.16	2.08
	SD	0.4 (0.01)	0.41	0.40	0.38
	Min	1.26 (0.07)	1.21	1.36	1.20
	Max	2.61 (0.06)	2.64	2.66	2.53
	Range	1.35 (0.06)	1.43	1.30	1.33
Cunningham Lake	Plots (n)	68.67 (0.47)	69	69	68
	Mean	2.73 (0.03)	2.71	2.71	2.78
	SD	0.3 (0.08)	0.35	0.35	0.19
	Min	2.33 (0.06)	2.29	2.29	2.41
	Max	4.17 (0.81)	4.74	4.74	3.02
	Range	1.83 (0.87)	2.45	2.45	0.60
Campbell Slough	Plots (n)	78 (24.06)	112	62	60
	Mean	2.63 (0.44)	2.01	2.92	2.95
	SD	0.61 (0.36)	1.12	0.38	0.32
	Min	1.78 (0.94)	0.45	2.38	2.51
	Max	3.91 (0.11)	4.02	3.94	3.76
	Range	2.12 (1.02)	3.56	1.56	1.25
Franz Lake	Plots (n)	69 (6.68)	71	76	60
	Mean	4.5 (0.1)	4.37	4.53	4.60
	SD	0.36 (0.1)	0.47	0.38	0.23
	Min	3.54 (0.29)	3.32	3.36	3.95
	Max	5.12 (0.13)	5.30	5.05	5.01
	Range	1.58 (0.39)	1.98	1.70	1.06

Inter-annual variation in inundation patterns is much greater at the upper estuary sites (Table 19, Figure 33-Figure 38), where seasonal flooding can result in months of continuous inundation during high-water years. In contrast, at the lower estuary sites dominated by tidal patterns, inundation lasts just a few hours

during high tide, but occurs frequently, usually one to two times daily. Inundation, as measured as a percent of time that the water surface level exceeds the ground surface is a means of comparing sites to each other and over time. The inundation at each site is dependent on the elevation, the position along the tidal and riverine gradient, and the seasonal and annual hydrologic conditions. The average % of inundation per each elevation for the month of August shown in Figure 33-Figure 38. The month of August was chosen because it is a critical time for plant development in the upper river sites, as the freshet draws down and exposes the marsh surface. Additionally, we have the most consistent amount of data for the month of August all sites and all years monitored. Generally, the trends in % time inundated identified in August correlate well with average % daily inundation for the year (unpublished data). Note that August 2021 has limited data available in this report.

The lower river sites, Ilwaco Slough, Welch Island, and Whites Island, showed similar and consistent trends of daily flooding during the month of August (Figure 33-Figure 35). The hydrology of these sites are more tidally driven than the mid and upper river sites, especially in the summer after the high winter and spring flows have dissipated, generally showing less annual variability in their hydrology and plant community compositions than the mid and upper river sites (Figure 33-Figure 38).

Ilwaco Slough

Percent Inundation in August vs. Marsh Elevation

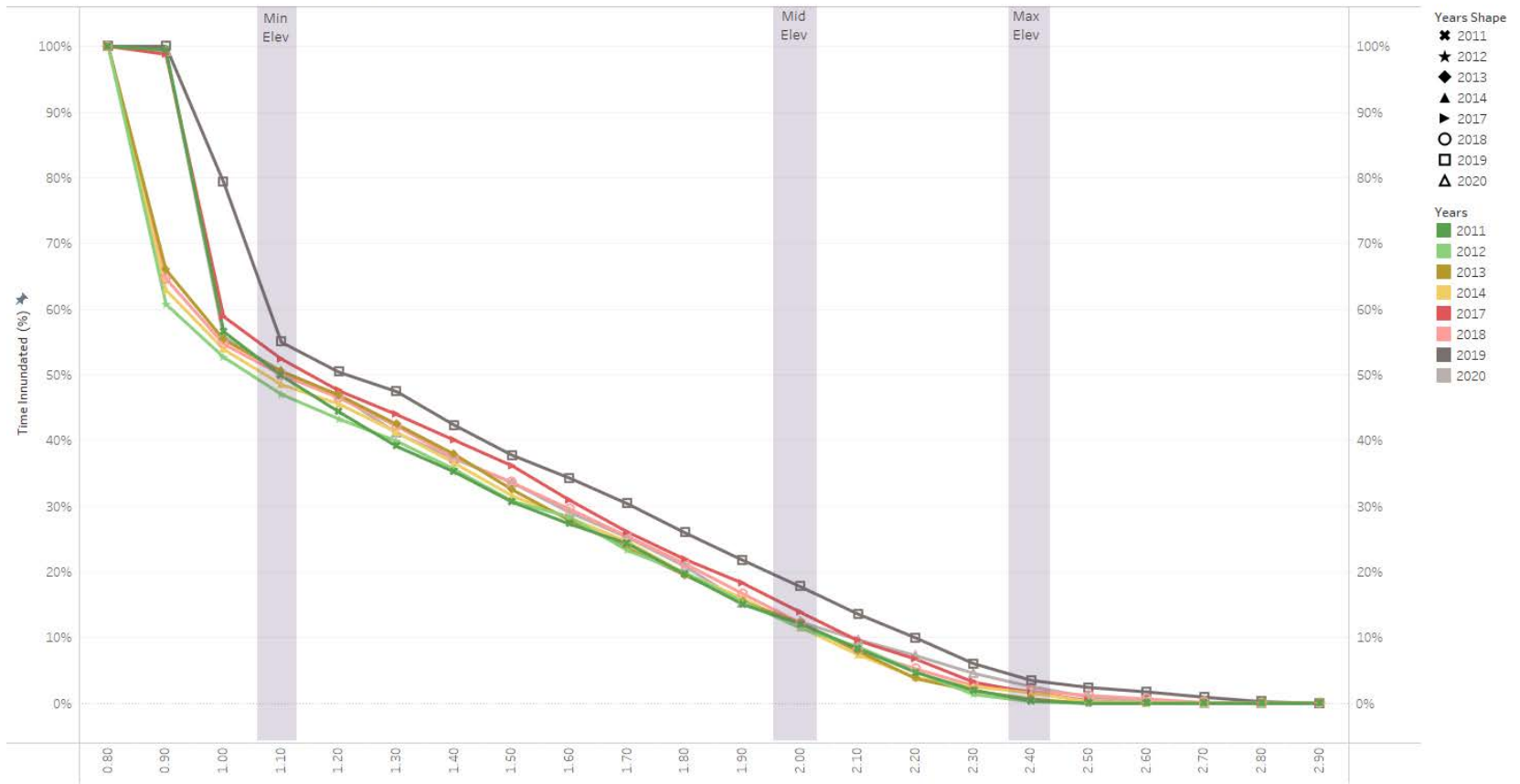


Figure 33: Ilwaco Slough: Percent time inundation for the month of August along the marsh elevation gradient between 2011-2021. Min Elevation = 1.1, mean elevation = 2.0, Max elevation = 2.4.

Welch Island

Percent Inundation in August vs. Marsh Elevation

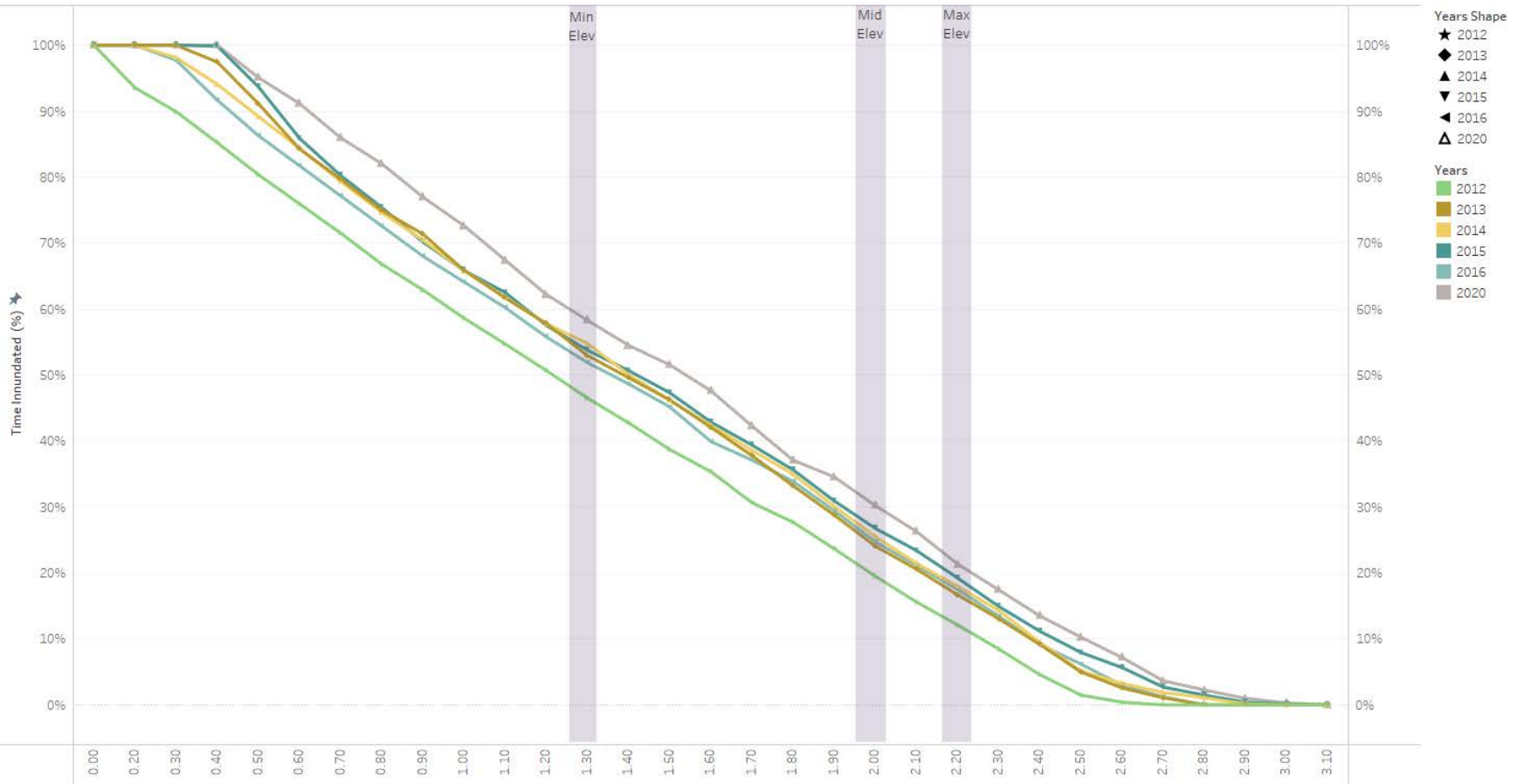


Figure 34: Welch Island: Percent time inundation for the month of August along the marsh elevation gradient between 2013-2021. Min = 1.3, Mean = 2.0, Max = 2.2

Whites Island

Percent Inundation in August vs. Marsh Elevation

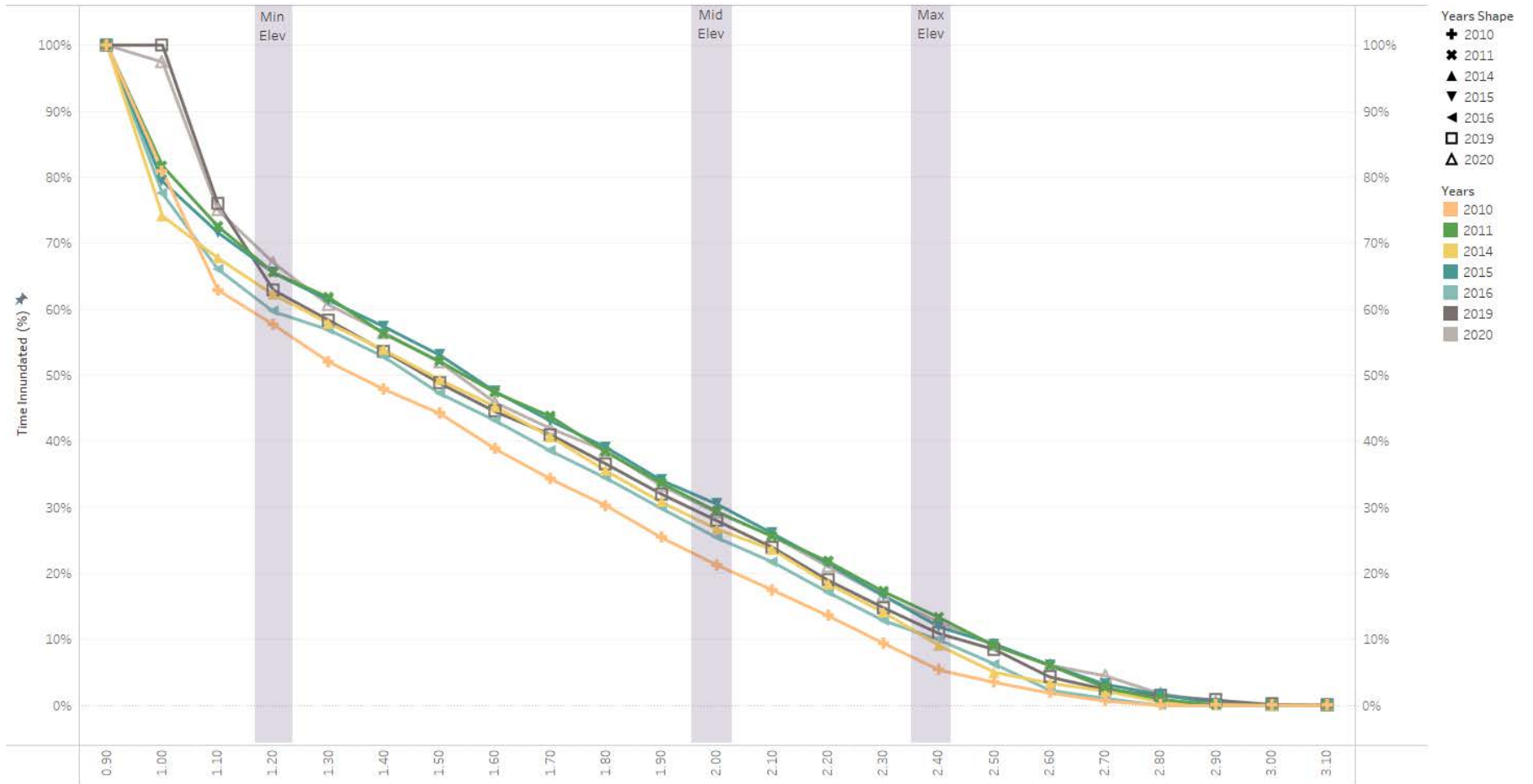


Figure 35: Whites Island: Percent time inundation for the month of August along the marsh elevation gradient between 2009-2021. Min = 1.2, Mean = 2.0, Max = 2.4

Consistently, for all years monitored, Cunningham Slough experiences greater levels of flooding than Campbell Slough (Figure 35, Figure 36). Cunningham Lake hydrology appears to be slightly more sensitive to shifts in the Columbia River discharge than Campbell Slough, likely due to differences in their connectivity and proximity to the mainstem (Figure 1).

Cunningham Lake

Percent Inundation in August vs. Marsh Elevation

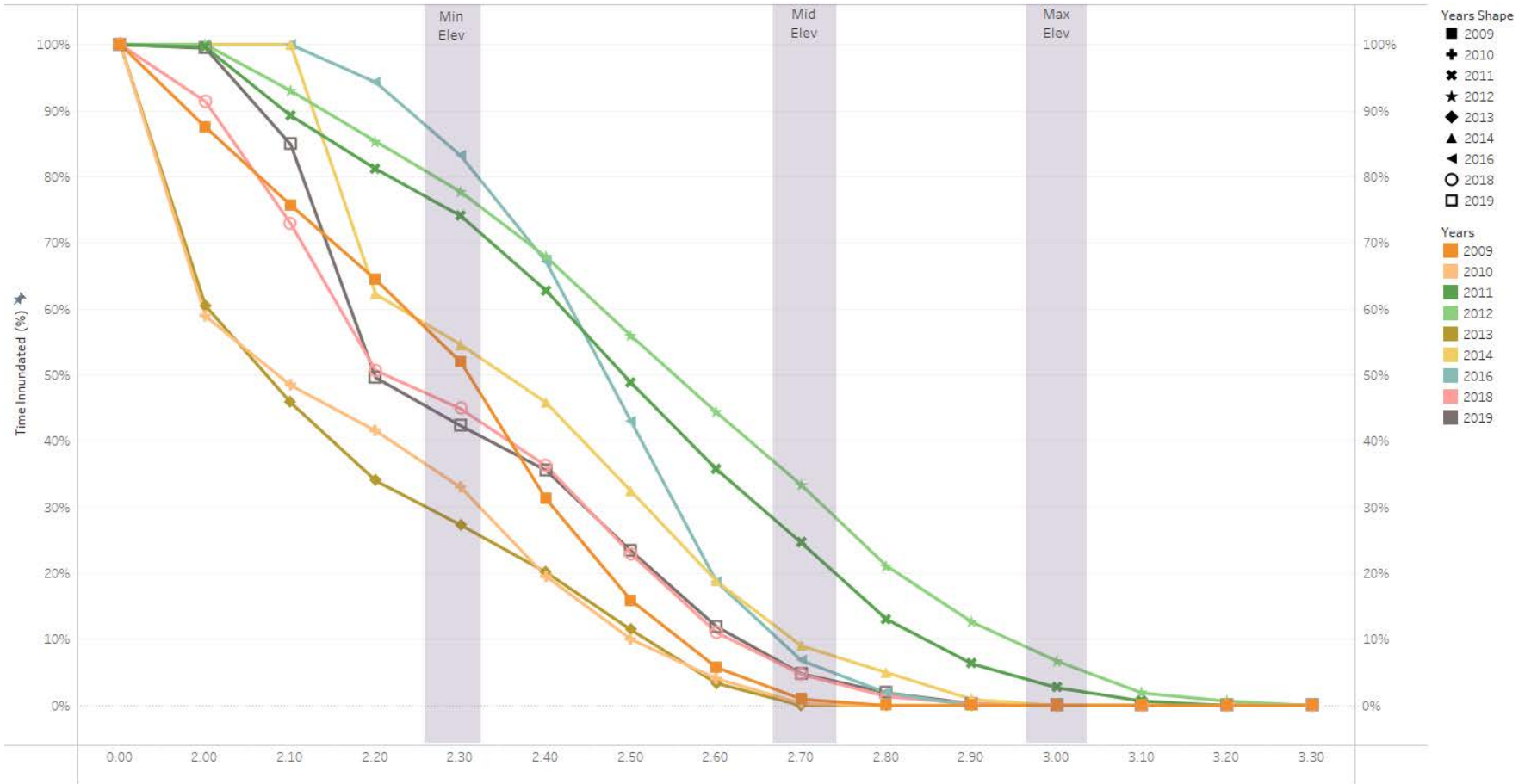


Figure 36: Cunningham Lake: Percent time inundation for the month of August along the marsh elevation gradient between 2009-2021. Min = 2.3, Mean = 2.7, Max = 3.0

Campbell Slough
Percent Inundation in August vs. Marsh Elevation

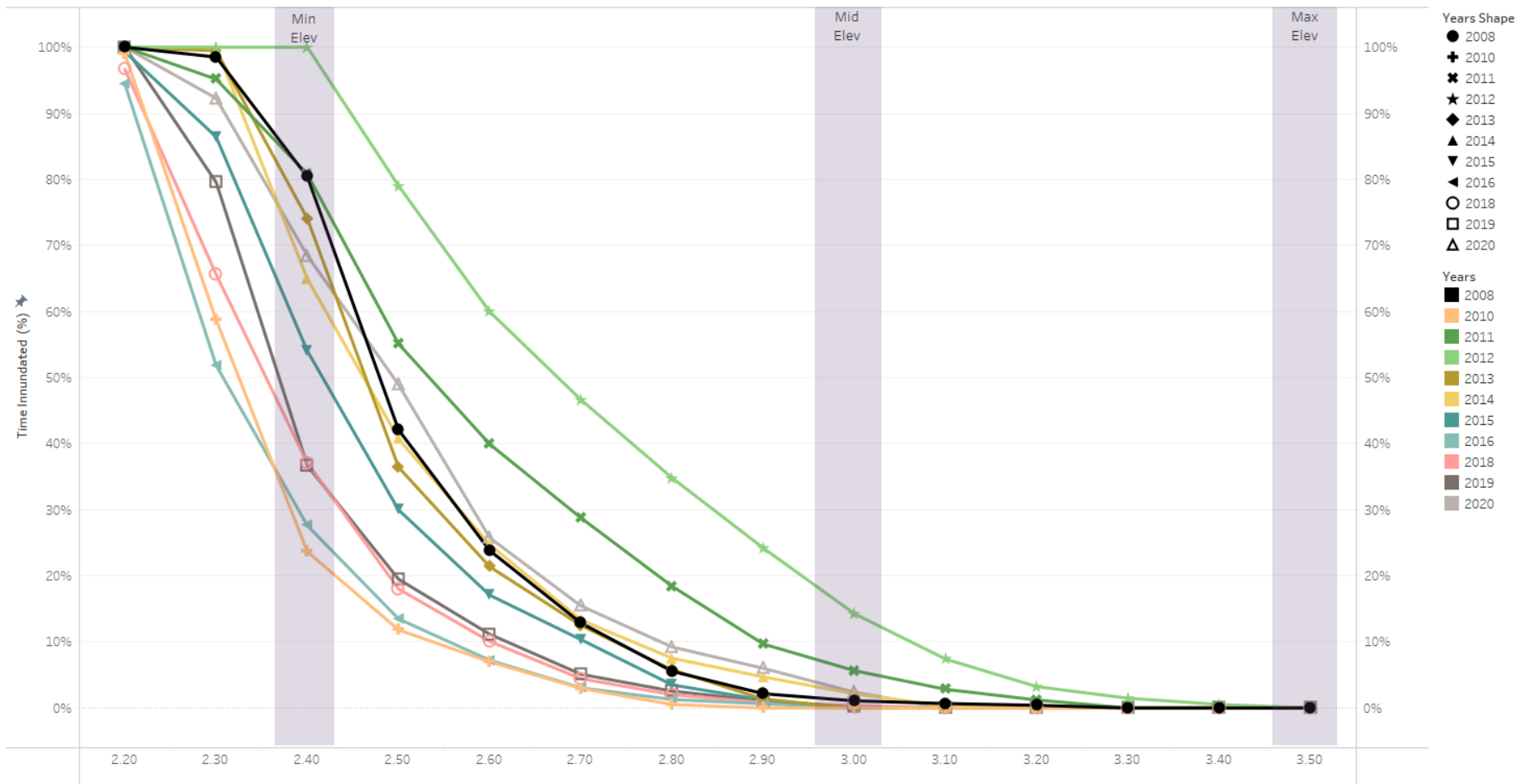


Figure 37: Campbell Slough: Percent time inundation for the month of August along the marsh elevation gradient between 2008-2021. Min = 2.4, Mean = 3.0, Max = 4.0

Significant flooding during August for the upper river (Franz Lake) and mid-river sites (Cunningham and Campbell) indicates flooding for a majority of the growing season, freshet levels being elevated for a longer duration than normal. Extended periods of flooding during the peak of the growing season can significantly alter wetland plant community compositions. For example, Franz Lake transitioned from being a *Phalaris arundinacea* dominated to a *Polygonum amphibium* dominant wetland following the 2011 and 2012 growing seasons, these years exhibiting extremely high and extended Columbia River discharge levels compared to previous and following years (Figure 38, Table 28). Franz Lake has begun to see an increase in the ratio of *P. arundinacea* to *P. amphibium* in the recent, dryer years.

Franz Lake

Percent Innundation in August vs. Marsh Elevation

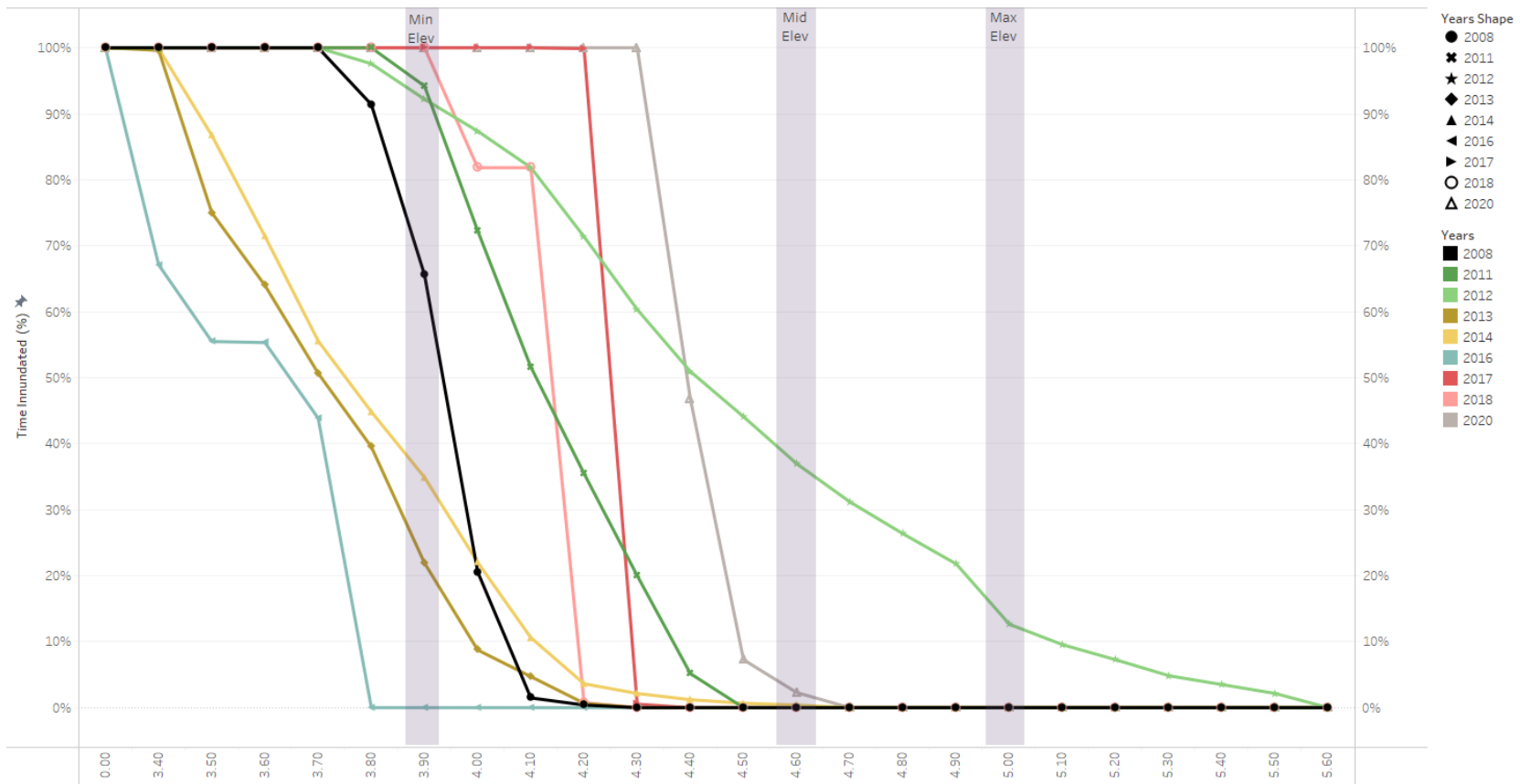


Figure 38: Franz Lake: Percent time inundation for the month of August along the marsh elevation gradient between 2008, 2012-2021. Min = 3.9, Mean = 4.6, Max = 5.0

3.3.2 Sediment Accretion Rates

In 2021, average sediment accretion or erosion rates at the five trend sites ranged from -6.7 to 6.0 cm per year. Note that Campbell Slough and Cunningham Lake both have large bovine populations, causing largely increased erosion and variability year to year. Of sites without cattle grazing, Franz Lake high marsh stakes had the highest rate of average erosion, with greatest variability (FLM-2: -0.47 ± 1.32 cm), which has been a consistent trend since installation of these stakes in 2015. Campbell slough showed large rates of erosion, likely (

Site Code:	BBM-1	BBM-2	WI2-1	WI2-2	WHC-1	WHC-2	CLM-1	CLM-2	CS1-1	CS1-2	CS1-3	FLM-1	FLM-2
Elevation (m, NAVD88)	2.61	2.49	2.83	2.71	3.09	2.46	3.53	3.25	3.71	4.08	4.081	5.28	5.71
Dominant Species	CALY	LIOC	CAOB	CALY	TYLA	CALY	PHAR/SALA	Mud	ELPA	PHAR	SALA	POAM	PHAR
2008-2009	ND	ND	ND	ND	-1.2	ND	ND	ND	ND	ND	ND		ND
2009-2010	ND	ND	ND	ND	1	ND	1.9	ND	0.4	ND	ND	ND	ND
2010-2011	1.7	ND	ND	ND	0.1	ND	1.6	ND	1.7	ND	ND	3	ND
2011-2012	0.1	ND	ND	ND	0.9	ND	1.4	ND	0.9	ND	ND	-0.2	ND
2012-2013	0.6	ND	0.8	ND	0.2	1.2	1.3	ND	0.2	ND	ND	3	ND
2013-2014	0.4	ND	0.6	ND	0.8	2.3	0.5	ND	1.5	ND	ND	0.7	ND
2014-2015	1	ND	0.7	ND	0	2.7	-0.5	ND	-2.4	ND	ND	1.2	ND
2015-2016	0	0.3	ND	1.0	ND	2.6	0.9	2.9**	1.4	0.8	ND	-0.6	-2.3
2016-2017	0.4	-2.5	0.6	1.8	0.4	3.7	0.1	ND	-4.2	-0.6	ND	0.6	-2.1
2017-2018	0.9	1.1	-2.5	4.0	2.1	2.4	1.5	ND	2.2	0.6	ND	3.3	1.4
2018-2019	-0.3	-0.5	1.7	-3.0	-0.3	1.3	-1.1	ND	-3.2	-1.2	ND	0.4	0.2
2019-2020	0.33	-0.16	1.8	-3	-1.36	-1.1	-0.3*	ND	3.9*	-0.4*	-9.2*	0.4	0.2
2020-2021	1.05	-0.22	.6	-0.16	0.62	1.6	-1.03*	-4.6*	6.0*	-6.7*	1.0*	.49	-0.2
Average	0.56	-0.33	0.54	0.11	0.27	1.86	0.52	-0.85	-0.24	-0.17	-4.1	1.12	-0.47
Std Dev	4.54	1.1	1.24	2.52	0.91	1.28	1.01	NA	2.73	0.69	NA	1.29	1.32

Table 21) this is attributed to cattle grazing and repeated trampling of the site. Sedimentation stakes installed in Whites Island low marsh displayed the maximum accretion rate (1.86 ± 1.28 cm). It should be noted that accretion and erosion rates in the longterm dataset are accompanied by high degree of variability, as shown in Figure 39.

Site Code:	BBM-1	BBM-2	WI2-1	WI2-2	WHC-1	WHC-2	CLM-1	CLM-2	CS1-1	CS1-2	CS1-3	FLM-1	FLM-2
Elevation (m, NAVD88)	2.61	2.49	2.83	2.71	3.09	2.46	3.53	3.25	3.71	4.08	4.081	5.28	5.71
Dominant Species	CALY	LIOC	CAOB	CALY	TYLA	CALY	PHAR/ SALA	Mud	ELPA	PHAR	SALA	POAM	PHAR
2008-2009	ND	ND	ND	ND	-1.2	ND	ND	ND	ND	ND	ND		ND
2009-2010	ND	ND	ND	ND	1	ND	1.9	ND	0.4	ND	ND	ND	ND
2010-2011	1.7	ND	ND	ND	0.1	ND	1.6	ND	1.7	ND	ND	3	ND
2011-2012	0.1	ND	ND	ND	0.9	ND	1.4	ND	0.9	ND	ND	-0.2	ND
2012-2013	0.6	ND	0.8	ND	0.2	1.2	1.3	ND	0.2	ND	ND	3	ND
2013-2014	0.4	ND	0.6	ND	0.8	2.3	0.5	ND	1.5	ND	ND	0.7	ND
2014-2015	1	ND	0.7	ND	0	2.7	-0.5	ND	-2.4	ND	ND	1.2	ND
2015-2016	0	0.3	ND	1.0	ND	2.6	0.9	2.9**	1.4	0.8	ND	-0.6	-2.3
2016-2017	0.4	-2.5	0.6	1.8	0.4	3.7	0.1	ND	-4.2	-0.6	ND	0.6	-2.1
2017-2018	0.9	1.1	-2.5	4.0	2.1	2.4	1.5	ND	2.2	0.6	ND	3.3	1.4
2018-2019	-0.3	-0.5	1.7	-3.0	-0.3	1.3	-1.1	ND	-3.2	-1.2	ND	0.4	0.2
2019-2020	0.33	-0.16	1.8	-3	-1.36	-1.1	-0.3*	ND	3.9*	-0.4*	-9.2*	0.4	0.2
2020-2021	1.05	-0.22	.6	-0.16	0.62	1.6	-1.03*	-4.6*	6.0*	-6.7*	1.0*	.49	-0.2
Average	0.56	-0.33	0.54	0.11	0.27	1.86	0.52	-0.85	-0.24	-0.17	-4.1	1.12	-0.47
Std Dev	4.54	1.1	1.24	2.52	0.91	1.28	1.01	NA	2.73	0.69	NA	1.29	1.32

Table 21. Sediment accretion rates at the trends sites between 2008 and 2021. Note that CS1-1 was decommissioned during Summer 2021 and a new stake was deployed nearby. Additionally, CLM-2 was lost in 2017 and redeployed in 2019.

ND No data.

* Large bovine presence.

** CLM-2 old stake; lost and redeployed.

Combined EMP Sed Bench Accretion Rates across low/high marsh plots
 Based on annual accretion rates

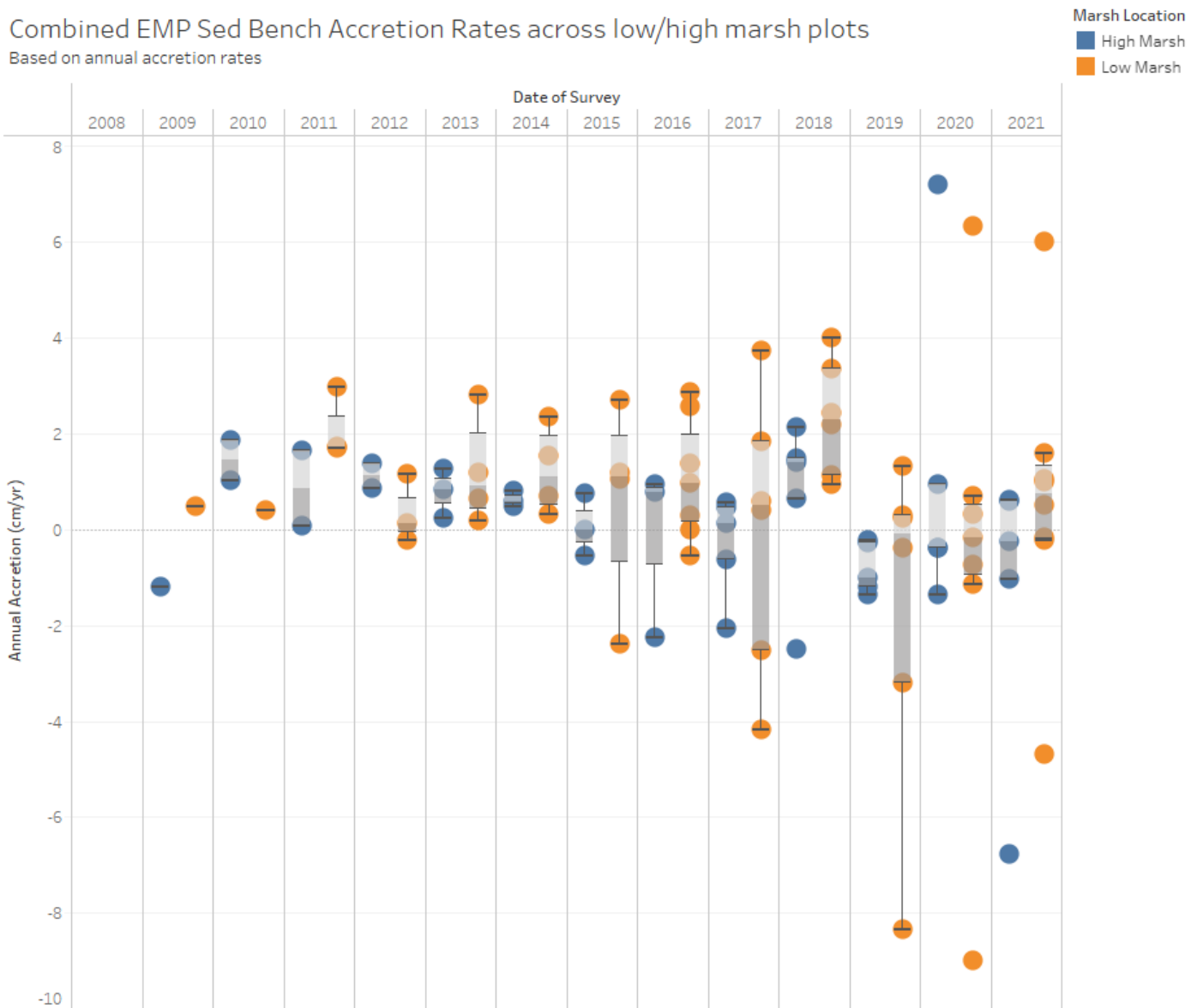


Figure 39: Longterm accretion rate variability across all 6 trend sites for 2010-2021.

When longterm accretion and erosion rates were plotted against marsh elevation (m,CRD, Figure 41), we obtained a significant ($R^2 = 0.761$, p-value = 0.002) correlation between marsh elevation and sediment accretion rates. Low marsh elevations at the trend sites having higher accretion rates than high marsh elevations, thereby supporting our previously stated hypothesis in Section 2.3.2.2 (Figure 40).

Regression analysis of mainstem cumulative discharge over average accretion and erosion rates at trend sites did not show any significant relationship ($R^2 = 0.034$, $p > 0.05$). This can be attributed to high variability of the longterm dataset (Figure 39). Future research will examine more nuanced relationships between site hydrology, sediment accretion, and marsh elevation, this analysis will be included in 2023.

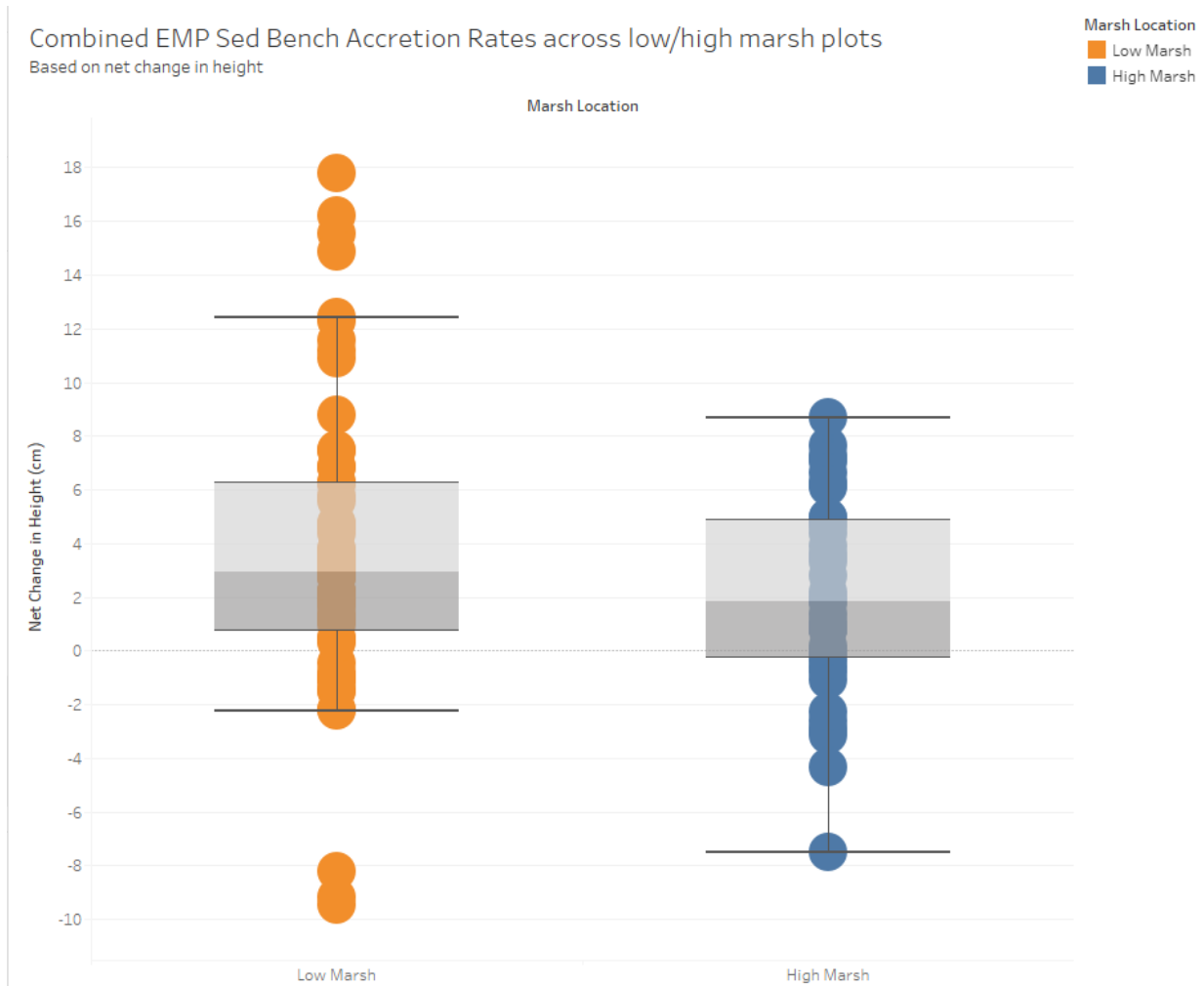


Figure 40: A box and whisker plot of the net change in height of all low marsh stakes and all high marsh stakes. The low marsh stakes have a median net accretion of 2.95 cm and the high marsh stakes have a median net accretion of 1.85 cm over the lifetime of all stakes.

EMP Sed Benches Elevations in CRD vs Long-Term Mean Sediment Accretion/Erosion (cm/year).

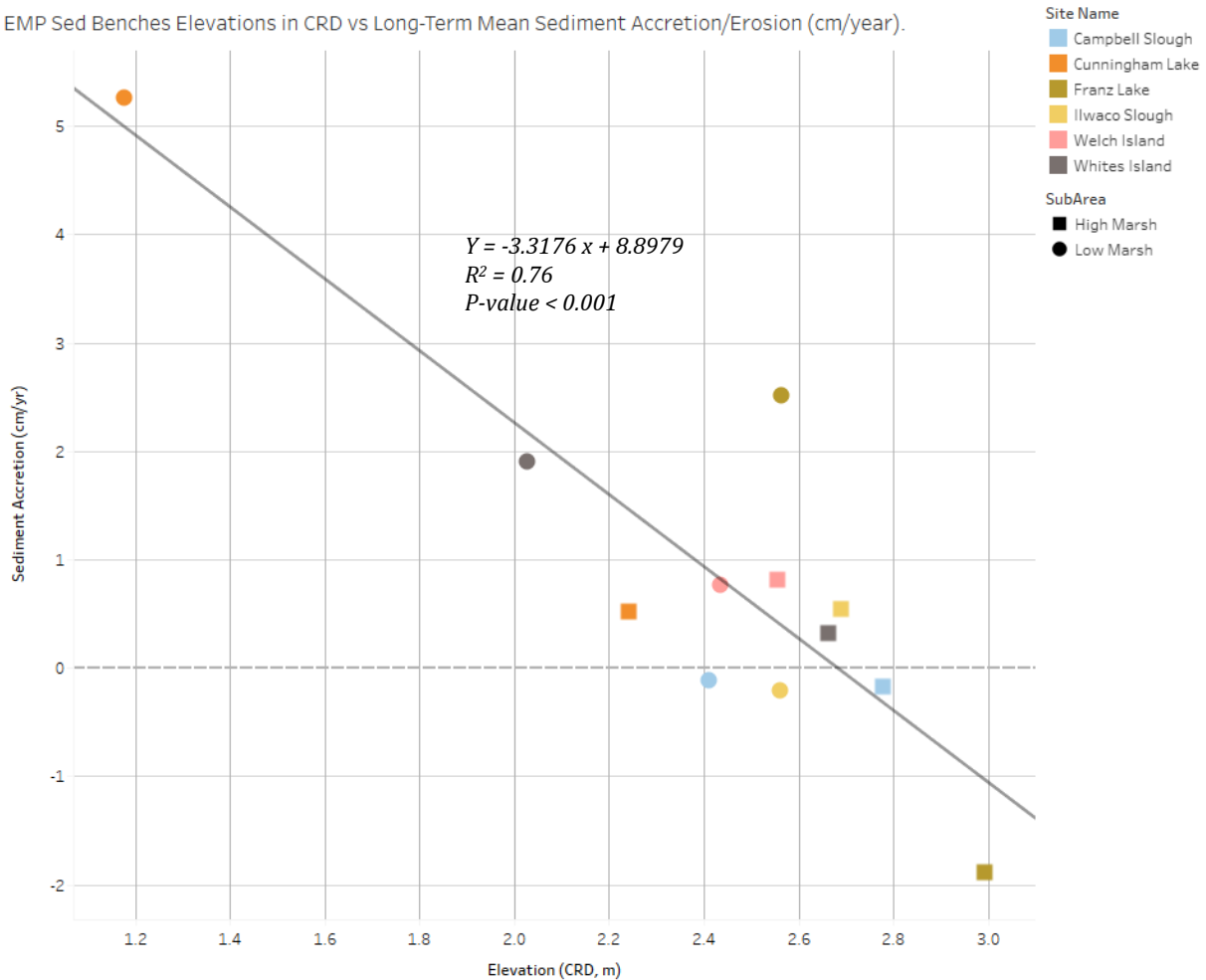


Figure 41: EMP site sediment bench elevations in CRD, meters vs. the longterm mean sediment accretion/erosion (+/-, cm). Low (circles) and high (squares) relative within marsh elevations highlighted for each site. No longterm data was available for Cunningham Lake high marsh. Linear regression ($y = -3.317x + 8.898$), $R^2 = 0.761$, $p\text{-value} = 0.002$. For full summary of these data see Table 21.

When looking at overall quantities of accretion, the low marsh tends to be more variable than the high marsh. Ilwaco Slough, Whites Island, and Franz Lake all received deposition and accretion in the low marsh while Cunningham Lake, Campbell Slough, and Welch Island saw erosion in the low marsh (Figure 42-Figure 47). In sites with high marsh stakes, all sites accreted besides Campbell Slough.

Net change in height - Ilwaco Slough
River kilometer 4

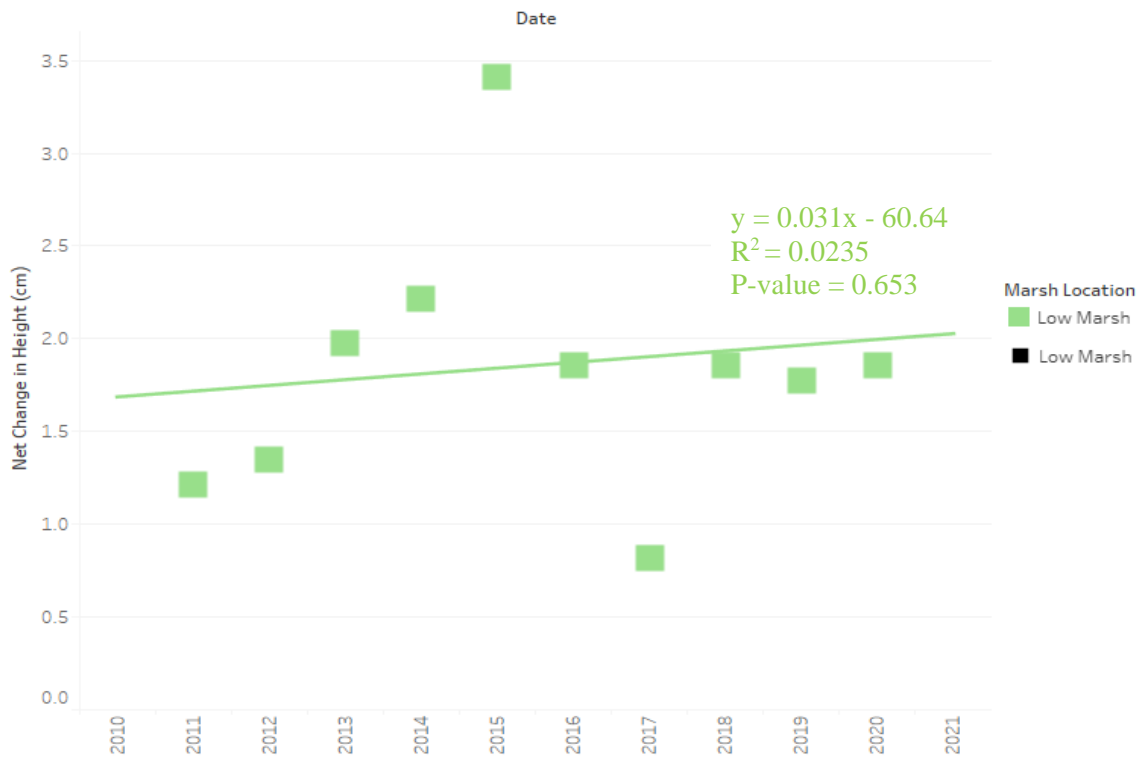


Figure 42: Ilwaco Slough net change in height (cm) per year. Overall, Ilwaco slough is fairly variable and is accreting at an average rate of 0.03 cm/year.

Net change in height - Welch Island
River kilometer 33

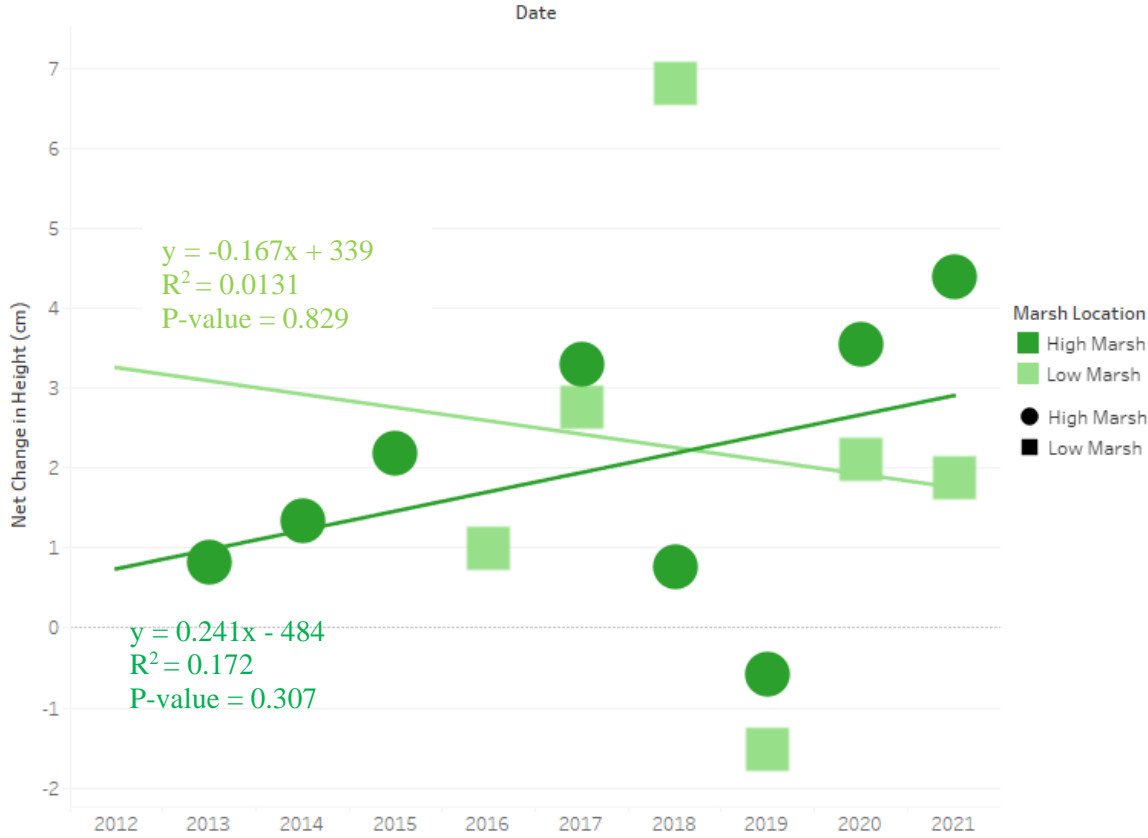


Figure 43: Welch Island net change in height (cm) per year. Overall, Welch Island is fairly variable in the low marsh with an average erosional rate of 0.17 cm/year. The high marsh is accreting at an average rate of 0.24cm/year.

Net change in height - Whites Island
River kilometer 45

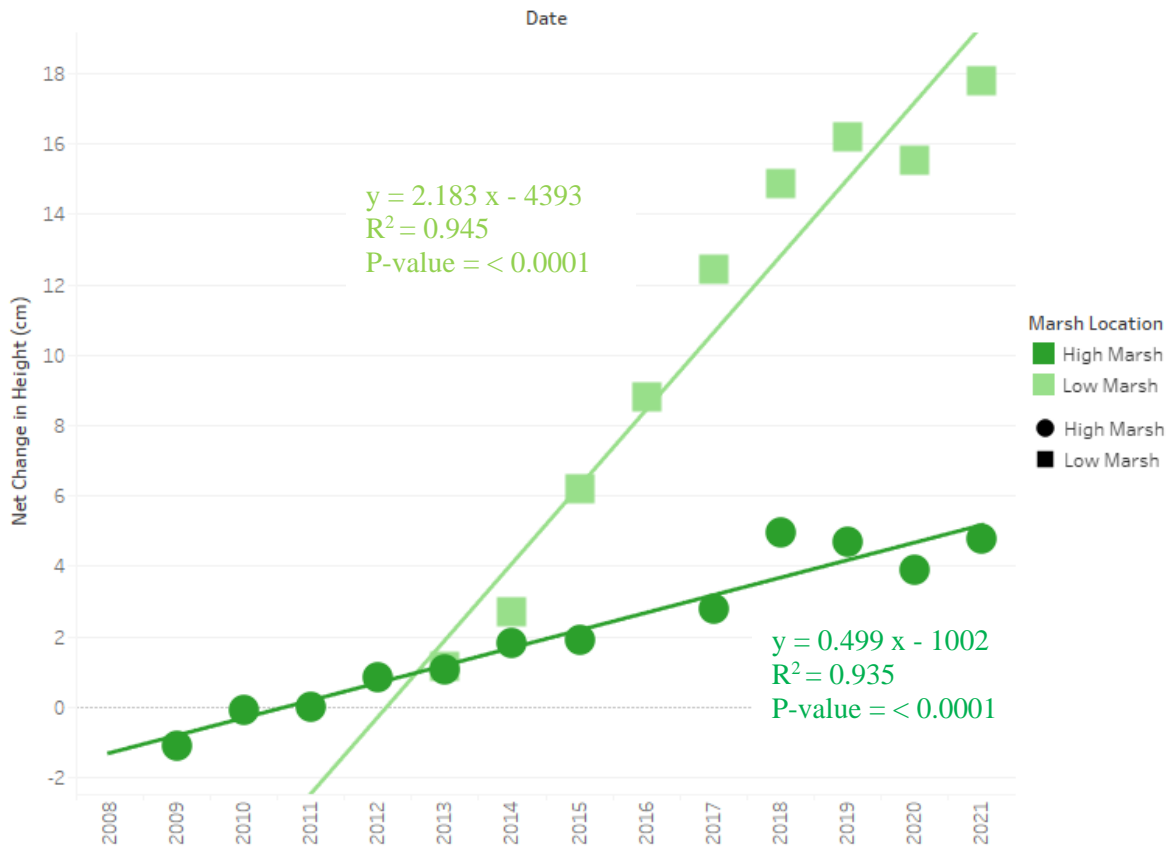


Figure 44: Whites Island net change in height (cm) per year. Overall, Whites Island is accreting in the low marsh with an average rate of 2.18 cm/year. The high marsh is accreting at a slower average rate of 0.50 cm/year.

Net change in height - Cunningham Lake
River kilometer 90

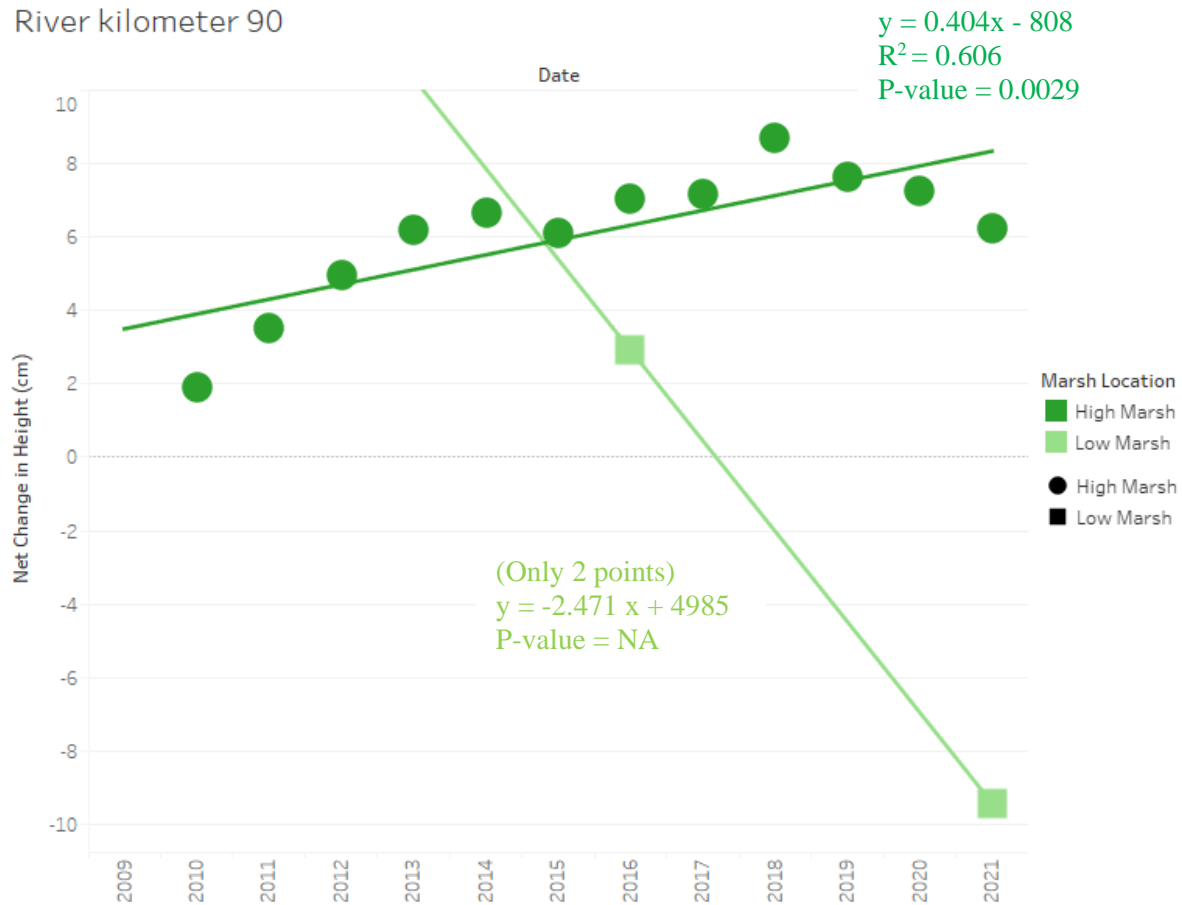


Figure 45: Cunningham Lake net change in height (cm) per year. Overall, Cunningham Lake is eroding in the low marsh at an average rate of with a rate of 2.47 cm/year. The high marsh is accreting at an average rate of 0.40 cm/year. Note that the low marsh stakes are lacking data due to being lost during 2017 and only reset in 2020.

Net change in height - Campbell Slough
River kilometer 93

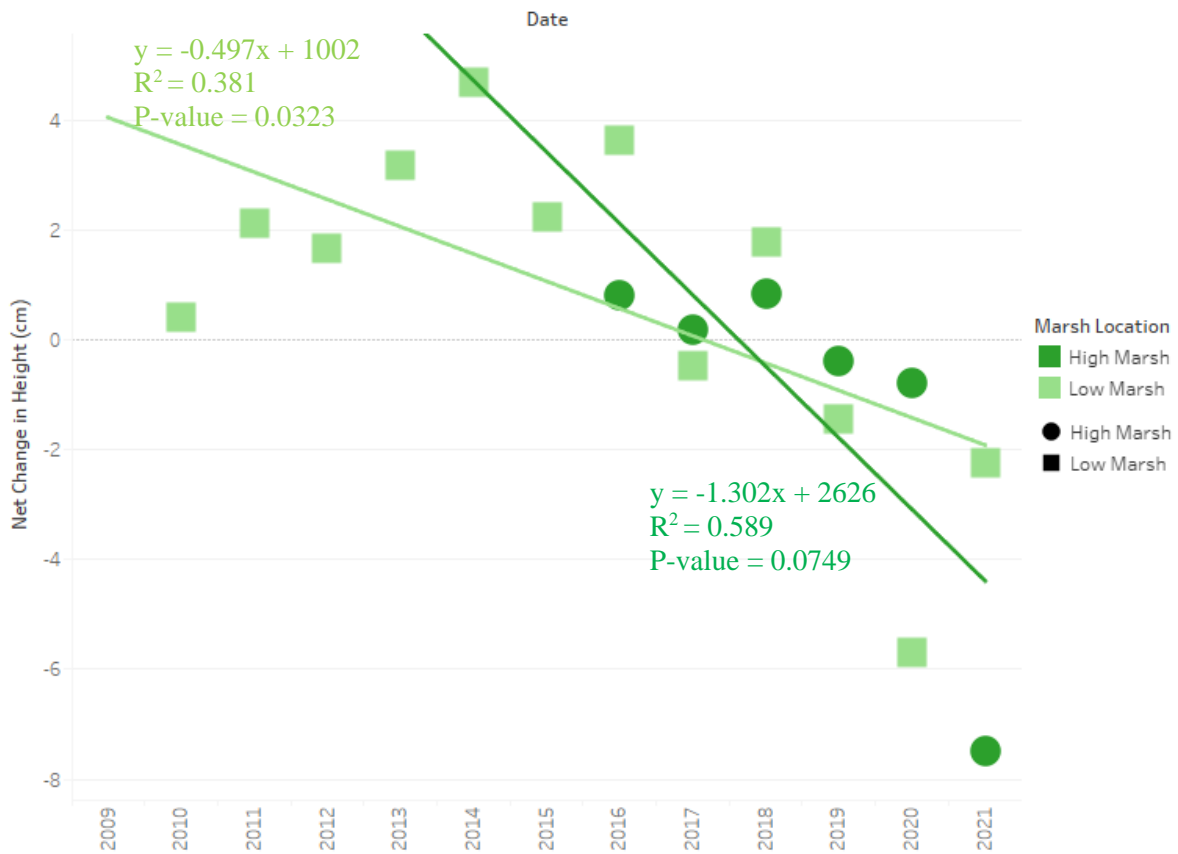


Figure 46: Campbell Slough net change in height (cm) per year. Overall, Campbell Slough is eroding in the low marsh with an average rate of 0.49 cm/year. The high marsh is eroding at a faster average rate at 1.30 cm/year.

Net change in height - Franz Lake
River kilometer 137

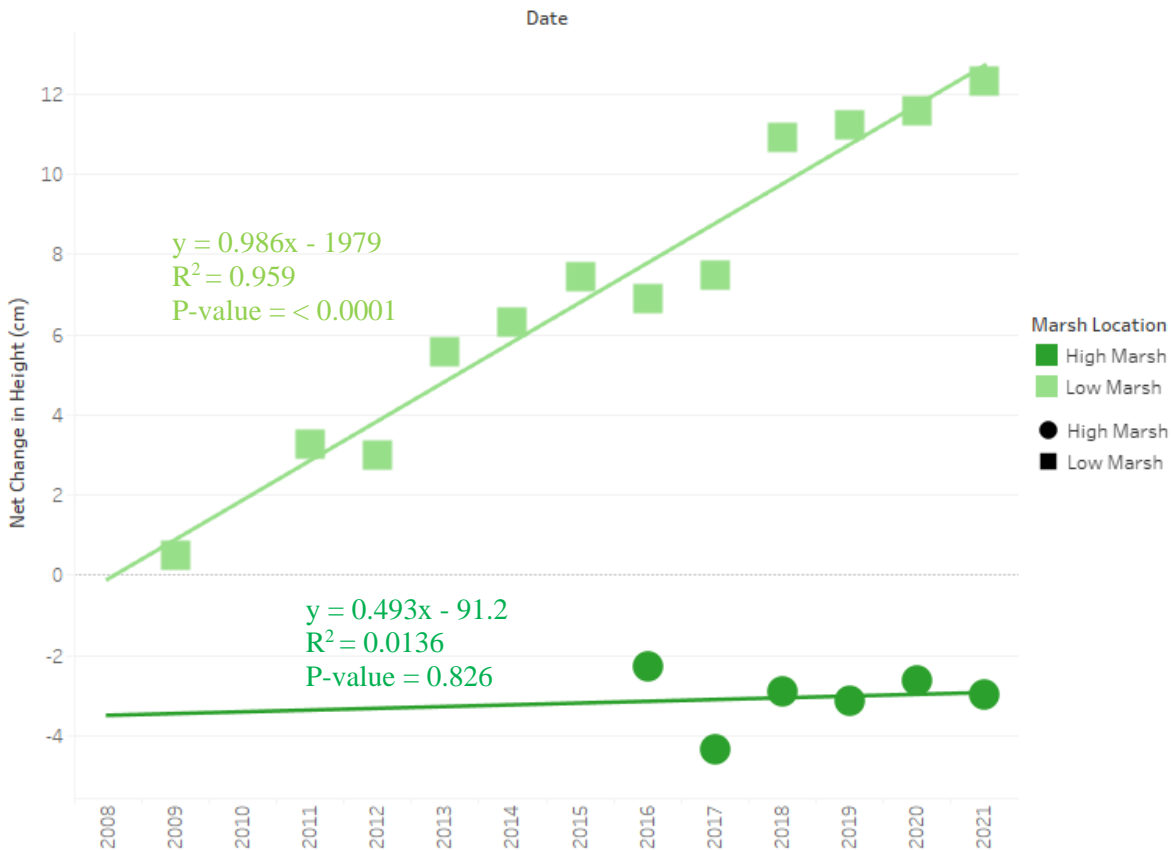


Figure 47: Franz Lake net change in height (cm) per year. Overall, Franz Lake is accreting in the low marsh with an average rate of 0.99 cm/year. The high marsh is accreting at a slower average rate of 0.13 cm/year.

3.3.2.1 *Sea Level Rise*

Forecasted Sea Level Rise

Understanding how our tidal wetlands and floodplains are keeping track with Sea Level Rise (SLR) is critical for considering how future restoration and management actions can address further potential wetland loss. For this preliminary analysis, we have used the USACE's 2020 Lower Columbia River Adaptive Hydraulics (AdH) Model Scenarios (Pevey et al. 2020).

These Scenarios (50, 75, and 100 yr.) are slightly more aggressive (greater rates of change) than the Miller et al. 2018 model which focuses on the Oregon and Washington Coast; however, they do provide a glimpse into how well our reference and restoration sites may be keeping up with increases in Water Surface Elevation across each reach of the Lower Columbia (Figure 48).

Each site, except for Franz Lake, is accreting slower than the most extreme forecasted sea level rise scenarios. Whites Island and Cunningham Lake are both expected to keep pace with the most conservative estimates of the Pevey et al. model. Continuing to track these conditions overtime will allow

us to evaluate how these conditions are changing. Further detailed analysis of these trends is planned for FY23.

Forecasted Sea Level Rise by River km and Site

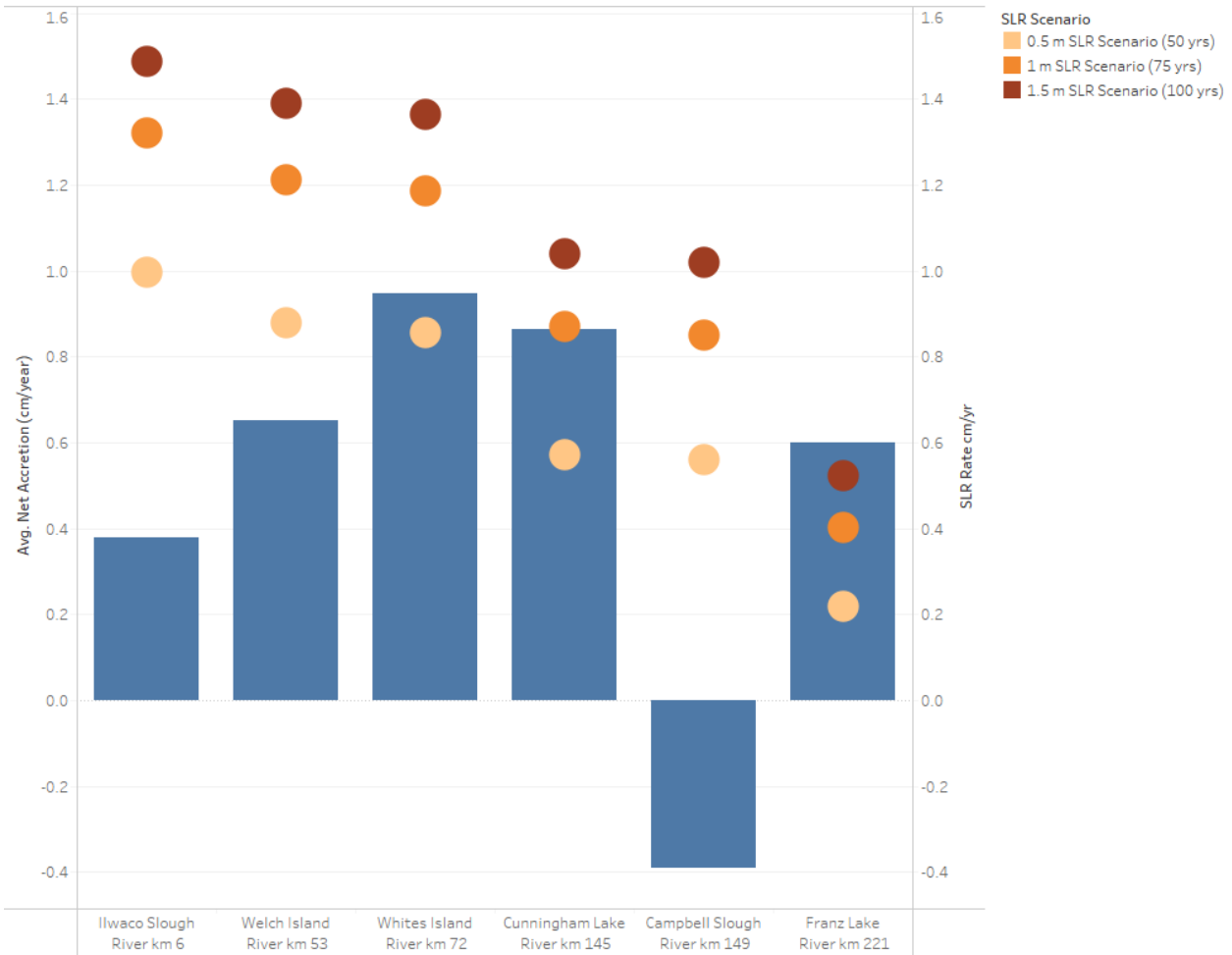


Figure 48: Forecasted sea level rise utilizing the Pevey et al. 2020 model by river km and site, plotted with average net accretion for each site.

3.3.3 Vegetation Species Assemblage

3.3.3.1 2020-2021 Vegetation Patterns Across Estuary Zones

Trends in species richness and diversity

In 2021, Whites Island had the highest total species richness of 43 species, followed by Welch Island with a total of 41 species, these levels of species richness fall within the longterm mean for both sites (Table 22). Welch Island and Whites Island are both located in wetland zone 2, in the lower river. As in previous years, the lowest species richness was at the brackish Ilwaco Slough (15 species) located in zone 1, near the mouth of the Columbia River. In wetland zone 4, mid-river sites, Campbell Slough, and Cunningham Lake both had similar richness (41, 26 respectively), and average richness per plot (5.6, 3.9 respectively). Campbell Slough’s jump in species richness over the years (longterm mean is 27) is due to the longterm grazing of the site which introduces species and causes disturbance to the wetland (grazing starting in

earliest in 2017), in 2021 - 16 of the 41 species were non-native. In an attempt to capture the slough plant community in an area less impacted by grazing we have added some transects across the main channel (cows tend not to swim across) and this area will now be monitored as well. In this report we have call this area Campbell Slough – Channel and it had a total species richness of 21 which is more in line with what would be expected without heavy grazing (and more similar to Campbell’s conditions prior to 2017), with only 4 non-native species observed (Table 22). In 2021, Franz Lake, wetland zone 5, the upper river site, had a total richness of 22, which is similar to the longterm mean of the site of 23. A summary of all plant community species richness data for 2020 and 2021 can be found in Table 22 and Table 23.

Generally, trends in site level mean plant species richness and diversity are consistent across all years of data collection, mean species richness being greatest at Welch Island (zone 2), followed by Whites Island (zone 2), Franz Lake (zone 5), Ilwaco (zone 1), and Cunningham and Campbell Slough (zone 4) (Figure 50). Additionally, across time, a slight increase in mean total species richness has been observed, with both native and non-native species richness increasing annually, non-native species richness has increased at a slightly greater rate than native species (Figure 49-Figure 52). This overall longterm increase in species richness over time could be caused by several factors including an increased survey effort and familiarity with site flora, increases in non-native introduced species which have been aided in recent years (2016-2021) at Campbell Slough and Cunningham Lake by exposure to cattle grazing, the mean and total species richness at the new Campbell monitoring location falls more in line with the number seen prior to 2017, 2017 being the year the cattle fence was washed out completely. The trends in mean species richness increasing across time are also seen in the Shannon Diversity values; these values are slightly increasing annually in response to increases in species richness (Figure 52, Table 24). Species evenness, a diversity measure of plant community cover and species richness distributions, show less change over time, species evenness remaining consistent across all sites over the longterm data set (Table 24). Indicating that while species compositions may be shifting slightly year to year the general distribution of species dominance have not changed substantially across the sites (Table 24). In 2021, Welch Island had the greatest Shannon Diversity index of 1.8, followed by Whites Island, 1.6, Campbell Slough and Ilwaco Slough at 1.2, Franz Lake at 1, and lastly Cunningham Lake at 0.8. Generally, these follow longterm trends, with Whites and Welch always having the most diverse communities, while Campbell, Cunningham, and Franz Lake have the least diverse across the trend sites (Table 24).

Table 22. Overall total species richness, total native and total non-native species richness over time at the six trend sites, longterm mean also shown for each site. In 2021, a second monitoring area was added to Campbell Slough to represent ungrazed conditions.

Total Species Richness		Mean	2021	2020	2019	2018	2017	2016	2015	2014	2013	2012	2011	2010	2009	2008	2007	2006	2005
Ilwaco Slough	Native	14	13	14	16	14	13	15	18	13	15	13	14						
	Non-native	2	2	5	4	3	1	1	1	3	2	2	2						
	Unknown	1					1	2	1	1	1	1	1						
	Total	17	15	19	20	17	15	18	20	17	18	16	17						
Welch Island	Native	32	29	32	34	32	29	32	36	34	34	30							
	Non-native	10	9	12	14	12	6	8	10	8	8	8							
	Unknown	3	3	1	2	2	3	2	2	7	3	1							
	Total	44	41	45	50	46	38	42	48	49	45	39							
Whites Island	Native	29	27	26	32	33	38	31	32	30	31	21	25	27	25				
	Non-native	11	14	14	14	14	9	10	11	13	11	9	13	9	6				
	Unknown	3	2	2	3	4	2	5	4	5	3	2	1	2	4				
	Total	43	43	42	49	51	49	46	47	48	45	32	39	38	35				
Cunningham Lake	Native	13	19	12	18	22	15	17	16	11	8	8	9	14	13	12	11	9	13
	Non-native	4	6	4	7	5	3	4	5	3	2	2	3	4	5	2	2	2	1
	Unknown	2	1	2	2	4	1	2	2	1	1	1	1	3	2		1	1	1
	Total	18	26	18	27	31	19	23	23	15	11	11	13	21	20	14	14	12	15
Campbell Slough	Native	16	23	17	17	19	13	24	26	17	22	15	12	17	14	12	8	9	7
	Non-native	8	16	9	15	12	6	12	8	8	12	5	3	8	8	5	9	3	2
	Unknown	3	2	2	3	4	1	2	3	4	5	3	1	2	2	5		1	
	Total	27	41	28	35	35	20	38	37	29	39	23	16	27	24	22	17	13	9
Campbell Slough – Channel (New 2021)	Native	16	16																
	Non-native	4	4																
	Unknown	1	1																
	Total	21	21																
Franz Lake	Native	18	17	16	18	20	21	24	24	21	15	14	16		15	9			
	Non-native	4	5	4	6	4	5	6	6	4	4	2	1		2	2			
	Unknown	2		2	1	2	2	2	3	2	2	1	2		1	1			
	Total	23	22	22	25	26	28	32	33	27	21	17	19		18	12			

Table 23. Total number of plots and average species richness, native and non-native species richness over time at the six trend sites, longterm mean also shown for each site. In 2021, a second monitoring area was added to Campbell Slough to represent ungrazed conditions.

Mean Species Richness	Mean	2021	2020	2019	2018	2017	2016	2015	2014	2013	2012	2011	2010	2009	2008	2007	2006	2005	
Ilwaco Slough	Native	3.7	4.3	3.5	3.6	4.4	4.1	3.8	3.5	3.3	3.3	3.2	3.6						
	Non-native	0.5	0.9	1.0	1.0	1.1	0.2	0.1	0.1	0.8	0.1	0.2	0.1						
	Total Mean	4.6	5.2	4.5	4.6	5.5	5.2	4.8	4.1	4.1	4.0	4.0	4.4						
	# of plots	39.6	38	40	40	40	40	39	39	40	40	40	40						
Welch Island	Native	9.2	9.4	9.0	9.9	10.5	8.0	9.3	9.7	9.1	8.9	8.2							
	Non-native	1.9	2.8	1.8	2.5	2.6	1.6	1.1	1.9	1.3	1.7	1.8							
	Total Mean	11.6	12.4	10.9	12.7	13.5	10.3	11.4	11.8	11.2	11.2	10.4							
	# of plots	40.4	41	41	41	40	41	40	40	40	40	40							
Whites Island	Native	4.6	4.3	4.2	5.7	5.2	5.0	5.4	4.5	4.5	4.7	3.4	3.5	5.1	4.4				
	Non-native	2.5	3.6	2.7	3.4	3.5	2.2	2.3	2.3	2.4	2.3	1.9	2.3	2.2	1.4				
	Total Mean	7.5	8.0	7.4	9.6	9.1	7.3	8.2	7.0	7.3	7.4	5.4	6.7	7.5	6.6				
	# of plots	40.8	43	43	43	44	44	43	42	43	41	42	42	35	25				
Cunningham Lake	Native	2.8	2.7	2.2	3.7	5.1	4.0	3.5	3.0	2.8	2.0	1.8	1.3	2.5	2.9	2.4	2.8	2.2	2.7
	Non-native	1.0	1.0	1.0	1.3	1.2	1.8	1.4	0.9	1.1	0.9	0.7	0.8	0.9	0.9	0.8	0.9	0.7	0.7
	Total Mean	4.0	3.9	3.3	5.2	7.1	6.3	5.0	4.1	3.9	3.1	2.5	3.4	3.7	3.8	3.2	3.7	3.0	3.5
	# of plots	59.1	62	66	70	68	69	69	68	36	34	60	59	62	64	63	64	62	28
Campbell Slough	Native	2.4	3.6	2.9	3.8	2.9	2.1	3.0	3.7	2.3	2.5	1.7	1.5	2.4	2.3	1.9	1.7	1.7	1.5
	Non-native	1.0	2.0	1.1	1.9	1.4	0.9	1.3	1.0	1.2	1.1	0.7	0.7	0.8	0.8	0.7	0.8	0.5	0.8
	Total Mean	3.7	5.6	4.0	5.8	4.8	3.2	4.6	5.0	3.6	3.9	2.6	3.0	3.2	3.2	3.0	2.4	2.3	2.3
	# of plots	59.5	60	62	62	61	65	61	62	61	61	61	61	62	61	64	62	61	24
Campbell Slough – Channel (New 2021)	Native	2.9	2.9																
	Non-native	1.0	1.0																
	Total Mean	3.9	3.9																
	# of plots	49.0	49																
Franz Lake	Native	3.8	2.9	2.7	4.9	5.3	4.9	4.2	4.1	3.3	4.2	2.6	3.3		3.8	2.5			
	Non-native	0.9	0.9	0.8	0.8	1.2	1.4	1.1	1.1	0.5	0.8	0.7	0.9		0.8	1.0			
	Total Mean	5.2	3.8	3.9	5.9	7.2	7.1	6.2	5.5	4.6	5.8	4.0	4.6		4.6	3.6			
	# of plots	59.0	64	67	70	67	61	61	62	61	58	62	58		36	40			

Table 24: Diversity indices over time at the six trend sites, longterm mean also shown for each site. In 2021, a second monitoring area was added to Campbell Slough to represent ungrazed conditions.

Diversity Indices		Mean	2021	2020	2019	2018	2017	2016	2015	2014	2013	2012	2011	2010	2009	2008	2007	2006	2005
Ilwaco Slough	Shannon	1.0	1.2	1.0	1.2	1.1	1.2	1.0	0.9	0.9	0.7	0.8	0.9						
	Evenness	0.6	0.7	0.7	0.7	0.6	0.7	0.6	0.6	0.7	0.5	0.6	0.7						
	Simpson	0.6	0.7	0.6	0.7	0.6	0.6	0.7	0.7	0.7	0.5	0.5	0.5	0.5					
Welch Island	Shannon	1.6	1.8	1.8	1.7	1.9	1.5	1.5	1.5	1.5	1.5	1.5							
	Evenness	0.7	0.7	0.8	0.7	0.7	0.6	0.6	0.6	0.6	0.6	0.6							
	Simpson	0.7	0.7	0.8	0.8	0.8	0.7	0.7	0.7	0.7	0.7	0.7							
Whites Island	Shannon	1.3	1.6	1.5	1.7	1.5	1.3	1.2	1.0	1.2	1.1	1.0	1.1	1.2	1.2				
	Evenness	0.6	0.7	0.7	0.7	0.7	0.6	0.6	0.5	0.6	0.6	0.6	0.6	0.6	0.6				
	Simpson	0.7	0.8	0.7	0.8	0.8	0.7	0.7	0.6	0.7	0.7	0.7	0.7	0.7	0.7				
Cunningham Lake	Shannon	0.8	0.8	0.6	1.0	1.2	1.1	1.0	0.8	0.7	0.5	0.6	0.9	0.6	0.8	0.7	0.8	0.6	0.5
	Evenness	0.6	0.6	0.6	0.6	0.6	0.6	0.6	0.6	0.5	0.5	0.5	0.6	0.5	0.6	0.6	0.7	0.6	0.5
	Simpson	0.7	0.5	0.7	0.6	0.7	0.8	0.7	0.6	0.8	0.6	0.9	0.8	0.5	0.6	0.7	0.6	0.8	0.3
Campbell Slough	Shannon	0.8	1.2	1.0	1.3	1.1	0.8	0.9	0.9	0.7	0.7	0.7	0.7	0.6	0.6	0.6	0.6	0.4	0.4
	Evenness	0.6	0.7	0.7	0.8	0.7	0.7	0.6	0.6	0.6	0.7	0.7	0.6	0.5	0.6	0.5	0.7	0.6	0.6
	Simpson	0.7	0.8	0.8	0.8	0.8	0.8	0.6	0.6	0.7	0.7	0.9	0.8	0.6	0.4	0.7	0.8	0.6	0.4
Campbell Slough (New 2021)	Shannon	0.8	0.8																
	Evenness	0.7	0.7																
	Simpson	0.5	0.5																
Franz Lake	Shannon	0.9	1.0	0.7	0.9	0.8	1.1	1.0	1.1	0.8	0.8	0.8	1.0		0.9	0.9			
	Evenness	0.5	0.7	0.6	0.5	0.5	0.5	0.5	0.6	0.5	0.4	0.5	0.6		0.6	0.7			
	Simpson	0.7	0.6	0.7	0.6	0.7	0.7	0.7	0.7	0.6	0.8	0.7	0.8		0.6	0.7			

Mean Total Species Richness Graph

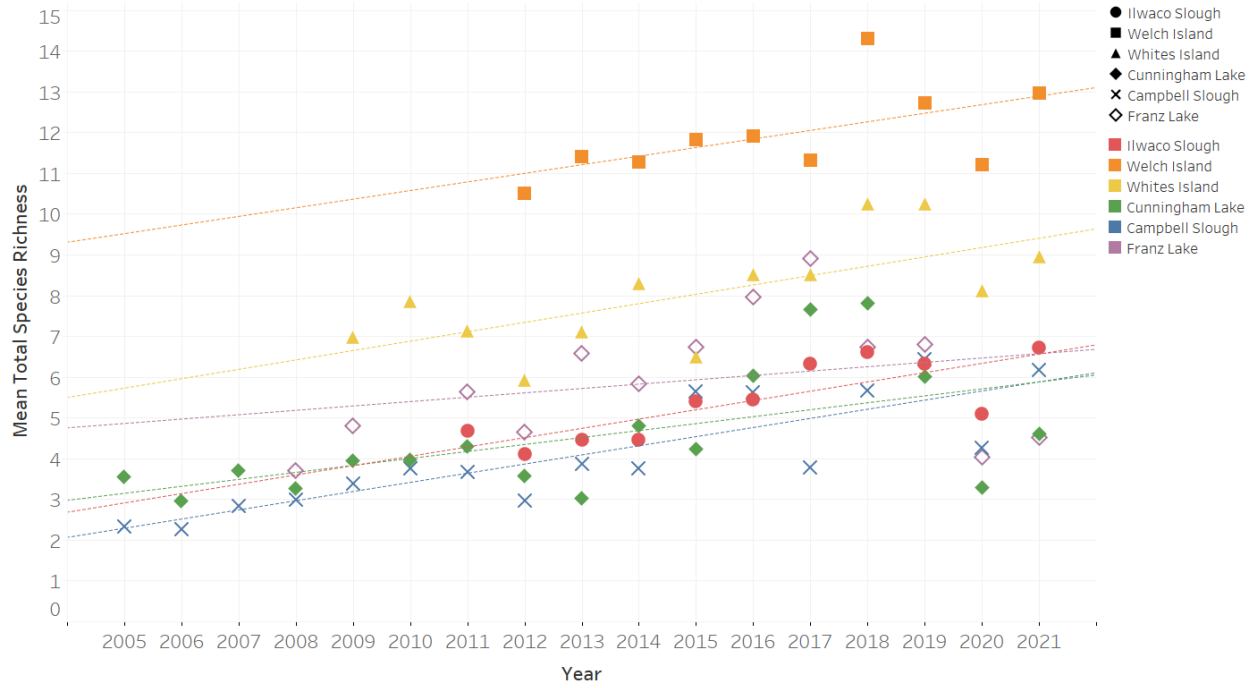


Figure 49. Changes in mean total species richness over time at each trend site.

Mean Total Non-native Species Richness Graph

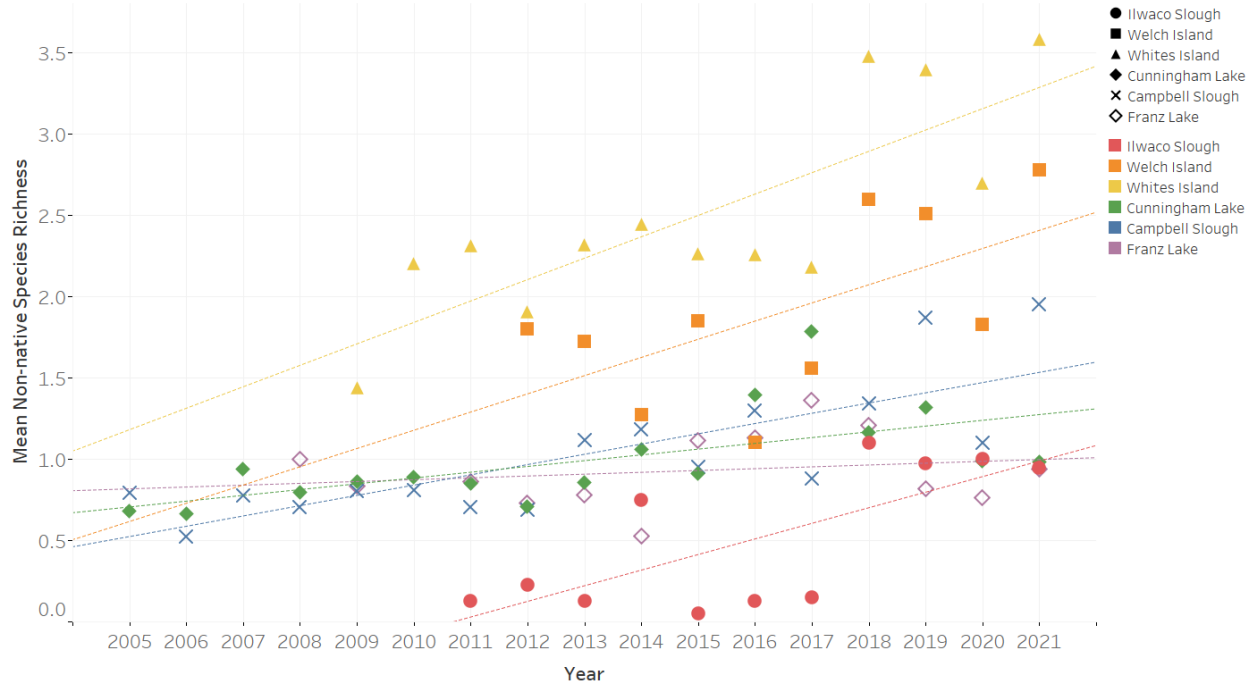


Figure 50. Changes in mean non-native species richness over time at each trend site.

Mean Total Native Species Richness Graph



Figure 51. Changes in mean native species richness over time at each trend site.

Shannon Diversity Graph

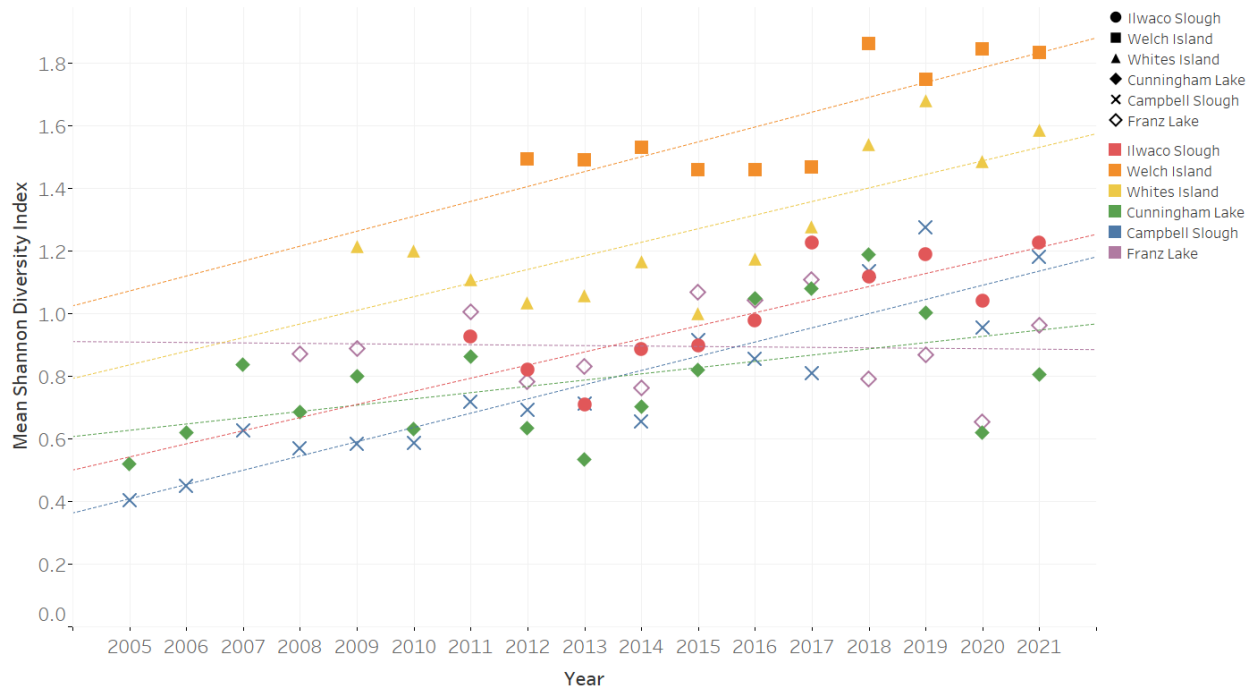


Figure 52. Changes in mean Shannon Diversity over time at each trend site.

Trends in plant cover

When comparing overall % total cover in 2020 and 2021, Campbell Slough had substantially lower % vegetative cover (67%) than all other sites (82%-155%) in 2020 (Table 30, Figure 53, Figure 54). This is likely due to extensive cattle grazing removing vegetation from the site, in addition to overall higher water levels observed across the upper river sites, from the late 2020 freshet, with Franz Lake and Cunningham Slough also experiencing lower than normal total cover. Comparatively, there was a significant increase in cover at Cunningham Lake between 2017-2021 from 87% to 105% which was also grazed in 2017 but not as heavily in 2021. Welch Island had the highest cover in 2020 and 2021 (155 and 160%), while the sites at the two ends of the tidal estuary, Ilwaco Slough (112%, 2020; 122%, 2021) and Franz Lake (86%, 2020; 136%, 2021) were similar to each other in 2021 (but not in 2020), with relatively high total cover. It is likely that the particularly low water year in 2021 affected the total cover at Franz Lake substantially (freshet conditions paired with beaver dam failure). Total cover estimates follow trends with mean total species richness, as total cover is accumulative as the number of species observed increases so does the total % cover (Table 22, Table 23, Table 30). Generally, with the longterm dataset we can clearly see how discharge conditions in the upper reaches of the estuary can impact growing conditions as these sites (Campbell, Cunningham, and Franz Lake), reducing total cover and species richness when water levels remain relatively high into July such as in 2017 and 2020 (Figure 57-Figure 63).

Relative cover of native and non-native plant communities across the sites have followed a less linear trend than total cover overtime (Table 25-Table 29, Figure 53-Figure 56). Generally, native and non-native cover are more similar from year to year in zone 1 and 2 sites (Ilwaco, Welch, Whites) compared to the zone 4 and 5 sites (Cunningham, Campbell, and Franz) (Figure 53-Figure 56), this is likely due to the general hydrology of these sites, inundation patterns being much more stable from year to year in the tidally driven lower river, zone 1 and 2, sites compared to the fluvially dominated mid and upper river, zone 4 and 5, sites (see section 3.3.1). In 2021, mean relative native cover was greatest at Ilwaco Slough (82%; longterm average 81%) and Franz Lake (69%; longterm average 77%), both sites saw generally similar conditions between 2020 (Table 25-Table 29, Figure 53-Figure 56). However in 2021, Franz Lake experienced an increase in *Phalaris arundinacea* cover from 22% (2020) to 30% on average (2021), generally *P. arundinacea* has been increasing at the site since 2018 (11), however historically (2009-2012) mean cover *P. arundinacea* was between 38-41% (Table 29, Figure 57). Franz Lake has also experienced a significant increase in Wapato in 2021, up from 11 in 2018 to 30 in 2021, this increase was mainly observed in the low marsh zone typically flooded by the longterm established beaver dam which was damaged and no longer holding water in 2021 (providing a template for Wapato growth in these areas). This is clear when looking at the typical open water cover for the site which is about 19-26% and down to 5% in 2021 (Table 27).

Campbell Slough showed a general increase in native relative cover between 2018 and 2020, before dropping slightly in 2021, shifting from 52% in 2018 to 65% in 2020 and 55% in 2021 (Table 25, Figure 55 & Figure 56). This shift can be accounted for by an increase in native herbs such as *Eleocharis ovata*, *Helenium autumnale*, *Lindernia dubia*, and *Ludwigia palustris* which were found growing in the plots heavily disturbed by grazing. This shift, caused by grazing, indicates that these native species are found in the seed bank but are normally (under no grazing) suppressed by more dominant non-native species such as *Phalaris arundinacea* (Kidd 2017). However, it should be noted that while non-native cover did not increase due to these grazing pressures, non-native species richness across the site jumped from 6 in 2017 up to 16 in 2021 (Table 22). Comparatively, Cunningham Lake, which has not experienced heavy grazing since 2017, had a decrease in native cover from 65% in 2018 to 46% in 2021 (Table 25, Figure 55 & Figure 56). This decrease in native cover was accompanied by a general increase in non-native cover including a 47% increase in *Phalaris arundinacea* cover between 2018 and 2021 (Table 29). Additionally, Cunningham Lake's native and non-native species diversity has remained relatively stable compared to Campbell Slough (Table 22).

It is also worth noting that in 2020 water levels were abnormally high at Campbell and Cunningham Slough during summer monitoring which resulted in a dip in total cover, native and non-native – in addition to a dramatic increase in open water across these sites (Table 27). This was seen the accumulative discharge and site water level data – which August 2020, having above normal conditions in these upper river reaches (see Section 3.3.1, and Figure 53-Figure 56).

Overall, relative native cover at Whites and Welch Islands has remained relatively stable only fluctuating around 7% at Whites Island and 15% between 2012-2021 at Welch Island. Welch Island (68%, longterm average 80%) and Whites Island (43%, longterm averages 42%) experienced very little change in their average relative native plant cover between 2018-2021 (Table 25, Figure 55 & Figure 56).

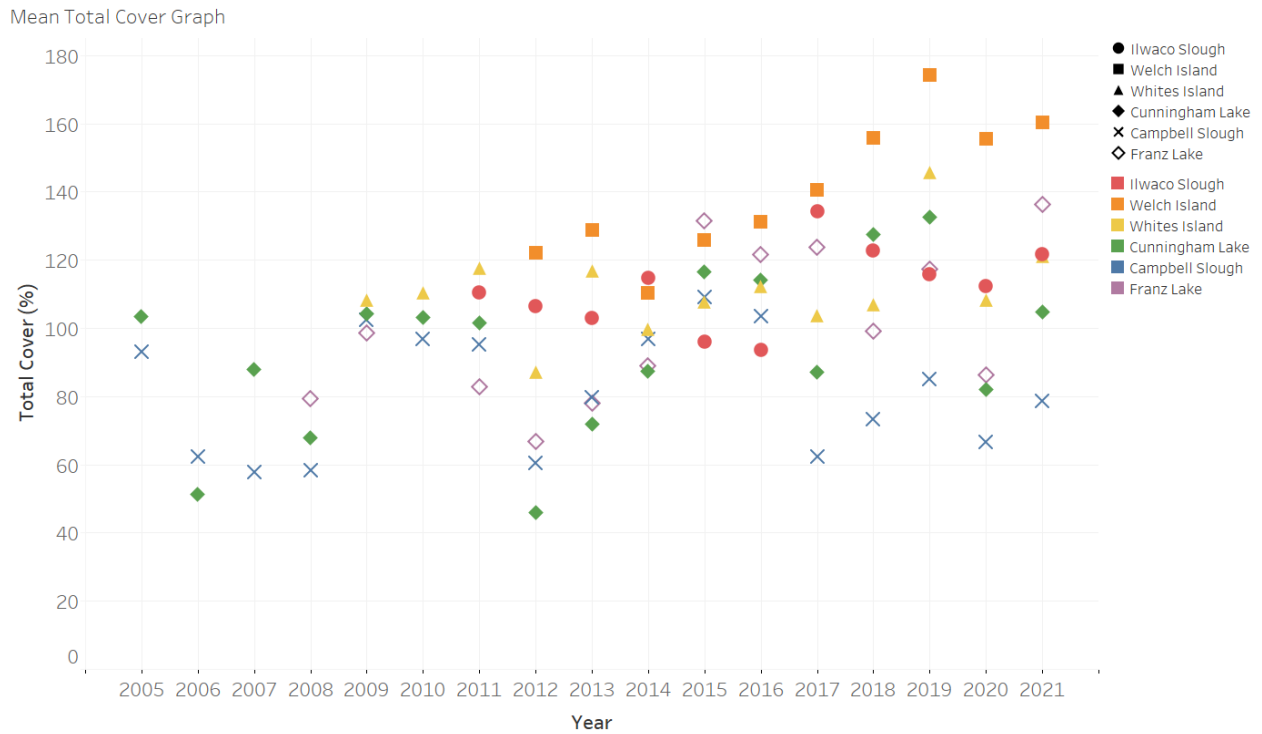


Figure 53. Changes in mean total cover (%) over time at each trend site.

Long-term Mean of Total Cover

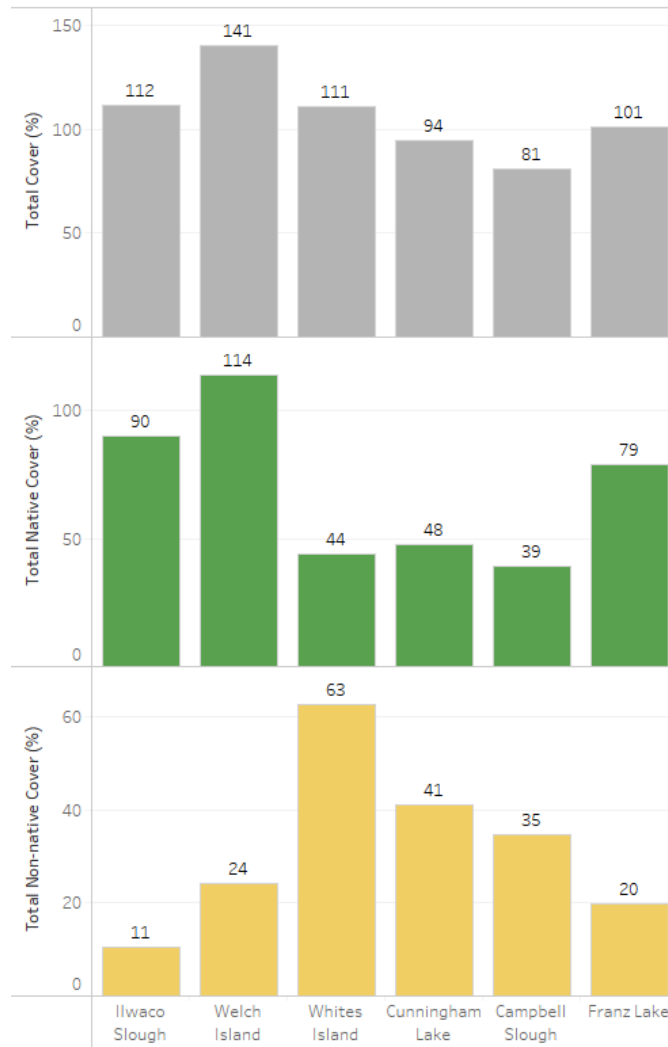


Figure 54. Average % total cover (not relative cover) of vegetation at each trend site through 2021.

Mean Native Relative Cover Graph

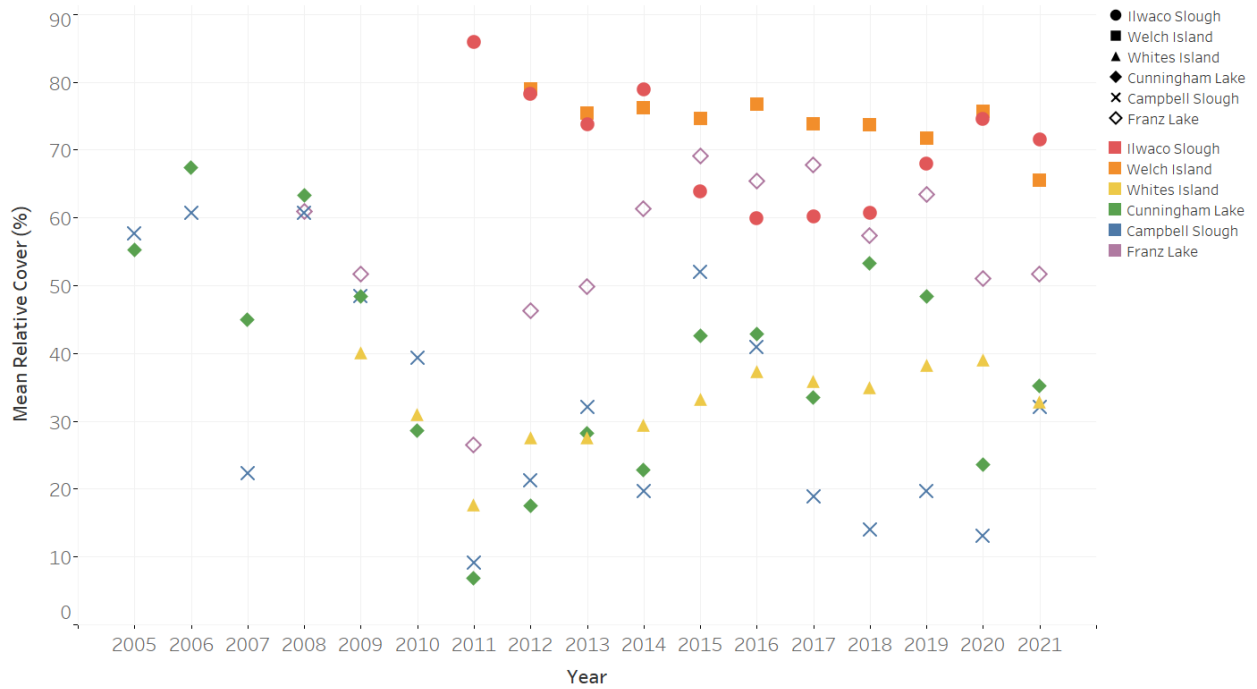


Figure 55. Changes in mean native species relative cover (%) over time at each trend site.

Mean Non-native Relative Cover Graph

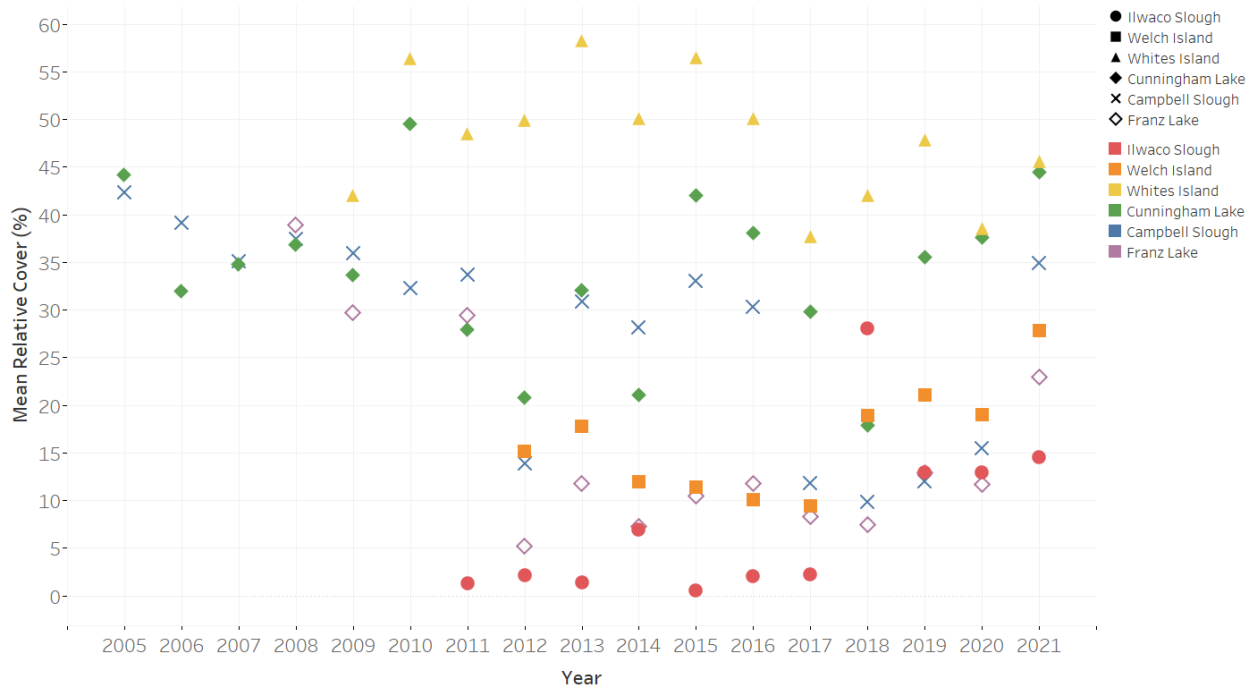


Figure 56: Changes in mean non-native species relative cover (%) over time at each trend site.

Table 25. Changes in average relative % cover of living native and non-native plant over time at the six trend sites, longterm mean also shown for each site. In 2021, a second monitoring area was added to Campbell Slough to represent ungrazed conditions.

Mean Relative Cover		Mean	2021	2020	2019	2018	2017	2016	2015	2014	2013	2012	2011	2010	2009	2008	2007	2006	2005
Ilwaco Slough	Native	81	82	84	81	69	69	73	81	88	85	85	90						
	Non-native	9	16	14	15	29	2	3	1	9	2	2	1						
Welch Island	Native	80	68	80	77	78	84	85	85	84	79	82							
	Non-native	18	31	20	23	20	11	11	14	14	18	16							
Whites Island	Native	42	43	49	43	46	49	44	39	40	36	43	27	39	44				
	Non-native	55	56	45	54	53	51	54	61	58	63	57	54	61	46				
Cunningham Lake	Native	53	46	51	59	65	56	55	51	50	44	54	14	41	60	63	63	67	55
	Non-native	40	53	48	40	21	39	43	43	33	35	46	42	52	38	37	37	32	44
Campbell Slough	Native	55	55	65	65	52	63	61	60	29	54	51	25	53	58	61	56	61	58
	Non-native	37	45	35	33	36	32	38	37	31	33	27	40	43	39	37	44	39	42
Campbell Slough – Channel (New 2021)	Native	54	54																
	Non-native	46	46																
Franz Lake	Native	78	74	82	86	88	86	85	87	85	80	72	49		66	61			
	Non-native	18	26	15	14	10	11	14	12	9	16	10	40		34	39			

Table 26. Changes in average relative % cover of living plants by wetland indicator status (WIS) over time at the six trend sites, longterm mean also shown for each site. In 2021, a second monitoring area was added to Campbell Slough to represent ungrazed conditions. Wetland indicator status broken down by FAC = Facultative, FACW= Facultative Wet, and OBL= Obligate.

Mean Relative Cover by WIS		Mean	2021	2020	2019	2018	2017	2016	2015	2014	2013	2012	2011	2010	2009	2008	2007	2006	2005
Ilwaco Slough	FAC	8	14	12	13	28	0	0	0	9	0	1	1						
	FACW	9	4	9	8	4	3	12	8	13	14	16	18						
	OBL	75	82	79	79	68	76	69	82	78	67	67	71						
Welch Island	FAC	3	4	3	3	3	2	2	3	3	2	3							
	FACW	23	37	29	28	25	12	17	24	23	21	17							
	OBL	72	59	67	69	71	79	76	73	74	75	80							
Whites Island	FAC	5	7	3	5	8	4	4	5	5	5	5	3	2	4				
	FACW	47	48	48	42	39	48	51	53	51	52	46	45	53	42				
	OBL	43	44	41	49	52	43	43	41	39	37	49	34	44	41				
Cunningham Lake	FAC	0	0	0	0	0	0	0	0	0	0	0	0	0	0	0	0	0	0
	FACW	41	40	51	42	26	56	45	37	48	44	54	38	46	33	31	30	26	25
	OBL	55	60	49	57	73	43	55	63	52	56	46	18	53	61	61	67	70	75
Campbell Slough	FAC	1	4	2	1	1	0	3	0	1	1	0	0	0	0	1	0	0	0
	FACW	33	30	32	31	34	37	30	32	32	43	28	27	36	36	32	35	43	29
	OBL	63	63	66	67	63	62	66	63	66	54	69	47	64	61	61	63	57	71
Campbell Slough – Channel (New 2021)	FAC	1	1																
	FACW	28	28																
	OBL	72	72																
Franz Lake	FAC	1	0	0	0	1	2	1	1	2	0	0	0		0	0			
	FACW	41	51	50	47	43	38	44	47	31	34	22	48		36	37			
	OBL	54	49	49	51	53	56	53	51	60	61	66	48		57	42			

Table 27. Changes in average relative % cover of living plants, dead plants, bare ground, and open water over time at the six trend sites, longterm mean also shown for each site. In 2021, a second monitoring area was added to Campbell Slough to represent ungrazed conditions. It should also be notes that bare ground, open water, and dead plant materials were not consistently recorded until 2011/2010, which is clearly seen in the historic data. Recent years with abnormal occurrences are highlighted in blue, see text summary for analysis.

Mean Relative Cover		Mean	2021	2020	2019	2018	2017	2016	2015	2014	2013	2012	2011	2010	2009	2008	2007	2006	2005
Ilwaco Slough	Living	80.7	80.3	86.7	75.0	82.2	75.0	72.4	62.6	82.1	85.5	91.9	93.9						
	Dead	4.8	3.5	5.0	8.8	1.9	11.2	1.9	6.1	4.1	8.5	1.2	0.3						
	Bare ground	6.0	5.4	5.0	4.3	3.7	2.6	17.1	13.5	3.4	5.4	3.9	2.0						
	Open water	3.1	4.3	2.6	3.2	5.1	2.3	2.6	5.3	3.6	0.3	2.2	2.4						
Welch Island	Living	92.1	94.0	95.0	93.2	94.0	86.9	89.9	86.3	90.3	95.3	95.7							
	Dead	2.6	5.1	1.8	2.5	3.1	9.3	2.7	0.1	0.5	0.9	0.1							
	Bare ground	2.4	0.3	0.3	0.2	0.2	1.1	5.7	3.0	6.0	2.7	4.0							
	Open water	2.9	0.5	2.9	4.1	2.7	2.7	1.7	10.6	3.1	1.1	0.2							
Whites Island	Living	81.9	79.0	83.3	86.8	77.6	73.1	88.0	90.1	80.0	86.8	77.6	66.5	87.3	88.5				
	Dead	9.4	16.2	9.5	9.9	14.6	21.4	2.9	4.0	6.6	4.0	6.2	19.6	3.8	3.9				
	Bare ground	6.4	3.6	6.7	1.6	3.2	2.4	7.5	3.8	7.2	6.9	14.4	11.6	8.8	5.2				
	Open water	2.0	0.9	0.4	1.2	4.7	3.0	1.4	2.2	6.1	2.2	1.9	1.8	0.0	0.0				
Cunningham Lake	Living	71.3	80.7	61.3	84.3	71.9	52.7	77.0	85.0	43.1	60.4	38.2	17.9	78.6	82.2	100.0	79.7	100.0	100.0
	Dead	6.7	10.5	1.3	6.4	4.8	17.9	9.7	1.0	8.4	3.0	5.9	39.5	3.0	2.8				
	Bare ground	12.6	5.7	0.5	6.6	12.8	22.8	7.8	10.1	21.4	31.6	55.1	12.4	12.5	14.3		1.0		
	Open water	7.7	3.1	36.9	2.4	4.2	4.7	5.1	1.4	20.5	0.4	0.7	28.3	4.1	0.0		19.3		
Campbell Slough	Living	64.5	67.1	51.8	59.5	45.9	43.2	69.8	77.5	46.9	63.5	35.6	37.4	71.6	84.7	100.0	42.7	100.0	100.0
	Dead	6.8	7.0	1.8	11.3	15.1	8.6	9.3	12.2	1.3	0.2	2.0	19.3	10.5	1.5		14.7		
	Bare ground	15.5	14.9	17.2	20.9	23.2	31.5	7.7	5.8	21.8	18.5	39.8	17.1	9.8	12.1		22.6		
	Open water	10.9	11.0	29.2	7.9	12.1	16.3	13.3	4.4	14.5	12.2	15.3	22.1	6.3			20.0		
Campbell Slough (New 2021)	Living	87.1	87.1																
	Dead	4.8	4.8																
	Bare ground	2.7	2.7																
	Open water	5.4	5.4																
Franz Lake	Living	70.8	74.5	62.9	76.5	65.1	72.8	75.3	71.8	71.8	64.1	55.8	48.1		81.5	100.0			
	Dead	7.3	14.1	5.9	4.4	2.3	10.4	7.4	17.0	4.4	5.5	8.7	13.0		1.8				
	Bare ground	12.1	6.8	6.4	0.5	6.9	9.8	9.9	5.8	21.5	29.4	27.9	15.3		16.7				
	Open water	9.2	4.6	24.8	18.6	25.7	6.9	7.4	5.4	2.1	1.1	5.5	17.9						

Trends in plant community composition

Between 2012-2021 the six most common plant species identified throughout the tidal estuary (across the 6 trend sites) in order of overall abundance are *Phalaris arundinacea* (PHAR, non-native), reed canarygrass, *Carex lyngbyei* (CALY, native), lyngby sedge, *Eleocharis palustris* (ELPA, native), common spikerush, *Sagittaria latifolia* (SALA, native), wapato, *Leersia oryzoides* (LEOR, native), rice cut grass, and *Ludwigia palustris* (LUPA, native), water purslane (Table 28, Figure 57-Figure 63). While these species are the most common and abundant across all sites over the years, they are not necessarily present at all sites every year. For example, *P. arundinacea* does not grow at Ilwaco, likely due to the saline conditions present at this wetland (Kidd 2017). However, it is found growing in abundance at all the other trend sites across the lower river (Table 28, Figure 57-Figure 63). In 2021, *P. arundinacea* cover levels stayed relatively consistent to those observed in 2020 and previous years, however, at Cunningham, there was a significant increase in *P. arundinacea* levels from 21% in 2018 to 68% in 2021. Franz Lake also experienced a small increase from 11% in 2018 to 30% in 2021. (Table 28-Table 29, Figure 57-Figure 63). *P. arundinacea* frequency (spread across the site) decreased at Cunningham, but only slightly from 74 plots in 2018 to 63 plots in 2021, and overall *P. arundinacea* frequency increased significantly at Franz Lake from 60 plots in 2018 to 75 plots in 2021 (Table 29). This shift in *P. arundinacea* levels observed at Cunningham and Franz Lake is likely a product of both very low freshet flooding conditions in 2021 (Figure 67) and, at Cunningham Lake, change in grazing pressure. The last several years cattle have heavily grazed Cunningham Lake wetlands; it is well known that cattle pressure can significantly reduce *P. arundinacea* abundance during the growing season (Kidd 2017). Generally, *P. arundinacea* abundance has been found to decrease in years of greater freshet discharge levels, especially in Cunningham Slough, Campbell Slough, and Franz Lake where wetland water levels are tightly correlated with Columbia River discharge conditions, higher water levels making growing conditions less favorable for *P. arundinacea* (Figure 67).

C. lyngbeyi grows in abundance at Ilwaco Slough, Welch Island, and Whites Island but is not found at Cunningham Lake, Campbell Slough, or Franz Lake (Table 30, Figure 58). In 2021, *C. lyngbeyi* levels increased slightly at Ilwaco, remained close to the historic mean at Whites Island, and decreased across Welch Island compared to historic levels. Both Ilwaco and Welch remained below longterm average cover conditions. In 2021, Ilwaco Slough *C. lyngbeyi* cover decreased by 8% compared to 2020, and Welch Island and Whites Island cover levels have stayed relatively stable 2018-2021 (Table 30, Figure 58). Generally, *C. lyngbeyi* abundance has been found to increase in years of greater freshet discharge levels, especially in Ilwaco Slough, where salinity levels are reduced during large discharge years, making growing conditions more favorable for *C. lyngbeyi* (Figure 67).

E. palustris is the only species found growing across all trend sites, however its abundance does range widely, only being found in trace amounts at Ilwaco Slough, and low levels at Whites Island, Welch Island, and Franz Lake, while it is generally found in abundance at Cunningham Lake and Campbell Slough (Table 30, Figure 59). In 2020 *E. palustris* levels were lower than longterm averages across all sites, this low marsh species was clearly impacted by the high water levels observed in 2020, and saw a rebound closer to longterm averages across sites in 2021 (Table 30, Figure 59).

S. latifolia follows a similar trend to *E. palustris*. However, it is not found growing in Ilwaco Slough. In 2021, *S. latifolia* levels were equivalent to longterm averages at Welch Island (7%), greater than the longterm average at Cunningham Lake (20%) and Franz Lake (30%), and lower at Campbell Slough (12%, but 22% at the new Campbell location) and Whites Island (10%; Table 30, Figure 60). *S. latifolia* has been found to have a delayed reaction to freshet conditions, with lower freshet conditions resulting in an increase in *S. latifolia* abundance the following year, which was clear shift between the 2020 and 2021 cover results.

Ludwigia palustris is a common and consistent species found across all sites (minus Ilwaco Slough), typically averaging less than 5% in overall relative cover. In 2021, *L. palustris* was not found on Welch or Whites. Comparatively, *L. palustris* levels were higher than longterm averages at Cunningham Lake and Campbell Slough and were equivalent to longterm averages at Franz Lake (Table 30, Figure 62).

Leersia oryzoides, is also a common and consistent species found across all sites (minus Ilwaco Slough), typically averaging less than 3% in overall relative cover, 2021 levels were similar to those observed historically across all sites (Table 30, Figure 61). The new Campbell Slough Channel (ungrazed) monitoring location had a robust 14% *L. oryzoides* mean abundance in 2021, which may indicate it is intolerant of grazing pressure observed commonly at Campbell Slough and Cunningham Lake.

While not a common species across all the trend sites *Polygonum amphibium* (POAM, native), water knotweed, it is an important species because it has become dominant at Franz Lake. *P. amphibium* levels have significantly increased since 2011, taking over dominance from *P. arundinacea* on the site in 2012 (an extreme high-water year for the site Figure 38) and generally increasing in cover (and *P. arundinacea* declining in cover) every year following (Table 30, Figure 63) until 2021. In 2021, *P. amphibium* level dropped (34%) slightly below the longterm average (37%) (Table 30, Figure 63)

Between 2011 and 2021, *P. amphibium* levels at Franz Lake have also be found to follow a similar trend to *S. latifolia* with a one year delayed reaction to decreased freshet conditions, lower freshet conditions (lower water levels across the wetland site) resulting in an increase in *P. amphibium* cover the following growing year (Figure 63). For both species this might be a result of increased rhizome stores from positive growing conditions (low water levels), providing for more robust growth in the following growing season, assuming the freshet conditions return to an average condition.

The average percent cover of all plant species at each trend site is provided in Appendix D, along with the wetland elevation ranges for each site.

Table 28. The overall longterm mean cover of the 6 most commonly occurring plant species across all six trend sites from 2012-2021. Species are listed in order of overall average relative % cover.

Scientific Name Common Name	Wetland Status	Category	Native	Relative Cover (%) between 2012-2021						
				Ilwaco	Welch	Whites	Cunningham	Campbell	Campbell -Channel	Franz Lake
<i>Phalaris arundinacea</i> reed canarygrass	FACW	grass	no	0.0	20.1	40.7	44.9	49.7	63.5	20.7
<i>Carex lyngbyei</i> lyngby sedge	OBL	sedge	yes	46.2	39.7	13.0	0.0	0.0	0.0	0.0
<i>Eleocharis palustris</i> common spikerush	OBL	sedge	yes	0.0	7.3	7.3	27.5	29.1	21.7	12.0
<i>Sagittaria latifolia</i> wapato	OBL	herb	yes	0.0	7.0	12.9	15.8	16.1	22.2	13.8
<i>Leersia oryzoides</i> rice cut grass	OBL	Grass	yes	0.0	2.2	4.0	5.7	3.1	14.2	3.9
<i>Ludwigia palustris</i> water purslane	OBL	herb	yes	0.0	6.3	1.9	9.2	6.6	3.7	2.8

Table 29. *Phalaris arundinacea* (reed canarygrass) average relative % cover and frequency (% of sample plots) at the trend sites between 2005 and 2021. Mean relative cover only calculated among plots that contain reed canarygrass, longterm mean also highlighted. ND indicates No Data.

Site (Rkm)	Ilwaco		Welch		Whites		Cunningham		Campbell		Campbell -		Franz	
	Slough		Island		Island		Lake		Slough		Channel		Lake	
	6		53		72		145		149		149		221	
	Rel Cover	% Freq	Rel Cover	% Freq	Rel Cover	% Freq	Rel Cover	% Freq	Rel Cover	% Freq	Rel Cover	% Freq	Rel Cover	% Freq
Mean	0	0	20	33	41	85	45	68	50	51	63	63	21	67
2021	0	0	14	59	25	81	68	63	44	50	63	63	30	75
2020	0	0	31	22	30	81	52	65	45	52	ND	ND	22	53
2019	0	0	14	44	29	91	43	79	31	60	ND	ND	21	60
2018	0	0	11	63	27	89	21	74	33	53	ND	ND	11	60
2017	0	0	17	32	37	82	21	81	43	42	ND	ND	10	75
2016	0	0	31	23	49	84	44	75	51	51	ND	ND	18	61
2015	0	0	22	25	54	86	61	68	54	50	ND	ND	16	61
2014	0	0	20	38	46	88	32*	64	50	48	ND	ND	16	46
2013	0	0	65	13	52	85	56	54	64	44	ND	ND	18	66
2012	0	0	33	18	45	83	33	62	24	49	ND	ND	8	69
2011	0	0	ND	ND	46	88	15	75	44	62	ND	ND	27	81
2010	ND	ND	ND	ND	49	86	70	69	53	58	ND	ND	ND	ND
2009	ND	ND	ND	ND	43	80	58	56	72	48	ND	ND	38	75
2008	ND	ND	ND	ND	ND	ND	58	60	70	47	ND	ND	41	93
2007	ND	ND	ND	ND	ND	ND	44	77	38	48	ND	ND	ND	ND
2006	ND	ND	ND	ND	ND	ND	50	63	79	49	ND	ND	ND	ND
2005	ND	ND	ND	ND	ND	ND	65	68	66	63	ND	ND	ND	ND

*A different sampling design was used at Cunningham Lake in 2014, so results are not directly comparable to the other years.

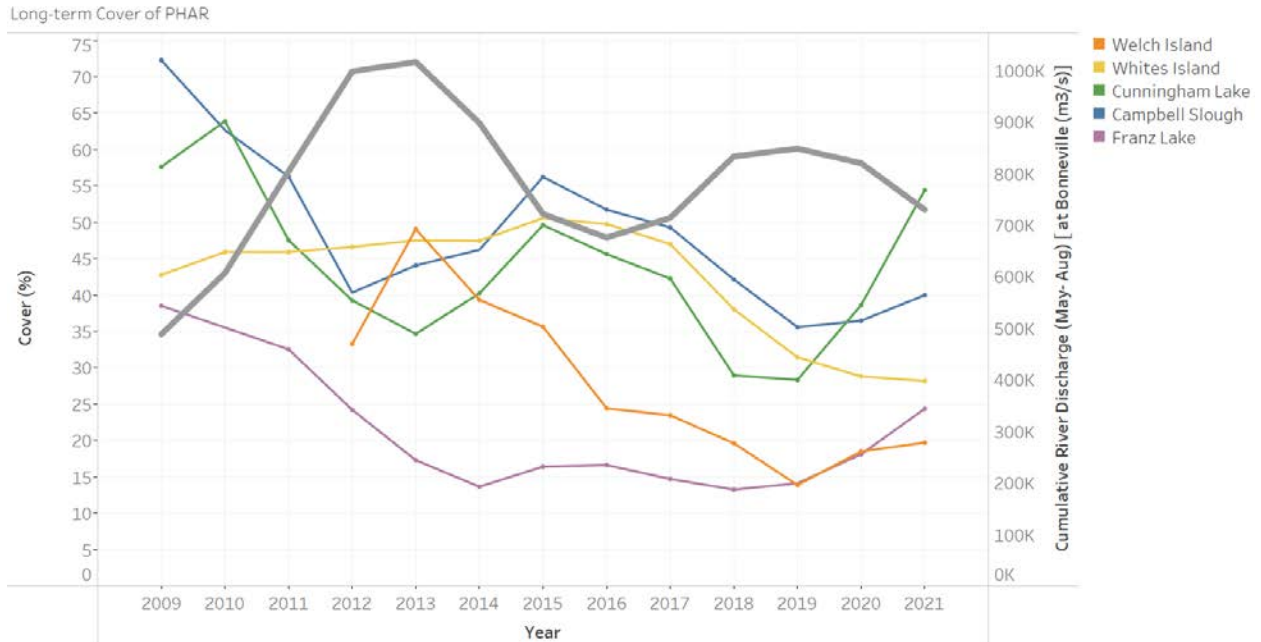


Figure 57. Annual mean relative % cover, *Phalaris arundinacea* (PHAR, non-native), reed canarygrass, for all trend sites. Annual cumulative river discharge from May-Aug included for annual water year context (line is in gray, see Section 3.3.1). Relative species cover data can also be found in Table 30.

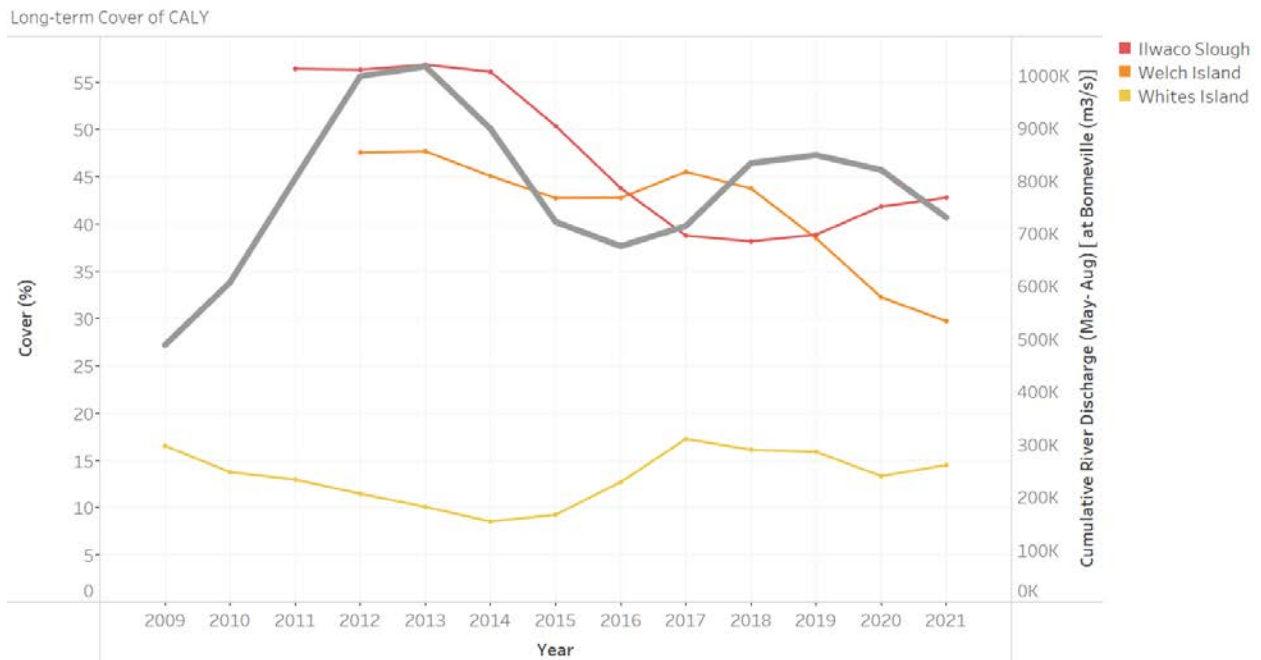


Figure 58: Annual mean relative % cover for *Carex lyngbyei* (CALY, native), lyngby sedge, for all trend sites. Annual cumulative river discharge from May-Aug included for annual water year context (line is in gray, see Section 3.3.1). Relative species cover data can also be found in Table 30.

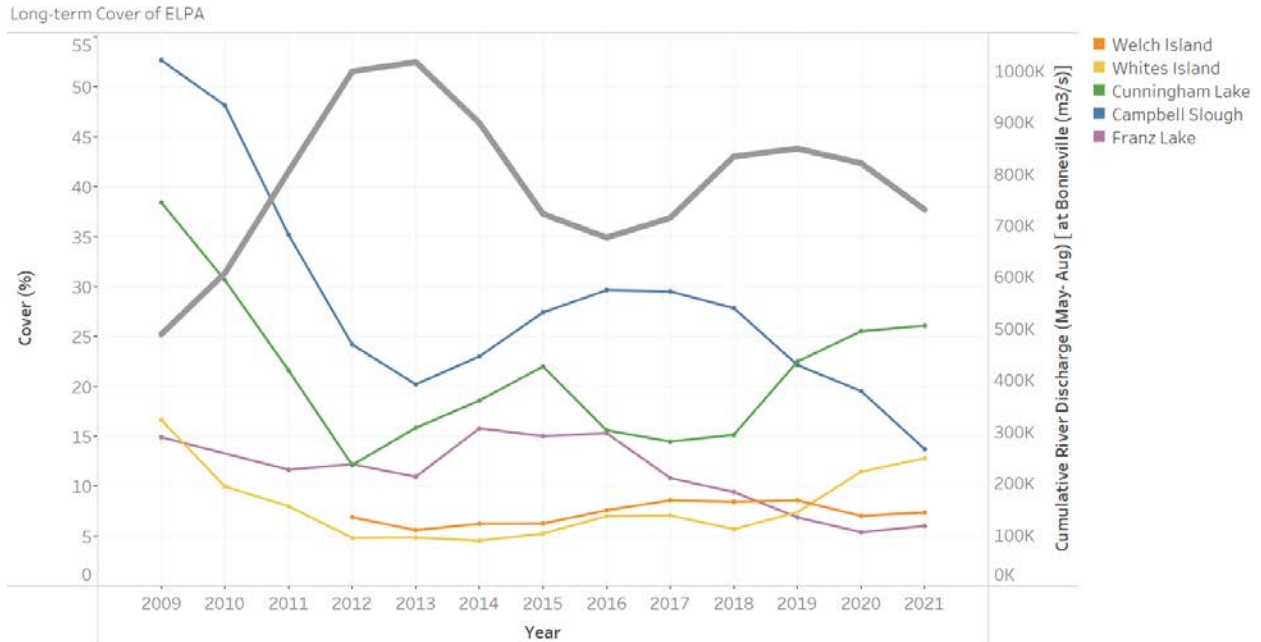


Figure 59. Annual mean relative % cover for *Eleocharis palustris* (ELPA, native), common spikerush. Annual cumulative river discharge from May-Aug included for annual water year context (line is in gray, see Section 3.3.1). Relative species cover data can also be found in Table 30.

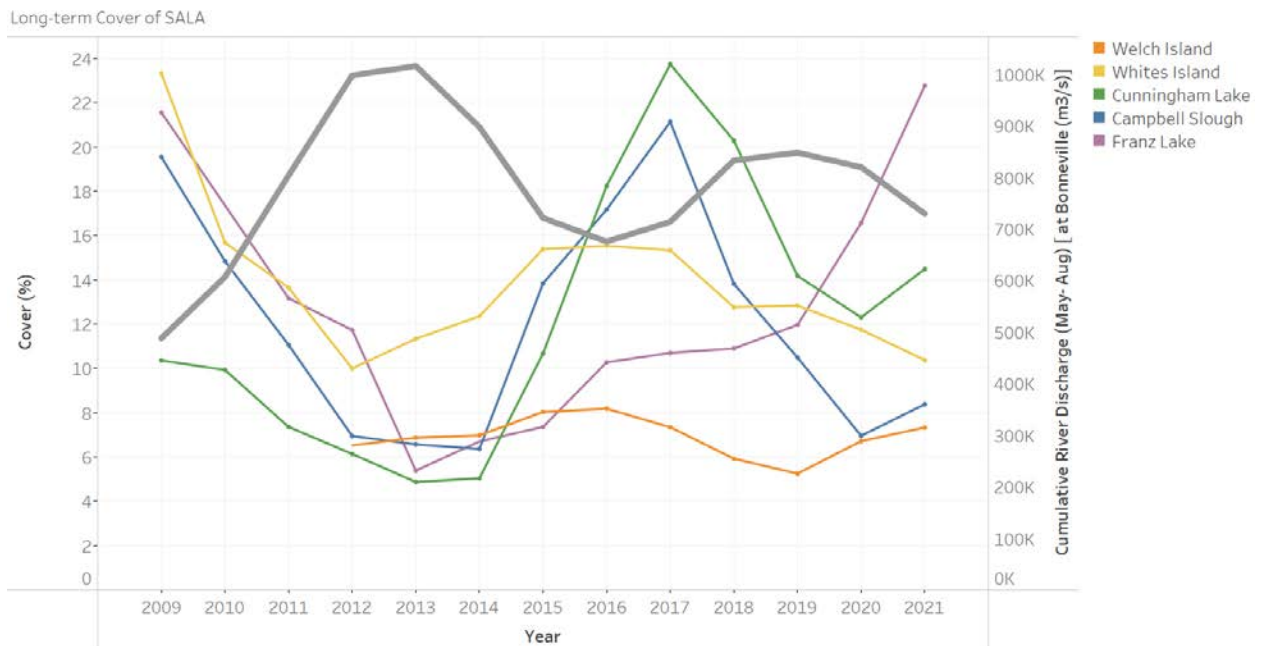


Figure 60. Annual mean relative % cover for *Sagittaria latifolia* (SALA, native). Annual cumulative river discharge from May-Aug included for annual water year context (line is in gray, see Section 3.3.1). Relative species cover data can also be found in Table 30.

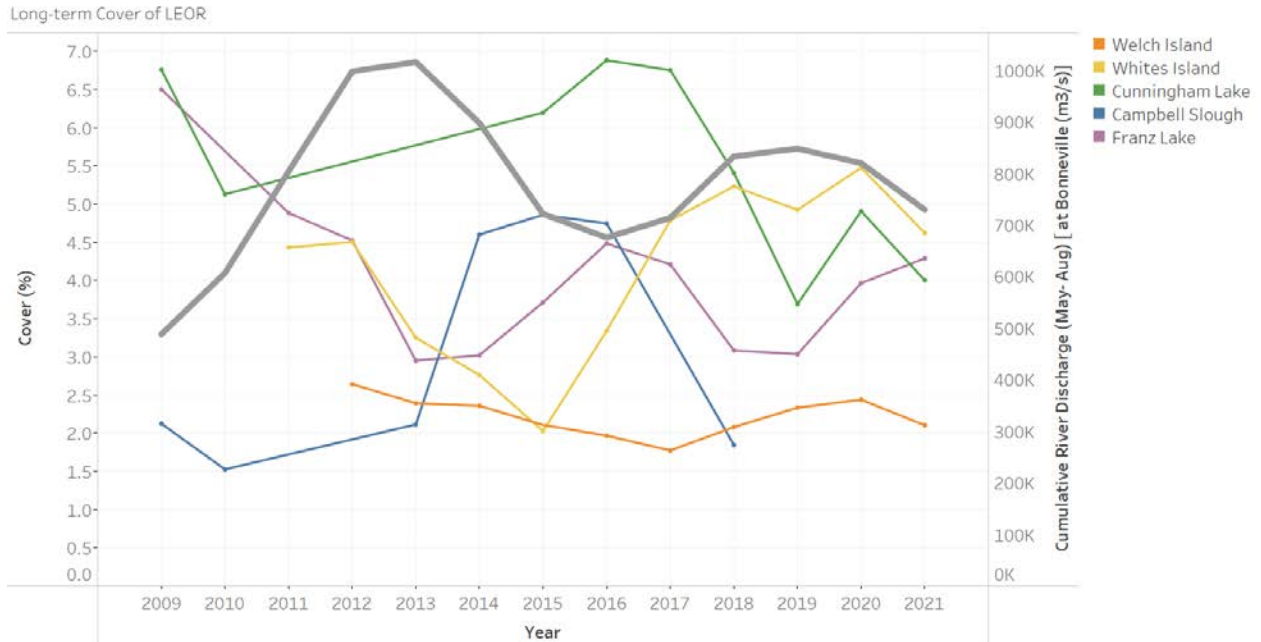


Figure 61. Annual mean relative % cover for *Leersia oryzoides* (LEOR, native), rice cut grass. Annual cumulative river discharge from May-Aug included for annual water year context (line is in gray, see Section 3.3.1). Relative species cover data can also be found in Table 30.

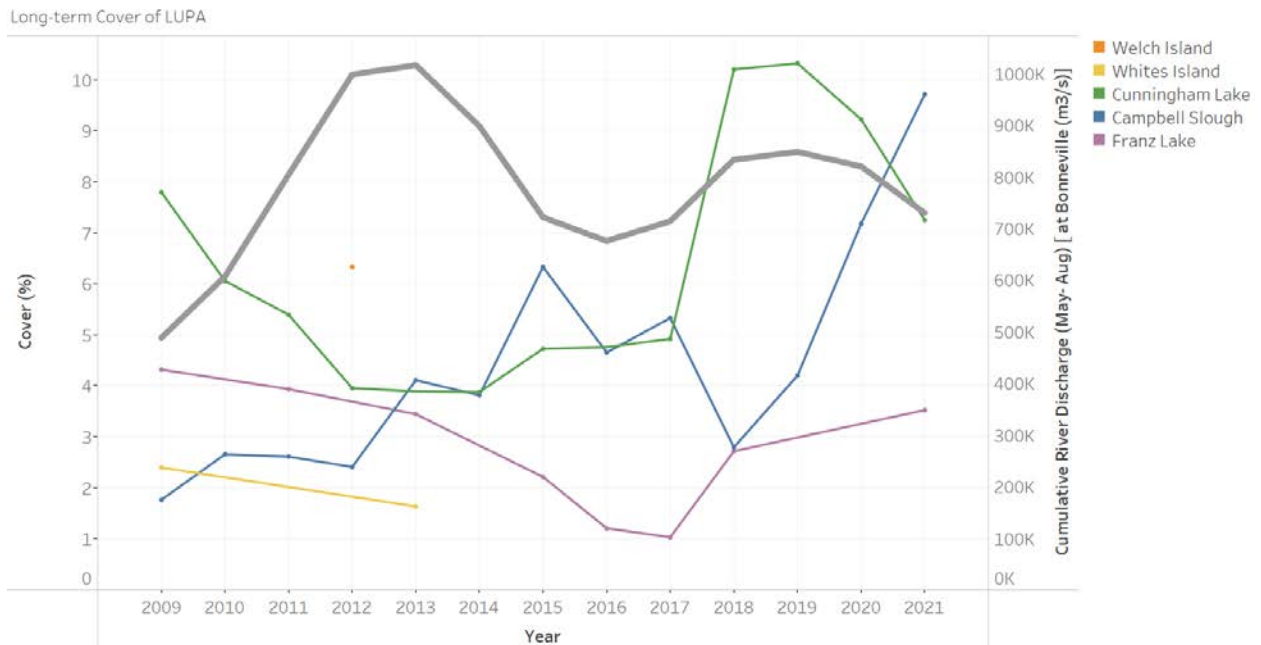


Figure 62. Annual mean relative % cover for *Ludwigia palustris* (LUPA, native), water purslane. Annual cumulative river discharge from May-Aug included for annual water year context (line is in gray, see Section 3.3.1). Relative species cover data can also be found in Table 30.

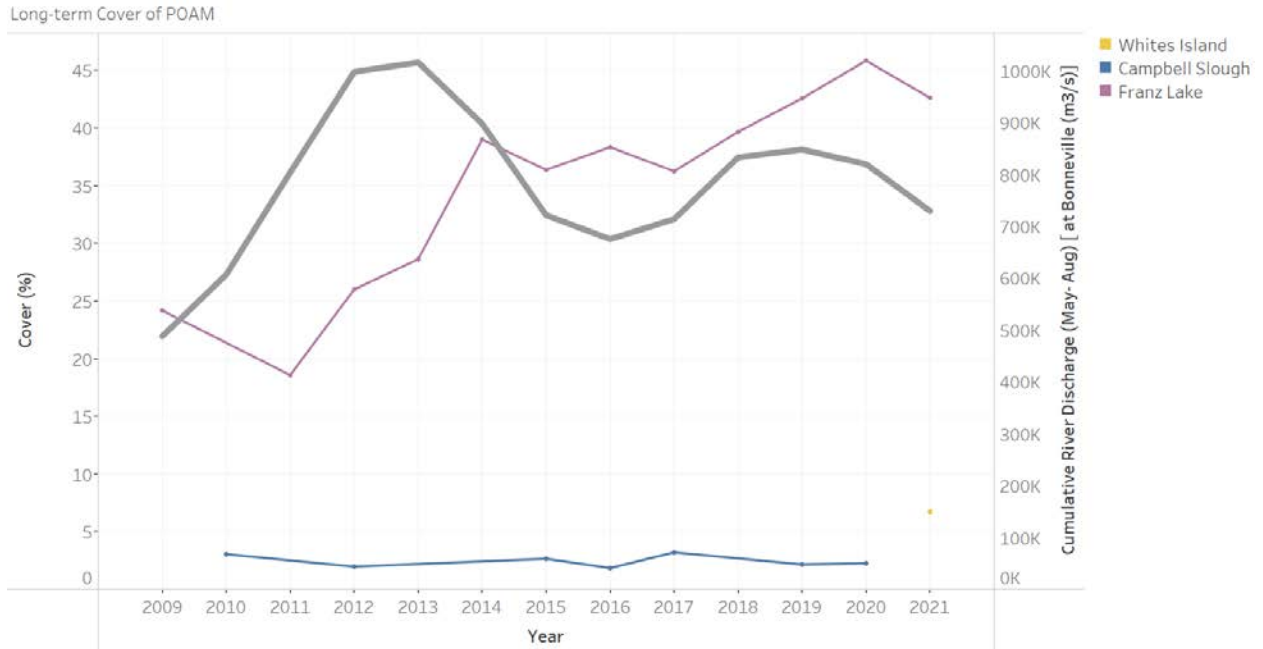


Figure 63. Annual mean relative % cover for *Polygonum amphibium* (POAM, native), water knotweed. Annual cumulative river discharge from May-Aug included for annual water year context (line is in gray, see Section 3.3.1). Relative species cover data can also be found in Table 30.

Table 30: Overall total cover of dominant and common plant species found across all six trend sites, mean relative cover calculated within plots where each species was identified. *Carex lyngbyei* (CALY, native), lyngby sedge, *Eleocharis palustris* (ELPA, native), common spikerush, *Leersia oryzoides* (LEOR, native), rice cut grass, *Ludwigia palustris* (LUPA, native), water purslane, *Phalaris arundinacea* (PHAR, non-native), reed canarygrass, *Sagittaria latifolia* (SALA, native), Wapato, and *Polygonum amphibium* (POAM, native), water knotweed.

	Plant Code	Mean	2021	2020	2019	2018	2017	2016	2015	2014	2013	2012	2011	2010	2009	2008	2007	2006	2005
Ilwaco Slough	CALY	46	40	48	40	37	39	38	39	54	58	56	56						
	ELPA	3							1		5								
Welch Island	CALY	40	28	29	32	35	48	48	41	40	48	48							
	ELPA	7	7	6	9	6	11	8	7	8	4	7							
	LEOR	2	2	2	2	3	2	2	2	2	2	3							
	LUPA	6										6							
	PHAR	26	14	31	14	11	17	31	22	20	65	33							
	SALA	7	7	9	6	5	5	8	10	7	7	7							
Whites Island	CALY	13	14	13	16	11	20	17	14	7	7	12	11	11	17				
	ELPA	8	9	15	14	5	3	9	9	3	3	7	4	3	17				
	LEOR	4	1	9	4	4	7	5	2	3	1	5	4						
	LUPA	2									1				2				
	PHAR	41	25	30	29	27	37	49	54	46	52	45	46	49	43				
	POAM	7	7																
	SALA	13	10	9	13	14	12	13	21	13	12	12	10	8	23				
Cunningham Lake	ELPA	27	24	17	37	22	8	15	20	12	34	10	4	23	38	44	29	59	55
	LEOR	5	2	7	4	4	3	9	8					3	7				
	LUPA	7	16	1	5	22	5	4	6	4	4	3	4	4	8	10	15		
	PHAR	47	68	52	43	21	21	44	61	32	56	33	15	70	58	58	44	50	65
	POAM	11																	11
	SALA	15	20	14	10	13	19	28	24	3	6	7	2	9	10	27	11	23	28
Campbell Slough	ELPA	30	10	9	21	28	17	38	33	18	32	20	9	44	53	46	26	52	61
	LEOR	3				1		3	2	10	3			1	2				

	Plant Code	Mean	2021	2020	2019	2018	2017	2016	2015	2014	2013	2012	2011	2010	2009	2008	2007	2006	2005
	LUPA	6	9	13	8	1	4	4	9	2	9	1	3	4	2	13	8		
	PHAR	51	44	45	31	33	43	51	54	50	64	24	44	53	72	70	38	79	66
	POAM	3		1	1		5	1	4			1		3				5	
	SALA	16	12	4	9	8	15	19	30	3	9	7	3	10	20	34	8	53	36
Campbell Slough (New 2021)	ELPA	22	22																
	LEOR	14	14																
	LUPA	4	4																
	PHAR	63	63																
	SALA	22	22																
Franz Lake	ELPA	11	9	5	4	7	9	12	11	23	11	13	8		15	17			
	LEOR	4	3	5	4	2	3	4	6	3	2	4	3		7				
	LUPA	3	3			6	2	1	1		2		4		4				
	PHAR	21	30	22	21	11	10	18	16	16	18	8	27		38	41			
	POAM	35	34	48	47	43	38	38	33	44	32	41	13		24	26			
	SALA	15	30	24	14	11	10	11	11	9	3	9	5		22	38			

3.3.3.2 Drivers of Plant Community Status and Trends

3.3.3.2.1 Wetland Hydrology

One of the largest mechanisms of change in the tidal wetlands of the Columbia River estuary is the annual timing, duration, and magnitude of the freshet. The freshet typically occurs in early spring following spring rain events which coincide with the melting of the regional snowpack. Since 2011 the freshet floods have occurred as early as March and as late as June. Timing of these annual flood events can determine the amount of time tidal marshes, especially in the upper estuary, are exposed during the growing season. Across all wetlands, a drawdown of flood waters is essential for plant growth and biomass accumulation. Two metrics represent these dynamic flooding conditions and correlate well with plant community change in the upper estuary fluvial dominated zone: 1) the mean daily marsh inundation (% time) during the month of August (see Section 3.3.1) and 2) the annual freshet accumulated discharge.

Comparing mean marsh elevation and common plant species distributions across all EMP sites (except Ilwaco which only shares *C. lyngbyei* in common), it is clear that within wetland plant community zonation is similar, even if the elevations (m, NAVD88) in which these species are found are different, increasing from the lower river sites to the upper river sites (Figure 64). By evaluating the mean % time these plant communities are inundated daily across all the sites (Figure 65), it is clear that inundation rates are important and consistent drivers of plant community establishment within each site. The graph of common species shows that they are found growing within similar inundation zones across the sites. However, the variability of daily inundation range increases from the lower river sites to the upper river sites (Figure 65). This variability is not surprising as hydrology in the upper river sites can heavily depend on water year and the freshet conditions (see Section 3.3.1).

Combining data from Welch Island, Whites Island, Cunningham Lake, and Campbell Slough, it was found that annual mean % *P. arundinacea* was strongly correlated with mean % daily inundation for the month of August across all sites (Figure 66). These data may provide useful information for future restoration planning, sites with an anticipated >30 % daily inundation (in August) rate may provide improved habitat opportunities for native wetland species such as *Carex lyngbyei* (CALY, native), lyngby sedge, *Eleocharis palustris* (ELPA, native), and *Sagittaria latifolia* (SALA, native), Wapato. The 30% daily inundation rate appears to be an important lower threshold in the distribution of *P. arundinacea* observed across multiple sites in the estuary (Figure 65 and Figure 66).

The annual Columbia River freshet accumulated discharge was also found strongly correlated with the year to year variability of % *P. arundinacea* cover within each site, greater freshet levels corresponding with lower % *P. arundinacea* cover at Cunningham Lake ($R^2 = 0.70$), Campbell Slough ($R^2 = 0.75$), and Franz Lake ($R^2 = 0.61$) (Figure 67). Indicating that annual flooding conditions within sites (% daily inundation) and across the river (freshet accumulated discharge) are important mechanisms driving much of the observed annual variability in *P. arundinacea* dominance across the estuary. These data are supporting the hypothesis that annual flooding conditions in the Columbia can dramatically impact year to year shifts in plant community dynamics, especially the non-native species *P. arundinacea* in the upper river sites. *P. arundinacea* mean annual cover was also found to be tightly negatively correlated with native plant community cover across all river zones except the mouth (Ilwaco has no *P. arundinacea* due to high salinity levels), annual increases in *P. arundinacea* resulting in an overall decrease in native plant cover (Figure 68). Summarizing these findings, site level daily inundation patterns in addition to season freshet flooding conditions are important drivers of native and non-native plant species across the EMP sites.

Dominant native wetland species were also found to have significant longterm trends in abundance tied to annual freshet conditions (water levels across sites during the growing season) including *Carex lyngbyei* (CALY, native), lyngby sedge, *Sagittaria latifolia* (SALA, native), Wapato, and *Polygonum amphibium* (POAM, native), water knotweed which has been discussed briefly in the section above (3.3.3.1). Further exploration of these longterm ecological relationships will be reported in the FY23 EMP synthesis report.

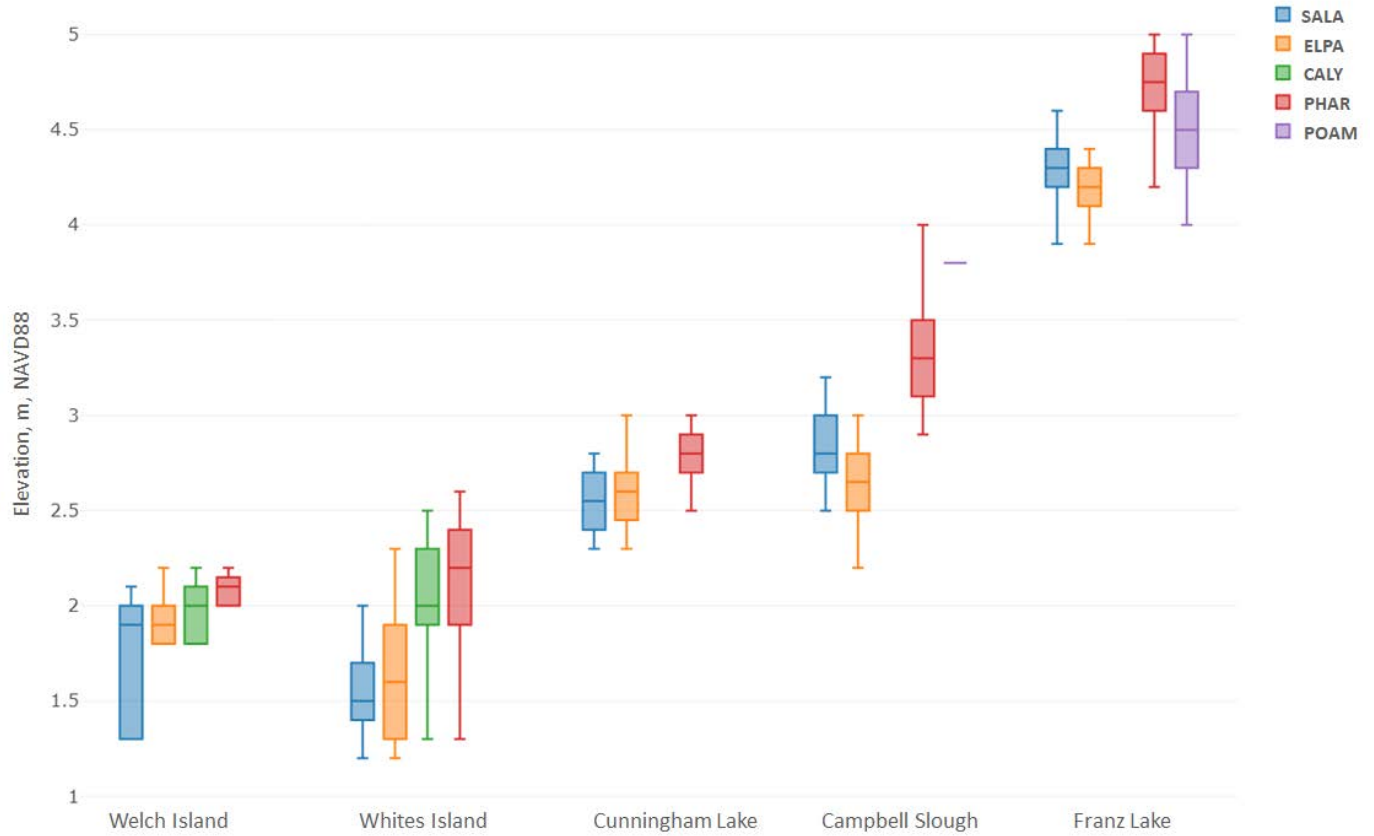


Figure 64: Box plot of elevation range of plant species across each site, sites in order from lower river to upper river from left to right. Species codes: *Carex lyngbyei* (CALY, native), lyngby sedge, *Eleocharis palustris* (ELPA, native), common spikerush, *Phalaris arundinacea* (PHAR, non-native), reed canarygrass, *Sagittaria latifolia* (SALA, native), Wapato, and *Polygonum amphibium* (POAM, native), water knotweed.

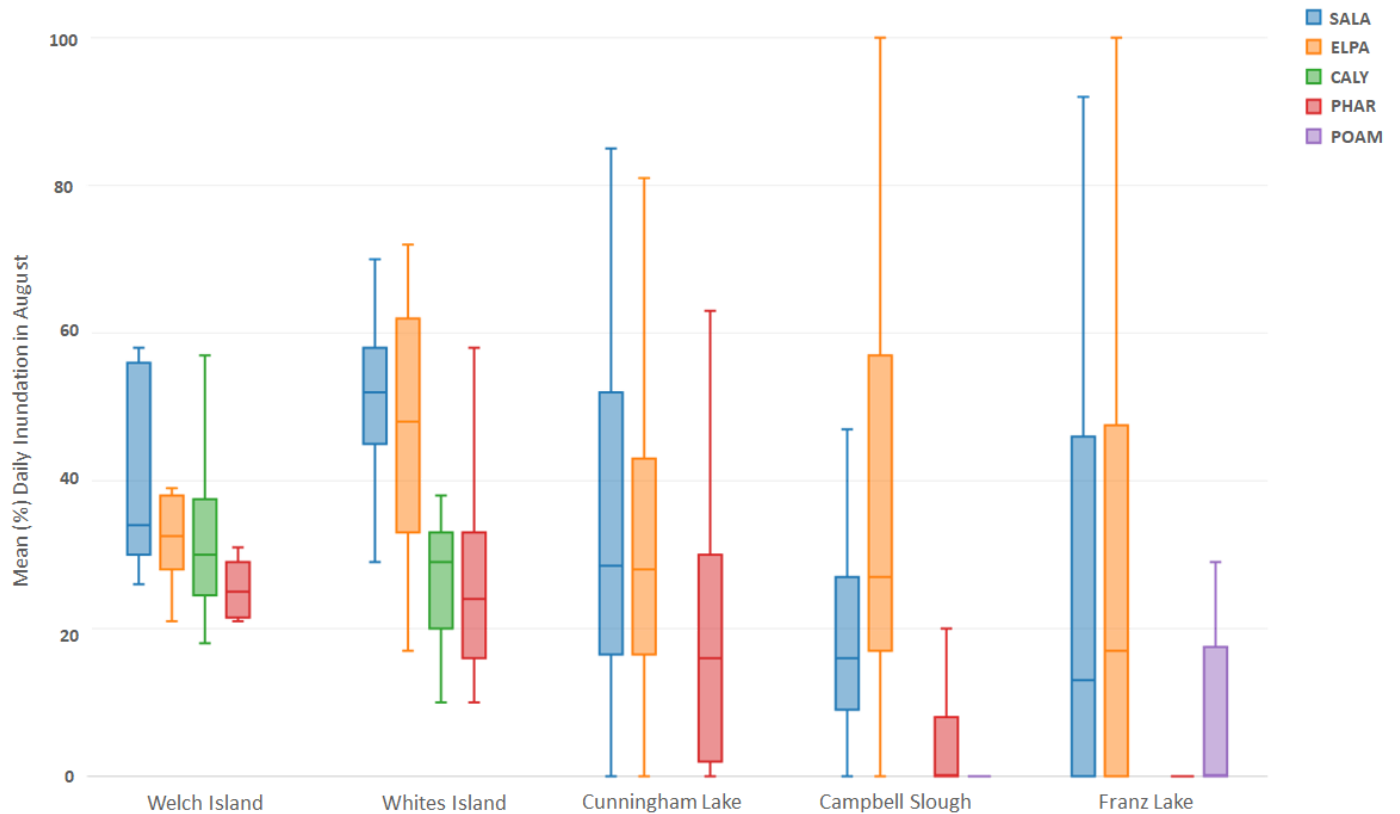


Figure 65: Box plot of daily mean inundation range (% , August - across all years) of plant species across each site, sites in order from lower river to upper river from left to right. Species codes: *Carex lyngbyei* (CALY, native), lyngby sedge, *Eleocharis palustris* (ELPA, native), common spikerush, *Phalaris arundinacea* (PHAR, non-native), reed canarygrass, *Sagittaria latifolia* (SALA, native), Wapato, and *Polygonum amphibium* (POAM, native), water knotweed.

Mean (%) PHAR Cover vs. Mean (%) Daily Inundation (August)

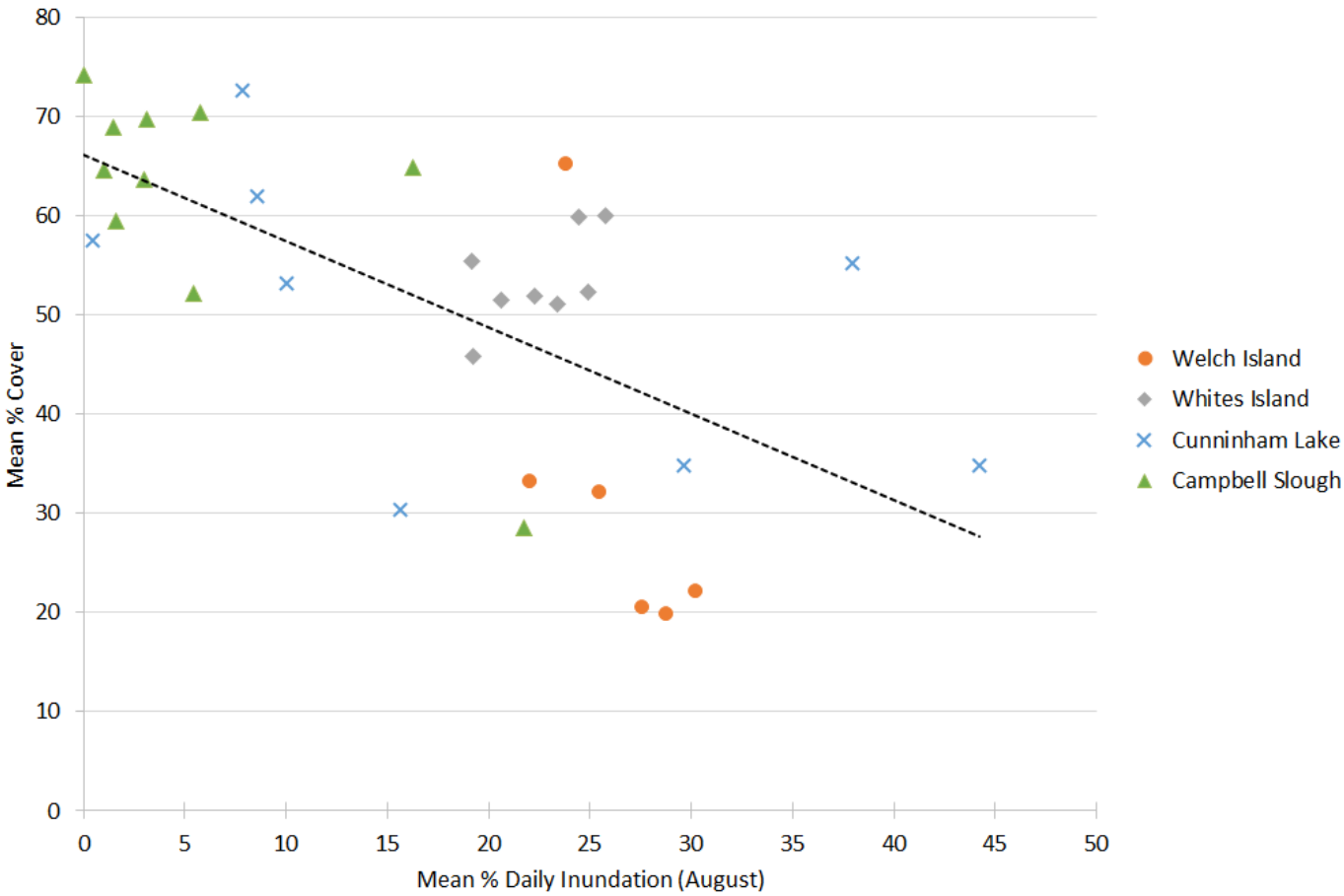


Figure 66: Mean Annual (%) *Phalaris arundinacea* (PHAR, non-native), reed canarygrass, vs. daily (%) inundation (August –2012-2018) of PHAR plots. Linear regression ($y = -0.8711x + 66.207$), $R^2 = 0.41$, $p < 0.001$.

Annual Freshet Discharge vs. Mean Relative PHAR Cover (%)

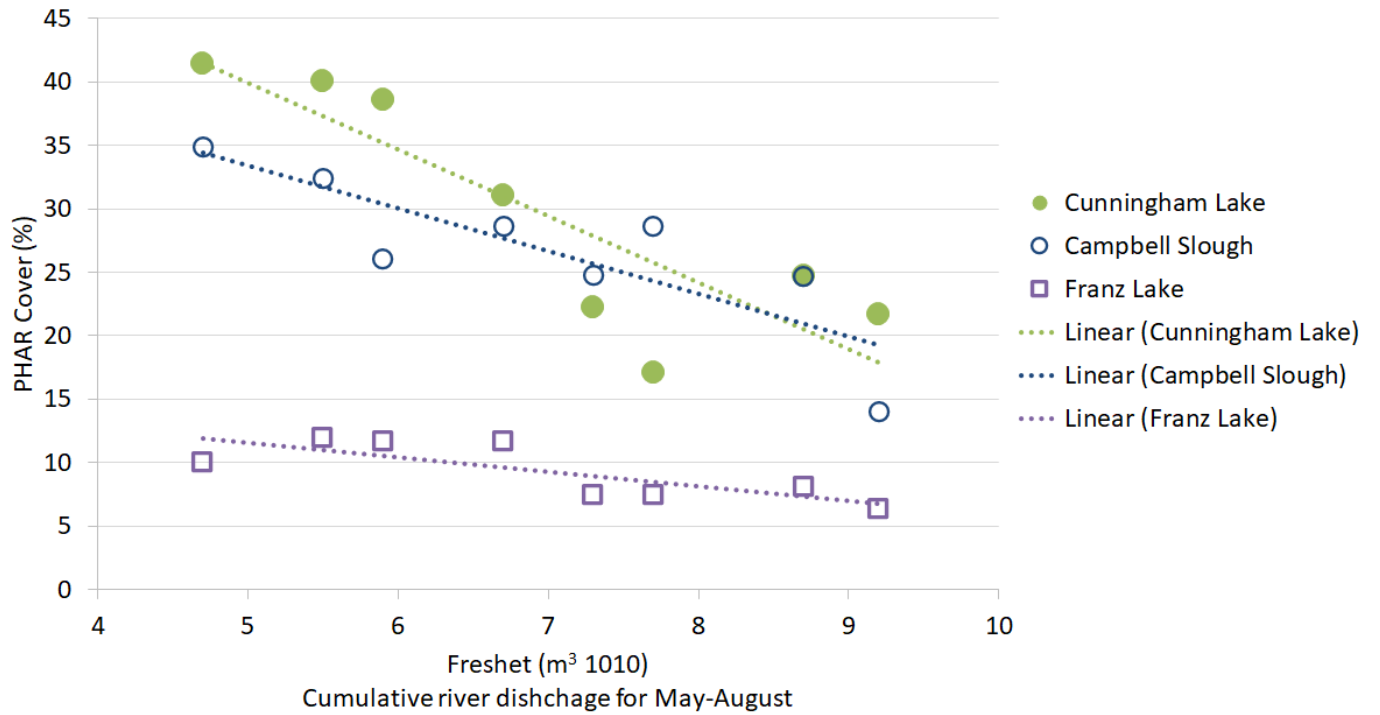


Figure 67: Annual Freshet Cumulative River Discharge (Bonneville Dam, May- August) vs. Mean Annual (%) *Phalaris arundinacea* (PHAR, non-native), reed canarygrass, (2012-2019). Cunningham Lake, linear regression ($y = -3.36x + 50.2$), $R^2 = 0.70$, $p < 0.001$; Campbell Slough linear regression ($y = -5.25x + 66.1$) $R^2 = 0.75$, $p < 0.001$; Franz Lake, linear regression ($y = -1.13x + 17.2$), $R^2 = 0.61$, $p < 0.001$.

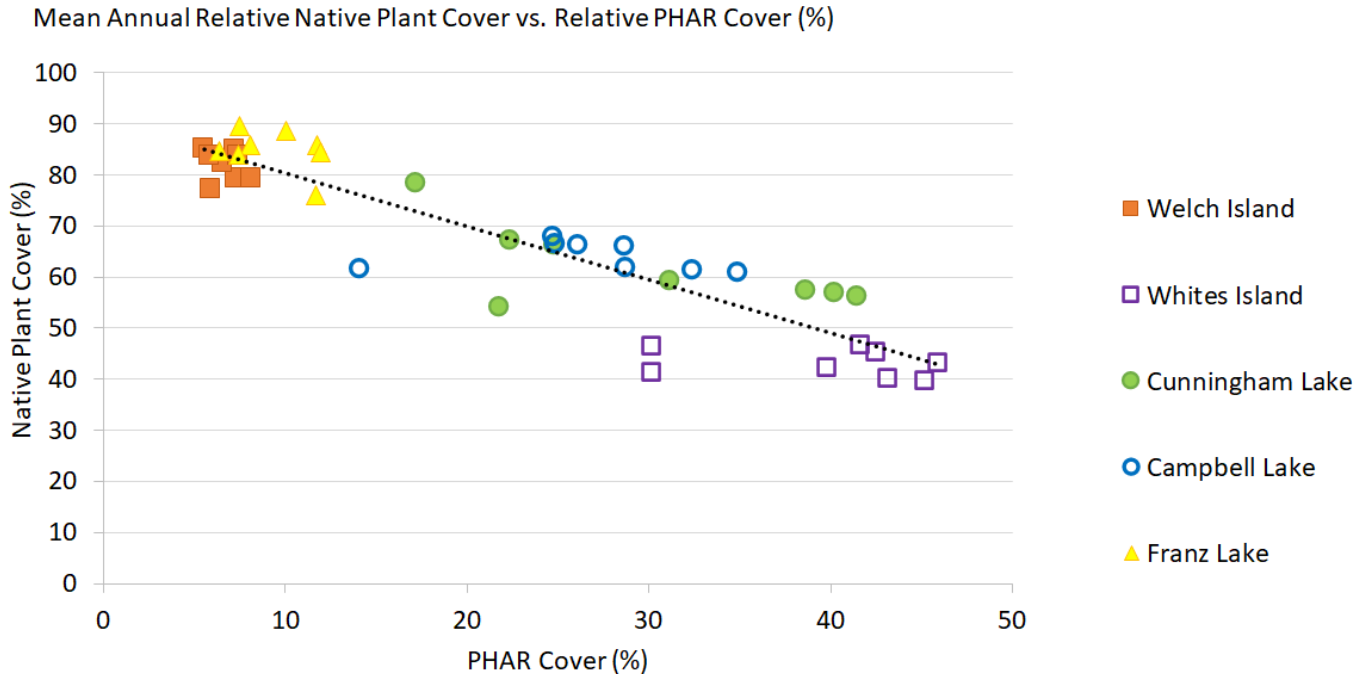


Figure 68: Mean Annual Relative Native Plant Cover vs. Mean (%) *Phalaris arundinacea* (PHAR, non-native), reed canarygrass cover (August –2012-2019). Linear regression ($y = -1.0443x + 90.774$), $R^2 = 0.83$, $p < 0.001$.

3.3.4 Channel Morphology

Channel morphology at the trends sites exhibited low inter-annual variability in years prior to 2016; therefore, only the channel mouth cross section was surveyed in 2016. Channel measurements from previous years are presented with the newly calculated inundation frequency results from 2016 in Table 31. The tidal channels measured at the sites were generally small, with most cross-sectional areas less than 10m² (see Appendix A for locations of the measured channels). Five of the tidal channels surveyed were primary channels feeding directly into the Columbia River, while the channels at the Welch and Whites Island sites were secondary channels that feed into a larger tidal channel. The channels varied in width from 1.3 m to 50.1 m; most becoming narrower with increasing elevation, with the exception of the Ilwaco Slough and Whites Island channels, which were slightly wider at the middle than at the mouth. Channel depth ranged from 0.3 m to 2.1 m, with most channels between 0.9 m and 1.2 m in depth. The Thalweg elevation of the channels was generally between 0.0 and 1.0 m and the channel bank between 1.0 and 2.0 m, relative to CRD. Channel Cross-sections are being re-surveyed in 2021 and 2022, and these data will be reported in the FY23 EMP report.

Table 31. Physical channel metrics measured at each site. The channel mouth (indicated with an *) was measured in 2016; the year of full channel cross section measurement is provided in parentheses after the site code. Channel cross-section and hydrology data collected in 2017 and 2021 are still under analysis and unavailable at the time this report was written, no cross-section data was collected in 2018, 2019, or 2020. The text below is adapted from the 2016 report.

Physical Metrics							
Site (year)	Cross Section	Thalweg Elevation (m, CRD)	Bank Elevation (m, CRD)	Channel Depth (m)	Cross Section Area (m²)	Channel Width (m)	Width: Depth Ratio
Ilwaco Slough (11)	1*	0.87	1.56	0.69	3.3	6.2	9.0
	2	0.70	1.86	1.16	8.94	9.30	8.04
	3	0.90	2.12	1.22	9.73	10.10	8.27
	4	1.01	2.00	0.99	4.33	5.20	5.23
	5	1.17	2.26	1.09	1.58	2.70	2.48
Welch Island (12)	1*	0.30	1.51	1.21	13.0	20.4	16.9
	2	0.36	1.65	1.29	8.75	9.20	7.13
	3	0.71	1.80	1.09	3.96	5.09	4.67
	4	0.78	1.74	0.96	2.07	3.30	3.44
	5	1.31	1.62	0.31	0.42	1.32	4.27
Whites Island (11)	1*	0.42	1.12	0.70	12.1	34.6	49.4
	2	0.34	1.41	1.07	10.8	20.5	19.1
	3	0.61	1.53	0.92	11.1	36.2	39.5
	4	0.92	1.93	1.00	34.0	50.1	50.0
	5	0.44	1.45	1.01	1.90	2.83	2.80
Cunningham Lake (15)	1	0.82	1.26	0.44	5.5	18.3	41.6
Campbell Slough (15)	1	0.80	1.47	0.67	11.7	23.0	34.3
Franz Lake (12)	0*	0.34	2.23	1.89	21.3	23.2	12.2
	3	0.40	1.39	0.99	4.20	14.3	14.4
	4	0.85	1.45	0.60	6.20	13.2	22.0

3.4 Food Web

3.4.1 Primary Production

3.4.1.1 *Emergent Wetland Vegetation*

Biomass sampling is grouped by season and year – such as Summer 2019 sample locations are re-sampled in Winter 2020 to identify season changes in biomass abundance. New sample locations are randomly stratified through the high/low marsh zones each Summer; biomass samples represent a subset of the dominant plant species composing each site. Starting in the summer of 2017 detritus sampling was included in the biomass sampling and analysis to evaluate detrital production and export. In the winter of 2018 (and all sampling events to follow through 2021), biomass sampling protocols changed slightly to accommodate detrital sampling and streamline data collection. This included shifting from “strata” mixed species designations to simple high and low marsh strata descriptions across all sites sampled. This change has also included species biomass weights to be recorded individually to assess species-specific contributions to each high and low marsh stratum (in the past mixes of species were assessed together). In general, these changes will allow for a more detailed understanding of species-specific biomass contributions and still allow for longterm comparisons to overall site, high and low marsh contributions. In 2020, we elected to only sample at Steamboat Slough and Franz Lake due to the COVID-19 pandemic. Furthermore, in 2021, we reduced the number of total plots of 18 per site to 10 per site; however, we sampled all four sites throughout 2021. These shifts in methods (see methods section for full details) should be considered when interpreting the below analysis.

Composition of Biomass

At each longterm monitoring site, aboveground biomass was sampled within the high and low marsh vegetation strata to reduce variability associated with sampling across strata. The dominant species for the strata are identified in Table 32; converted to a percentage of total biomass dry weight/biomass density. In 2021, at Welch Island, the high marsh biomass species stratification remained similar to the longterm abundances, dominated by *Carex lyngbyei*, CALY, native, and *Phalaris arundinacea*, PHAR, non-native; however, the low marsh biomass samples at Welch Island shifted to being dominated completely by *Eleocharis palustris*, ELPA, native. At Steamboat Slough, the high marsh samples remain fairly consistent to previous years, being dominated by both *Juncus effuses*, JUEF, non-native, and *P. arundinacea*, PHAR. Conversely, the low marsh biomass samples at Steamboat Slough have shifted to being dominated by *Sagittaria latifolia*, SALA, native. Whites Island biomass sampling has seen a large increase in *Myosotis laxa*, MYLA/MYSC, and an increase in *C. lyngbyei*, CALY, native. The low marsh biomass samples at Whites Island are dominated by *E. palustris*, ELPA, and *C. lyngbyei*, CALY. The Franz Lake high marsh biomass sampling also remained similar to longterm averages of around 40% *P. arundinacea*, PHAR, and 60% *Polygonum amphibium*, POAM, native. The low marsh biomass sampling at Franz Lake has been focused on *S. latifolia*, SALA dominated areas.

In Table 32 the relative % of each strata by biomass density can be seen changing from year to year and season to season. These trends highlight how low marsh species (across all sites) such as *E. palustris*, ELPA and *S. latifolia*, SALA tend to only have abundant biomass in the summer and when re-surveyed in winter months these species above ground biomass have died off and the detritus has mostly been fluxed out of the site, comparatively species like *Phalaris arundinacea*, PHAR, *Juncus effuses*, JUEF, *Polygonum amphibium*, POAM, and *C. lyngbyei*, CALY, tend to contribute much more to the winter biomass composition, these species retaining dormant stems and stolon's above ground during the winter season. Additionally, we have found *Myosotis laxa*, MYLA/MYSC, biomass increases in the winter, as these other plants die back providing it with more light and room to grow. Over the last several years

winter abundance of *Myosotis laxa*, MYLA/MYSC has grown significantly at Welch Island, this species growing year round.

Table 32. The overall proportion of biomass density of the dominant species ($\geq 5\%$ of total sample by dry biomass) across high and low marsh strata sampled for Welch Island, Steamboat Slough, Whites Island, and Franz Lake. When evaluating changes note that sampling is grouped by season and year – such as Summer 2019 sample locations are re-sampled in Winter 2020. New sample locations are stratified through the high/low marsh zones each summer. There was reduced sampling for Summer 2020 and Winter 2021 due to the COVID-19 pandemic. See Appendix D for all plant code information. Welch Island low marsh strata and Franz Lake (both strata) were not sampled until summer 2018.

Code		Welch Island (Rkm 53)			Steamboat Slough (Rkm 57)					Whites Island (Rkm 72)			Franz Lake (Rkm 221)				
		Summer 2021	Winter 2020	Summer 2019	Summer 2021	Winter 2021	Summer 2020	Winter 2020	Summer 2019	Summer 2021	Winter 2020	Summer 2019	Summer 2021	Winter 2021	Summer 2020	Winter 2020	Summer 2019
High Marsh	BICE								6%								
	CALY	41%	24%	44%						40%							
	IRPS											11%					
	JUEF				47%	42%	52%	37%	19%								
	MYSC		30%							23%		6%					
	PHAR	59%	46%	50%	53%	58%	48%	63%	75%	37%	100%	84%	49%	50%	34%	33%	44%
	POAM												51%	50%	66%	67%	56%
	SALA			6%													
Low Marsh	AGSP										7%						
	BICE				6%				21%								
	CAHE										1%						
	CALY		35%	33%						39%	2%	55%					
	ELCA		2%								3%	7%					
	ELPA	100%		52%					32%	61%							7%
	PHAR										84%						
	POAM					100%									34%	100%	49%
	POHY		62%	15%					7%		4%						
	POPE				8%		4%	100%									
	SALA				81%		71%		17%			38%	100%		66%		44%
	SCAM				5%				23%								

Overall proportion of biomass contribution from living, dead, and detritus biomass contribution varied across the seasons, living biomass contributing the most during the summer season, standing dead and detritus contributing the most during the winter, with biomass contributions being more evenly split between living, dead, and detritus in the spring reflecting new plant growth across all sites (Table 33). This seasonal look at biomass composition shows the largest flux of standing biomass (living + dead) is between the summer and winter time-period, some of this living and dead biomass shifting to detrital material and most being exported from the sampling areas. The largest flux of detritus out of the wetland occurs during the spring-summer time-period, detrital material showing a gradual increase from summer to spring and then a sharp decline between the spring and summer sampling events (Table 33, Figure 69). While the overall amount of biomass contributed is lower coming out of the low marsh compared to the high marsh strata's, they follow similar patterns of living, dead, and detritus biomass contribution over the seasonal shifts. This is with the exception of Steamboat Slough which showed a decline in low marsh and increase in high marsh biomass production between summer 2017 and 2018 (Figure 70). Following the shift in species contributions on this site (such as shifting from non-native *J. effusus* and *P. arundinacea* to native *S. tabernaemontani*, *E. palustris*, and *S. latifolia* in the low marsh zone), this change is likely reflective of plant community shifts stemming from restoration efforts (

Table 32). Between 2021 and previous years, there was very little change between the proportions of live and dead species for all sites besides Franz Lake. Franz Lake saw a slight decrease in the percentage of dead material and an increase in detritus across the site in from 2019 to later years (Table 33) which may be due to the dynamic changes in hydrology observed at this site from the loss and then re-installation of a longterm beaver dam at the site in 2021, this increased the low marsh productivity (more exposed mudflat for robust plant growth).

Table 33. Overall proportion (by dry biomass) of living (live), dead, and detritus across high and low marsh strata sampled between the winter of 2019 and summer 2021. When evaluating changes note that sampling is grouped by season and year – such as Summer 2019 sample locations are re-sampled in Winter 2020. New sample locations are stratified through the high/low marsh zones each summer. Note that there was reduced sampling for Summer 2020 and Winter 2021 due to the COVID-19 pandemic.

		High Marsh			Low Marsh			Overall		
		Live	Dead	Detritus	Live	Dead	Detritus	Live	Dead	Detritus
Welch Island (Rkm 53)	Summer 2021	94%	1%	5%	95%	1%	4%	94%	1%	5%
	Winter 2020	21%	58%	22%	39%	45%	15%	23%	56%	21%
	Summer 2019	88%	4%	8%	94%	4%	2%	90%	4%	7%
	Winter 2019	19%	49%	32%	39%	39%	22%	31%	43%	26%
	Average	73%	15%	12%	65%	23%	12%	71%	17%	12%
Steamboat Slough (Rkm 57)	Summer 2021	77%	20%	3%	93%	5%	2%	80%	17%	3%
	Winter 2021	41%	52%	7%		100%		40%	53%	7%
	Summer 2020	86%	12%	2%	84%	10%	6%	86%	11%	3%
	Winter 2020	56%	26%	18%		11%	89%	54%	25%	21%
	Summer 2019	83%	6%	11%	97%	1%	2%	85%	5%	9%
	Winter 2019	24%	31%	45%	4%	32%	64%	24%	31%	45%
Average	69%	19%	12%	86%	7%	7%	72%	17%	11%	
Whites Island (Rkm 72)	Summer 2021	86%	9%	5%	92%	3%	5%	87%	8%	5%
	Winter 2020	25%	50%	26%	38%	49%	13%	26%	50%	24%
	Summer 2019	81%	4%	14%	96%		4%	85%	3%	12%
	Winter 2019	20%	59%	21%	29%	29%	41%	22%	51%	27%
	Average	59%	25%	16%	76%	12%	12%	62%	22%	15%
Franz Lake (Rkm 221)	Summer 2021	58%	33%	10%	84%	11%	5%	65%	27%	8%
	Winter 2021	12%	54%	35%			100%	11%	53%	36%
	Summer 2020	62%	35%	3%	57%	11%	32%	61%	30%	9%
	Winter 2020	18%	48%	35%			100%	18%	47%	36%
	Summer 2019	58%	29%	12%	98%	0%	2%	65%	24%	11%
	Winter 2019	3%	43%	54%		2%	98%	3%	43%	55%
	Average	41%	38%	21%	76%	7%	17%	46%	34%	20%

Biomass Dry Weight for All Sites

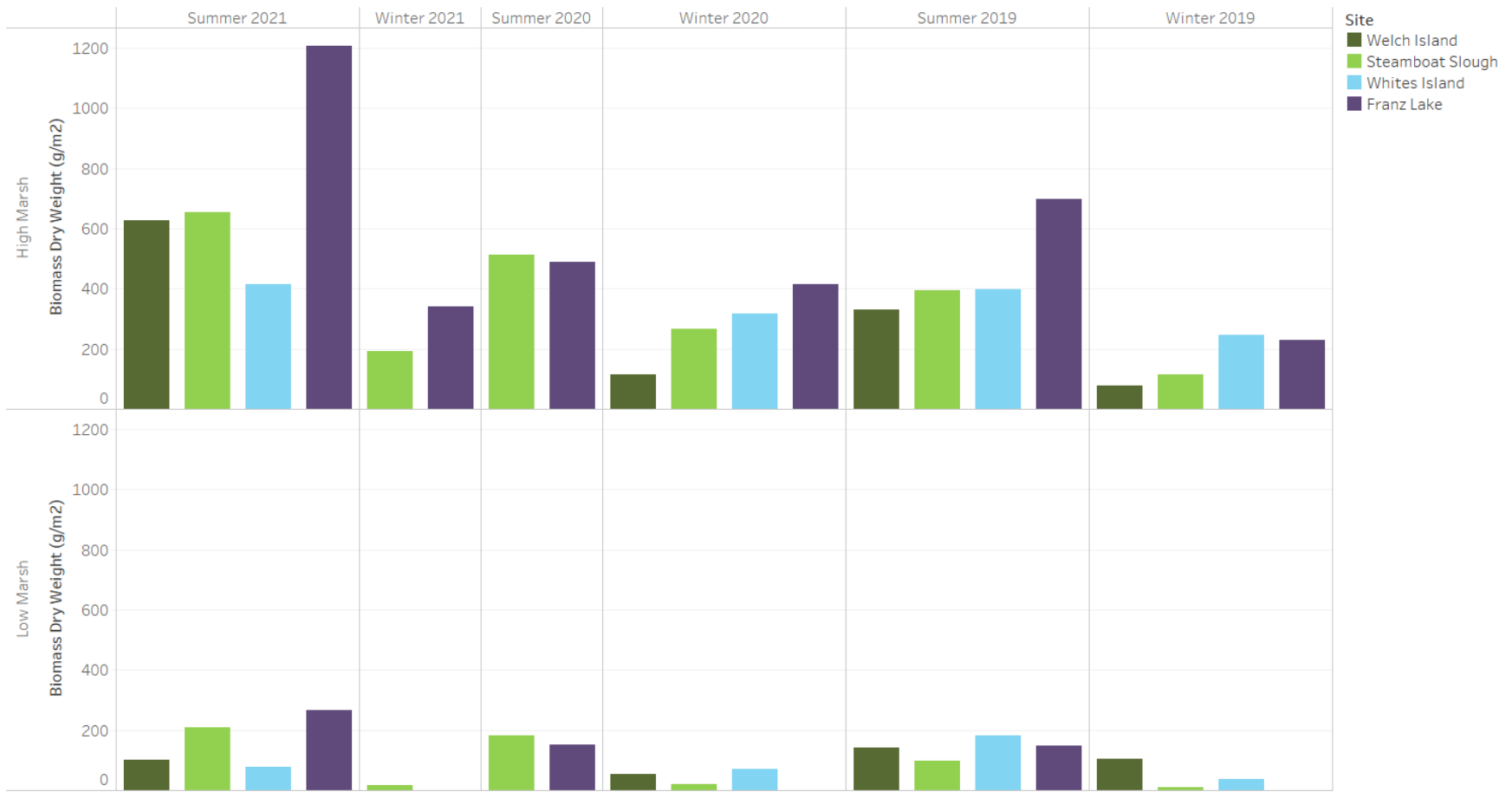


Figure 69: Average aboveground standing stock biomass (living + dead, dry weight g/m²) for summer 2021, through winter 2019 for both the high and low marsh strata across sites sampled. Sites shown in order of rkm from mouth of the Columbia River to the Bonneville dam. Note that sampling was reduced from 16 plots per site to 10 plots per site beginning in Summer 2020. Additionally, note that there was reduced sampling for Summer 2020 and Winter 2021 due to the COVID-19 pandemic. See

			Summer					Winter					Annual
Site	High/Low Marsh	Biomass Year	Elevation	Count	Living + Dead	Detritus	Total (g/m ²)	Count	Living + Dead	Detritus	Total (g/m ²)	Export (g/m ²)	
Welch Island	High	2021-2022	2.16	5	1,758	190	1,948						
		2019-2020	2.06	9	1,252	226	1,479	9	378	212	590	888	
		2018-2019	2.09	9	1,233	80	1,313	5	401	380	781	532	
		2017-2018	2.07	14	922	34	957	12	167	210	378	579	
	Low	2021-2022	1.38	5	253	23	276						
		2019-2020	1.09	9	424	16	441	8	59	21	80	360	
2018-2019		1.59	9	820	75	895	9	376	210	586	308		
Steamboat Slough	High	2021-2022	2.17	5	1,829	111	1,941						
		2020-2021	2.03	8	1,156	48	1,204	8	579	86	664	540	
		2019-2020	2.00	9	1,096	269	1,365	9	560	251	811	554	
		2018-2019	2.03	9	1,459	106	1,565	9	292	472	764	801	
		2017-2018	2.05	7	948	177	1,126	6	470	243	714	412	
	Low	2021-2022	1.53	5	498	25	523						
		2020-2021	1.23	7	495	65	560	7	3	0	3	557	
		2019-2020	1.24	9	254	12	266	9	6	52	59	207	
		2018-2019	1.27	9	153	5	158	8	6	23	29	129	
2017-2018	1.57	14	700	35	735	13	140	75	215	520			
Whites Island	High	2021-2022	1.96	5	1,327	138	1,465						
		2019-2020	2.37	9	1,194	405	1,599	9	740	511	1,251	348	
		2018-2019	2.54	9	1,458	252	1,710	4	867	463	1,330	380	
		2017-2018	2.18	13	1,042	274	1,316	12	710	310	1,020	296	
	Low	2021-2022	1.18	5	284	28	312						
		2019-2020	1.50	9	507	39	546	10	100	30	130	416	
		2018-2019	1.97	10	402	35	437	10	95	135	230	206	
		2017-2018	1.51	6	204	4	208	6	51	47	99	109	

			Summer					Winter				Annual
Site	High/Low Marsh	Biomass Year	Elevation	Count	Living + Dead	Detritus	Total (g/m ²)	Count	Living + Dead	Detritus	Total (g/m ²)	Export (g/m ²)
Franz Lake	High	2021-2022	5.23	4	2,080	404	2,484					
		2020-2021	4.89	9	1,469	99	1,568	9	623	660	1,283	284
		2019-2020	4.06	9	1,709	487	2,196	9	832	882	1,714	482
		2018-2019	4.99	9	1,419	242	1,661	9	384	904	1,287	374
	Low	2021-2022	4.17	4	670	75	745					
		2020-2021	4.17	8	322	297	619	8	0	24	24	595
		2019-2020	3.09	9	394	13	407	9	0	61	61	346
		2018-2019	4.32	9	640	37	677	4	0	43	43	634

Table 34 for all values and standard deviations.

Detritus Dry Weight

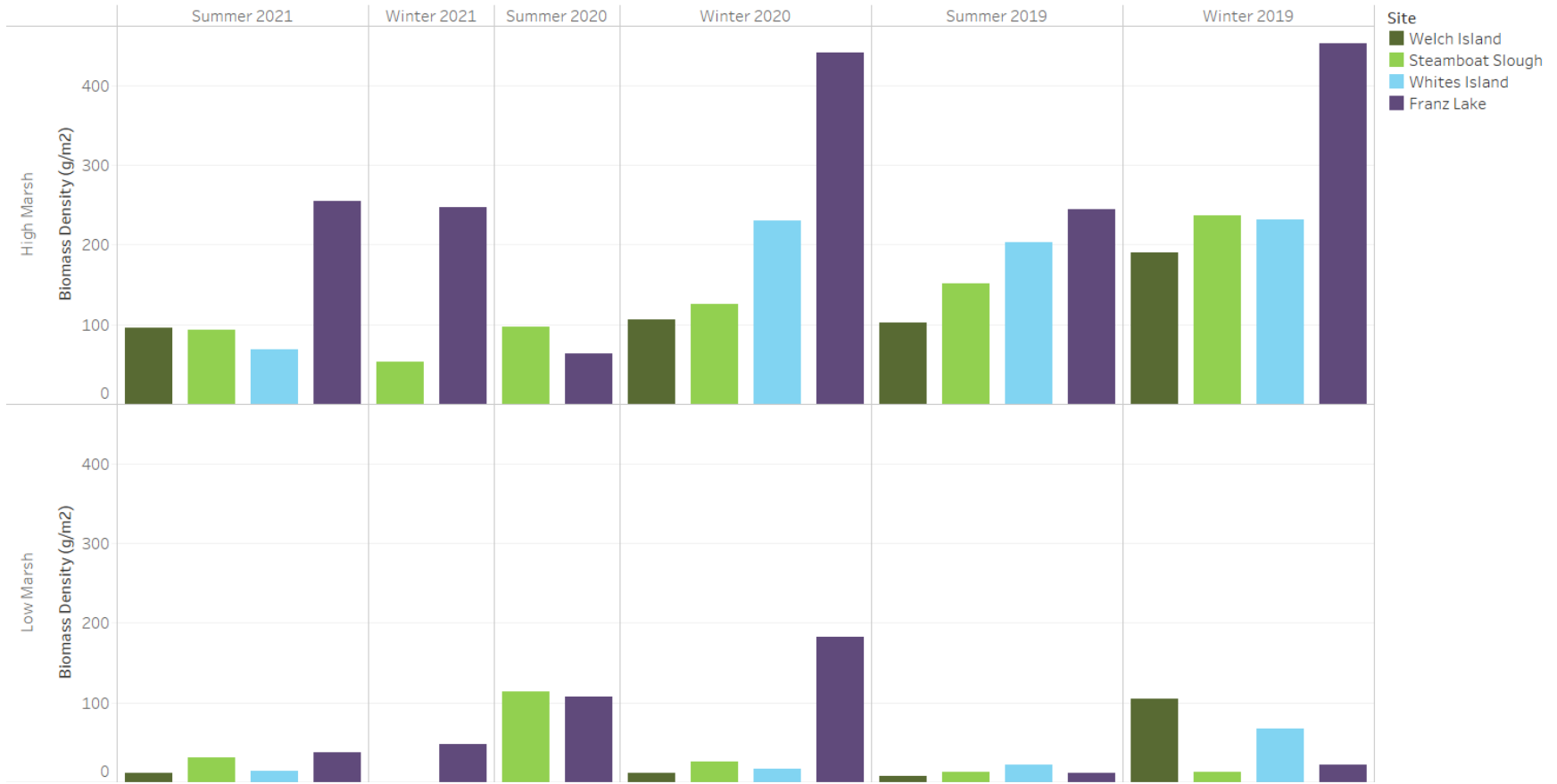


Figure 70: Average detrital biomass (dry weight g/m²) for summer 2021, winter 2021, summer 2020, and winter 2020 for both the high and low marsh strata across sites sampled. Sites shown in order of rkm from mouth of the Columbia River to the Bonneville dam. Note that sampling was reduced from 16 plots per site to 10 plots per site beginning in Summer 2020. Additionally, note that there was reduced sampling for Summer 2020 and Winter 2021 due to the COVID-19 pandemic. See

			Summer					Winter				Annual
Site	High/Low Marsh	Biomass Year	Elevation	Count	Living + Dead	Detritus	Total (g/m ²)	Count	Living + Dead	Detritus	Total (g/m ²)	Export (g/m ²)
	High	2021-2022	2.16	5	1,758	190	1,948					

			Summer					Winter					Annual
Site	High/Low Marsh	Biomass Year	Elevation	Count	Living + Dead	Detritus	Total (g/m ²)	Count	Living + Dead	Detritus	Total (g/m ²)	Export (g/m ²)	
Welch Island		2019-2020	2.06	9	1,252	226	1,479	9	378	212	590	888	
		2018-2019	2.09	9	1,233	80	1,313	5	401	380	781	532	
		2017-2018	2.07	14	922	34	957	12	167	210	378	579	
	Low	2021-2022	1.38	5	253	23	276						
		2019-2020	1.09	9	424	16	441	8	59	21	80	360	
		2018-2019	1.59	9	820	75	895	9	376	210	586	308	
Steamboat Slough	High	2021-2022	2.17	5	1,829	111	1,941						
		2020-2021	2.03	8	1,156	48	1,204	8	579	86	664	540	
		2019-2020	2.00	9	1,096	269	1,365	9	560	251	811	554	
		2018-2019	2.03	9	1,459	106	1,565	9	292	472	764	801	
		2017-2018	2.05	7	948	177	1,126	6	470	243	714	412	
	Low	2021-2022	1.53	5	498	25	523						
		2020-2021	1.23	7	495	65	560	7	3	0	3	557	
		2019-2020	1.24	9	254	12	266	9	6	52	59	207	
		2018-2019	1.27	9	153	5	158	8	6	23	29	129	
		2017-2018	1.57	14	700	35	735	13	140	75	215	520	
Whites Island	High	2021-2022	1.96	5	1,327	138	1,465						
		2019-2020	2.37	9	1,194	405	1,599	9	740	511	1,251	348	
		2018-2019	2.54	9	1,458	252	1,710	4	867	463	1,330	380	
		2017-2018	2.18	13	1,042	274	1,316	12	710	310	1,020	296	
	Low	2021-2022	1.18	5	284	28	312						
		2019-2020	1.50	9	507	39	546	10	100	30	130	416	
		2018-2019	1.97	10	402	35	437	10	95	135	230	206	
		2017-2018	1.51	6	204	4	208	6	51	47	99	109	

			Summer					Winter					Annual
Site	High/Low Marsh	Biomass Year	Elevation	Count	Living + Dead	Detritus	Total (g/m ²)	Count	Living + Dead	Detritus	Total (g/m ²)	Export (g/m ²)	
Franz Lake	High	2021-2022	5.23	4	2,080	404	2,484						
		2020-2021	4.89	9	1,469	99	1,568	9	623	660	1,283	284	
		2019-2020	4.06	9	1,709	487	2,196	9	832	882	1,714	482	
		2018-2019	4.99	9	1,419	242	1,661	9	384	904	1,287	374	
	Low	2021-2022	4.17	4	670	75	745						
		2020-2021	4.17	8	322	297	619	8	0	24	24	595	
		2019-2020	3.09	9	394	13	407	9	0	61	61	346	
		2018-2019	4.32	9	640	37	677	4	0	43	43	634	

Table 34 for all values and standard deviations.

			Summer					Winter					Annual
Site	High/Low Marsh	Biomass Year	Elevation	Count	Living + Dead	Detritus	Total (g/m ²)	Count	Living + Dead	Detritus	Total (g/m ²)	Export (g/m ²)	
Welch Island	High	2021-2022	2.16	5	1,758	190	1,948						
		2019-2020	2.06	9	1,252	226	1,479	9	378	212	590	888	
		2018-2019	2.09	9	1,233	80	1,313	5	401	380	781	532	
		2017-2018	2.07	14	922	34	957	12	167	210	378	579	
	Low	2021-2022	1.38	5	253	23	276						
		2019-2020	1.09	9	424	16	441	8	59	21	80	360	
		2018-2019	1.59	9	820	75	895	9	376	210	586	308	
Steamboat Slough	High	2021-2022	2.17	5	1,829	111	1,941						
		2020-2021	2.03	8	1,156	48	1,204	8	579	86	664	540	
		2019-2020	2.00	9	1,096	269	1,365	9	560	251	811	554	
		2018-2019	2.03	9	1,459	106	1,565	9	292	472	764	801	
		2017-2018	2.05	7	948	177	1,126	6	470	243	714	412	
	Low	2021-2022	1.53	5	498	25	523						
		2020-2021	1.23	7	495	65	560	7	3	0	3	557	
		2019-2020	1.24	9	254	12	266	9	6	52	59	207	
		2018-2019	1.27	9	153	5	158	8	6	23	29	129	
		2017-2018	1.57	14	700	35	735	13	140	75	215	520	
Whites Island	High	2021-2022	1.96	5	1,327	138	1,465						
		2019-2020	2.37	9	1,194	405	1,599	9	740	511	1,251	348	
		2018-2019	2.54	9	1,458	252	1,710	4	867	463	1,330	380	
		2017-2018	2.18	13	1,042	274	1,316	12	710	310	1,020	296	
	Low	2021-2022	1.18	5	284	28	312						
		2019-2020	1.50	9	507	39	546	10	100	30	130	416	
		2018-2019	1.97	10	402	35	437	10	95	135	230	206	
		2017-2018	1.51	6	204	4	208	6	51	47	99	109	

			Summer					Winter				Annual
Site	High/Low Marsh	Biomass Year	Elevation	Count	Living + Dead	Detritus	Total (g/m ²)	Count	Living + Dead	Detritus	Total (g/m ²)	Export (g/m ²)
Franz Lake	High	2021-2022	5.23	4	2,080	404	2,484					
		2020-2021	4.89	9	1,469	99	1,568	9	623	660	1,283	284
		2019-2020	4.06	9	1,709	487	2,196	9	832	882	1,714	482
		2018-2019	4.99	9	1,419	242	1,661	9	384	904	1,287	374
	Low	2021-2022	4.17	4	670	75	745					
		2020-2021	4.17	8	322	297	619	8	0	24	24	595
		2019-2020	3.09	9	394	13	407	9	0	61	61	346
		2018-2019	4.32	9	640	37	677	4	0	43	43	634

Table 34: Average aboveground standing stock biomass (living + dead, dry weight g/m²) and average detrital biomass (dry weight g/m²) for 2018-2021 for both the high and low marsh strata across sites sampled. Winter 2022 data still under analysis and post-processing. Sites shown in order of rkm from mouth of the Columbia River to the Bonneville dam. Count= number of samples, Elevation = meters NAVD88, all units in g/m². Annual Export is the mean predicted contribution of organic matter (dry weight g/m²/year) both including and excluding detrital material.

Contribution of Biomass

The difference between the plant standing stock in the summer and that remaining in the winter can be considered the amount of organic matter contributed by the plants during that year. Presumably, some material continues to breakdown during the next growing season, but for the purposes of this analysis, we consider the summer-winter difference to represent the annual organic matter contribution. Specifically, the contribution of organic matter is typically calculated as the summer standing stock (live and dead) minus the following winter’s standing stock (live and dead). With the addition of detritus data, it can also be calculated as standing stock plus detritus. Including detritus into the equation allows for understanding how much biomass materials leave the sampling area altogether (not just shift from living to the dead to detritus). This calculation shows that not all of the standing stock is exported from the site, with some staying onsite as detritus; however the amount of detritus retained on the site varies across the sites, generally being less than 100 g/m²/year, but we’ve found it to be very dynamic from site to site and year to year (Table 35). In Table 35 this retention of detritus on the sites is highlighted as “change of export estimate” which negative numbers representing how our export of materials using standing stock alone, can over estimated export. In this column positive numbers indicating an underestimate of export, with a loss of detritus adding to the overall export estimate. Across the sites, low marsh areas tend to export more detritus than the high marsh, with those areas retaining more detritus than not. In general, between 2018-2021 detritus biomass contributions have varied greatly across sites and years (Table 34, Table 35). Overall, 2020 and 2021 resulted in a high production of standing stock and detritus biomass across all sites, with some of the largest values seen to date – likely a result of the longer growing seasons observed during the lower freshet conditions these years experienced. This was especially true for Franz lake (Figure 69, Figure 70, Table 34, Table 35), where the longer growing season was compounded with the removal of the beaver dam, proving a larger area for low marsh plant community establishment.

Annual Export

Location	High/Low Marsh	Biomass Year	Standing Stock Only (g/m ²)	Including Detritus (g/m ²)	Change in Export Estimate (g/m ²)	% Change
Welch Island	High	2019-2020	874	888	14	2%
		2018-2019	832	532	-300	-36%
		2017-2018	755	579	-176	-23%
	Low	2019-2020	365	360	-5	-1%
		2018-2019	443	308	-135	-30%
Steamboat Slough	High	2020-2021	577	540	-37	-6%
		2019-2020	535	554	18	3%
		2018-2019	1,167	801	-366	-31%
		2017-2018	478	412	-66	-14%
	Low	2020-2021	492	557	65	13%
		2019-2020	248	207	-41	-16%
		2018-2019	147	129	-17	-12%
		2017-2018	560	520	-40	-7%
Whites Island	High	2019-2020	454	348	-106	-23%
		2018-2019	591	380	-211	-36%

		2017-2018	332	296	-36	-11%
	Low	2019-2020	407	416	9	2%
		2018-2019	307	206	-100	-33%
		2017-2018	152	109	-43	-28%
Franz Lake	High	2020-2021	845	284	-561	-66%
		2019-2020	877	482	-395	-45%
		2018-2019	1,035	374	-662	-64%
	Low	2020-2021	322	595	273	85%
		2019-2020	394	346	-48	-12%
		2018-2019	640	634	-6	-1%

Table 35: Annual Export is the mean predicted contribution of organic matter (dry weight g/m²/year) both including and excluding detrital material, the change in the estimated export by incorporating the detritus is highlighted (negative means more material is kept on site than estimated with standing stock change alone, and positive means more material is exported than estimated without including detritus). Winter 2022 data still under analysis and post-processing. Sites shown in order of rkm from mouth of the Columbia River to the Bonneville dam.

Multi-Year Analysis

Multi-year patterns in biomass production for 2019-2021 are still under analysis; hence, the historic dataset has been further explored. Additionally, a full biogeochemical analysis is planned for these data in the 2023 reporting season. Above ground biomass data from 2011 – 2018 were analyzed to determine if differences exist in summer biomass (production) and annual organic matter contribution (hereafter termed contribution) between 1) high marsh vs. low marsh, and 2) across survey years. Clear trends in biomass production between high and low marsh strata are evident, low marsh plant communities producing lower weight dry biomass compared to high marsh plant communities across all sites (EMP 2018, Figure 71). In 2018, Welch Island low marsh composed approx. 40% of the overall site summer standing stock, Steamboat Slough the low marsh composed approx. 10%, Whites Island 22%, and Franz Lake 31% (Table 36).

Relative to other years 2018 was an average biomass production year for Welch Island and Whites Island, however the low marsh strata on Whites Island exhibited greater levels of biomass production than previous years, but this may be due to slightly higher elevations being included in the “low marsh strata” compared to previous years (Table 36). Franz lake mean biomass production in 2018 was slightly higher than in previous years, but this could also be due to the new method of sampling both the high and low marsh strata on the site, the low marsh strata not historically separated out of samples from Franz Lake when averaging site biomass levels (Table 36, Figure 71).

At Whites Island, which has the longest consistent annual record of high and low marsh biomass sampling, the contribution from the low marsh (Summer-Winter) standing stock is relatively consistent from year to year (~150-200 g/m²/year) compared to the high marsh (~1184-332 g/m²/year), which is much more variable (Table 36, Figure 71). Across time, differences in summer biomass production between high and low marsh strata follow a consistent pattern with the low marsh producing less biomass than the high marsh (Figure 71 and Figure 72). The high marsh contribution is, however, much more variable from year to year (Figure 72).

The annual freshet magnitude appears to influence biomass production across all sites, greater magnitudes such as in 2011, 2012, and 2017 generally producing less summer biomass (in August, when it is

sampled) compared to lower magnitude years (2013, 2015, 2016) (Figure 72, Figure 73). This is likely directly related to the amount of time these marsh areas are exposed during the growing season; a lower magnitude freshet would result in a longer growing season (marsh exposed) resulting in greater plant biomass accumulation. The mean annual summer total standing stock for all sites (Whites, Welch, Franz) shows a strong correlation ($R^2 = 0.63$, p-value < 0.001) with the cumulative Columbia River discharge for the month of August, higher discharge correlated with lower biomass production, further supporting this conclusion (Figure 73).

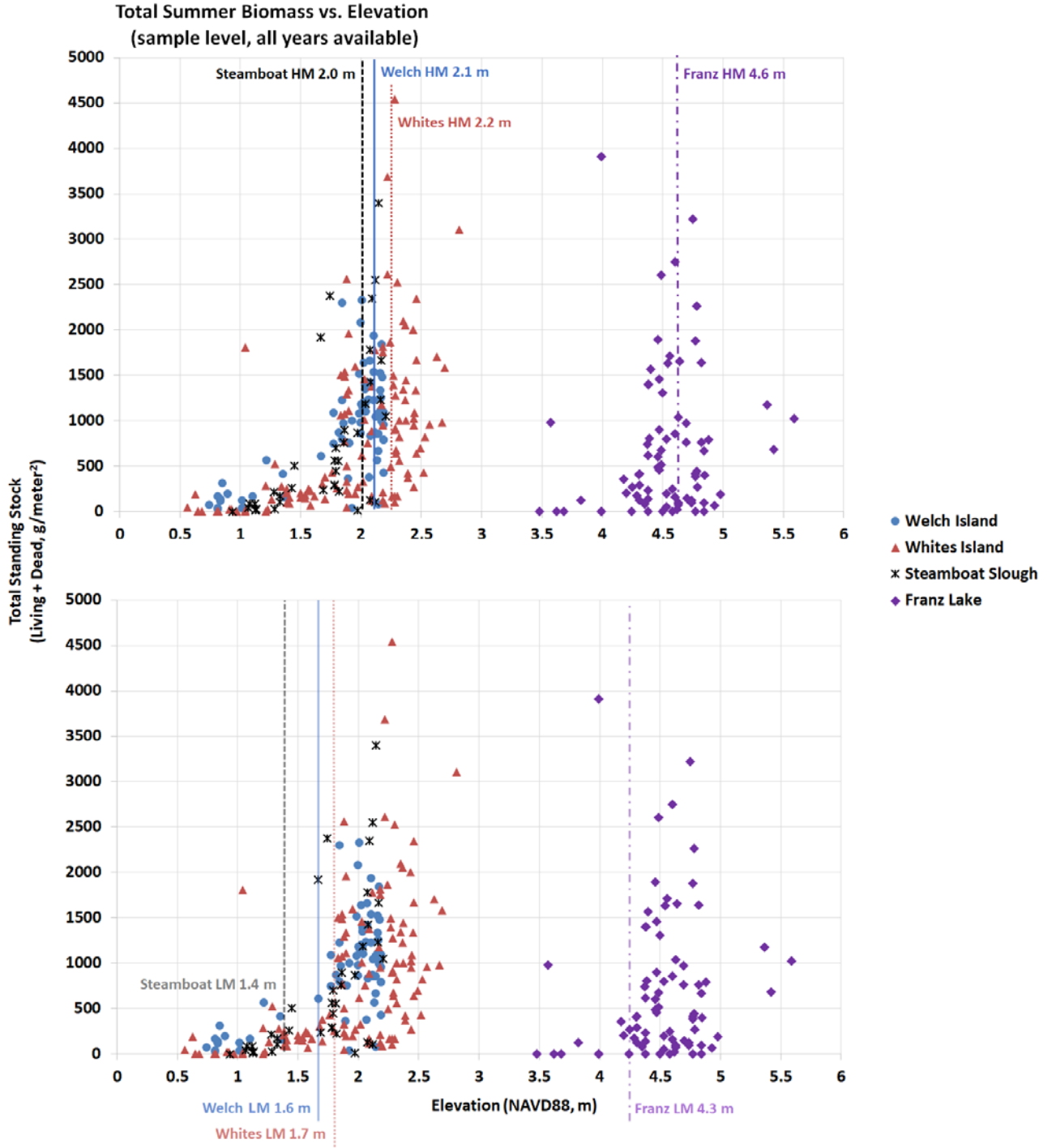


Figure 71: Total summer standing stock biomass (dry weight, g/m²) data by elevation for all year's data was collected at each site. Mean high and mean low marsh sample elevations (averaged across all years) highlighted as vertical lines on graph. A shows HM elevations, B shows LM elevations. HM = High Marsh, LM = Low Marsh.

Table 36: Total mean summer standing stock biomass (dry weight, g/m²) data split by high and low marsh plant community strata by survey year. Mean elevation of strata, and standard deviation (SD) of standing stock biomass also presented. Data also depicted in Figure 72.

Site	Strata	Biomass (g/m ²)	2018	2017	2016	2015	2013	2012	2011
Welch Island	High Marsh	Elevation	2.09	2.07	2.12		2.13	1.99	
		n	9	14	12		9	5	
		Mean	1233	922	1095		1361	1142	
		SD	374	456	320		647	322	
	Low Marsh	Elevation	1.59					1.64	
		n	9					4	
		Mean	820					401	
		SD	638					362	
Steamboat Slough	High Marsh	Elevation	2.03	2.05					
		n	9	7					
		Mean	1459	948					
		SD	1099	659					
	Low Marsh	Elevation	1.27	1.57					
		n	9	14					
		Mean	153	700					
		SD	160	1231					
Whites Island	High Marsh	Elevation	2.54	2.18	2.19	2.10	2.14	2.22	2.27
		n	9	13	12	12	9	8	6
		Mean	1458	1042	1802	1372	1359	739	1152
		SD	823	527	1161	462	834	623	844
	Low Marsh	Elevation	1.97	1.51	1.53	1.73	1.78	1.78	1.16
		n	10	6	6	6	6	3	2
		Mean	402	204	198	261	163	114	88
		SD	226	68	32	152	126	102	89
Franz Lake	High Marsh	Elevation	4.99		4.41	4.51	4.60	4.63	4.61
		n	9		12	12	9	7	8
		Mean	1419		1287	893	434	672	203
		SD	862		1205	719	317	557	152
	Low Marsh	Elevation	4.32						
		n	9						
		Mean	640						
		SD	485						

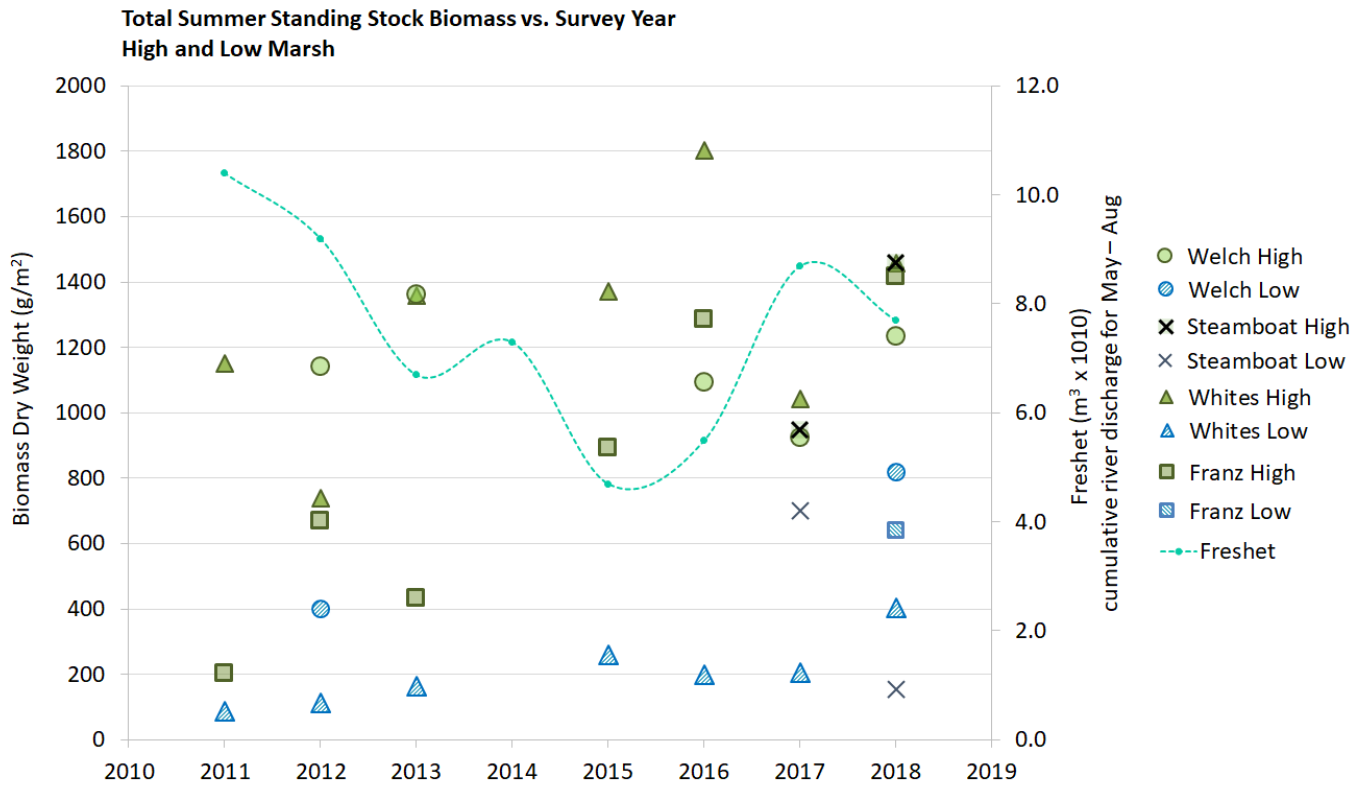


Figure 72: Total summer standing stock biomass (dry weight, g/m²) data split by high and low marsh plant community strata by survey year. Freshet magnitude is shown as the right axis for reference (see section 3.3.1. for details). Biomass data and standard deviation is shown in Table 36.

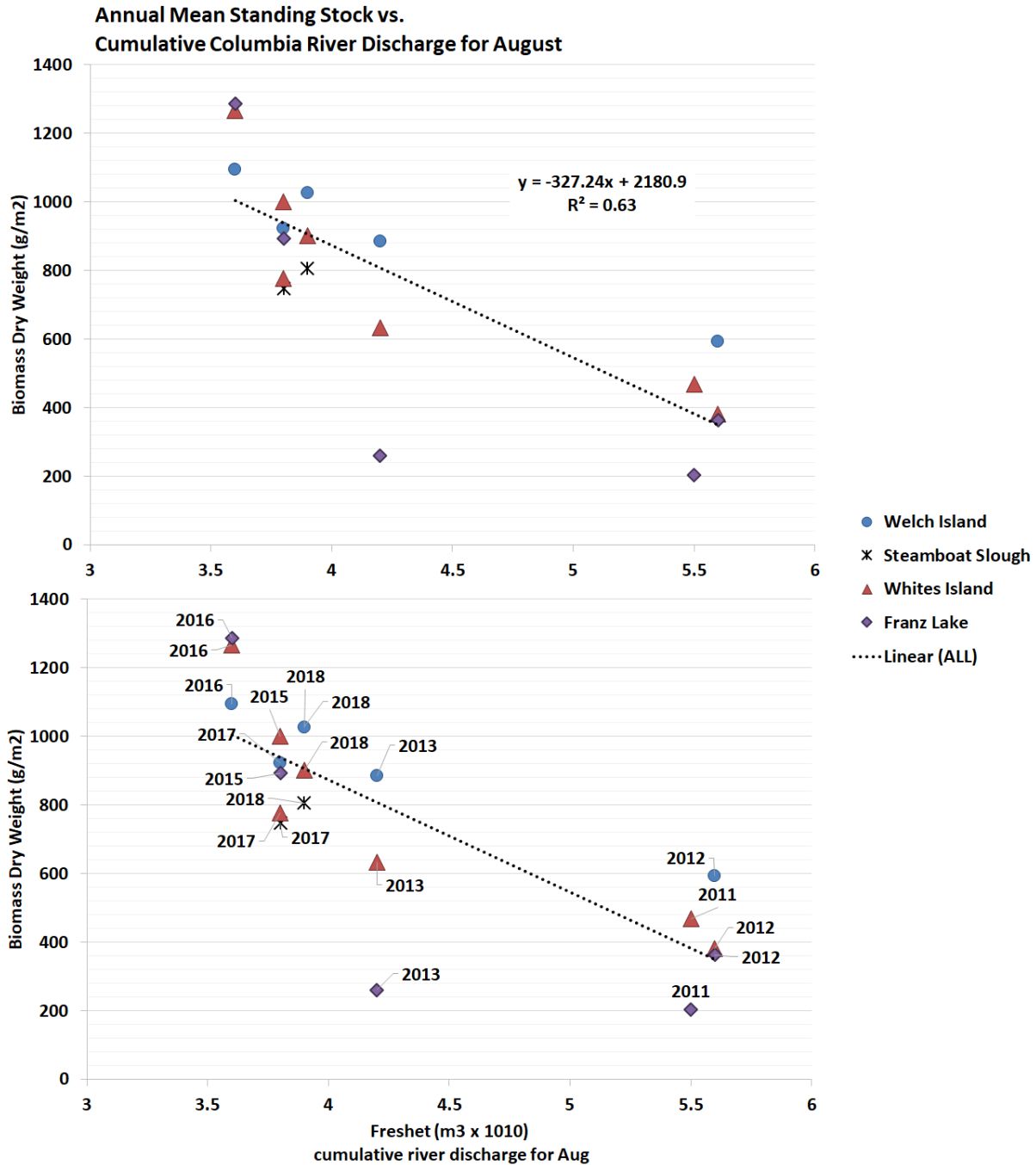


Figure 73: Overall annual mean total standing stock biomass (dry weight, g/m²/year) vs. the Freshet cumulative river discharge for the month of August. Second graph has annual labels for emphasis.

Biomass and Soil Nutrient Composition

In 2018, a sub-sample of live biomass and detritus samples were tested for nitrogen, carbon, and ADF lignin content. These data provide information on the nutrient content of the living biomass and decomposing detritus. Additionally, the soil nutrient content and texture were analyzed at the location of the biomass samples. Overall, Carbon (C) content was greatest in the living above ground biomass across all sites, followed by detritus, and soil (Figure 74, Table 37). In the living aboveground biomass mean C

content ranging from $41.9 \pm 2.3\%$ at Welch Island to $36.0 \pm 8.8\%$ at Steamboat Slough (restoration site). Generally, the mean above ground living biomass C content was similar across sites, with Steamboat Slough showing the overall lowest C content (Figure 74, Table 37). Mean detritus C content was more variable than living biomass C content and ranged from $34.7 \pm 5.1\%$ at Steamboat Slough to $21.9 \pm 10.2\%$ at Whites Island. Mean soil C content ranged from $6.2 \pm 2.2\%$ at Welch Island to $2.6 \pm 0.9\%$ at Whites Island.

Nitrogen (N) content was greatest in the living above ground biomass across all sites, followed by detritus, and soil (Figure 74, Table 37). In the living aboveground biomass mean N content ranging from $2.1 \pm 1.0\%$ at Whites Island to $1.3 \pm 0.4\%$ at Welch Island. Generally, the mean above ground living biomass N content was similar across sites, with Welch Island showing the overall lowest N content (Figure 74, Table 37). Mean detritus N content was more variable than living biomass N content and ranged from 1.5% at Steamboat Slough and Welch Island to $1.0 \pm 0.4\%$ at Whites Island. Mean soil N content ranged from $0.5 \pm 0.2\%$ at Welch Island to $0.2 \pm 0.1\%$ at Whites Island.

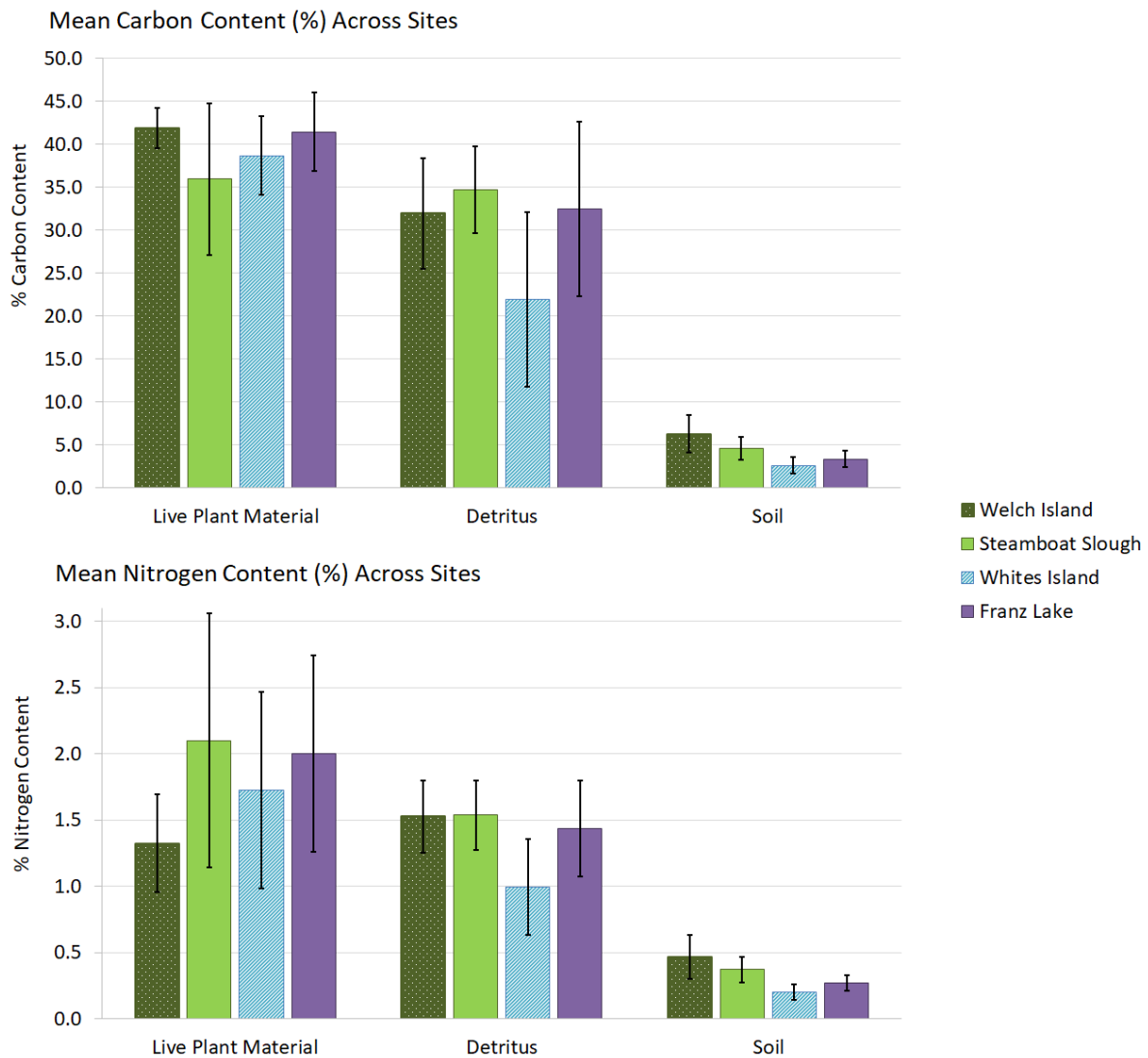


Figure 74: Mean % Carbon and Nitrogen content of above ground living biomass, detritus, and soil across sites, samples collected in the Summer of 2018. Data provided in Table 37.

The C:N ratio was greatest in the living above ground biomass across all sites, followed by detritus, and soil (Figure 75, Table 37). In living aboveground biomass mean C: N content ranging from $34.7 \pm 11.1\%$ at Welch Island to $23.1 \pm 7.9\%$ at Franz Lake. Mean detritus C: N content was less variable than living biomass C:N content and ranged from $21.3 \pm 4.7\%$ at Welch Island to $23.6 \pm 10.2\%$ at Franz Lake. Mean soil C: N content ranged from $13.9 \pm 2.0\%$ at Welch Island to $12.3 \pm 1.7\%$ at Steamboat Slough.

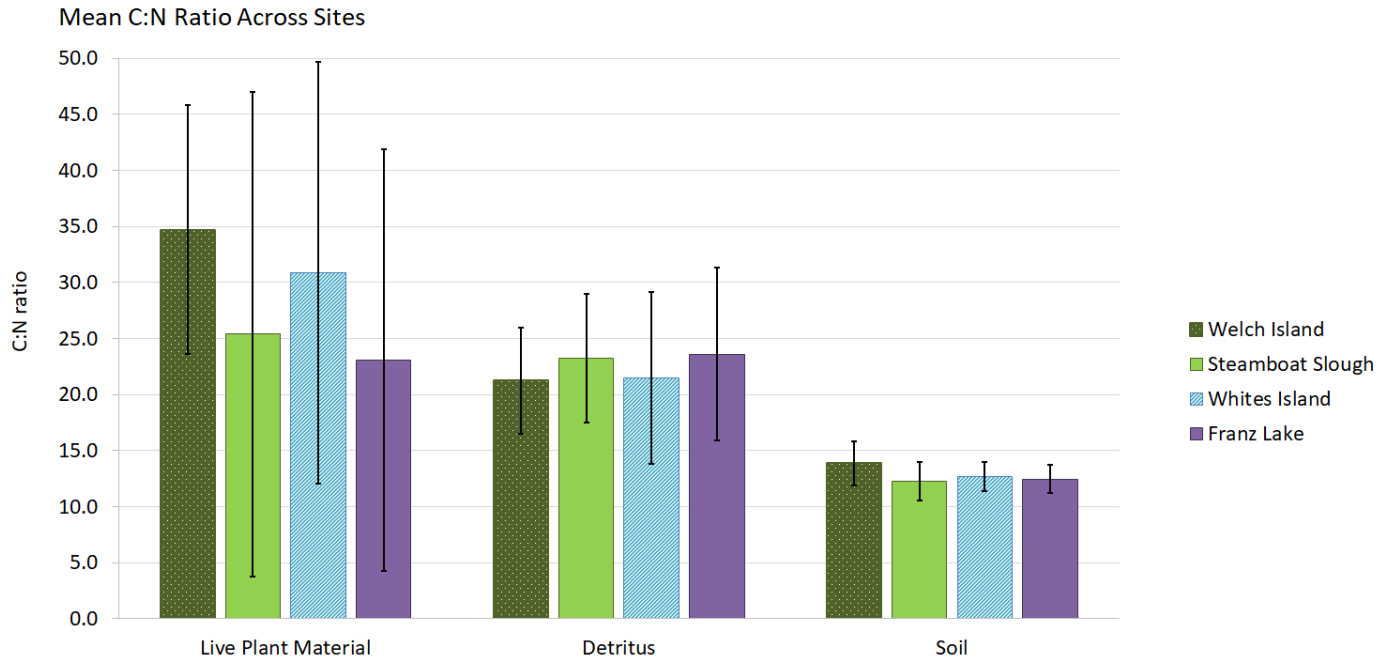


Figure 75: Mean Carbon and Nitrogen ratio of above ground living biomass, detritus, and soil across sites, samples collected in the Summer of 2018. Data provided in Table 37.

Table 37: Mean % Carbon and Nitrogen content of above ground living biomass, detritus, and soil across sites, samples collected in the Summer of 2018. For comparative graphs see Figure 74 and Figure 75.

Site		Carbon (%)			Nitrogen (%)			C: N Ratio		
		Live Plant Material	Detritus	Soil	Live Plant Material	Detritus	Soil	Live Plant Material	Detritus	Soil
Welch Island	n	12	16	10	12	16	10	12	16	10
	Mean	41.9	32.0	6.2	1.3	1.5	0.5	34.7	21.3	13.9
	SD	2.3	6.5	2.2	0.4	0.3	0.2	11.1	4.7	2.0
Steamboat Slough	n	17	7	10	17	7	10	17	7	10
	Mean	36.0	34.7	4.6	2.1	1.5	0.4	25.4	23.3	12.3
	SD	8.8	5.1	1.4	1.0	0.3	0.1	21.6	5.7	1.7
Whites Island	n	19	16	11	19	16	11	19	16	11
	Mean	38.7	21.9	2.6	1.7	1.0	0.2	30.9	21.5	12.7
	SD	4.5	10.2	0.9	0.7	0.4	0.1	18.8	7.7	1.3
Franz Lake	n	18	16	10	18	16	10	18	16	10
	Mean	41.5	32.4	3.4	2.0	1.4	0.3	23.1	23.6	12.5
	SD	2.7	8.1	0.9	0.6	0.5	0.1	7.9	6.2	0.9

At Steamboat Slough, a strong positive correlation was identified between C content in living above ground biomass and sample elevation within the wetland, higher elevations having greater C content (Figure 76). This relationship was not identified across the other EMP sites and may be a factor of the Steamboat’s recent re-flooding through restoration and this impact on wetland plant development along the elevation gradient within this site (Figure 76). No relationship in detrital carbon content and elevation was identified across the research sites, while strong positive correlations in soil C content and wetland elevation were found across all the EMP sites (Figure 76). Steamboat Slough did not show this trend in soil content, again, likely due to the recent soil biochemical changes occurring on that site from the restoration.

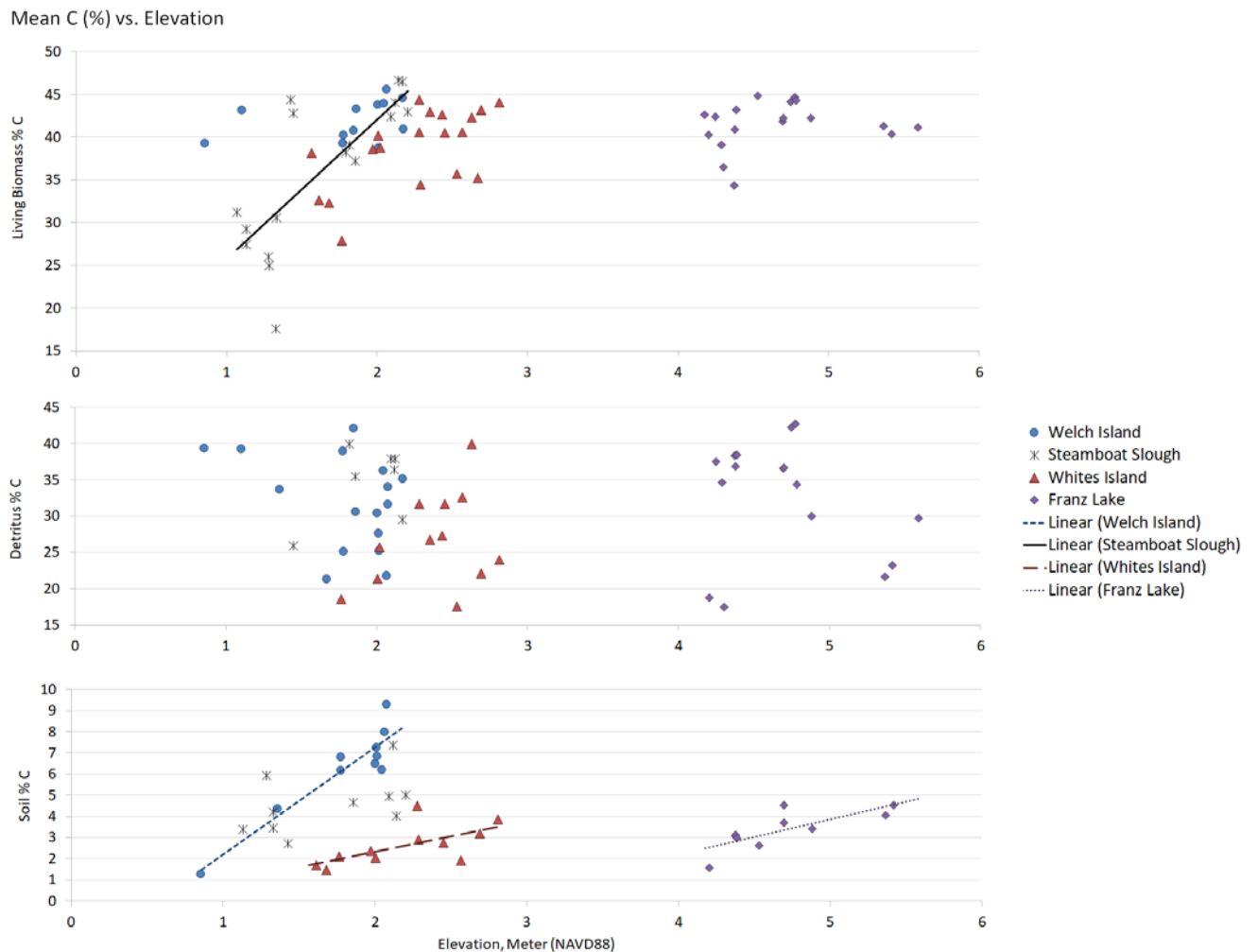


Figure 76: Carbon content (%) of above ground living biomass, detritus, and soil (graphs from top to bottom) vs. sample elevations in meters NAVD88. Significant within site correlations shown in each graph, site summary data provided in Table 37.

All sites including Steamboat Slough showed a strong negative correlation between N content in living above ground biomass and sample elevation within the wetland, lower elevations having greater N content (Figure 77). No relationships in detrital N content and elevation were identified across the research sites, while strong positive correlations in soil N content and wetland elevation were found across all the sites (Figure 77).

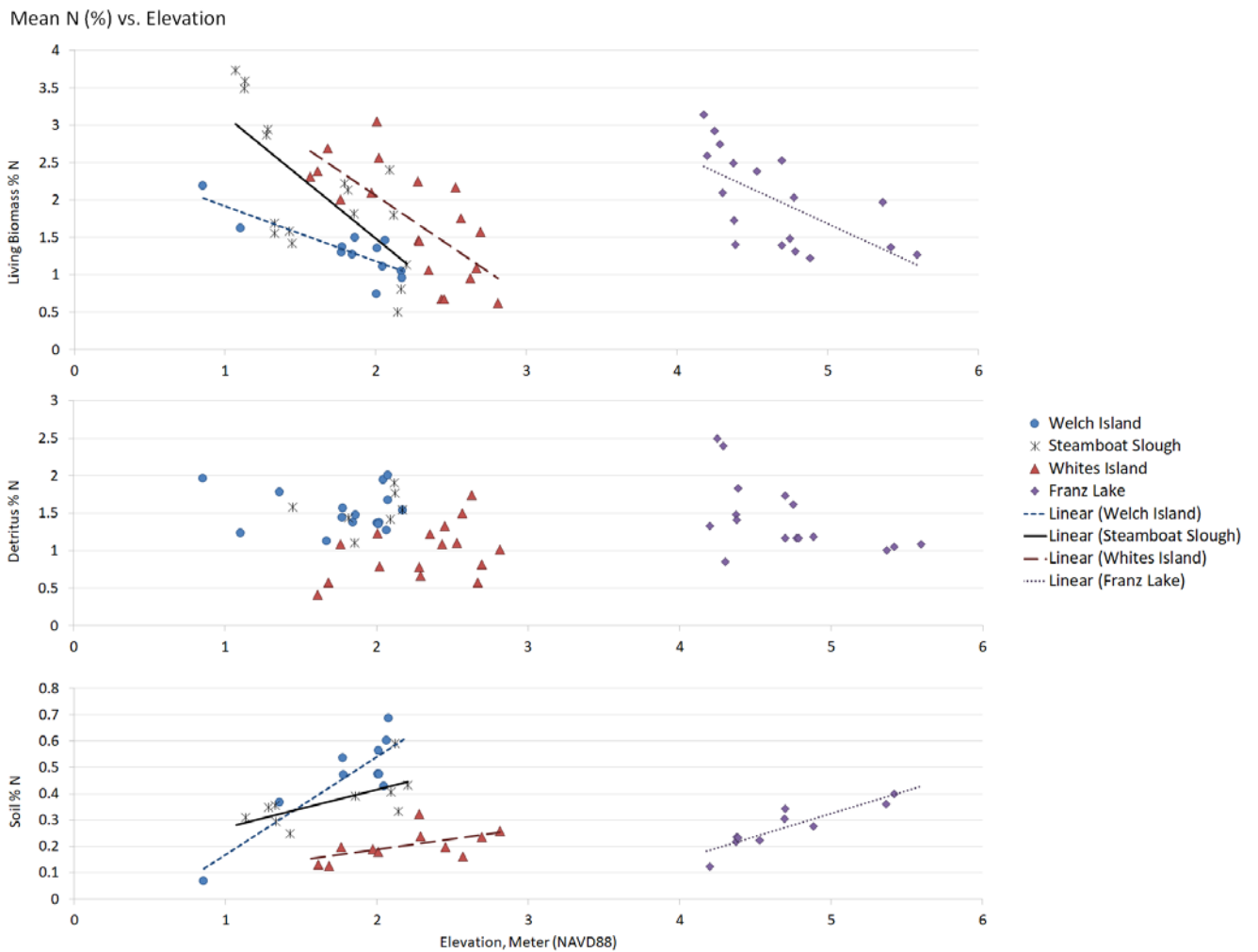


Figure 77: Nitrogen content (%) of above ground living biomass, detritus, and soil (graphs from top to bottom) vs. sample elevations in meters NAVD88. Significant within site correlations shown in each graph, site summary data provided in Table 37.

All sites including Steamboat Slough showed a strong positive correlation between C:N ratio in living above ground biomass and sample elevation within the wetland, lower elevations having lower C:N ratios (Figure 78). No relationships in detrital C:N ratio and elevation were identified across the research sites (Figure 78). Strong positive correlations in soil C:N ratios and wetland elevation were found across all the sites, except Franz Lake where a negative correlation in soil C:N ratio and wetland elevation was identified (Figure 78). This is particularly interesting, as the soil N content was lowest in the lower wetland elevation and living plant biomass in these elevations had the highest N content. This potentially reflects the shift in plant species and plant species nutrient use along the high to low marsh gradient. The low marsh species having lower carbon content, and lower C:N ratios overall, indicating less decomposition time required for the plant species found in the low marsh zone; C: N Ratio under 25 indicating no N limitation to decomposition (Wang et al. 2016). These results have potential implications for decomposition differences in the high and low marsh plant biomass corresponds to the overall differences found in detritus accumulation between the high and low marsh zone across sites, less detritus accumulation occurring in the low marsh zone (Figure 70). The above ground living biomass Lignin:

Nitrogen (L: N) ratio is also known as a good predictor of plant biomass decomposition rates, smaller ratios indicate more N and less Lignin, and quicker decomposition (Taylor et al. 1989, Talbot et al. 2011). L:N ratios across the wetlands were found to also correlate with elevation, following the N content trend, with smaller ratios in the lower marsh zones across sites (Figure 83).

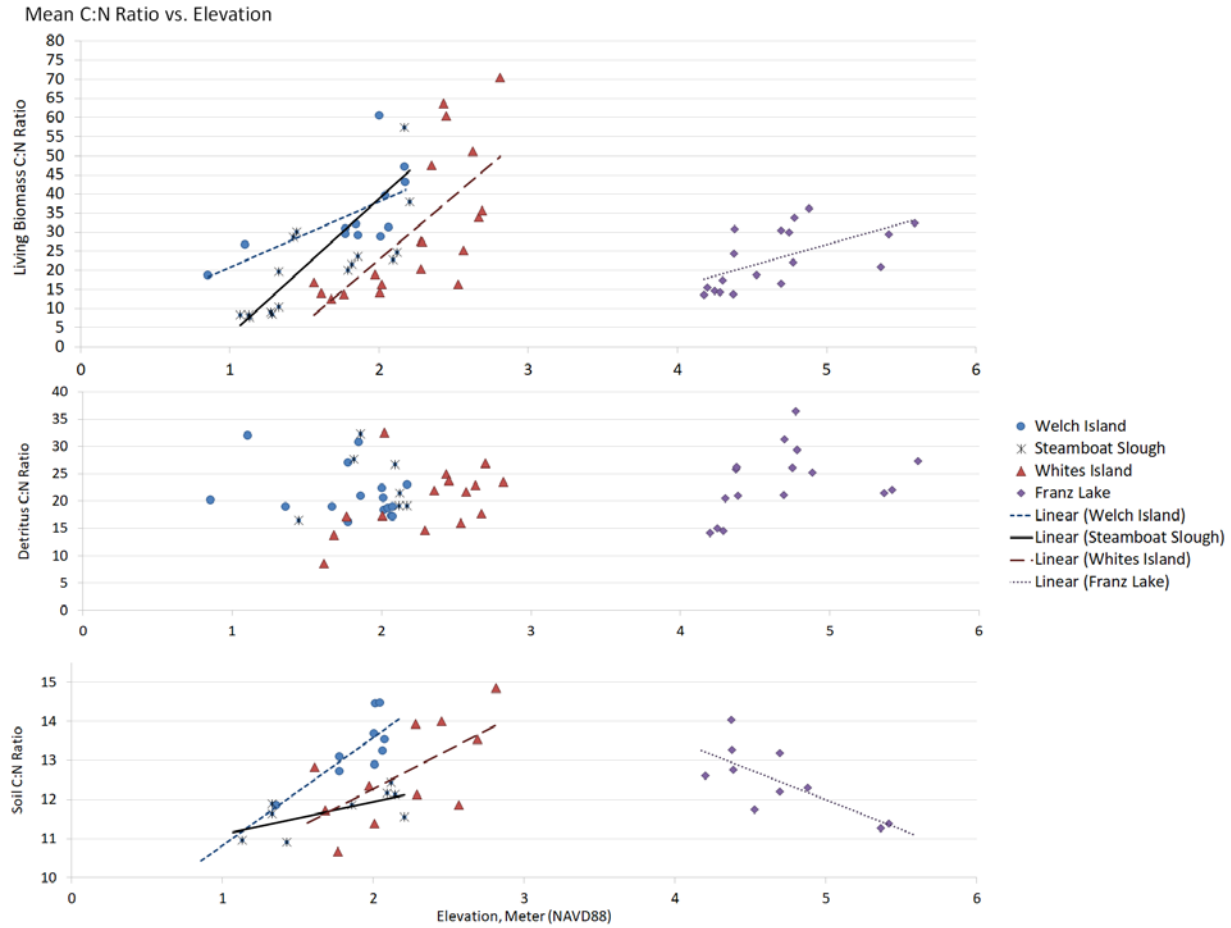


Figure 78: Carbon and Nitrogen ratio of above ground living biomass, detritus, and soil (graphs from top to bottom) vs. sample elevations in meters NAVD88. Significant within site correlations shown in each graph, site summary data provided in Table 37.

The mean soil N and C content showed a strong positive correlation, increases in soil C content corresponding to higher levels of N content (Figure 79). This relationship was also found in the detritus, with detrital C and N having a positive correlation across all sites (Figure 82). No relationship was found between mean living above ground biomass C and N content, indicating that this relationship becomes clearer once decomposition begins (detritus) and the decaying plant matter and associated microbial communities are incorporated into the soil within these sites.

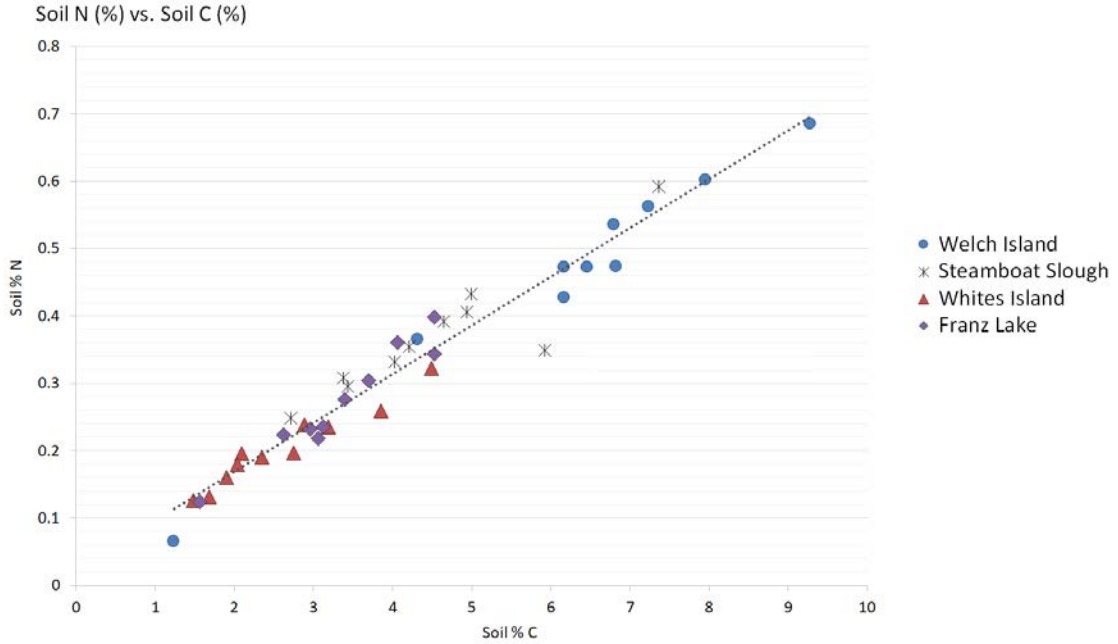


Figure 79. Soil N content (%) vs. Soil C content (%), a strong correlation was shown across all sites ($r^2 = 0.95$, $p < 0.001$). Summary data provided in Table 37.

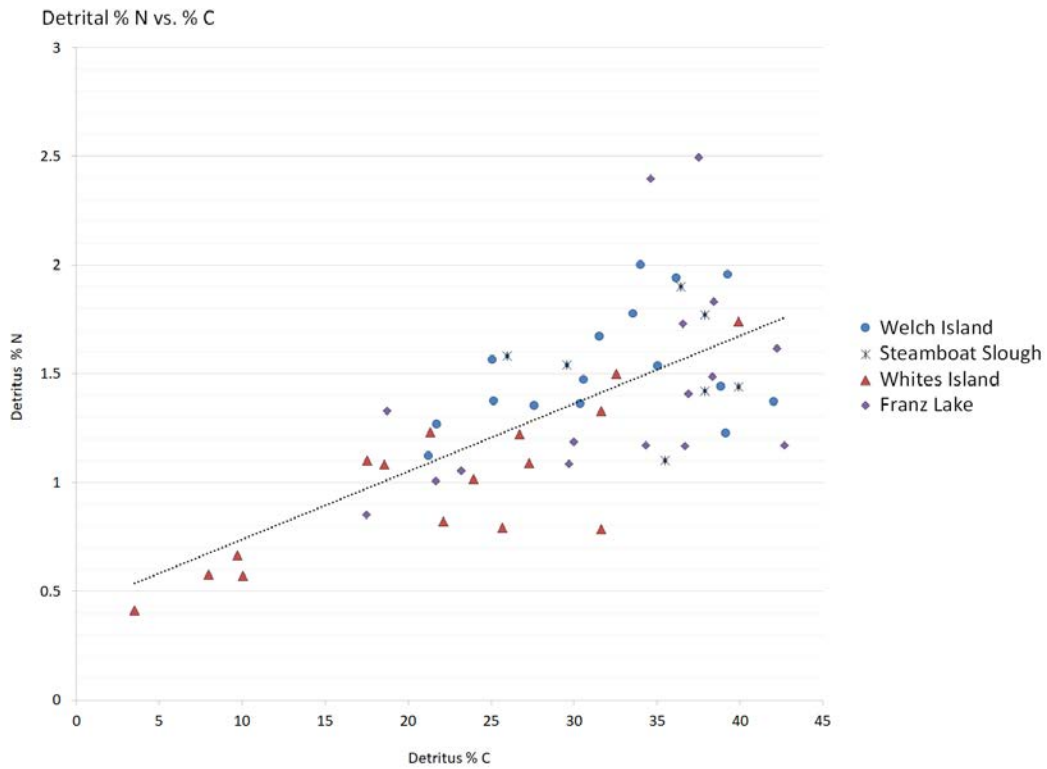


Figure 80: Detritus N content (%) vs. Detritus C content (%), a strong correlation was shown across all sites ($r^2 = 0.47$, $p < 0.001$). Summary data provided in Table 37.

Overall, mean summer ADF Lignin content was greatest in the detritus samples compared to the living plant biomass (Figure 81, Table 38), this follows the expected trend of ADF Lignin concentrations increasing in the detritus as decomposition occurs (lignin and associated compounds resisting decomposition (Taylor et al. 1989, Talbot et al. 2011). The greatest ADF Lignin content was found in the detritus from Franz Lake, $19.8 \pm 7.0\%$, and the living above ground biomass from Franz Lake, $12.9 \pm 6.6\%$, followed by the detritus, $15.4 \pm 9.0\%$, and biomass at Welch Island, to $9.0 \pm 15.4\%$. The lowest ADF Lignin levels were identified within the living above ground biomass at Steamboat Slough, $5.8 \pm 1.7\%$, and the lowest detritus ADF Lignin levels were identified at Whites Island, $6.6 \pm 8.8\%$. Detrital ADF Lignin content was found to be positively correlated with detrital carbon content, greater carbon levels within the detritus corresponding with greater levels of lignin. Similarly, detritus L:N ratio was also positively correlated with detritus carbon content, higher levels of Lignin and lower levels of N corresponding with greater levels of carbon (Figure 82, Figure 83). This result is expected, as others have found that as the biomass breaks down, the ratio of Lignin and C will increase compared to N (Taylor et al. 1989, Talbot et al. 2011). This relationship is essentially showing N limitation in the longterm breakdown of organic matter with high C and Lignin content (Taylor et al. 1989, Talbot et al. 2011).

Table 38: Mean % ADF Lignin content of above ground living biomass, and detritus across sites, samples collected in the Summer of 2018.

Site	ADF Lignin (%)		
		Live Plant Material	Detritus
Welch Island	n	12	17
	Mean	9.0	15.4
	SD	5.1	6.0
Steamboat Slough	n	17	7
	Mean	5.8	13.0
	SD	1.7	2.2
Whites Island	n	19	16
	Mean	6.6	8.8
	SD	2.2	7.4
Franz Lake	n	18	17
	Mean	12.9	19.8
	SD	6.6	7.0

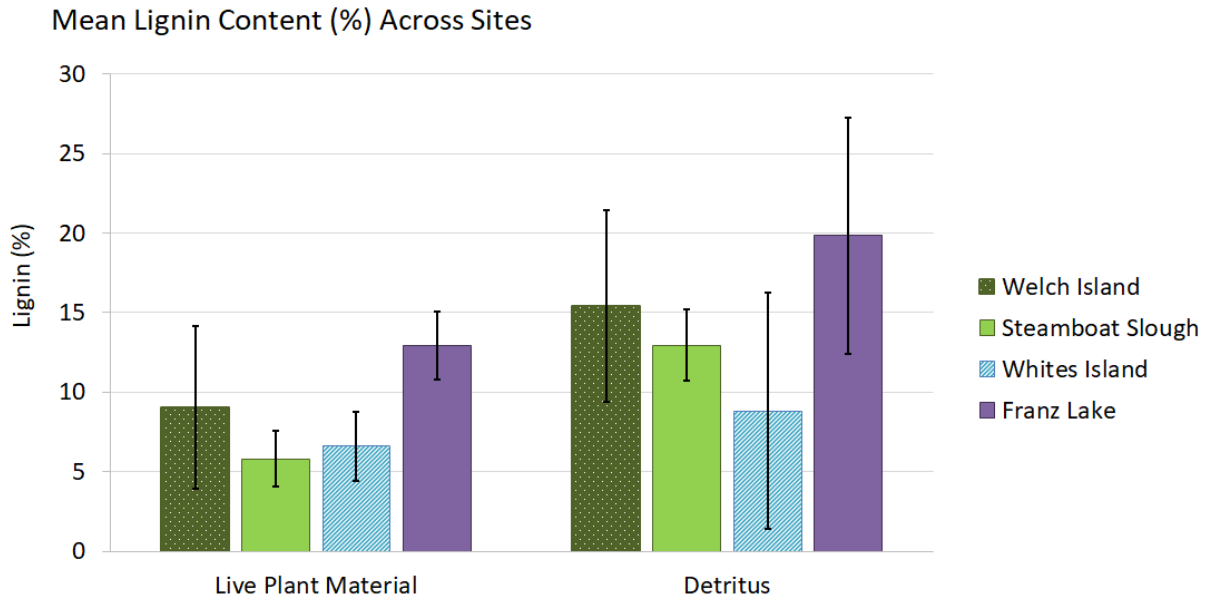


Figure 81: Mean % ADF Lignin content of above ground living biomass, and detritus across sites, samples collected in the Summer of 2018. For summary data see Table 38.

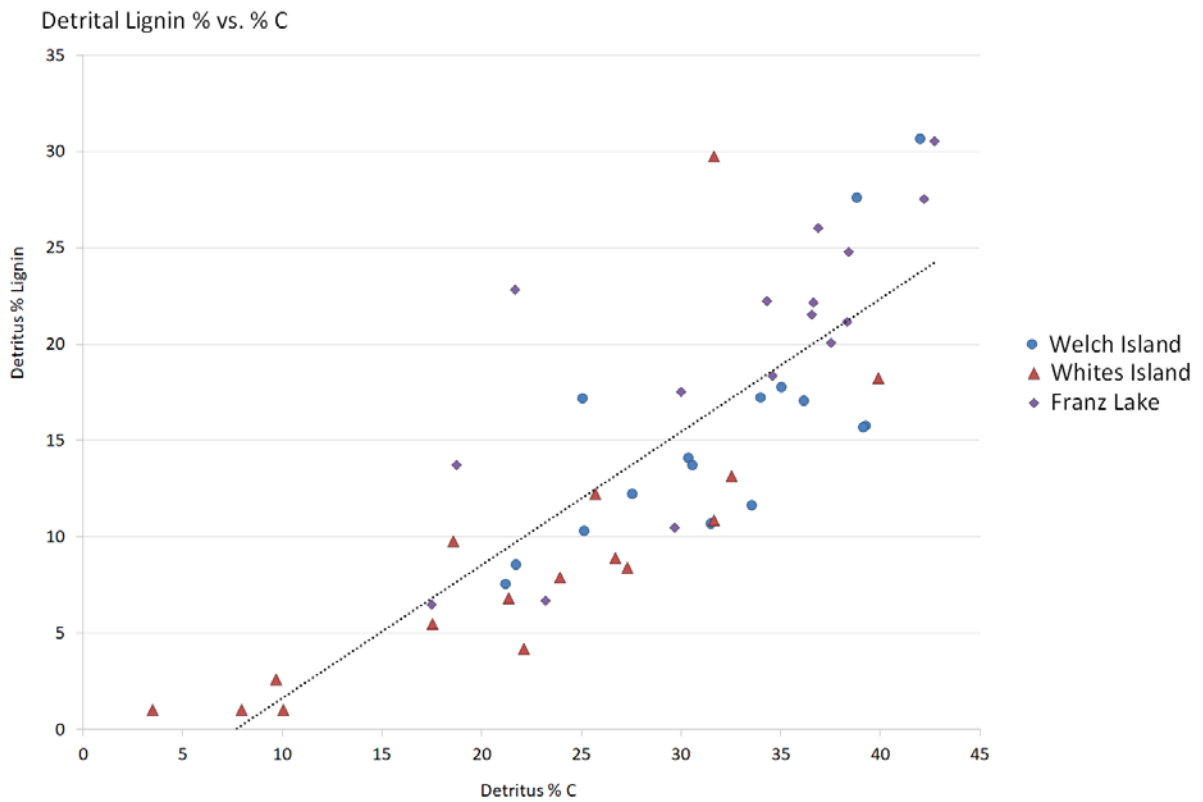


Figure 82: Detritus ADF Lignin content (%) vs. Detritus C content (%), a strong correlation was shown across all sites ($r^2 = 0.67$, $p < 0.001$). Summary data provided in Table 38.

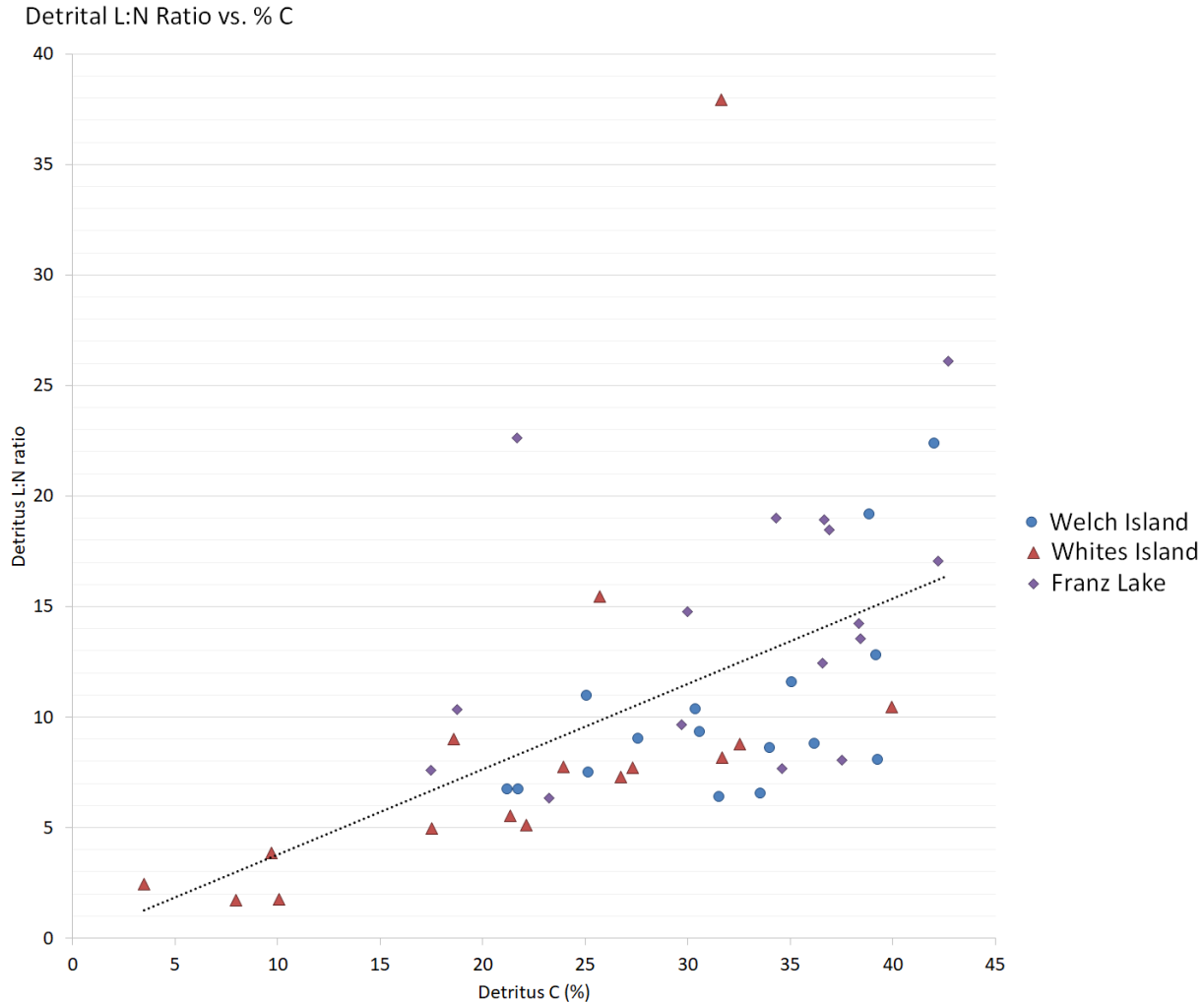


Figure 83: Detritus ADF Lignin: Nitrogen (L:N) content (%) vs. Detritus C content (%), a strong correlation was shown across all sites ($r^2 = 0.30$, $p < 0.05$). Summary data provided in Table 38.

General variability in the mean living above ground biomass and detritus carbon, nitrogen, and lignin content can be attributed to several factors including the general variability of these components across different wetland plant species (Table 39, Table 40) and variability between leaf and stem composition. Additionally, due to how the biomass data were collected and the degree of decay associated with detritus samples, detritus could not be associated specifically with any one species. This can make comparing across living and detritus samples challenging because no direct species to species comparison can be made. In general, the living above ground biomass results reflects a mix of stem and leaf materials and it is assumed the detritus samples are also a mix of decaying leaf and stem components.

Comparison among species of the above ground living biomass carbon, nitrogen, and lignin content shows that there is a large range of variability, however, species-specific trends were generally found to be consistent across all sites sampled (Table 39, Table 40). Of the most common species, *Polygonum amphibium* and *Polygonum hydropiperoides* were found to have the highest overall lignin to nitrogen ratios (L: N), 11.7 ± 3.3 and 14.7 ± 4.9 , this is not particularly surprising as these species have woody (high in lignin) perennial stems (especially when compared to the other common wetland grass and herb species) that persist throughout the winter months. These species were followed in L: N content by *P. arundinacea*, 6.7 ± 2.8 , and *C. lyngbyei*, 6.0 ± 3.2 for the high marsh species, and *S. latifolia*, 2.9 ± 0.6 and *E.*

palustris, 2.4 ± 0.9 , for the low marsh species. These L:N ratios mirror observations of decomposition in the field with *P. arundinacea* generally being retained on the site as standing dead biomass, followed in abundance by *C. lyngbyei*, and low marsh species, *S. latifolia*, and *E. palustris*, generally not found as standing dead due to its quick state of decay and location in the low marsh which is exposed to more active hydrologic flushing compared to the high marsh. *P. amphibium* and *P. hydropiperoides* are an interesting comparison to the other marsh species because they do lose their leaves annually without much dead leaf accumulation, but their stems tend to fall dormant (not actually standing dead), indicating that their L:N ratios may vary dramatically between the two plant structures (more in the perennial stems and less in the leaves). Additionally, the C:N ratio of the *P. amphibium*, 24.8 ± 7.0 , and *P. hydropiperoides*, 29.8 ± 6.3 , species were found to be below that of *P. arundinacea*, 46.2 ± 19.2 , and *C. lyngbyei*, 38.2 ± 9.1 , and above that of *S. latifolia*, 15.7 ± 3.1 , and *E. palustris*, 21.2 ± 4.9 . Further testing and distinction between leaves and stems of all species will help us better understand these functional plant traits and how they inform plant decomposition and detrital production within these sites moving forward.

Table 39: Plant species-specific mean (\pm SD) living above ground biomass elevation (m, NAVD88), ADF Lignin, C:N ratio, %C, %N, and dry biomass (g/m^2) across all sites sorted by mean elevation within each site (low to high marsh). Y = Native, N = Non-native. Data from summer 2018 biomass data collection.

Site	Sp. Code	Scientific Name	Native (Y/N)	n	Elevation	ADF Lignin %	C: N	%C	%N	Biomass g/m^2
Welch Island	ELPA	<i>Eleocharis palustris</i>	Y	2	0.98 (0.18)	3.8 (0.1)	24.8 (2.5)	42.3 (1.1)	1.7 (0.1)	122 (160)
	POHY	<i>Polygonum hydropiperoides</i>	Y	3	1.8 (0.04)	22 (1.3)	32.6 (3.4)	42.4 (2.1)	1.3 (0.1)	244 (265)
	EQFL	<i>Equisetum fluviatile</i>	Y	3	1.88 (0.12)	4 (1)	28.6 (3.1)	37.2 (1.4)	1.3 (0.1)	332 (374)
	PHAR	<i>Phalaris arundinacea</i>	N	3	2.01 (0.16)	6.5 (0.7)	52.4 (20.5)	43.6 (0.3)	1 (0.5)	629 (322)
	CALY	<i>Carex lyngbyei</i>	Y	4	2.07 (0.07)	7.4 (1.8)	39.3 (10.1)	44.6 (0.9)	1.2 (0.3)	368 (358)
	MYLA	<i>Myosotis laxa</i>	Y	1	2.18	11.5	43.1	40.9	1	289
Steamboat Slough	POHY	<i>Polygonum hydropiperoides</i>	Y	1	1.33	9.6	19.6	30.6	1.6	14
	ELPA	<i>Eleocharis palustris</i>	Y	2	1.44 (0.01)	6.2 (2.7)	26.9 (4.6)	43.2 (0.5)	1.6 (0.3)	165 (148)
	BICE	<i>Bidens cernua</i>	Y	3	1.82 (0.03)	11.7 (2.4)	19.7 (4.6)	39 (3.1)	2 (0.3)	12 (5)
	PHAR	<i>Phalaris arundinacea</i>	N	5	1.95 (0.18)	3.8 (1.7)	33.9 (3.8)	40.6 (2.4)	1.2 (0.2)	420 (520)
	SALA	<i>Sagittaria latifolia</i>	Y	2	1.97 (0.17)	7.3 (1)	15.2 (4.1)	41.9 (3.5)	2.9 (1)	405 (361)
	SCTA	<i>Schoenoplectus tabernaemontani</i>	Y	1	2.12	1.5	22.8	45.6	2	1579
	JUEF	<i>Juncus effusus</i>	N	2	2.16 (0.02)	5.5 (0.6)	74.9 (24.7)	46.6 (0.1)	0.7 (0.2)	2164 (1404)
Whites Island	POHY	<i>Polygonum hydropiperoides</i>	Y	1	1.97	15.5	21.4	82.3	1.9	126
	SALA	<i>Sagittaria latifolia</i>	Y	8	1.98 (0.31)	7.5 (1.4)	16.2 (3.8)	43.1 (17.1)	2.4 (0.4)	123 (147)
	ELPA	<i>Eleocharis palustris</i>	Y	2	2.01 (0.01)	6 (2.1)	21.6 (0.6)	44.1 (3)	2 (0.2)	59 (45)
	EQFL	<i>Equisetum fluviatile</i>	Y	1	2.29	4.2	28.7	36.7	1.3	88
	PHAR	<i>Phalaris arundinacea</i>	N	9	2.54 (0.17)	5.9 (0.7)	54 (17.2)	40.8 (2.5)	0.9 (0.5)	648 (550)
	CALY	<i>Carex lyngbyei</i>	Y	1	2.63	4.3	33.7	44.8	1.3	61

Franz Lake	SALA	<i>Sagittaria latifolia</i>	Y	4	4.24 (0.06)	6 (0.8)	14.8 (1)	39.1 (3.4)	2.7 (0.4)	204 (86)
	ELPA	<i>Eleocharis palustris</i>	Y	1	4.25	5.4	13.2	41.3	3.1	22
	POAM	<i>Polygonum amphibium</i>	Y	11	4.55 (0.23)	20.1 (2.7)	24.8 (7)	46.4 (14.2)	1.8 (0.5)	679 (654)
	PHAR	<i>Phalaris arundinacea</i>	N	5	5.19 (0.38)	6.3 (1.2)	28.5 (10.6)	40.8 (0.5)	1.6 (0.6)	475 (376)

Table 40: Overall plant species-specific mean (\pm SD) living above ground biomass elevation (m, NAVD88), Lignin:Nitrogen (L:N) content, C:N ratio, %C, %N, ADF Lignin %, and dry biomass (g/m^2). Y = Native, N = Non-native. Data from summer 2018 biomass data collection. Summary of common plant species combining all EMP site data (Welch Island, Whites Island, and Franz Lake).

General Elevation	Sp. Code	Scientific Name	Native (Y/N)	Count	L: N	C: N	C%	N%	ADF Lignin %	Biomass g/m^2
High Marsh	PHAR	<i>Phalaris arundinacea</i>	N	17	6.7 (2.8)	46.2 (19.2)	41.3 (2.1)	1.1 (0.6)	6.1 (0.9)	598 (438)
	CALY	<i>Carex lyngbyei</i>	Y	5	6.0 (3.2)	38.2 (9.1)	44.6 (0.8)	1.2 (0.3)	6.8 (2.1)	302 (270)
	POAM	<i>Polygonum amphibium</i>	Y	11	11.7 (3.3)	24.8 (7.0)	46.4 (14.2)	1.8 (0.5)	20.1 (2.7)	639 (570)
Low Marsh	POHY	<i>Polygonum hydropiperoides</i>	Y	4	14.7 (4.9)	29.8 (6.3)	52.4 (20.0)	1.5 (0.3)	20.4 (3.4)	220 (245)
	SALA	<i>Sagittaria latifolia</i>	Y	12	2.9 (0.6)	15.7 (3.1)	41.8 (13.9)	2.5 (0.4)	7.0 (1.4)	125 (137)
	ELPA	<i>Eleocharis palustris</i>	Y	5	2.4 (0.9)	21.2 (4.9)	42.8 (2.0)	2.1 (0.6)	5.0 (1.6)	77 (105)

Mean soil texture of the sites (Welch Island, Steamboat Slough, Whites Island, and Franz Lake) can generally be described as silt loam (Table 41, Figure 84). The exact amount of silt, sand, and clay did vary within and among sites, with Welch Island having the highest levels of sand, $33.3 \pm 19.2\%$, followed by Steamboat Slough, $27.7 \pm 7.3\%$, Whites Island, $24.7 \pm 9.1\%$, and Franz Lake, $11.0 \pm 6.4\%$. Correspondingly, Silt levels were greatest at Franz Lake, $77.2 \pm 5.8\%$, followed by Whites Island, $69.9 \pm 6.7\%$, Welch Island, $59 \pm 15.4\%$, and Steamboat Slough $57.5 \pm 8\%$. Steamboat Slough showed the greatest soil clay content, $14.8 \pm 4.8\%$, followed by Franz Lake, $11.7 \pm 1.3\%$, Welch Island $7.6 \pm 4.3\%$, and Whites Island, $5.3 \pm 3.3\%$. Generally, it appears sand and silt soil content are correlated with a location within the estuary, greater silt levels in the upper river site (Franz Lake) and greater sand content at the site located closest to the mouth of the Columbia River (Welch Island) (Figure 84). Soil bulk density was found similar across sites, with the highest bulk density found at Whites Island, followed by Steamboat Slough, Franz Lake, and Welch Island (Figure 84, Table 38).

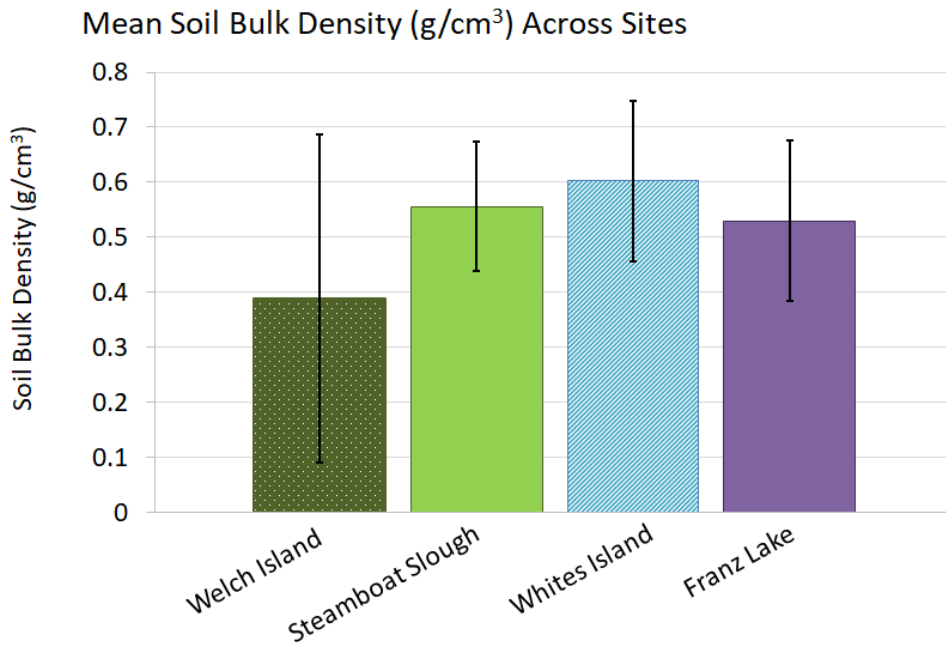
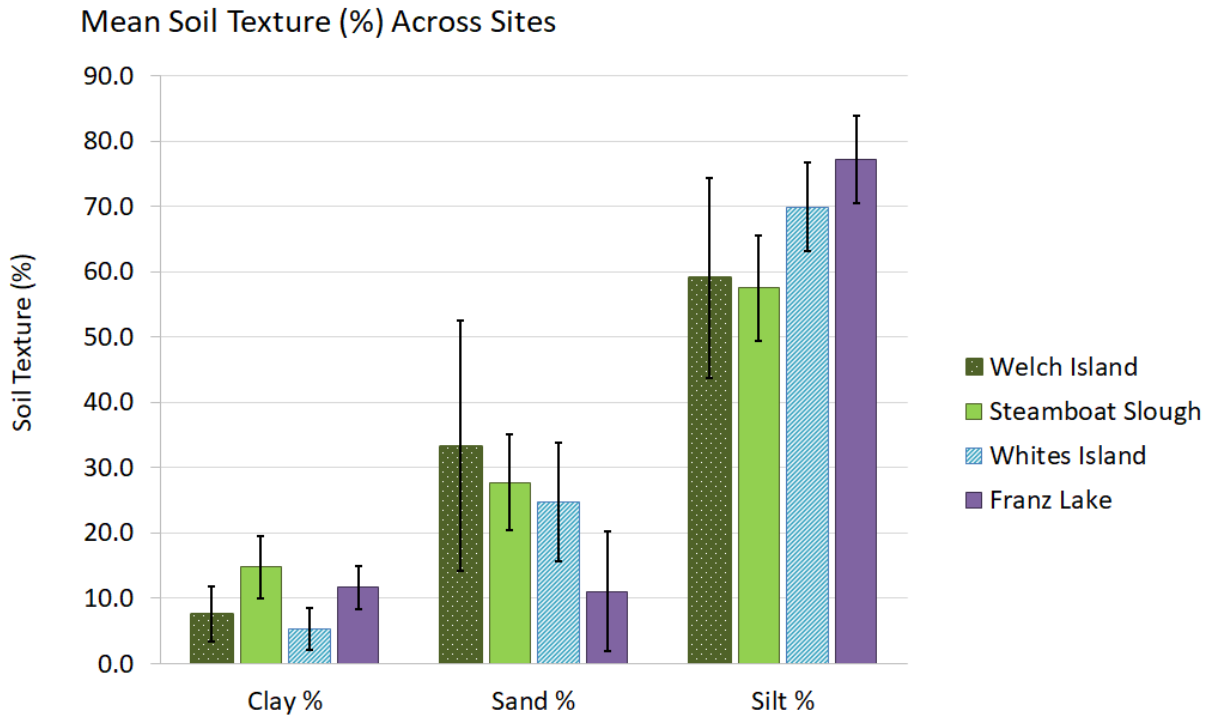


Figure 84. Mean soil texture composition (%) and bulk density (g/cm³) across sites, samples collected in the Summer of 2018. For summary data see Table 38.

Table 41: Mean soil texture composition (%) and bulk density (g/cm³) across sites, samples collected in the Summer of 2018. For comparative graphs see Figure 84.

Site	Soil Characteristics				
	Clay (%)	Sand (%)	Silt (%)	Bulk Density (g/cm ³)	
Welch Island	n	10.0	10.0	10.0	10
	Mean	7.6	33.3	59.0	0.39
	SD	4.3	19.2	15.4	0.30
Steamboat Slough	n	10.0	10.0	10.0	10
	Mean	14.8	27.7	57.5	0.56
	SD	4.8	7.3	8.0	0.12
Whites Island	n	11.0	11.0	11.0	11
	Mean	5.3	24.7	69.9	0.60
	SD	3.3	9.1	6.7	0.15
Franz Lake	n	10.0	10.0	10.0	10
	Mean	11.7	11.0	77.2	0.53
	SD	1.3	6.4	5.8	0.15

3.4.1.2 *Pelagic*

Primary production contributed by phytoplankton in the water column was estimated by the concentration of the pigment, chlorophyll *a*, which is found in all photosynthetic organisms. In addition to hourly fluorescence-based measurements of chlorophyll *a*, whole water samples were analyzed by extracting the chlorophyll *a* pigment from particulate matter collected on filters. This step is necessary to validate fluorescence data from in situ sensors. Together these data provide information about the amount of biomass associated with fluvial phytoplankton. The sonde data collected at high frequency provide additional context to the whole water grab samples, which is important for determining water quality. At the time of writing, samples are still being processed and analyzed for 2020 and 2021 at Ilwaco and Whites Island. The compiled data from 2011-2019 are shown here for context for the sites where data are available.

The highest chlorophyll concentrations observed in 2020-21 were found at Campbell Slough and Franz Lake Slough, similar to previous years (Figure 85-Figure 86). These sites are prone to the development of algal blooms in the summer months, which often discolor the water. In previous years, the lowest chlorophyll *a* values were observed at Ilwaco Slough. No chlorophyll measurements exceeded 25 µg L⁻¹ in 2020-21. If a benchmark of 15 µg L⁻¹ is used, four observations were above the recommended threshold over the 2020-21 time period, suggesting poor water quality (Oregon State Water Quality Standards). However, since a body of water is only considered impaired when the threshold is exceeded in observations from three consecutive months, no site met this criterion.

Primary production, as approximated by chlorophyll *a* concentration, tends to be highest in March at the lower river sites (Welch Island and Whites Island) and in August at the more upriver sites (Campbell Slough and Franz Lake Slough). However, there were not enough data to determine a trend in 2020 (Figure 85-Figure 86); in 2021, the trend seemed to hold true at Franz and at Welch, but not at Campbell, where higher chlorophyll was observed in March-April compared to later in the year (Figure 85-Figure 86).

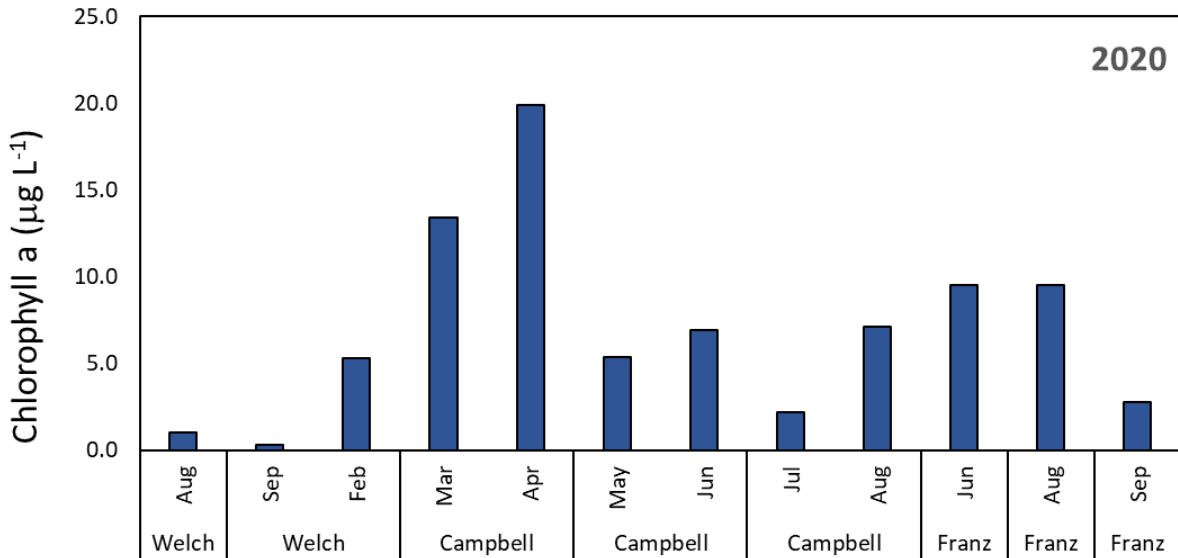


Figure 85: Chlorophyll *a* concentrations (µg L⁻¹) at Welch Island (Welch), Campbell Slough (Campbell), and Franz Lake Slough (Franz) in 2020.

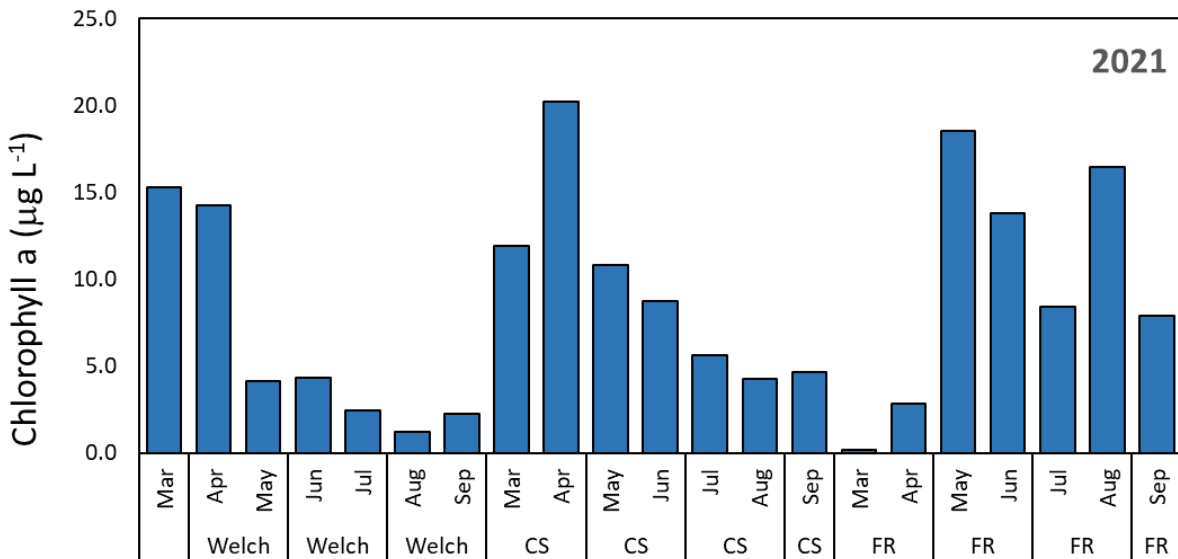


Figure 86. Chlorophyll *a* concentrations (µg L⁻¹) at Welch Island (Welch), Campbell Slough (CS), and Franz Lake Slough (FR) in 2021.

Aside from the very high value observed in May at Franz Lake Slough, primary production, as approximated by chlorophyll *a* concentration, was highest in March at the lower river sites (Welch Island and Whites Island) and in August at the more upriver sites (Campbell Slough and Franz Lake Slough), 2019 (Figure 87).

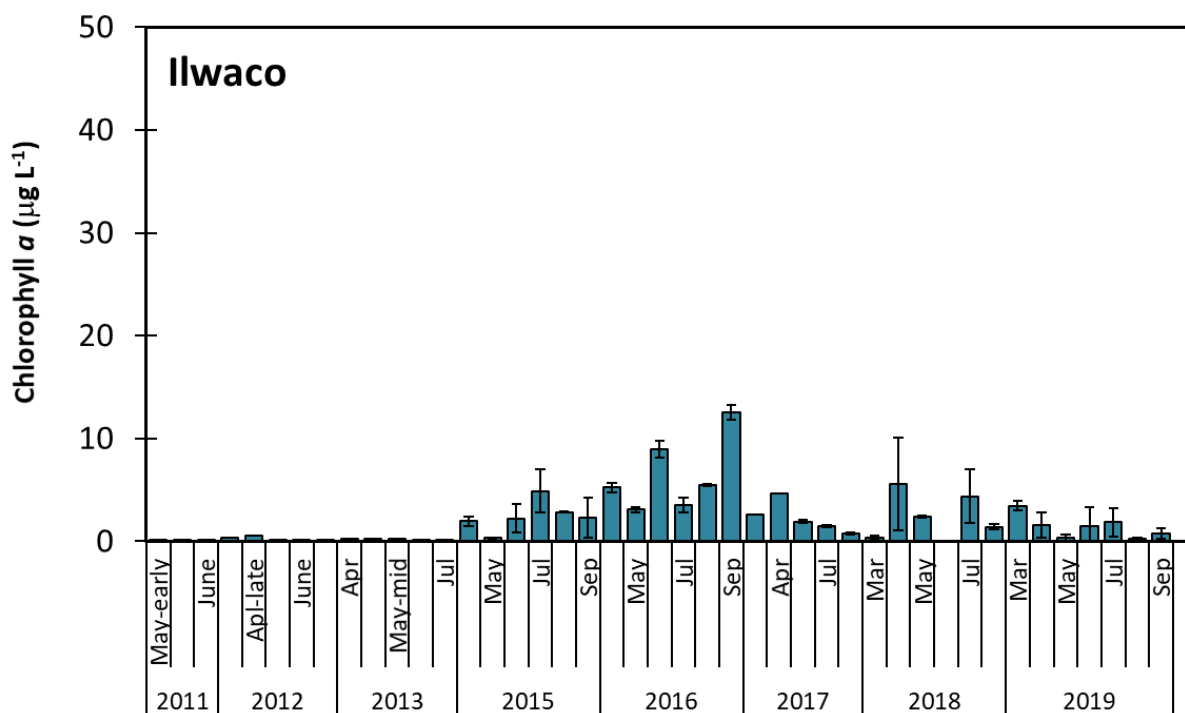


Figure 87. Chlorophyll *a* concentration in discrete samples collected from Ilwaco (2011–2019).

The magnitude of primary production tends to be lower at Ilwaco than at the other sites (compare Figure 87 with Figure 88, Figure 89; throughout the lower Columbia, chlorophyll values tend to be highest in March and lowest in May and August, associated with the spring freshet in May-June and with lower nutrient availability in the summer months at sites other than Ilwaco. At Ilwaco, marine conditions prevail in August and chlorophyll concentrations can reach their annual peak at that site. At Ilwaco, chlorophyll concentrations are almost always less than at the other sites, with values generally <10 µg L⁻¹ throughout the time series.

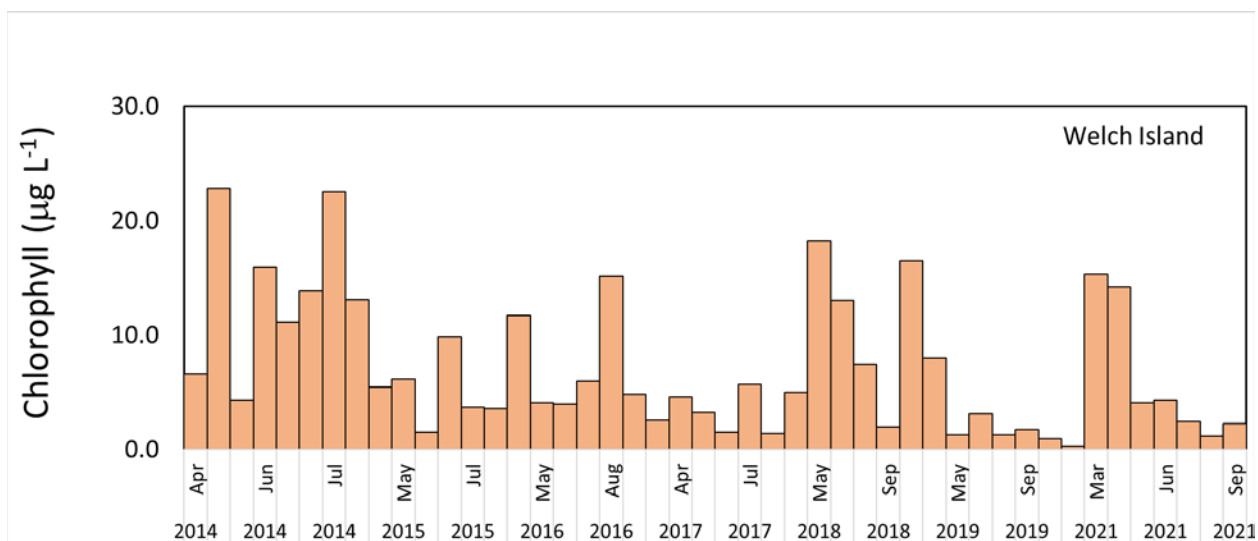


Figure 88. Chlorophyll *a* concentration at Welch Island (2014–2021).

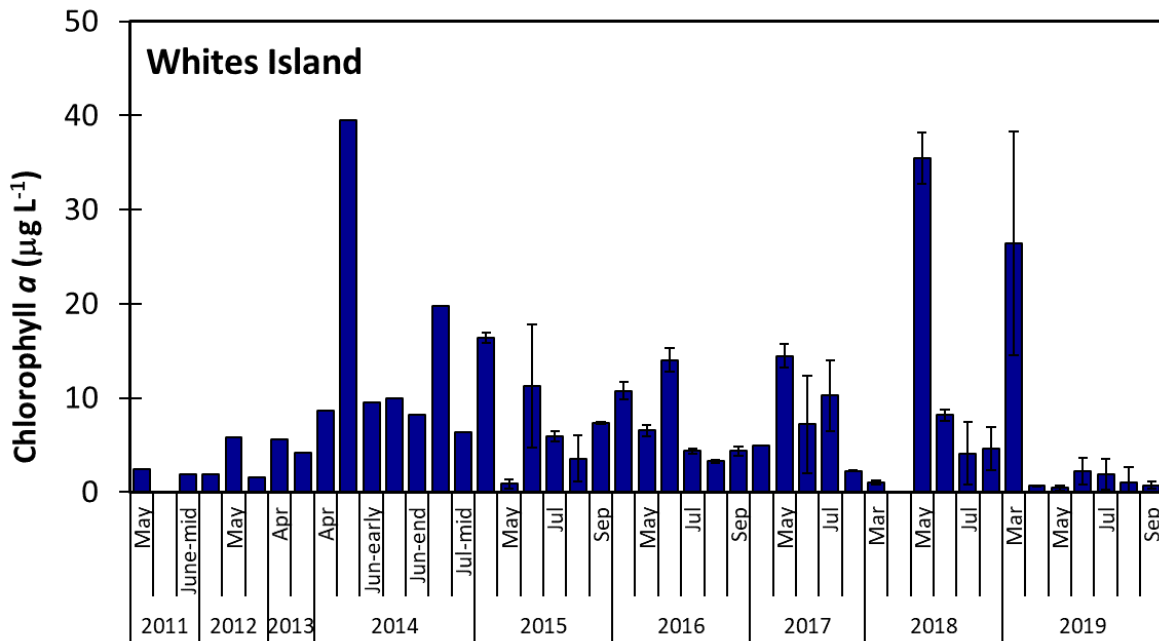


Figure 89. Chlorophyll *a* concentration in discrete samples collected from Whites Island (2011–2019).

As shown in the 2011-2019 time series, pre-freshet primary production tends to be high at Whites Island, with high peaks occurring in some years (Figure 89, Figure 90). In general, chlorophyll concentrations decline after the freshet subsides, although reasonably high values have been observed in June and July in some years. For example, in 2016, the highest chlorophyll *a* concentration observed that year was in June, while in 2014, concentrations observed in early July were second only to the peak in May (Figure 89).

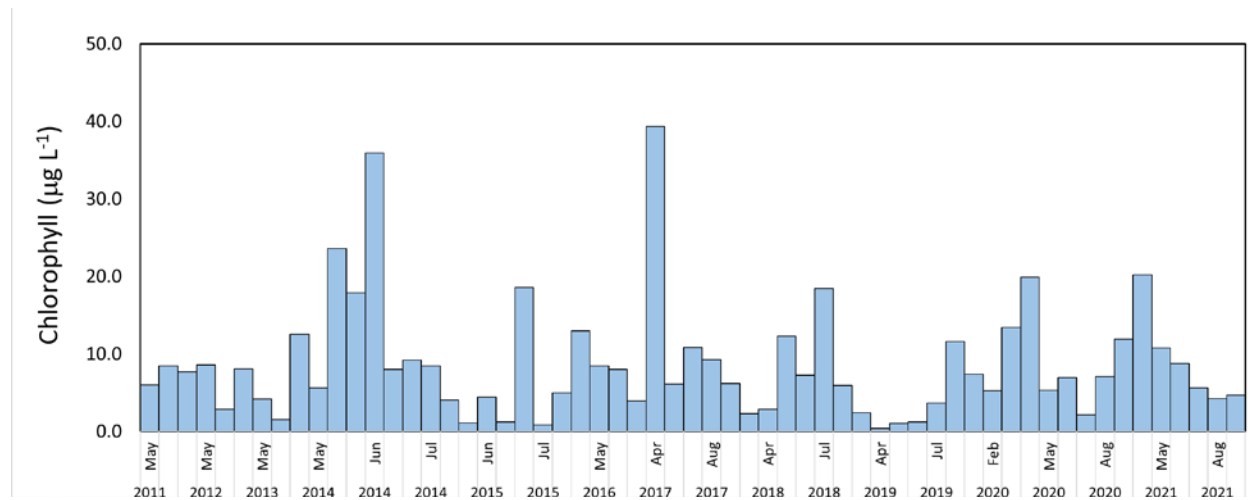


Figure 90. Chlorophyll *a* concentrations at Campbell Slough (2011–2021).

At Campbell Slough, peaks in chlorophyll *a* values were highest in 2014 and in 2017 (Figure 90). The latter was a year characterized by higher-than-average river flow. Chlorophyll concentrations were lower than average in 2015 and 2019, two years where water levels were very low. At this site, chlorophyll peaks have occurred at different times during the spring and summer, unless other sites where the peak generally occurs after the onset of spring and before the spring freshet.

Franz Lake Slough had a large peak in chlorophyll during 2019, a very dry year, with high concentrations also observed in 2018 (Figure 91). Moderate concentrations of chlorophyll *a* were observed in 2020 and 2021.

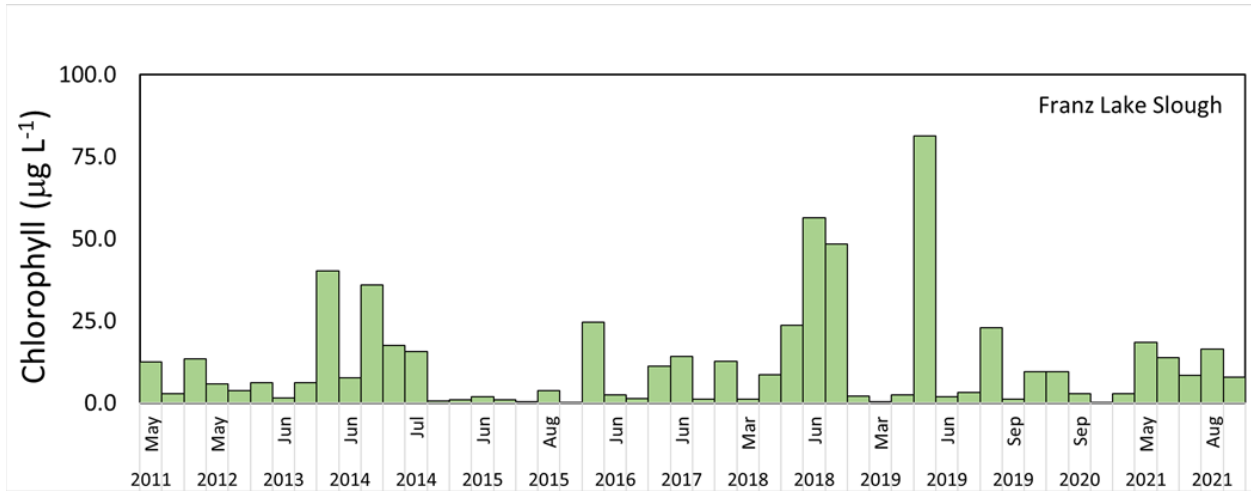


Figure 91. Chlorophyll *a* concentrations at Franz Lake Slough (2011–2021).

Looking at a summary of chlorophyll data from the five trend sites, it is clear that the highest episodic values are seen at Franz Lake Slough (Figure 92). The distribution of data is similar at Campbell Slough, Welch Island, and Whites Island. The fewest high values are observed at Ilwaco Slough, where the bulk of the chlorophyll concentrations are low and consistent throughout the sampling periods.

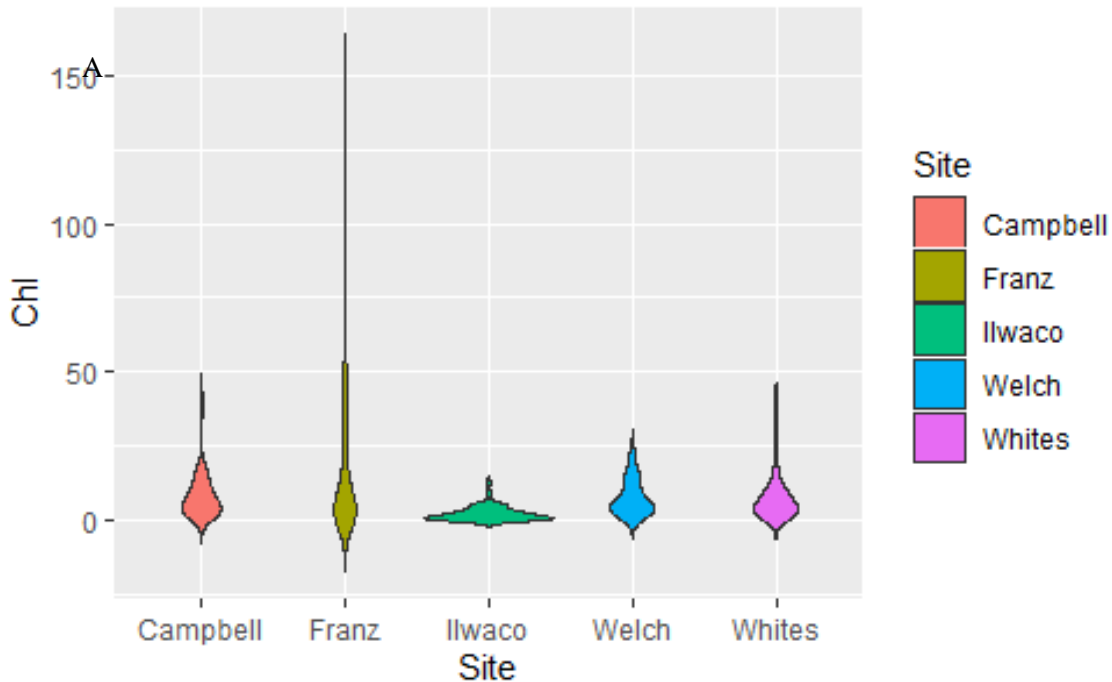


Figure 92. Violin boxplots showing chlorophyll concentrations determined at the five off-channel trends sites between 2011 and 2021.

3.4.1.3 *Phytoplankton Species Composition*

Sampling for phytoplankton species composition took place between March and September from 2011-2019, although sampling was not performed during each of these months for all years. In 2020, sampling was limited to February, March, June, August, and September due to travel restrictions associated with covid-19. In 2021, sampling returned to near normal, but sample processing times were delayed due to modified operations in laboratories at OHSU.

Phytoplankton taxa were placed in the following groupings: diatoms (Class Bacillariophyceae), chlorophytes (Class Chlorophyceae), chrysophytes (Class Chrysophyceae), cryptophytes (Class Cryptophyceae), cyanobacteria (Class Cyanophyceae), and dinoflagellates (Class Dinophyceae). Also, ciliates were enumerated, since there are some species that can be photosynthetic (e.g., *Mesodinium rubrum*; Lindholm et al., 1985, Herfort et al., 2011a, 2011b), particularly at Ilwaco Slough. However, ciliate abundances were relatively low and therefore were not included in plots. The following sections report out on longterm species composition at trend sites between 2011-2019, as well as the more limited observations from 2020 and 2021. Analysis of 2021 samples is ongoing at the time of the writing of this report.

Overview

Over the full time series, diatoms (Class Bacillariophyceae) have been found to dominate the phytoplankton assemblage in the spring, prior to the annual snowmelt-driven freshet. During the freshet, populations decline due to dilution by the increased water volume. In the summer, a shift from diatoms to green algae and unicellular flagellates tends to occur at the off-channel sites, with the exception of Ilwaco, which becomes increasingly influenced by tidal exchange with the coastal ocean. At this site, benthic diatoms are prevalent, both from fresh and marine sources. In addition, marine species are found in the summer and autumn months, including diatoms (e.g., *Ditylum brightwellii* and *Asterionellopsis* sp.) and the photosynthetic ciliate, *Mesodinium* cf. *rubrum*. At Campbell Slough and Franz Lake Slough, cyanobacteria abundance increases to high levels in the summer months, particularly from July through September. This has consistently been observed, year after year.

Over the years of study, we observed a similar succession pattern among the diatoms, with early spring assemblages dominated by small centric species (mainly *Cyclotella* spp.). Following the small centrics is *Asterionella formosa*, which occurs either in advance of, or coincident with, *Aulacoseira* spp. Next comes *Fragilaria* (*F. crotonensis* and *F. intermedia*), and finally *Skeletonema potamos*. In some years, *Tabellaria* spp. occurs at the same time as *Skeletonema*. In different years, we observe these key species at different times, depending on environmental conditions and when we were able to collect samples. Observing and documenting these succession patterns is useful, because a disruption in the sequence can signal a flow-driven disturbance (for example resulting from pluvial flow or an early or delayed freshet) that influences the availability of organic matter for secondary and tertiary producers. Further, different species have different size characteristics, susceptibility to parasitism, and occupy different physical niches (e.g., benthic vs. pelagic habitats), which influence the degree to which fluvial primary production enters the food web and fuels growth of juvenile salmonids and other species.

In 2020, fewer samples were examined, so it is difficult to ascertain whether the succession patterns observed from 2011-2019 occurred in 2020. However, broadly, cyanobacteria and chlorophytes increased in numerical abundance from winter through spring and summer at the EMP sites (Figure 93). Although high abundances of small cells (including cyanobacteria and some of the chlorophytes and chrysophytes) were observed at some of the sites in 2020 (similar to other years), it is worth noting that the amount of carbon associated with these smaller cells tends to be much smaller than the amount associated with larger cells such as diatoms.

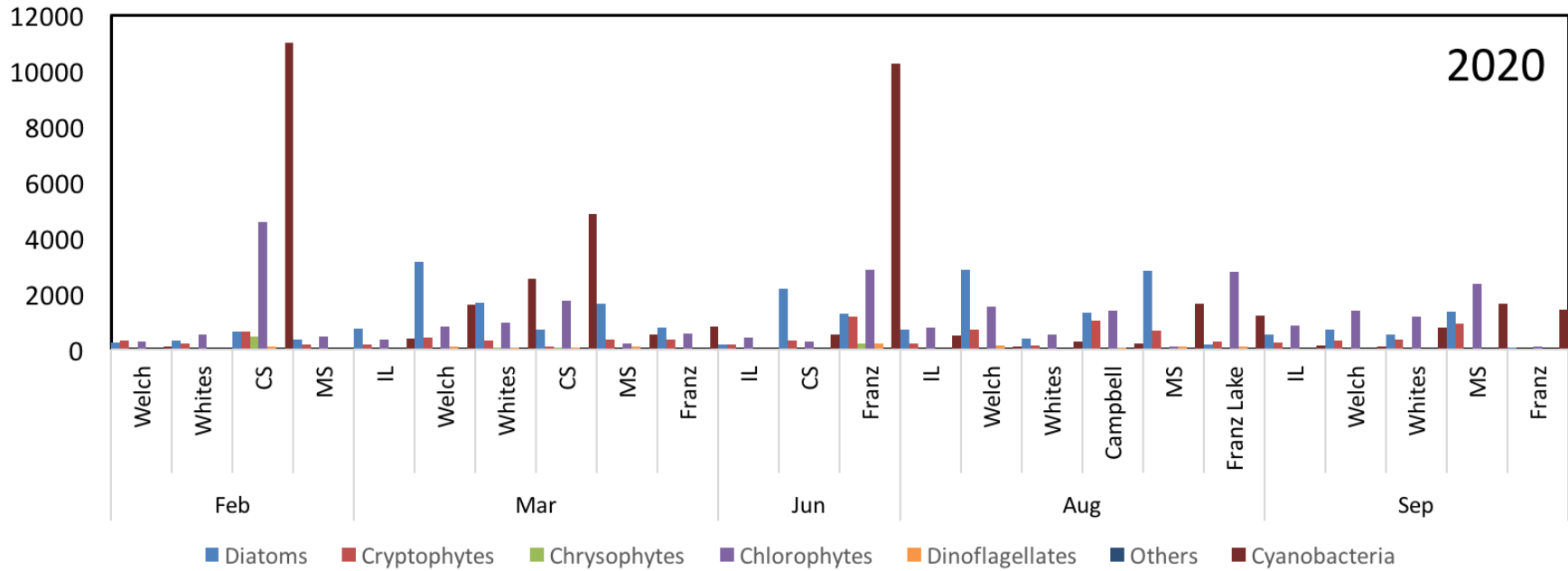
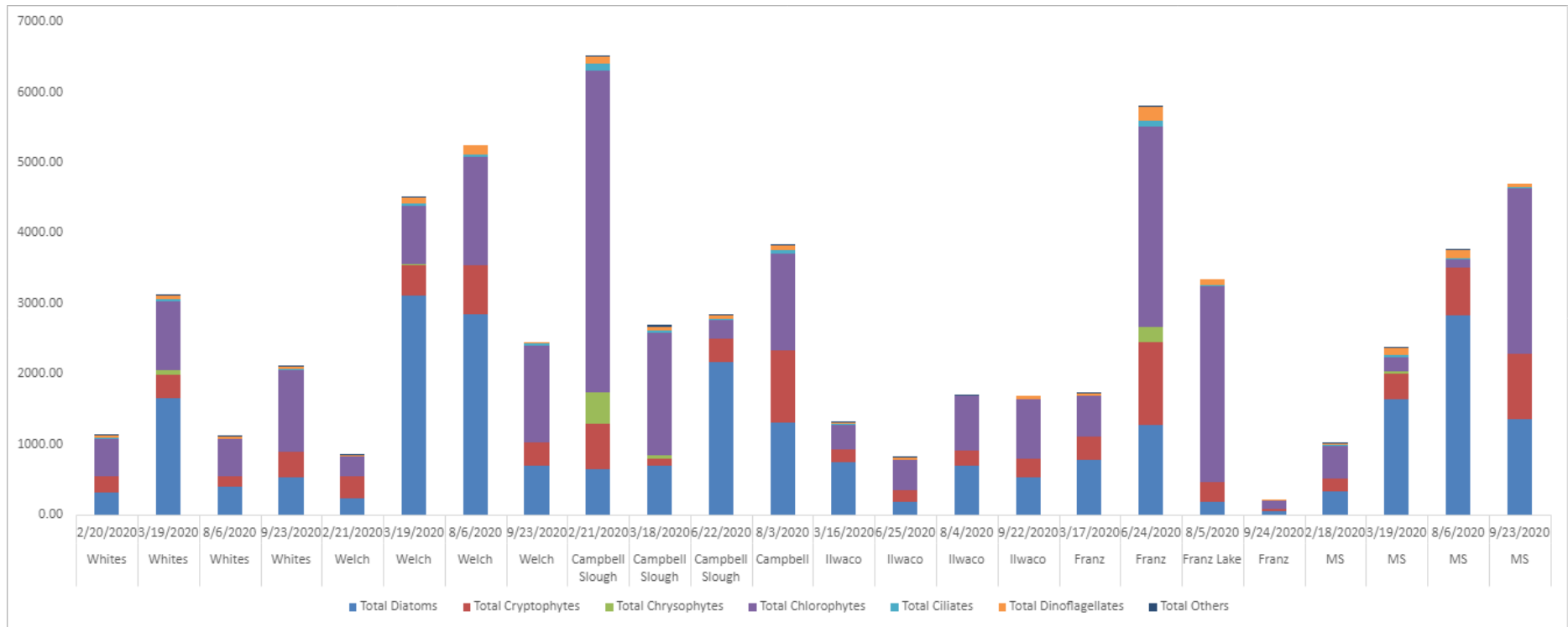


Figure 93. Phytoplankton data for EMP sites in 2020. Sites include Ilwaco Slough (IL), Welch Island, Whites Island, Campbell Slough (Campbell), Franz Lake Slough (Franz), and samples from the mainstem river at the Port of Camas, Washington (MS).



When the data are considered in terms of percent of total abundance, the relative contribution by diatoms, a taxonomic group generally considered to be of high nutritional value, was more variable at the two sites often characterized by cyanobacteria blooms – Campbell Slough and Franz Lake Slough (Figure 94). At Whites Island, diatoms accounted for 20-30% of total phytoplankton and at Welch Island, the contribution was between 25 and 50%. Much lower contributions (<10%) were observed at Campbell Slough and Franz Lake Slough on some of the sample dates. The contribution of diatoms at Ilwaco was similar to Whites and Welch, although marine species were present at Ilwaco in the summer months, unlike the other two.

2020

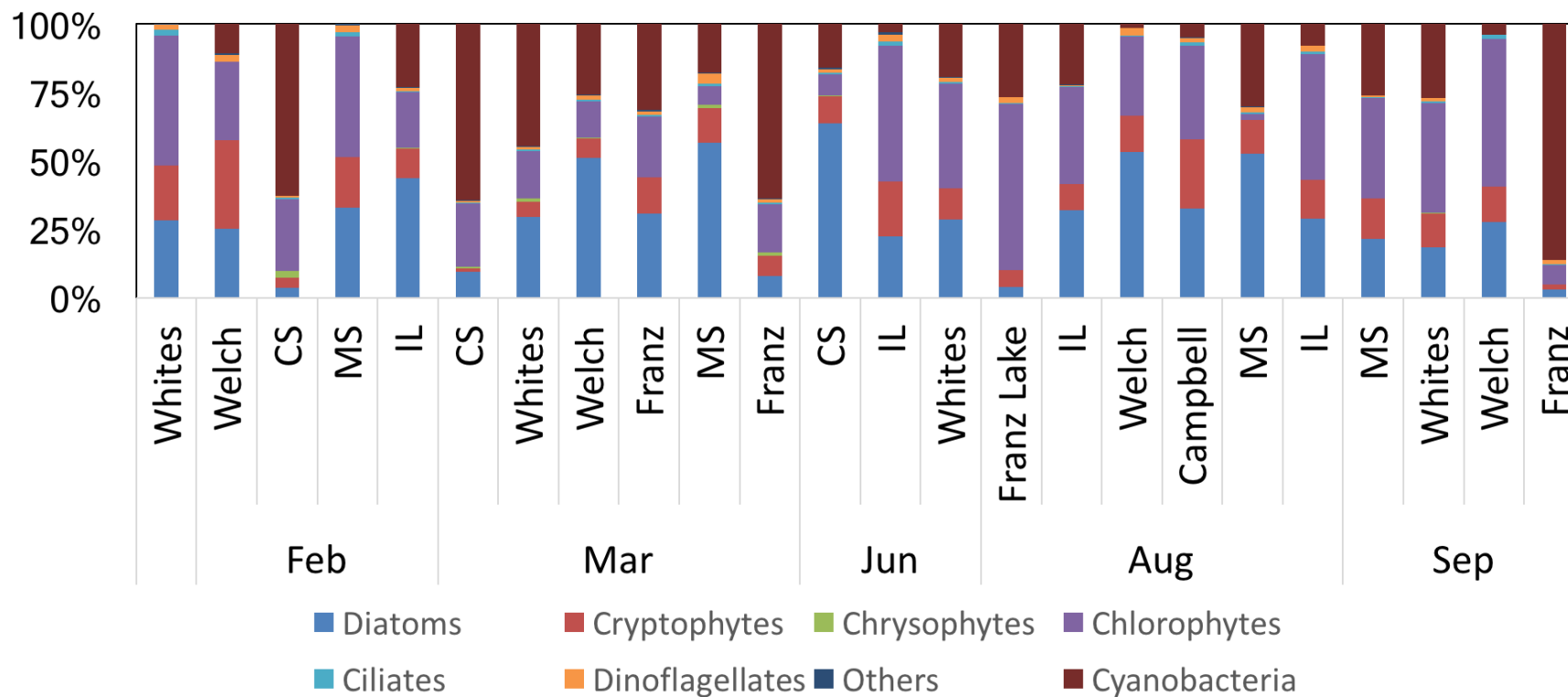


Figure 94. Summary of species composition data collected in 2020 at EMP sites and the mainstem Columbia River at the Port of Camas, Washington (mainstem = MS), including Whites Island (Whites), Welch Island (Welch), Ilwaco (IL), Campbell Slough (CS), and Franz Lake Slough (Franz)

Ilwaco Slough

The phytoplankton assemblage at Ilwaco varies seasonally, with riverine conditions dominating until after the spring freshet subsides. Assemblages tend to look more similar to the other sites in early to mid-spring (March-May), with diatoms dominating the assemblage (Figure 96 and Figure 94). During the transition to summer where conditions become more marine, the assemblage includes a greater proportion of cryptophytes and other flagellate species (e.g., chrysophytes). In 2019, we observed a higher abundance of cyanobacteria species at Ilwaco compared to previous years in both April-May and August; this was not observed in 2020, where the proportional numerical contribution of cyanobacteria (~20% in spring) was approximately half that of the diatoms (Figure 95). Diatoms dominated the phytoplankton assemblage in March and were co-dominant with small flagellates in August and September in 2020.

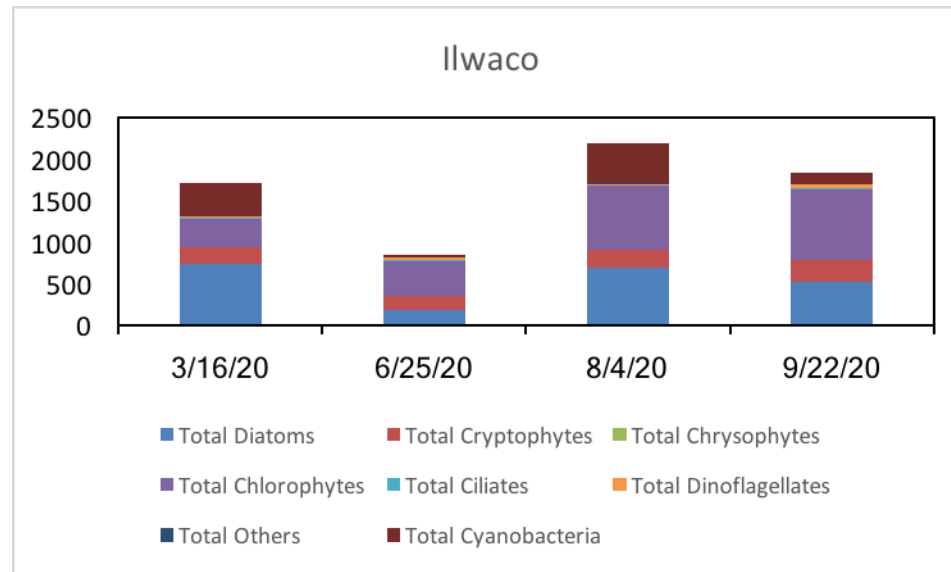


Figure 95. Densities (in cells mL⁻¹) of different phytoplankton taxonomic groups at the EMP site, Ilwaco, in 2020.

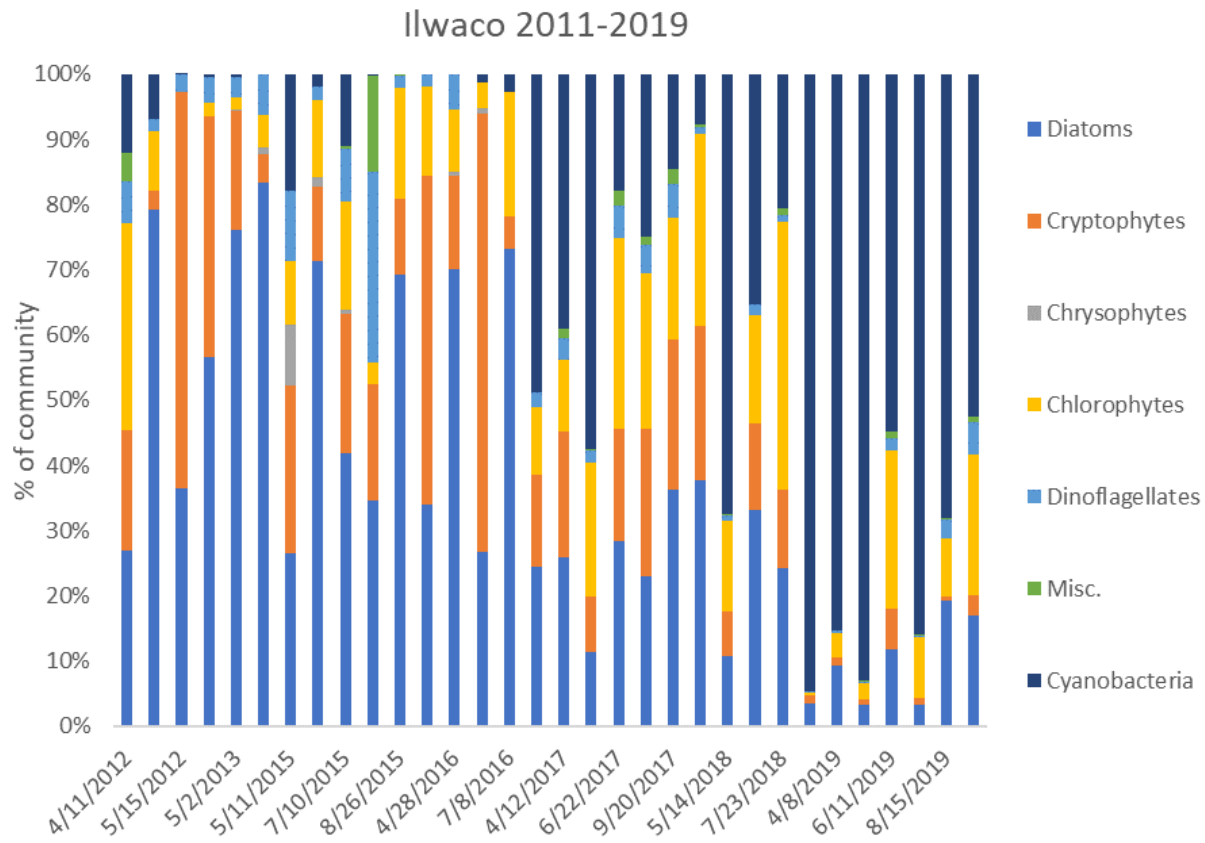


Figure 96. Relative percentages of different phytoplankton classes at Ilwaco observed during the spring and summer months between 2011 and 2019.

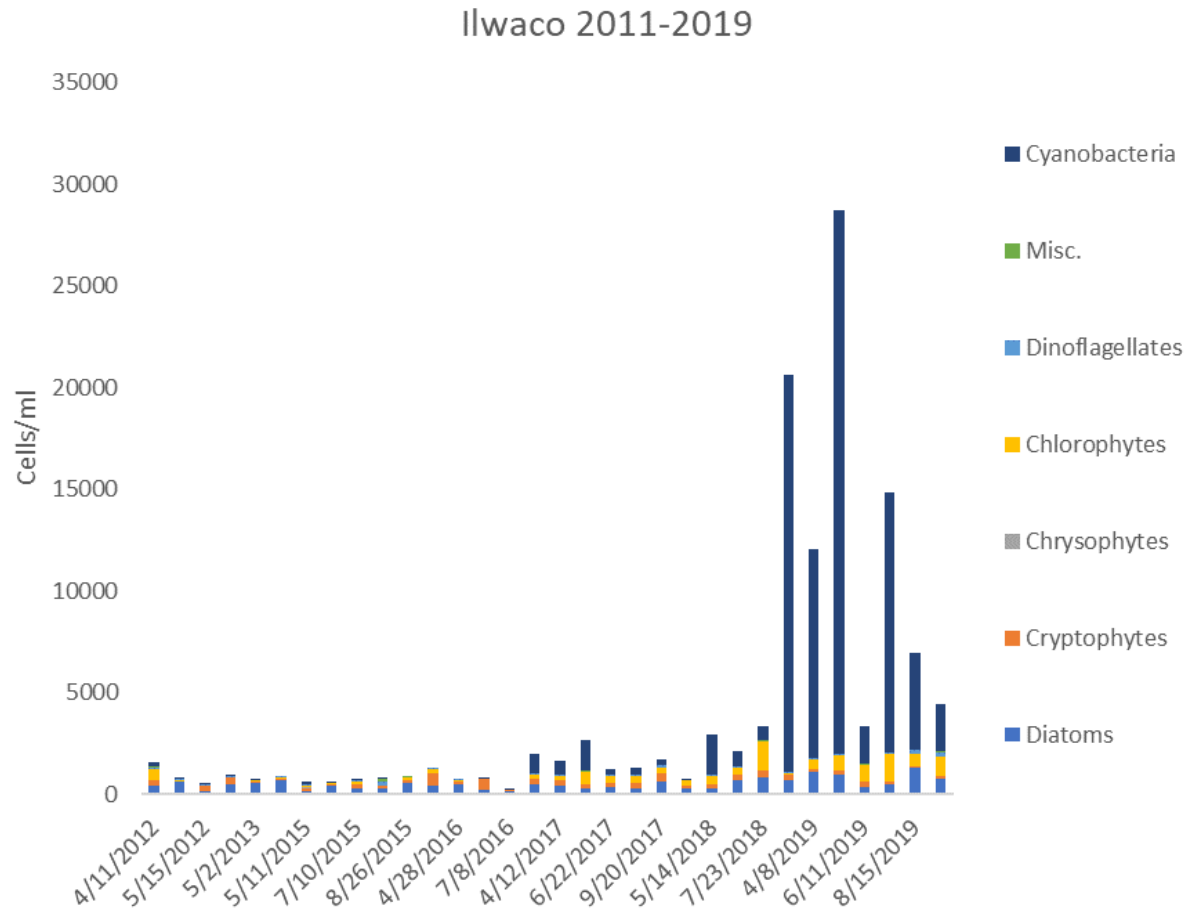


Figure 97. Absolute abundances of phytoplankton classes at Ilwaco from 2011 to 2019.

Welch Island and Whites Island

In previous years, the phytoplankton assemblages at Welch Island and Whites Island have been numerically dominated by diatoms, particularly in early spring (Figure 98 and Figure 101). Notably, abundances of cyanobacteria were higher in 2017, 2018 and 2019 than in previous years, particularly in the summer months at Welch Island (Figure 98) and abundances of cyanobacteria were higher at Whites Island in 2017 and 2018 compared to 2019. In 2020, of the samples we were able to obtain, diatoms were not numerically dominant (Figure 99); instead, cyanobacteria and

chlorophytes were most abundant. It is important to note that most of the species encompassed by the cyanobacteria and chlorophyte groups are much smaller than the diatoms, so in terms of contributions to carbon associated with pelagic primary producers, diatoms were still the most important group at this site. Data for Welch Island in 2020 were not available at the time of this report, nor were data from 2021 for either site.

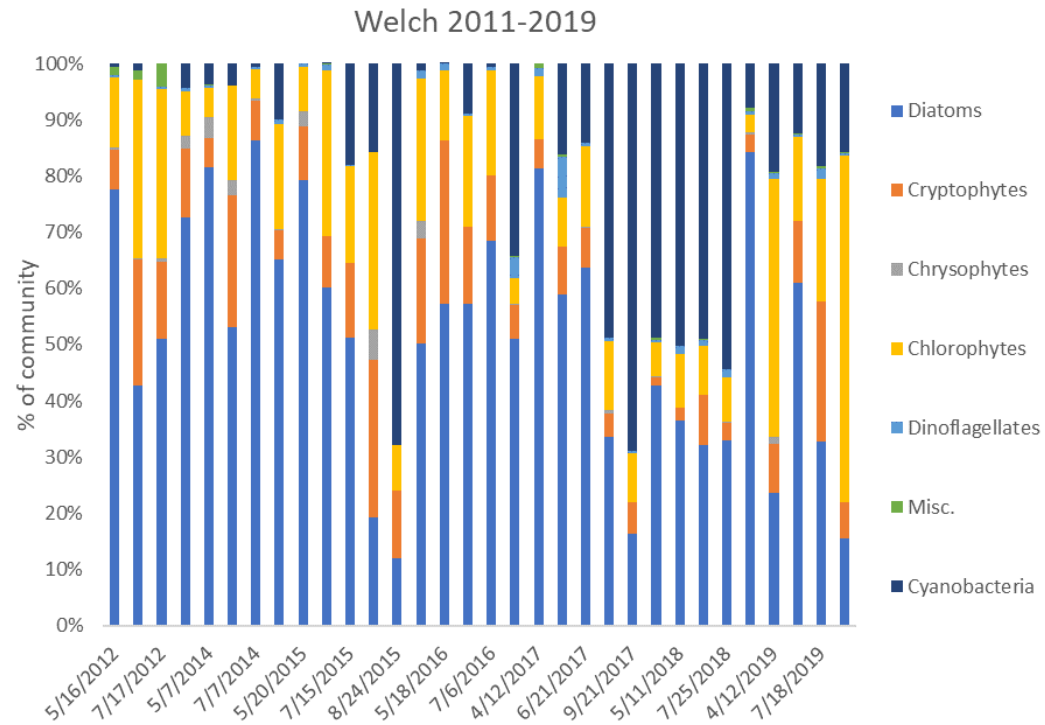


Figure 98. Relative percentages of different phytoplankton classes at Welch Island from 2011 to 2019.

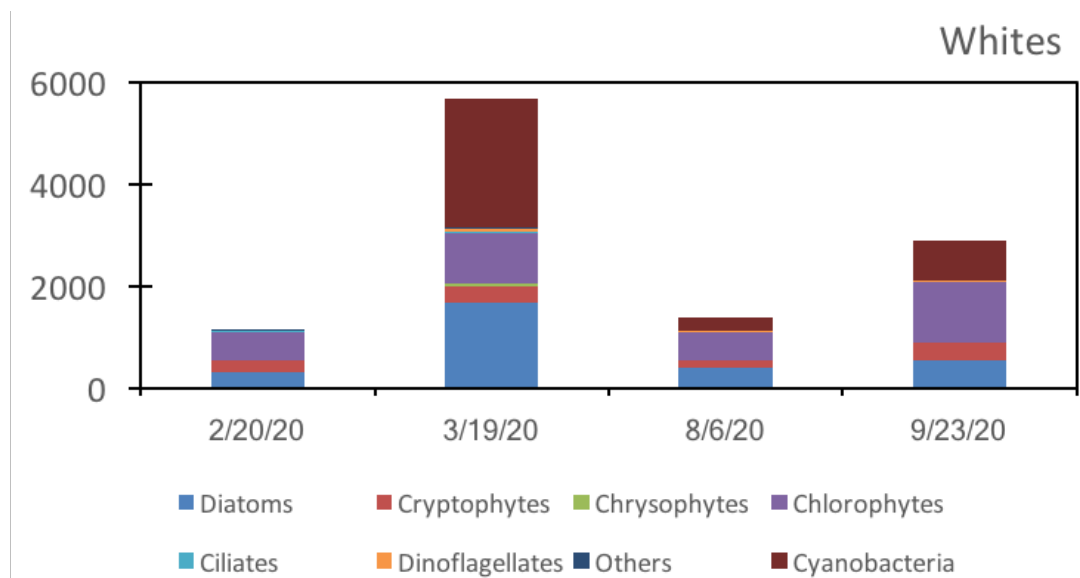


Figure 99. Densities (in cells mL⁻¹) of different phytoplankton taxonomic groups at the EMP site, Whites Island, in 2020. Data for April and May are missing due to travel restrictions associated with the covid-19 pandemic.

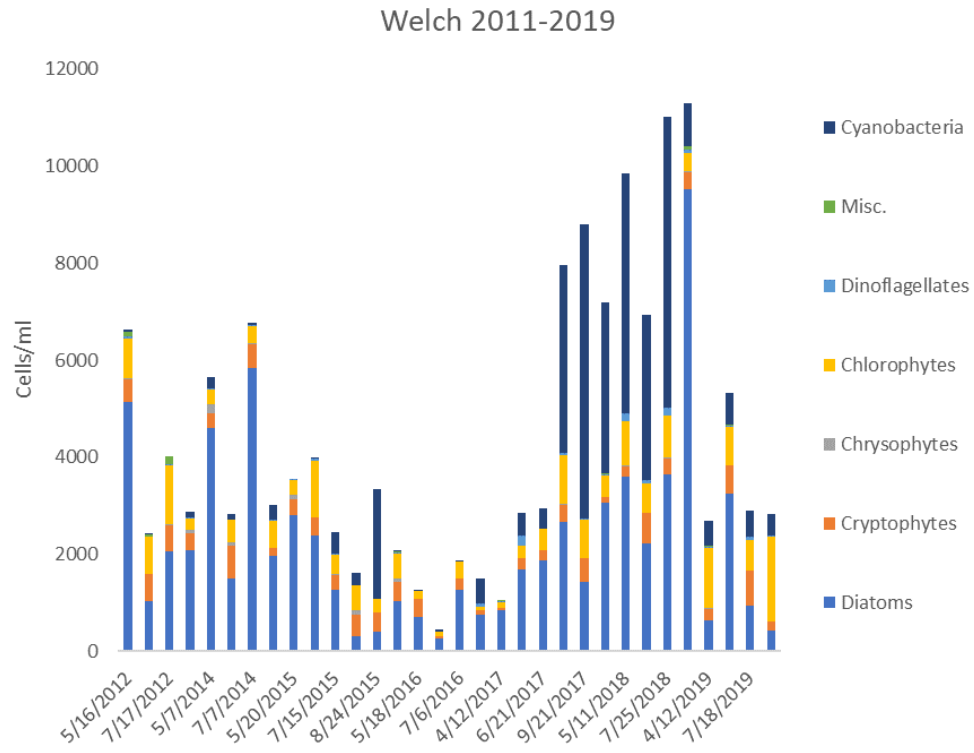


Figure 100. Absolute abundances of phytoplankton classes at Welch Island from 2011 to 2019.

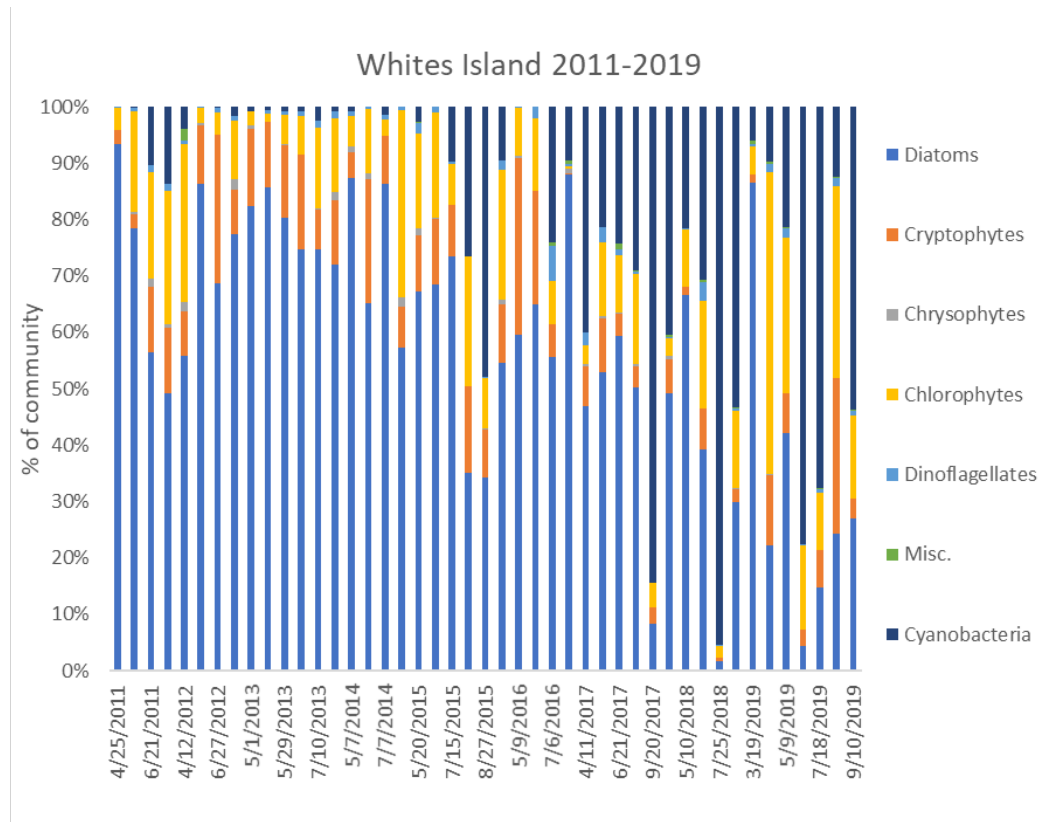


Figure 101. Relative percentages of different phytoplankton classes at Whites Island from 2011 to 2019

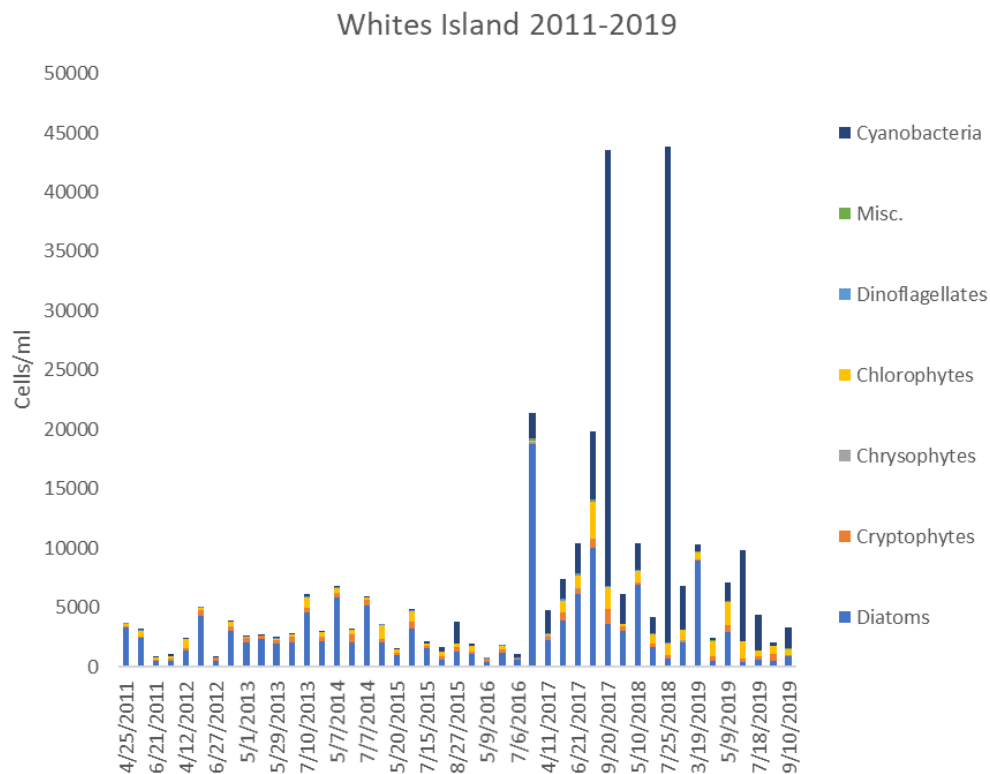


Figure 102. Abundances of different phytoplankton classes (in cells/mL) at Whites Island from 2011 to 2019.

Campbell Slough and Franz Lake Slough

Phytoplankton assemblages in the upriver sites have evolved since summer 2015, showing a growing dominance of cyanobacteria at both Campbell and Frank Lake Sloughs, with a short hiatus in 2016 (Figure 103 and Figure 105). Abundance of cyanobacteria were greater in 2018 than in 2019 at Campbell (Figure 104). Cyanobacteria abundance in 2019 at Franz Lake slough was significantly lower than previous years (Figure 106).

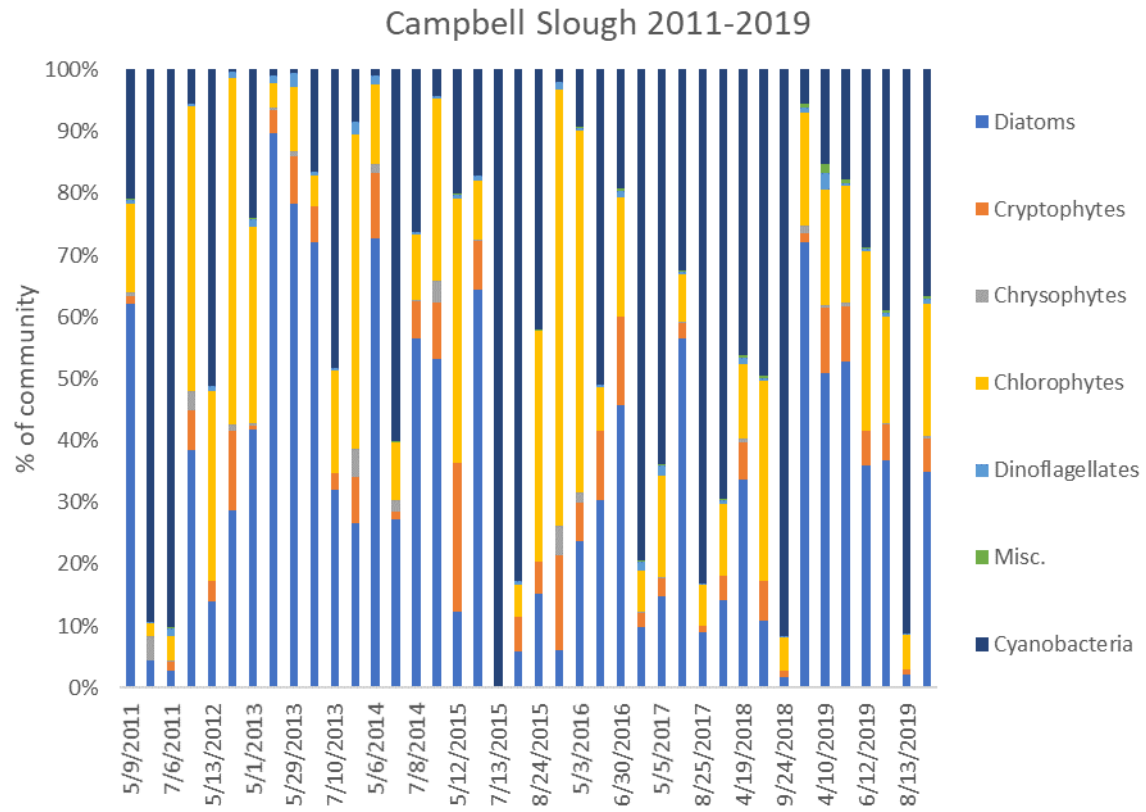


Figure 103. Relative percentages of different phytoplankton classes at Campbell Slough from 2011 to 2019.

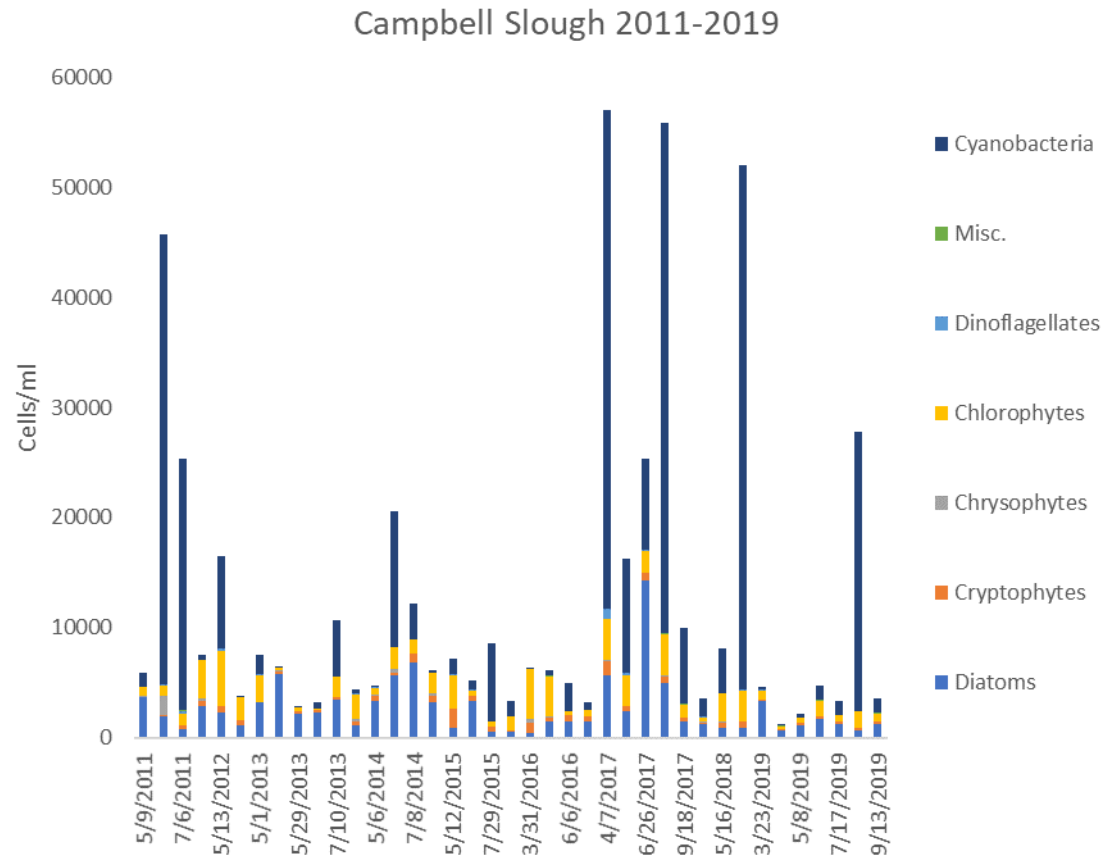


Figure 104 Abundances of different phytoplankton classes (in cells/mL) at Campbell Slough from 2011 to 2019.

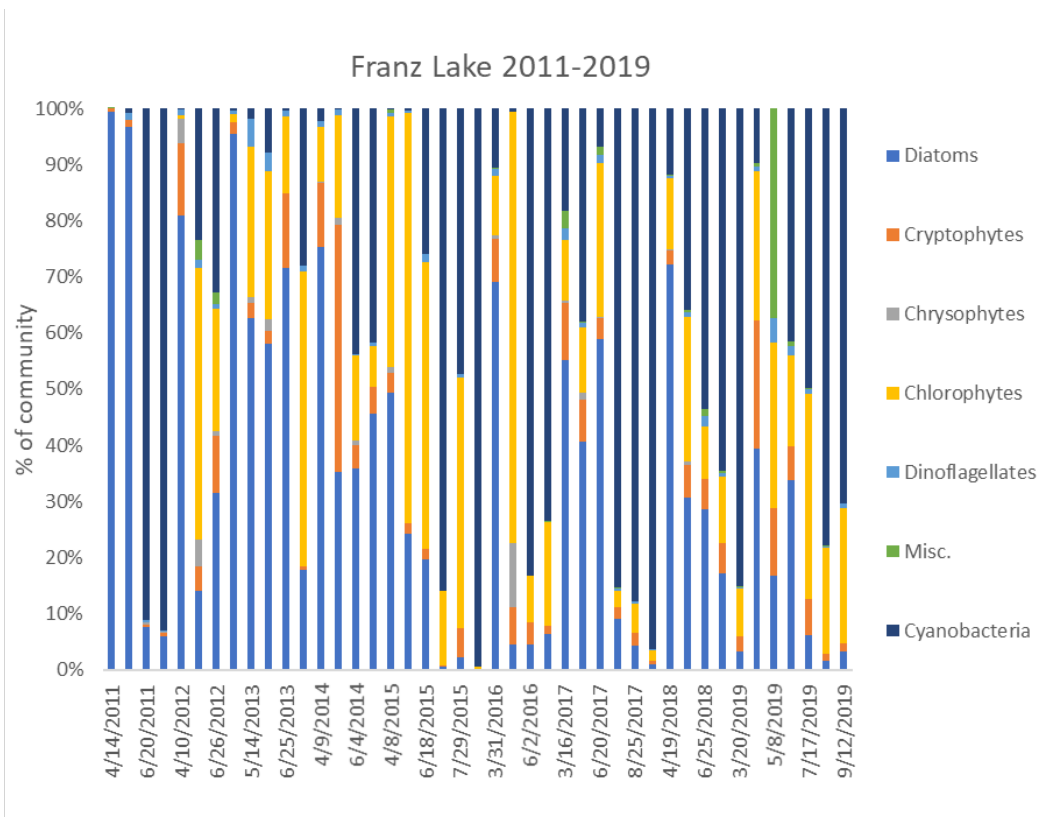


Figure 105. Relative percentages of different phytoplankton classes at Franz Lake Slough from 2011 to 2019.

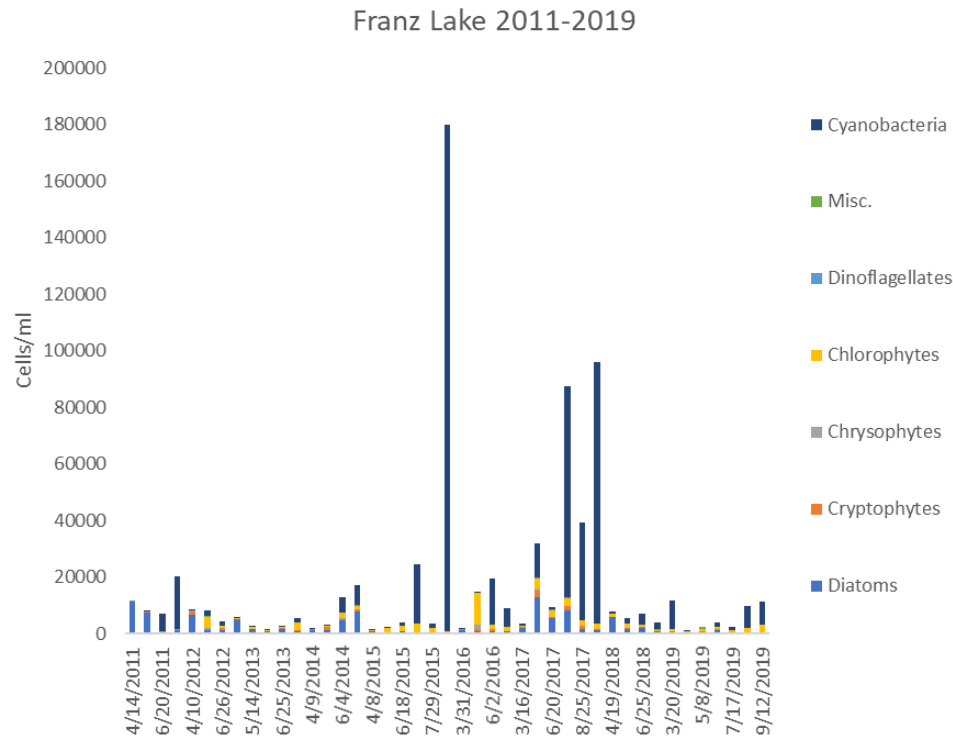


Figure 106. Abundances of different phytoplankton classes (in cells/mL) at Franz Lake Slough from 2011 to 2019.

3.4.1.4 *Phytoplankton and environmental variables*

To look for relationships between environmental variables and phytoplankton assemblages, we performed canonical correspondence analysis on phytoplankton and environmental data collected between 2012 and 2021 (Figure 107). The plot shows a greater spread along the second axis of variability, which was most closely related to nitrate concentration, temperature, and percentage of maximum discharge. Positive associations were observed between temperature and abundance of chlorophytes, dinoflagellates, and cryptophytes, while negative associations were observed between temperature and the abundance of diatoms and chrysophytes. The first axis was most closely associated with variation in phosphate concentration, which was most closely associated with variations in the abundance of cyanobacteria and negatively associated with the abundance of diatoms. The CCA also showed that high levels of nitrate and the highest percentages of maximum yearly discharge were associated with diatoms, while cryptophytes, dinoflagellates, and chlorophytes were negatively related to nitrate concentration.

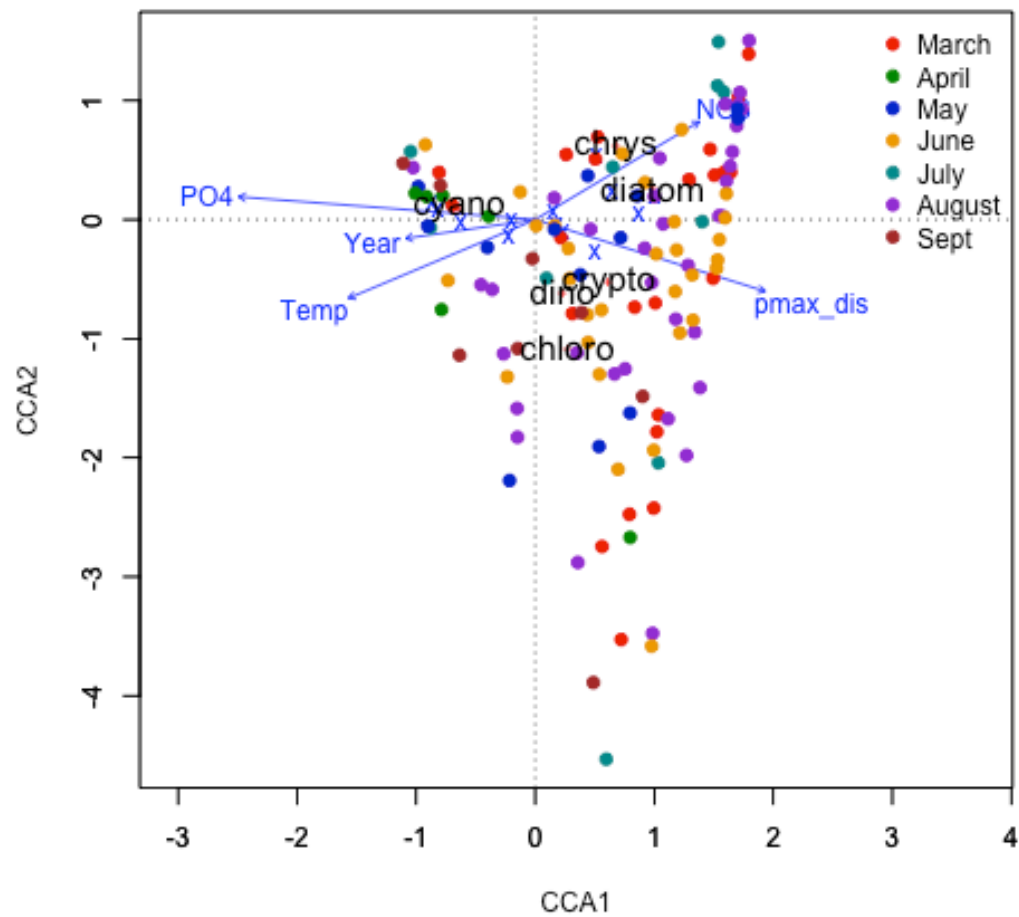


Figure 107. Biplot generated from canonical correspondence analysis relating phytoplankton taxonomic groups (labeled according to month sampled) to environmental variables: PO₄ = phosphate, NO₃ = nitrate, Temp = river temperature

3.4.2 Spring Zooplankton Assemblages

Data from 2011 to 2019 show that, numerically, rotifers accounted for a large percentage of the zooplankton assemblages at all sites prior to 2017. Copepods and cladocerans together dominated the zooplankton assemblages, with different taxa found at Ilwaco compared to the rest of the EMP sites. The greatest density and diversity of cladocerans was observed at Campbell Slough, particularly in 2017. In general, copepods were found to increase in abundance in the spring before cladocerans did, except at Ilwaco, where cladocerans were not as abundant compared to the other sites. New data from 2020 and 2021 are unavailable for this report.

Among the copepods, cyclopoids generally dominated the zooplankton assemblages across sites, except in a few cases where either harpacticoids or calanoids co-dominated alongside the cyclopoids (e.g., Whites Island in June 2019 and Franz Lake Slough in 2017). There was less of a dominance of cyclopoid taxa at Ilwaco, where harpacticoid and calanoid taxa were co-dominant in May/June 2018. Cyclopoid densities peaked earlier in 2017 (May) than 2018 (June-July) at Whites Island, Campbell Slough, and Franz Lake Slough. At Ilwaco, harpacticoid abundances peaked in May in both 2017 and 2018.

In 2017, dipteran larvae were present early in the season at Ilwaco, while they appeared at Whites and Franz during the summer months.

Ilwaco

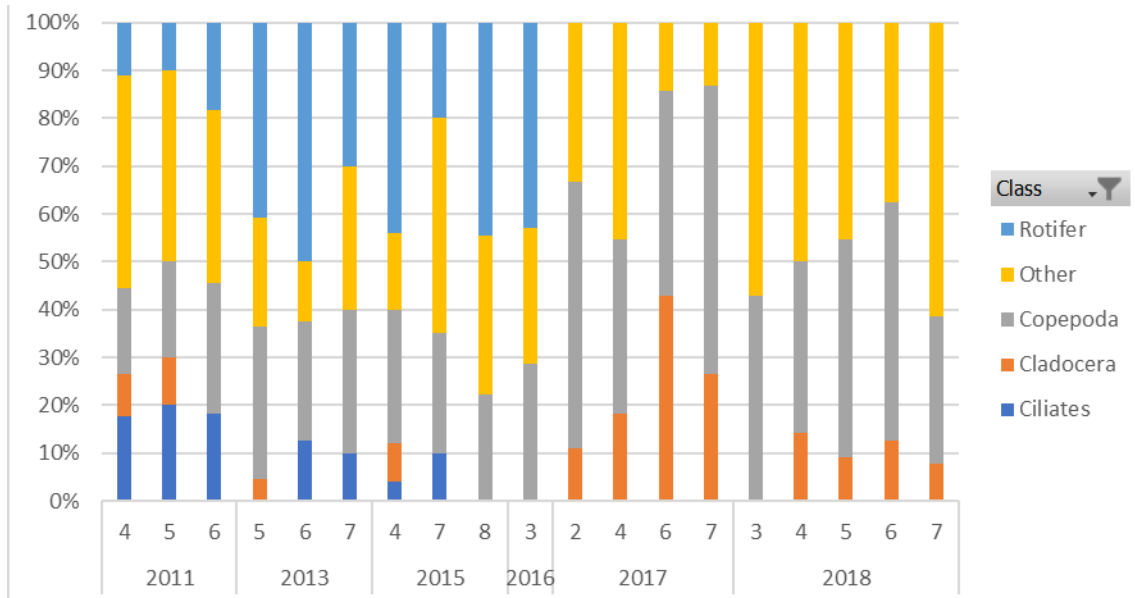


Figure 108. Percentage of total zooplankton community accounted for by different groups (rotifers, copepods, cladocerans, ciliates, and ‘other’, which includes taxa not included in the other groups listed. These include, for example, nematodes, polychaetes, chironomid larvae, ostracods, etc.) at Ilwaco (including Ilwaco Slough and Ilwaco Marina) from 2011 to 2018.

Welch Island

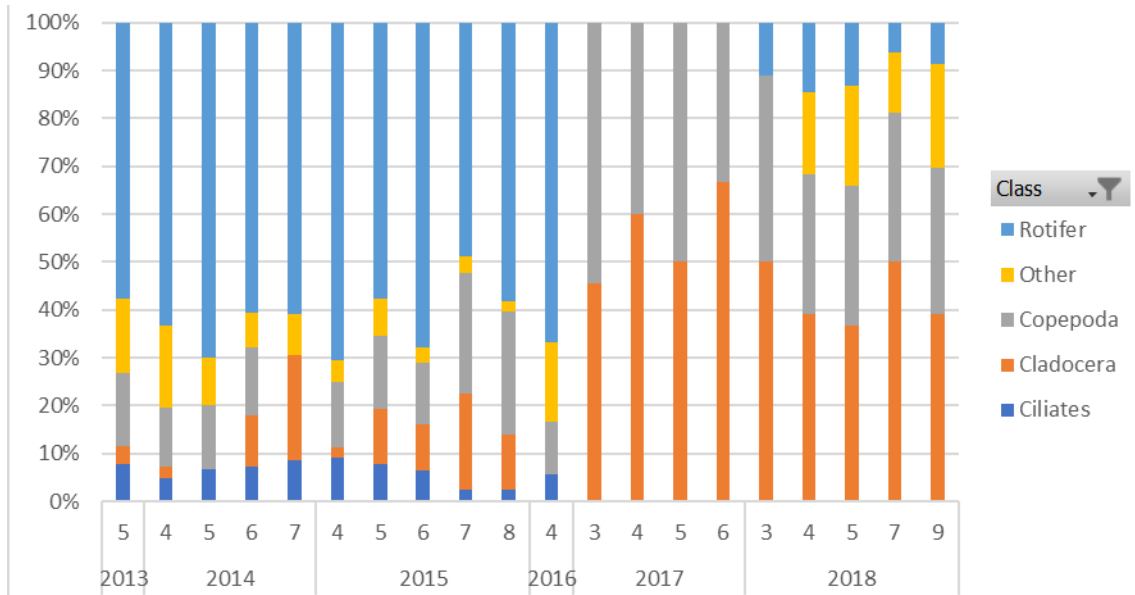


Figure 109. Percentage of total zooplankton community accounted for by different groups (rotifers, copepods, cladocerans, ciliates, annelids, and ‘other’, which includes taxa not included in the other groups listed. These include taxa that are present at low abundance, for example nematodes) at Welch Island from 2011 to 2018.

Whites Island

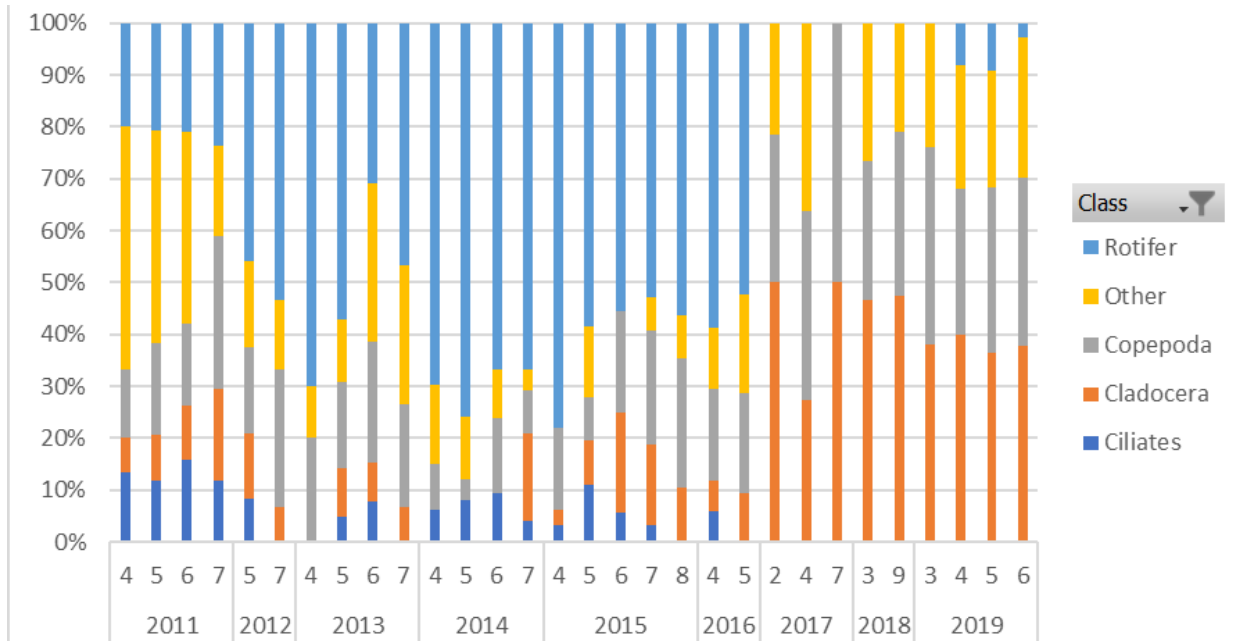


Figure 110. Percentage of total zooplankton community accounted for by different groups (rotifers, copepods, cladocerans, ciliates, annelids, and ‘other’, which includes taxa not included in the other groups listed. These include taxa that are present at low abundance, for example nematodes) at Whites Island from 2011 to 2019.

Campbell Slough

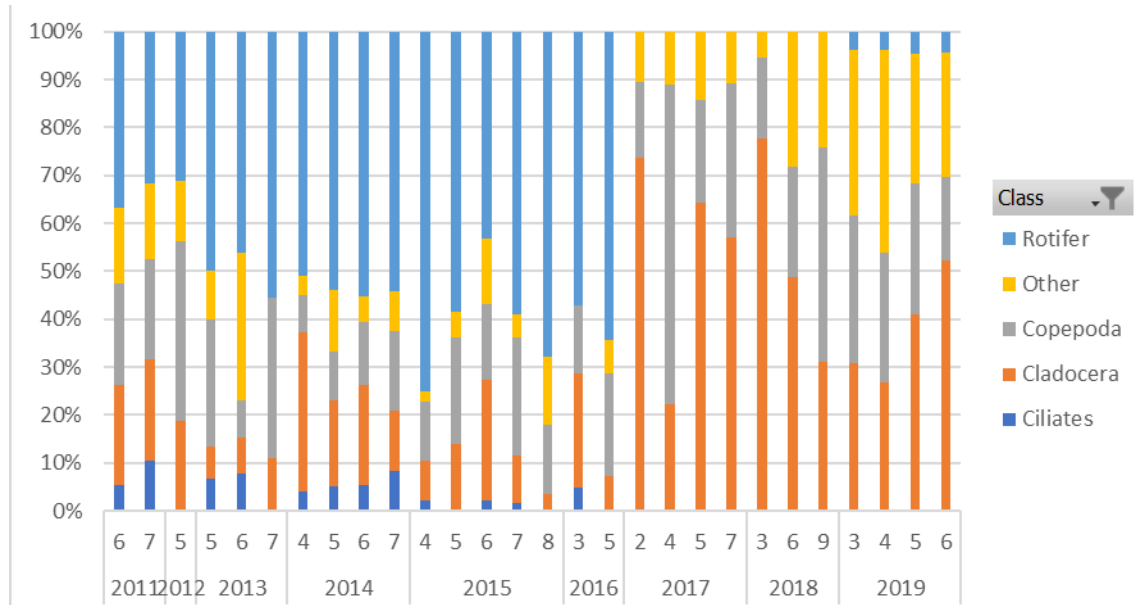


Figure 111. Percentage of total zooplankton community accounted for by different groups (rotifers, copepods, cladocerans, ciliates, annelids, and ‘other’, which includes taxa not included in the other groups listed. These include taxa that are present at low abundance, for example nematodes) at Campbell Slough from 2011 to 2019.

Franz Lake Slough

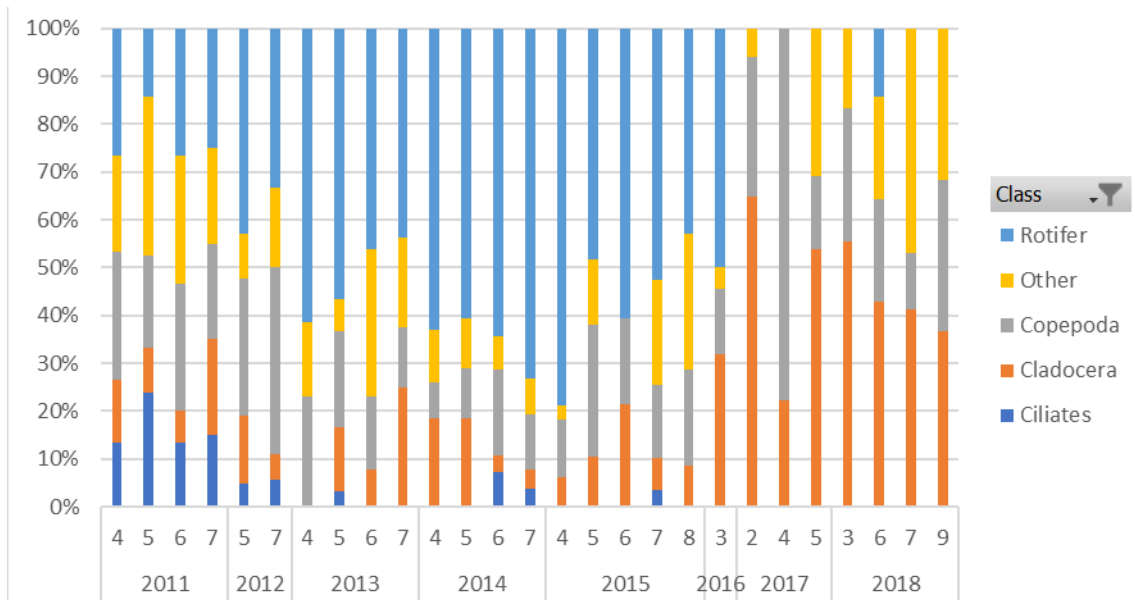


Figure 112. Percentage of total zooplankton community accounted for by different groups (rotifers, copepods, cladocerans, ciliates, annelids, and ‘other’, which includes taxa not included in the other groups listed. These include taxa that are present at low abundance, for example nematodes) at Franz Lake Slough from 2011 to 2018.

A comparison of two sites, Whites Island in Reach C and Campbell Slough in Reach F shows that the zooplankton densities and assemblage composition were more similar between the two sites during April and May than in March and June, likely reflecting a combination of water connectivity, resuspension (in the case of the Nematoda), and invertebrate life cycles (e.g., for the Diptera).

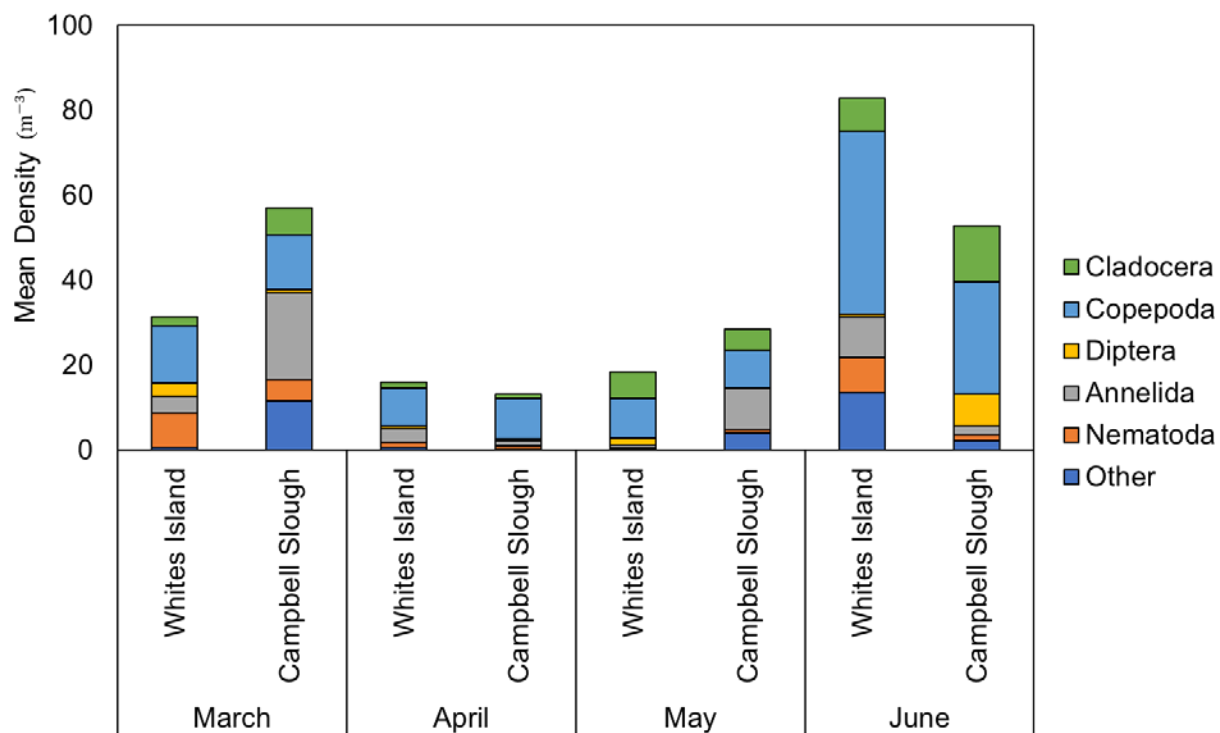


Figure 113. Comparison of zooplankton densities at Whites Island (Reach C) and Campbell Slough (Reach F) in 2019 showing the mean total density and relative contributions to mean total density at the two sites.

In general, rotifers – a group that includes species which tend to be much smaller than copepods and cladocerans - are numerically dominant, particularly in the early spring, prior to the spring freshet. Among the Crustacea, copepods tend to dominate the mesozooplankton assemblages at all sites (Figure 113), with the highest densities observed at Campbell Slough and the highest proportional contributions observed at Ilwaco. Cyclopoids tend to be ~10 times denser at Campbell Slough than at the other sites. Franz Lake Slough tends to have the lowest copepod densities, which consist mainly of calanoid and harpacticoid species. At Ilwaco Slough, zooplankton assemblages tend to be dominated by harpacticoid and cyclopoid species.

The zooplankton assemblage at most of the sites shifts from one dominated by copepods to one dominated by cladocerans from spring to summer. The cladoceran assemblages are generally dominated by *Bosmina* spp. (with and without eggs) at all sites, except Ilwaco, with greatest diversity seen at Campbell Slough, where *Chydoridae* spp. *Alona* spp., and *Ceriodaphnia* spp. co-dominate. At Ilwaco, the predominant cladoceran taxon is *Daphnia* spp.

3.4.3 Stable Isotope Ratios of Carbon and Nitrogen

Stable isotopes were not analyzed in 2020 nor 2021; however, these data have been further analyzed. Carbon isotopes can be used to determine the source of organic matter to a consumer, while nitrogen isotopes can be used to determine the trophic level of a consumer. Most terrestrial plants have $\delta^{13}\text{C}$ values between -24 and -34‰, seaweeds, and marine plants between -6 and -19‰, and algae and lichens -12 to -23‰. According to Cloern (2002), $\delta^{13}\text{C}$ values for freshwater phytoplankton are between -29.5 and -27.5‰, which overlaps with emergent vascular plant matter, which typically has $\delta^{13}\text{C}$ values ranging from -28.1 to -27.2‰. Sediments and soils tend to have heavier isotopic signatures, while runoff can have lighter values. In 2019, Isotopic values of carbon in particulate organic matter ($\delta^{13}\text{C}$ -POM) collected onto filters revealed $\delta^{13}\text{C}$ signatures in the range of freshwater phytoplankton most of the time, with values closer to terrestrial vascular plants in May and June at Campbell Slough and Franz Lake Slough. $\delta^{13}\text{C}$ -POM at Ilwaco was closer to marine values. It is interesting that the signatures of $\delta^{13}\text{C}$ -POM would be close to that of vascular plants, since POM was collected by filtering whole water onto glass fiber filters and much of the material collected onto the filters was composed of phytoplankton (the same collection method is used to determine chlorophyll *a* concentrations).

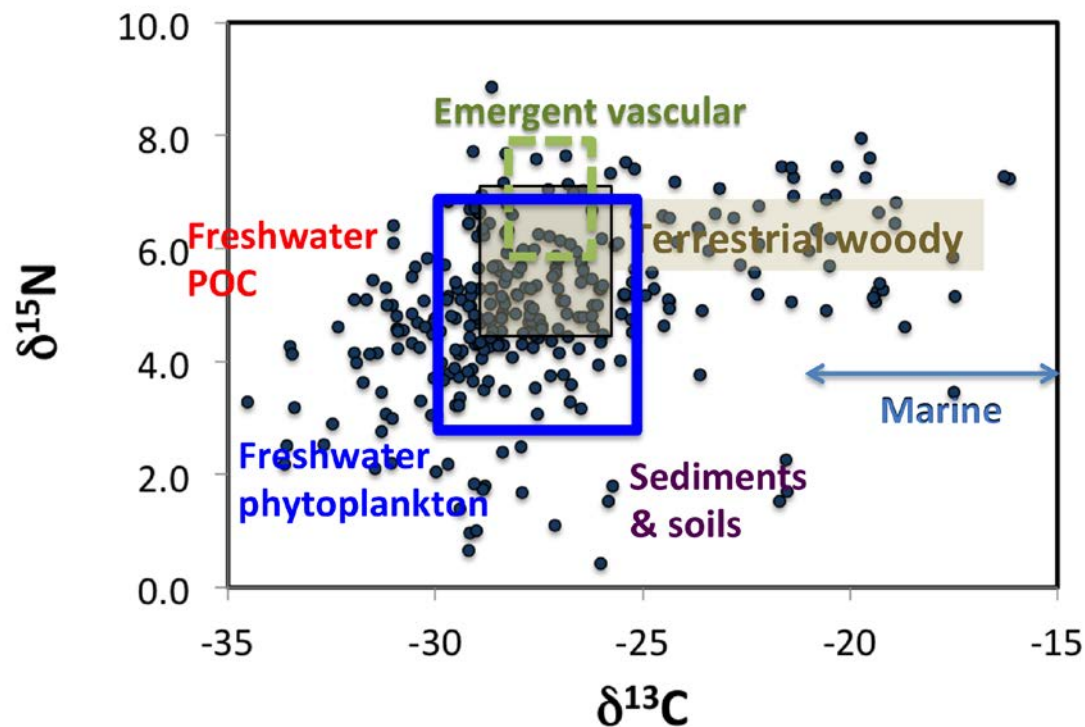


Figure 114. Plot of particulate organic matter (POM) data from off-channel trends sites (circles) in isopach; typical isotopic signature ranges for different organic matter sources are shown (derived from Cloern, 2002). The contribution of various sources to measured POM in the lower Columbia is evident in the data spread.

When all the data from particulate organic matter are placed in context with typical values for different sources (e.g., sediments, marine phytoplankton, woody debris), the spread in isotopic signatures (Figure 114) suggests that there are several sources contributing to POM in the lower Columbia, with several samples resembling freshwater phytoplankton, while others appeared to include some woody debris or soil organic compounds. There is considerable overlap in the stable isotope signatures of emergent vascular plants, freshwater phytoplankton, and terrestrial woody debris, with a narrower range for emergent vascular plant material.

3.4.3.1 *Stable Isotope Ratios of Carbon and Nitrogen of Primary Producers*

All primary producers

When stable isotope signatures for carbon and nitrogen associated with all primary producers is combined, two broad patterns emerge (Figure 115). The average $\delta^{13}\text{C}$ (ratio of ^{13}C to ^{12}C) is slightly higher in very dry years (for example, 2015) as well as very wet years (for example, 2017), and lower for more moderate years. In the case of nitrogen, this effect is more pronounced with bi-modal features during moderate, dry, and very dry years.

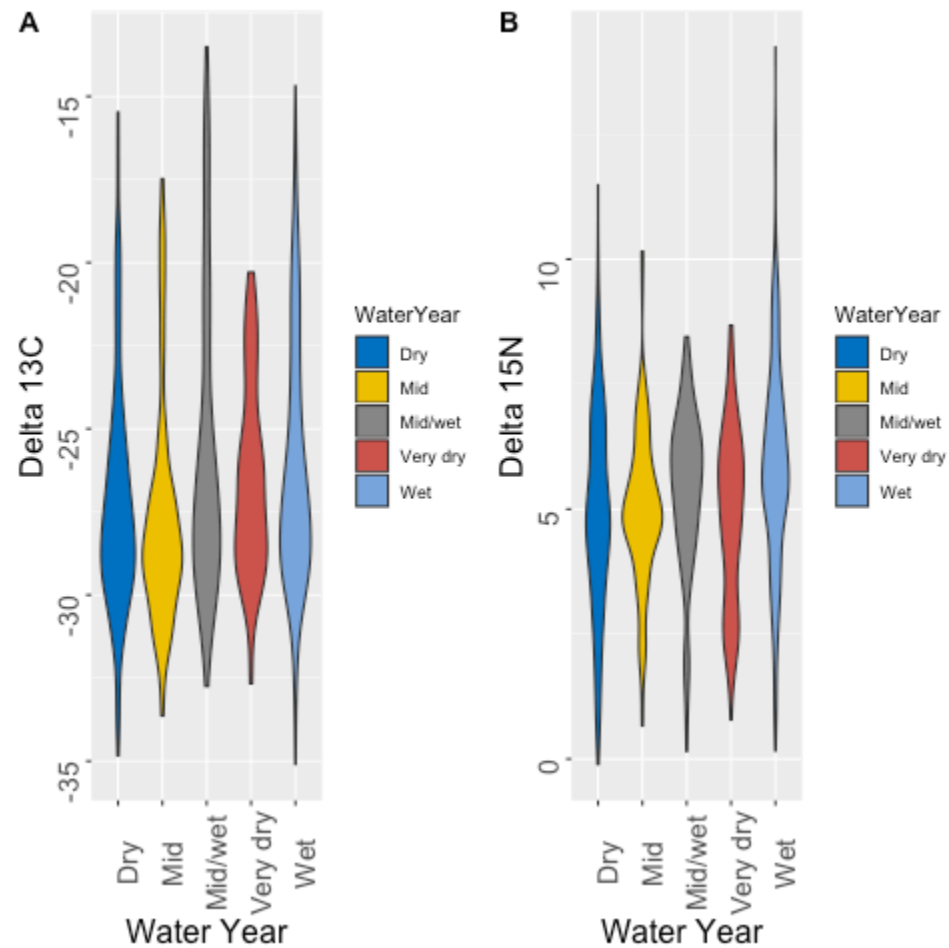


Figure 115. Plots showing stable isotope signatures of all primary producers according to the type of water year (Dry, moderate (“mid”), wet-to-moderate (“Mid/wet”), Very dry, and Wet). The data spread for $^{13}\text{C}/^{12}\text{C}$ was greatest for moderately wet, wet, and dry years, while for $^{15}\text{N}/^{14}\text{N}$ was greatest for wet and dry years.

Pelagic primary producers: Particulate Organic Matter (POM)

The data suggest that heavier carbon isotope signatures in particulate organic matter (POM) were associated with dry years, while wet years were associated with lighter carbon isotope values in POM (Figure 116). In very dry years, like 2015, the average $\delta^{13}\text{C}$ was -25.6‰ , which was significantly heavier than in dry, moderately wet, and wet years ($p < 0.05$). Wet and moderately wet years did not differ in the carbon isotopic signature of POM ($p = 0.99$). In contrast, there were no significant differences in the stable isotope signatures of nitrogen ($^{15}\text{N}/^{14}\text{N}$) in POM, with the exception of the difference between very dry (4.75‰) and dry (4.14‰) years ($p = 0.05$).

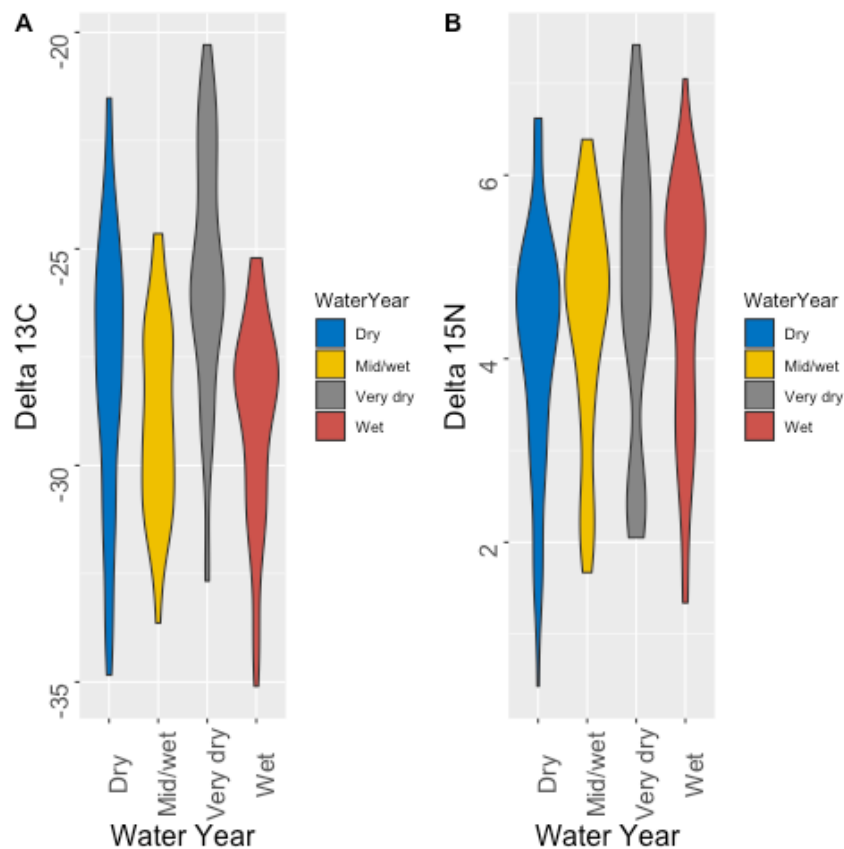


Figure 116. Plots showing average stable isotope signatures ($^{13}\text{C}/^{12}\text{C}$, or Delta 13C, and $^{15}\text{N}/^{14}\text{N}$, or Delta ^{15}N) for particulate organic matter (POM) in different water years. (Dry years, $n=63$; very dry years, $n = 63$; wet years, $n = 51$; moderately wet years, $n=77$).

Since there were more data points from samples collected at Campbell Slough and Whites, the average values of delta C and delta N for POM over the 2011-2019 time series were compared (Figure 117). The carbon data showed a wider spread at Campbell Slough compared to Whites Island, although the mode values were similar. Similarly, delta N values showed a wider spread at Campbell Slough compared to Whites Island with similar mode values at the two sites.

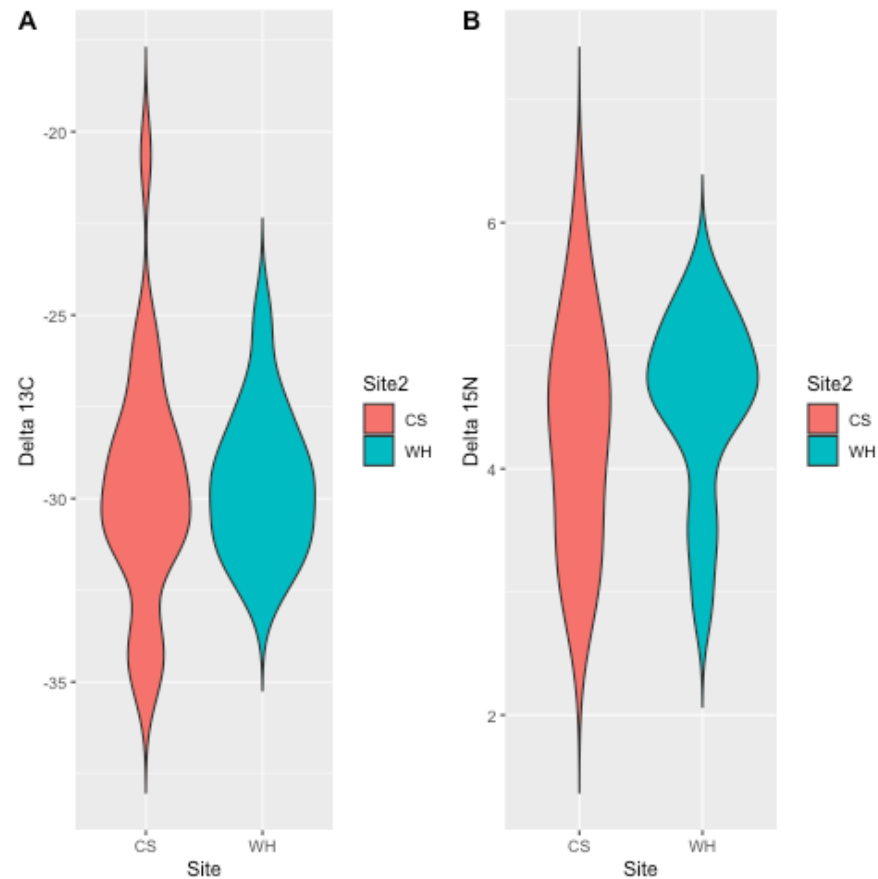


Figure 117. Violin boxplots showing the $\delta^{13}\text{C}$ and $\delta^{15}\text{N}$ signatures of particulate organic matter at Campbell Slough and Whites Island. The data included samples collected between 2011-2019.

Stable isotope signatures of periphyton

The stable isotope signatures of periphyton collected across the trends sites between 2011 and 2019 varied widely across the data set. When the samples were divided to compare wet vs. dry years, there were a few notable observations. Average values of $\delta^{13}\text{C}$ were higher during moderately wet and wet years (Figure 118), although there was considerable spread in the data. There was an increase in the average $\delta^{15}\text{N}$ over a gradient of dry to wet years, with the largest spread in data observed for wet years.

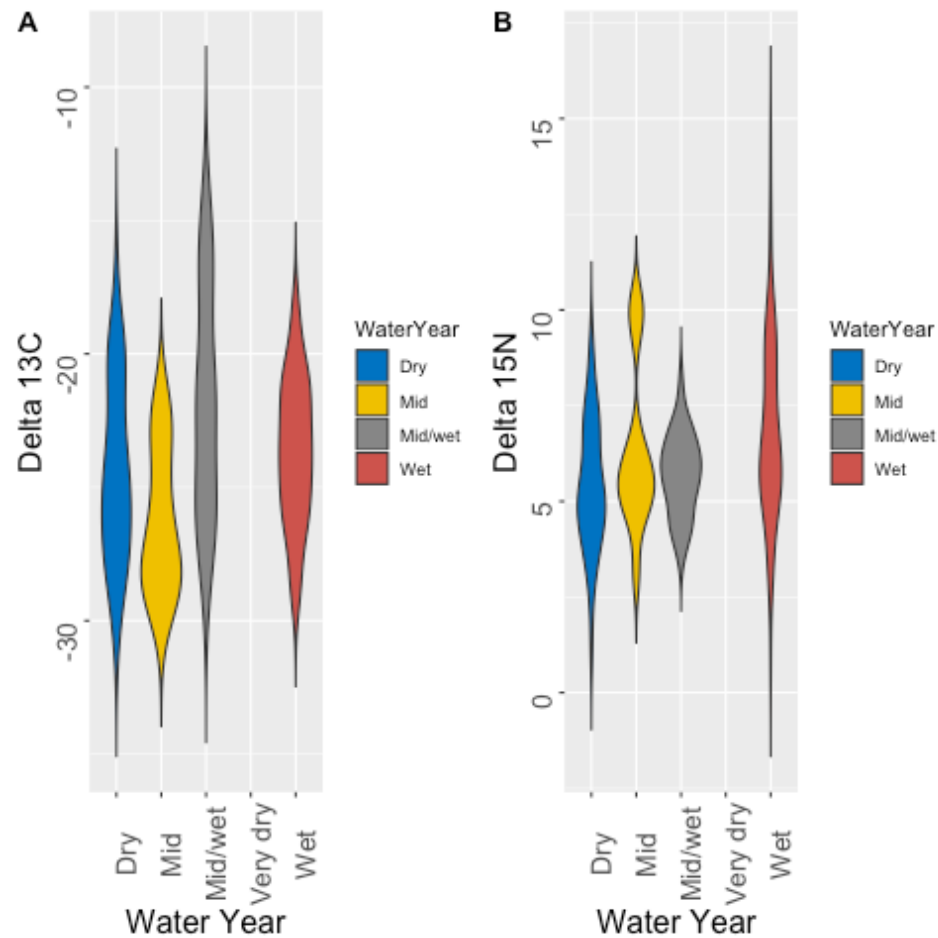


Figure 118. Plots showing stable isotope signatures ($^{13}\text{C}/^{12}\text{C}$, or $\delta^{13}\text{C}$, and $^{15}\text{N}/^{14}\text{N}$, or $\delta^{15}\text{N}$) associated with periphyton in different water years. The data from all sites were pooled.

Stable isotope signatures of vegetation

Comparison among sites

When the stable isotope signatures of carbon associated with vegetation (Figure 119) were compared among the sites five EMP sites according to a one-way analysis of variance, values from Ilwaco were different from all other sites ($p < 0.01$). Similarly, $\delta^{15}\text{N}$ values differed at Ilwaco compared to the other sites. We performed a second set of ANOVAs excluding the data from Ilwaco followed by Tukey post hoc multiple comparisons tests. These revealed that for $\delta^{13}\text{C}$, there were significant differences between Franz Lake Slough and Campbell Slough, Whites Island and Campbell Slough, and between Welch Island and Franz Lake Slough, as well as Welch Island and Whites Island. Whites Island and Franz Lake Slough also differed significantly. Interestingly, Welch Island and Campbell Slough were not different ($p = 0.90$). In the case of $\delta^{15}\text{N}$, signatures at Campbell Slough and Franz Lake Slough were similar while $\delta^{15}\text{N}$ signatures at Welch Island and Whites Island were similar. The two groups differed significantly from each other.

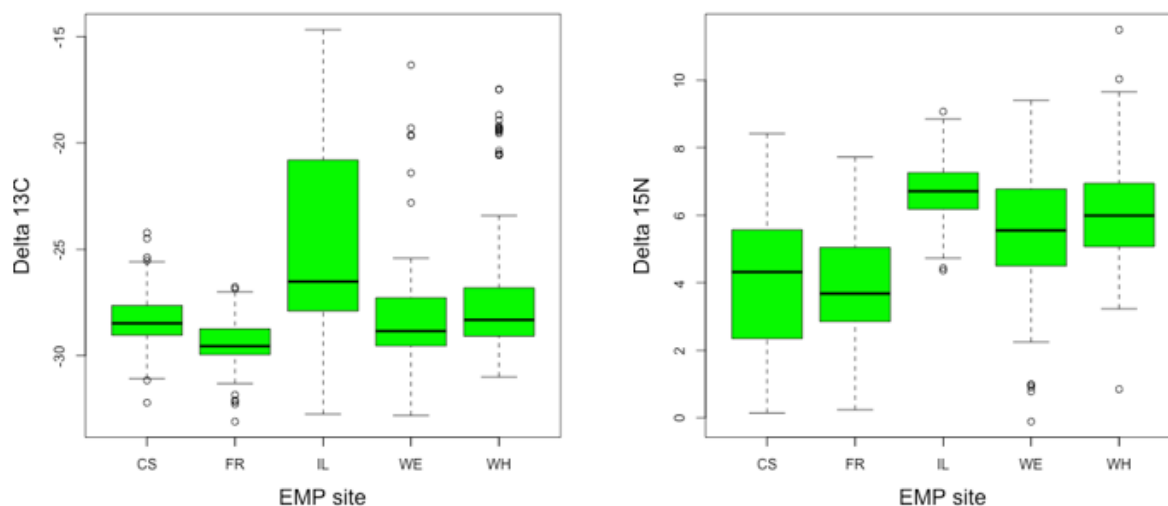


Figure 119. Boxplots showing the distribution of data for stable isotope of carbon ($\delta^{13}\text{C}$) and nitrogen ($\delta^{15}\text{N}$) from vegetation at EMP sites, CS = Campbell Slough, FR = Franz Lake Slough, IL = Ilwaco, WE = Welch Island, WH = Whites Island.

Comparison among years

When the samples were grouped according to whether they came from years with low, moderate, or high cumulative discharge (very dry, dry, moderate, wet), there were significant differences in average $\delta^{13}\text{C}$, but not in $\delta^{15}\text{N}$ (Figure 120). The only non-significant differences among year types were between moderately wet and wet years.

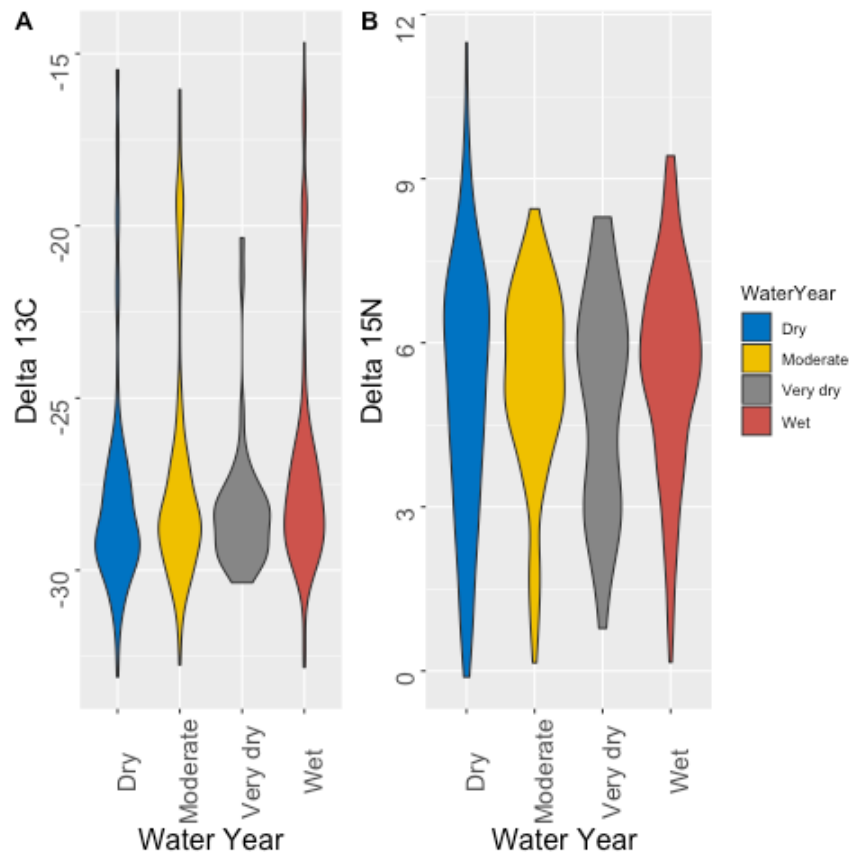


Figure 120. Plots showing average stable isotope signatures ($^{13}\text{C}/^{12}\text{C}$, or $\delta^{13}\text{C}$, and $^{15}\text{N}/^{14}\text{N}$, or $\delta^{15}\text{N}$) for vegetation in different water years. Data from all sites were pooled.

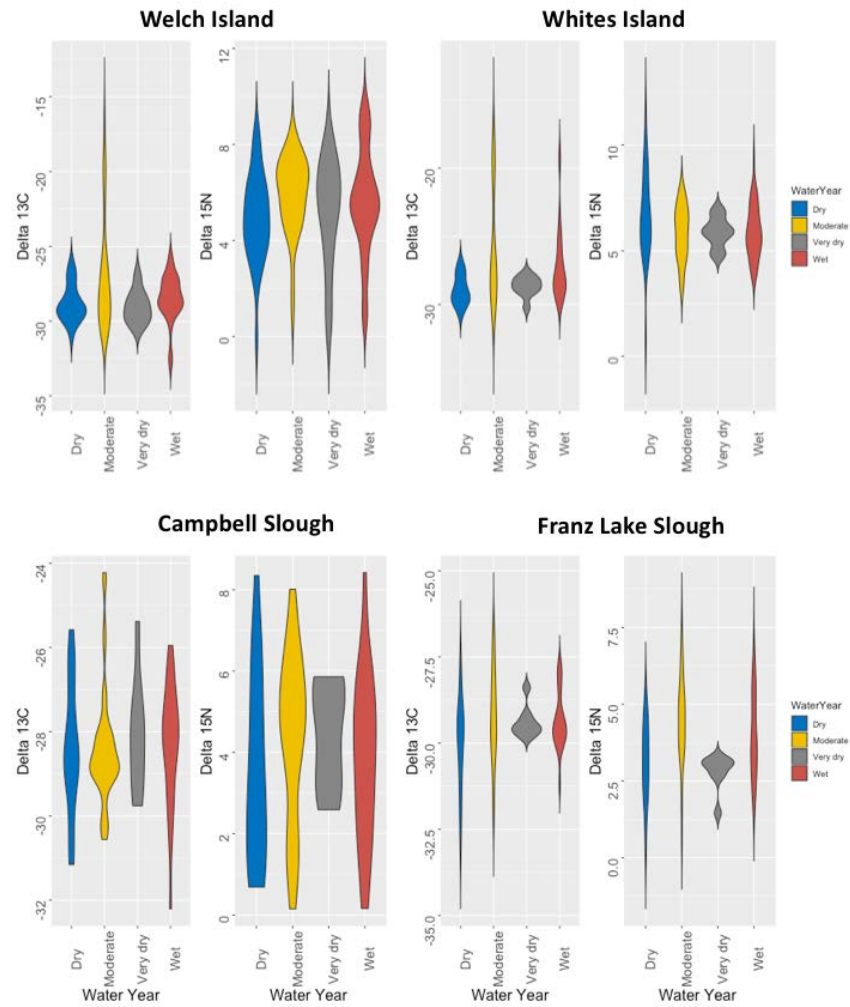


Figure 121. Stable isotope ratios of carbon and nitrogen for vegetation tissues at four of the EMP sites: Welch Island, Whites Island, Campbell Slough, and Franz Lake Slough.

3.4.3.2 *Stable Isotope Ratios Associated with Potential Salmon Prey*

According to direct observations from fish stomach contents, juvenile salmonids in the lower Columbia appear to rely primarily on chironomids and amphipods in their diets. However, the energy ration associated with other taxa, particularly the large, terrestrial insects, can be higher and might contribute to growth of juvenile salmonid, so we explored how the isotopic signatures of potential prey items varied with habitat. For this analysis, prey was divided into four different habitat types: benthic, pelagic, terrestrial, or 'other' (i.e., uncertain). Pelagic prey had the largest spread in $\delta^{13}\text{C}$ values, while the spread of $\delta^{15}\text{N}$ values was similar for all habitat types. The mode of $\delta^{15}\text{N}$ values for terrestrial prey was lighter than that for benthic or pelagic prey (Figure 122).

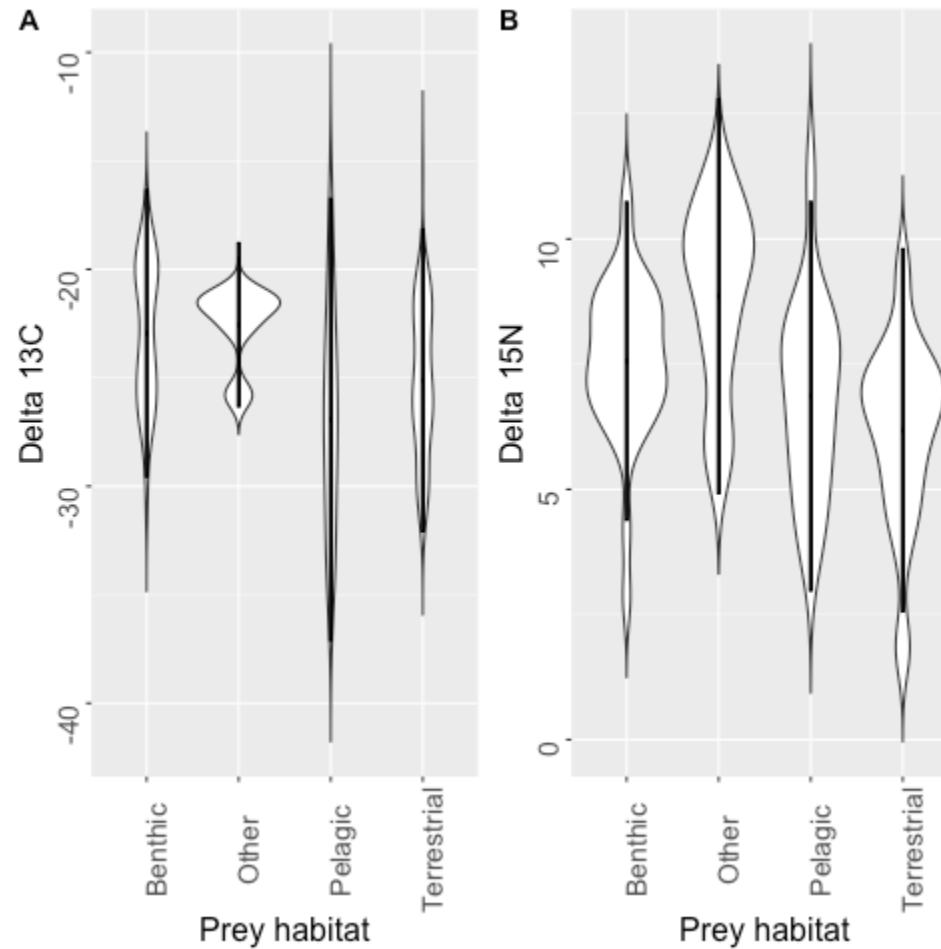


Figure 122. Stable isotope ratios of carbon ($\delta^{13}\text{C}$) and nitrogen ($\delta^{15}\text{N}$) for prey sources divided according to their typical habitat (benthic, pelagic, terrestrial, or 'other' [unknown, or mixed]). The graphs show the data distribution over the range of observed values, with narrow shapes indicating few data points per observed value (relative to the total number of observations), and wider shapes indicating more data points per observed value. For benthic prey, $n=60$; for pelagic prey (copepods and cladocerans), $n = 16$; for terrestrial prey, $n =100$; for 'Other', $n = 5$.

We were also interested in investigating how the stable isotope signatures of organic matter (i.e., primary producers) related to those of the two primary salmonid prey taxa (chironomids and amphipods). When the $\delta^{13}\text{C}$ and $\delta^{15}\text{N}$ values of vascular plants primary producers (VegA and VegB; Veg A groups those plant tissues with heavier $\delta^{13}\text{C}$ and $\delta^{15}\text{N}$, while Veg B includes those having light $\delta^{13}\text{C}$ and $\delta^{15}\text{N}$), particulate organic matter (a proxy for pelagic phytoplankton), and periphyton were compared with salmon prey (chironomids), there was overlap with periphyton, POM, and the VegA group (Figure 123). Some of the chironomid tissues, however, were lighter in terms of nitrogen isotopes than any of the organic matter sources (i.e., $<5\text{‰}$) and one was lighter than any of the carbon isotope values observed in organic matter sources (i.e., $<-29\text{‰}$).

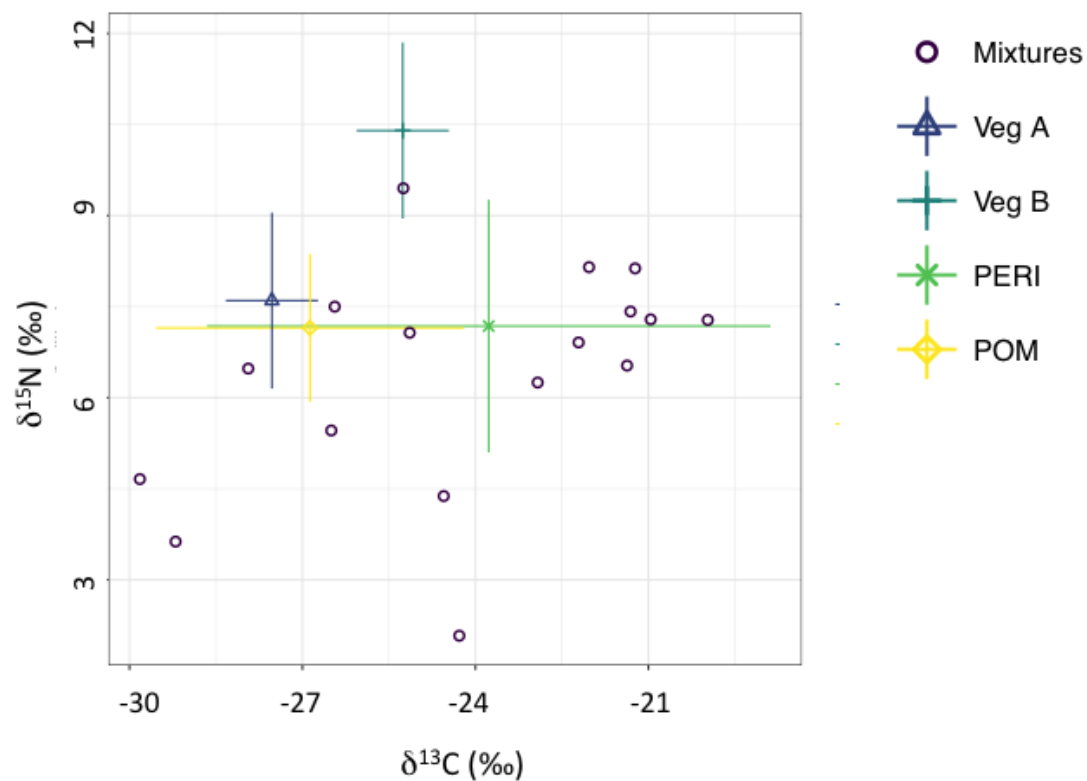


Figure 123. Isopace plot showing stable isotope signature of chironomids (“mixtures”) compared to vascular plant matter with heavier $\delta^{13}\text{C}$ and $\delta^{15}\text{N}$ (Veg A) and those having light $\delta^{13}\text{C}$ and $\delta^{15}\text{N}$ (Veg B) as well as to periphyton (PERI) and particulate organic matter (POM).

3.4.3.3 *Stable Isotope Ratios Associated with Salmon*

Among salmonid muscle tissues, there was a positive relationship between $\delta^{13}\text{C}$ and $\delta^{15}\text{N}$ (Figure 124). Some of the observed values associated with salmon were heavier in both C and N than were the prey items, which suggests that not all prey sources were accounted for.

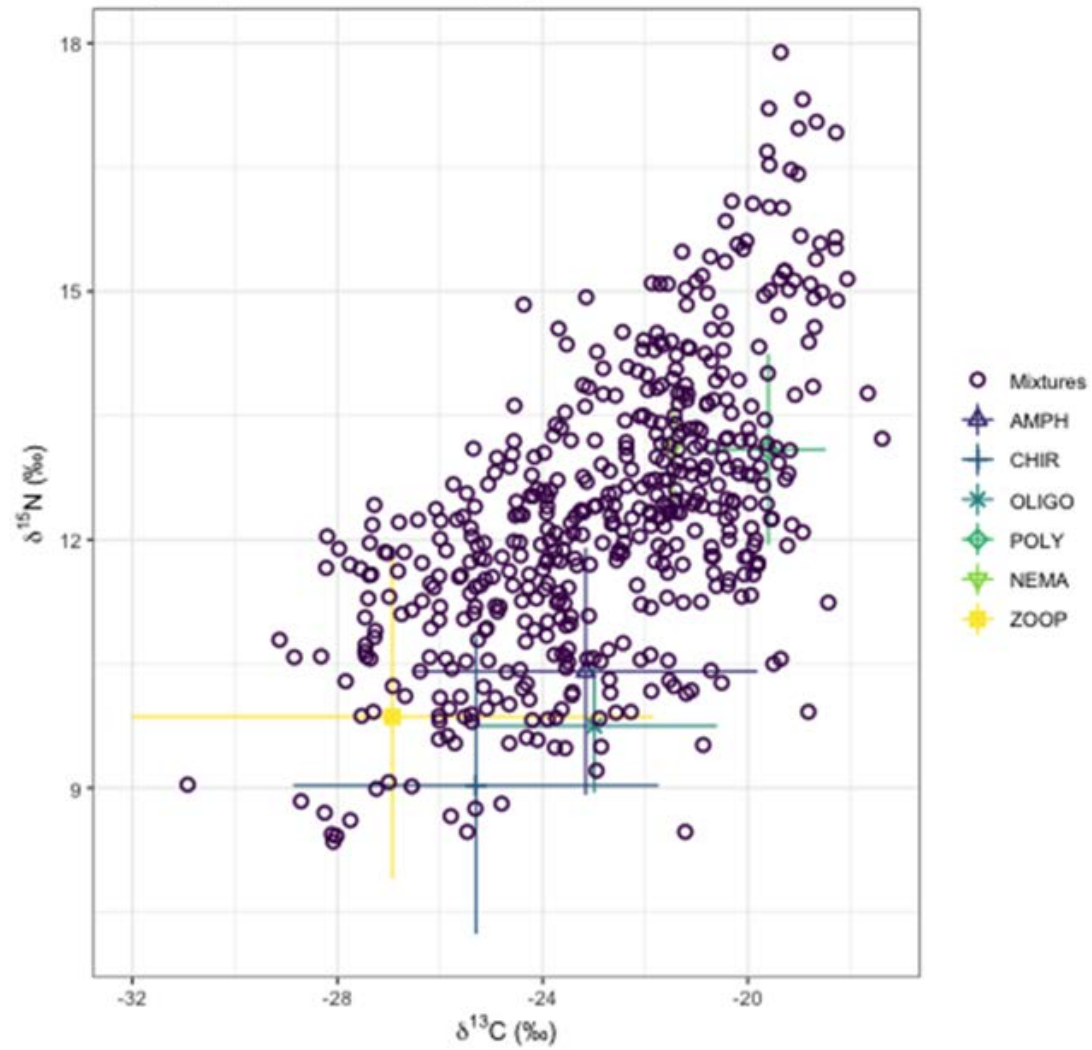


Figure 124. Isospace plot showing isotopic signatures for salmon tissue (“Mixtures”) as well as prey sources (AMPH = amphipods, CHIR = chironomids, OLIGO = oligochaetes, POLY = polychaetes, NEMA = nematodes, and ZOOP = copepods and cladocerans).

When isotope signatures from juvenile salmonid tissues were divided according to water year (i.e., wet vs. dry), the average $^{13}\text{C}/^{12}\text{C}$ and $^{15}\text{N}/^{14}\text{N}$ values were heaviest in years of moderate flow (Figure 125), with wide ranges around the average in all years observed. The lowest $\delta^{13}\text{C}$ values were observed during wet years; interestingly, there was a bimodal pattern in the $\delta^{13}\text{C}$ value during the wet years, with fewer data points occurring between lower and higher values.

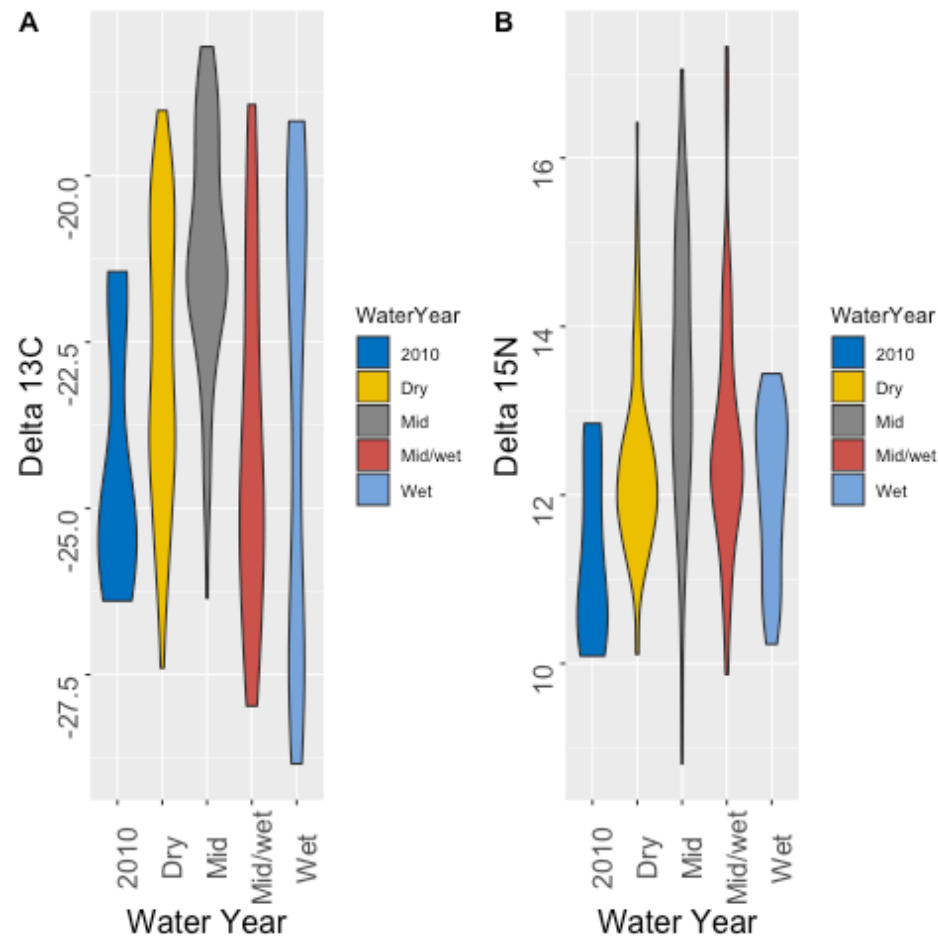


Figure 125. Isotope ratios (delta 13C and delta 15N) of juvenile salmonid tissues pooled according to years categorized by variations in river flow.

When the isotopic signatures were grouped according to site, the largest differences in $\delta^{13}\text{C}$ and $\delta^{15}\text{N}$ were observed between Franz Lake Slough and all the other sites (Figure 124). In addition, the $\delta^{15}\text{N}$ values were lower at Campbell Slough than the other sites. This is exemplified in the data from 2014 (Figure 125), a year when data were available from multiple sites, which is not always the case (i.e., in some years and at some sites, fish catches are not large enough to provide samples for isotope analysis of fish tissue). The 2014 data show a wider spread in isotopic values of both carbon and nitrogen, with a lower average than at the other sites.

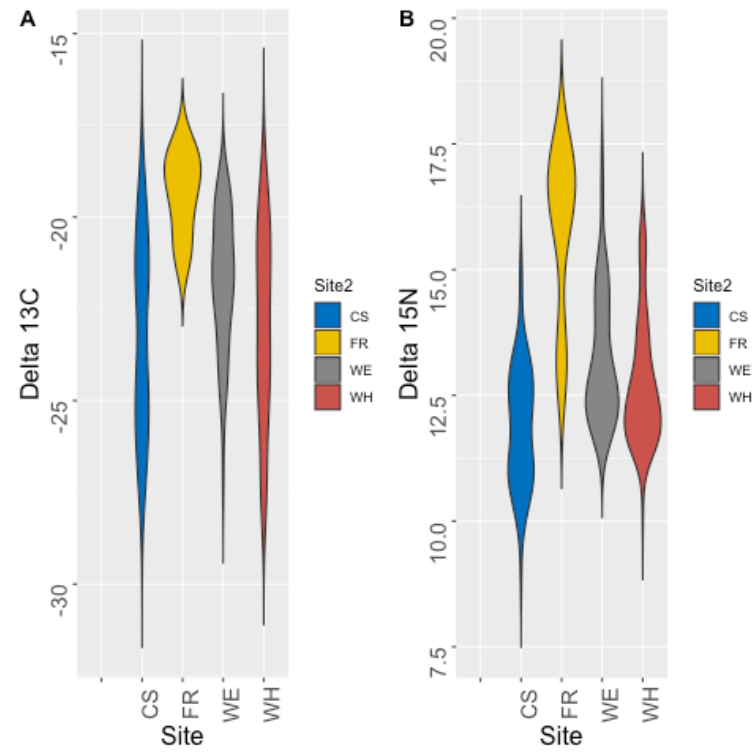


Figure 126. Violin plots showing (A) delta 13C ($^{13}\text{C}/^{12}\text{C}$) in juvenile salmon tissue collected from Campbell Slough (CS), Franz Lake Slough (FR), Welch Island (WE), and Whites Island (WH).

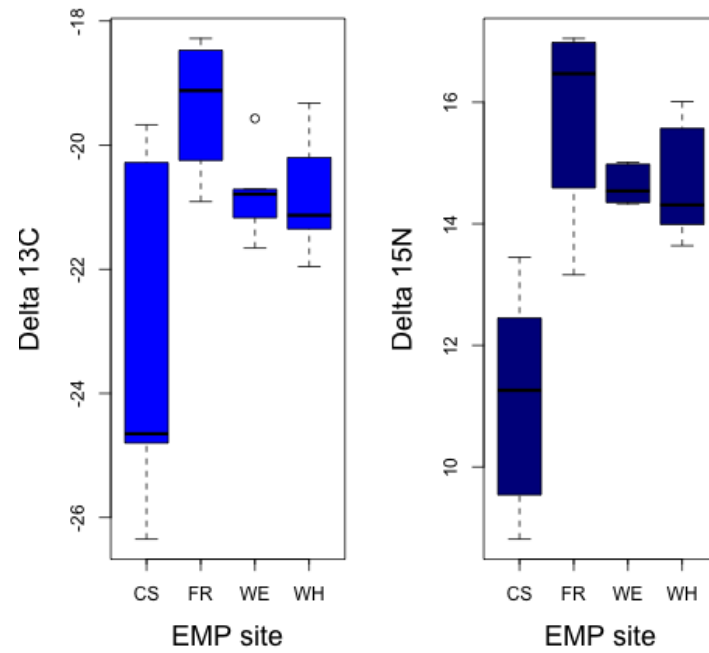


Figure 127. Boxplot showing delta 13C and 15N values for salmon muscle tissue in April 2014 at four EMP sites: CS = Campbell Slough, FR = Franz Lake Slough, WE = Welch Island, and WH = Whites Island. According to a one-way anova with Tukey's HSD post hoc testing, signatures of tissues at Campbell Slough were significantly different than those at the other sites.

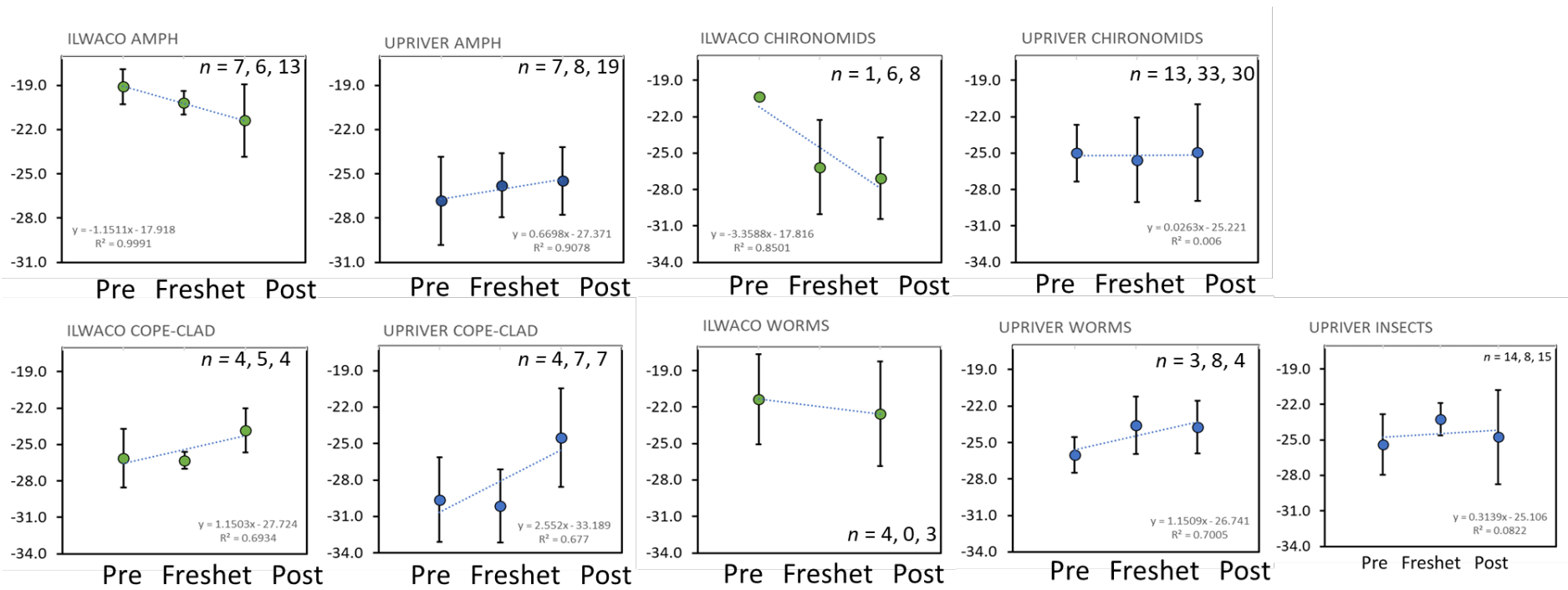


Figure 128. Ratios of $^{13}\text{C}/^{12}\text{C}$ in tissues from salmon prey, including amphipods (AMPH), chironomids, copepods and cladocerans (COPE-CLAD), worms, and insects from sites considered ‘Upriver’ (upstream of the Willamette-Columbia confluence) and ‘Downriver’ (downstream of the Willamette-Columbia confluence).

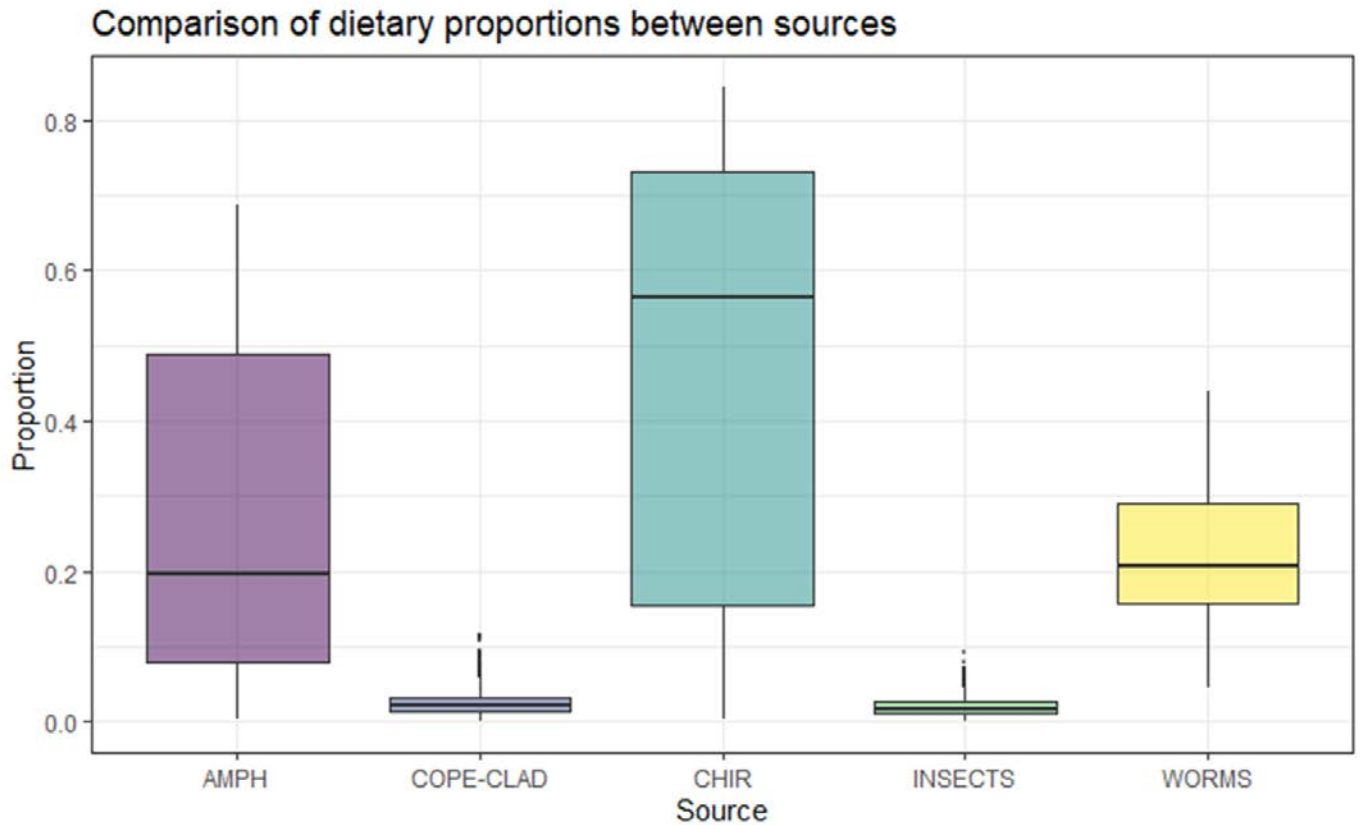


Figure 129. Estimate of the dietary proportion of juvenile salmon accounted for by different prey items based on output from a Bayesian mixing model. AMPH = amphipods; COPE-CLAD = copepods and cladocerans; CHIR = chironomids; INSECTS = a pool of insects of mixed taxonomy; WORMS = polychaetes, oligochaetes, and nematodes. Horizontal line represents the median, whiskers show the range of estimated proportional contributions arising from model output

3.5 Macroinvertebrates

3.5.1 Salmon Prey Availability

2020 data, sampled February – March, is reported below. 2021 data is still under analysis.

3.5.1.1 *Benthic*

Interannually and among sites, the numeric composition of benthic core samples was consistently dominated by oligochaete worms (Figure 130). Nematode worms and dipteran fly larvae and pupae were present at all sites but were numerically abundant at Welch Island, Whites Island, Campbell Slough, and Franz Lake. At Ilwaco Slough, polychaete worms comprised a large proportion of the numeric and gravimetric composition of samples but were relatively rare at other sites. Amphipods, mainly comprised of *Americorophium* spp., were present predominantly at Ilwaco Slough and Whites Island in most years, and at Welch Island in 2020.

Across most sites and years, oligochaete worms were large contributors to benthic core samples, especially those from Welch Island, Campbell Slough, and Franz Lake. While not always numerically abundant, the large body size of amphipods, bivalves, gastropods, Hirudinea (leeches), and isopods made relatively large additions to the gravimetric composition when they were present (Figure 131). In particular, bivalves had a relatively high biomass at Whites Island. At Welch Island, a variety of taxa have added to gravimetric composition through the years, mainly consisting of oligochaete worms, dipterans, bivalves, and gastropods.

Two common orders of juvenile salmon prey, Amphipoda and Diptera, have small yet consistent numerical and gravimetric presence in benthic data, with amphipods contributing mostly at Ilwaco Slough and Whites Island, and dipterans contributing at all sites. Amphipod abundance declined upstream with highest densities at Ilwaco Slough (Figure 132), low densities at Welch Island and White Island and none at Campbell Slough and Franz Lake in 2020. Dipterans, including Chironomidae - the family primarily consumed by juvenile salmon, were collected at sites in nearly all the years (including all months). The highest gravimetric contributions by dipterans were at Franz Lake in 2019, with higher numeric contributions in 2019 and 2020.

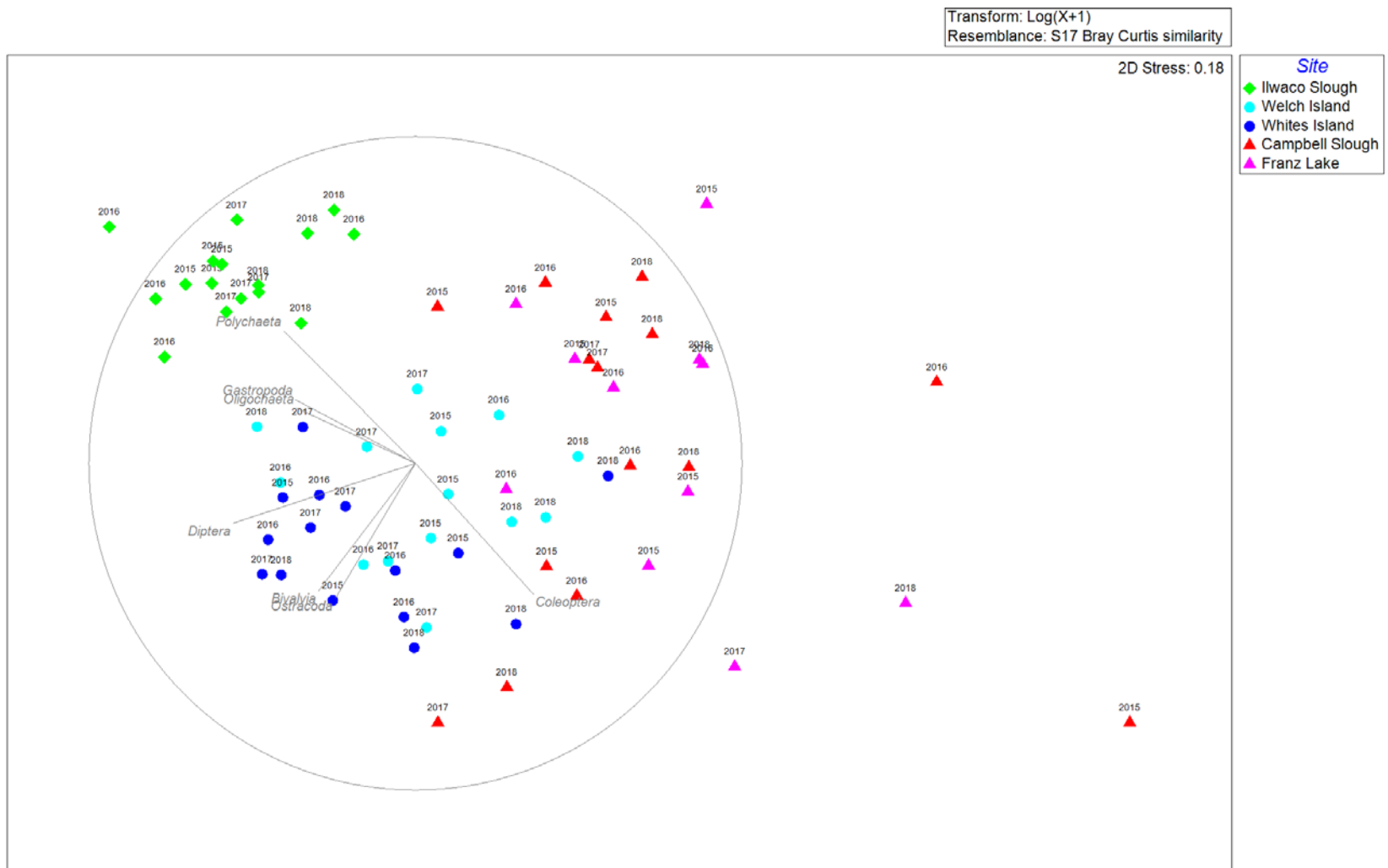


Figure 130. Two-dimensional NMDS plot based on Bray-Curtis similarities between log transformed numeric abundances of taxa collected in benthic cores between 2015 and 2018. Each point represents the composition of the average monthly abundance of taxa collected between April and July within a site and year. Correlation with taxa (Pearson $R > 0.4$) are represented as gray vectors.

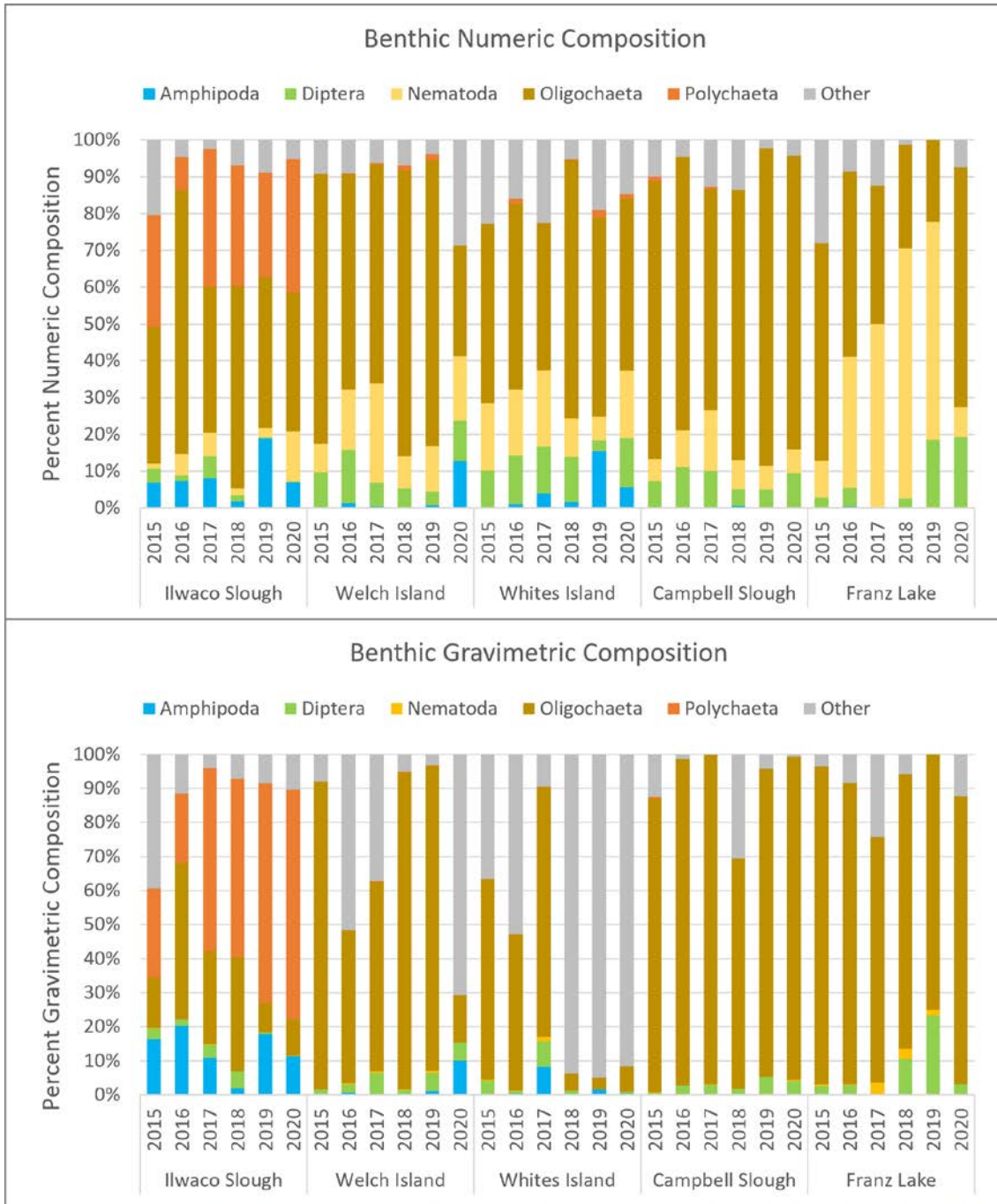


Figure 131. Percent numeric (top) and gravimetric composition (bottom) of benthic core samples collected 2015 – 2020. Percent numeric and gravimetric compositions are sorted by site and year.

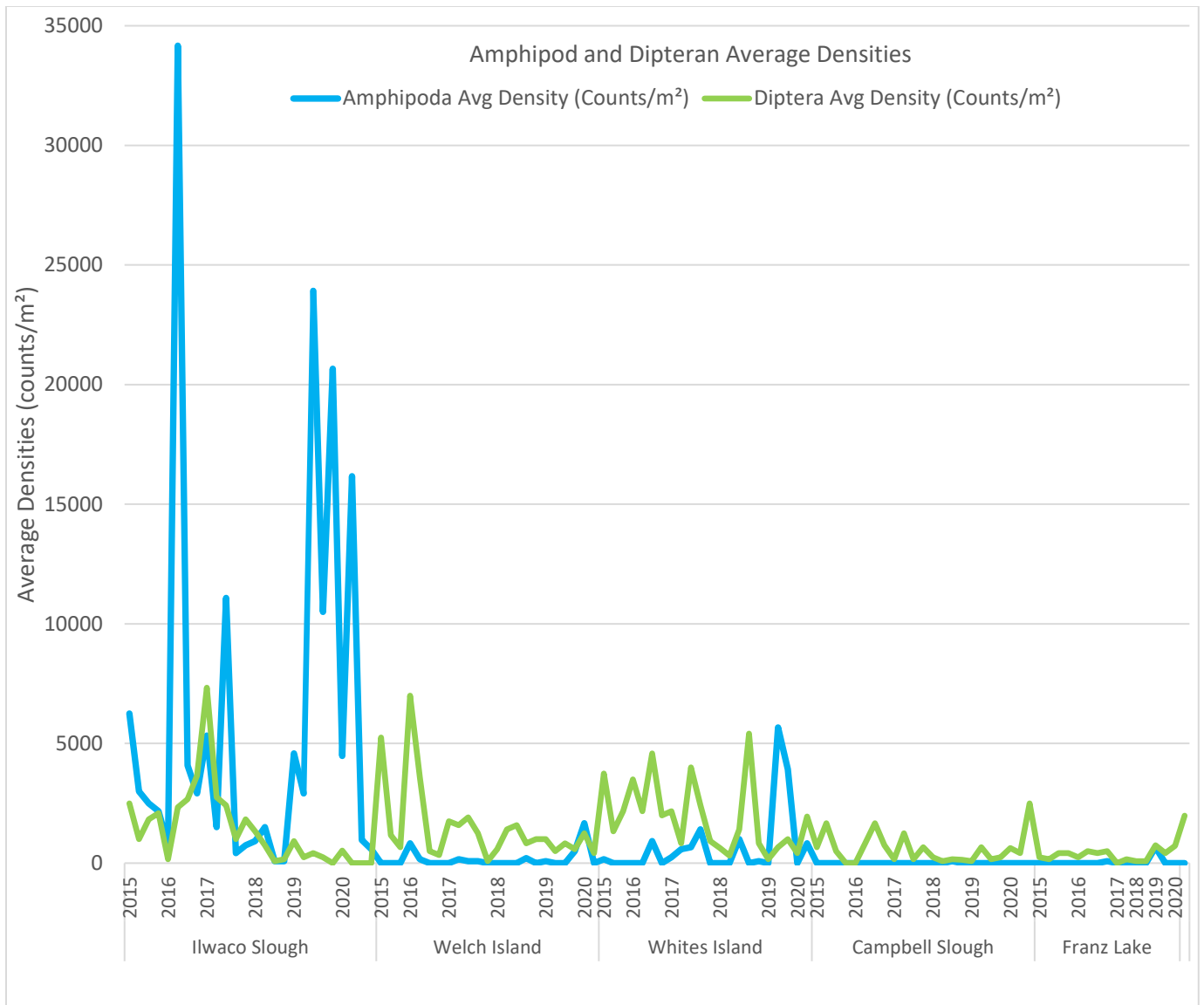


Figure 132. Average density (counts/meter²) of major juvenile salmonid prey taxa in benthic core samples. Major prey taxa include amphipods (blue) and dipterans (green). Densities were sorted by site and year. Uneven year spacing on x-axis reflects sampling events spaced, by month, each year sampled. For example, a year spaced further from the previous year indicates more sampling events in the first year.

3.5.1.2 *Neuston*

Due to attenuated sampling in 2020 associated with the coronavirus pandemic, neuston sampling occurred only from February to March. To compare 2020 neuston data to other sampling years, and to account for seasonal changes in neuston prey fields, numeric and gravimetric composition plots in this report include only February-March. In general, neuston samples have a diverse array of benthic/epibenthic, terrestrial riparian, and planktonic taxa (Figure 133-Figure 142). Interannually, small planktonic taxa, such as copepods and cladocerans, were numerically abundant in both the open water and emergent vegetation and more so in open water. Both taxa have lower contributions to gravimetric composition. Collembolans (springtails) and insects have been relatively abundant interannually and among sites in both sampling strata (emergent vegetation and open water), but with higher presence in emergent vegetation relative to open water. The 2020 numeric composition of neuston samples was dominated by insects, copepods, collembolans, and cladocerans, depending on site and sampling strata. The large body size of amphipods, gastropods, and isopods made large gravimetric contributions when they were present even if their densities were low ((Figure 133-Figure 142).

Amphipods and dipterans had relatively high spatial and temporal weight contributions in both sampling strata. In emergent vegetation samples, average densities of dipterans were typically low at Ilwaco Slough and Welch Island, and higher at Whites Island, Campbell Slough, and Franz Lake. Amphipod densities were relatively low in all locations (Figure 133-Figure 142). In open water samples, amphipod densities were highest at Ilwaco Slough, but were generally low across sites and years, while dipteran densities were generally higher at sites upstream of Ilwaco Slough. Cladoceran densities were highest at Campbell Slough in emergent vegetation as well as open water samples. Two cladoceran sampling peaks (emergent vegetation, 2017; open water, 2019) exceeded 1000 individuals/meter towed (Figure 133-Figure 142). Interannual cladoceran densities at all remaining sites were relatively low.

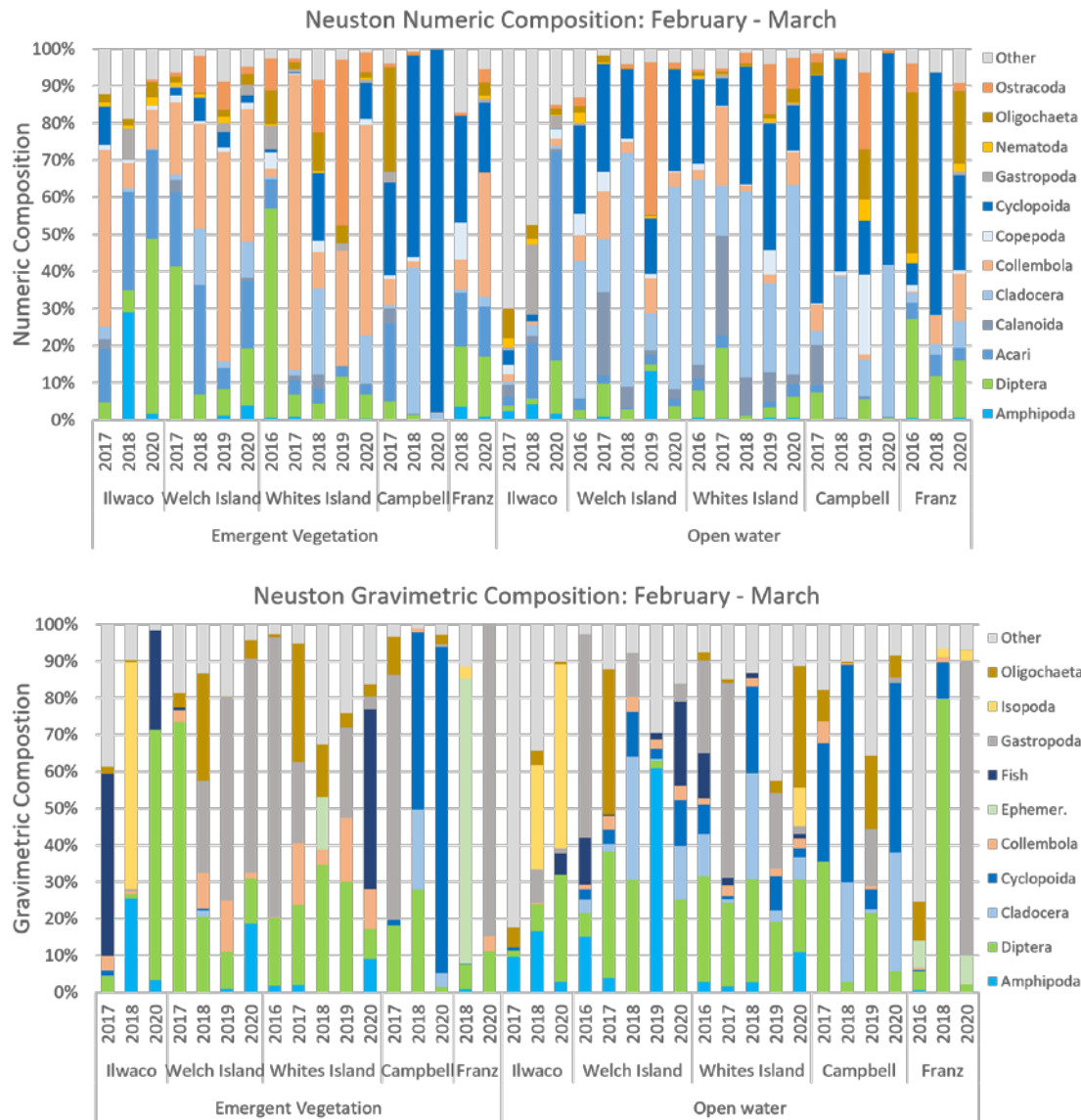


Figure 133. Percent numeric (above) and gravimetric (below) composition of neuston samples collected 2016-2020. Samples were collected between February and March (2020), and April-July (2017-2019), sorted by site and year.

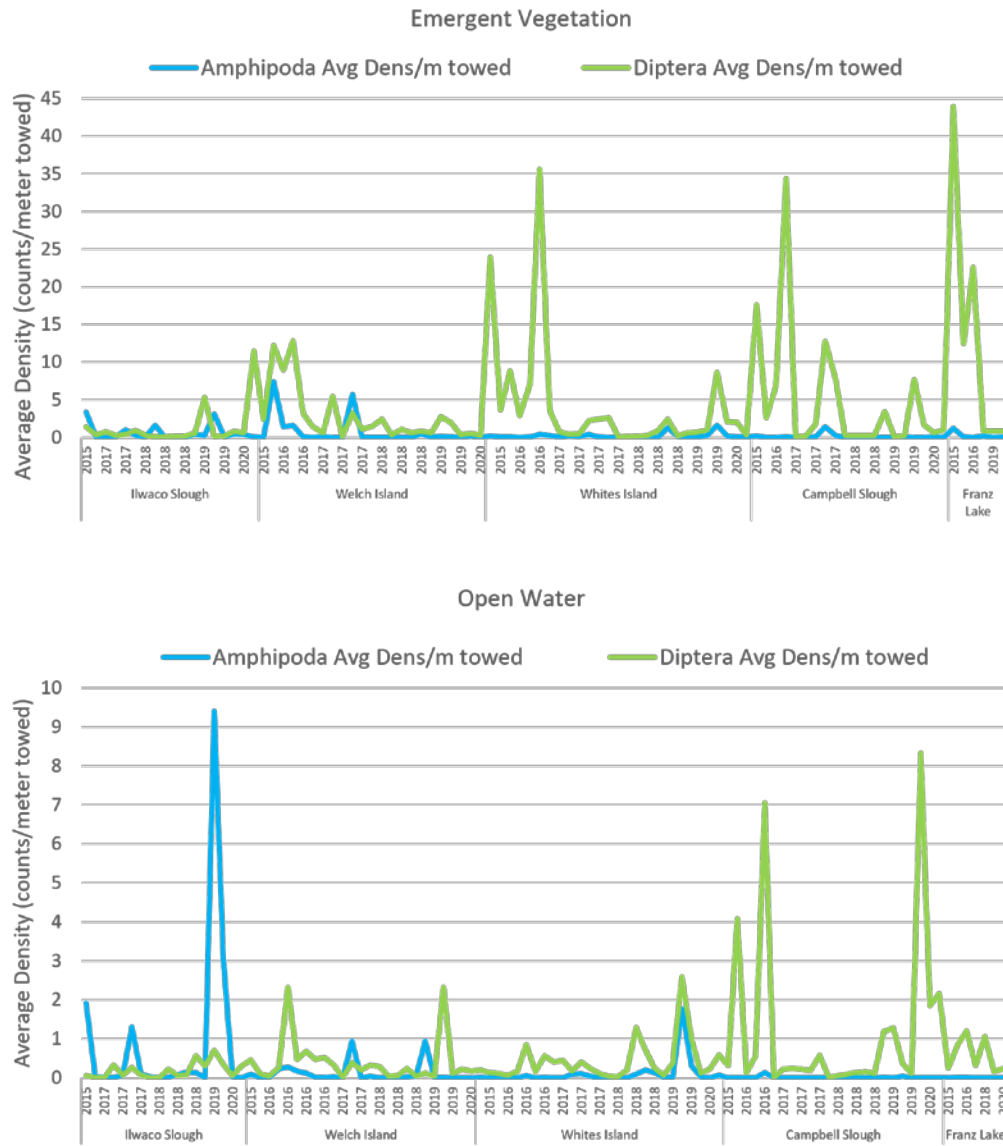


Figure 134. Average density (count per meter towed) of Amphipoda by neuston tow. Samples are sorted by strata (top: emergent vegetation; bottom: open water) and color sorted by prey taxa (Amphipoda: blue; Diptera: green). Note that scales differ.

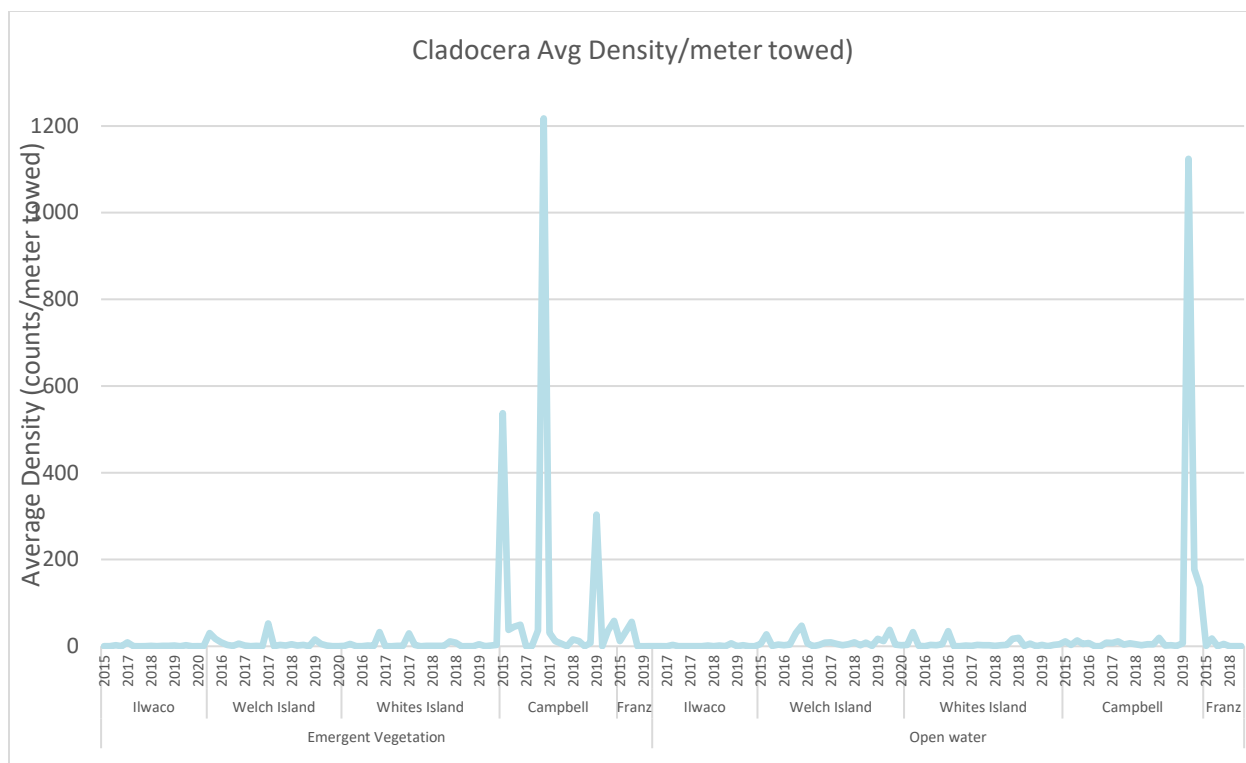


Figure 135. Average density (count per meter towed) of Cladocera collected by neuston tow for sampling years 2015 – 2020. All years are plotted regardless of presence on the x-axis. Samples are sorted by sampling strata (left: emergent vegetation; right: open water), site, and year

3.5.2 Salmon Diet

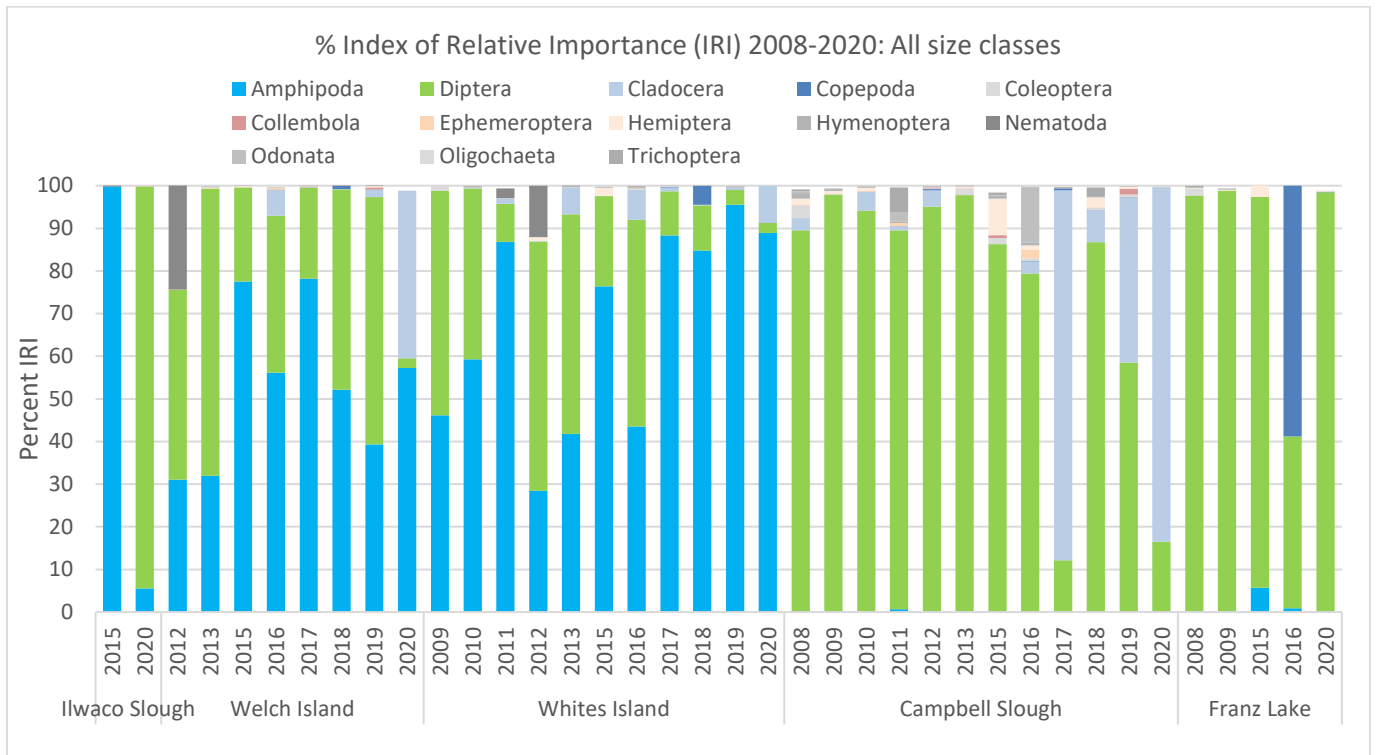
Due to attenuated sampling in 2020 associated with the coronavirus pandemic, 2020 juvenile Chinook salmon diet sampling took place February-March. All salmon collected were 30-59 mm fork length (FL). Interannually, all February-March fish were the 30-59 FL; however, all 30-59 mm fish were not sampled in February-March. Index of Relative Importance results from years preceding 2020 were from April – June sampling. Note that 2021 data is still under analysis.

3.5.2.1 Salmon Diet

With a few exceptions, juvenile Chinook salmon diets from the study sites have followed annual geographic trends consisting of primarily dipterans and other wetland insects at Franz Lake and Campbell Slough, primarily dipterans and amphipods at Whites Island and Welch Island, and primarily amphipods at Ilwaco Slough near the estuary mouth (Figure 136). Prey with highest % IRIs for fish in all size classes have been amphipods, dipterans, and cladocerans. Although common prey taxa like amphipods and dipterans were often identified by Order, prey species in each group were nearly entirely comprised of *Americorophium* spp. (amphipods) and Chironomidae (dipterans). Since 2015, when prey taxa began being identified to family or genus, chironomids have comprised 90% of both the counts and wet weights of order Diptera. By life stage, larva account for 73% of all chironomid densities (counts/meter towed), followed by adults (21%), pupa (4%), and emergent (2%). Less than 1% are unidentified by their life stage. *Americorophium* spp. account for 93% and 88% of the total counts and wet weights, respectively, of amphipods.

2020 diets, sampled February to March, were also dominated by amphipods, dipterans, and cladocerans, particularly *Americorophium* spp., chironomids, and *Daphnia* spp. 2020 salmon also followed the annual

trend of consuming primarily dipterans and cladocerans at Franz Lake and Campbell Slough and amphipods and dipterans at the downstream sites (Figure 137). An exception to this was that dipterans dominated 2020 Ilwaco slough diets (94% IRI), similar to Franz Lake (98% IRI), which differed from 2015, where Ilwaco diets were nearly entirely amphipods (99.7% IRI) (Figure 136). Campbell Slough followed a recent trend of increased IRI for cladocerans in diets (83%). Whites Island and Welch Island diets consisted predominantly of amphipods (89%, 57% IRI) with a minority of cladocerans (9%, 39% IRI), dipterans, and fish. Welch Island diets had the highest cladoceran IRIs since the beginning of the study (39%).



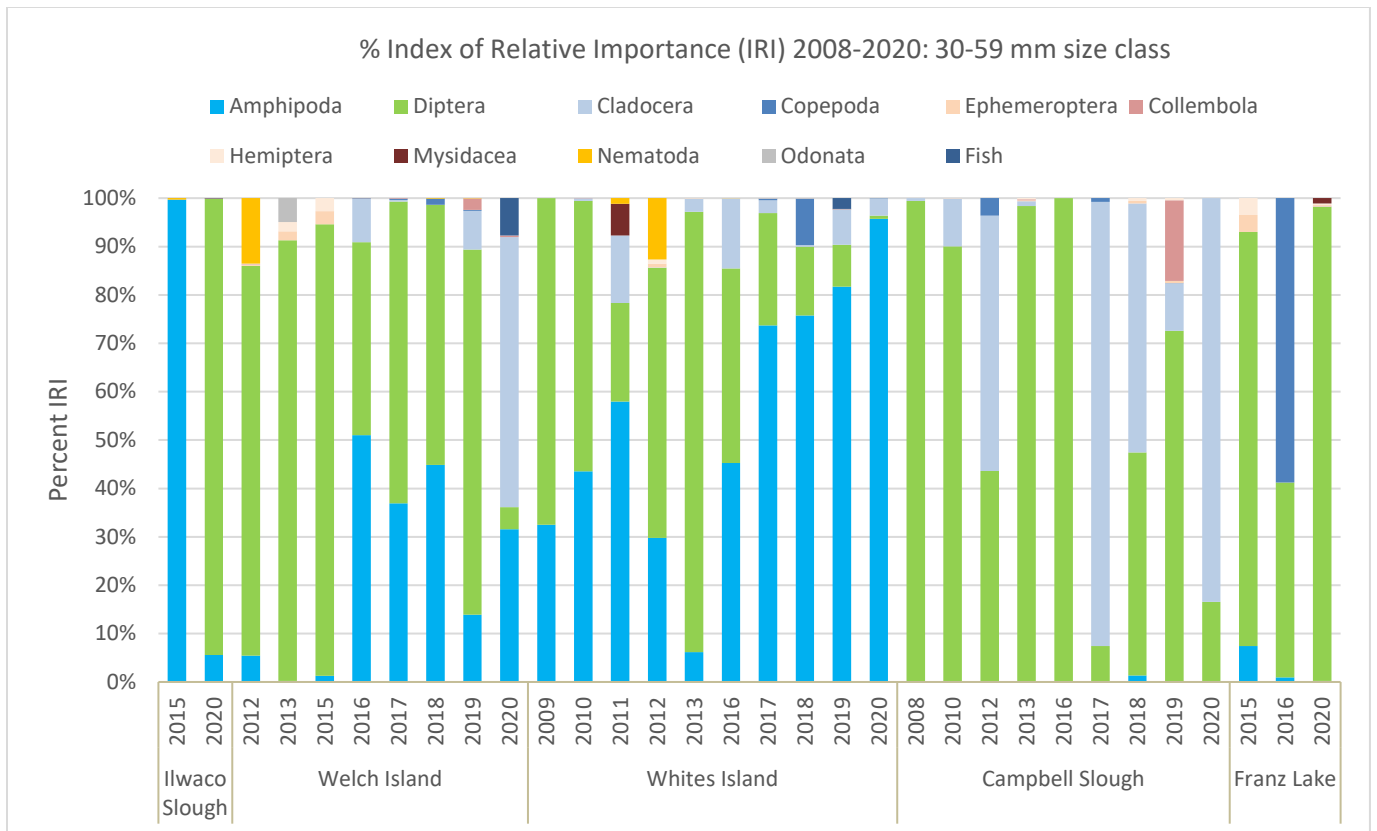


Figure 136: Percent Index of Relative Importance (IRI) by site and year for juvenile salmon 2008-2020. IRIs are calculated for all size classes (top) and in the 30-59 mm size class (bottom). Note: 2020 fish were collected February-March, while the remaining years represent fish collected April – June.

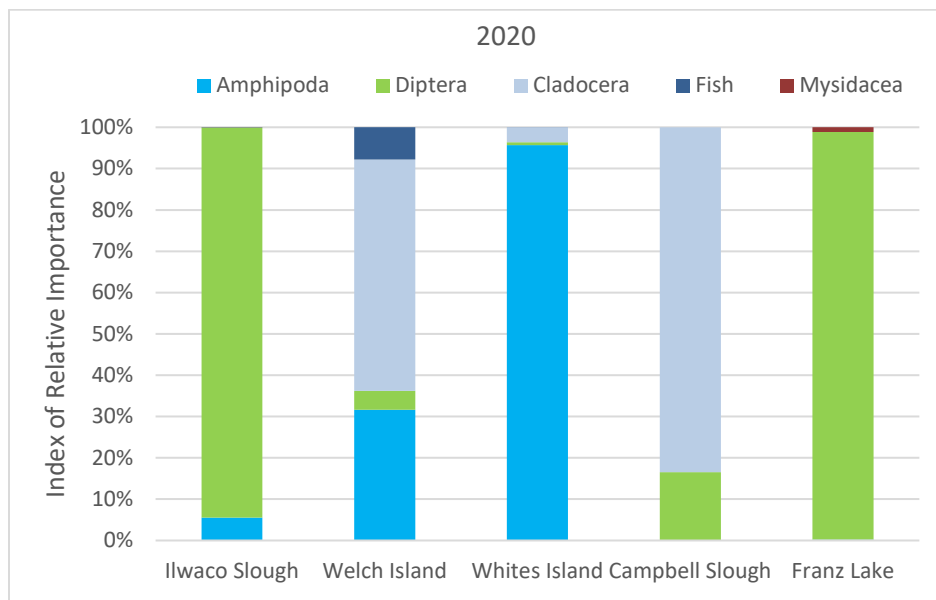


Figure 137: 2020 Percent Index of Relative Importance (IRI), by site, collected February-March. 2020 fish were in the 30-59 mm fork length size class. Sample size ranged from 5-33 individuals.

A comparison of the instantaneous ration (IR) and energy ration (ER) of fish collected in 2020 (Figure 138) indicate that highest IR and ER occurred at Ilwaco Slough, where juvenile Chinook predominantly

consumed insects, specifically Chironomidae and Psychodidae adults. IR and ER were lowest at Campbell Slough, where salmon consumed a mixture of cladocerans and insects, specifically *Daphnia* spp. and chironomids. IR and ER generally increased as fish grew, with largest increases appearing to occur at Ilwaco Slough (Figure 138).

Early interannual season salmon diets reflect highest instantaneous and energy rations at Ilwaco Slough and Welch Island, and generally low IR and ER values at Campbell Slough and Whites Island (Figure 139). As fish length increased, IR and ER values appear to increase most at Ilwaco Slough, while IR and ER values appeared to decrease at Whites Island and did not change at Welch Island. Linear trends for Franz Lake were not calculated due to infrequency of interannual February-March sampling.

A comparison of the instantaneous ration (IR) and energy ration (ER) of fish collected in 2020 to those collected in previous years during the same sampling months (February-March; 30 – 59 mm) shows that in all years, IR and ER trends appear to be relatively stable in this size class of salmon (Figure 140).

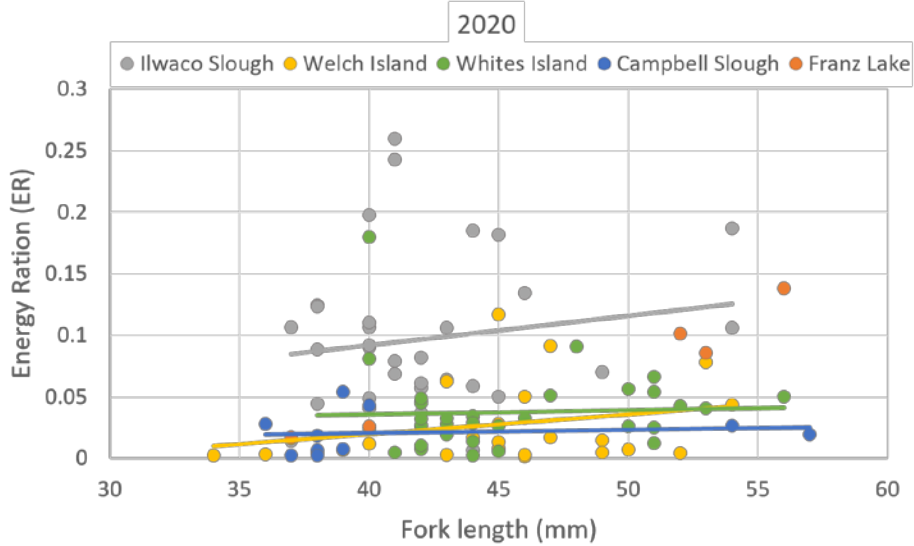
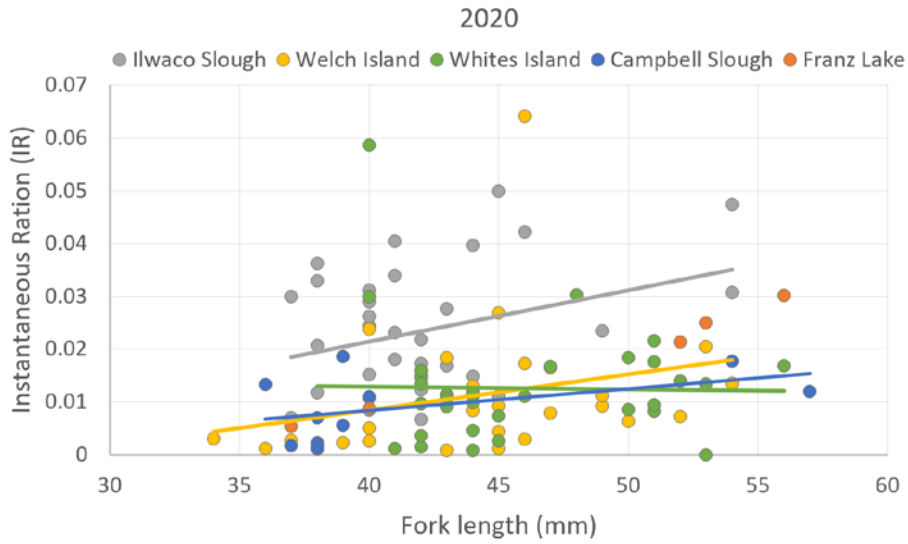


Figure 138: Instantaneous ration (IR) and energy ration (ER) for individual juvenile salmon in 2020. IR (top) and ER (bottom) indices are color sorted by site. Trendline is not calculated for Franz Lake due to small sample sizes.

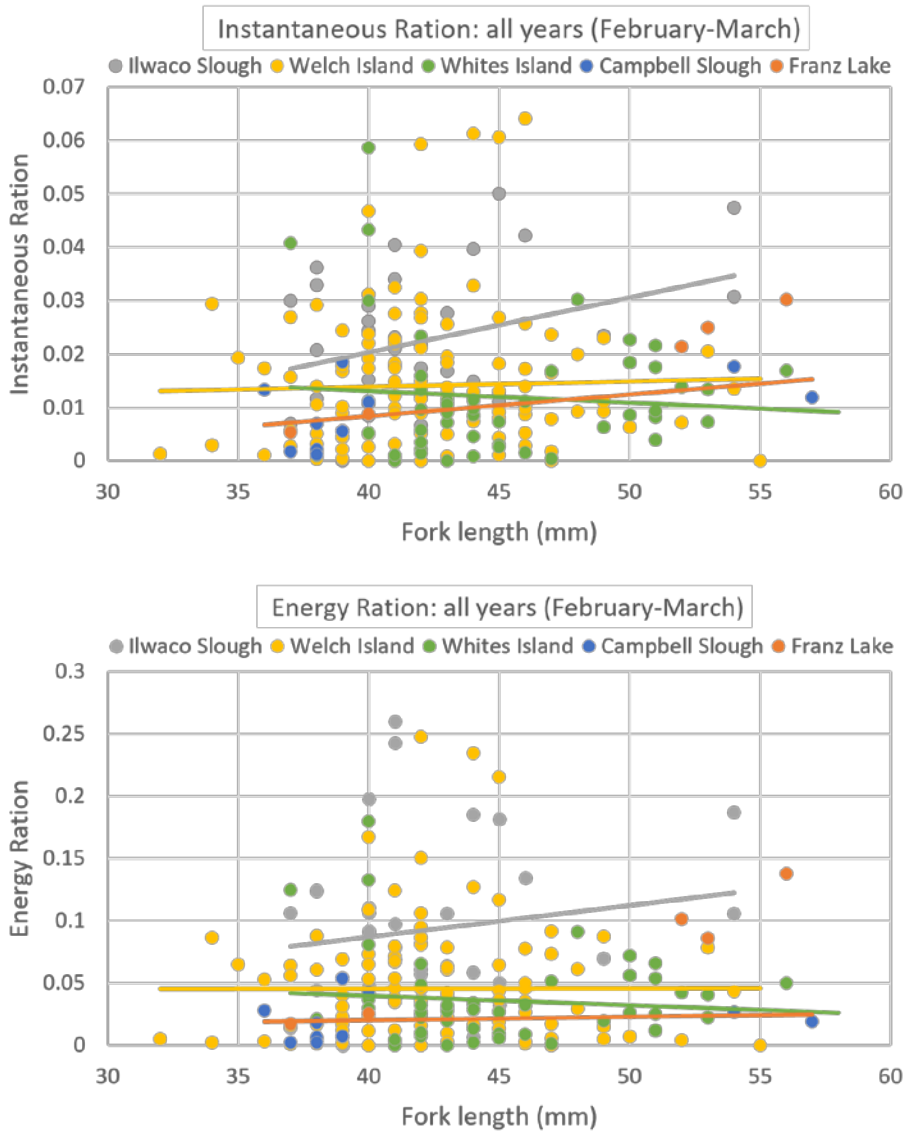


Figure 139: All year (Feb-March) instantaneous ration (IR) and energy ration (ER) for juvenile salmon. IR (top) and ER (bottom) indices are color sorted by site. Trendlines not calculated for Franz Lake due to infrequent interannual February-March sampling.

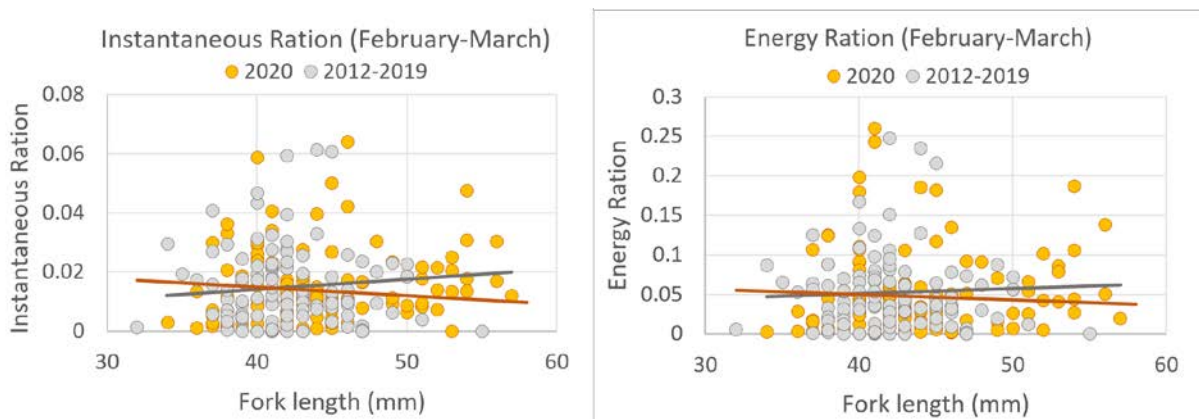


Figure 140: Instantaneous ration (IR) and energy ration (ER) for all salmon collected 2012 – 2020. IR (left) and ER (right) indices 2012-2013, 2017-2019 (gray) and 2020 (orange) are calculated for February-March. The solid line is the linear trendline.

Figure 141 provides a graphic representation, plotting mean maintenance metabolism against mean ER for all fish sampled in 2020. Samples with high energy assimilation and low metabolic costs (lower right quadrant) reflect conditions especially conducive to juvenile salmon growth, while samples with low energy assimilation and high metabolic costs (upper left quadrant) reflect less favorable conditions for juvenile salmon growth. Energy assimilation was typically low for all sites except Ilwaco Slough. The highest observations of J_m occurred at Ilwaco Slough, with a few observations occurring at Whites and Welch Islands. Campbell Slough reflected conditions less conducive to salmon growth, with high metabolic costs and low energy assimilation. Franz Lake and Whites Island had above average energy assimilation paired with above average metabolic costs. Due to attenuated sampling, connecting all-season 2020 growing conditions to specific sites is challenging. Interannual comparisons (Figure 141; bottom) demonstrate above average metabolic costs in 2020, and higher metabolic costs compared to previous years (February – March).

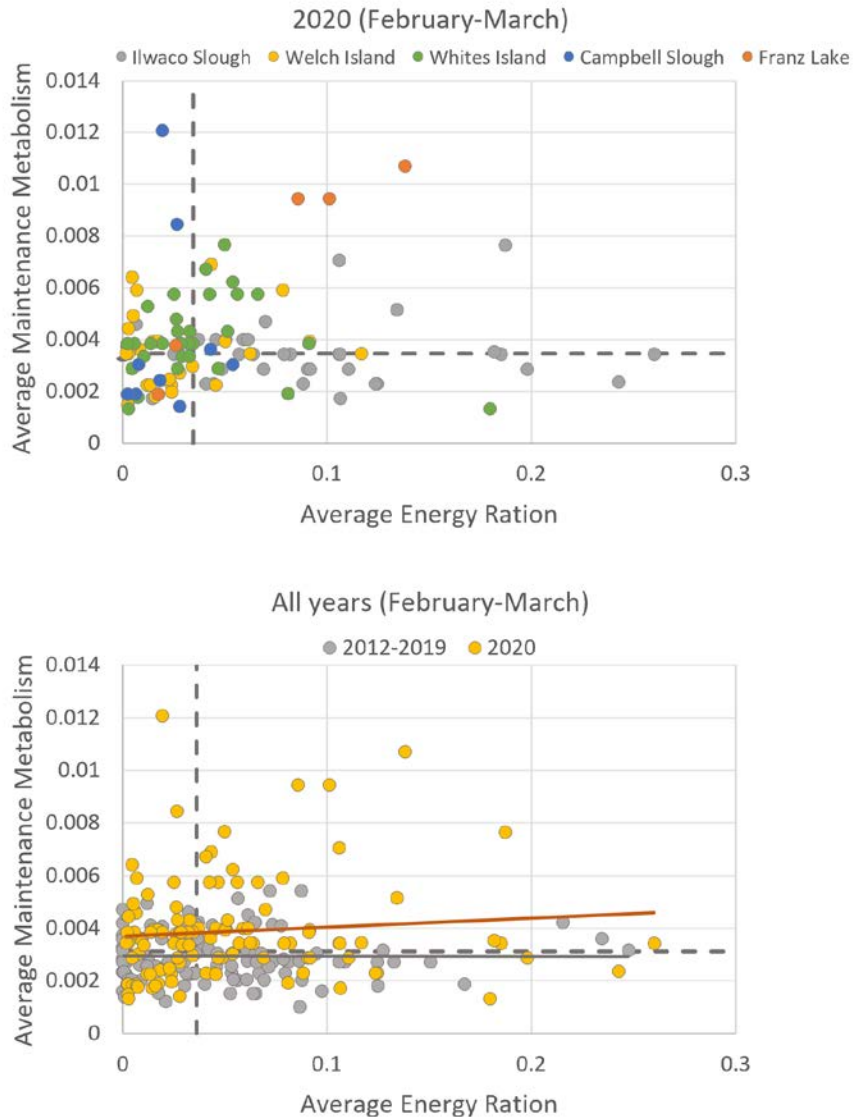


Figure 141: Quadrant charts of juvenile salmon average maintenance metabolism (J_m) and energy ration. Maintenance metabolism is calculated for 2020 (top) and among all years (bottom), and color sorted by site (top) and time (bottom, 2012-2019 – gray; 2020 – orange).

The NMDS ordination shows dissimilarity between Campbell Slough and Welch and Whites Islands, while interpretation for Ilwaco Slough and Franz Lake was challenging due to low sample sizes (Figure 142). There was higher contribution to diets by dipterans and cladocerans at Campbell Slough, and similarity of diet composition at Welch and Whites Islands, with majority contributions by amphipods and dipterans. Among sites, Campbell Slough and Franz Lake juvenile Chinook prey compositions were statistically different from Welch and Whites Islands' prey compositions (Table 42). Most non-significant group interactions, including group comparisons among Welch Island, Whites Island, and Ilwaco Slough, were not included in the table.

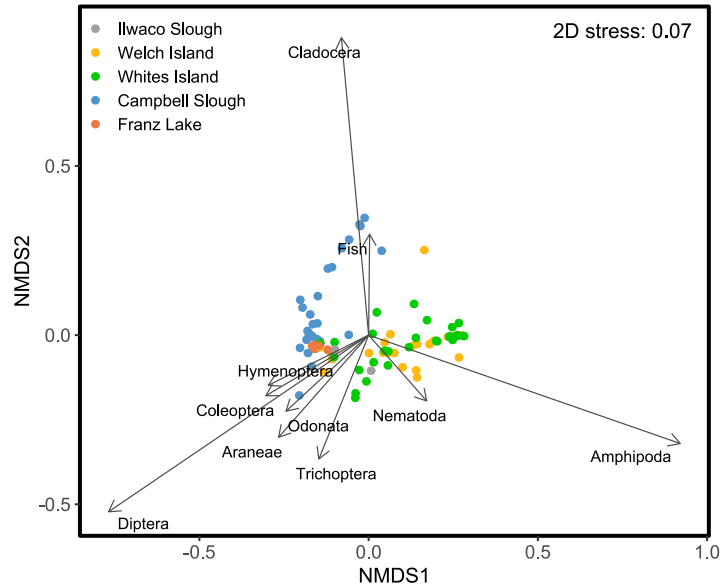


Figure 142: Two-dimensional NMDS plot for % IRI for major prey in juvenile Chinook diets. Percent IRIs are square-root transformed percent IRI and sampled between 2008 and 2020. Each point represents fish collected between April and June within the defined size class (fish fork length in mm) (2008-2017) and all fish collected (2020). Black vectors depict significant species loadings ($p = 0.05$), with strongest weights for Cladocera, Amphipoda, and Diptera.

Pairwise comparisons were used to identify the cumulative contribution of each species to the overall dissimilarity. The taxa listed account for more than 70% of the differences between groups. Amphipods and dipterans explain most of the dissimilarity between groups for all significant site pairings, except for Campbell Slough and Franz Lake, where dipterans and cladocerans contribute to most of the dissimilarity between diets. To illustrate, Campbell Slough and Whites Island have statistically different prey communities in which amphipods and dipterans contribute to 74% of the dissimilarity between the diets at these sites. Inversely, the diet composition at these sites was 26% similar.

Table 42: Analysis of similarities of juvenile salmon prey composition differences between paired sites. Includes R-value and adjusted p-value for each significant pairwise comparison. Most non-significant comparisons were not listed. Cumulative contribution of influential species include species that contribute 70% or more to the difference in prey composition between sites.

Pairwise comparisons	R-value	Bonferroni p	Cumulative Contribution of influential species		
			Amphipoda	Diptera	Cladocera
Campbell – Ilwaco	0.45	0.096	0.41	0.77	
Campbell – Welch	0.44	0.006	0.39	0.73	
Campbell – Whites	0.44	0.006	0.39	0.74	
Franz – Ilwaco	0.63	0.042	0.46	0.91	
Franz – Welch	0.49	0.006	0.86	0.44	
Franz – Whites	0.36	0.006	0.86	0.45	
Campbell – Franz	-0.16	1		0.44	0.71

3.6 Fish

In 2020, NOAA safety protocols associated with the COVID-19 pandemic limited the fish sampling at all trend sites to February and March for Ilwaco Slough, Welch Island, White Islands and Campbell Slough and only February for Franz Lake. In 2021, fish community sampling was able to resume for the five

trend sites and was conducted March–June and November, with the exception of June for Campbell Slough when water temperatures were too high for handling fish. Data for this section of the report includes 2020–2021, however the results will focus on 2021 data unless specified. A more comprehensive overview of annual trends, including 2020 data is presented in the discussion in Section 4.6.

3.6.1 Fish Community Composition

In 2021, fourteen different families of fishes were present and within those families there were 24 different taxonomic categories which included a combination of specific species and/or unidentified species within family/genus categories (Figure 143 and Appendix Table E-2). Threespine stickleback and banded killifish were the only species that were consistently present at all five sites. Three salmon species were captured, with Chinook the most common and often the most abundant species occurring at all sites except Ilwaco Slough. Chum was captured at three sites (Welch and White Islands, Campbell Slough) but were not always numerically dominant. Coho were only captured at Campbell Slough. Campbell Slough had the highest diversity of taxonomic categories (17) followed by Franz Lake (14) and Whites Island (9). Franz Lake had the highest percent of introduced fishes in the total catch (35%) followed by Campbell Slough (14%). Threespine stickleback was the dominant species at Welch Island (92%) and Campbell Slough (79%); Chinook salmon was the dominant species at White Island and Franz Lake which is an increase in comparison to previous years for those sites.

Although relative abundances of fish species varied among sites, patterns of community structure can be discerned through multivariate analyses. The ANOSIM test on species abundance indicated a significant difference in fish community structure among trend sites from 2008–2021 (global $R = 0.274$, $P = 0.01$). Pairwise tests show that the community structure at all sites were significantly different from other sites except for Welch and Whites Islands ($P = 0.461$). The nMDS plot of community structure by site (Figure 144) shows the separation and overlap of sites and the driving factors. There is high overlap between Welch and Whites Islands, which is driven by threespine sticklebacks. Ilwaco Slough tends to separate from Welch and Whites Islands based on the presence of marine species. Campbell Slough and Franz Lake are more similar with each other than with the lower river sites.

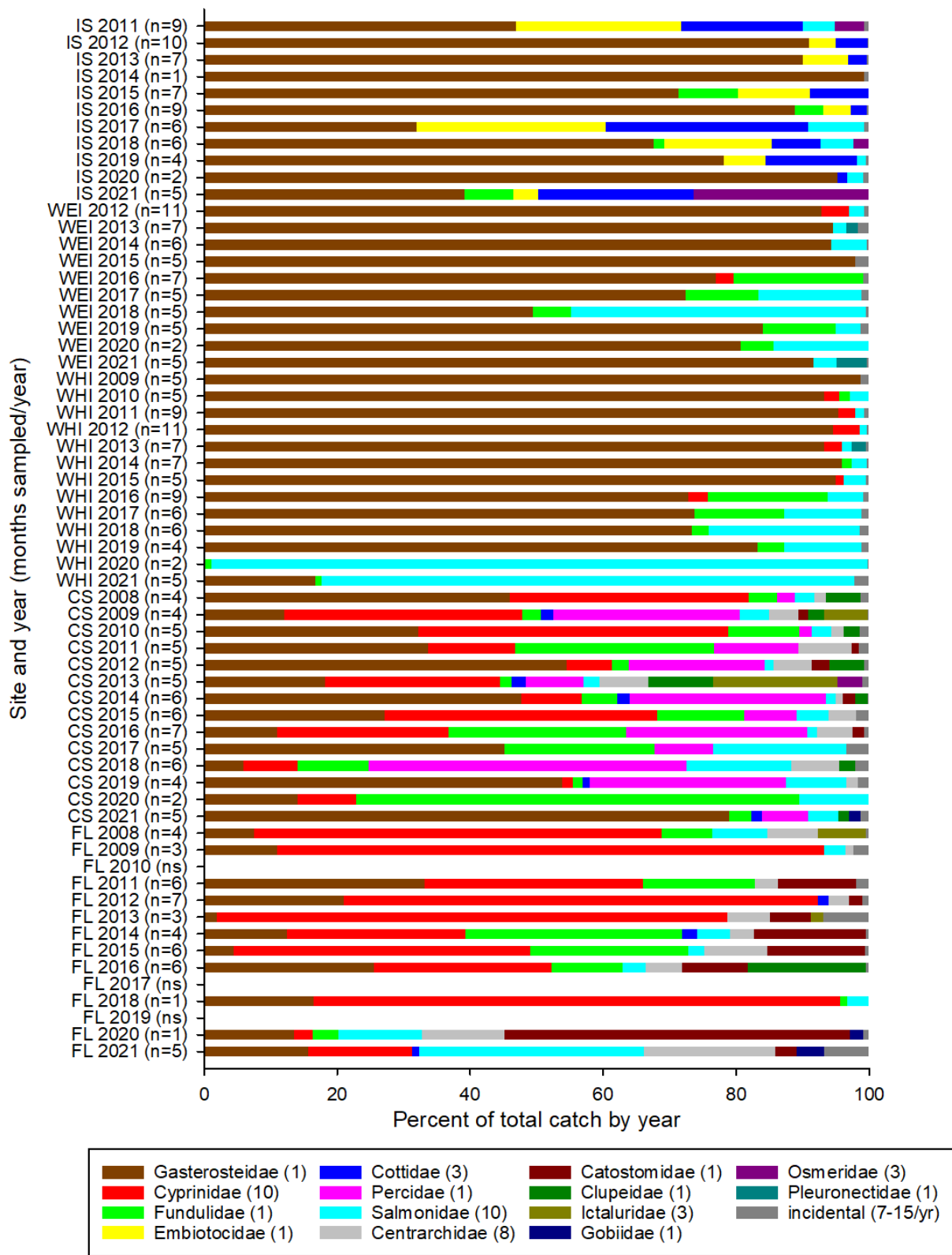


Figure 143. Fish community composition at EMP trend sites sampled from 2008-2021, presented by Family. For each year, the total number of sampling months is presented in parentheses. IS = Ilwaco Slough, WEI = Welch Island, WHI = Whites Island, CS = Campbell Slough, FL = Franz Lake.

Non-metric MDS

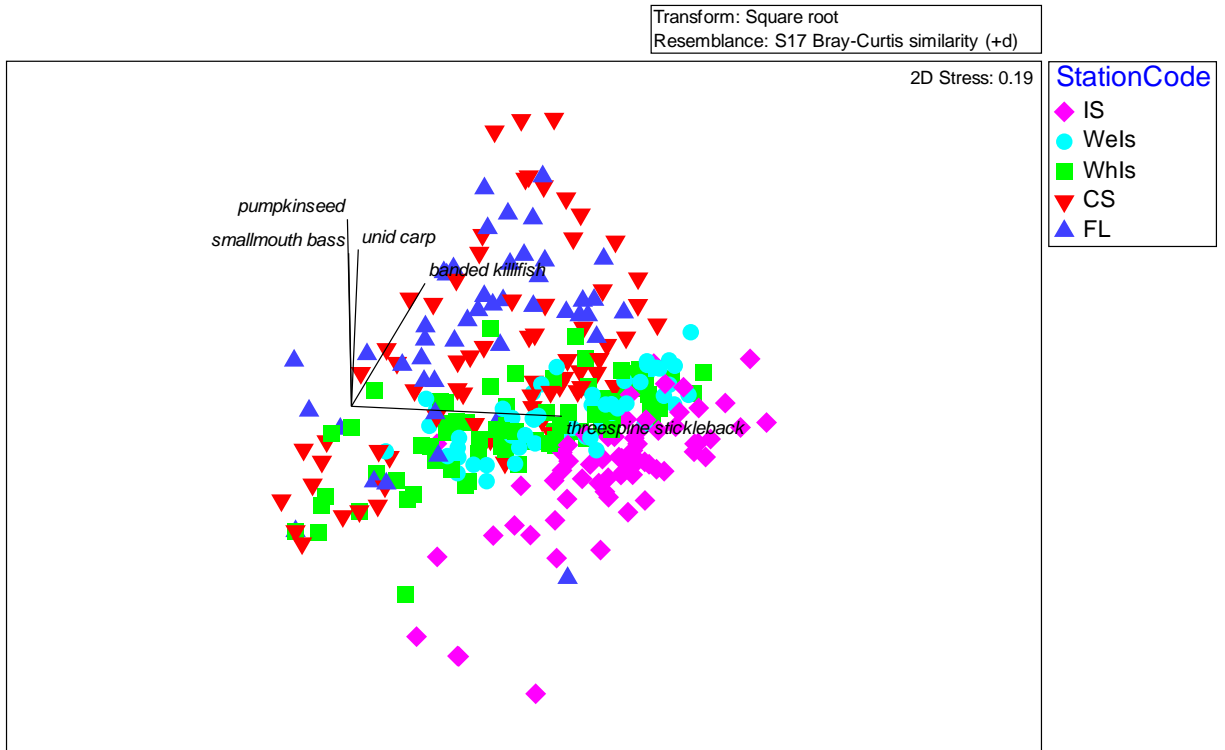


Figure 144. Nonmetric multidimensional scaling (NMDS) plot based on square-root transformed species abundance at five trend sites, 2008-2021. Significant correlation with variables (Pearson $R > 0.5$) are represented as vectors. IS = Ilwaco Slough, WEI = Welch Island, WHI = Whites Island, CS = Campbell Slough, FL = Franz Lake. Note that 2020 data, while limited, is included.

Mean species richness and associated ranges for each year of sampling at Ilwaco Slough, Welch Island, and Whites Island all fall between 0-10 species and remain similar from year to year (Figure 145-Figure 146). Campbell Slough and Franz Lake reflect a more diverse community (ranging from 0-24 species) that is dominated by introduced species which can tolerate warm water. The same trend is observed in the Shannon-Weiner diversity indices (Figure 146), where the values can vary minimally, yet tend to be the highest at Campbell Slough and Franz Lake. Typical trends in both the Shannon-Weiner diversity index and Species Richness were seen in 2021 (Figure 147).

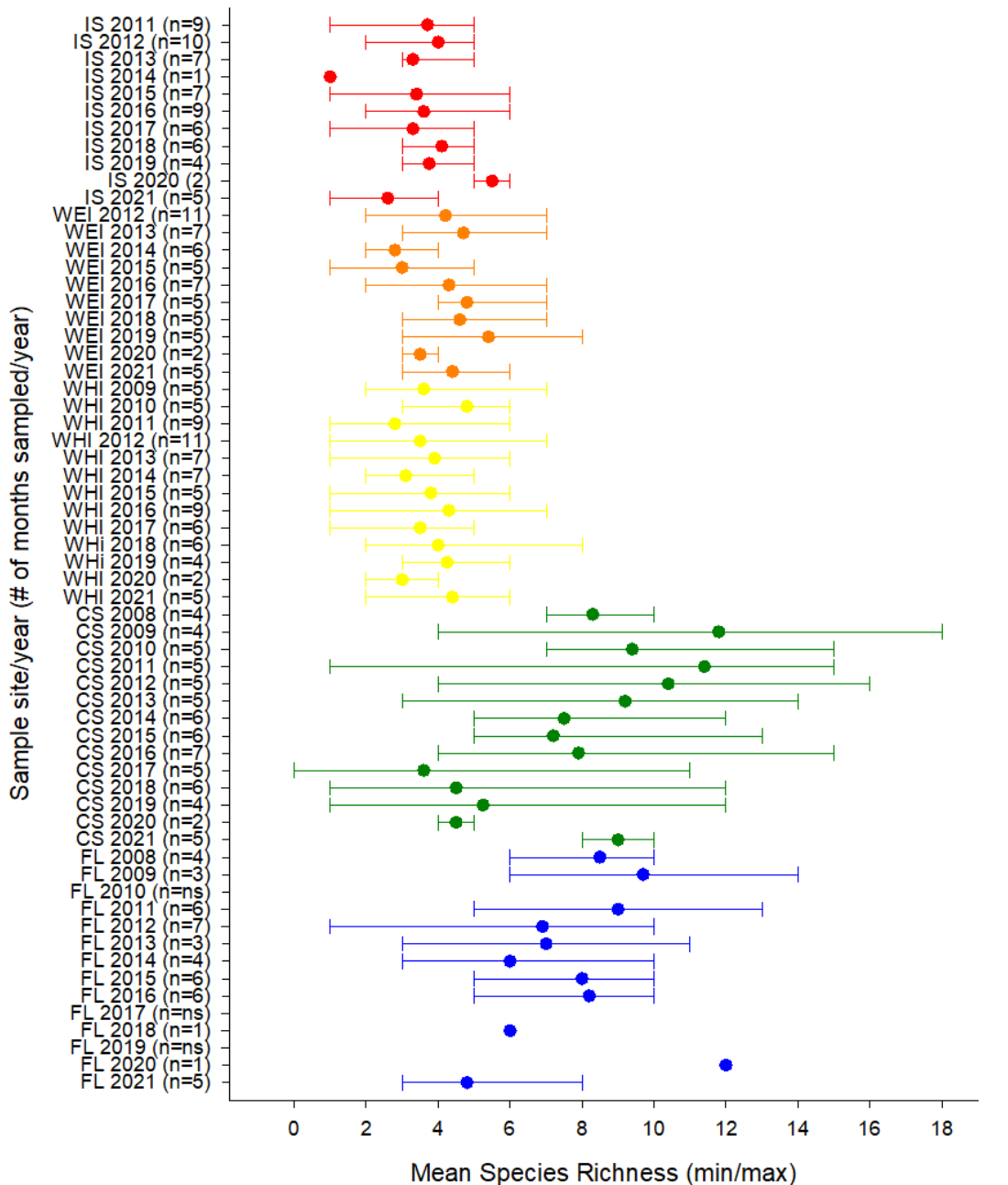


Figure 145. Mean species richness with minimum/maximum ranges for EMP trend sites sampled from 2008-2021. For each year, the total number of sampling months is presented in parentheses. IS = Ilwaco Slough, WEI = Welch Island, WHI = Whites Island, CS = Campbell Slough, FL = Franz Lake.

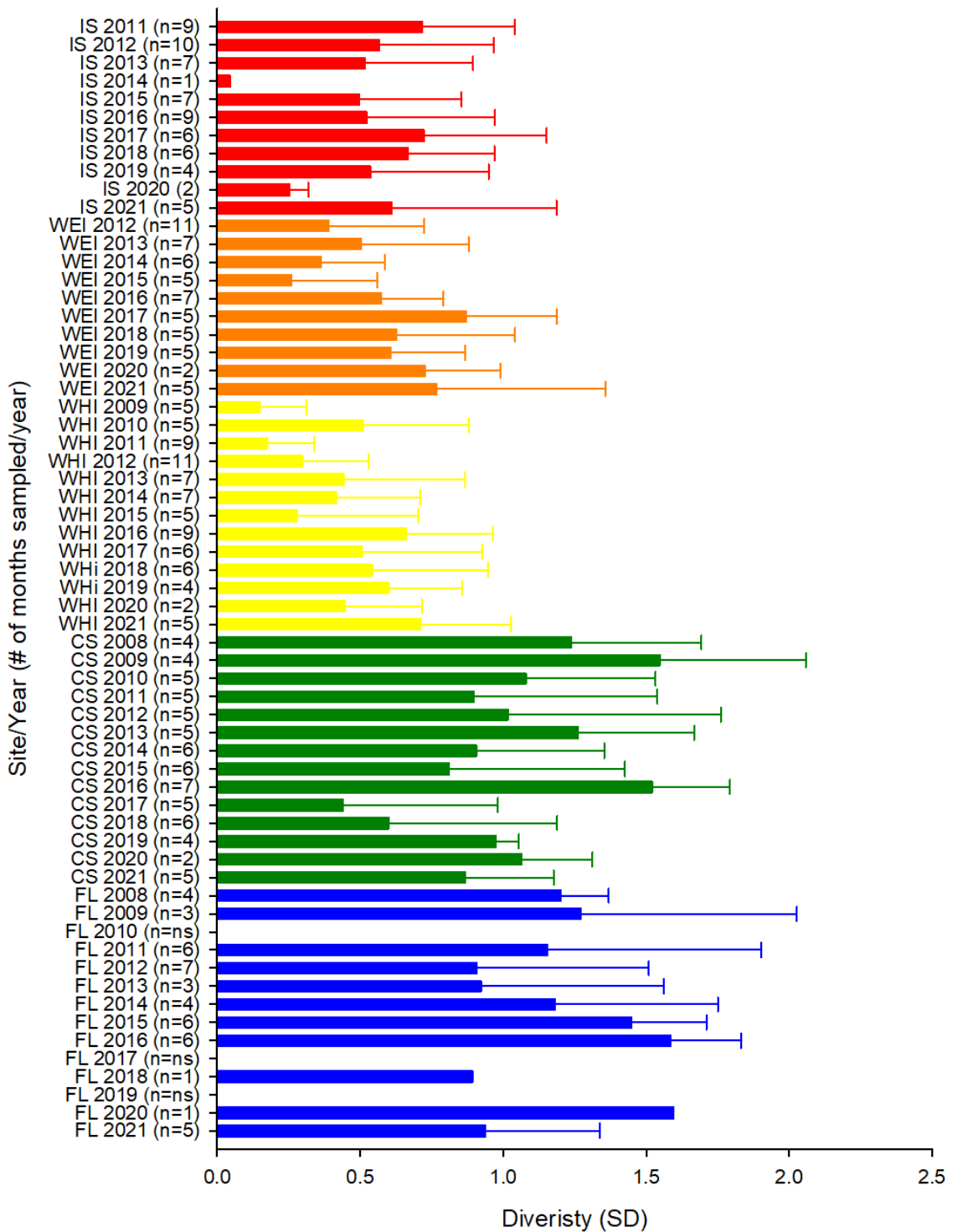


Figure 146. Mean Shannon-Weiner diversity index with standard deviation from EMP trend sites sampled from 2008-2021. For each year, the total number of sampling months is presented in parentheses. IS = Ilwaco Slough, WEI = Welch Island, WHI = Whites Island, CS = Campbell Slough, FL = Franz Lake.

In 2019, the monthly sampling at each site did not show any distinct pattern of species richness and diversity (Figure 147). The number of species each month typically ranged from 1-6, the only exception occurred at Campbell Slough in June where the total number of species reached 12. Campbell Slough also had the greatest range in diversity (0.0-1.1) which reflects the higher number of species and the overall total catch of those species.

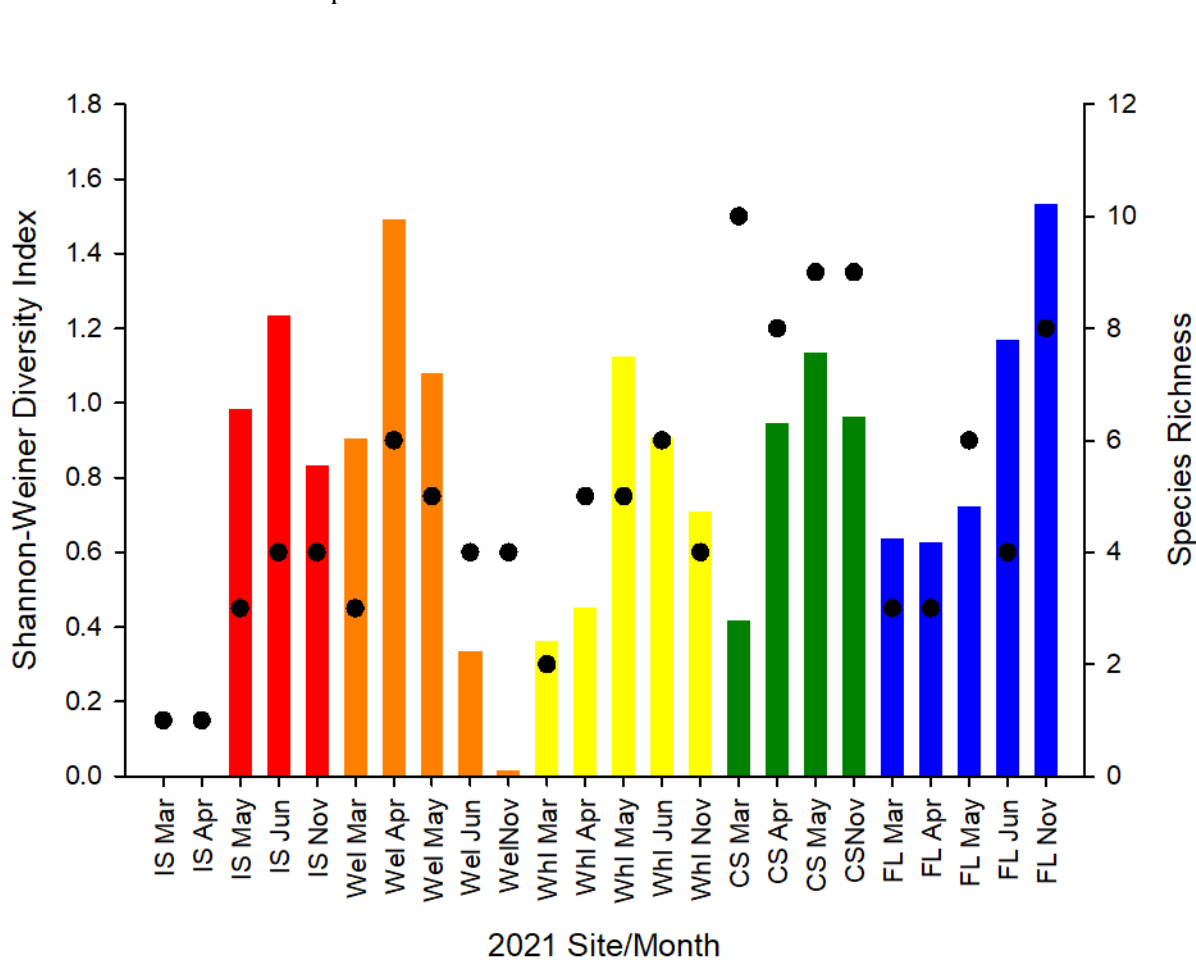


Figure 147. Shannon-Weiner diversity index (bars) and species richness (closed circles) for EMP trend sites sampled monthly in 2021. IS = Ilwaco Slough, WEI = Welch Island, WHI = Whites Island, CS = Campbell Slough FL = Franz Lake.

Non-native fish species occur at all five trend sample sites over all sampling years; their presence is highly variable and likely very dependent on water levels and temperature (Figure 148). The highest number of non-native fishes occurs at Campbell Slough where the catch rates have exceeded 50% (range from 13-76%) for eight out of the last fourteen years. At Campbell Slough, banded killifish, yellow perch, and unidentified juvenile carp comprise the majority of the non-native species. Franz Lake has the second highest numbers of non-native species exceeding 20% for eight out of the last eleven years of sampling and ranging from 1-54%. At Franz Lake, banded killifish, unidentified juvenile carp, and five categories in the Centrarchidae family are the predominant non-native fishes.

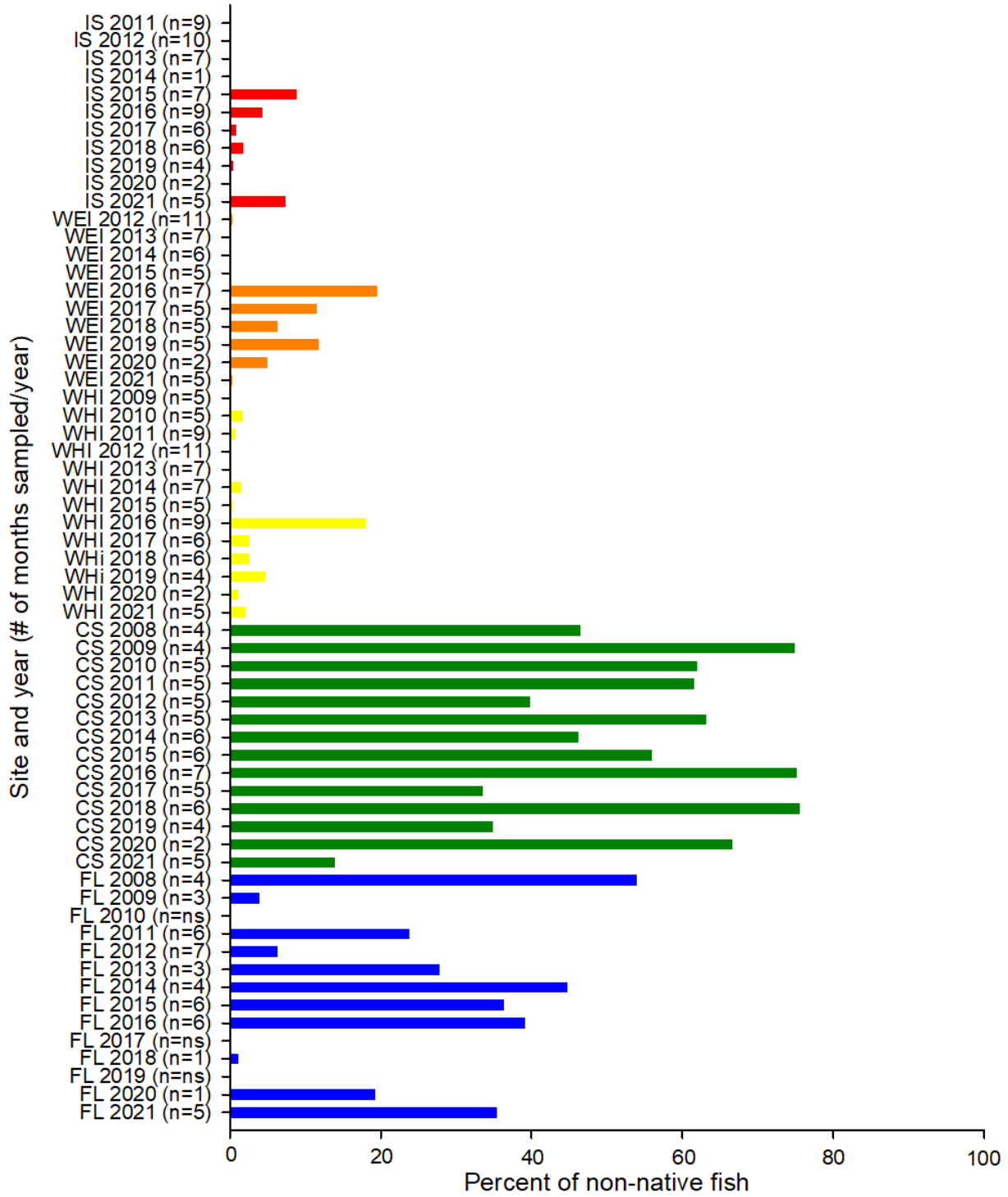


Figure 148. Percent of total fish catches per year that are non-native species for EMP trend sites sampled in 2008-2021. For each year the total number of sampling months is presented in parentheses. IS = Ilwaco Slough, WEI = Welch Island, WHI = Whites Island, CS = Campbell Slough, FL = Franz Lake.

There are five non-native (small and largemouth bass, walleye, warmouth, and yellow perch) and one native (northern pikeminnow) fish species that produce mature stages that can prey on juvenile salmon. These fish are freshwater species that primarily occur at Campbell Slough and Franz Lake and minimally occur at Welch and Whites Islands (Figure 149).

No predatory species have been captured in the Ilwaco Slough site, which is the only site with marine water influence. At the four freshwater sites yellow perch is the most common species followed by northern pikeminnow. Smallmouth bass is the third most common species has been captured at Campbell Slough and Franz Lake exclusively. In 2021, yellow perch comprised 76% of the total number of predatory fish captured.

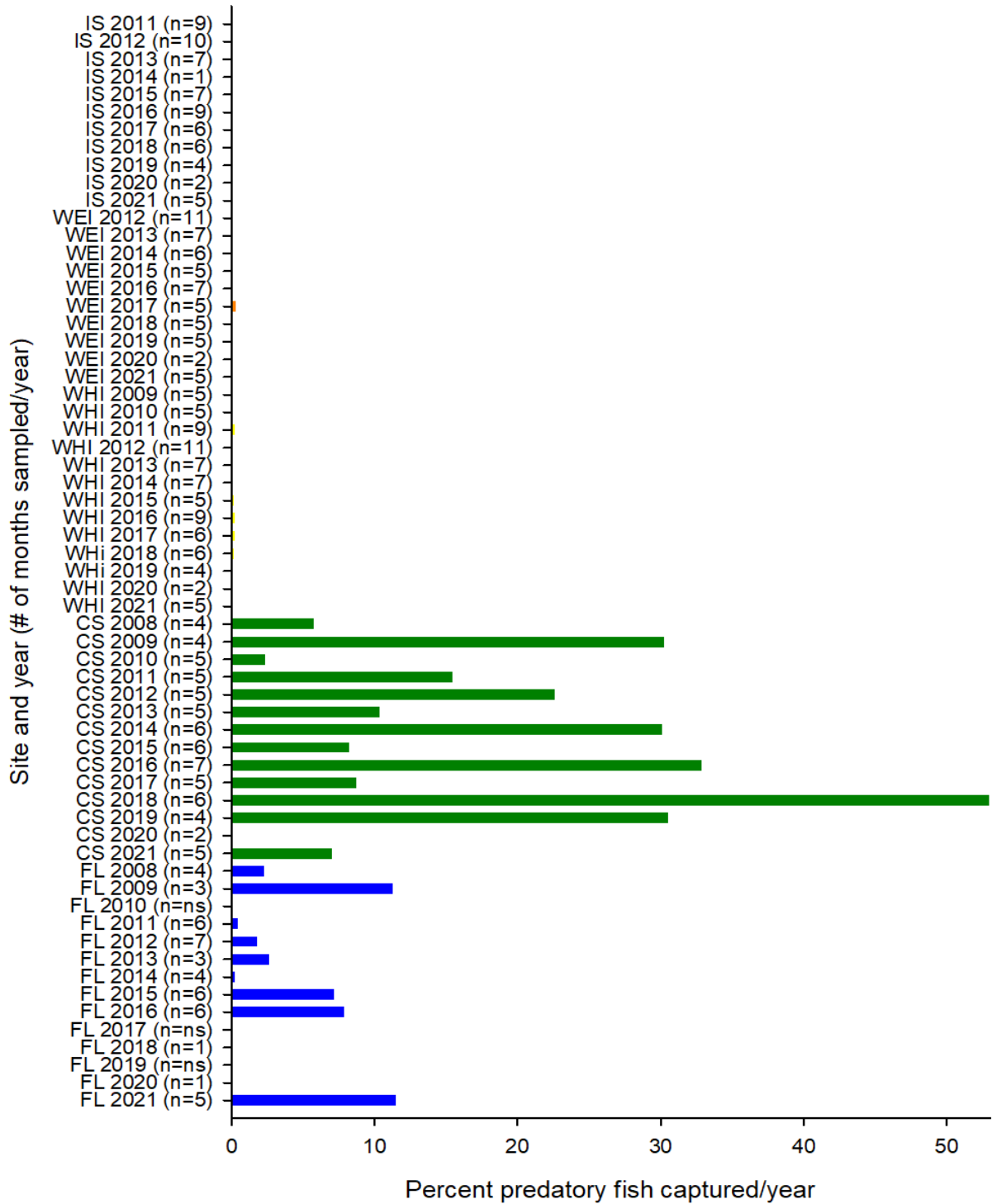


Figure 149. Total percentage of the yearly (2008-2021) catch of fish species that have mature stages that could be predatory toward juvenile salmon. Species include small and largemouth bass, northern pikeminnow, walleye, warmouth, and yellow perch. For each year the total number of sampling months is presented in parentheses. IS = Ilwaco Slough, WEI = Welch Island, WHI = Whites Island, CS = Campbell Slough, FL = Franz Lake.

3.6.2 Salmon Species Composition

In 2020, NOAA safety protocols associated with the COVID-19 pandemic limited the fish sampling at all trend sites to February and March for Ilwaco Slough, Welch Island, White Islands and Campbell Slough and only February for Franz Lake. In 2021, fish community sampling was able to resume for the five trend sites and was conducted March - June and November, with the exception of June for Campbell Slough when water temperatures were too high for handling fish. Data for this section of the report includes 2020–2021, however the results will focus on 2021 data unless specified. A more comprehensive overview of annual trends, including 2020 data is presented in the discussion in Section 4.6.

Similar to previous sampling years, 2021 salmon species composition varied by site, showing distinct patterns associated with hydrogeomorphic reach (Figure 150). In 2021, Chinook salmon were caught at four of the five sampled sites and were the dominant salmon species at Welch Island in reach B, Whites Island in reach C, Campbell Slough in reach F and Franz Lake in reach H. At these sites, Chinook salmon comprised 90 to 100% of salmonid catches. In 2021, unmarked (presumably wild) Chinook were more abundant at all four sites where Chinook were sampled than marked hatchery Chinook (Figure 151). In addition to Chinook salmon, small numbers of chum salmon were found at Welch Island, Whites Island and Campbell Slough. This pattern is typical for Welch and Whites Islands and has been evident since 2012. Only two unmarked coho salmon were collected at Campbell Slough in 2021 (Figure 152). No trout or sockeye salmon were caught in 2021.

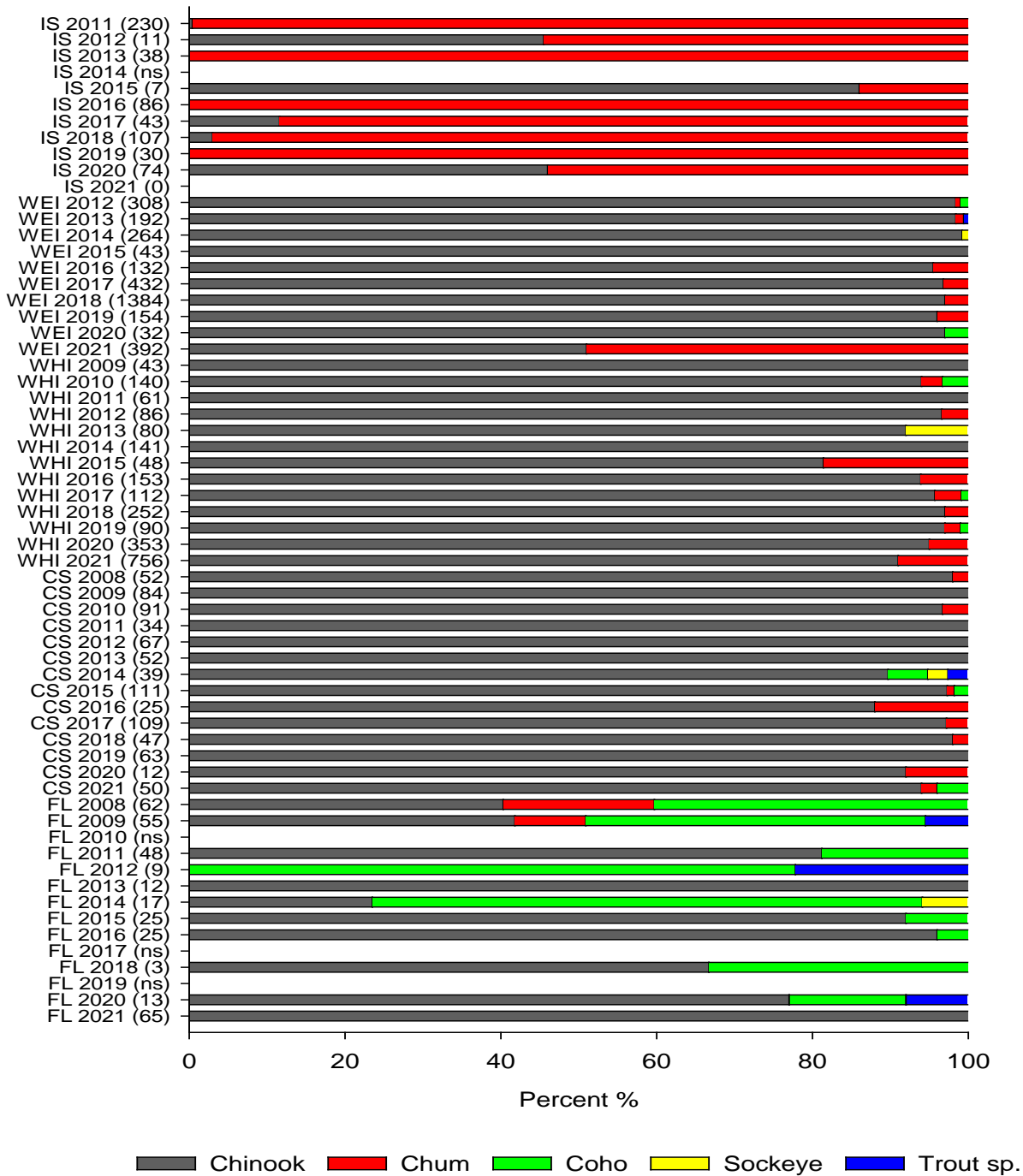


Figure 150. Percentage of salmonid species collected at EMP trends sites from 2008 - 2021. Total number of salmonids captured at a given site and year are presented in parentheses. WEI = Welch Island, WHI = Whites Island, CS = Campbell Slough, FL = Franz Lake.

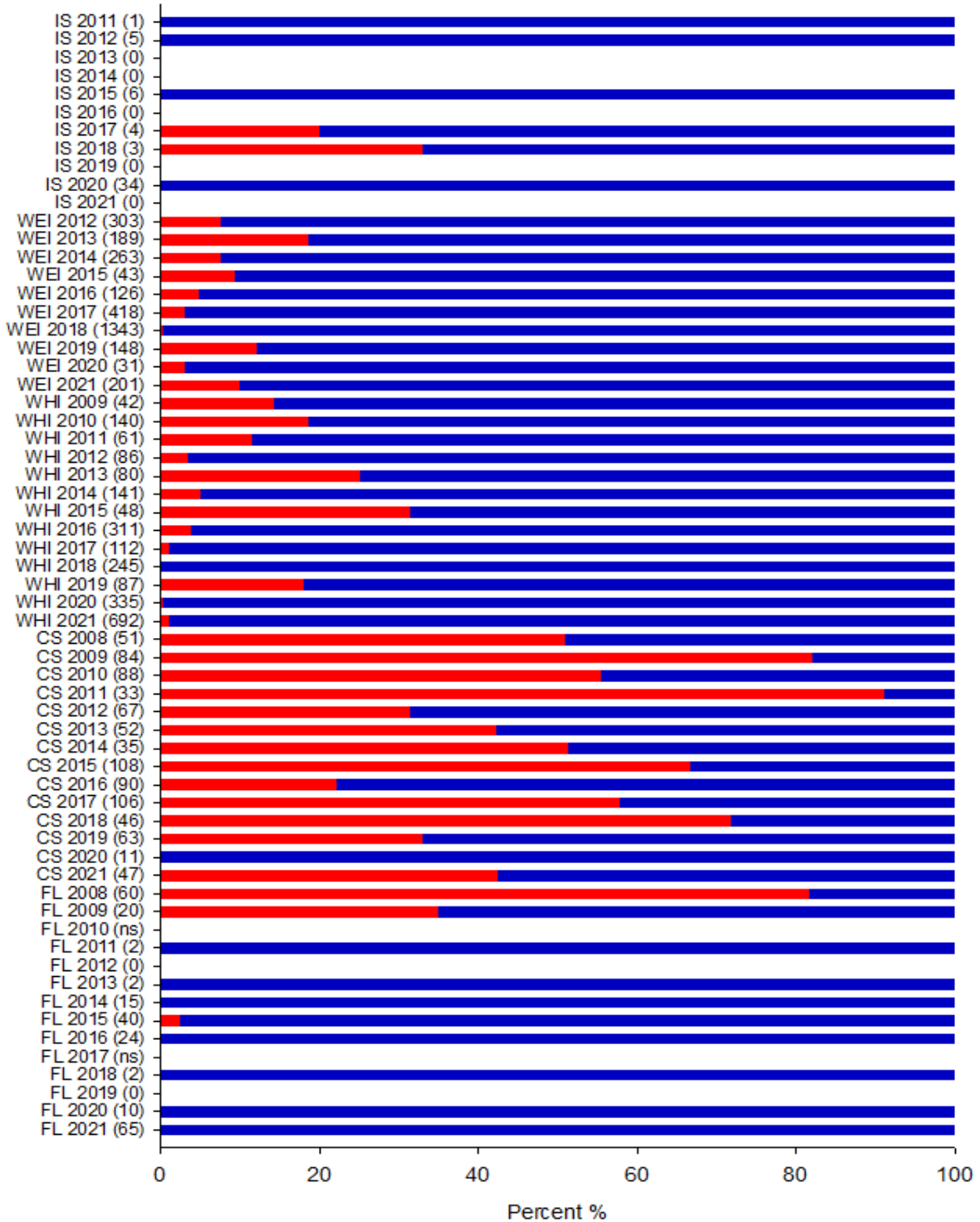


Figure 151a. Percentage of marked (red) and unmarked (blue) Chinook salmon captured at the EMP sampling sites from 2008- 2021. The vertical axis represents site and year of sampling. Total number of the specified salmon species captured at a given site are presented in parentheses. IS = Ilwaco Slough; WEI = Welch Island, WHI = Whites Island, CS = Campbell Slough, FL = Franz Lake.

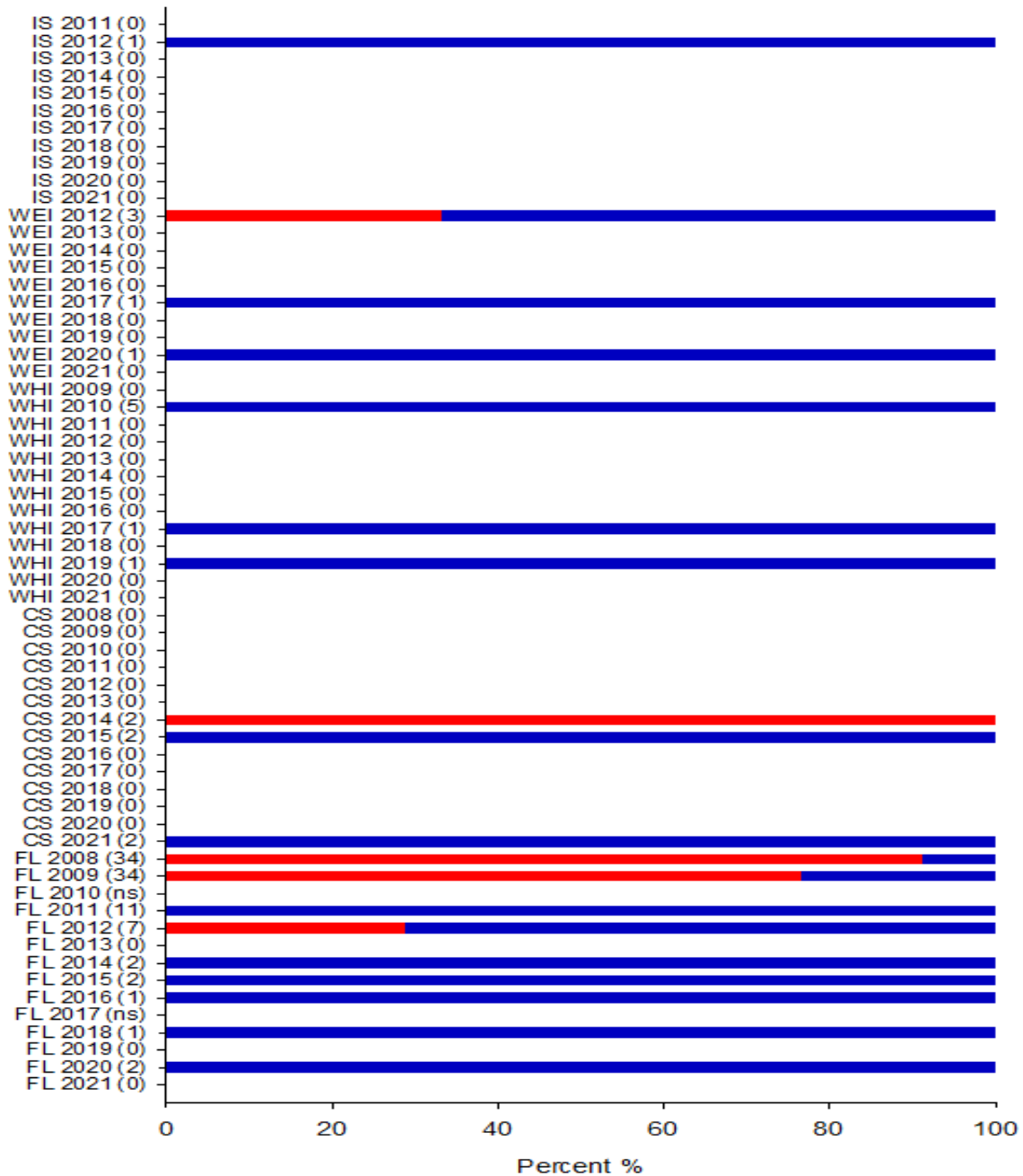


Figure 152b. Percentage of marked (red) and unmarked (blue) coho salmon captured at the EMP sampling sites from 2008- 2021. Vertical Axis represents site and year of sampling. Total number of the specified salmon species captured at a given site are presented in parentheses. IS = Ilwaco Slough; WEI = Welch Island, WHI = Whites Island, CS = Campbell Slough, FL = Franz Lake.

3.6.2.1 *Salmon Density*

Chinook salmon

In 2021, unmarked Chinook salmon were captured at the EMP trend sites from March through June and again in November. The highest average densities of unmarked juvenile Chinook salmon were 144.63 per 1000 m² in April. Marked Chinook salmon were captured from March through June, with the highest average densities of 14.81 fish per 1000 m² in May (Figure 153-Figure 154). Mean Chinook salmon densities by site and year are shown in (Figure 153-Figure 154). In 2021 the density of unmarked Chinook salmon was highest at Whites Island (398.39 fish per 1000 m²) and Welch Island (54.03 fish per 1000 m²) and lowest at Campbell Slough (10.67 fish per 1000 m²). Franz Lake had a strong year for Chinook catches with a density of (29.11 fish per 1000 m²). No Chinook were captured at Ilwaco Slough in 2021. Densities of marked Chinook salmon in 2021 were greatest at Campbell Slough, however with a density of (7.95 fish per 1000 m²) catches were slightly less than previous years. The densities of marked Chinook salmon in 2021 were generally within similar ranges as seen from 2008-2020 at all sites (Figure 153-Figure 154).

Coho salmon

In 2021, only two unmarked coho salmon were collected at Campbell Slough in November (152). Coho salmon have been captured only sporadically at Ilwaco Slough, Campbell Slough and Welch Island, so their lack of abundance was not unusual compared to previous years. Sampling was conducted at Franz Lake in 2021, however no coho were captured. Franz Lake is traditionally the only site where coho salmon have been consistently collected. Coho salmon density at Franz Lake was at its lowest reported level in 2016 and has shown a consistent decline since 2011. However, low sampling efforts in 2017, 2018 and no sampling in 2019 have made it difficult to determine any recent trends in coho abundance levels at Franz Lake. Marked coho salmon, which were common at Franz Lake in 2008 and 2009, have not been observed since 2012.

Chum salmon

In 2021, chum salmon were found at the trends sites in March, April and May with the highest average density in May (91.78 fish per 1000 m²; (Figure 153-Figure 154). Chum salmon were present at Welch Island, Whites Island and Campbell Slough in 2021 (Figure 153-Figure 154). In 2021 the density of chum salmon was highest at Whites Island (65.52 fish per 1000 m²) and lowest at Campbell Slough (0.43 fish per 1000 m²). However, no chum were captured at Ilwaco Slough and Franz Lake in 2021. Chum Salmon was not seen in the sample at Ilwaco Slough for the first time since sampling began in 2011. This is worth noting due to Ilwaco slough traditionally having the highest density of chum salmon of all five sample sites. Chum salmon been found at all the sampling sites at varying densities, although not consistently. Chum salmon have not been observed at Franz Lake since 2009.

Sockeye salmon and trout species

In 2021, Sockeye salmon and trout were not caught. Historic densities for sockeye salmon and trout for all sampling have been extremely low.

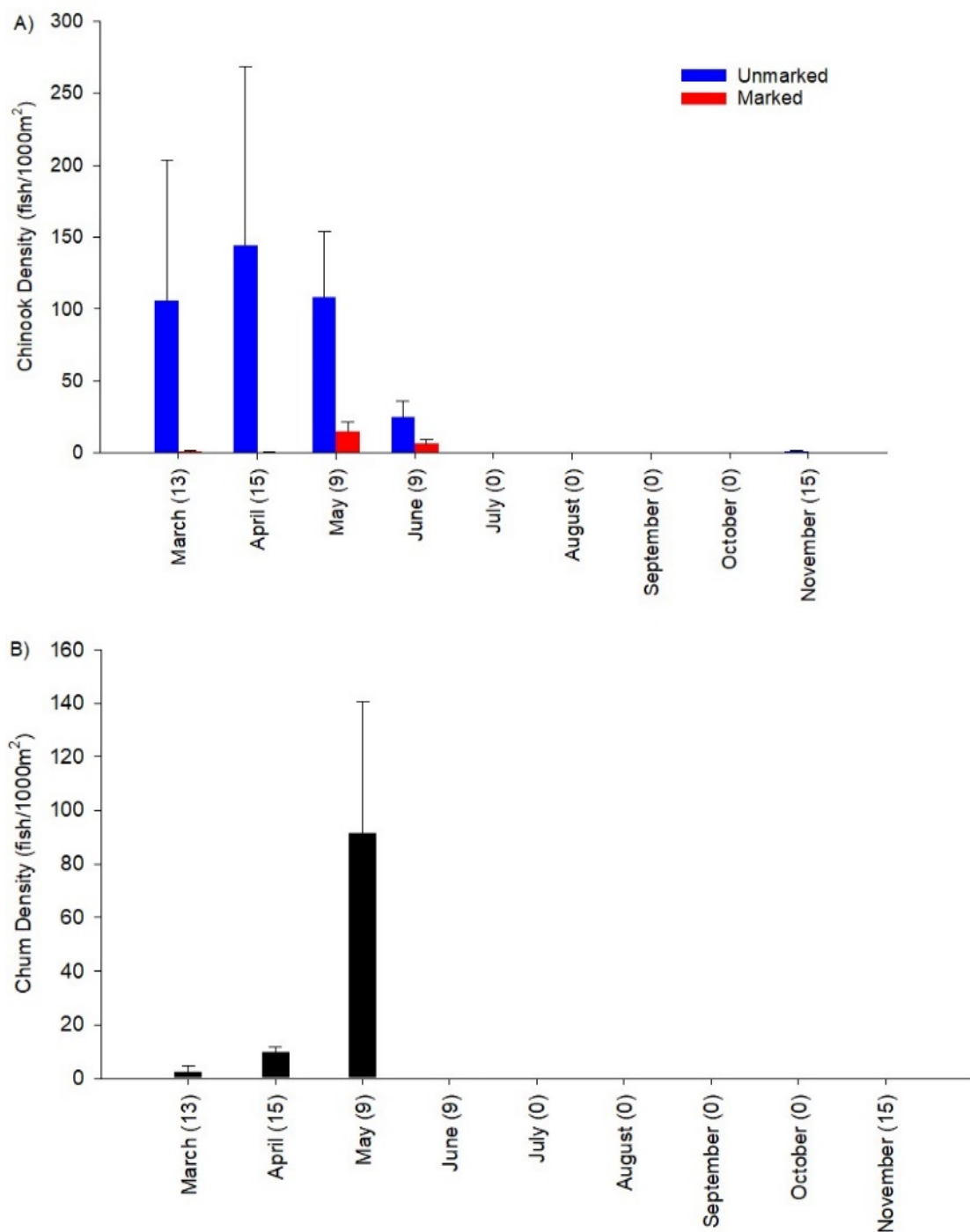


Figure 153. Monthly Mean (SE) densities (fish per 1000 m²) of a) marked (red bars) and unmarked (blue bars) juvenile Chinook salmon, b) chum salmon in 2021 (all sites combined). Total number of sampling efforts per month are presented in parentheses. Only two coho salmon were captured at all sites in 2021 therefore no monthly density for coho salmon is shown.

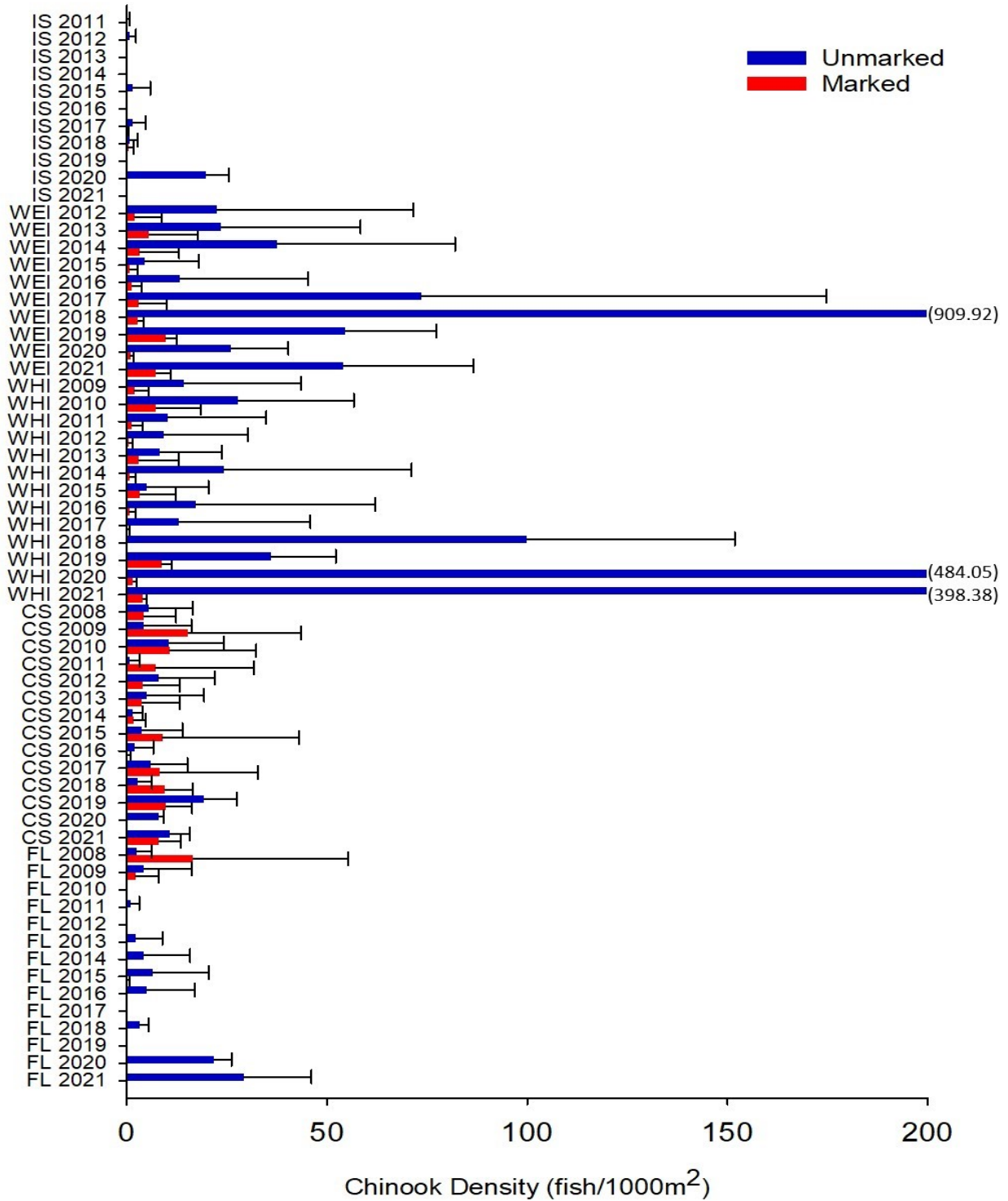


Figure 154. Marked (red bars) and unmarked (blue bars) juvenile Chinook salmon densities (fish per 1000 m²) by site and year. Welch 2018, Whites 2020 and 2021 were truncated for ease of viewing. IS = Ilwaco Slough, WEI = Welch Island, WHI = Whites Island, CS = Campbell Slough, FL = Franz Lake.

3.6.3 Salmon Metrics

3.6.3.1 Genetic Stock Identification

Genetic analysis has been halted by COVID-19 related safety protocols that closed the NOAA laboratories responsible for processing the samples, therefore no samples collected in 2021 have been analyzed. Here we present results from the two months of sampling in 2020 (February and March) that occurred prior to COVID-19 related closures. For 2020, genetics data were collected from Chinook salmon at all five trend sites. To maintain the highest level of confidence in stock assignments, we only reported stock assignments for fish that had an assignment probability greater than or equal to 0.90. We applied this criterion across all reporting years. On average, 86% of genetic samples assigned at 0.90 or greater.

3.6.3.1.1 Unmarked Chinook

In 2020, a substantial amount of Chinook salmon was collected at Ilwaco Slough which is typically a site with low Chinook catches. The entirety of the Chinook catch was unmarked, and the majority were West Cascade fall with a few Spring Creek Group. The trend for West Cascade fall stock to predominate unmarked catches at Ilwaco and at Welch and Whites Islands in Reaches B and C was maintained in February and March of 2020. This trend has persisted since 2010 and 2012 when Whites and Welch Islands were first sampled by this study (Figure 155). The diversity of stocks represented in unmarked fish at Campbell Slough was less in 2020 and was limited to West Cascade fall and Spring Creek group. This uncharacteristic lack of stock diversity is likely due to the limited sampling that occurred in 2020. The February-March timeframe is usually too early in the season for other stocks we typically see at Campbell (i.e., upper Columbia summer/fall, Snake River fall, and Deschutes River fall) to be present. The greatest diversity of unmarked Chinook in Feb-Mar 2020 occurred at Franz Lake where four stock groups were represented. The largest number of unmarked Chinook were yearling-sized mid and upper Columbia River spring stock. Subyearling-sized West Cascade fall, Spring Creek Group, and upper Columbia summer/fall were also present at Franz Lake.

3.6.3.1.2 Marked Chinook

Only two marked Chinook salmon were collected in February-March 2020; one each at Welch and Whites Island. A yearling-sized West Cascade fall Chinook was collected at Whites Island and a yearling-sized Willamette River spring Chinook was collected at Welch Island. No marked Chinook were collected at Ilwaco, Campbell, or Franz (Figure 155).

3.6.3.1.3 Seasonal Trends

We cannot address trends across the entirety of the 2020 season, but we can examine how the February-March catches of 2020 compared to previous February-March catches (Figure 156). As observed in previous years, West Cascade fall stock was the predominant stock during February and March. This is a typical pattern that is indicative of the almost constant presence of West Cascade fall in the lower Columbia River and estuary. A few Spring Creek group were present which is also in keeping with historical trends. New for 2020 was the number of mid and upper Columbia River spring Chinook that were observed at Franz Lake in February. Previously this stock had been seen rarely at EMP trend sites; showing up in marked Chinook at Campbell Slough in 2019 and an unmarked fish at Whites Island in 2011.

Data from 2020 was added to the non-parametric analysis of genetic stock composition at the five trend sites. A non-parametric multidimensional scaling (nMDS) and an analysis of similarity (ANOSIM) were performed using Primer-e version 7 (Clarke and Warwick 1994, Clarke and Gorley 2006). These analyses

look for similarities and differences in the community structure (in this case genetic stock composition) at our five sites. ANOSIM analysis indicates a significant difference in stock composition among sites (global $R = 0.328$, $P = 0.001$). Pairwise tests indicate significant dissimilarities between all sites and Campbell Slough and all sites and Franz Lake. Stock composition at Welch and Whites Islands is not dissimilar ($P = 0.72$). In previous years Franz and Ilwaco were also not dissimilar, but with the increased sample size at Ilwaco in 2020 and increase stock diversity at Franz, these two sites became significantly dissimilar ($P = 0.05$). Again, we must note that these differences are based on 2020 data from February-March only. Had we sampled a full season the strong trends early in the year may have been diminished by later-season trends. The nMDS plot (Figure 157) shows high overlap between Welch and Whites Islands and greater separation of Campbell and Franz, as indicated by ANOSIM. Ilwaco has few data points that are highly dispersed indicating no clear pattern of stock composition.

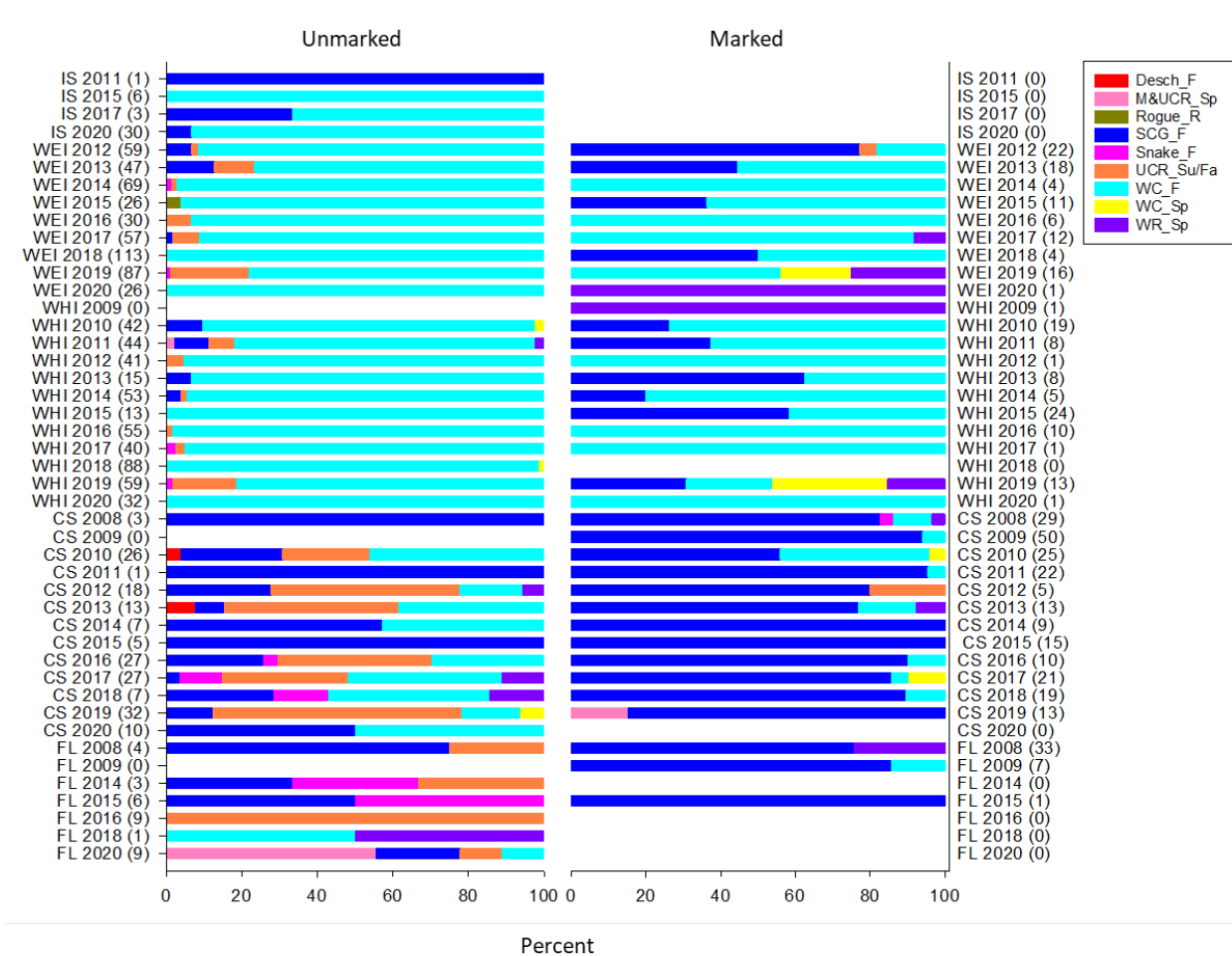


Figure 155. Genetic stock composition of unmarked (left column) and marked (right column) Chinook Salmon at trend sites from 2008–2020. Genetic sample sizes (probability ≥ 0.90) for each site are presented in parentheses. IS = Ilwaco Slough, WEI = Welch Island, WHI = Whites Island, CS = Campbell Slough, FL = Franz Lake. Chinook salmon stocks: Desch_F = Deschutes River fall, M&UCR_Sp = mid and upper Columbia River spring, Rogue_R = Rogue River, SCG_F = Spring Creek Group fall, Snake_F = Snake River fall, Snake_Sp/Su = Snake River spring/summer, UCR_Su/Fa = Upper Columbia River summer/fall, WC_F = West Cascade fall, WC_Sp = West Cascade spring, WR_Sp = Willamette River Spring.

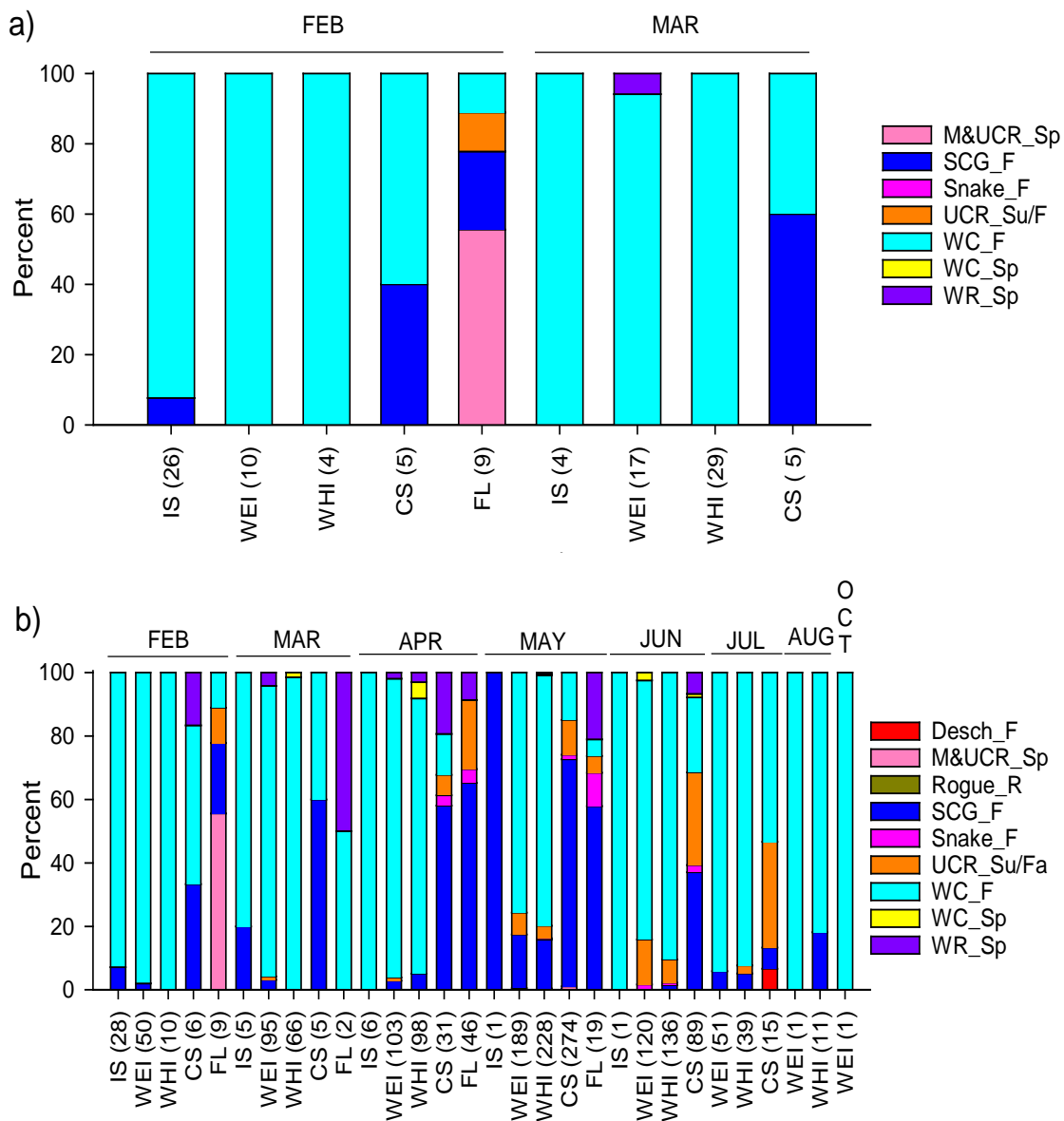


Figure 156. Seasonal percent stock composition per site for Chinook Salmon collected in a) 2020 and b) 2008–2020. Note that only February and March were sampled in 2020. Plots include both unmarked and marked Chinook Salmon. Genetic sample sizes for each site are presented in parentheses. IS = Ilwaco Slough, WEI = Welch Island, WHI = Whites Island, CS = Campbell Slough, FL = Franz Lake. Chinook salmon stocks: Desch_F = Deschutes River fall, M&UCR_Sp = mid and upper Columbia River spring, Rogue_R = Rogue River, SCG_F = Spring Creek Group fall, Snake_F = Snake River fall, UCR_Su/Fa = Upper Columbia River summer/fall, WC_F = West Cascade fall, WC_Sp = West Cascade spring, WR_Sp = Willamette River Spring.

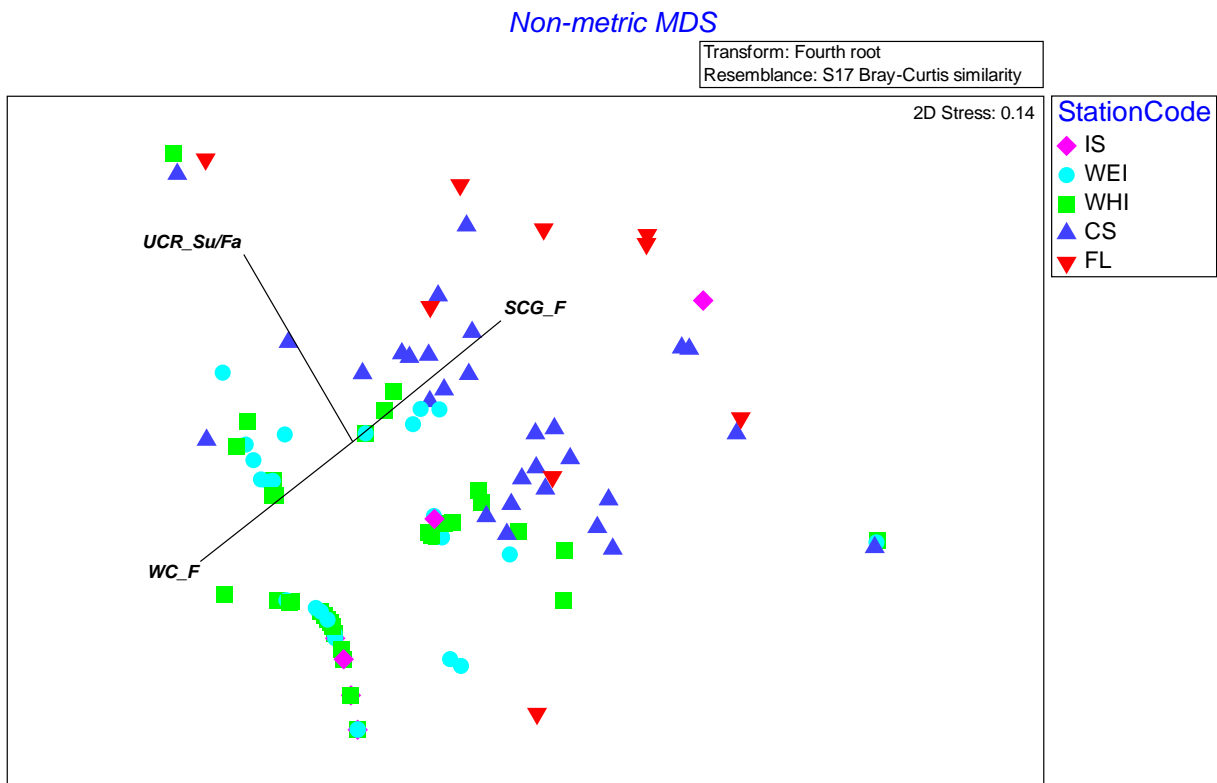


Figure 157. Nonmetric multidimensional scaling (NMDS) plot based on fourth-root transformed genetic stock abundance at five trend sites, 2008-2020. Significant correlation with genetic stock (Pearson $R > 0.5$) are represented as black vectors. IS = Ilwaco Slough, WEI = Welch Island, WHI = Whites Island, CS = Campbell Slough, FL = Franz Lake. SCG_F = Spring Creek Group fall, UCR_Su/Fa = Upper Columbia River summer/fall, WC_F = West Cascade fall.

3.6.3.2 *Salmon Size and Condition*

Chinook salmon

Length, weight, and condition factor

As stated previously, NOAA safety protocols associated with the COVID-19 pandemic limited the fish sampling at all trend sites in 2020 to February and March for Ilwaco Slough, Welch Island, White Islands and Campbell Slough and only February for Franz Lake. In 2021, fish community sampling was able to resume for the five trend sites and was conducted March - June and November, with the exception of June for Campbell Slough when water temperatures were too high for handling fish. Data for this section of the report includes 2020–2021, however the results will focus on 2021 data unless specified. A more comprehensive overview of annual trends, including 2020 data is presented in the discussion in Section 4.6.

Chinook salmon were caught at all sampled locations except Ilwaco Slough in 2021. In 2021, the average length, weight and condition factor for unmarked Chinook captured at Welch Island, Whites Island, Campbell Slough and Franz Lake are presented in Table 43. No average length, weight and condition

factor was calculated for Ilwaco due to no Chinook being sampled. The length, weight, and condition of unmarked Chinook salmon in 2021 showed similar patterns to previous years, with the largest fish typically captured at Campbell Slough (Figure 158). Within sites, there was some variation among years, though no clear increasing or decreasing trends. Unmarked Chinook sampled at Whites Island in 2021 appeared to have a slightly larger average weight than seen in 2018 and 2019. However, the condition appears to follow the overall trend on Whites Island over the past 5 years. Unmarked Chinook sampled at Welch Island in 2021, had a larger average fork length, weight and condition similar to the 2019 sample. However, this is likely due to no June sampling at Welch Island in 2018 and 2017, which would have likely contributed to the decreased averages of all measured indices.

In 2021, marked Chinook salmon were caught at three of the five sampled locations. Welch Island, Whites Island and Campbell Slough experienced significant enough catches to examine marked Chinook size and condition. The average length, weight and condition factor for marked Chinook captured are presented in Table 43. Campbell Slough shows little variation in length, weight, and condition across the past three sampled years (Figure 158-Figure 177). Similar to unmarked Chinook sampled at Welch Island in 2019, marked Chinook size, weight and condition were all greater than previous seen in last 8 sampling seasons (Figure 158-Figure 177).

Table 43: Average length, weight and Fulton's Index (k) for unmarked and marked chinook in 2019

Site	Length (mm)	SD	Weight (g)	SD	Fulton's Index	SD
Welch Island						
<i>Unmarked</i>	54.7	1.64	2.21	0.30	1.02	0.03
<i>Marked</i>	85.2	1.70	6.8	0.64	1.09	0.02
Whites Island						
<i>Unmarked</i>	55.90	1.00	2.10	0.12	1.03	0.05
<i>Marked</i>	80.40	2.06	5.52	0.68	1.04	0.04
Campbell Slough						
<i>Unmarked</i>	68.04	4.61	5.20	1.30	1.16	0.05
<i>Marked</i>	82.00	1.66	6.12	0.35	1.09	0.04
Franz Lake						
<i>Unmarked</i>	47.20	0.61	0.77	0.04	0.90	0.02

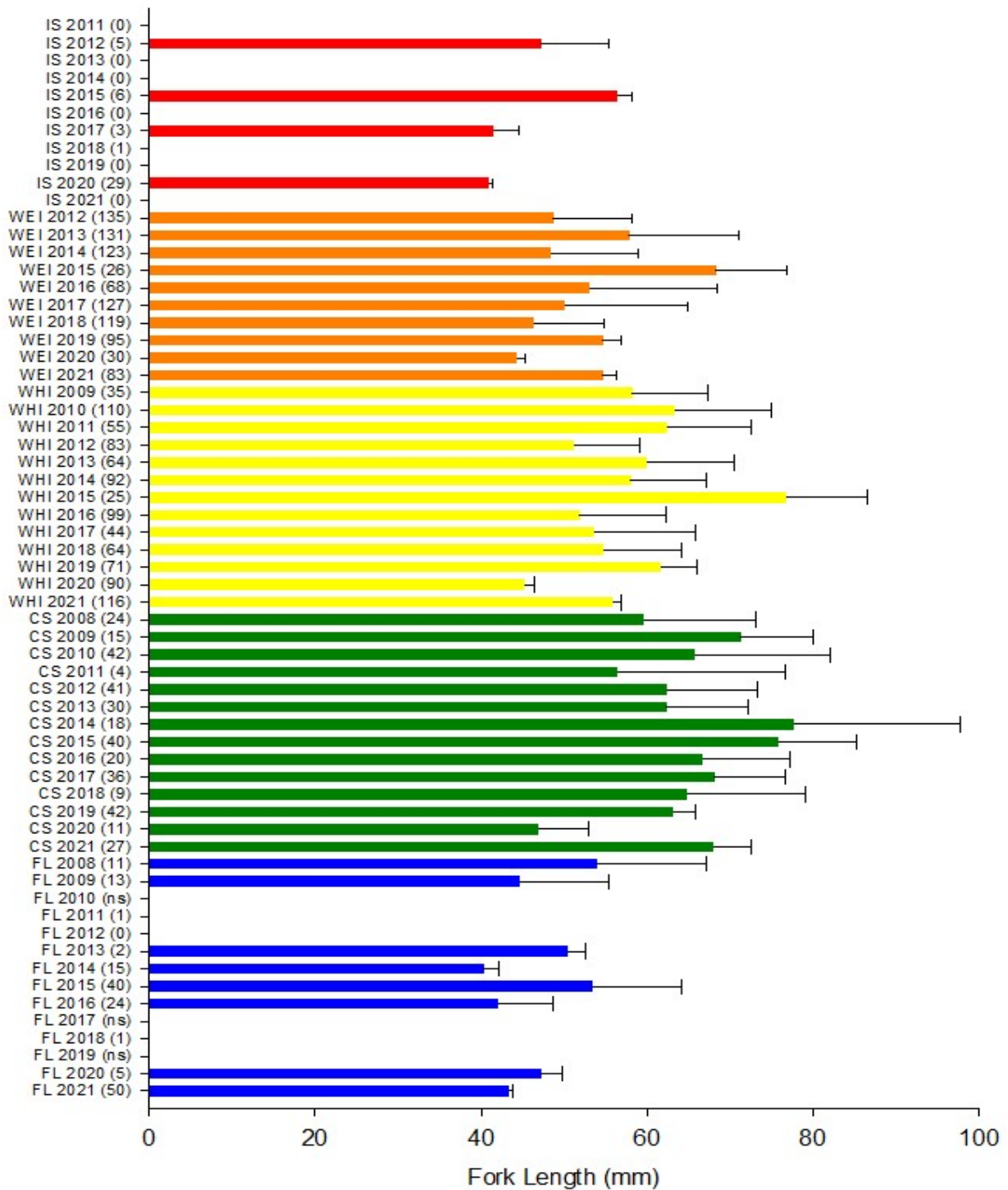


Figure 158. Mean (SD) length (mm) of unmarked juvenile Chinook salmon at trends sites in 2021 as compared to previous years. Total number of Chinook salmon weighed and/or measured per year at a site are presented in parentheses. IS = Ilwaco Slough; WEI = Welch Island, WHI = Whites Island, CS = Campbell Slough, FL = Franz Lake.

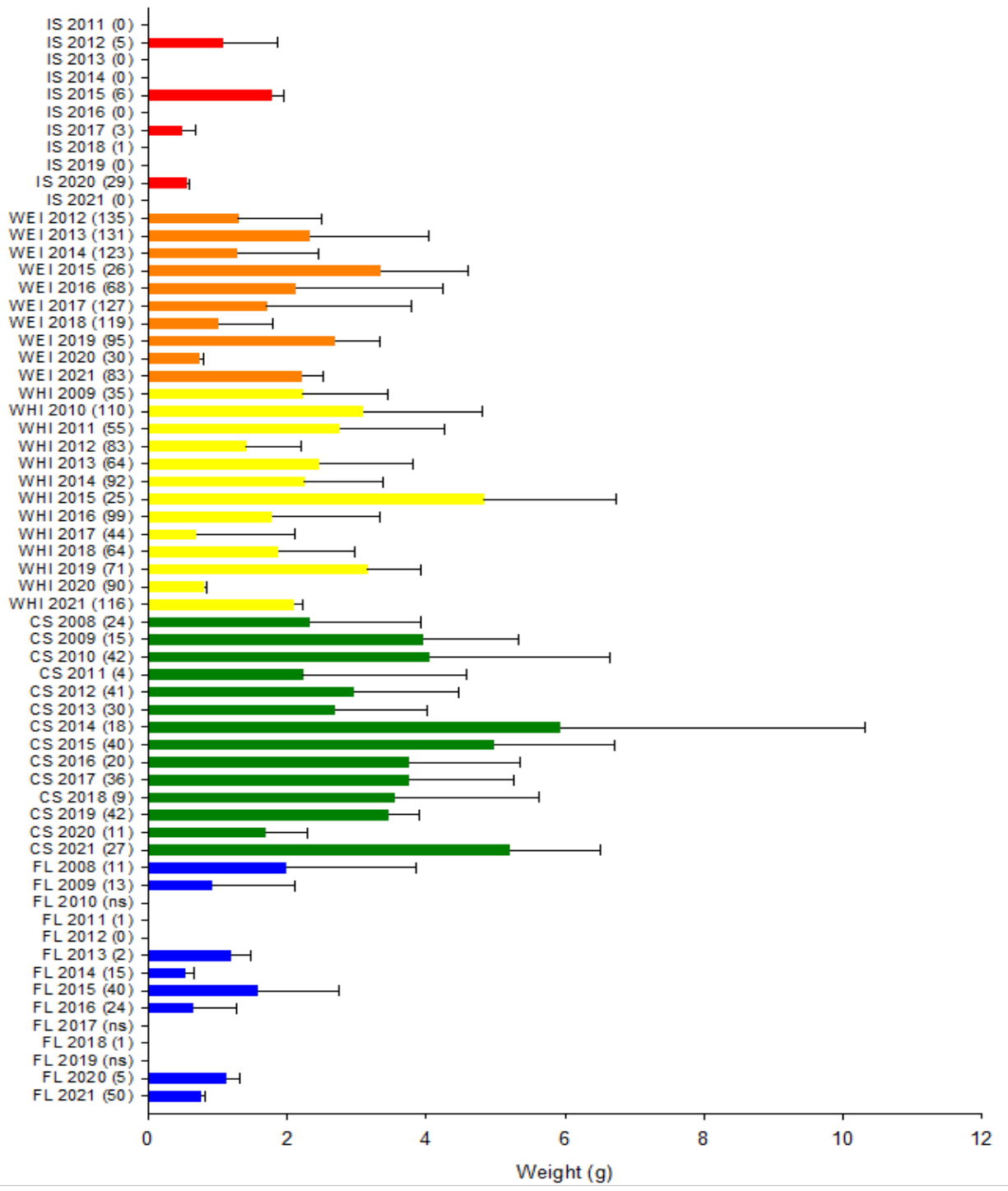


Figure 159: Mean (SD) weight (g) of unmarked juvenile Chinook salmon at trends sites in 2021 as compared to previous years. Total number of Chinook salmon weighed and/or measured per year at a site are presented in parentheses. IS = Ilwaco Slough; WEI = Welch Island, WHI = Whites Island, CS = Campbell Slough, FL = Franz Lake.

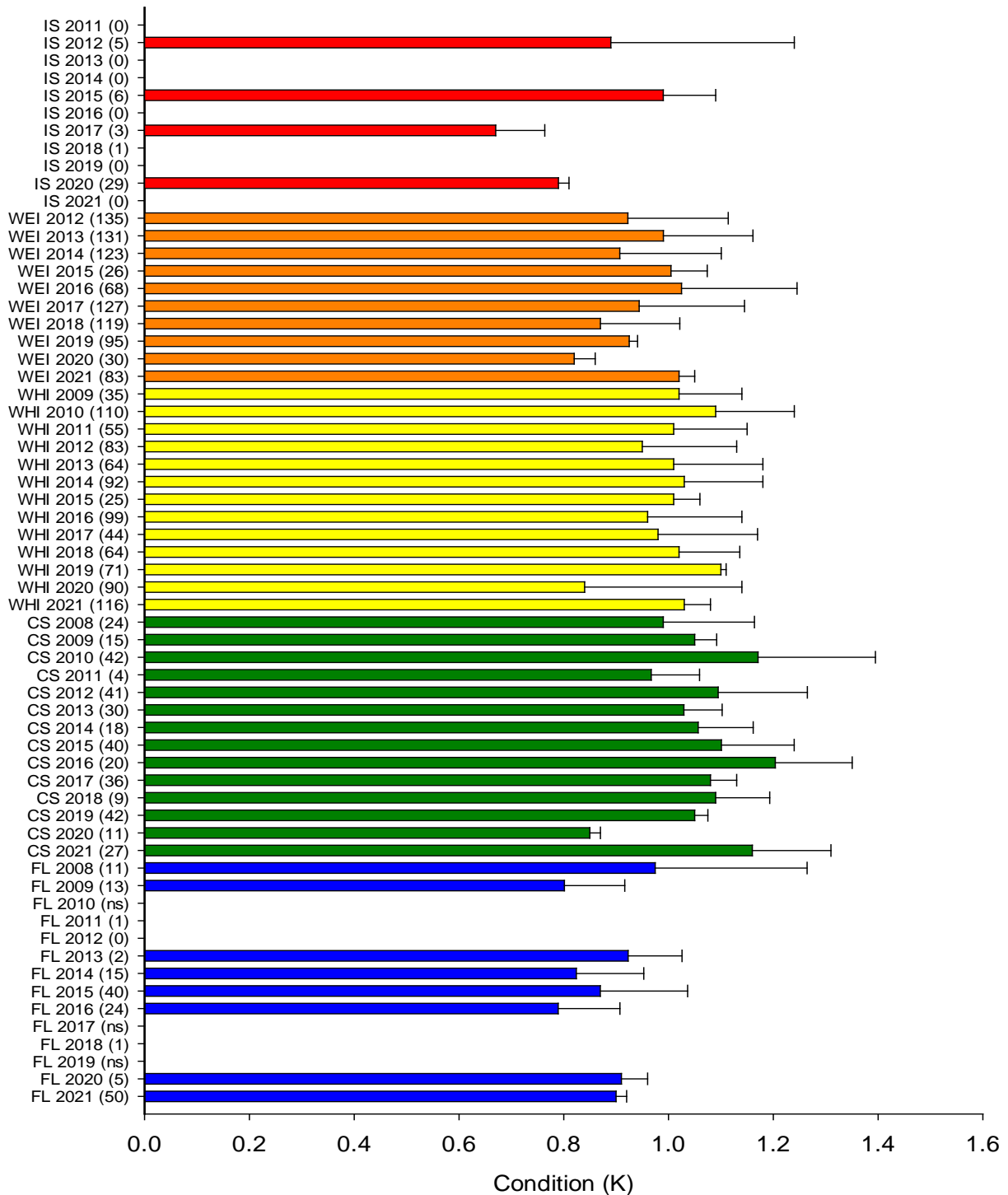


Figure 160. Mean (SD) condition factor of unmarked juvenile Chinook salmon at trends sites in 2021 as compared to previous years. Total number of Chinook salmon weighed and/or measured per year at a site are presented in parentheses. IS = Ilwaco Slough; WEI = Welch Island, WHI = Whites Island, CS = Campbell Slough, FL = Franz Lake.

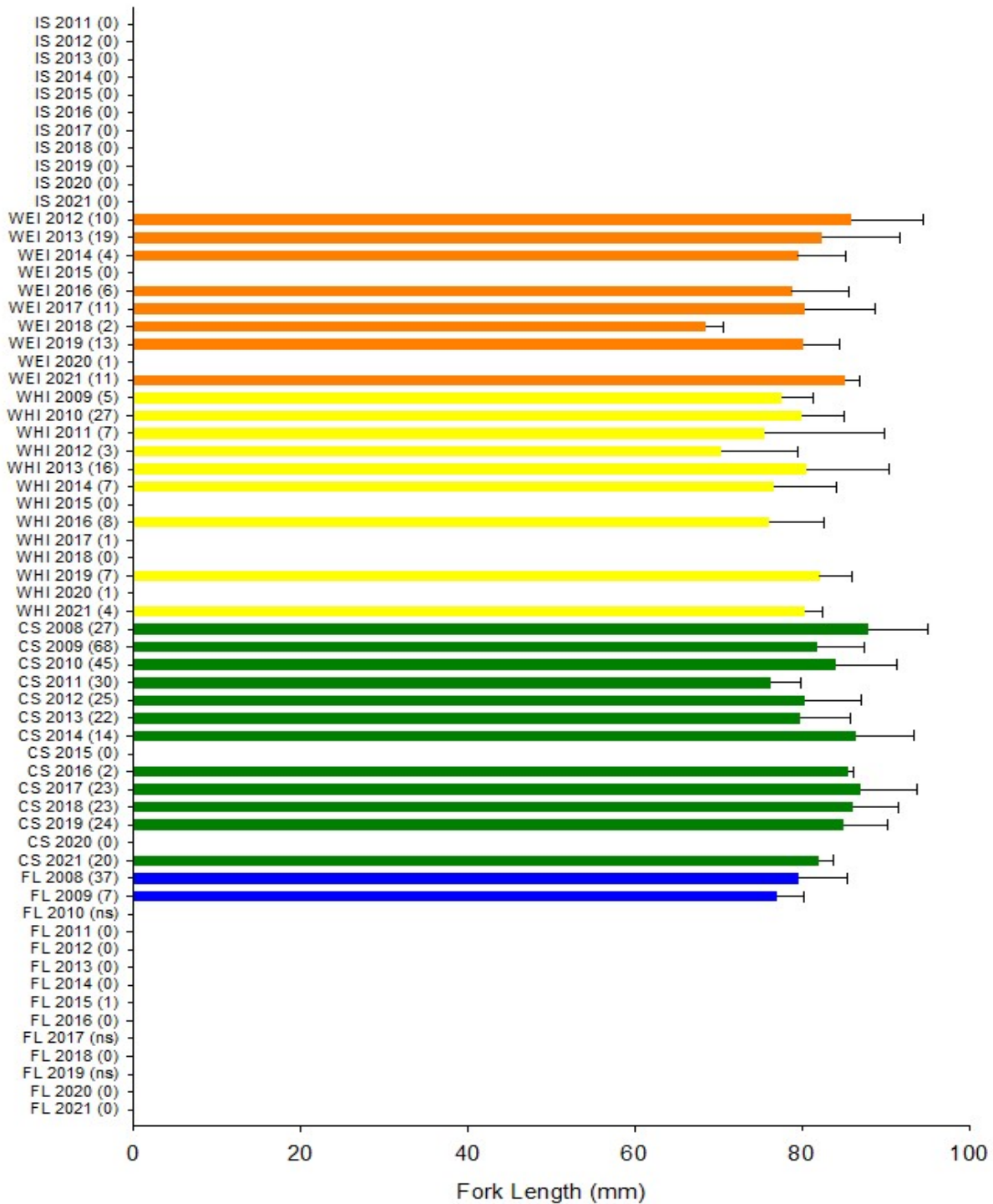


Figure 161. Mean (SD) length (mm) of marked Chinook salmon at trends sites in 2021 as compared to previous years. Total number of Chinook salmon weighed and/or measured per year at a site are presented in parentheses. IS = Ilwaco Slough; WEI = Welch Island, WHI = Whites Island, CS = Campbell Slough, FL = Franz Lake.

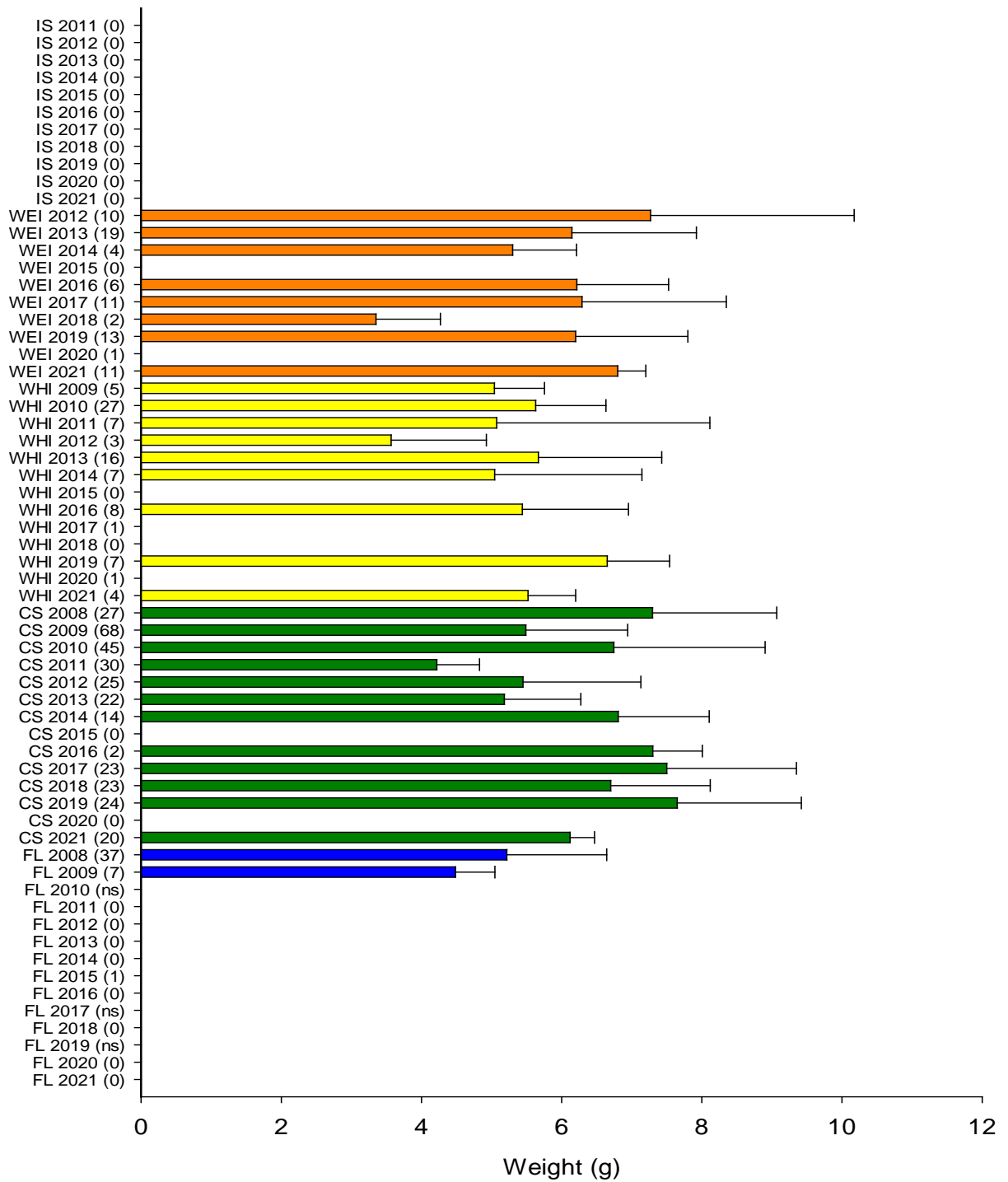


Figure 162. Mean (SD) weight (g) of marked Chinook salmon at trends sites in 2021 as compared to previous years. Total number of Chinook salmon weighed and/or measured per year at a site are presented in parentheses. IS = Ilwaco Slough; WEI = Welch Island, WHI = Whites Island, CS = Campbell Slough, FL = Franz Lake.

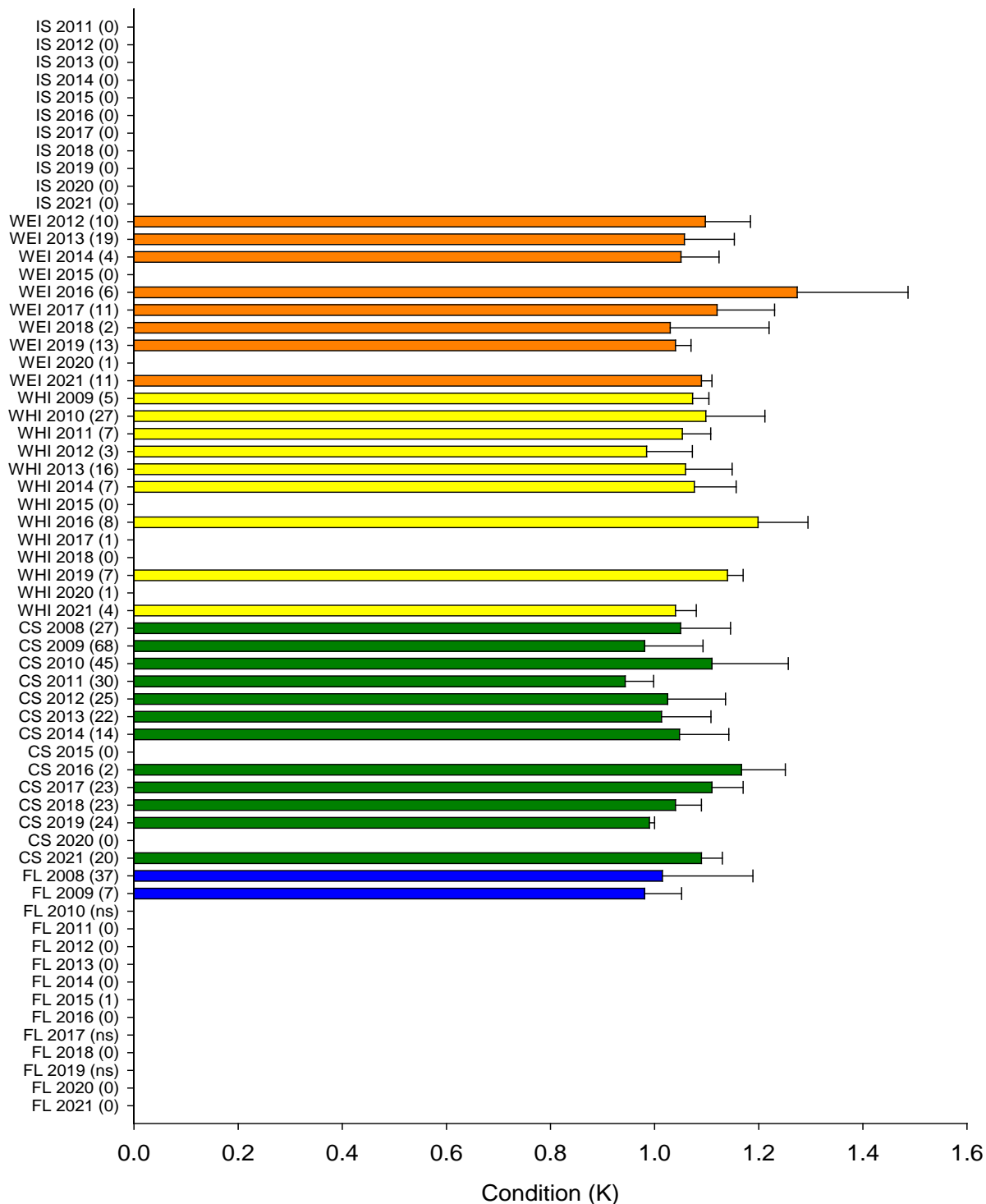


Figure 163 Mean (SD) condition factor of marked Chinook salmon at trends sites in 2021 as compared to previous years. Total number of Chinook salmon weighed and/or measured per year at a site are presented in parentheses. IS = Ilwaco Slough; WEI = Welch Island, WHI = Whites Island, CS = Campbell Slough, FL = Franz Lake.

Life History

At the trend sites in 2021, the majority (74%) of unmarked Chinook salmon were fry, 25% were fingerlings, and 1% were yearlings (Figure 164). Fry were the dominate group caught at all sites in 2021. Campbell Slough and Whites Island showed a slightly more even distribution of fry and fingerling of unmarked Chinook salmon. In comparison to previous years, the percentage of fry at all of the trend sites was slightly higher than in recent years.

A total of 47 (91%) marked Chinook salmon caught at the trends sites in 2021 were fingerlings (Figure 165). In comparison to previous sampling years, the proportion of yearlings encountered in 2021 was slightly lower. This does appear to differ from the overall trend; however, sample size is relatively low. Similar to all previous years, no marked Chinook fry were observed in 2021 at any of the sampled locations.

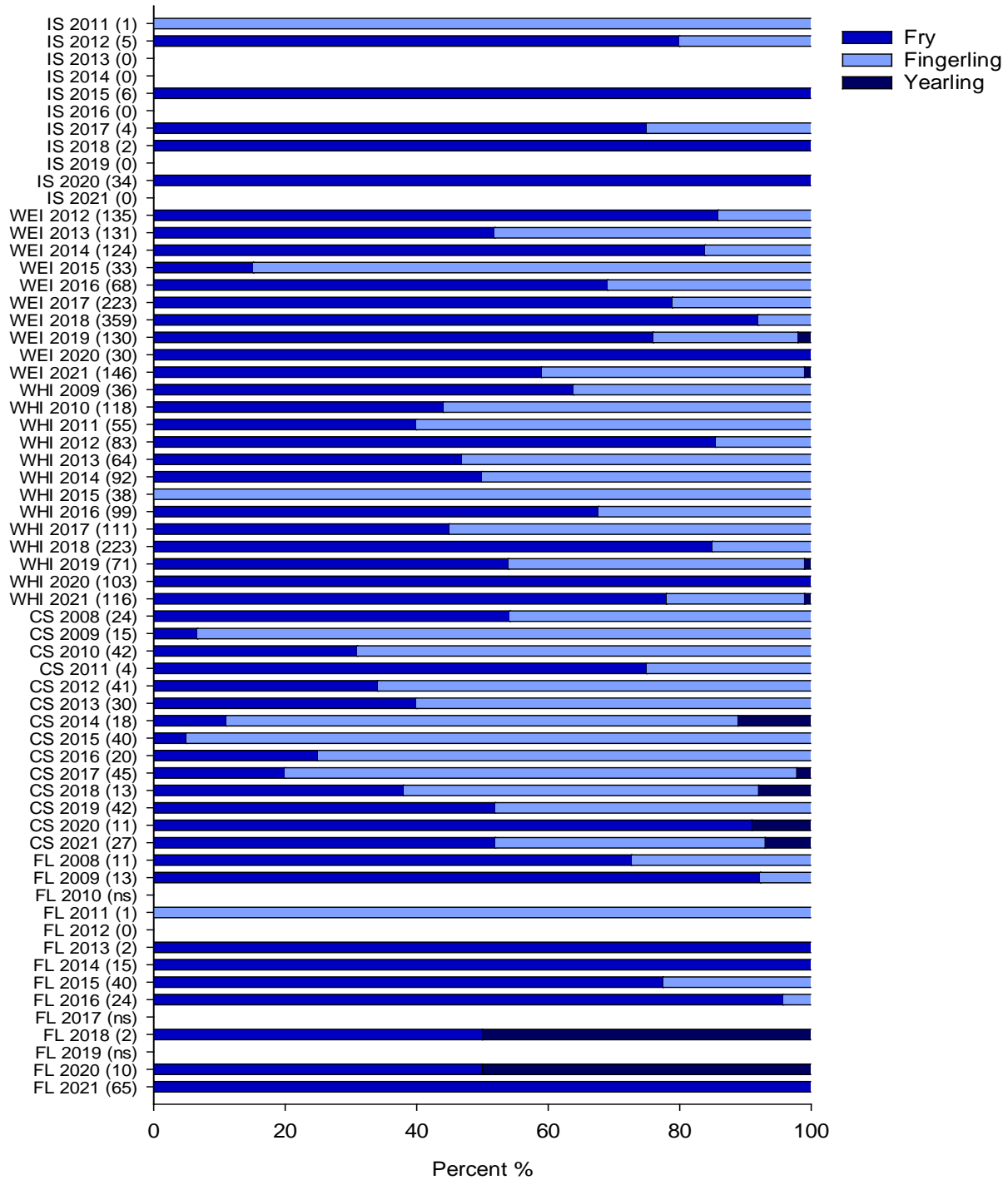


Figure 164. Percentages of life history types of unmarked juvenile Chinook salmon captured at trends sites in 2021 and in previous sampling years. Total numbers of Chinook salmon captured per year at a site are presented in parentheses. IS = Ilwaco Slough; WEI = Welch Island, WHI = Whites Island, CS = Campbell Slough, FL = Franz Lake.

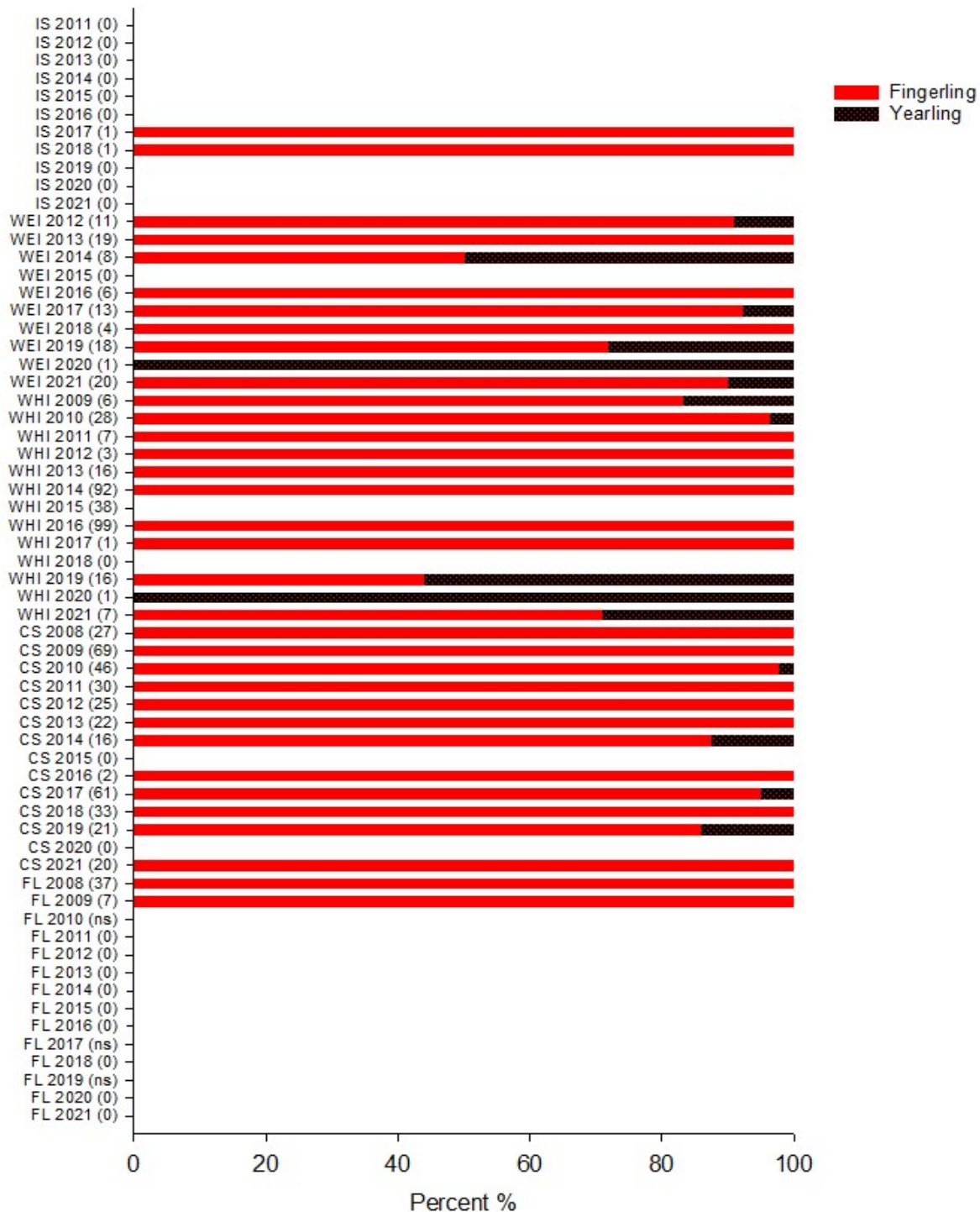


Figure 165. Percentages of life history types of marked juvenile Chinook salmon captured at trends sites in 2021 and in previous sampling years. Total numbers of Chinook salmon captured per year at a site are presented in parentheses. IS = Ilwaco Slough; WEI = Welch Island, WHI = Whites Island, CS = Campbell Slough, FL = Franz Lake.

Other salmon species

Chum salmon

A total of 79 chum salmon were captured in 2021, 58 at Whites Island, 13 at Welch Island and 1 at Campbell Slough. All Chum were caught between March and May. In 2021 the average length, weight, and condition factor of chum salmon captured were as follows: Welch Island 62.03 ± 1.96 mm, 2.27 ± 0.24 g, and 0.88 ± 0.03 ; Whites Island 52.01 ± 1.30 mm, 1.23 ± 0.09 g, and 0.83 ± 0.03 (Figure 166-Figure 174). Only 1 chum was collected at Campbell Slough in 2021. The chum salmon collected in 2021 were comparable in size to those that have been collected in previous years. Welch Island did see an overall increase in all three indices; however, this could be due to low sample size. Similarly, the mean 2021 value for condition factor was intermediate, between a high of 1.10 in 2008 and a low of 0.58 in 2013—noting that 2018 and 2019 had very low sample sizes due to no weights taken in the field at Ilwaco Slough where the majority of chum salmon are caught each year. The largest fish, in terms of length and weight, are generally found at Whites Island and Campbell Slough, and condition factor tended to be highest at Campbell Slough. This site is located second farthest upstream of all currently sampled sites. Although chum salmon were captured sporadically, some variation by year is found at Ilwaco Slough, Welch Island, and Whites Island (Franz Lake is not considered in this comparison, as no chum salmon have been captured at the site since 2009).

Coho Salmon

Only two coho salmon were caught in 2021, both unmarked coho were captured at Campbell Slough in November. Franz Lake is the only site where coho salmon have been caught consistently enough to compare size measurements by sampling year. However, low sampling efforts in 2017, 2018 and no sampling in 2019 have made it difficult to determine any recent trends in coho at Franz Lake. No coho were caught at Franz in 2021 despite an increased effort due to favorable condition. Overall size and condition of unmarked and marked coho sampled at Franz Lake are shown below in Figure 166-Figure 174.

Sockeye salmon

Sockeye salmon and trout were not caught at any of the trends sites in 2021. Sockeye salmon were last sampled at Welch Island in 2014 and trout were last caught at Franz Lake in 2020.

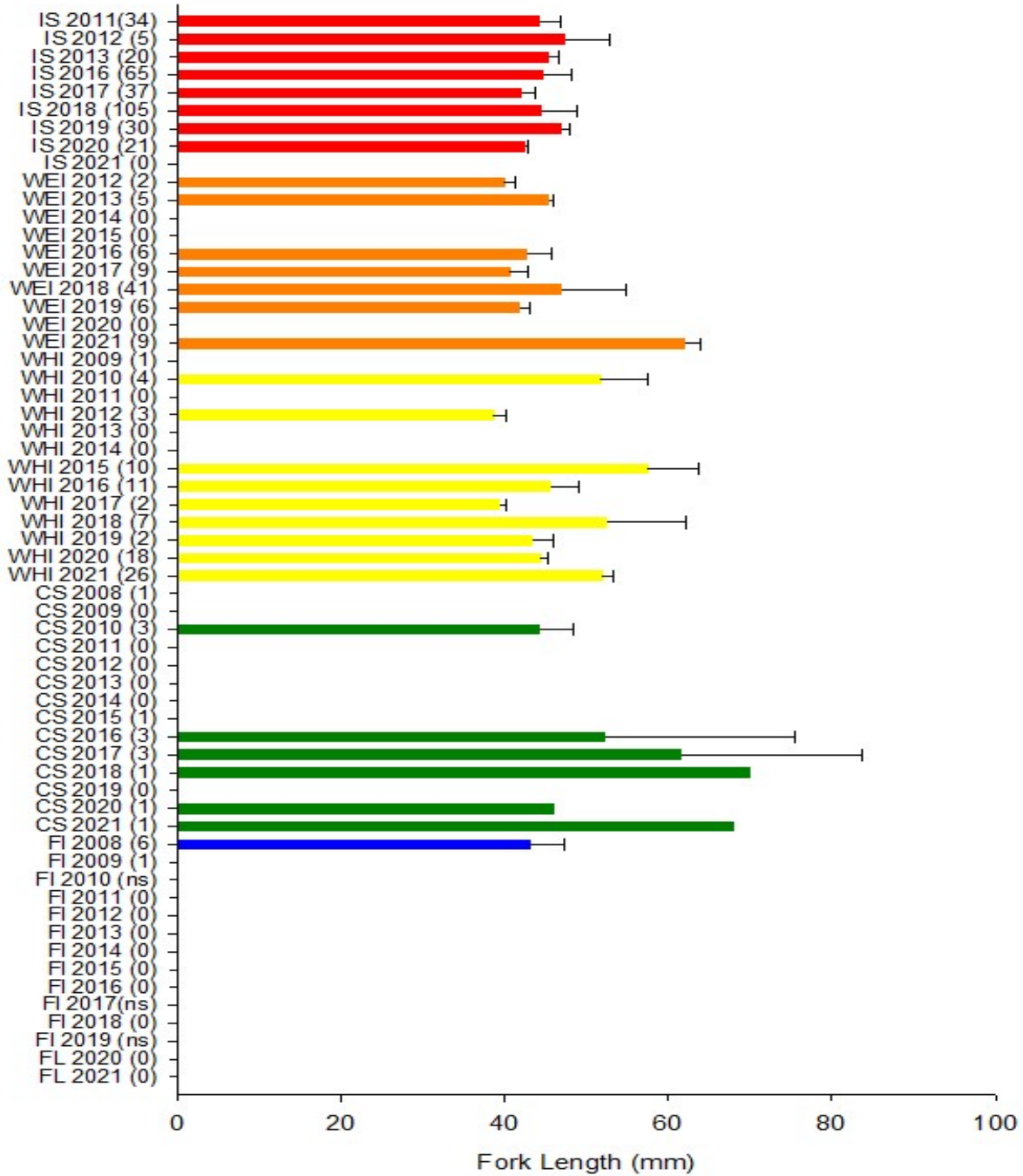


Figure 166. Mean (SD) length (mm) of chum salmon at trends sites in 2021 compared to previous sampling years. Total number of chum salmon weighed and/or measured per year at a site are presented in parentheses. IS = Ilwaco Slough; WEI = Welch Island, WHI = Whites Island, CS = Campbell Slough, FL = Franz Lake.

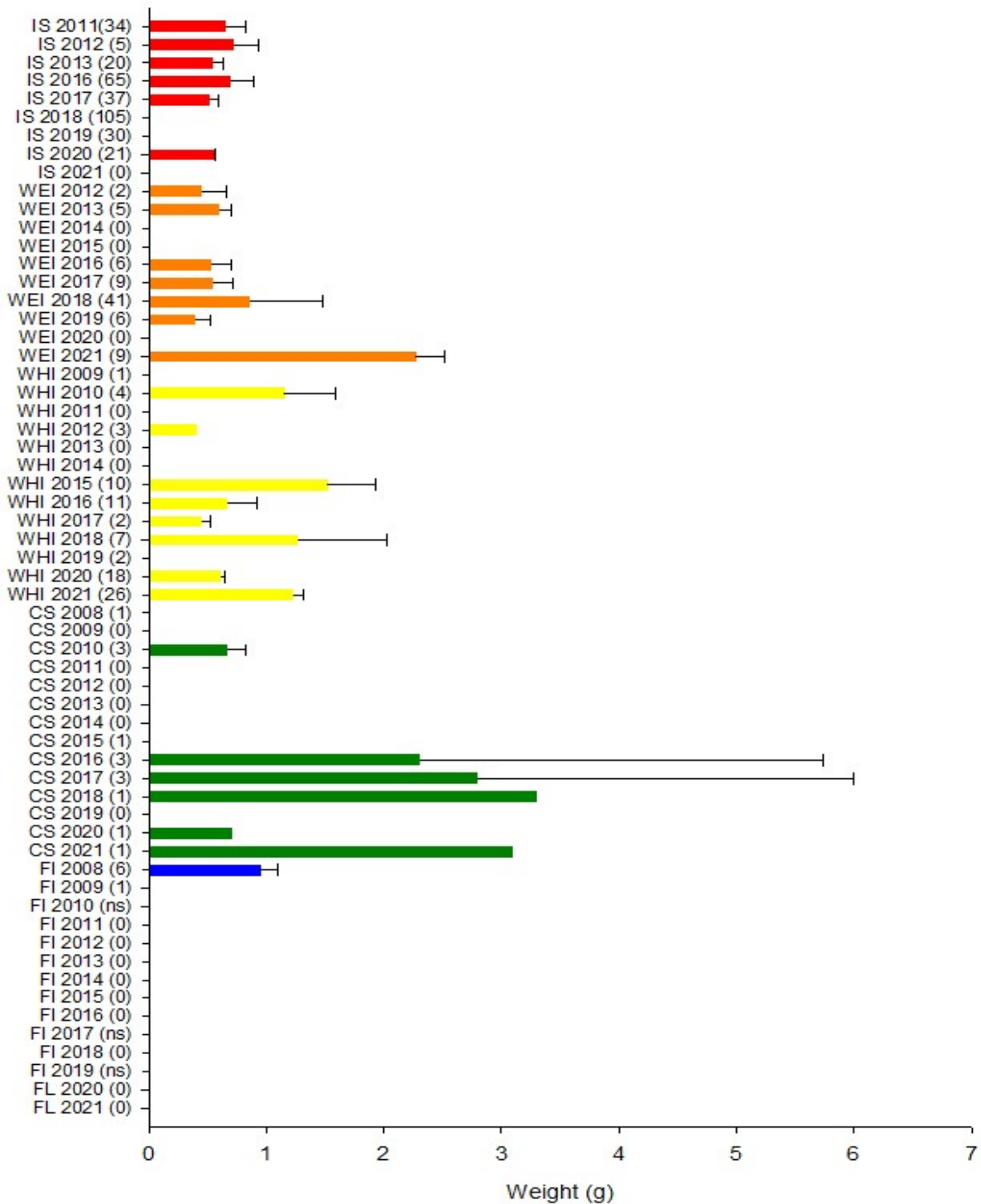


Figure 167 Mean (SD) weight (g) of chum salmon at trends sites in 2021 compared to previous sampling years Total number of chum salmon weighed and/or measured per year at a site are presented in parentheses. IS = Ilwaco Slough; WEI = Welch Island, WHI = Whites Island, CS = Campbell Slough, FL = Franz Lake.

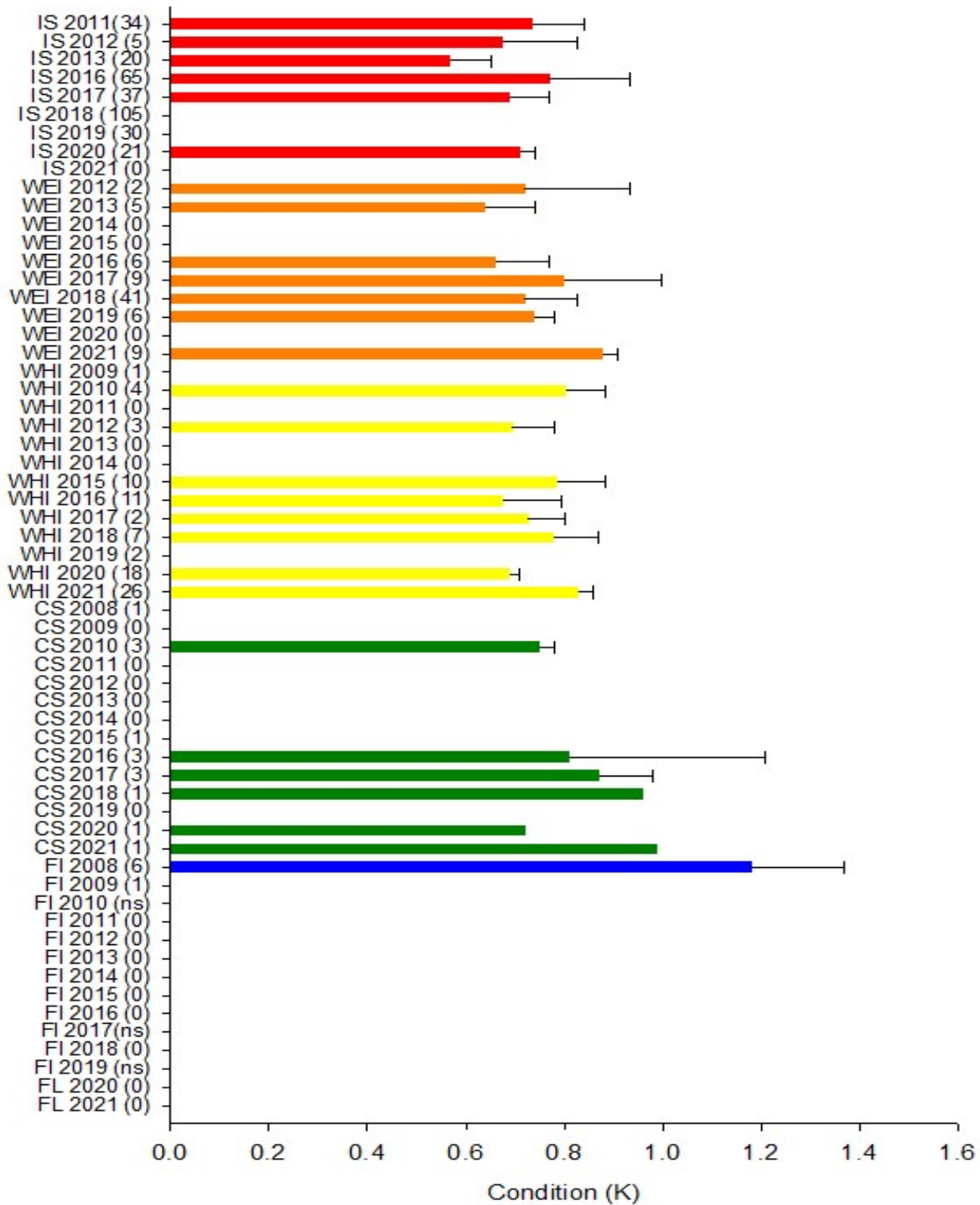


Figure 168. Mean (SD) condition factor (k) of chum salmon at trends sites in 2021 compared to previous sampling years. Total number of chum salmon used per year at a site are presented in parentheses. IS = Ilwaco Slough; WEI = Welch Island, WHI = Whites Island, CS = Campbell Slough, FL = Franz Lake.

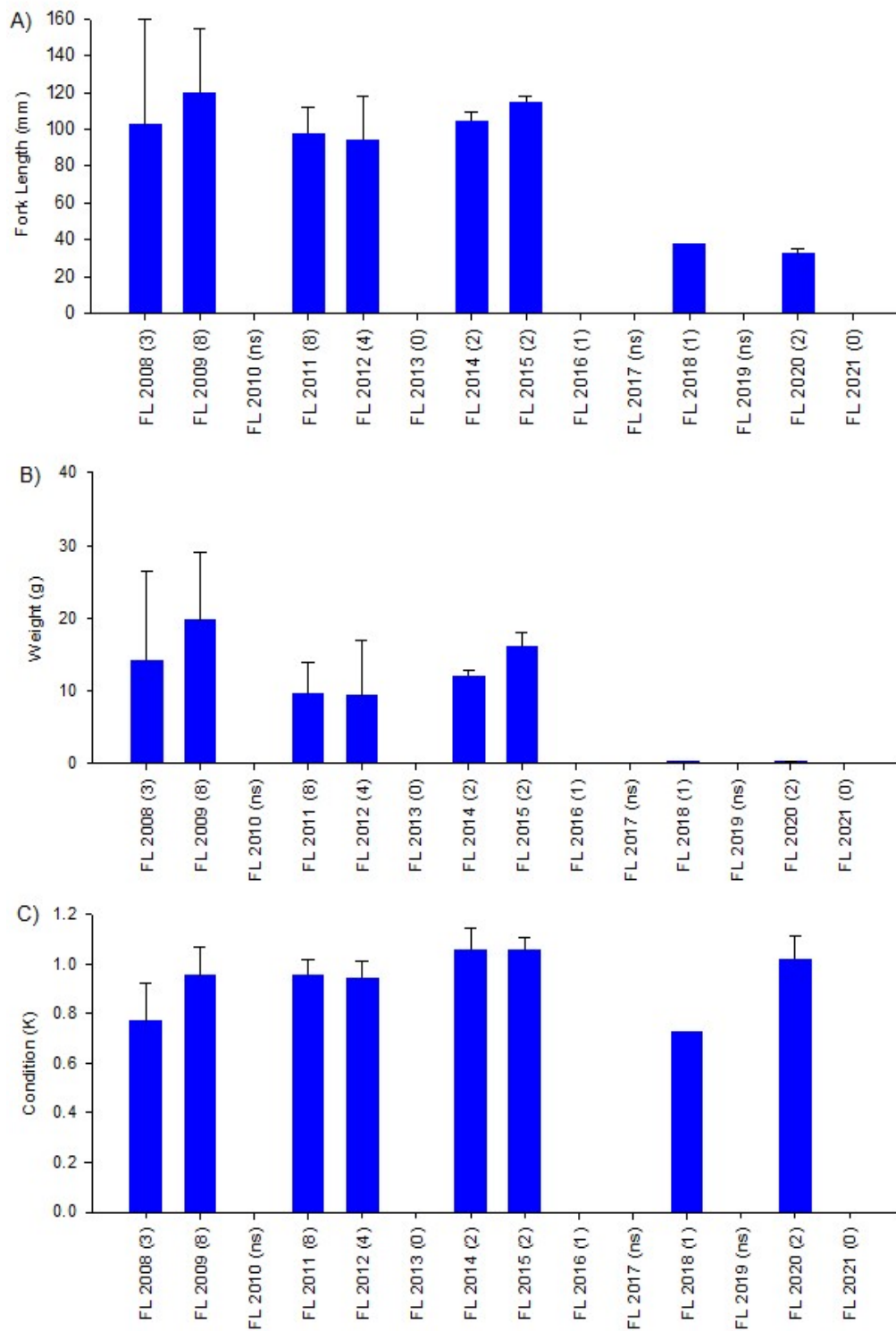


Figure 169 Mean (SD) a) length (mm), b) weight (g), and c) condition factor of unmarked coho salmon at Franz Lake by sampling year. Total number of coho salmon captured at Franz Lake per year are presented in parentheses.

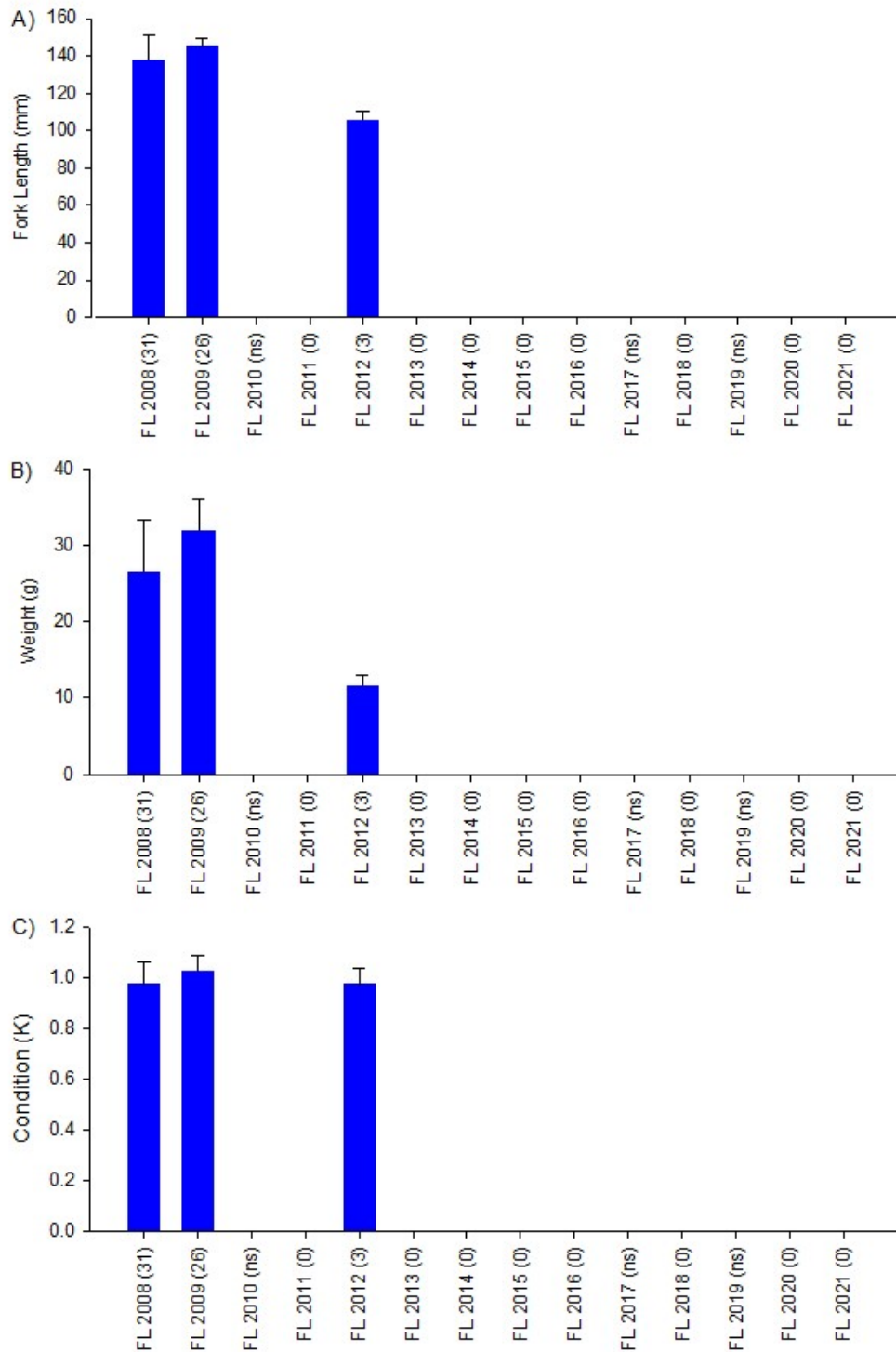


Figure 170.. Mean (SD) a) length (mm), b) weight (g), and c) condition factor of marked coho salmon at Franz Lake by sampling year. Total number of coho salmon captured at Franz Lake per year are presented in parentheses.

3.6.3.3 Somatic Growth Analyses

Otolith analyses for fish collected in 2019-2021 has not been completed due to mandatory closures of the NWFSC laboratories during the COVID-19 pandemic. Otoliths are used to estimate somatic growth rates in fish. Patterns in somatic growth rate can represent variations in growth in response to genetic stocks or environmental conditions. Previous analyses of otolith data find that somatic growth rate in Chinook salmon ranged from 0.31 to 0.87 mm/day with an average of 0.54 mm/day (Chittaro et al. 2018). These analyses included sites representing mainstem and off-channel habitats that have been sampled as part of the Ecosystem Monitoring Program from 2005–2018. In 2018 we ran separate analyses for mainstem and off-channel habitat to better align with the reporting of trend site data. Sample sizes were large enough at Welch, Whites, and Campbell sites to accommodate site-specific analyses. Specific years used in each analysis is provided below. See Chittaro et al. 2018 for locations of non-trend site sampling locations.

Main stem: Fish (n=100) collected in main stem habitat were obtained across several years (2005, 2008, 2013) and sites (Beaver, Columbia city, confluence, Point Adams, & Warrendale). Our GLM analysis indicated that the model that best explained variability in growth rate (mm/day) only included discharge. Specifically, we detected a significant ($p < 0.05$) negative relationship between growth rate and discharge (Figure 171-Figure 175).

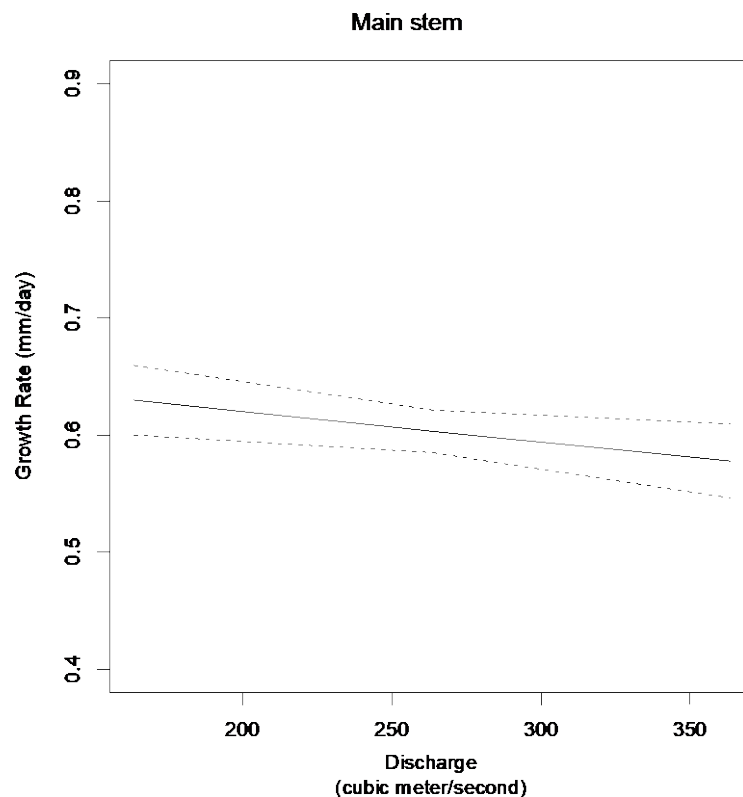


Figure 171. Relationship between growth rate and discharge for juvenile Chinook Salmon collected at mainstem Columbia River sites, 2005, 2008, and 2013.

Off-channel: Fish (n=652) collected in off-channel habitat were obtained across several years (2007-2014, 2016-2018) and sites (Beacon, Bradwood, Burke, Campbell, Deer, Franz, Goat, Jackson, Lemon, Lord/Walker, Mirror Lake 1 & 4, Pierce, Ryan, Sand, Secret, Wallace, Washougal, Welch, & Whites). Our GLM analysis indicated that the model that best explained variability in growth rate (mm/day) included year, river kilometer, stock, hatchery/unmarked, and fork length. Specifically, we observed a significant ($p < 0.01$) (curvilinear) positive relationship to river km and fork length. Also, fish collected in 2007 had significantly faster growth than those from 2011 and 2014 (Figure 172).

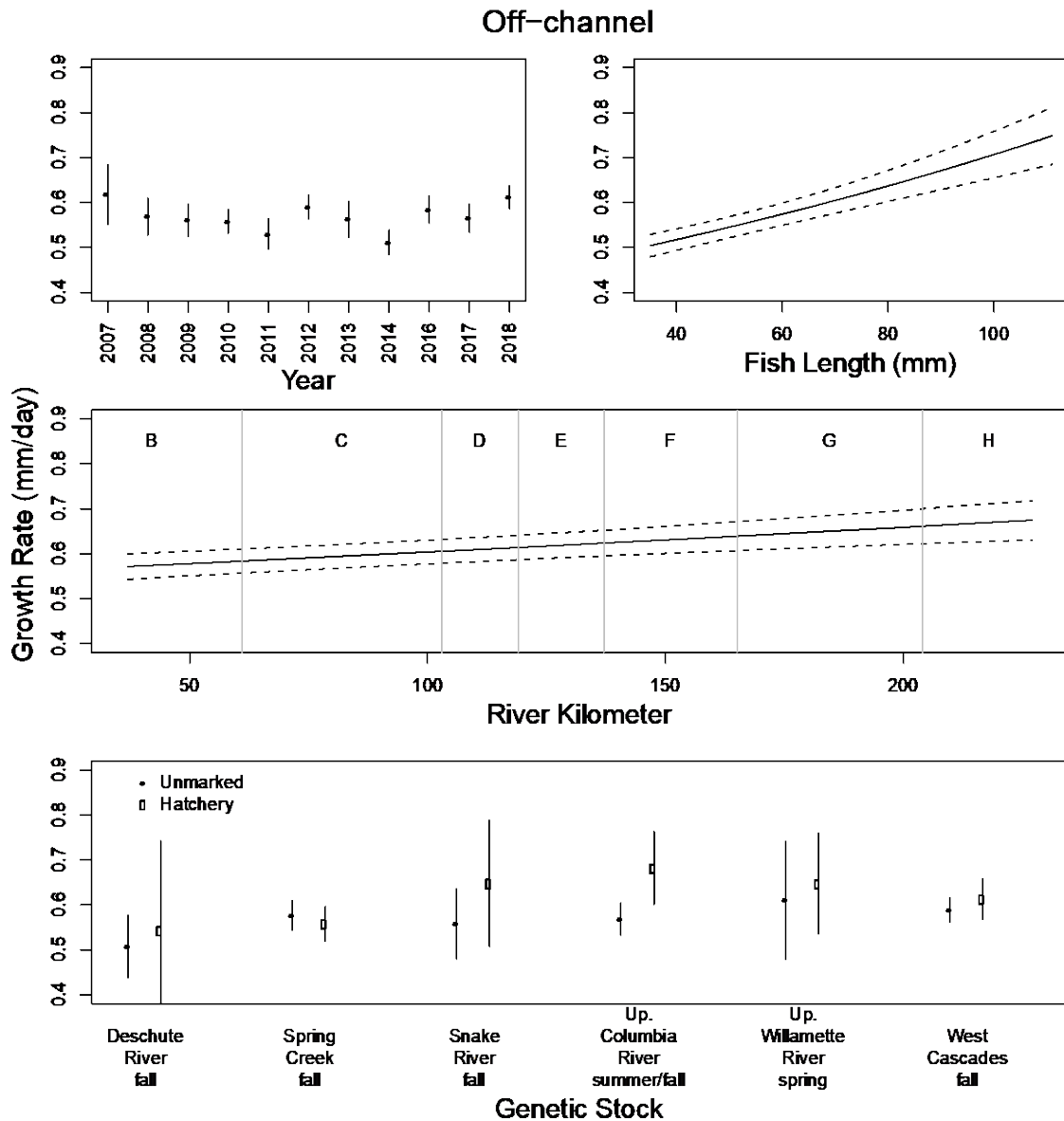


Figure 172. Relationships between growth rate and a suite of variables for juvenile Chinook Salmon collected at off-channel Columbia River sites, 2007–2014, and 2016–2018.

Welch Island: Fish (n=141) collected from Welch Island were obtained across several years (2012-2014, 2016-2018). Our GLM analysis indicated that the model that best explained variability in growth rate (mm/day) consisted of year and fork length. Specifically, we detected a significant ($p < 0.05$) positive relationship between growth rate and fork length. Also, fish collected in 2014 had significantly ($p < 0.01$) slower growth than those from 2012, 2016, & 2017 (Figure 173).

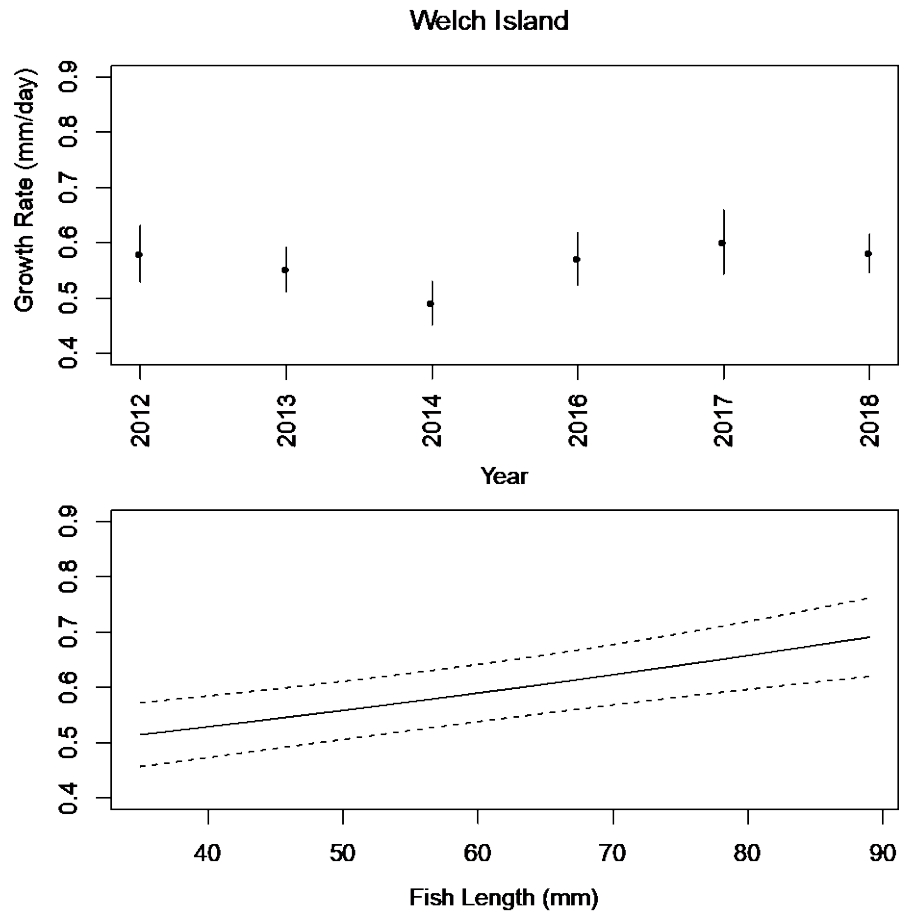


Figure 173. Relationships between growth rate and a suite of variables for juvenile Chinook Salmon collected at Welch Island, 2012–2014, and 2016–2018.

Whites Island: Fish (n=136) collected from Whites Island were obtained across several years (2009-2014, 2016-2018). Our GLM analysis indicated that the model that best explained variability in growth rate (mm/day) consisted of year and fork length. Specifically, we detected a significant ($p < 0.05$) positive relationship between growth rate and fork length. Also, fish collected in 2012, 2013, 2016, and 2018 had significantly ($p < 0.05$) faster growth than those from 2014, and those from 2013 grew significantly faster than those from 2011, 2017 (Figure 174).

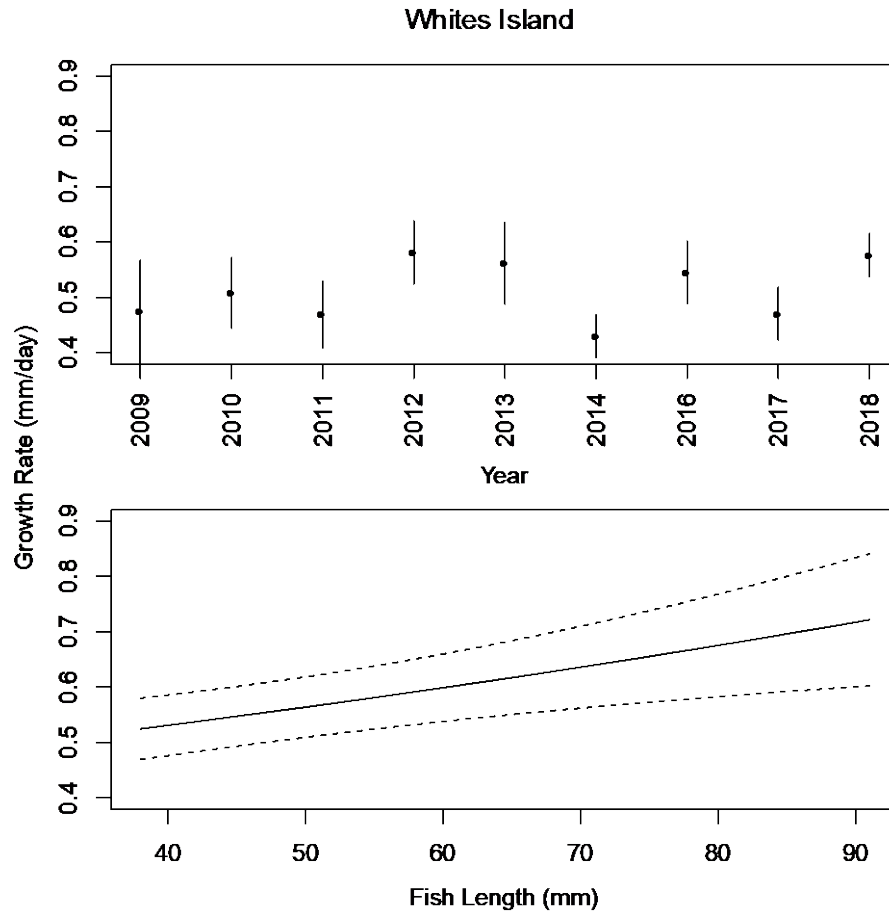


Figure 174. Relationships between growth rate and year and fish length for juvenile Chinook Salmon collected at Whites Island, 2009–2014, and 2016–2018.

Campbell Slough: Fish (n=112) collected from Campbell Slough were obtained across several years (2007-2014, 2016-2018). Our GLM analysis indicated that the model that best explained variability in growth rate (mm/day) consisted of fork length and the interaction between stock and hatchery/wild. Specifically, we detected a significant ($p < 0.05$) positive relationship between growth rate and fork length (Figure 175).

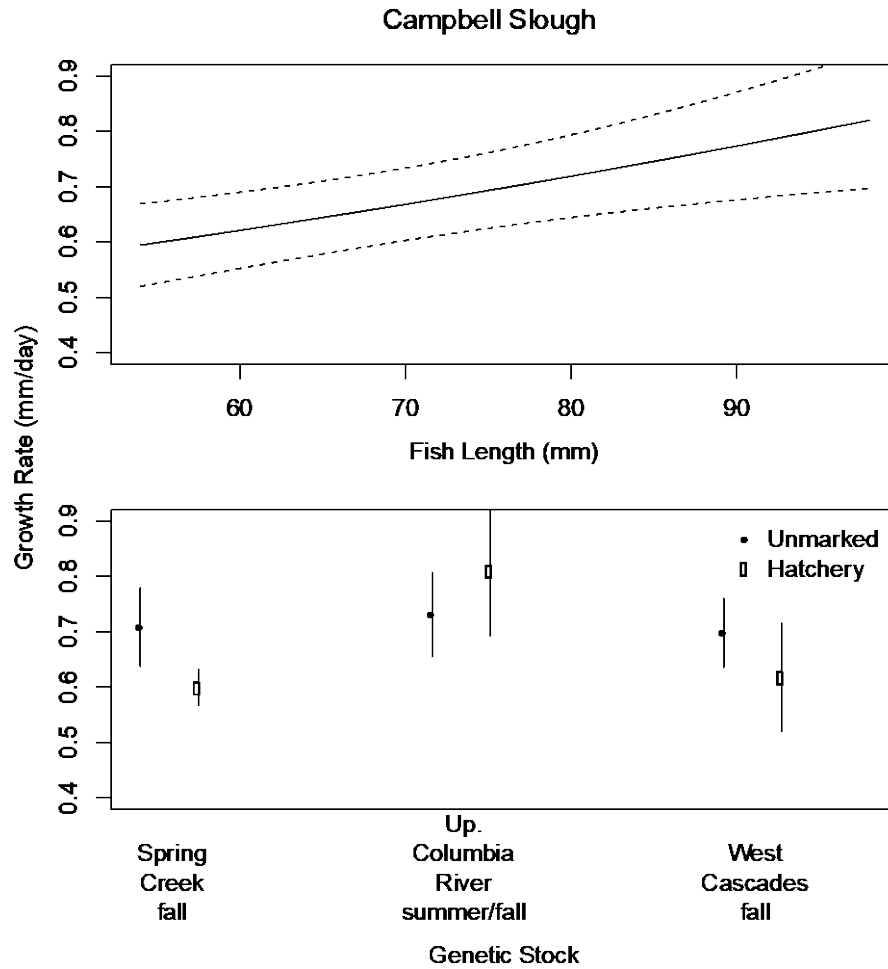


Figure 175. Relationships between growth rate and fish length and genetic stock for juvenile Chinook Salmon collected at Campbell Slough, 2007–2014, and 2016–2018.

3.6.3.4 *Lipid Content of Juvenile Chinook Salmon*

Lipid analyses for fish collected in 2019 has not been completed. The following are the results up to 2018. Lipid content can be a useful indicator of salmon health such that higher content is associated with improved survival (Biro et al. 2004). In this report we present data on percent lipid content and the percent of lipid present as triglycerides in juvenile Chinook salmon between 2007 and 2018 (Figure 176). Because these measures did not differ significantly between marked and unmarked fish, samples from both groups of fish were pooled, increasing sample size. Juvenile Chinook whole body samples collected in 2014 for lipid determinations were compromised due to a freezer failure, so no data are reported for that sampling year.

Overall, we observed considerable overlap in both percent lipid and triglycerides through space (i.e., among sites and within years) and time (i.e., among years and within sites) suggesting little change in the relative health of Chinook during this study. Some of the lowest percent lipid and triglyceride values were found in 2009-2013, which might indicate reductions in health during these years. In addition, median percent triglycerides in 2018 increased with respect to river kilometer, yet this pattern was not present in previous years.

Significant differences ($p < 0.05$) in percent lipid content among years were observed at each sampling site. Only at Welch Island did Tukey's post hoc pairwise comparisons indicate significant differences in percent lipids between 2018 and any of the previous sampling years. Specifically, fish collected in 2018 had significantly lower percent lipid content relative to those from 2015.

Significant differences ($p < 0.05$) in percent triglycerides were observed among years for Campbell Slough, Welch Island, and Whites Island, but not Franz Lake. At Welch Island, Tukey's post hoc pairwise comparisons indicated significantly lower percent triglycerides in fish collected in 2018 relative to those collected in 2013 and 2015. At Whites Island, percent triglycerides for fish collected in 2018 were significantly lower than those collected in 2013. In contrast, fish from Campbell Slough in 2018 had significantly higher percent triglycerides compared to the fish collected in 2007. To date, only one composite sample from Ilwaco Slough has been analyzed, so trends at this site cannot be evaluated.

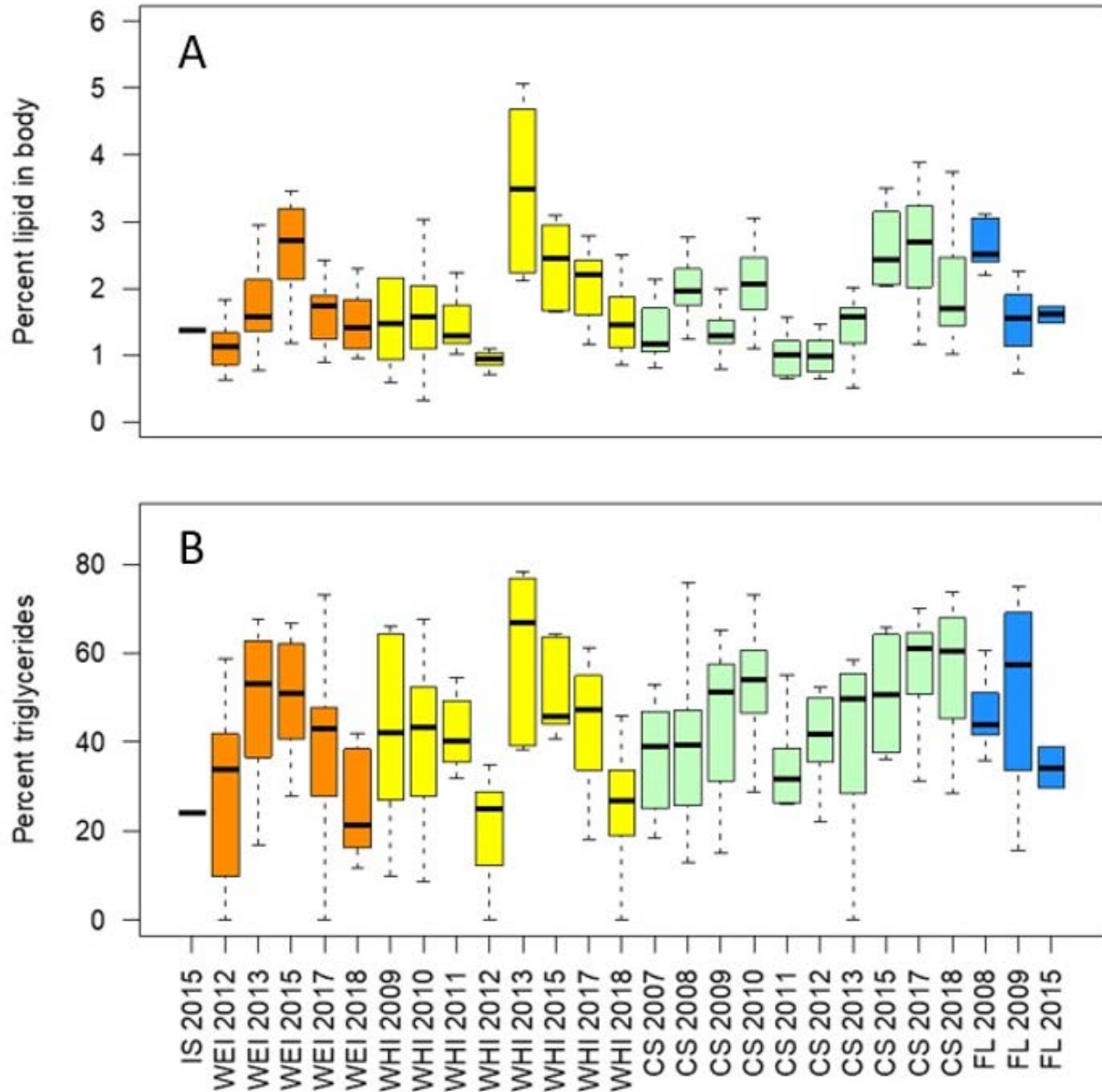


Figure 176. Percent lipid content (A) and percent total lipids that were triglycerides (B) determined in whole bodies of juvenile Chinook salmon collected from the trend sites in 2018 compared to previous sampling years. Unlike letters indicate 2018 values within each site that differ significantly from those determined in other years (Kruskal-Wallis, Tukey's post hoc test, $p < 0.05$). Sites are organized in increasing distance from the mouth of the Columbia River. Site abbreviations: IS = Ilwaco Slough, WEI = Welch Island, WHI = Whites Island, CS = Campbell Slough, FL = Franz Lake.

3.6.4 PIT-Tag Array Monitoring of Juvenile Salmon Residence

The PIT tag detection system at Campbell Slough was not operational in 2020. COVID-19 related suspension of fieldwork precluded routine operation and maintenance of the site. We were first able to inspect the site in October 2020. During that visit we discovered that the site had been vandalized. Fortunately, the transceiver, cellular modem, and batteries had been removed for the 2019-2020 winter season and had not been replaced prior to suspension of field activities. However, there was damage to the electronics box and theft of solar panels. At the October inspection we also discovered that a large tree with an intact root wad had entered the channel and damaged some of the antennas. The site remained inoperable in 2021 as we removed equipment when fieldwork was permitted and started designing a new array for the site. In 2022, we will transition the site to a flexible antenna system that will have better channel coverage and will consist of two sets of interrogation lines to determine directionality.

Similarly, the array at Horsetail was inoperable in 2020 and 2021 due to the inability to get to the site to turn on the equipment and perform maintenance. During a visit in February 2021, it was discovered that a large amount of logs and debris had accumulated on the upstream side of the culvert resulting in damage to many of the antennas. There was also considerable damage on the downstream set of antennas. We are in the process of decommissioning this site as a new site will be placed at the Steigerwald Lake restoration area in 2022.

4 Status and Trends Discussion

4.1 Mainstem Conditions

The 2020 hydrograph resembled that of 2019 in terms of low flows in March and August through October; however, 2020 had stronger winter flows in February and the peak flow was both delayed and more Gaussian in shape (i.e., peak in April in 2019 vs. late May in 2020). Peak river flow in 2020 was similar in timing (but not magnitude) to 2011 and was preceded by the lowest spring flows of the time series. The 2010 freshet was well-defined, unlike many of the years examined, beginning in mid-April and persisting through early July. Peak river flow was about average for the data set in 2020, while flows in February were among the highest. The high river flows observed in February, November, and December at Beaver Army Terminal (RM-53) coincided with high flows from the Willamette River.

In 2021, river flows were among the lowest on record from March through September when data collected ceased. Winter flows in January and February were close to average; however, by March, river flow was almost as low as observed in 2020 and there was no perceptible freshet in the spring/early summer, similar to 2015. There were small peaks in flow in early and late May/early June that were not seen in 2015. These peaks were associated with flows from the Columbia and not the Willamette River when data collected from Bonneville Dam were compared with those collected in the Willamette River at the Morrison Bridge in downtown Portland. Notably, summer flows in 2021 were similar or lower than those observed in 2015, 2018, and 2019.

The low-flow summer conditions observed in many of the study years are consistent with hydrologic models that predict intensified late summer drought in the Pacific Northwest (Hamlet and Lettenmaier, 2007, Hamlet and Littell, 2012, Lutz et al., 2012) due to earlier snowpack melt (Cayan et al., 2001, Nayak et al., 2010, Stewart et al., 2005). Hydrologic changes are rooted in increased air temperatures observed throughout the Pacific Northwest (Littell et al., 2011), which has changed the size of annual snowpacks (Hamlet et al., 2005, Mote, 2003). As a result of these changes, high water temperatures have been recorded in the lower Columbia over the last few years, particularly in 2015 when the atmosphere was very warm (Gentemann et al., 2016).

In 2020, water temperatures in the mainstem were warmer than average until May and then similar to the 10-year average for the remainder of the year. The number of days exceeding 19°C – a threshold above which juvenile salmonid populations are negatively affected – was below average in 2020 by almost one standard deviation; in contrast, the number of days exceeding the 19°C threshold was above average by almost two standard deviations in 2021, and was second only to 2015, which had the highest number of warm days meeting the threshold. Interestingly, although 2019 had very low flows from June through the end of the calendar year, the number of days exceeding the 19°C threshold was similar to the average for the data set at ~60. While there was a similar number of days where temperatures exceeded thresholds of 19°C, 20°C, and 21°C in 2019 compared to the previous few years (~80 and 62-65, 42-45, respectively), there were fewer days with temperatures exceeding higher thresholds shown to be deleterious to juvenile salmonids in 2019 compared to 2018 or 2017: whereas in 2018 there were ~25 day-equivalents with temperatures >22°C, there were <10 days in 2019 that were this warm, and there were no day-equivalents with temperatures exceeding 23°C, whereas there were a few days in each of 2018 and 2017 that were this warm. Climate change, generally manifested through warmer ocean temperatures over a sustained period, has been linked to shifts in survival, distribution, and biomass of marine organisms (Schwing et al., 2010, Doney et al., 2012, Chust et al., 2014, Cheung et al., 2015). In addition, recent work has shown that temperature strongly influences food consumption by juvenile salmonids, with consumption increasing during warm periods (Daly and Brodeur, 2016). This is significant since decreased survival of juvenile

Chinook salmon has been linked to higher temperatures, which is thought to occur due to reduced food availability (Burke et al., 2013, Daly et al., 2013).

4.1 Abiotic Site Conditions

The last several years of temperatures data from the trends sites shows that, in general, the months of July and August include a high percentage of days where the average daily temperature exceeds 19°C or 22°C. Therefore, it is instructive to look at May and particularly, June, to assess habitat suitability for juvenile salmonids. While there are missing data in 2015, the available data show that 32% of daily average observations in June at Campbell Slough exceeded 19°C. In 2020, no days in May exceed 19°C, while in 2021, 23% of days in April and 32% of days in May exceeded the 19°C threshold at Campbell Slough. A small percentage of days exceeded the 19°C threshold at Ilwaco in 2019, and 2020; 2021 data were not incorporated into these calculations at the time of this report. A look at the time series of available sonde data shows that Campbell Slough exhibits the longest period of high-temperature conditions, while July and August show consistent high temperatures across sites. The percentage of daily average temperature observations across June, July, and August at Campbell Slough in 2021 was not as high as 2015, but higher than 2019.

Dissolved oxygen concentrations are generally lowest at Ilwaco, followed by Franz Lake Slough (Sagar et al. 2016, Hansen et al. 2017), which was also the case in 2020 and 2021. There were very few observations of dissolved oxygen levels below a critical threshold of 2 mg L⁻¹, which is considered hypoxic and detrimental to survival of aquatic species, including salmonids, at Ilwaco.

Unlike other years, pH measurements exceeded the range upper threshold indicating good water quality at all sites with the exception of Ilwaco in both 2020 and 2021 (however, note that there were no pH measurements at Whites Island in 2020). Values were both of the greatest magnitude and duration at Campbell Slough, where hourly pH measurements in 2020 exceeded the threshold for good water quality from April through July, and again in August-September. Measurements exceeded thresholds in April and after mid-July in 2021. These high values coincided with peaks in dissolved oxygen and chlorophyll, indicating strong primary production during these periods. The daily averages at the other sites did not show these strong peaks, indicating that conditions on the whole fall within acceptable standards. Thus, with the exception of Campbell Slough, pH values were in the target range for good water quality throughout the sampling season in 2020 and 2021, with short-term fluctuations in pH occasionally falling outside the range for good water quality according to the Washington Department of Ecology's acceptable limits (7–8.5).

Due to limitations in sample collection imposed by travel restrictions in 2020, we have limited nutrient data in April and May. The data that are available suggest that winter and late spring nitrate concentrations were lower in both 2020 and 2021 by ~10-20 µM in 2020 at the EMP sites compared to previous years, for example 2019. Both 2020 and 2021 had relatively high winter flows, suggest that dilution may have been a factor in reducing nitrate concentrations relative to other years. Similar to previous years, nitrate concentrations were highest earlier in the sampling season (i.e., March and April) at all the of the sites except for Ilwaco, where nutrient concentrations are strongly influenced by ocean inputs in the summer. In 2021, the strongest drawdown of nitrate was observed between late winter/early spring and early May. Since there are no April or May data points from 2020, it is not clear how much drawdown occurred versus dilution by the freshet at that time, but since there was no discernible freshet in 2021, it is likely that the decline in nitrate reflects the combination of biological drawdown and limited inputs. During the growing season, nitrate concentrations never exceeded benchmarks for good water quality (<0.399 mg L⁻¹, or 28.5 µM; Oregon's National Rivers and Streams Assessment 2008-2009).

Similar to nitrate, phosphate concentrations in 2020 were generally higher in the winter prior to biological drawdown and lowest in the summer, with the exception of Ilwaco and Franz Lake Slough. The former is influenced by marine inputs in the summer that transport deep, nutrient-rich coastal water into the estuary during periods of seasonal upwelling. At Franz Lake Slough, phosphate concentrations were highly variable, with a large peak occurring in late July. In 2021, with reduced river flows, phosphate concentrations actually increased from winter to summer as water levels fell. Peak phosphate concentrations at Franz Lake were lower in 2021 compared to 2020. The very low levels of nitrate in early July 2021 at Franz Lake Slough coincided with high phosphate concentrations; low-nitrate-high phosphate concentrations provide conditions that foster the growth of nitrogen-fixing cyanobacteria species. Data from 2021 illustrate how periods of low river flow influence nutrient concentrations in a way that encourages proliferation of nuisance species, particularly when temperature are high.

Following the period of spring growth of phytoplankton nitrate concentrations tend to decline, and fluxes of nitrate associated with the spring freshet are small; combined, levels of nitrate tend to be lower from May through the end of the summer. In previous years, elevated phosphate levels at Campbell Slough and Franz Lake Slough in the summer months coincided with high proportional contributions of cyanobacteria to the total phytoplankton assemblage at these two sites, which is expected for 2020 and 2021.

4.2 Habitat Structure

4.2.1 Hydrology and Sediment Dynamics

Marsh Hydrology

Hydrologic processes are the primary environmental driver dictating wetland sediment accretion and erosion dynamics, soil biogeochemistry, plant species assemblages, vegetation productivity, and overall wetland condition. Understanding hydrologic processes and variability across tidal wetland sites in the lower Columbia River is critical to informing conservation and restoration efforts throughout the estuary.

Akin to 2019 and past years, the maximum flood levels in both 2020 and 2021 occurred during the peak freshet for all upper river sites: Franz Lake, Campbell Slough, and Cunningham Lake. As one progresses down the river, the high flow conditions become less apparent during the freshet periods, specifically at Whites Island, Welch Island, and Steamboat Slough. The mid-river sites see their maximum flood conditions in the winter at peak tide events during winter storms. Ilwaco has little to no influence from the freshet. These trends are similar to past years; however, the maximum flood levels across the estuary occurred in January 2021. In 2020, the maximum for the mid and lower river occurred in November 2020 with the upper river peaking during the freshet in June 2020.

In general, we have found that inter-annual variation in inundation patterns is much greater at the upper river sites, Franz Lake, Campbell Slough, and Cunningham Lake where seasonal flooding (both winter and freshet) can result in months of continuous inundation during high-water years. In contrast, the mid and lower estuary sites, Whites Island, Welch Island, Steamboat Slough, and Ilwaco Slough, are dominated by tidal patterns where inundation lasts just a few hours during high tide, but occurs frequently, usually two times daily. Inundation, as measured as a percent of time that the water surface level exceeds the ground surface is a means of comparing sites to each other and over time. The average inundation daily at each site is dependent on the elevation, the position along the tidal and riverine gradient, and the seasonal and annual hydrologic conditions. The average % of the day the mean marsh elevation is inundated for the month of August is critical for plant development in the upper river sites because the freshet draws down and exposes the marsh surface. Generally, the trends in % time inundated

identified in August correlate well with average % daily inundation for the year (unpublished data). It does not, however, always correlate with the overall magnitude of the annual freshet. This is because the timing of the freshet can vary from year to year, in some years such as 2011 and 2012, the high flows from the freshet have lasted into August, resulting in significantly greater daily inundation patterns at the upper river sites (Figure 33-Figure 38), while other years, such as 2017, freshet levels were high but receded quickly resulting in low inundation levels in August and generally more of the growing season. These shifts in daily inundation are critical for plant community development and can have major implications for not only plant species composition but also biomass production. Lower water years (in August), such as 2015, 2017, and 2021, produce greater plant biomass than high August water years (Figure 72). We hypothesize that the annual timing, magnitude, and duration of the freshet may also impact the longterm status and trends of tidal wetland fish utilization, macroinvertebrate assemblages, and plankton productivity.

Sediment Dynamics

Sediment accretion rates are variable within the Columbia River estuary and within individual sites, likely due to variation in elevation, sediment loading, and flood inundation frequency (Kadlec & Robbins, 1984, Chmura et al., 2003, Woods & Kennedy, 2011) and may even be affected by the vegetation present (Larsen et al., 2010; Mudd et al., 2010, Marani et al., 2013). In 2021, sediment accretion and erosion rates at the five trend sites and Cunningham Lake ranged between -6.7 cm and 6.0 cm. The greatest sediment accretion rates have been measured at Campbell Slough and can likely be explained by the large bovine presence in the years before. The next largest accretion rate, and the highest average accretion rate, occurs at Whites Island in a patch of *C. lyngbyei* located at a mid- to low-marsh elevation (2.46 m, NAVD88) very close to the primary tidal channel at the site (<10 m from marsh edge). This is a good example of conditions conducive to high accretion rates: proximity to the tidal channel, high inundation frequency (about 50 percent), and vegetation that produces high amounts of organic material and effectively traps mineral and organic material, both important sources of sediment accretion in tidal freshwater marshes (Neubauer 2008). Additionally, Campbell Slough had an average erosional rate of around 0.2 cm/year with a standard deviation of 2.73. The high variability in the data set is likely explained by the open grazing, the higher energy system with close proximity to the channel, the very high inundation frequency, as well as the high sediment supply.

Overall, the erosion rates at Campbell slough and Cunningham Lake can be attributed to constant cattle grazing trampling, which affects soil compaction and removal of above ground biomass (Trimble, 1994; Nolte et al., 2013). In both 2020 and 2021, large variation in accretion and erosion rates were observed at all five trend sites and Cunningham Lake. The 2020 and 2021 sediment accretion and erosion data for the EMP were included with the 2021 sediment dataset and were included into the longterm dataset. This inclusion is one possible cause of change in trends observed in rates.

Site Code:	BBM-1	BBM-2	WI2-1	WI2-2	WHC-1	WHC-2	CLM-1	CLM-2	CS1-1	CS1-2	CS1-3	FLM-1	FLM-2
Elevation (m, NAVD88)	2.61	2.49	2.83	2.71	3.09	2.46	3.53	3.25	3.71	4.08	4.081	5.28	5.71
Dominant Species	CALY	LIOC	CAOB	CALY	TYLA	CALY	PHAR/SALA	Mud	ELPA	PHAR	SALA	POAM	PHAR
2008-2009	ND	ND	ND	ND	-1.2	ND	ND	ND	ND	ND	ND		ND
2009-2010	ND	ND	ND	ND	1	ND	1.9	ND	0.4	ND	ND	ND	ND
2010-2011	1.7	ND	ND	ND	0.1	ND	1.6	ND	1.7	ND	ND	3	ND
2011-2012	0.1	ND	ND	ND	0.9	ND	1.4	ND	0.9	ND	ND	-0.2	ND
2012-2013	0.6	ND	0.8	ND	0.2	1.2	1.3	ND	0.2	ND	ND	3	ND
2013-2014	0.4	ND	0.6	ND	0.8	2.3	0.5	ND	1.5	ND	ND	0.7	ND
2014-2015	1	ND	0.7	ND	0	2.7	-0.5	ND	-2.4	ND	ND	1.2	ND
2015-2016	0	0.3	ND	1.0	ND	2.6	0.9	2.9**	1.4	0.8	ND	-0.6	-2.3
2016-2017	0.4	-2.5	0.6	1.8	0.4	3.7	0.1	ND	-4.2	-0.6	ND	0.6	-2.1
2017-2018	0.9	1.1	-2.5	4.0	2.1	2.4	1.5	ND	2.2	0.6	ND	3.3	1.4
2018-2019	-0.3	-0.5	1.7	-3.0	-0.3	1.3	-1.1	ND	-3.2	-1.2	ND	0.4	0.2
2019-2020	0.33	-0.16	1.8	-3	-1.36	-1.1	-0.3*	ND	3.9*	-0.4*	-9.2*	0.4	0.2
2020-2021	1.05	-0.22	.6	-0.16	0.62	1.6	-1.03*	-4.6*	6.0*	-6.7*	1.0*	.49	-0.2
Average	0.56	-0.33	0.54	0.11	0.27	1.86	0.52	-0.85	-0.24	-0.17	-4.1	1.12	-0.47
Std Dev	4.54	1.1	1.24	2.52	0.91	1.28	1.01	NA	2.73	0.69	NA	1.29	1.32

Table 21. Similar observations were noticed in a study researchers in the marshes along Gulf of Mexico (Callaway et al., 1997).

When combining longterm sediment accretion rates across sites we found that marsh elevation (m, CRD) was negatively correlated with sediment accretion rates, meaning that low-marsh zones accrete more sediment than high marsh zones. This pattern of sediment accretion is well supported by other studies (Harrison & Bloom, 1977; Cahoon et al., 1996). Locally, Kidd (2017) found similar patterns within wetland sites in Young Bay. The mechanism driving these observations are the differences in daily and seasonal tidal ranges that can manifest in differences in sediment loading across the marsh elevation gradient. Sediment depositions being more pronounced in low marshes near marsh channels, which receive more daily inundation and sediment exposure than high marsh zones (Hassan et al., 2005; Larsen et al., 2010; Jay et al., 2015).

While we have found a significant trend in sediment accretion across the EMP sites, in general our study of sediment dynamics at the trend sites is has limitations. Firstly, the overall lack of sufficient sedimentation stakes prevents us from making definitive connections with inundation and flooding frequency, effects of vegetation of accretion rates as well as studying the influence of cumulative discharge.

Site Code:	BBM-1	BBM-2	WI2-1	WI2-2	WHC-1	WHC-2	CLM-1	CLM-2	CS1-1	CS1-2	CS1-3	FLM-1	FLM-2
Elevation (m, NAVD88)	2.61	2.49	2.83	2.71	3.09	2.46	3.53	3.25	3.71	4.08	4.081	5.28	5.71
Dominant Species	CALY	LIOC	CAOB	CALY	TYLA	CALY	PHAR/ SALA	Mud	ELPA	PHAR	SALA	POAM	PHAR
2008-2009	ND	ND	ND	ND	-1.2	ND	ND	ND	ND	ND	ND		ND
2009-2010	ND	ND	ND	ND	1	ND	1.9	ND	0.4	ND	ND	ND	ND
2010-2011	1.7	ND	ND	ND	0.1	ND	1.6	ND	1.7	ND	ND	3	ND
2011-2012	0.1	ND	ND	ND	0.9	ND	1.4	ND	0.9	ND	ND	-0.2	ND
2012-2013	0.6	ND	0.8	ND	0.2	1.2	1.3	ND	0.2	ND	ND	3	ND
2013-2014	0.4	ND	0.6	ND	0.8	2.3	0.5	ND	1.5	ND	ND	0.7	ND
2014-2015	1	ND	0.7	ND	0	2.7	-0.5	ND	-2.4	ND	ND	1.2	ND
2015-2016	0	0.3	ND	1.0	ND	2.6	0.9	2.9**	1.4	0.8	ND	-0.6	-2.3
2016-2017	0.4	-2.5	0.6	1.8	0.4	3.7	0.1	ND	-4.2	-0.6	ND	0.6	-2.1
2017-2018	0.9	1.1	-2.5	4.0	2.1	2.4	1.5	ND	2.2	0.6	ND	3.3	1.4
2018-2019	-0.3	-0.5	1.7	-3.0	-0.3	1.3	-1.1	ND	-3.2	-1.2	ND	0.4	0.2
2019-2020	0.33	-0.16	1.8	-3	-1.36	-1.1	-0.3*	ND	3.9*	-0.4*	-9.2*	0.4	0.2
2020-2021	1.05	-0.22	.6	-0.16	0.62	1.6	-1.03*	-4.6*	6.0*	-6.7*	1.0*	.49	-0.2
Average	0.56	-0.33	0.54	0.11	0.27	1.86	0.52	-0.85	-0.24	-0.17	-4.1	1.12	-0.47
Std Dev	4.54	1.1	1.24	2.52	0.91	1.28	1.01	NA	2.73	0.69	NA	1.29	1.32

Table 21 shows standard deviation much greater than the mean of accretion at all the trend sites and Cunningham Lake, suggesting high variability of the dataset.

There are still several questions that need to be answered. The interplay of mineral sediment accretion and the accumulation of organic material is important in determining the rates of sediment accretion and also the rates of carbon sequestration (Craft 2007). In Tidal Freshwater marshes, carbon accumulation in the sediment comes from organic material associated with mineral sediments in the water column and from in situ biomass production and breakdown (Neubauer 2008). Similar to sediment accretion variability, carbon density and accumulation rates are likely variables in the Tidal Freshwater marshes of the LCRE. Carbon density is often greater at higher marsh elevations with lower flooding frequency and lower sediment loading; however, the inverse may be true of carbon accumulation rates (Chmura et al., 2003). Overall, in LCRE marshes, carbon in the surface sediments (~10 cm) accounts for approximately 3 to 10 percent of the sediment (Borde et al., 2011; Sagar et al., 2013). This carbon content is similar to those amounts found in a prograding riverine brackish marsh with high mineral sediment accretion rates (Thom 1992), but lower than some other Tidal Freshwater marsh sediments (Craft 2007; Thom 1992) where organic material may account for more of the accretion. In general, Tidal Freshwater wetlands store more carbon and have higher carbon accumulation rates than salt marshes (Craft 2007) but understanding the variability of this process in the LCRE will be important to gain a better understanding of the overall storage capacity of these wetlands now and in the future.

In the future, it may be informative to relate site hydrology and sediment dynamics between and among both EMP sites as well as AEMR sites throughout the lower Columbia. This effort may require more detailed tracking of sediment accretion and erosion rates within and across sites due to the high level of variability seen in the historic data and generally inherent to monitoring sediment dynamics (Takekawa et al. 2010). Furthermore, it is vital to compare rates of sediment accretion to forecasted sea level rise to determine the rate of drownage across wetlands; we have found that many sites across the lower Columbia are not keeping pace with forecasted sea level rise (Figure 48). Further study to quantify the rates of accretion across all sites of the lower Columbia, including both the AEMR and EMP sites; additional analyses of forecasted sea level rise; and the impact of both on overall extent and quality of marsh habitats are planned for FY23.

4.2.2 Vegetation Community Condition and Dynamics

Overall trends in plant community composition

Overall, 2021 total plant cover was relatively stable across Ilwaco Slough, Welch Island, Whites Island, and Franz Lake compared to historic, longterm averages. Cunningham Lake total cover has continued to increase through 2021, beginning to rebound from the heavy cattle grazing observed in 2017. Campbell Slough has exhibited a small increase in total cover levels in 2021, however the overall cover at Campbell is still low compared to non-grazed conditions; a new vegetation grid was established at Campbell Slough in 2021 to capture non-grazed conditions and will continue to be used for comparisons moving forward. Cattle grazing has continued at Campbell Slough since 2017, with fencing efforts failing to keep the cattle out of the wetland.

Generally, native and non-native cover are more similar from year to year in the zone 1 and 2 sites (Ilwaco, Welch, Whites) compared to the zone 4 and 5 sites (Cunningham, Campbell, and Franz) (Figure 55 & Figure 56), this is likely due to the general hydrology of these sites, inundation patterns being much more stable from year to year in the tidally drive lower river, zone 1 and 2, sites compared to the fluvially dominated mid and upper river, zone 4 and 5, sites (see section 3.3.1). These trends were generally observed in 2019, with Ilwaco Slough, Whites Island, Welch Island, and Franz Lake retaining similar native cover conditions as to previous years. At Ilwaco Slough this was account for through a general reduction in non-native *Agrostis stolonifera* cover and a corresponding increase in native *Carex lyngbyei* cover, in addition to increases in other natives such as *Argentina egedii ssp. Egedii*, *Deschampsia*

cespitosa, *Lilaeopsis occidentalis*, and *Symphyotrichum subspicatum*. At Franz Lake, this shift was a result of a general mixed increase in native species cover including *Argentina egedii* ssp. *Egedii*, *Fraxinus latifolia*, *Salix lucida*, and *Helenium autumnale*.

Comparatively, Campbell Slough showed a marginal increase in native relative cover (Table 25, Figure 55 & Figure 56). This shift can be accounted for by an increase in native herbs such as *Eleocharis ovata*, *Helenium autumnale*, *Lindernia dubia*, and *Ludwigia palustris* which were found growing in the plots heavily disturbed by grazing. This shift, caused by grazing, indicates that these native species are found in the seed bank but are normally (under no grazing) suppressed by more dominant non-native species such as *P. arundinacea* (Kidd 2015). Comparatively, Cunningham lake, which has not experienced heavy grazing since 2017, had a decrease in native cover from a historic high of 65% in 2018 to a mere 46% in 2021 (Table 25, Figure 55 & Figure 56). This decrease in native cover was accompanied by a general increase in non-native cover including a 47% increase in *P. arundinacea* cover between 2018 and 2021 (Figure 57). This increase in *P. arundinacea* is to be expected both because of the reduced grazing pressure and because of the lower water conditions experienced during the 2021 growing season, which favors *P. arundinacea* growth (see more on this below).

Between 2012-2021 the six most common plant species identified throughout the tidal estuary (across the 6 trend sites) in order of overall abundance are *Phalaris arundinacea* (PHAR, non-native), reed canarygrass, *Carex lyngbyei* (CALY, native), lyngby sedge, *Eleocharis palustris* (ELPA, native), common spikerush, *Sagittaria latifolia* (SALA, native), wapato, *Leersia oryzoides* (LEOR, native), rice cut grass, and *Ludwigia palustris* (LUPA, native), water purslane (Table 28, Figure 57-Figure 63). While these species are the most common and abundant across all sites over the years, they are not necessarily present at all sites every year. For example, *P. arundinacea* does not grow at Ilwaco, likely due to the saline conditions present at this wetland (Kidd 2017). However, it is found growing in abundance at all the other trend sites across the lower river (Table 29 & Table 30, Figure 57-Figure 63).

Trends in P. arundinacea abundance

In 2021, *P. arundinacea* cover levels stayed relatively consistent to those observed in 2020 and previous years, however, at Cunningham, there was a significant increase in *P. arundinacea* levels from 21% in 2018 to 68% in 2021. Franz Lake also experienced an increase from 11% in 2018 to 30% in 2021. (Table 29 & Table 30, Figure 57). *P. arundinacea* frequency (spread across the site) decreased at Cunningham, but only slightly from 74 % of plots in 2018 to 63 % of plots in 2021, and overall *P. arundinacea* frequency increased significantly at Franz Lake from 60 % of plots in 2018 to 75 % of plots in 2021 (Table 29). This shift in *P. arundinacea* levels observed at Cunningham and Franz Lake is likely a product of both very low freshet flooding conditions in 2021 (Figure 67) and, at Cunningham Lake, a reduction of grazing pressure. The last several years cattle have heavily grazed Cunningham Lake wetlands; it is well known that cattle pressure can significantly reduce *P. arundinacea* abundance during the growing season (Kidd 2017). Generally, *P. arundinacea* abundance has been found to decrease in years of greater freshet discharge levels, especially in Cunningham Slough, Campbell Slough, and Franz Lake where wetland water levels are tightly correlated with Columbia River discharge conditions, higher water levels making growing conditions less favorable for *P. arundinacea* (Figure 67).

Water year conditions and impacts of plant community composition

In 2021, data continued to support our findings that annual shifts in *P. arundinacea* cover are strongly correlated with Columbia River discharge levels and site water levels during the growing season (Figure 66), with lower water levels (and lower discharge levels) favoring *P. arundinacea* growth and observed abundance. These findings indicate that annual flooding conditions within sites (% daily inundation) and across the river (freshet accumulated discharge) are important mechanisms driving much of the observed annual variability in *P. arundinacea* dominance across the estuary. Additionally, these data support the

hypothesis that annual flooding conditions in the Columbia can dramatically impact year to year shifts in plant community dynamics, especially the non-native species *P. arundinacea* in the upper river sites. *P. arundinacea* mean annual cover was also found to be tightly negatively correlated with native plant community cover across all river zones except the mouth (Ilwaco has no *P. arundinacea* due to high salinity levels), annual increases in *P. arundinacea* resulting in an overall decrease in native plant cover (Figure 68).

The longterm trends in the abundance of native species *C. lyngbeyi*, *S. latifolia*, *P. amphibium* have also been found to be strongly (and significantly) linked to annual river discharge conditions. Generally, *C. lyngbeyi* abundance has been found to increase in years of greater freshet discharge levels, especially in Ilwaco Slough, where salinity levels are reduced during large discharge years, making growing conditions more favorable for *C. lyngbeyi* (Figure 58). *S. latifolia* has been found to have a delayed reaction to freshet conditions, with lower freshet conditions resulting in an increase in *S. latifolia* abundance the following year. Additionally, *P. amphibium* levels at Franz Lake have also been found to follow a similar trend to *S. latifolia* with a one year delayed reaction to decreased freshet conditions, lower freshet conditions (lower water levels across the wetland site) resulting in an increase in *P. amphibium* cover the following growing year (Figure 43). For both species, this might be a result of increased rhizome stores from positive growing conditions (low water levels), providing for more robust growth in the following growing season.

Summarizing these findings, site level daily inundation patterns in addition to season freshet flooding conditions are important drivers of native and non-native plant communities across the estuary. Publication of these data and further investigations of these relationships will be explored in the FY23 report.

4.3 Food Web

4.3.1 Primary Production

4.3.1.1 Emergent Wetland Vegetation

Overall, 2020 and 2021 resulted in a high production of standing stock and detritus biomass across all sites, with some of the largest values seen to date – likely a result of the longer growing seasons observed during the lower freshet conditions these years experienced. This was especially true for Franz lake (Figure 69, Figure 70, Table 34, Table 35), where the longer growing season was compounded with the removal of the beaver dam, proving a larger area for low marsh plant community establishment.

Net aboveground primary productivity (NAPP) is the rate of storage of organic matter in aboveground plant tissues exceeding the respiratory use by the plants during the period of measurement (Odum 1971). Many methods exist to estimate NAPP; however, for our ecosystems in which there is a clear seasonality, a good method is a single harvest at peak biomass (Sala and Austin 2000). Our analysis of the proportion of live versus dead material indicated that for most species the live proportion of the summer samples averaged greater than 90 percent; a confirmation that we indeed were sampling at or near the biomass peak. Starting in the summer of 2017 detritus sampling was included in the biomass sampling and analysis to evaluate detrital production and export. In the winter of 2018 (and all sampling events to follow), biomass sampling protocols changed slightly to accommodate detrital sampling and streamline data collection. This included shifting from “strata” mixed species designations to simple high and low marsh strata descriptions across all sites sampled. This change has also included species biomass weights to be recorded individually to assess species specific contributions to each high and low marsh stratum (in the past mixes of species were assessed together). In general, these changes will allow for a more detailed

understanding of species-specific biomass contributions and still allow for longterm comparisons to overall site, high and low marsh contributions.

Generally, productivity in the high marsh strata has been very high and similar in quantity to the most productive North American marshes (Brinson et al. 1981; Bernard et al. 1988; Windham 2001). Average summer biomass of 1000 to 1500 g dry weight/m² in the high marsh strata is not an uncommon observation throughout the estuary (Kidd et al. 2018). In 2021, the highest average summer biomass was observed at Welch Island high marsh strata, with 1,255 g/m², however, the multi-year analysis of the summer biomass revealed high variability between years at Welch Island. Across sample sites, year to year variability in overall total biomass contribution was found to be negatively correlated with cumulative river discharge for August, indicating the importance of river conditions on annual wetland biomass production and export, even at the lower river wetland locations, Whites and Welch Island (Figure 73).

Overall proportion of biomass contribution from living, dead, and detritus varied across the seasons, living biomass contributing the most during the summer season, standing dead and detritus contributing the most during the winter, with biomass contributions being more evenly split between living, dead, and detritus in the spring, reflecting new spring plant growth across all sampled sites (Table 33, Table 34). This seasonal look at biomass composition shows the largest flux of standing biomass (living + dead) out of these wetlands is between the summer and winter time-period, some of this living and dead biomass shifting to detrital material and most being exported from the sampling areas altogether. The largest flux of detritus out of the wetland occurs during the spring-summer time-period, detrital material showing a gradual increase from summer to spring and then a sharp decline between the spring and summer sampling events (Table 33, Figure 69). While the overall amount of biomass contributed is lower coming out of the low marsh compared to the high marsh strata, they were found to follow similar patterns of living, dead, and detritus biomass contribution over the seasonal shifts.

The EMP biomass sampling efforts continue to highlight the significant organic plant material contribution from these wetland sites to the estuary ecosystem annually; however, this contribution relative to the energy needs of the estuary food web is still unknown. Overall, across sites the high marsh strata dominated by a mix of native sedge *C. lyngbyei*, native herb *P. amphibium*, and the non-native grass *P. arundinacea* contributed the highest and most consistent amount of organic material, signifying the importance of the high marsh plant community complex to the estuary food web. The low marsh strata dominated by a mix of native *P. hydrophoroides*, *S. latifolia*, and *E. palustris* also contributes a consistent flux of organic material, while much lower in overall biomass weight, these low marsh contributions are generally less variable than the high marsh on a site to site and year to year basis. If organic material from marsh plants is indeed a limiting factor for the detrital based food web in the lower river, the restoration of additional marsh area dominated by native high and low marsh species could improve those conditions.

4.3.1.2 *Emergent Wetland Vegetation Nutrient Dynamics*

One factor in the EMP biomass analysis conducted in 2018 was the evaluation of the living above ground biomass, detritus, and soil nutrients Carbon (C), Nitrogen (N), and ADF lignin (L, lignin) composition. This research has continued through 2021, with the exception of the soil analyses. These data provide insight into the quality and nutrient dynamics of the biomass contributions and highlight the variability in nutrient composition between plant species and the high and low marsh strata. Species-specific functional plant traits such as C:N ratio and L:N ratio can also provide insight into the potential decomposition rates of species, with low C:N and L:N ratio species having greater decomposition potential than species with higher C:N and L:N ratios. The C:N ratio is commonly used to define the N immobilization-mineralization gradient, a greater C:N ratio promoting N up take by microbes (immobilization) and

detrital accumulation, while a lower C:N ratio promotes N mineralization (release) by microbes and detrital decomposition (Reddy and Delaune 2008). The quality and rate of decomposition provides insight into the direct food web contributions provided by different species found in the high and low marsh stratas across wetlands.

Nutrient Conditions Observed Across Strata

Comparing C, N, and C:N ratios between the above ground living biomass, detritus, and soil across the elevation gradient can provide insight into plant species nutrient use efficiency and decomposition.

Trends in C, N, and C:N ratios across the elevation gradient within wetlands were particularly interesting with living above ground biomass and soil C content both increasing along the elevation gradient; low in the low marsh strata and high in the high marsh strata. Soil N followed a similar pattern being higher in the high marsh strata and lower in the low marsh strata. Living above ground biomass N content followed a reverse trend with lower N levels in the high marsh strata and higher levels in the lower marsh. These results generally translated into greater C:N ratios in the high marsh soil and living above ground biomass and lower C:N ratios in the low marsh soil and living above ground biomass. These results potentially reflect both a shift in plant species and plant species nutrient use efficiency along the high to low marsh gradient. The low marsh species having lower carbon content, and lower C:N ratios overall, indicating less decomposition time required for the plant species found in the low marsh zone, C: N Ratio under 25 indicating no N limitation to decomposition (Wang et al. 2016). The high to low marsh shift in C:N ratios also corresponds to the overall differences found in detritus accumulation between the high and low marsh zone across sites, less detritus accumulation occurring in the low marsh zone (Figure 70). L:N ratios across the wetlands were found to also correlate with elevation, following the N content trend, with smaller ratios in the lower marsh zones across sites (Figure 83). The above ground living biomass L:N ratio is also known as a good predictor of plant biomass decomposition rates, smaller ratios indicate more N and less lignin, and quicker decomposition (Taylor et al. 1989, Talbot et al. 2011).

Overall, mean summer lignin content was greatest in the detritus samples compared to the living plant biomass (Figure 81, Table 38), this follows the expected trend of lignin concentrations increasing in the detritus as decomposition occurs, lignin and associated compounds resisting decomposition (Taylor et al. 1989, Talbot et al. 2011). Detrital lignin content was found to be positively correlated with detrital carbon content, greater carbon levels within the detritus corresponding with greater levels of lignin. Similarly, detritus L:N ratio was also positively correlated with detritus carbon content, higher levels of lignin and lower levels of N corresponding with greater levels of carbon (Figure 82, Figure 83). This result is expected, as others have found that as the biomass breaks down, the ratio of lignin and C will increase compared to N (Taylor et al. 1989, Talbot et al. 2011). This relationship is essentially showing N limitation in the longterm breakdown of organic matter with high C and Lignin content (Taylor et al. 1989, Talbot et al. 2011).

The mean soil N and C content showed a strong positive correlation, increases in soil C content corresponding to higher levels of N content (Figure 79). This relationship was also found in the detritus, with detrital C and N having a positive correlation across all sites (Figure 82). No relationship was found between mean living above ground biomass C and N content, indicating that this relationship becomes clearer once decomposition begins (detritus) and the decaying plant matter and associated microbial communities are incorporated into the soil within these sites.

Incorporating these nutrient dynamics into the longterm status and trends monitoring will provide additional insight and confidence in our understanding of the detrital and nutrient flux within these sites and their contributions to the greater estuary food web.

Species Specific Traits Observed

Specific species analysis of the above ground living biomass C, N, and lignin content showed a large range of variability in these traits from species to species, however, species specific trends were generally found consistent across all sites sampled (Table 39, Table 40). Species specific C: N and L:N ratio results have provided insight into the quality of biomass and detritus being produced by dominant species. It has long been hypothesized that non-native grass *P. arundinacea* produces lower quality biomass (higher L: N and C:N ratios) than the native sedge *C. lyngbyei*, preliminary results from summer biomass sampling in 2018 support this hypothesis (Hanson et al. 2016). The common high marsh non-native species, *P. arundinacea*, was found to have a higher mean L: N and C:N ratios than *C. lyngbyei*. These differences in L: N and C:N ratios mirror observations of decomposition in the field with more *P. arundinacea* being retained on the site as standing dead biomass than *C. lyngbyei* (Hanson et al. 2016).

Common native low marsh species *S. latifolia*, and *E. palustris*, were found to have much lower L:N and C:N ratios than the high marsh species (Table 40), indicating these species have more N in their living above ground biomass than *P. arundinacea* and *C. lyngbyei*, aiding fast decomposition rates. *S. latifolia*, and *E. palustris*, are not generally found as standing dead due this faster decomposition and location in the low marsh which is exposed to more active hydrologic flushing (exporting the dead biomass) compared to the high marsh.

Other common species, *Polygonum amphibium* (Franz Lake, High Marsh) and *Polygonum hydropiperoides* (Whites and Welch Island, Low Marsh) were found to have the highest overall L:N ratios, this is not particularly surprising as these species have woody (high in lignin) perennial stems (especially when compared to the other common wetland grass and herb species) that persist throughout the winter months. *P. amphibium* and *P. hydropiperoides* are an interesting comparison to the other marsh species because they do lose their leaves annually without much dead leaf accumulation, but their stems tend to fall dormant (not actually standing dead), indicating that their L:N ratios may vary dramatically between the two plant structures (more in the perennial stems and less in the leaves). Further testing and distinction between leaves and stems of all species will help us better understand these functional plant traits and how they inform plant decomposition and detrital production within these sites moving forward.

4.3.1.3 Pelagic

Further discussion will be provided in the FY23 report, due to Covid related restrictions on time, these data were still in process at the time of this report, for a partial update of these conditions see Section 3.4.2. In 2019, total algal biomass, as estimated by concentrations of chlorophyll *a*, was highest in March, prior to the spring freshet, at Welch Island and Whites Island; in contrast, the highest algal biomass at Campbell Slough and Franz Lake Slough was observed in August, with an exceptional peak in biomass at Franz Lake Slough in May. While there were a number of years between 2011 and 2019 where samples were not obtained in March, the values observed in March 2019 are relatively high for the early spring period. The low river flows in winter 2019 coincided with relatively high algal biomass, consistent with previous analyses that showed a negative correlation between river flow and algal biomass during the winter and spring months (Maier, 2014). The low levels of chlorophyll *a* observed after the freshet subsided and flows were reduced to some of the lowest rates in the 2011-2019 time series is also consistent with previous observations that in the summer months, river flow is positively associated with algal biomass (Maier, 2014).

The contrast in timing of maximum pelagic algal biomass between Welch and Whites Islands compared to Campbell Slough and Franz Lake Slough reflects the differences in species responsible for the bulk of the pelagic primary production. Whereas at Welch and Whites Islands the assemblages were dominated by diatoms, peak biomass at Campbell Slough and Franz Lake Slough was dominated by cyanobacteria and chlorophytes. This is an important distinction due to the differences in nutritional quality among the

different groups of phytoplankton; studies have shown that feeding rates of zooplankton are very low on cyanobacteria (Schmidt and Jonasdottir, 1997). However, that same study showed that a supplementation of diatom diets by cyanobacteria can lead to an increase in feeding rates among copepods, as indicated by egg production rates; they observed that a 3:1 ratio of diatoms to small, unicellular cyanobacteria could result in an elevated feeding rate relative to diatoms alone (Schmidt and Jonasdottir, 1997). It is possible that the higher diversity in algal taxonomic classes observed at Campbell Slough and Franz Lake Slough contributes to the high densities of zooplankton there, in addition to slower presumed flushing rates that prevent dilution of standing stocks.

Over the last number of years, pelagic productivity has been high at Franz Lake Slough, which reached a peak $>100 \mu\text{g chl } a \text{ L}^{-1}$ in 2017. In 2019, cyanobacteria accounted for a large proportion of the phytoplankton assemblage in the summer; however, the cell densities (of cyanobacteria and other phytoplankton) were not as high as in 2017 or 2018 at most of the trends sites, with the exception of Campbell Slough, which had high abundances of cyanobacteria in August. There were also relatively high densities of cyanobacteria in 2019 at Ilwaco. Total phytoplankton biomass (as estimated by chlorophyll *a*) was highest in early spring at Ilwaco, Welch Island, and Whites Island (i.e., March, April); in contrast, peak biomass occurred after June at Campbell Slough. Phytoplankton biomass was high both before and after the freshet at Franz Lake Slough. At Franz Lake Slough the first peak coincided with high nitrate concentrations while the second peak (after the freshet) coincided with high phosphate concentrations. The species composition of the first peak was dominated by diatoms and chlorophytes, whereas the second peak was dominated by cyanobacteria, where the assemblage was dominated by *Anabaena* spp. and *Microcystis* spp. *Anabaena* was also abundant at Campbell Slough, in addition to *Merismopedia* spp., in August. *Microcystis* and *Pseudo-anabaena* were the most abundant cyanobacteria taxa at Whites Island, Welch Island, and Ilwaco.

The availability of phosphorus without available nitrate tends to stimulate the predominance of cyanobacteria (Andersson et al., 2015) since many of them are able to fix atmospheric nitrogen (Vahtera et al., 2007). The in-situ fluorescence data showed a peak in phycocyanin, a pigment associated with cyanobacteria, in August, when phosphate concentrations were high. Although the proportional contributions by cyanobacteria to the phytoplankton assemblages was high, the cell densities were not as high as those observed in 2017 or 2018. Cyanobacteria blooms have been regularly observed in off-channel habitats during the mid to late summer months throughout the duration of the Ecosystem Monitoring Program (Sagar et al., 2016, Hansen et al., 2017), and each year of observations contributes to a better understanding of factors that control the initiation and development of blooms in these habitats. It is interesting to note that although cyanobacteria blooms tend to be associated with high temperatures (Paerl and Huisman, 2009, Paerl et al., 2013), the blooms observed during the warmest of recent years (2015) was associated with species that were not toxin-producing (i.e., *Merismopedia*, Tausz, 2015, Peterson et al., in prep.). In 2019, river flows and nutrient concentrations were not as high as in previous years; thus, while temperatures were favorable for the development of cyanobacteria blooms-and the proportional contributions to the total assemblage were high-the absolute densities were likely limited by low fluxes of nutrients to the system. This highlights the interplay between species composition and environmental conditions that influence the development of blooms, especially nutrient supply, temperature, and transport and colonization of organisms. Since nutrient supply to the lower Columbia River appear to come from different sources, including particulate matter (phosphorus), direct inputs from tributaries (nitrogen; especially from the Willamette), and the ocean (nitrogen or phosphorus, depending on the season; especially at Ilwaco), it is important to better understand how temporal patterns in nutrient supply influence the timing and magnitude of phytoplankton blooms, especially when they are dominated by noxious species such as toxin-producing cyanobacteria.

Outside of the warm summer months, the phytoplankton assemblage at Whites Island and Welch Island tends to be dominated by diatoms, with *Asterionella formosa* repeatedly being most abundant in the early

part of the period of spring growth, while other diatoms, including *Skeletonema potamos* increased in abundance later in the year. *S. potamos* is a species typically associated with warmer waters; this species was present in high abundance in 2015 and was observed during the summer months during most years. In 2019, *S. potamos* was observed in relatively high abundance in May at Whites Island and in June at Welch Island and Campbell Slough, but was not observed at Franz Lake Slough, nor at Ilwaco. In each of the years between 2009 and 2019, *A. formosa* has constituted the early succession species that initiates the spring bloom in the river (Maier, 2014, Maier and Peterson, 2017, Maier et al., in review). This species is prone to heavy parasitism by flagellated chytrid fungi in the river mainstem (Maier and Peterson, 2014); the degree to which shallow water habitats with longer residence time influence rates and prevalence of parasitism upon primary producers that fuel aquatic food webs is currently being investigated (Cook and Peterson, unpubl. data). Since parasitism is often dependent on temperature (Ibelings et al., 2011), it is likely that periods of higher temperature would have a different prevalence of parasitism and thus influence carbon cycling and transfer through the lower food web.

Analysis of relationships between environmental variables and phytoplankton assemblages revealed that high relative proportions of diatoms are associated with high concentrations of dissolved oxygen and high dissolved oxygen saturation relative to the atmosphere. Diatom growth is also associated with a reduction in nutrient concentrations (accomplished through drawdown associated with growth). High dissolved oxygen saturation and low-to-moderate nutrient concentrations are indicative of good water quality. Diatoms tend to dominate in the spring months, where populations can get quite large; most of the annual growth of phytoplankton occurs in the spring and is accomplished by diatoms (Maier and Peterson, in prep.).

According to a Bayesian Inference stable isotope mixing model, phytoplankton carbon contributes to the juvenile salmonid food web as part of the diet of chironomid prey, based on stable isotope signatures of carbon; this carbon is incorporated as particulate organic matter and as periphyton (attached organisms). Models looking at how different sources of primary production contribution to additional prey sources are being investigated as more data are gathered, but analysis thus far suggests that periphyton constitutes an important source of organic matter for the preferred prey of juvenile salmonids (i.e., amphipods and chironomids). Estimates of dietary contributions from different prey items inferred from stable isotope mixing models suggest that juvenile salmonid growth is supported by amphipods, chironomids, and other crustacean prey, which is consistent with observations derived from stomach analysis.

4.3.2 Zooplankton

Zooplankton assemblages differ along the spatial gradient from Ilwaco Slough to Franz Lake Slough and over time from early spring to summer. Ilwaco Slough is consistently dominated by copepods, with inputs from rotifers, but very few cladoceran taxa. At the other sites, copepods generally dominated the zooplankton assemblages. At Welch Island and Whites Island, there was an increase in the proportional contribution by cladocerans from spring to summer in each of 2017, 2018, and 2019. At Campbell Slough and Franz Lake Slough, an increase in the proportional contribution of cladocerans was observed from March to June; however, by July, the relative proportions of cladocerans decreased at both sites in 2017 and 2018.

4.4 Macroinvertebrates

We examined trends in the availability of major juvenile Chinook salmon prey taxa, including amphipods, dipteran flies, cladocerans, and copepods. Amphipod abundance in benthic core samples was greatest at

Ilwaco Slough. Relatively few amphipods were collected from Welch Island and Whites Island, although 2020 Welch Island benthic samples had the highest amphipod contribution to date. Amphipods were typically not present in the furthest upriver sites, Campbell Slough and Franz Lake. The distribution of benthic invertebrates in the environment is not uniform, and high variation has occurred among benthic samples. Regardless, the pattern of declining abundance in amphipods upriver is consistent over time and is also reflected in the diets of juvenile Chinook salmon.

Benthic dipteran larvae abundances have been variable, yet typically low across sites and years. In contrast, with the exception of 2020, dipterans have higher contributions to neuston tow samples, and greatest peaks, at higher reach sites. Campbell Slough and Franz Lake have lower connectivity to the mainstem, especially during low water periods, and aquatic insects, like chironomids and other dipterans, may be retained more within these sites than at more open sites like Ilwaco Slough and Welch Island. The extent of invertebrate export from tidal marsh systems is influenced by the size and geomorphology of wetland channels as well as the energy associated with oscillating water levels and velocities. Connectivity to the mainstem is likely a factor in the potential for fluvial export of wetland insects and may help explain the disconnect between our benthic and neuston sampling. Continued monitoring of patterns in benthic and neuston dipteran densities at the trend sites will help inform the complexity of prey availability in these tidal wetlands. There were no 2020 dipteran density peaks, which is likely due to the shortened sampling season.

In Pacific Northwest estuaries, including the Columbia River estuary, juvenile Chinook salmon diet composition is typically dominated by amphipods and dipterans (Simenstad et al. 1982, Lott 2004, David et al. 2016). The EMP study has consistently described a dietary transition from wetland insects to amphipods as juvenile Chinook salmon grow and move toward the estuary mouth. Beginning in 2017, however, Campbell Slough juvenile salmon diets have transitioned more to cladocerans relative to previous years, when they typically consumed Chironomidae and other dipteran taxa. A 2020 sampling peak that exceeded 1100 cladocerans per meter towed may be similar to a 2017 peak (1200 individuals per meter towed) that occurred after a spike in Chlorophyll a concentration caused substantial increases in zooplankton abundance (Kidd 2017).

2020 multivariate analyses corroborated previous annual reports of juvenile salmon diets consisting mostly of amphipods and dipterans, with higher contributions of cladocerans at Campbell Slough. Conditions affecting the growth potential of juvenile Chinook salmon, including prey availability, varies over both spatial and temporal scales in the estuary. For the fish, habitat opportunity metrics including site accessibility, temperature, water depth, and salinity interacts with habitat capacity metrics such as prey availability, competition, and predation to determine salmon feeding success, growth, and survival (D. Bottom et al. 2005). Examining average metabolic costs and energy assimilation may allow us to evaluate habitat quality across various time scales by informing us how habitat changes at the scale of a single juvenile Chinook migration season, or at the scale of years. The method may also be useful in comparing among different sites to understand where salmon experience relatively good or poor growing conditions. For example, salmon sampled from a new restoration site could be plotted along with the longterm averages from the trend sites to provide an evaluation of the new habitat relative to other areas in the estuary.

4.5 Fish

In 2021, fish community composition was sampled at five trend sites—Ilwaco Slough, Welch Island, Whites Island, and Campbell Slough and Franz Lake. There is much overlap in overall species composition at all five trend sites with specific attributes that either separate or link sites in terms of similarity. Ilwaco stands apart with a greater influence of marine species while Welch and Whites Islands

tend to resemble each other and overlap Ilwaco and the upriver sites at Campbell Slough and Franz Lake. The catches at Welch and Whites Islands are composed primarily of native species and most often are dominated by a single species (Threespine stickleback), however, Chinook salmon can also dominate numerically as in 2020 and 2021 at White Island. Catches at Campbell Slough and Franz Lake most often have the highest values of species richness and diversity. The increased species diversity in the upper reaches of the estuary is primarily driven by non-native species, many of which have mature stages that could prey upon juvenile salmon. The greater proportion of non-natives species in this part of the estuary and river is likely due to several factors including reduced marine influence, summer water temperatures, and the predominance of back water sloughs connected to the mainstem through tide gates and water control structures. Studies have shown that these areas can be hotspots for non-native species and foster environmental conditions, such as high temperature and low dissolved oxygen, which many non-native species can tolerate (Scott et al. 2016, McNatt et al. 2017).

Patterns of salmon species composition vary by year and more strongly by site. While Chinook salmon are the most prevalent salmonid observed at four of the five sites, chum is the dominant salmonid observed at Ilwaco. Coho are observed at higher frequencies at Franz Lake than all other sites, but Chinook are still numerically dominant at Franz Lake. Chinook salmon are more abundant than any other salmonid species at Welch and Whites Islands, Campbell Slough, and Franz Lake. The majority of Chinook caught at all sites are unmarked fry and fingerlings except at Campbell Slough where the proportion of unmarked and marked fish varies. Highest densities of unmarked Chinook salmon are observed at Welch Island except in 2021 when highest densities were observed at Whites Island. Abundance and density of Chinook increases seasonally from February and peaks in April-May for unmarked Chinook, and May for marked Chinook. These findings support the results of other studies of juvenile salmon use in the lower river and estuary (Bottom et al. 2011, McNatt et al. 2016, Roegner et al. 2012, Sather et al. 2016). The lack of Chinook at Ilwaco Slough is consistent across years yet difficult to explain. It is possible that prevailing currents cause smolts to bypass the area or that the site's location adjacent to a vast mud flat limits juvenile salmon access to later stages of incoming tides. One noteworthy exception to this pattern is February of 2020 when 29 Chinook were captured at Ilwaco. This "anomaly" serves as a reminder that our samples are merely snapshots of fish abundance and distribution at specific points in time and variability is high. For example, in 2021 no salmonids were observed at Ilwaco despite three completed beach seine sets each sampling date. Coho abundance at Franz Lake is variable. Most coho are unmarked fingerling or yearling-sized fish, with exceptions in 2008-2009 when large numbers of marked coho were observed in May. Unmarked coho at Franz Lake are observed throughout the season with a notable peak in December of 2011.

Site-specific trends in the stock composition are evident. Unmarked West Cascade fall are the predominant stock of Chinook observed at Welch and Whites Islands. These sites are located downstream of tributaries such as the Lewis, Kalama, and Cowlitz rivers, which produce large numbers of West Cascade fall stock. Franz Lake is located upstream of West Cascade fall tributaries, and this is reflected in the higher percentage of interior and Spring Creek Group stocks observed there. The greatest diversity of stocks is located at Campbell Slough in Reach F, where salmon from interior Columbia Basin, Willamette River, and lower river stocks converge. Results from this study support the findings of Teel et al. (2014) who sampled hydrogeomorphic reaches throughout the estuary and found the greatest diversity of stocks in Reaches E and F. Specific to 2020, five Chinook of mid and upper Columbia spring stock were observed at Franz Lake. Previous observations of this endangered stock at EMP trend sites are rare. In 2019 two marked individuals were captured at Campbell Slough and in 2011 one unmarked individual was captured at Whites Island. The reason for this increase is unknown, but patchiness in the distribution of the stock coupled with coarse temporal sampling frequency (monthly) could play a role, whereby in previous years we may have missed individuals of this stock. Additionally, the spring Chinook observed in 2020 were captured at Franz Lake during February and were yearling sized. This pattern could indicate

the use of this floodplain lake habitat by mid and upper Columbia River spring Chinook for overwintering.

Spring Creek group stock dominates catches of marked Chinook at Campbell Slough and Franz Lake in the upper portions of the estuary. This is likely due to the close proximity to, and a large number of hatchery fish of this stock released from hatcheries just above and below Bonneville Dam. Spring Creek Group stock comprise a larger percentage of marked than unmarked Chinook at Welch and Whites Islands, but West Cascade fall stocks remain the predominant stock of both unmarked and marked fish at these sites. In 2020, only two marked Chinook were collected; a marked West Cascade fall at Whites Island and a marked Willamette River Spring at Welch Island. It is not unusual to have such a low number of marked fish during February and March as most hatchery fish tend to arrive at EMP trend sites in May.

The seasonal distribution of stocks is similar to what has been found in previous studies (Roegner et al. 2012, Teel et al. 2014). West Cascade fall stock are present throughout the year. Spring Creek group stock tend to increase in proportion during April–May, concurrent with large hatchery releases, and interior stocks tend to show up beginning in April and through summer. Seasonal trends for February–March of 2020 were not dissimilar to previous years except for the presence of an interior stock (mid and upper Columbia River spring) in February.

The temporal distributions of Chinook and chum salmon indicate separation in the timing of estuary use. Chum salmon densities peak in March or early April, whereas Chinook salmon densities increase through April, peak in May, and then start to decline. This pattern of estuary use is similar to patterns of abundance found by Roegner et al. (2012). The consistency with which juvenile salmon are captured at EMP trend sites demonstrates the importance of tidal wetlands to juvenile Chinook salmon. Chinook are rearing in these areas during times of low and high flows. The predominance of Chinook salmon in tidal wetland habitats is consistent with findings of other studies within the Columbia River estuary and elsewhere (Levy and Northcote 1982, Healey 1991, Bottom et al. 2011, Hanson et al. 2017).

The abundance of food resources in tidal wetlands is a likely attractant of juvenile Chinook. This study and others have demonstrated that prey items originating from tidal wetlands are an important part of Chinook diet (Lott 2004, Maier and Simenstad 2009, Hanson et al. 2017, Weitkamp et al. 2018) and Chinook have been observed entering wetland channels against water flow during times of peak diel prey abundance (McNatt et al. 2016). Condition factors at EMP trend sites are consistent, with little variability over the years. Measures of percent lipids and triglycerides are variable over time and across sites. The value ranges of lipid content for juvenile Chinook within the Columbia River estuary (1.4–2.3%) are consistent with values observed in Chinook salmon shortly after ocean entry. Daly et al. (2010) measured percent lipid of juvenile Chinook salmon in May and June off the coast of the Columbia River and southern Washington and found average (SD) values of 1.3% (0.7), whereas other marine fishes tended to have much higher values, e.g., Liparidae = 5.8% (0.5) and Cottidae = 6.8% (1.5).

Somatic growth analyses from otoliths indicate that fish collected in this study (2005–2018, over a range of mainstem and off-channel sites, historically sampled) are growing at rates similar to or greater than what other studies in the Columbia River estuary have observed (this study: 0.54 mm/d, Chittaro et al. 2018; 0.41 mm/d, Campbell 2010; 0.23 mm/d, Goertler et al. 2016; 0.53 mm/d, McNatt et al. 2016). At off-channel sites, fish length correlated with growth rates, as larger fish grew faster than smaller fish. Chittaro et al. (2018) also found that fish collected in the upper reaches of the estuary grew at faster rates than those collected at lower reaches of the estuary. This pattern seems contrary to conventional thinking—that growth rates increase as the salmon move from colder tributary waters to warmer estuarine habitats with large capacities of prey production. A number of factors could contribute to this observation. The transition from freshwater to saltwater environments and maintaining position in an increasingly tidal

habitat may require additional energetic resources. At off-channel sites, growth rates have been consistent from 2007–2018, implying that differences in flow regimes from year-to-year have little impact on the growth rates of juvenile Chinook that utilize tidal wetlands. Of note is that otoliths sampled from 2015, which was an extreme low flow and high temperature year, were lost and not processed, so any impacts from such extreme conditions cannot be ascertained.

Additionally, as juvenile salmon pass through lower reaches of the river, the input of highly estuary-dependent stocks such as West Cascade falls increases. This could lead to density-dependent impacts on fish utilizing tidal wetlands. Given that 70% of vegetated tidal wetlands in the Columbia River estuary have been lost (Marcoe and Pilson 2017) the reduced capacity of the estuary to produce adequate prey resources may exacerbate increased competition for food.

Data from off-channel PIT detection arrays indicate that off-channel habitat is used by a wide variety of stocks and species including Chinook and coho salmon, as well as steelhead. The extent of use varies among stock. Fall Chinook typically are the most abundant in these areas and reside longer than other stocks. However, at Horsetail Creek individual steelhead have been shown to reside for several months. One caveat to off-channel use is that northern pikeminnow, a known predator of juvenile Chinook salmon has also been detected in these habitats and tend to reside for weeks to months. Thus, extended use of these habitats could increase juvenile salmon vulnerability to predation.

The ecological trade-off between predation risk and foraging opportunity in tidal wetlands, as in tributaries and the ocean, is the mechanistic driver of survival. Increases in foraging opportunities through habitat restoration and efforts to decrease predators (especially non-native predators) may help tilt the scale towards improved salmon survival.

5 Juvenile Chinook Salmon Food Web Synthesis Discussion

5.1 Introduction

The EMP has been collecting ecosystem condition data in the lower Columbia since 2005, focusing its efforts on collecting on-the-ground data from relatively undisturbed emergent wetlands to provide information about habitat structure, fish use, abiotic site conditions, salmon food web dynamics, and river mainstem conditions to assess the biological integrity of the lower river, enhance our understanding of estuary function, and support recovery of threatened and endangered salmonids. The creation and maintenance of longterm datasets are vital for documenting the history of change within important resource populations. Therefore, through this program, we aim to assess the status (i.e., spatial variation) and track the trends (i.e., temporal variation) in the overall condition of the lower Columbia River, provide a better basic understanding of ecosystem function, provide a suite of reference sites for use as endpoints in regional habitat restoration actions, and place findings from other research and monitoring efforts (e.g., action effectiveness monitoring) into context with the larger ecosystem. The synthesis below is a summary of *juvenile salmon food web* information which has been developed as part of this program from the past 12 years of data collection in the lower Columbia River.

5.2 Characterization of Salmonids in the lower Columbia River

5.2.1 Salmon Tidal Wetlands Use Patterns

All anadromous salmonids common in the Columbia River basin have been observed in tidal emergent wetland and backwater slough sites typical of the Lower Columbia Estuary Partnership's Ecosystem Monitoring Program (EMP) sites. The degree of wetland utilization varies with species and life history type. For example, species with yearling life histories, such as sockeye salmon, steelhead, and cutthroat trout, are rarely observed. However, coho salmon, which also has a yearling life history strategy, are caught in Reach H closest to Bonneville Dam. Chum salmon, which have a subyearling life history, are the second most frequent species observed. Chum have been seen at all sites, and their use of tidal wetlands peaks in April and is limited temporally from March-May.

Chinook salmon, which have both yearling and subyearling life histories, are described as the most estuary-dependent species (Healey 1982, Levy and Northcote 1982). Indeed, Chinook salmon are the predominant species observed in tidal wetlands by this study and others. Bottom et al. (2011) sampled tidal wetlands and mainstem beaches in Reaches A-B, from 2002-2008 and found distinct size-related patterns of juvenile Chinook salmon use. Wetlands were dominated by fry (<60 mm fork length) and fingerlings rarely larger than 90 mm, while a larger range of sizes were sampled at beach sites. Further upriver in Reaches D-E, Sather et al. (2016) also saw a wider range of size classes in mainstem beach sites versus wetland channels.

Residence data indicates that subyearling Chinook salmon may reside in tidal wetlands for extended periods. McNatt et al. (2016) marked, and PIT tagged juvenile Chinook salmon in an emergent wetland near rkm 36. While there was a wide range of residence times recorded, 33% of recaptured individuals resided for more than one week, despite being forced to exit the wetland during low tides. However, PIT tag data from tidal wetlands suggest that the size-related patterns of wetland use may be biased by gear type. McNatt et al. (2015) have observed that larger salmon from interior stocks tend to enter wetlands at high tide, implying that yearlings may be under-represented by traditional sampling methods.

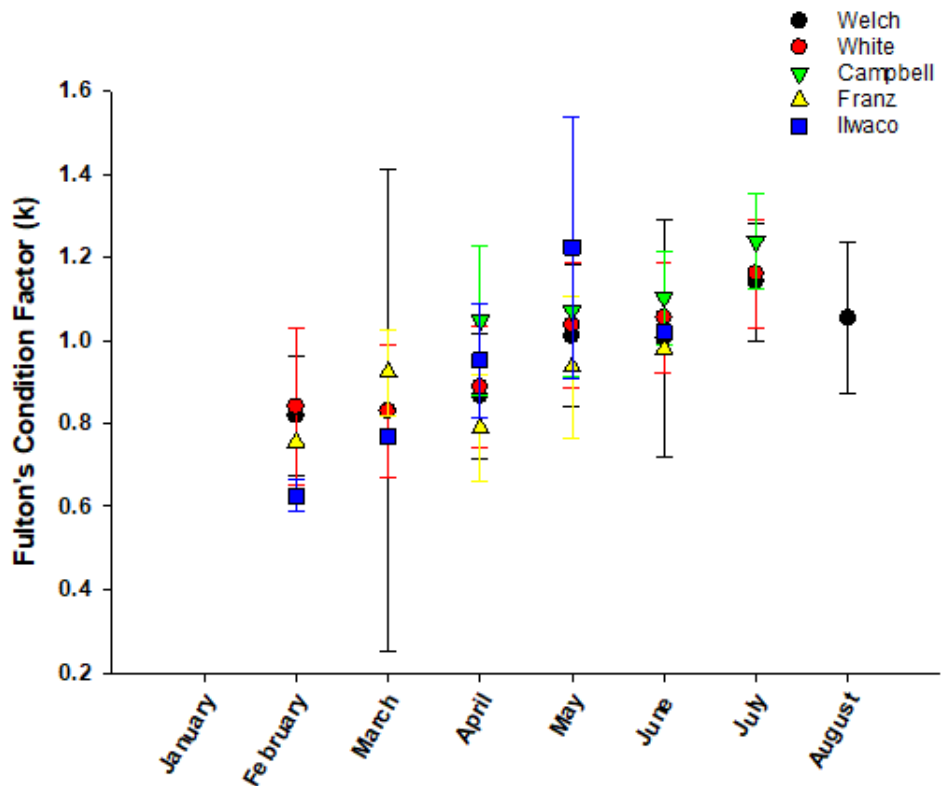
5.2.2 Fish Condition and Growth

Foraging opportunities likely attract juvenile Chinook salmon to tidal wetlands. Wetlands are productive habitats that provide a variety of ecological services (Nixon 1980, Boesch and Turner 1984, Peterson et al. 2008) In the lower Columbia River it has been estimated that up to 1 million macroinvertebrates are exported from a single wetland channel during an ebb tide and that the majority of the exported taxa are chironomids (C. Roegner, pers. comm.). Chironomids are known to be an important component of juvenile Chinook salmon diets. In the first comprehensive diet study of Columbia River juvenile Chinook salmon collected in tidal wetlands, Lott (2004) found that chironomids accounted for 85.3% of the total IRI. Since that time chironomids have been documented as a major element of juvenile Chinook salmon diets throughout the lower Columbia River and estuary (Kidd et al. 2018, Goertler et al.2016, Sather et al.2009). Juvenile Chinook salmon have been observed entering wetland channels against water flow during times of peak diel prey abundance (McNatt et al.2016) further supporting the tenet that foraging opportunities attract juvenile Chinook salmon to these habitats.

Growth and fish condition are used to measure the capacity of wetland habitats to support salmon populations. Growth rates for juvenile Chinook salmon in the estuary indicate that fish collected in this study are growing at rates similar to or greater than what other studies in the Columbia River estuary have observed (this study: 0.54 mm/d, Chittaro et al. 2018; 0.41 mm/d, Campbell 2010; 0.23 mm/d, Goertler et al. 2016; 0.53 mm/d, McNatt et al. 2016). Subyearling Chinook salmon that reside in tidal wetlands can achieve substantial growth. McNatt et al. (2016) measured increases of 20 mm for individuals that resided in a tidal wetland for 15 days or more. The condition of unmarked Chinook salmon is more variable than that of marked fish, yet, in both groups, condition increases over the course of the migration period at all trend sites (Figure 177). Limited data indicated that after July condition starts to decline, likely due to high water temperature.

Measures of performance such as condition factor and growth, coupled with residence time, indicate that tidal wetlands are productive and beneficial habitats for juvenile salmon. The abundance of prey items and refuge from piscine predators and high flows creates beneficial rearing habitat to allow juvenile salmon to grow and adjust to an increasingly marine environment as they migrate seaward.

Unmarked Chinook Condition By Month



Marked Chinook Condition by Month

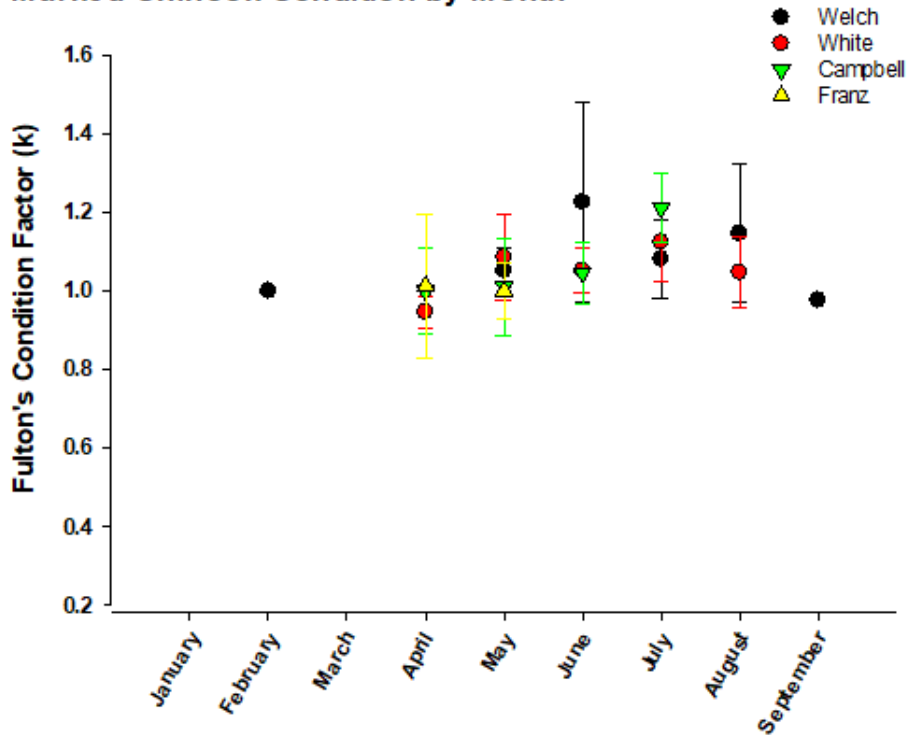


Figure 177. Monthly mean (SD) Fulton's condition factor of unmarked and marked Chinook Salmon, 2008-2017.

5.3 Characterization of Salmonid Prey Conditions in the lower Columbia River

5.3.1 Juvenile Salmon Prey and Diet

While there may be considerable diversity of prey taxa in juvenile Chinook diets overall, the EMP study has consistently identified two main prey items consumed by juvenile Chinook salmon collected at the emergent wetland and backwater slough trends sites. These taxa, the crustacean order Amphipoda and the insect order Diptera dominate consumption patterns quantified by the Index of Relative Importance (IRI). A third prey item, the order Cladocera (water fleas), dominated prey in 2017 and 2020 Campbell Slough IRIs and the 2020 Welch Island IRI.

Since 2015, prey have been identified to a lower taxonomic level than in previous years, and this revealed that the two species in the genus *Americorophium* (*A. salmonis* and *A. spinicorne*) accounted for 93% and 88% of the total counts and wet weights, respectively, of amphipods in Chinook diets. *Americorophium* spp. are estuarine amphipods, commonly found in brackish to freshwater environments. They build tubes in sand and mud flats and adjoining shallow water habitats that are intermittently exposed with the tide along larger channels in emergent marshes and along the mainstem river. *Americorophium* becomes available as prey for juvenile salmon and other fish when they leave their burrows to migrate or as part of reproductive behavior (e.g., males looking for mates, Davis 1978, Wilson 1983).

Chironomidae are a food source for a wide range of predators throughout their life cycle (Armitage 1995). They have comprised 90% of both the counts and wet weights of order Diptera in EMP juvenile Chinook diets. The family is regularly reported as the dominant insect group from wetland and estuarine systems, including the lower Columbia River (Stagliano et al. 1998, Williams and Williams 1998, Lott 2004, Ramirez 2008). They are diverse, with estimates as high as 15,000 species, and the most widespread of all aquatic insect families, occurring on all continents (Ferrington 2008). Some taxa can tolerate diverse climates and water quality conditions (Cranston 1995, Ferrington 2008). A study on chironomid distribution in an emergent marsh of the Columbia River estuary showed that abundance peaked in mid-June with temporal and microhabitat patterns in distribution driven by three dominant genera (Ramirez 2008). These genera exhibited microhabitat preferences within a tidal channel, but not habitat specialization. As non-specialists, these insects can adapt to a variety of conditions (Cranston 1995, Ferrington 2008). Lott (2004) found that emerging adults were the dominant life history stage appearing in the diets of juvenile Chinook salmon in shallow water wetland habitats of the Columbia River estuary. However, the EMP study found that juvenile Chinook salmon fed primarily on larval and adult stages of chironomids, specifically 73% larva, 21% adults, and 4% pupa.

Several studies have described a dietary transition from wetland insects to amphipods as juvenile Chinook salmon grow and move toward the estuary mouth (McCabe et al. 1986, Lott 2004). Juvenile Chinook salmon diets from the trends sites located further upriver and less connected sites (Campbell Slough and Franz Lake), are dominated by chironomids and other wetland insects. Fish collected from Welch and Whites Island, respectively, mainly consume a combination of amphipods and chironomids or other dipteran flies, with certain years dominated by cladocerans (2017, 2020). At Ilwaco Slough near the estuary mouth, juvenile Chinook feed almost exclusively on amphipods, except for 2020, which was dominated by dipterans during the shortened sampling season. According to stable isotope signatures of carbon and nitrogen (Peterson and Fry 1987, (Phillips et al. 2014), the organic matter source supporting chironomids appears to be primarily periphyton, similar to a study in which grazing larval chironomids fed on periphyton and diatoms in a shallow, hypertrophic lake in Poland (Tarkowska-Kukuryk 2013). Corophiid amphipods bore carbon isotopic signatures that were heavier on average than those of vascular plants or particulate organic matter (presumed to be dominated by fluvial phytoplankton), indicating that their primary dietary source of organic matter is heavier than either of those two sources. A likely

candidate is benthic diatoms (Maier & Simenstad 2009), although there were times when periphyton also appeared to be an important food source for corophiids.

While prey consumption patterns vary along the estuarine gradient, there is annual variation in within site consumption patterns. For example, amphipods dominated the 2015 Ilwaco Slough IRI for salmon 30 – 59 mm, while the 2020 IRI was dominated by dipterans. For the same size class, 2016 Franz Lake IRI copepods comprised the majority of the IRI, while the 2020 IRI was nearly entirely comprised of dipterans. And in 2020, cladocerans had larger contributions to Welch Island and Campbell Slough IRIs relative to previous years. 2020 and interannual instantaneous and energy rations (IR/ER) were highest at Ilwaco Slough, where prey is predominantly amphipods or dipterans. 2020 and interannual ERs were lowest at Campbell Slough, where fish were consuming energy-poor cladocerans, while IR values were similar to Welch and White Islands. This indicates the fish were consuming numbers of small-bodied cladocerans to maintain stomach fullness but were not acquiring the same number of calories compared to other sites (e.g., Ilwaco Slough).

Juvenile Chinook growth may be influenced by prey changes associated with flood and drought conditions. Goertler et al. (Goertler et al. 2018) found that juvenile Chinook in a floodplain-tidal slough complex of the Sacramento River, California, fed primarily on higher calorie aquatic-riparian insects during flood conditions and lower calorie zooplankton during drought conditions. These authors also found that drought years resulted in higher temperatures and higher metabolic costs for the salmon. More comprehensive analyses and modeling incorporating patterns in hydrology, quality, and quantity of salmon diets and prey fields, and salmon condition metrics could identify variation in realized benefits for salmon in space (EMP sites) and time (seasonal and interannual sampling).

Prey sampling methods at EMP trends sites included benthic cores and neuston tows. *Americorophium* spp. occur mainly within the sediment and are patchy in distribution. It may be informative to conduct distributional studies of *Americorophium* spp. at the trends sites to determine which microhabitats they use at each site (e.g., Bottom et al. (2011)). This would allow for refinement of sample locations for benthic cores within each site. While the distribution of amphipods has not been effectively assessed across trends sites, the sampling locations at Welch and Whites Island are within large distributary channels adjacent to intermittently exposed shallow-water habitats. These areas would presumably support greater abundances of amphipods than the backwater sloughs further upriver at Campbell Slough and Franz Lake where flats are not as well developed. Furthermore, Levy et al. (Levy et al. 1979) found chironomids were more prominent in the Fraser River estuary tidal channel diets within the marsh complex than those of mudflat and adjoining shallow-water habitats. The results from both studies highlight the importance in associating fish diets with specific locations, because small habitat shifts can alter macroinvertebrate availability and diet composition.

5.4 Characterization of Food Web Primary Productivity in the lower Columbia River

5.4.1 Marsh Plants Fuel the Salmon Food Web

The energy that supports a food web, and constrains its productivity, is provided by the system's primary producers, including plants, phytoplankton, and benthic microalgae. The productivity of invertebrate prey for salmon depends in part on the volume, quality, and timing of delivery of biomass from the marsh (Hanson et al. 2016a, Figure 178). Marsh plants provide more biomass and are a higher source of energy than phytoplankton or microalgae (Hanson et al. 2016 b). The productivity of marsh plants varies over both space and time, in response to changes in key biophysical drivers like water levels, sediment dynamics, invasive species, and other sources of stress. When plant biomass production or its quality

declines, there is less food to fuel the invertebrate food web that supports salmon. For this reason, it is important to understand the biophysical interactions that drive variation in plant productivity and how this productivity feeds into the salmonid food web. Stable isotope signatures of carbon within salmonid muscle and prey items do not provide a direct match to that of marsh plants, and therefore it is possible that degradation of plant material through microbial or fungal processing may be important to the assimilation of this high-energy material. These processes should be characterized to identify the mechanisms by which energy flows from primary production to salmonids and other ecosystem components. Elsewhere, the lability of carbon compounds within vascular plants was significantly altered through decomposition processes, increasing carbon assimilation rates later in the growing season when higher temperatures lead to higher growth rates of decomposers that include bacteria and fungi (Campeau et al., 1994).

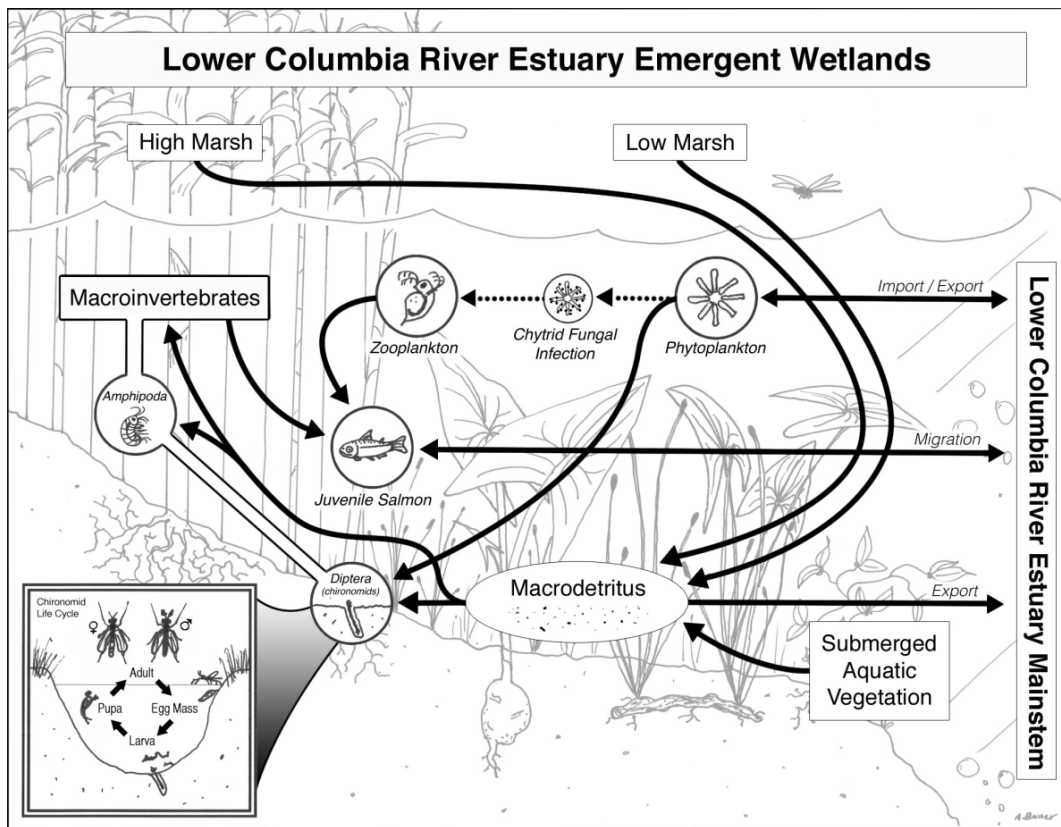


Figure 178: Conceptual model of food web interactions within Lower Columbia River emergent wetlands.

In addition to overall biomass productivity, the quality of biomass varies in ways that may affect its contribution as food for salmon prey. Low marsh plants contribute 80-93% of their annual aboveground biomass to the detrital food web, with particularly high values for *Sagittaria latifolia*, *Eleocharis palustris*, and submerged aquatic vegetation. Within the high marsh, communities that are dominated by the native sedge, *Carex lyngbyei*, contribute 68-80% of their annual aboveground biomass to the food web each year. In contrast, communities dominated by the non-native reed canarygrass, *Phalaris arundinacea*, contribute only 37-72% of their annual biomass to the food web in the same year. In addition to contributing less of its annual biomass to the detrital food web that supports salmon prey, *P. arundinacea*'s contribution is also substantially more variable. Overall, wetlands dominated by the native sedge *C. lyngbyei* contributed the highest and most consistent amount of organic material, signifying the importance of this species to the food web in the estuary.

Furthermore, there is some evidence that the non-native plant species, *P. arundinacea*, produces biomass with a higher concentration of lignin which is difficult to decompose and may reduce the proportion of annual biomass that enters the detrital food web. This potential difference in biomass quality may reduce the food available to support salmon prey. Biomass quality is a new area of investigation and may lead to new insights about the importance of adjusting restoration and management strategies to favor native wetland species.

5.4.1.1 *Plant Assemblages in Columbia River Tidal Marshes*

Many different vegetation assemblages occur in tidal marshes, but for simplicity, we generalize the major groupings into three main strata: high marsh, low marsh, and submerged aquatic vegetation (SAV). Within a site, those three categories occupy different places in the elevation spectrum, from high to low. For the purposes of this discussion, we'll focus on just the high and low marsh assemblages.

Species richness in tidal marshes ranged from 15 – 43 species in 2021, with the lower value at the downstream-most site at Ilwaco Slough and the highest value at Whites Island. In the same year, total percent cover of plants ranged from a low of 66% at Campbell Slough to a high of 153% at Welch Island. The dominant plant species throughout the estuary are shown in Table 30. The two most common species are the native sedge, *Carex lyngbyei*, and the non-native grass, *Phalaris arundinacea*, which appear to have different effects on the detrital food web that supports salmon prey.

5.4.1.2 *Key Drivers of Marsh Productivity*

There are several key biophysical drivers of marsh productivity including water levels, sediment dynamics, salinity, herbivores, and invasive species. Of these, variations in water level are the biggest driver of both the distribution and abundance of different plant species.

The depth of inundation strongly affects plant growth, as does the timing, frequency, and duration of inundation. All of these hydrologic characteristics vary annually and seasonally as the river flows change. Tidal fluctuations add a daily variable to inundation periods. At sites closer to the river mouth (Ilwaco Slough and Welch Island), tidal influence and winter storms have a stronger influence on water level dynamics than the spring freshet. The influence of the freshet increases farther upstream and contributes to a mixed set of tidal and freshet drivers at Whites Island. At Cunningham Lake and Campbell Slough, the primary driver shifts to the freshet. And finally, at the farthest upstream trend site at Franz Lake, the tidal signal is difficult to discern from the influence of dam operations. There, the marsh surface is inundated much of the time during high river levels in winter and spring. Beavers also play a role in Franz Lake water levels, elevating them in years with an active dam and lowering them when the dam is absent.

In general, marsh surface inundation times increase upriver as the influence of the winter and spring high flows increases. In addition, the inter-annual variability in inundation increases along with the relative influence of the river flows. This can be illustrated by looking at the variability in the cumulative inundation experienced by the wetlands over the course of a growing season. We do this using Sum Exceedance Values (SEV) which measure of the cumulative inundation. As can be seen in Figure 33-Figure 38 in section 3.3.1, downstream trends sites have much lower cumulative inundation periods and those periods are experienced as daily tidal flooding that lasts for a few hours at a time. These sites also show limited variability among years, regardless of river flow volume because their hydrology is dominated by the tidal signal. Farther upstream, cumulative inundation periods increase substantially as river flow comes to dominate hydrological patterns and the freshet keeps marsh surfaces flooded for days or weeks at a time. In addition, the cumulative inundation varies greatly from year to year, depending on climate impacts on river flows. These differences in inundation patterns have significant implications for plant biomass production.

5.4.1.3 *Inundation Periods Affect Marsh Productivity*

Plant species composition and productivity responds to inundation periods and to the amount of variability in inundation. In the Columbia estuary, the species composition and % cover increase in variability at upper river sites, just as inundation periods increase in variability. Furthermore, the range of variability increases with time, with the sites that have been monitored the longest having changed the most. This is a clear indicator of the importance of longterm monitoring since data from any single year tells only a small part of the story of how marsh dynamics may affect the larger food web.

In general, plant productivity declines as the inundation period increases. High marsh generally produces greater biomass than low marsh (Figure 179). This pattern is consistent in the lower estuary but becomes more variable in the upper estuary. In the upper estuary, freshet flows can inundate high marsh for extended periods of time, which can reduce productivity compared to sites closer to the river mouth (Figure 180). Low marsh is consistently flooded more often than high marsh, regardless of location in the upper or lower estuary, and there was no statistical difference in productivity in the low marsh strata between the lower and upper estuary sites.

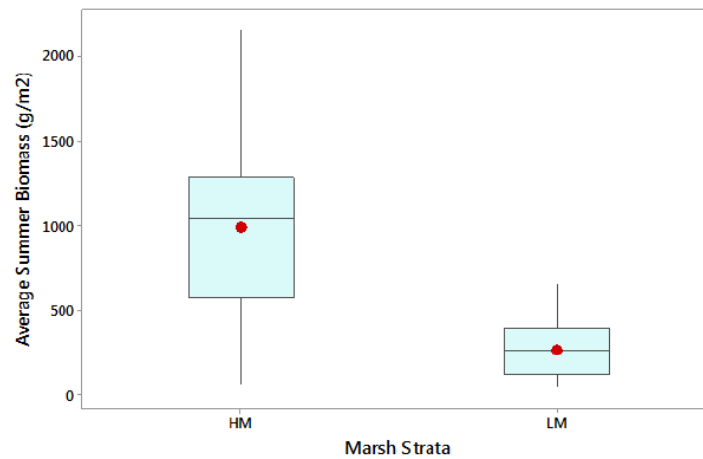


Figure 179. Overall average summer biomass (g dry weight/m²) from the high marsh (HM) and low marsh (LM) strata.

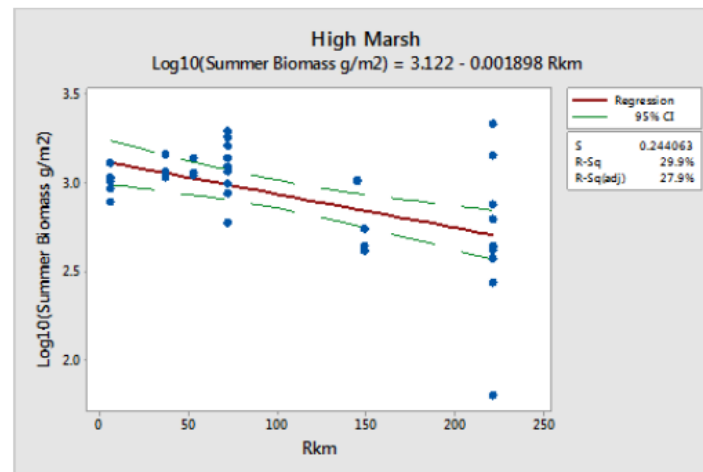


Figure 180. Average annual summer biomass (g dry weight/m²) compared to river km for the high marsh strata. Results are transformed by Log10 for statistical analysis.

Plant species differ not only in their annual biomass production, but also in the proportion of their annual production that enters the detrital food web. We estimate the organic matter contribution to the annual food web by subtracting the winter standing stock from the summer standing stock and calculating the

proportion of summer production that has been contributed. Low marsh plants contribute 80–93% of their annual aboveground biomass to the detrital food web, with particularly high values for *Sagittaria latifolia*, *Eleocharis palustris*, and SAV. Within the high marsh, communities that are dominated by the native sedge, *Carex lyngbyei*, contribute 68–80% of their annual aboveground biomass to the food web each year, averaging 882 ± 277 g dry weight/m². In contrast, communities dominated by the non-native reed canarygrass, *Phalaris arundinacea*, contribute only 37–72% of their annual biomass to the food web in the same year, averaging just 425 ± 381 g dry weight/m². In addition to contributing less of its annual biomass to the detrital food web that supports salmon prey, *P. arundinacea*'s contribution is also substantially more variable. Overall, wetlands dominated by the native sedge *C. lyngbyei* contributed the highest and most consistent amount of organic material, signifying the importance of this species to the food web in the estuary.

Macroinvertebrates have carbon isotopic signatures more similar to periphyton and the fluvial-phytoplankton-dominated particulate organic matter than to vascular and aquatic plants, suggesting that other roles in addition to direct consumption of plant material may be important in plant communities.

5.4.1.4 *Phytoplankton Distribution*

Fluvial phytoplankton distributions are strongly influenced by the hydrograph, with high flows being characterized almost exclusively by colonial diatoms in the mainstem Columbia upstream of the salt-influenced estuary (Maier 2014, Breckenridge et al. 2015). Lower in the estuary, seasonality in phytoplankton abundance and composition comes from river discharge and the seasonality in ocean influence. In general, the system is dominated by diatoms throughout much of the year and throughout most of the river (Lara-Lara et al. 1990). Through the Ecosystem Monitoring Program, we have documented the dominance of diatoms in phytoplankton assemblages at sites downstream of the Willamette-Columbia confluence; in contrast, at Campbell Slough and Franz Lake Slough, phytoplankton communities are not as strongly dominated by diatom and instead include greater proportions of chlorophytes, cryptophytes, cyanobacteria, and euglenophytes. Compared to diatoms, these latter groups tend to be smaller in size, with lower quality fatty acids that make them less nutritious to consumers than diatoms.

Although diatoms are more nutritious than other phytoplankton groups, colonial diatoms are often considered inaccessible to many grazers due to their large size; if they are not consumed, diatoms may be rapidly exported from the system in the mainstem, or else they may become deposited in back channels and sloughs within the system. An alternative pathway, however, arises when they become infected with lethal fungal parasites, called chytrids. These infections repackaging carbon from inedible, large colonial diatoms into small, nutritious zoospores which are easily consumed by zooplankton grazers. The presence of chytrid zoospores has been demonstrated in the Columbia (Maier and Peterson, 2016) and downstream increases in infection of diatom hosts demonstrates that infections actively occur during downstream transit toward the river mouth (Maier and Peterson, 2017). This process reduces export losses of carbon associated with fluvial phytoplankton and has the potential to shunt carbon into zooplankton and the salmonid food web.

Through the EMP, we have also shown that dissolved oxygen levels are influenced by the quantity of diatoms, suggesting that they have an important effect on water quality in salmonid habitats. When other types of phytoplankton dominate the assemblages and are present in high abundance, pH levels and dissolved oxygen concentrations can become unsuitable for salmonids and other aquatic organisms, underscoring the important role that aquatic microbiota play in determining water quality and habitat characteristics.

Prior to the spring freshet, colonial diatoms dominate the phytoplankton assemblage, with high similarity among all sites except Ilwaco Slough (Hanson et al. 2016, Hanson et al. 2017). At Ilwaco Slough, the phytoplankton assemblage contains a significant proportion of benthic diatoms, which have been resuspended in the water column. At the other sites, the spring freshet dilutes populations of phytoplankton, leading to lower abundances during that period. Once water levels begin to decrease, phytoplankton populations once again increase, and the loss of connectivity to the mainstem at Campbell Slough and Franz Lake Slough result in the development of distinct phytoplankton assemblages characterized by higher proportions of flagellate taxa, including chlorophyte, cryptophyte, and chrysophyte algae. These algal groups are less nutritious than are diatoms, likely resulting in a less high-quality organic matter source supporting consumers such as microzooplankton and macrozooplankton. In addition, at both of these sites, cyanobacteria populations increase as temperatures rise, often resulting in noxious blooms (Sagar et al. 2015, Tausz 2015, Hanson et al. 2016, Hanson et al. 2017).

5.5 Conclusions

Despite the number of research studies completed in the lower Columbia River and estuary that provided valuable habitat data (focused mainly in Reaches A and B), the EMP is currently the only longterm monitoring program that consistently collects longterm habitat data in the lower river from the mouth to the upper, freshwater reaches. Data collected under the EMP provides context for action effectiveness monitoring results and EMP sites often act as reference sites to which habitat restoration sites are compared. These longterm observations are valuable for capturing the range of annual variability of environmental conditions, and the longer the monitoring program is implemented, the more descriptive the dataset becomes. This longterm data set provides a basis for evaluating how future environmental fluctuations predicted to be associated with climate change may impact salmonid habitat and food web dynamics. Future EMP research will focus on synthesizing these environmental observations and identifying how shifting climatic, and habitat conditions will impact the salmonid food web.

6 Adaptive Management & Lessons Learned

Habitat restoration practitioners look to the best available science to inform restoration design. Despite the number of research studies completed in the lower Columbia River and estuary that provided valuable habitat data (focused mainly in Reaches A and B), the EMP is currently the only longterm monitoring program that consistently collects longterm habitat data in the lower river from the mouth to the upper, freshwater reaches. Information provided under the EMP provides context for action effectiveness monitoring results and EMP sites often act as reference sites to which habitat restoration sites are compared. Longterm observations are essential for capturing the range of and potential drivers of annual variability in environmental conditions, and the longer a monitoring program is implemented, the more descriptive the dataset becomes.

The lower river and estuary provide rearing and refugia habitat for juvenile salmonid stocks originating from across the Columbia River basin. Longterm monitoring of the various stocks that use lower river habitats, migration timing through the lower river, and the extent to which salmonids use these habitats is valuable information for resource managers. Tracking fish habitat use in conjunction with abiotic variables at reference sites provides information about conditions necessary for juvenile salmon survival and, in turn, can inform habitat restoration design. In addition, EMP data track annual patterns in fish presence, size, condition, growth, and diet of juvenile salmon during their migration period. These patterns vary according to genetic stock, life history type, and whether the fish is marked or unmarked (e.g., marked fish catches correspond to the timing of hatchery releases). Such monitoring data can be used to track how fish from these different groups utilize lower river habitats during this critical time of their life cycle. However, new data suggest that the current sampling methods (specifically the timing of fish collection with respect to the tidal cycle) may not be fully inclusive of all life history types, with yearlings potentially being underrepresented in catches. The lack of new sampling methods also results in low to no catches in Franz Lake, which is a unique EMP site based on its abiotic conditions and plankton assemblages. Efforts to conduct additional sampling across the tidal range and at high tide may produce results that differ from those derived using traditional methods and provide additional information to further explore the influence of tidal ranges.

Non-native fish species are consistently caught throughout all reaches of the lower river and estuary. It is unclear to what degree non-natives compete with juvenile salmon for resources such as food and space. Juvenile Chinook salmon consume a wide range of prey functional groups from benthic to pelagic to terrestrial-derived. As such, there is a high likelihood that prey items consumed by juvenile Chinook salmon overlap with prey items consumed by non-native species. A comprehensive examination of diet contents of non-native fish that overlap spatially and temporally with juvenile Chinook salmon would help illuminate some of these interactions that may have a substantial impact of juvenile salmon foraging success. Additionally, some non-native fish species, such as smallmouth bass and yellow perch, are predators of juvenile salmon in their adult form. Management options for controlling the numbers of these predators need to be explored.

Non-native species can pose risks to native species (e.g., increasing competition for resources, predation, the introduction of disease, reducing biodiversity, altering ecosystem function). For example, reed canarygrass (*Phalaris arundinacea*) is known to out-compete native wetland plants, and above-ground biomass data indicate that this species does not contribute the same quantity and quality of macrodetritus to the system as native species. Wetland plant distribution is highly dependent on elevation and hydrology, thus vegetation community structure and % cover can vary from year-to-year based on river discharge patterns. Longterm vegetation monitoring in emergent wetlands offers valuable information to managers seeking to control non-native plant species by helping them predict how vegetation at a recently

restored site will respond to annually fluctuating river flows. These data are especially critical when trying to evaluate if restoration actions used to control *P. arudinacea* have been successful or if *P. arudinacea* abundances are changing due to natural variability.

Physical, biogeochemical, and ecological habitat characteristics across varied hydrologic years may offer insight into how environmental factors (e.g., water temperature, dissolved oxygen levels) play into the survival success of juvenile salmon. Unsuitable conditions in off-channel habitats can have negative implications for rearing juvenile salmon. Water temperatures in 2019 were higher than 2018 during late spring and summer; so were the average number of days where water temperatures exceeded relevant thresholds for salmon survival. Similar observations were made in 2015 and 2016, which were dry years, with low discharge freshets. River discharge for 2019 were generally low, similar to 2015, except for high freshet flows observed in April. These conditions, in combination with patterns observed over the past decade indicate a shift in climate patterns, which needs to be explored further.

Water quality can vary within a watershed based on season and location. Even though the EMP sites are considered to be relatively undisturbed, our results indicate that water quality values sometimes exceed water quality standards and could pose a risk to aquatic organisms. In addition, connectivity between off-channel areas and the mainstem river is important for flushing and exchange of biotic and abiotic material. In poorly flushed sites, water chemistry characteristics such as very low dissolved oxygen and high chlorophyll concentrations may cause hypoxic conditions that are harmful to aquatic life, as well as nutrient inputs that can trigger further algae growth, including the proliferation of cyanobacteria.

Based on EMP data collected over the last several years, there are a number of potential threats to the survival and growth of salmonids associated with poor water quality. For example, over the last several years, the tidal intrusion of ocean waters in Baker Bay at Ilwaco Slough in the summer months has led to increasing poor water quality in terms of dissolved oxygen saturation and pH; 2018-2021 had the greatest number of observations of hours with low dissolved oxygen over the last several years. In 2019-2021, while pH at Ilwaco slough were largely in the range of good water quality, in contrast, Campbell slough exceeded standard in June, and remained high through September. In some years, pH fluctuations have been outside of the range for good water quality, and chlorophyll concentrations have exceeded water quality standards, particularly at Franz Lake Slough (e.g., in 2017). High abundances of cyanobacteria have been consistently observed at both Campbell Slough and Franz Lake Slough during the summer months, with high abundances occurring occasionally in the spring as well. In general, these threats to water quality mainly occur in the summer months when water temperatures are highest.

To some extent, the threats can be mitigated through increase water volume and flushing; however, as atmospheric temperatures increase and snowpack declines with global climate change, high flows do not necessarily provide as strong a temperature buffer as they have in the past. Flows in 2017 were high relative to the longterm average; yet there was a higher number of days with temperatures exceeding recommended values for salmonid growth and survival compared to all years but 2015, which had both low flows and high atmospheric temperatures. When water temperatures are high despite relatively high flows, cold water refugia become extremely important for salmonids. Monitoring the water quality in the lower river provides contextual information that identifies critical times periods and locations that should be targeted for management.

Water volume and quality (temperature, dissolved oxygen, pH, nutrients, chlorophyll) are driven by river flows under the influence of climatic factors that include atmospheric temperature and precipitation patterns. Biological production at the base of aquatic food webs depends directly on some these features (e.g., water residence time, temperature, nutrients) and also influences some of these features (e.g., pH, dissolved oxygen). The growth and survival of salmonids depend on food availability—which is directly tied to primary and secondary production—and to water quality parameters that influence growth and

physiology (e.g., dissolved oxygen, pH, and temperature). We are developing models to infer the diet of juvenile salmon so that we can relate hydrologic characteristics to components of the food web to improve our ability to predict how hydrology will influence salmon production and survival. In particular, habitat restoration efforts should consider how interventions influence water retention time and volume; EMP data show that when waters have long retention times during warm periods, they are vulnerable to the proliferation of noxious phytoplankton blooms, which impairs water quality in terms of dissolved oxygen, temperature, and pH. Additionally, it is important for managers to consider future fluctuations predicted to be associated with climate change and the consequences of rising water temperatures when planning habitat projects.

There are a number of questions that emerge based on several years of observations in the lower Columbia. Some of these have been presented below. Based on the longterm dataset available, we recommend an EMP Synthesis study addressing some of these questions:

- ***How important are biogeochemical processes upstream of Bonneville Dam for the tidal freshwater estuary?*** It is unclear how conditions above Bonneville Dam influence water chemistry and plankton stocks observed downstream. Measurements of water quality and food web components from above the dam would help to determine the degree to which advection is important versus in situ processes such as growth and gas equilibration with the atmosphere.
- ***What is the importance of decomposition of organic matter by microbial organisms in determining its quality for salmon prey?*** Microbial decomposition often results in “trophic upgrading”, whereby less labile compounds are transformed through microbial metabolism to compounds that are more easily assimilated. How are these processes influenced by water chemistry, temperature, and nature of the organic matter (e.g., non-native vs. native plant species)?
- ***What factors contribute to cyanobacteria blooms in Franz Lake Slough? Do these blooms pose a problem for wildlife, and if so, what is the extent of the problem?*** Over the last few years, elevated phosphorus concentrations have been observed at Franz Lake Slough in advance of cyanobacteria blooms, although the source is unknown.
- ***How do pulses in primary production from different sources vary in space and time, and how does this influence secondary production and salmon food webs?*** The timing of availability of different sources of organic matter produced through primary production varies between pelagic phytoplankton and marsh vegetation. It would be helpful to compare the magnitude of these stocks to identify patterns that could inform food web models. In addition, pulse events, such as the production and deposition of pollen, could produce reservoirs of organic matter originating from vascular plants in the water column that is independent of detritus transport.
- ***How does prey quality and quantity vary spatially and temporally across the estuary?*** While studies have shown that emergent wetlands are important for prey production and export, accurate assessments of information on prey source in the mainstem and floodplain habitats are yet to be made in the lower Columbia River. The spatial and temporal variation of energy densities of chironomids and amphipods in these undisturbed sites of the lower Columbia River would provide an important functional tool for restoration design. Maintenance metabolism and energy ration calculations from juvenile salmon diet data, or future calculations of modeled growth, may address questions about habitat quality for juvenile Chinook salmon. High prey quality and quantity may help mitigate effects of suboptimal temperatures and hydrological conditions.
- ***How does mainstem cumulative discharge affect prey availability and juvenile salmon health and habitat use?*** Additional information is needed to explore the effect of different mainstem hydrologic conditions on the food web and habitat structure for the EMP. Since many EMP sites serve as reference sites for restoration projects, additional information about changes in habitat use and structure under various freshet conditions would help determine crucial actions in restoration design and mitigate effects of climate change.

- ***How much do specific environmental factors impact growth, fish condition, residence time, age at maturation and survival of anadromous salmonids in the estuary?*** Habitat use in the lower Columbia depends on a myriad of abiotic conditions, and a closer look into specific characteristics such as temperature, DO, discharge, etc. would provide critical information about juvenile salmonid behavior which can be used to inform landscape principles in restoration planning. Bioenergetics analysis of subyearling Chinook could be a useful tool for determining impacts of temperature, flow-based variation in food availability, and habitat availability on subyearling growth and presumed survival. (Links with topic above on discharge and prey availability).
- ***How does sediment carbon interact with Greenhouse gases in EMP Trend Sites?*** In order to understand the effects of climate change on the EMP sites, another aspect that needs to be explored further are the exchanges between carbon and greenhouse gases in emergent wetlands. While some data is available from sediment analysis, further exploration is required in terms of accretion and nutrients and carbon sequestration.
- ***How does discharge and river flow impact availability of off-channel habitat including restored areas?*** Availability of alternate migration pathways and rearing opportunities is important for building population resiliency. Impacts of climate change may limit access to rearing habitat as flows decrease. Applying habitat connectivity models used in Puget Sound to the lower Columbia River could help identify under what flows habitat connectivity is constrained or maximized throughout the entire lower river or specific reaches.

The Estuary Partnership shares results from the monitoring program with other resource managers in the region and results from this multi-faceted program are applied to resource management decisions. Results from the EMP are presented and discussed at an annual Science Work Group meeting. The Science Work Group is composed of over 60 individuals from the lower Columbia River basin representing multiple regional entities (i.e., government agencies, tribal groups, academia, and private sector scientists) with scientific and technical expertise who provide support and guidance to the Estuary Partnership. In addition, EMP results will also be shared with regional partners at various conferences throughout the year. Data are often provided to restoration practitioners for use in restoration project design and project review templates (e.g., ERTG templates). Finally, data from the EMP are used to compare and contextualize results from the Action Effectiveness Monitoring Program (see 2022 AEMR report, [link](#)). Furthermore, the Estuary Partnership is working on shifting all EMP and AEMR data into a regional database to store, share, and conduct additional, largescale synthesis analyses of these data by utilizing Tableau.

7 References

- Achord, S., R.W. Zabel, and B.P. Sandford. 2007. Migration timing, growth, and estimated parr-to-smolt survival rates of wild Snake River spring-summer Chinook salmon from the Salmon River basin, Idaho, to the lower Snake River. *Transactions of the American Fisheries Society*. 136:142-154.
- Aiken, C.M., W. Petersen, F. Schroeder, M. Gehrung, P.A. Ramirez von Holle. 2011. Ship-of-opportunity monitoring of the Chilean fjords using the pocket FerryBox. *Journal of Atmospheric and Oceanic Technology*, 28: 1338-1350.
- Akaike, H. 1973. Information theory as an extension of the maximum likelihood principle. Pages 267-281 in B. N. Petrov and F. Csaki, editors. *Second international symposium on information theory*. Akademiai Kiado, Budapest, Hungary.
- Amoros, C. and G. Bornette. 2002. Connectivity and biocomplexity in waterbodies of riverine floodplains. *Freshwater Biology* 47:761-776.
- Andersson, A., Hoglander, H., Karlsson, C., Huseby, S. 2015. Key role of phosphorus and nitrogen in regulating cyanobacterial community composition in the northern Baltic Sea. *Estuarine, Coastal and Shelf Science* 164: 161-171.
- Araya, Y.N., J. Silvertown, D.J. Gowing, K.J. McConway, H.P. Linder and G. Midgley. 2010. A fundamental, eco-hydrological basis for niche segregation in plant communities. *New Phytologist* 189(1):1-6.
- Arelija Werner, Katrina Bennett, Joanna Runnells, Rick Lee, & David Rodenhuis. (2007). *Climate Variability and Change in the Columbia River Basin*. 69.
- Armitage, P.D. 1995. Behaviour and ecology of adults. Pages 194-224 in P.D. Armitage, P.S. Cranston, and L.C.V. Pinder, editors. *The Chironomidae: Biology and Ecology of Non-biting Midges*. Chapman & Hall, London.
- Beechie, T., H. Imaki, J. Greene, A. Wade, H. Wu, G. Pess, P. Roni, J. Kimball, J. Stanford, P. Kiffney, and N. Mantua. 2013. Restoring salmon habitat for a changing climate. *River Research and Applications*. 29:939-960.
- Biro P.A., A.E. Morton, J.R. Post, and E.A. Parkinson. 2004. Over-winter lipid depletion and mortality of age-0 rainbow trout (*Oncorhynchus mykiss*). *Canadian Journal of Fisheries and Aquatic Science* 61:1513-1519.
- Birtwell, I. K., & Kruzynski, G. M. (1989). In situ and laboratory studies on the behaviour and survival of Pacific salmon (genus *Oncorhynchus*). *Hydrobiologia*, 188(1), 543-560.
- Bonada, N., Rieradevall, M., Prat, N., & Resh, V. H. (2006). Benthic macroinvertebrate assemblages and macrohabitat connectivity in Mediterranean-climate streams of northern California. *Journal of the North American Benthological Society*, 25(1), 32–43. [https://doi.org/10.1899/0887-3593\(2006\)25\[32:BMAAMC\]2.0.CO;2](https://doi.org/10.1899/0887-3593(2006)25[32:BMAAMC]2.0.CO;2)

- Borde A.B., V.I. Cullinan, H.L. Diefenderfer, R.M. Thom, R.M. Kaufmann, J. Sagar, and C. Corbett. 2012. Lower Columbia River and Estuary Ecosystem Restoration Program Reference Site Study: 2011 Restoration Analysis. PNNL-21433, prepared for the Lower Columbia River Estuary Partnership by Pacific Northwest National Laboratory, Marine Sciences Laboratory, Sequim, Washington.
- Borde, A.B., S.A. Zimmerman, R.M. Kaufmann, H.L. Diefenderfer, N.K. Sather, and R.M. Thom. 2011. Lower Columbia River and Estuary Restoration Reference Site Study: 2010 Final Report and Site Summaries. PNWD-4262, prepared for the Lower Columbia River Estuary Partnership by the Battelle Marine Sciences Laboratory, Sequim, Washington.
- Bottom, D.L., A. Baptista, J. Burke, L. Campbell, E. Casillas, B. Craig, C. Eaton, S. Hinton, K. Jacobson, D. Jay, M.A. Lott, R. McNatt, G.C. Roegner, S. Schrode, C.A. Simenstad, S. Spilseth, V. Stamatiou, D. Teel, and J.E. Zamon. 2011. Salmon life histories, habitat, and food webs in the Columbia River estuary: final report 2002–2008. Report by the National Oceanic and Atmospheric Administration Fisheries, Fish Ecology Division to the U.S. Army Corps of Engineers, Portland District, Contract W66QKZ20374382, Portland, Oregon. Available: <http://nwfsc.noaa.gov/publications/scientificpubs.cfm>.
- Bottom, D.L., C.A. Simenstad, J. Burke, A.M. Baptista, D.A. Jay, K.K. Jones, E. Casillas, and M. Schiewe. 2005. Salmon at River's End: The Role of the Estuary in the Decline and Recovery of Columbia River Salmon. U.S. Department of Commerce, National Oceanic and Atmospheric Administration, Technical Memorandum NMFS-NWFSC-68, Northwest Fisheries Science Center, Seattle, Washington.
- Breckenridge, J.K., S.M. Bollens, G. Rollwagen-Bollens, and G.C. Roegner. 2015. Plankton assemblage variability in a river-dominated temperate estuary during late spring (high-flow) and late summer (low-flow) periods. *Estuaries and Coasts* 38:93-103.
- Burke, B.J., W.T. Peterson, B.R. Beckman, C.A. Morgan, E.A. Daly, M. Litz. 2013. Multivariate models of adult Pacific salmon returns. *PLoS ONE* 8(1):e54134.
- Burnham, K.P. and D.R. Anderson. 2002. Model selection and multimodel inference: a practical information-theoretic approach. Springer-Verlag, New York.
- Caffrey, J.M. 2004. Factors controlling net ecosystem metabolism in U.S. estuaries. *Estuaries* 27:90-101.
- Campbell, L. A. 2010. Life histories of juvenile Chinook Salmon (*Oncorhynchus tshawytscha*) in the Columbia River estuary as inferred from scale and otolith microchemistry. Master's thesis, Oregon State University, Corvallis.
- Cayan, D. R., S. A. Kammerdiener, M. D. Dettinger, J. M. Caprio, and D. H. Peterson (2001), Changes in the onset of spring in the western United States, *Bull. Am. Meteorol. Soc.*, 82, 399–415
- Cheung, W.W.L., R.D. Brodeur, T.A. Okey, D. Pauly. 2015. Projecting future changes in distributions of pelagic fish species of Northeast Pacific shelf seas. *Progress in Oceanography* 130:19-31.
- Chittaro, P.M., L. Johnson, D. Teel, P. Moran, S. Sol, K. Macneale, and R. Zabel. In press. Variability in the performance of juvenile Chinook salmon is explained primarily by when and where they reside in estuarine habitats. *Ecology of Freshwater Fish*.

- Chittaro, P.M., R.W. Zabel, B. Beckman, D.A. Larsen, and A. Tillotson. 2015. Validation of daily increment formation in otoliths from spring Chinook salmon. *Northwest Science* 89:93-98.
- Chust, G., J.I. Allen, L. Bopp, C. Schrum, J. Holt, K. Tsarias, K. et al. 2014. Biomass changes and trophic amplification of plankton in a warmer ocean. *Global Change Biology* 20: 2124-2139.
- Clarke, K.R. and R.M. Warwick. 1994. *Change in marine communities: An approach to statistical analysis and interpretation*. Natural Environment Research Council, London.
- Clarke, K.R. and R.N. Gorley. 2006. *PRIMER v6: User Manual/Tutorial*. PRIMER-E Plymouth.
- Cloern, J.E., Canuel, E.A., and Harris, D. (2002). Stable carbon and nitrogen isotope composition of aquatic and terrestrial plants of the San Francisco Bay estuarine system. *Limnology & Oceanography* 47: 713-729.
- Coutant, C.C. 1977. Compilation of temperature preference data. *Journal of the Fisheries Board of Canada* 34:739-745.
- Craig, J. K., & Crowder, L. B. (2005). Hypoxia-induced habitat shifts and energetic consequences in Atlantic croaker and brown shrimp on the Gulf of Mexico shelf. *Marine Ecology Progress Series*, 294, 79-94
- Cranston, P.S. 1995. Introduction to the Chironomidae. Pages 1-7 in P.D. Armitage, P.S. Cranston, and L.C.V. Pinder, editors. *The Chironomidae: The Biology and Ecology of Non-biting Midges*. Chapman & Hall, London.
- D'Avanzo, C., & Kremer, J. N. (1994). Diel oxygen dynamics and anoxic events in an eutrophic estuary of Waquoit Bay, Massachusetts. *Estuaries*, 17(1), 131-139
- Daley, E.A., C.E. Benkwitt, R.D. Brodeur, M.N.C.Litz, L.A.Copeman. 2010. Fatty acid profiles of juvenile salmon indicate prey selection strategies in coastal marine waters. *Marine Biology* 157:1975–1987.
- Daly, E.A. and R.D. Brodeur. 2015. Warming ocean conditions relate to increased trophic requirements of threatened and endangered salmon. *PLoS ONE* 10(12): e0144066. doi: 10.1371/journal.pone.0144066.
- Daly, E.A., Auth, T.D., Brodeur, R.D., Peterson, W.T. 2013. Winter ichthyoplankton biomass as a predictor of early summer prey fields and survival of juvenile salmon in the northern California Current. *Marine Ecology Progress Series* 484: 203-217.
- David, A.T., C.A. Simenstad, J.R. Cordell, J.D. Toft, C.S. Ellings, A. Gray, H.B. Berge. 2016. Wetland loss, juvenile salmon foraging performance, and density dependence in Pacific Northwest estuaries. *Estuaries and Coasts* 39:767-780.
- Davis, J.S. 1978. Diel activity of benthic crustaceans in the Columbia River estuary. MS thesis Oregon State University, 170 p.
- DeLaune, Ronald D., and K. Ramesh Reddy. 2008. *Biogeochemistry of Wetlands: Science and Applications*. CRC press.

- Diefenderfer, H.L. and D.R. Montgomery. 2009. Pool spacing, channel morphology, and the restoration of tidal forested wetlands of the Columbia River. U.S.A. *Restoration Ecology* 17:158–168.
- Diefenderfer, H.L., A.M. Coleman, A.B. Borde, and I.A. Sinks. 2008. Hydraulic geometry and microtopography of tidal freshwater forested wetlands and implications for restoration, Columbia River, USA. *Ecohydrology and Hydrobiology* 8(2):339-361.
- Doney, S.C., M.H. Ruckelshaus, J.E. Duffy, J.P. Barry, F. Chan, C.A. English, H.M. Galindo, J.M. Grebmeier, A.B. Hollowed, N. Knowlton, J. Polovina, N.N. Rabalais, W.J. Sydeman, and L.D. Talley. 2012. Climate change impacts on marine ecosystems. *Annual Reviews in Marine Science* 4:11-37.
- Elskus, A., T.K. Collier and E. Monosson. 2005. Interactions between lipids and persistent organic pollutants in fish. In: *Environmental Toxicology*, T.P. Mommsen and T.W. Moon (Eds), Elsevier, San Diego. pp. 119-152.
- Ferrington, L.C. 2008. Global diversity of non-biting midges (Chironomidae; Insecta-Diptera) in freshwater. *Hydrobiologia* 595: 447-455.
- Fiechter, J., D.D. Huff, B.T. Martin, D.W. Jackson, C.A. Edwards, K.A. Rose, E.N. Curchitser, K.S. Hedstrom, S.T. Lindley, and B.K. Wells. 2015. Environmental conditions impacting juvenile Chinook salmon growth off central California: An ecosystem model analysis. *Geophysical Research Letters* 42:2910-2917.
- France, R.L. 1995. Stable isotopic survey of the role of macrophytes in the carbon flow of aquatic food webs. *Vegetatio [Belgium]* 124:67-72.
- Fresh, K.L., D.J. Small, H. Kim, C. Waldbillig, M. Mizell, M.I. Carr, and L. Stamatiou. 2006. Juvenile Salmon Use of Sinclair Inlet, Washington, in 2001 and 2002. Report FRT-05-06. Olympia: Washington State Department of Fish and Wildlife.
- Fresh, K.L., E. Casillas, L.L. Johnson, and D.L. Bottom. 2005. Role of the Estuary in the Recovery of Columbia River Basin Salmon and Steelhead: An Evaluation of the Effects of Selected Factors on Salmonid Population Viability. NOAA Technical Memorandum NMFS-NWFSC-69. U.S. Department of Commerce.
- Fulton, T. 1902. Rate of growth of seas fishes. *Sci. Invest. Fish. Div. Scot. Rept.* 20.
- Gentemann, C.L., Fewings, M.R., Garcia-Reyes, M. 2016. Satellite sea surface temperature along the West Coast of the United States during the 2014-2016 Pacific marine heat wave. *Geophysical Research Letters* 44: 312-319.
- Gowing, D.J.G., C.S. Lawson, E.G. Youngs, K.R. Barber, and J.S. Rodwell. 2002. The water regime requirements and the response to hydrological change of grassland plant communities, Rep. BD1310, 98 pp., Cranfield Univ., Bedford, U.K.
- Hamlet, A.F. and D.P. Lettenmaier. 2007. Effects of 20th century warming and climate variability on flood risk in the western U.S. *Water Resources Research* 43: W06427. Doi: 10.1029/2006WR005099.

- Hamlet, A.F., M.M. Elsner, G.S. Mauger, S.Y. Lee, I. Tohver, and R.A. Norheim. 2013. An overview of the Columbia Basin Climate Change Scenarios Project: Approach, methods, and summary of key results. *Atmosphere-Ocean* 51(4):392-415.
- Hanson, A.C., A.B. Borde, J.R. Cordell, M. Ramirez, V. Cullinan, J. Sagar, E.E. Morgan, J. Toft, M. Schwartz, C.A. Corbett, R.M. Thom, 2016. Lower Columbia River Reed Canarygrass Macroinvertebrate and Macrodetritus Production Study. Prepared by the Lower Columbia Estuary Partnership for the Bonneville Power Administration. Available from the Lower Columbia Estuary Partnership, Portland, OR.
- Hanson, A.C., A.B. Borde, L.L. Johnson, T.D. Peterson, J.A. Needoba, J. Cordell, M. Ramirez, S.A. Zimmerman, P.M. Chittaro, S.Y. Sol, D.J. Teel, P. Moran, G.M. Ylitalo, D. Lomax, R. McNatt, V.I. Cullinan, C.E. Tausz, M. Schwartz, C. Gunn, H.L. Diefenderfer, C.A. Corbett. 2017. Lower Columbia River Ecosystem Monitoring Program Annual Report for Year 12 (October 1, 2015 to September 30, 2016). Prepared by the Lower Columbia Estuary Partnership for the Bonneville Power Administration. Available from the Lower Columbia Estuary Partnership, Portland, OR.
- Hanson, A.C., A.B. Borde, L.L. Johnson, T.D. Peterson, J.A. Needoba, J. Cordell, M. Ramirez, S.A. Zimmerman, P.M. Chittaro, S.Y. Sol, D.J. Teel, P. Moran, G.M. Ylitalo, D. Lomax, and C.E. Tausz, M. Schwartz, H.L. Diefenderfer, C.A. Corbett. 2016. Lower Columbia River Ecosystem Monitoring Program Annual Report for Year 11 (October 1, 2014 to September 30, 2015). Prepared by the Lower Columbia Estuary Partnership for the Bonneville Power Administration. Available from the Lower Columbia Estuary Partnership, Portland, OR.
- Healey, M. 1991. Life history of Chinook salmon (*Oncorhynchus tshawytscha*). In Pacific salmon life histories. C. Groot and L. Margolis (Eds.). UBC Press, Vancouver. 313-393.
- Herfort L., T.D. Peterson, L.A. McCue, B.C. Crump, F.G. Prahl, A.M. Baptista, V.C. Campbell, R. Warnick, M. Selby, G.C. Roegner, P. Zuber. 2011b. *Myrionecta rubra* population genetic diversity and its cryptophyte chloroplast specificity in recurrent red tides in the Columbia River estuary. *Aquatic Microbial Ecology* 62:85–97.
- Herfort L., T.D. Peterson, V. Campbell, S. Futrell, P. Zuber. 2011a. *Myrionecta rubra* (*Mesodinium rubrum*) bloom initiation in the Columbia River estuary. *Estuarine, Coastal and Shelf Science* 95:440–446.
- Houser, J. N., (Ed.) (2005). Multiyear synthesis of limnological data from 1993 to 2001 for the Long Term Resource Monitoring Program. U.S. Geological Survey Technical Report I 74.15/2:2005-T 003: 59 pp.
- Houser, J.N. and W.B. Richardson. 2010. Nitrogen and phosphorus in the Upper Mississippi River: transport, processing, and effects on the river ecosystem. *Hydrobiologia* 640:71-88.
- Ibelings, B.W., A.S. Gsell, W.M. Mooij, E. van Donk, S. Van Den Wyngaert, L.N. De Senerpont Domis. 2011. Chytrid infections and diatom spring blooms: paradoxical effects of climate warming on fungal epidemics in lakes. *Freshwater Biology* 56(4):754-766.
- Jassby, A.D., Cloern, J.E. 2000. Organic matter sources and rehabilitation of the Sacramento-San Joaquin Delta (California, USA). *Aquatic Conservation: Marine and Freshwater Ecosystems* 10: 323-352.

- Jay, D.A., A.B. Borde, and H.L. Diefenderfer. 2016. Tidal-Fluvial and Estuarine Processes in the Lower Columbia River: II. Water Level Models, Floodplain Wetland Inundation, and System Zones. *Estuaries and Coasts* 39(5):1299-1324.
- Jay, D.A., K. Leffler, H.L. Diefenderfer, and A.B. Borde. 2015. Tidal-fluvial and estuarine processes in the lower Columbia River: I. along-channel water level variations, Pacific Ocean to Bonneville Dam. *Estuaries and Coasts* 38(2):415-433.
- Johnson GE and KL Fresh (eds.). 2018. Columbia Estuary Ecosystem Restoration Program, 2018 Synthesis Memorandum. 95% draft submitted by PNNL and NMFS to U.S. Army Corps of Engineers, Portland District, Portland, Oregon. Available at: <https://www.cbfish.org/EstuaryAction.mvc/Index>.
- Junk, W. J., Bayley, P. B., & Sparks, R. E. (1989). The flood pulse concept in river-floodplain systems. *Canadian Special Publication of Fisheries and Aquatic Sciences*, 106(1), 110-127
- Kalinowski, S.T., K.R. Manlove, and M.L. Taper. 2007. ONCOR a computer program for genetic stock identification. Montana State University, Department of Ecology, Bozeman. Available: montana.edu/kalinowski/Software/ONCOR.htm.
- Kentula, M.E., R.P. Brooks, S.E. Gwin, C.C. Holland, A.D. Sherman, and J.C. Sifneos. 1992. An approach to improving decision making in wetland restoration and creation. U.S. Environmental Protection Agency, Corvallis, Oregon.
- Kidd, S. 2011. Summary of standard parameter ranges for salmonid habitat and general stream water quality. Water Quality Monitoring Grant Report, Oregon Watershed Enhancement Board, Salem, Oregon. Published July 2011.
- Kidd, S., and J. Yeakley. 2015. Riparian Wetland Plant Response to Livestock Exclusion in the Lower Columbia River Basin. *Natural Areas Journal*, October, 504–14. <https://doi.org/10.3375/043.035.0403>.
- Kidd, Sarah. 2017. Ecosystem Recovery in Estuarine Wetlands of the Columbia River Estuary. Dissertations and Theses, June. <https://doi.org/10.15760/etd.5521>.
- Kozloff, E.N. 1996. *Marine Invertebrates of the Pacific Northwest*. Seattle: University of Washington Press. 511 pp.
- Lara-Lara J.R., B.E. Frey, and L.F. Small. 1990. Primary production in the Columbia River Estuary I. Spatial and temporal variability of properties. *Pacific Science* 44:17-37.
- Larned, S. T., Datry, T., & Robinson, C. T. (2007). Invertebrate and microbial responses to inundation in an ephemeral river reach in New Zealand: Effects of preceding dry periods. *Aquatic Sciences*, 69(4), 554–567. <https://doi.org/10.1007/s00027-007-0930-1>
- Lassiter, R.R. and T.G. Hallam. 1990. Survival of the fattest: implications for acute effects of lipophilic chemicals on aquatic populations. *Environmental Toxicology and Chemistry* 9:585–595.
- Leigh, C., Sheldon, F., Kingsford, R. T., & Arthington, A. H. (2010). Sequential floods drive “booms” and wetland persistence in dryland rivers: A synthesis. *Marine and Freshwater Research*, 61(8), 896. <https://doi.org/10.1071/MF10106>

- Lewis W.M., S.K. Hamilton, M.A. Lasi, M. Rodriguez, and J.F. Saunders. 2000. Ecological determinism on the Orinoco floodplain. *BioScience* 50:681-692.
- Liao, H., C.L. Pierce, and J.G. Larscheid. 2001. Empirical Assessment of Indices of Prey Importance in the Diets of Predacious Fish. *Transactions of the American Fisheries Society* 130:583-591.
- Lindholm, T. 1985. *Mesodinium rubrum* – a unique photosynthetic ciliate. *Advances in Aquatic Microbiology* 3:1-48.
- Littell, J.S., Elsner, M.M., Mauger, G.S., Lutz, E., Hamlet, A.F., Salathe, E. 2011. Regional climate and hydrologic change in the northern US Rockies and Pacific Northwest: Internally consistent projections of future climate for resource management (Project report for USFS JVA 09-JV-11015600-039. Prepared by the Climate Impacts Group, University of Washington, Seattle.
- Lott, M.A. 2004. Habitat-specific feeding ecology of ocean-type Chinook salmon in the lower Columbia River estuary. M.Sc. Thesis. University of Washington, Seattle. 124 pp.
- Ludsin, S. A., Zhang, X., Brandt, S. B., Roman, M. R., Boicourt, W. C., Mason, D. M., & Costantini, M. (2009). Hypoxia-avoidance by planktivorous fish in Chesapeake Bay: implications for food web interactions and fish recruitment. *Journal of Experimental Marine Biology and Ecology*, 381, S121-S131.
- Lutz, E.R., A.F. Hamlet, J.S. Littell. 2012. Paleoreconstruction of cool season precipitation and warm season streamflow in the Pacific Northwest with applications to climate change assessments. *Water Resources Research* 48:W01525. Doi:10.1029/2011WR010687.
- Magurran, Anne E. 1988. *Ecological Diversity and Its Measurement*. Princeton university press.
- Maier, G.O. and C.A. Simenstad. 2009. The role of marsh-derived macrodetritus to the food webs of juvenile Chinook salmon in a large altered estuary. *Estuaries and Coasts* 32:984-998.
- Maier, M. A., & Peterson, T. D. (2014). Observations of a diatom chytrid parasite in the lower Columbia River. *Northwest Science*, 88(3), 234-245.
- Maier, M.A. 2014. Ecology of diatoms and their fungal parasites in the Columbia River. Ph.D. Dissertation, Oregon Health & Science University.
- Maier, M.A. and T.D. Peterson. 2017. Prevalence of chytrid parasitism among diatom opulations in the lower Columbia River (2009-2013). *Freshwater Biology* 62:414-428.
- Manel, S., O.E. Gaggiotti, and R.S. Waples. 2005. Assignment methods: matching biological questions with appropriate techniques. *Trends in Ecology and Evolution* 20:136-142.
- Marcoe, K. and S. Pilson. 2017. Habitat change in the lower Columbia River estuary, 1870-2009. *Journal of Coastal Conservation* 21(5):1-21.
- Marine, K.R. and J.J. Cech. 2004. Effects of high water temperature on growth, smoltification, and predator avoidance in juvenile Sacramento River Chinook salmon. *North American Journal of Fisheries Management* 24:198-210.

- Mason, W.R.M. 1993. Chapter 5: Key to superfamilies of Hymenoptera. In: H. Goulet and J.T. Huber (eds.). *Hymenoptera of the world: an identification guide to families*. Centre for Land and Biological Resources Research, publication 1894/E:65-101, Ottawa, Ontario.
- McCabe, G.T., Jr., R.L. Emmett, W.D. Muir, and T.H. Blahm. 1986. Utilization of the Columbia River estuary by subyearling Chinook salmon. *Northwest Science* 60: 113-124.
- McNatt R.A., D.L. Bottom, and S.A. Hinton. 2016. Residency and movement of juvenile Chinook salmon at multiple spatial scales in a tidal marsh of the Columbia River Estuary. *Transactions of the American Fisheries Society* 145:774-785.
- McNatt RA, B Cannon, SA Hinton, LD Whitman, R Klopfenstein, TA Friesen, DL Bottom. 2017. Multnomah Channel Wetland Restoration Monitoring Project. Report prepared by NMFS and ODFW for Sustainability Center, Oregon Metro Natural Areas Program, Portland, Oregon.
- Merritt, R.W. and K.W. Cummins (eds). 1996. *An Introduction to the Aquatic Insects of North America*, 3rd ed. Dubuque (IA): Kendall/Hunt Publishing Company. 862 pp.
- Merz J.E. 2001. Diet of juvenile fall-run Chinook salmon in the lower Mokelumne River, California. *California Fish and Game* 87:102-114.
- Moreira-Turcq P., M-P. Bonnet, M. Amorim, M. Bernardes, C. Lagane, L. Maurice, M. Perez, and P. Seyler. 2013. Seasonal variability in concentration, composition, age, and fluxes of particulate organic carbon exchanged between the floodplain and Amazon River. *Global Biogeochemical Cycles* 27:119-130.
- Mote, P.W. 2003. Trends in snow water equivalent in the Pacific Northwest and their climatic causes. *Geophysical Research Letters* 30: 1601-1604.
- Myers, J.M., C. Busack, D. Rawding, A.R. Marshall, D.J. Teel, D.M. Van Doornik, M.T. Maher. 2006. Historical population structure of Pacific salmonids in the Willamette River and lower Columbia River basins. U.S. Dept. of Commerce, NOAA Tech. Memo., NMFS-NWFSC-73, 311 p.
- Nayak, S. K. 2010. "Probiotics and Immunity: A Fish Perspective." *Fish & Shellfish Immunology* 29 (1): 2-14.
- Neill, C. and J.C. Cornwell. 1992. Stable carbon, nitrogen, and sulfur isotopes in a prairie marsh food web. *Wetlands* 12(3):217-224.
- Netboy, A. 1980. *The Columbia River Salmon and Steelhead Trout, Their Fight for Survival*. Seattle: University of Washington Press.
- Nilsson, C., & Renöfält, B. (2008). Linking Flow Regime and Water Quality in Rivers: A Challenge to Adaptive Catchment Management. *Ecology and Society*, 13(2). <https://doi.org/10.5751/ES-02588-130218>
- Otten, T. G., Crosswell, J. R., Mackey, S., & Dreher, T. W. 2015. Application of molecular tools for microbial source tracking and public health risk assessment of a *Microcystis* bloom traversing 300km of the Klamath River. *Harmful Algae*, 46, 71-81
- Paerl H.W. and J. Huisman. 2008. Blooms Like It Hot. *Science* 320:57-58.

- Paerl, H. W., Pinckney, J. L., Fear, J. M., & Peierls, B. L. 1998. Ecosystem responses to internal and watershed organic matter loading: consequences for hypoxia in the eutrophying Neuse River Estuary, North Carolina, USA. *Marine Ecology Progress Series*, 166, 17-25
- Paerl, H.W., Huisman, J. 2009. Climate change: a catalyst for global expansion of harmful cyanobacterial blooms. *Environmental Microbiology* 1: 27-37.
- Paerl, H.W., Otten, T.G. 2013. Harmful cyanobacterial blooms: causes, consequences, and controls. *Microbial Ecology* 65: 995-1010.
- Peterson B.J. and B. Fry. 1987. Stable isotopes in ecosystem studies. *Annual Reviews in Ecology and Systematics* 18:293-320.
- Pevey, Kimberley, Gaurav Savant, Hans Moritz, and Elvon Childs. "Lower Columbia River Adaptive Hydraulics (AdH) Model : Development, Water Surface Elevation Validation, and Sea Level Rise Analysis." Engineer Research and Development Center (U.S.), April 20, 2020. <https://doi.org/10.21079/11681/36295>.
- Phillips D.I., R. Inger, S. Bearhop, A.L. Jackson, J.W. Moore, A.C. Parnell, B.X. Semmens, and E.J. Ward. 2014. Best practices for use of stable isotope mixing models in food-web studies. *Canadian Journal of Zoology* 92:823-835.
- Phillips DI, Inger R, Bearhop S, Jackson AL, Moore JW, Parnell AC, Semmens BX and Ward EJ .2014. Best practices for use of stable isotope mixing models in food-web studies. *Canadian Journal of Zoology* 92:823-835
- R Development Core Team. 2018. R: A language and environment for statistical computing. R Foundation for Statistical Computing, Vienna, Austria. ISBN 3-900051-07-0, <http://www.R-project.org>.
- Ramirez, M.F. 2008. Emergent aquatic insects: assemblage structure and patterns of availability in freshwater wetlands of the lower Columbia River estuary. M.Sc. Thesis. University of Washington, Seattle.
- Rannala B. and J.L. Mountain. 1997. Detecting immigration by using multilocus genotypes. *Proceedings of the National Academy of Sciences* 94:9197-9201.
- Reed, P.B. 1988. National list of plant species that occur in wetlands: Northwest (Region 9). Biological Report 88 (26.9). 90 p. U.S. Fish and Wildlife Service, St. Petersburg, Florida.
- Ricker, W.E. 1975. Computation and interpretation of biological statistics of fish populations. *Bulletin of the Fisheries Research Board of Canada* 191:1-382.
- Roegner, G.C., A.M. Baptista, D.L. Bottom, J. Burke, L.A. Campbell, C. Elliot, S.A. Hinton, D.A. Jay, M. Lott, T.A. Lundrigan, R.A. McNatt, P. Moran, C.A. Simenstad, D.J. Teel, E. Volk, J.E. Zamon, and E. Casillas. 2008. Estuarine Habitat and Juvenile Salmon Current and Historical Linkages in the Lower Columbia River and Estuary, 2002-2004. Report by National Marine Fisheries Service to the U.S. Army Corps of Engineers Portland District, Seattle, Washington, 139 p.

- Roegner, G.C., E.W. Dawley, M. Russell, A. Whiting, D.J. Teel. 2010. Juvenile salmonid use of reconnected tidal freshwater wetlands in Grays River, lower Columbia River basin. *Transactions of the American Fisheries Society*. 139:1211-1232.
- Roegner, G.C., H.L. Diefenderfer, A.B. Borde, R.M. Thom, E.M. Dawley, A.H. Whiting, S.A. Zimmerman, and G.E. Johnson. 2009. Protocols for monitoring habitat restoration projects in the lower Columbia River and estuary. U.S. Dept. Commer., NOAA Tech. Memo. NMFS-NWFSC-97, 63 p.
- Roegner, G.C., R. McNatt, D.J. Teel, and D.L. Bottom. 2012. Distribution, size, and origin of juvenile Chinook salmon in shallow-water habitats of the lower Columbia River and Estuary, 2002-2007. *Marine and Coastal Fisheries* 4:450-472.
- Rolls, R. J., Leigh, C., & Sheldon, F. (2012). Mechanistic effects of low-flow hydrology on riverine ecosystems: Ecological principles and consequences of alteration. *Freshwater Science*, 31(4), 1163–1186. <https://doi.org/10.1899/12-002.1>
- Sagar, J.P., A.B. Borde, L.L. Johnson, C.A. Corbett, J.L. Morace, K.H. Macneale, W.B. Temple, J. Mason, R.M Kaufmann, V.I. Cullinan, S.A. Zimmerman, R.M. Thom, C.L. Wright, P.M. Chittaro, O.P. Olson, S.Y. Sol, D.J. Teel, G.M. Ylitalo, N.D. Jahns. 2013. Juvenile Salmon Ecology in Tidal Freshwater Wetlands of the Lower Columbia River and Estuary: Synthesis of the Ecosystem Monitoring Program, 2005–2010. Prepared by the Lower Columbia Estuary Partnership for the Bonneville Power Administration. Available from the Lower Columbia Estuary Partnership, Portland, OR.
- Sagar, J.P., A.B. Borde, L.L. Johnson, T.D. Peterson, J.A. Needoba, K.H. Macneale, M. Schwartz, A. Silva, C.A. Corbett, A.C. Hanson, V.I. Cullinan, S.A. Zimmerman, R.M. Thom, P.M. Chittaro, O.P. Olson, S.Y. Sol, D.J. Teel, G.M. Ylitalo, M.A. Maier and C.E. Tausz. 2015. Juvenile Salmon Ecology in Tidal Freshwater Wetlands of the Lower Columbia River and Estuary: Synthesis of the Ecosystem Monitoring Program, Trends (2005–2013) and Food Web Dynamics (2011-2013). Prepared by the Lower Columbia Estuary Partnership for the Bonneville Power Administration. Available from the Lower Columbia Estuary Partnership, Portland, OR.
- Sagar, J.P., A.C. Hanson, A. B. Borde, L.L. Johnson, T. Peterson, K.H. Macneale, J.A. Needoba, S.A. Zimmerman, M.J. Greiner, C.L. Wright, P.M. Chittaro, O.P. Olson, S.Y. Sol, D.J. Teel, G.M. Ylitalo, D. Lomax, A. Silva and C.E. Tausz. 2014. Lower Columbia River Ecosystem Monitoring Program Annual Report for Year 9 (October 1, 2012 to September 30, 2013). Prepared by the Lower Columbia Estuary Partnership for the Bonneville Power Administration. Available from the Lower Columbia Estuary Partnership, Portland, OR.
- Sather, N.K., E.M. Dawley, G.E. Johnson, S.A. Zimmerman, A.J. Storch, A.B. Borde, D.J. Teel, C. Mallette, J.R. Skalski, R. Farr, T.A. Jones. 2009. Ecology of Juvenile Salmon in Shallow Tidal Freshwater Habitats in the Vicinity of the Sandy River Delta, Lower Columbia River, 2008. May 2009. Prepared for Bonneville Power Administration under an agreement with the U.S. Department of Energy Contract DE-AC05-76RL01830. Pacific Northwest National Laboratory, Richland, Washington 99352.
- Sather, N.K., G.E. Johnson, D.J. Teel, A.J. Storch, J.R. Skalski, V.I. Cullinan. 2016. Shallow tidal freshwater habitats of the Columbia River: spatial and temporal variability of fish communities and density, size, and genetic stock composition of juvenile Chinook salmon. *Transactions of the American Fisheries Society* 145:734-753.

- Schwartz M.S., S. Kidd, G. Brennan, A. Silva, N. Elasmr, R. Fueller, and K. Poppe. 2019. Action Effectiveness Monitoring for the Lower Columbia River Estuary Habitat Restoration Program. October 2017 – September 2018, Project Number: 2003-007-00.
- Schwartz M.S., S.A. Kidd, A.B. Borde, A. Silva, N. Elasmr, C. Kenny, and M. Vesh. 2018. Action Effectiveness Monitoring for the Lower Columbia River Estuary Habitat Restoration Program (October 2016 – September 2017). Prepared by the Lower Columbia River Estuary Partnership for the Bonneville Power Administration. Available from the Lower Columbia Estuary Partnership, Portland, OR.
- Schwing, F.B., R. Mendelsohn, S. Bograd, J.E. Overland, M. Wan, S-I. Ito. 2010. Climate change, teleconnection patterns, and regional processes forcing marine populations in the Pacific. *Journal of Marine Systems* 70: 245-257.
- Scott, D. C., M. Arbeider, J. Gordon, and J. W. Moore. 2016. Flood control structures in tidal creeks associated with reduction in nursery potential for native fishes and creation of hotspots for invasive species. *Canadian Journal of Fisheries and Aquatic Sciences* 73: 1138-1148. Seeb, L.W., A. Antonovich, M.A. Banks, T.D. Beacham, M.R. Bellinger, S.M. Blankenship, M.R. Campbell, N.A. Decovich, J.C. Garza, C.M. Guthrie III, T.A. Lundrigan, P. Moran, S.R. Narum, J.J. Stephenson, K.T. Supernault, D.J. Teel, W.D. Templin, J.K. Wenburg, S.F. Young, and C.T. Smith. 2007. Development of a standardized DNA database for Chinook salmon. *Fisheries* 32:540–552.
- Shannon, C.E. and W. Weaver. 1949. *The mathematical theory of communication*. The University of Illinois Press, Urbana, 117 pp.
- Sherwood, C.R., D.A. Jay, R.B. Harvey, P. Hamilton, and C.A. Simenstad. 1990. Historical Changes in the Columbia River Estuary. *Progress in Oceanography* 25:299-357.
- Simenstad, C.A. and J.R. Cordell. 2000. Ecological assessment criteria for restoring anadromous salmonid habitat in Pacific Northwest estuaries. *Ecol. Engineering* 15:283-302.
- Simenstad, C.A., J.L. Burke, J.E. O’Connor, C. Cannon, D.W. Heatwole, M.F. Ramirez, I.R. Waite, T.D. Counihan, and K.L. Jones. 2011. *Columbia River Estuary Ecosystem Classification—Concept and Application*: U.S. Geological Survey Open-File Report 2011-1228, 54 p.
- Simon, S.D., M.E. Cardona, B.W. Wilm, J.A. Miner, and D.T. Shaw. 1997. The sum exceedance value as a measure of wetland vegetation hydrologic tolerance. In: Macdonald, K.B. and F. Weinmann (eds). 1997. *Wetland and Riparian Restoration: Taking a Broader View*. Proceedings of Society for Ecological Restoration, 1995 International Conference, September 14-16, University of Washington, USA. Publication EPA 910-R-97-007, USEPA, Region 10, Seattle, Washington
- Sommer, T.R., M.L. Nobriga, W.C. Harrell, W. Batham, and W.J. Kimmerer. 2001. Floodplain rearing of juvenile Chinook salmon: evidence of enhanced growth and survival. *Canadian Journal of Fish and Aquatic Science* 58:325–333.
- Spilseth, S.A. and C.A. Simenstad. 2011. Seasonal, Diel, and Landscape Effects on Resource Partitioning between Juvenile Chinook Salmon (*Oncorhynchus tshawytscha*) and Threespine Stickleback (*Gasterosteus aculeatus*) in the Columbia River Estuary. *Estuaries and Coasts*. 34:159-171.

- Stagliano, D.M., A.C. Benke, and D.H. Anderson. 1998. Emergence of aquatic insects from two habitats in a small wetland of the southeastern USA: temporal patterns of numbers and biomass. *Journal North American Benthological Society* 17(1):37-53.
- Stanley, D. W., & Nixon, S. W. 1992. Stratification and bottom-water hypoxia in the Pamlico River estuary. *Estuaries*, 15(3), 270-281
- Stewart, I.T., Cayan, D.R., Dettinger, M.D. 2005. Changes toward earlier streamflow timing across western North America. *Journal of Climate* 18: 1136-1155.
- Strauss, E. A., Richardson, W. B., Bartsch, L. A., Cavanaugh, J. C., Bruesewitz, D. A., Imker, H., Heinz, J. A. & Soballe, D. M. 2004. Nitrification in the Upper Mississippi River: patterns, controls, and contribution to the NO₃-budget. *Journal of the North American Benthological Society*, 23(1), 1-14
- Takekawa, John Y., Isa Woo, Nicole D. Athearn, Scott Demers, Rachel J. Gardiner, William M. Perry, Neil K. Ganju, Gregory G. Shellenbarger, and David H. Schoellhamer. 2010. Measuring Sediment Accretion in Early Tidal Marsh Restoration. *Wetlands Ecology and Management* 18 (3): 297–305. <https://doi.org/10.1007/s11273-009-9170-6>.
- Talbot, Jennifer M., Daniel J. Yelle, James Nowick, and Kathleen K. Treseder. 2012. Litter Decay Rates Are Determined by Lignin Chemistry. *Biogeochemistry* 108 (1–3): 279–95. <https://doi.org/10.1007/s10533-011-9599-6>.
- Tarkowska-Kukuryk M. 2013. Periphytic algae as food source for grazing chironomids in a shallow phytoplankton-dominated lake. *Limnologica - Ecology and Management of Inland Waters* 43:254-264.
- Tausz, C.E. 2015. Phytoplankton dynamics in off-channel habitats of the lower Columbia River. M.S. Thesis, Oregon Health & Science University, 92 pp.
- Taylor, Barry R., Dennis Parkinson, and William F. J. Parsons. 1989. Nitrogen and Lignin Content as Predictors of Litter Decay Rates: A Microcosm Test. *Ecology* 70 (1): 97–104. <https://doi.org/10.2307/1938416>.
- Teel, D. J., D.L. Bottom, S.A. Hinton, D.R. Kuligowski, G.T. McCabe, R. McNatt, G.C. Roegner, L.A. Stamatiou, and C.A. Simenstad. 2014. Genetic identification of Chinook salmon in the Columbia River estuary: stock-specific distributions of juveniles in shallow tidal freshwater habitats. *North American Journal of Fisheries Management* 34:621-641.
- Teel, D.J., C. Baker, D.R. Kuligowski, T.A. Friesen, and B. Shields. 2009. Genetic stock composition of subyearling Chinook salmon in seasonal floodplain wetlands of the Lower Willamette River. *Transactions of the American Fisheries Society* 138:211-217.
- Thorp, J.H. and A.P. Covich. 2001. *Ecology and Classification of North American Freshwater Invertebrates*. 2nd ed. San Diego: Academic Press. 1021 pp.
- Thorpe, J. E. 1994. Salmonid fishes and the estuarine environment. *Estuaries* 17:76-93.
- Triplehorn, C.A. and N.F. Johnson. 2005. Borror and DeLong's Introduction to the Study of Insects, 7th ed. Belmont (CA): Brooks/Cole. 864 pp.

- Tyler, R. M., Brady, D. C., & Targett, T. E. 2009. Temporal and spatial dynamics of diel-cycling hypoxia in estuarine tributaries. *Estuaries and Coasts*, 32(1), 123-145
- Vahtera, E., Conley, D.J., Gustafsson, B.G., Kuosa, H., Pitkanen, H., Savchuk, O.P., Tamminen, T., Viitasalo, M., Voss, M., Wasmund, N., Wulff, F. 2007. Internal ecosystem feedbacks enhance nitrogen-fixing cyanobacteria blooms and complicate management in the Baltic Sea. *Ambio* 36: 186-194.
- van Wezel, A.P., D.A.M. de Vries, S. Kostense, D.T.H.M. Sijm, and Q. Opperhuizen. 1995. Intraspecies variation in lethal body burdens of narcotic compounds. *Aquatic Toxicology* 33:325–342.
- Venterink H.O., F. Wiegman, G.E.M. Van der Lee, and J.E. Vermaat. 2003. Role of active floodplains for nutrient retention in the river Rhine. *Journal of Environmental Quality* 32:1430-1435.
- Vigg S. and C.C. Burley. 1991. Temperature-dependent maximum daily consumption of juvenile salmonids by northern squawfish (*Ptychocheilus oregonensis*) from the Columbia River. *Canadian Journal of Fisheries and Aquatic Sciences* 48:2491-2498.
- Volk, E.C., D.L. Bottom, K.K. Jones, and C.A. Simenstad. 2010. Reconstructing Juvenile Chinook Salmon Life History in the Salmon River Estuary, Oregon, Using Otolith Microchemistry and Microstructure. *Transactions of the American Fisheries Society* 139:535-549.
- Wang, Junjing, Junhong Bai, Qingqing Zhao, Qiongqiong Lu, and Zhijian Xia. 2016. Five-Year Changes in Soil Organic Carbon and Total Nitrogen in Coastal Wetlands Affected by Flow-Sediment Regulation in a Chinese Delta. *Scientific Reports* 6 (February): 21137. <https://doi.org/10.1038/srep21137>.
- Ward J.V. and J.A. Stanford. 1982. Thermal responses in the evolutionary ecology of aquatic insects *Annual Review of Entomology* 27:97-117.
- Weitkamp, L.A. 2008. Buoyancy regulation by hatchery and wild coho salmon during the transition from freshwater to marine environments. *Transactions of the American Fisheries Society* 137:860–868.
- Weitkamp, L.A., G. Goulette, J. Hawkes, M. O'Malley, and C. Lipsky. 2014. Juvenile salmon in estuaries: comparisons between North American Atlantic and Pacific salmon populations. *Reviews in Fish Biology and Fisheries* 24:713-736.
- Williams, D.D. and N.E. Williams. 1998. Aquatic insects in an estuarine environment: densities, distribution, and salinity tolerance. *Freshwater Biology* 39: 411-421.
- Wilson, S.L. 1983. The life history of *Corophium salmonis* in the Columbia River estuary. MS thesis Oregon State University, 66 p.
- Xu H., H.W. Paerl, B. Qin, G. Zhu, and G. Gaoa. 2010. Nitrogen and phosphorus inputs control phytoplankton growth in eutrophic Lake Taihu, China. *Limnology and Oceanography* 55:420-432.
- Ylitalo, G.M., G.K. Yanagida, L.C. Hufnagle Jr., M.M. Krahn. 2005. Determination of lipid classes and lipid content in tissues of aquatic organisms using a thin layer chromatography/flame ionization detection (TLC/FID) microlipid method. In Ostrander, G.K. (Ed.) *Techniques in Aquatic Toxicology*. CRC Press, Boca Raton, FL. Pages 227-237.

8 Appendices

Appendix A. Site Maps and Habitat Change Analysis

Site maps and habitat change analysis were conducted in 2015. UAV flights have been performed between 2019-2022 and these data will be included here in a future report.









Contents:

Site Maps (most recent mapping effort; 2015 in most cases)	A.2
Table A.1. Habitat change analysis results	A.9
Habitat Change Maps.....	A.12






Baker Bay, 2015

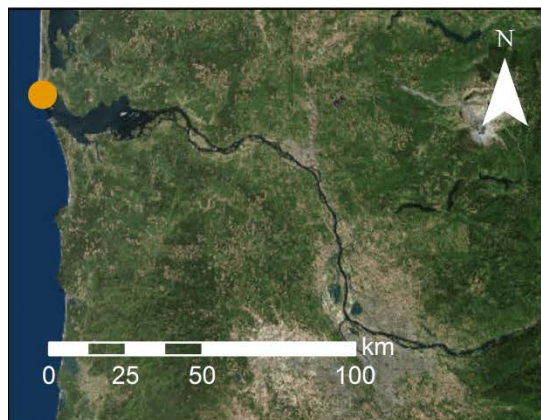
GPS Mapping

Vegetation Communities

-  Carex lyngbyei
-  Isolepis cernua
-  Scirpus americanus, Agrostis spp., C. lyngbyei (stunted)
-  Typha spp.
-  Bare ground
-  Channel
-  Mixed grass
-  Pan

Monitoring Locations

-  Cross section endpoints
-  Depth sensor
-  Photo point
-  Sediment accretion stakes
-  Vegetation/Elevation









Secret River Marsh, 2013

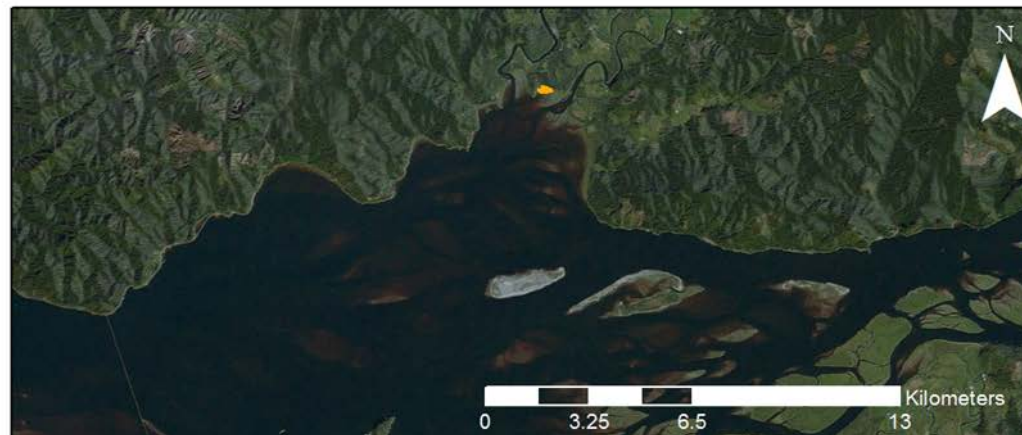
GPS Mapping

-  Bare ground
-  Carex lyngbyei/P. arundinacea
-  Channel
-  D. cespitosa and P. arundinacea
-  Deschampsia cespitosa
-  E. palustris and S. tabernaemontani
-  Lythrum salicaria
-  Mixed P. arundinacea
-  Phalaris arundinacea
-  Schoenoplectus tabernaemontani
-  Sparganium eurycarpum
-  Sparganium eurycarpum/P. arundinacea
-  Submerged aquatic vegetation



Monitoring Locations

-  Photo point
-  Depth sensor
-  Sediment accretion stakes
-  Sediment accretion stakes/Photo point
-  Cross section
-  Vegetation/Elevation Transect








Welch Island, 2012

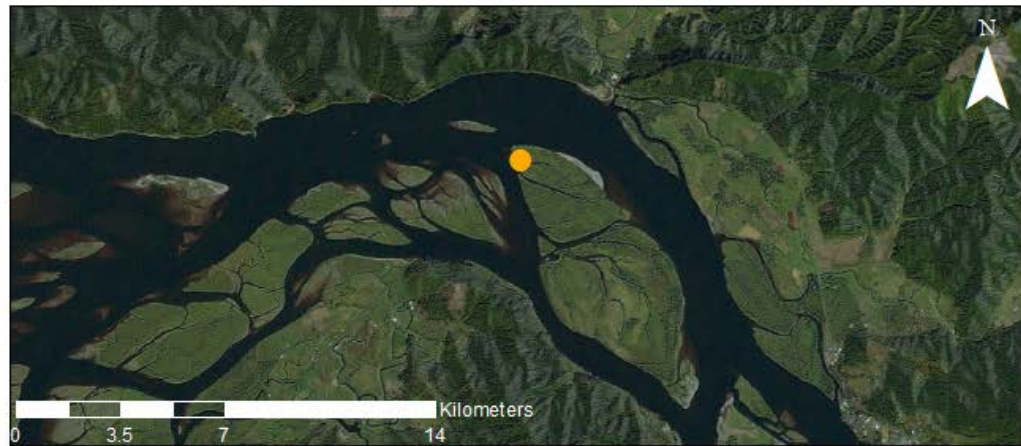
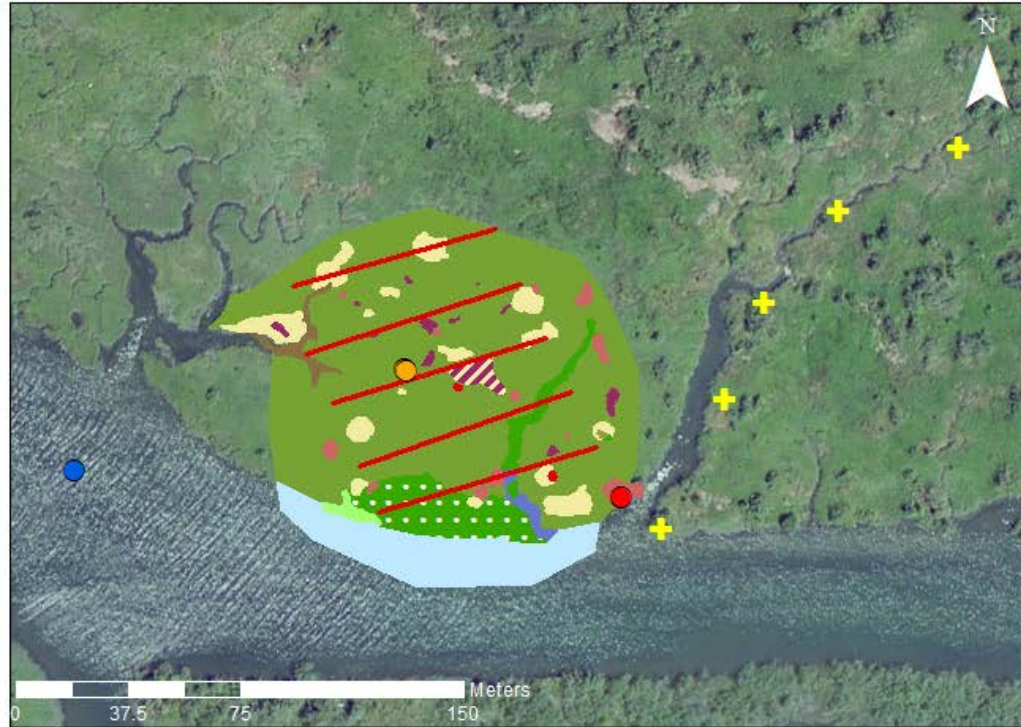
GPS Mapping

Vegetation communities

-  *C. obnupta*, *S. latifolia*
-  *Carex lyngbyei*
-  Channel
-  *Eleocharis palustris*
-  *Lythrum salicaria*
-  Open Water
-  *P. arundinacea*, *L. salicaria*
-  *P. arundinacea*, *S. latifolia*
-  *Phalaris arundinacea*
-  *S. latifolia*, *P. hydropiper*
-  *Sagittaria latifolia*
-  *Salix* spp.
-  *Salix* spp., *L. salicaria*

Monitoring Locations










-  Sediment accretion stakes
-  Depth sensor
-  Cross section
-  PhotoPoint
-  Vegetation Survey Line








White's Island, 2015

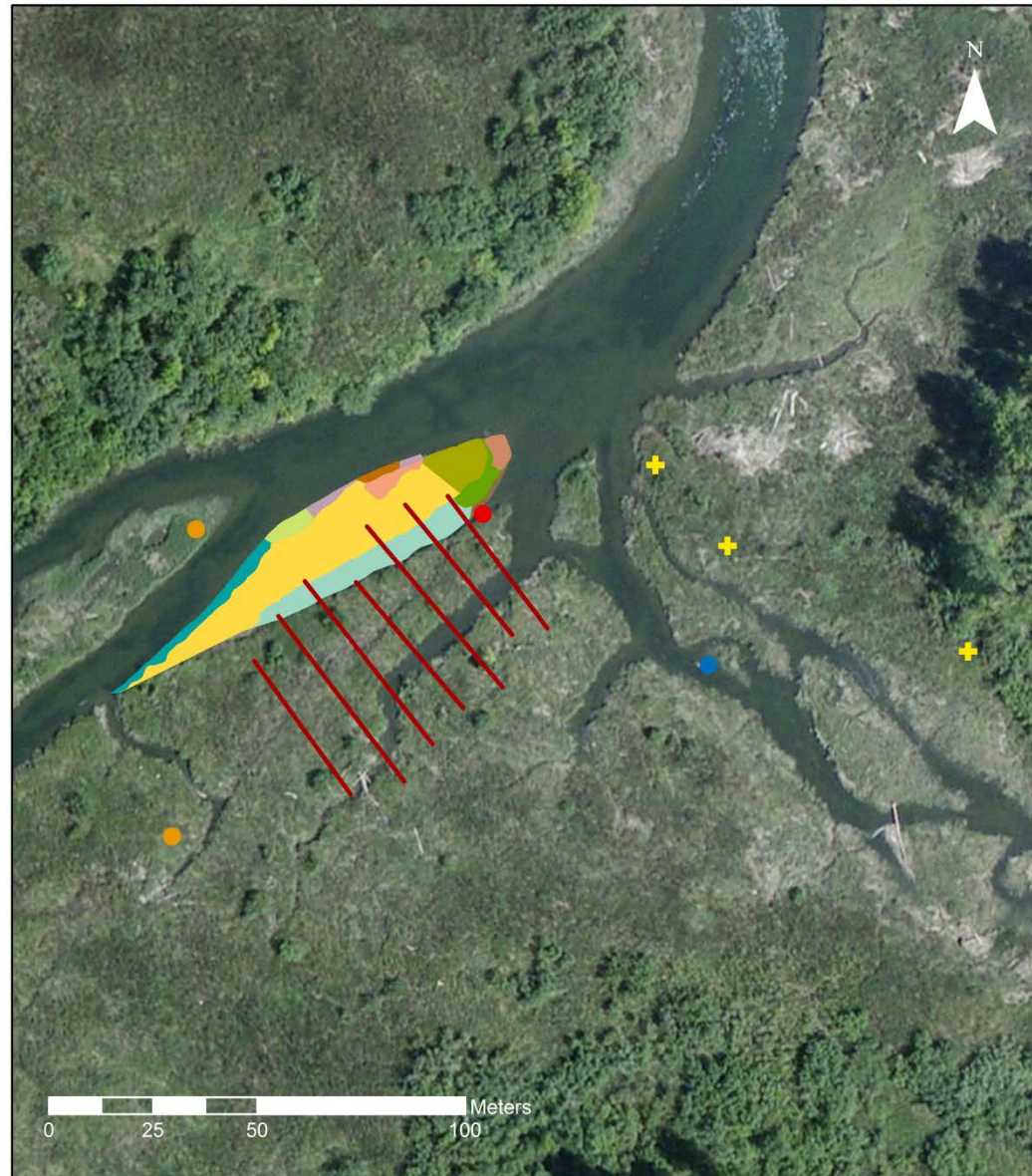
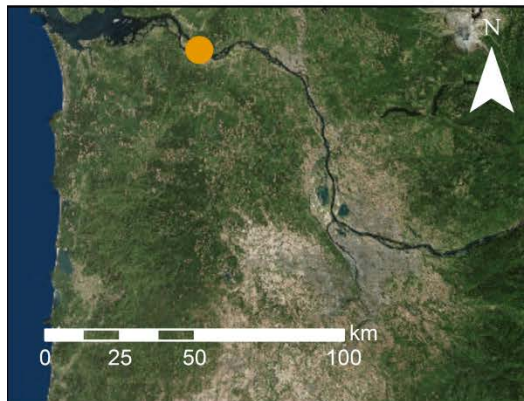
GPS Mapping

Vegetation Communities

-  *Alisma triviale*, *Bidens cernua*
-  *A. triviale*, *B. cernua*, *S. latifolia* (sparse)
-  *Carex lyngbyei*
-  *Eleocharis palustris*
-  *Phalaris arundinacea*
-  *Sagittaria latifolia*
-  *Schoenoplectus americanus*
-  *Schoenoplectus americanus*, *C. lyngbyei*
-  *S. americanus*, *Mimulus guttatus*
-  *S. latifolia*, *E. palustris*, *B. cernua*
-  Mud

Monitoring Locations







-  Cross section endpoints
-  Depth sensor
-  Photo point
-  Sediment accretion stakes
-  Vegetation/Elevation Transect








Cunningham Lake, 2015

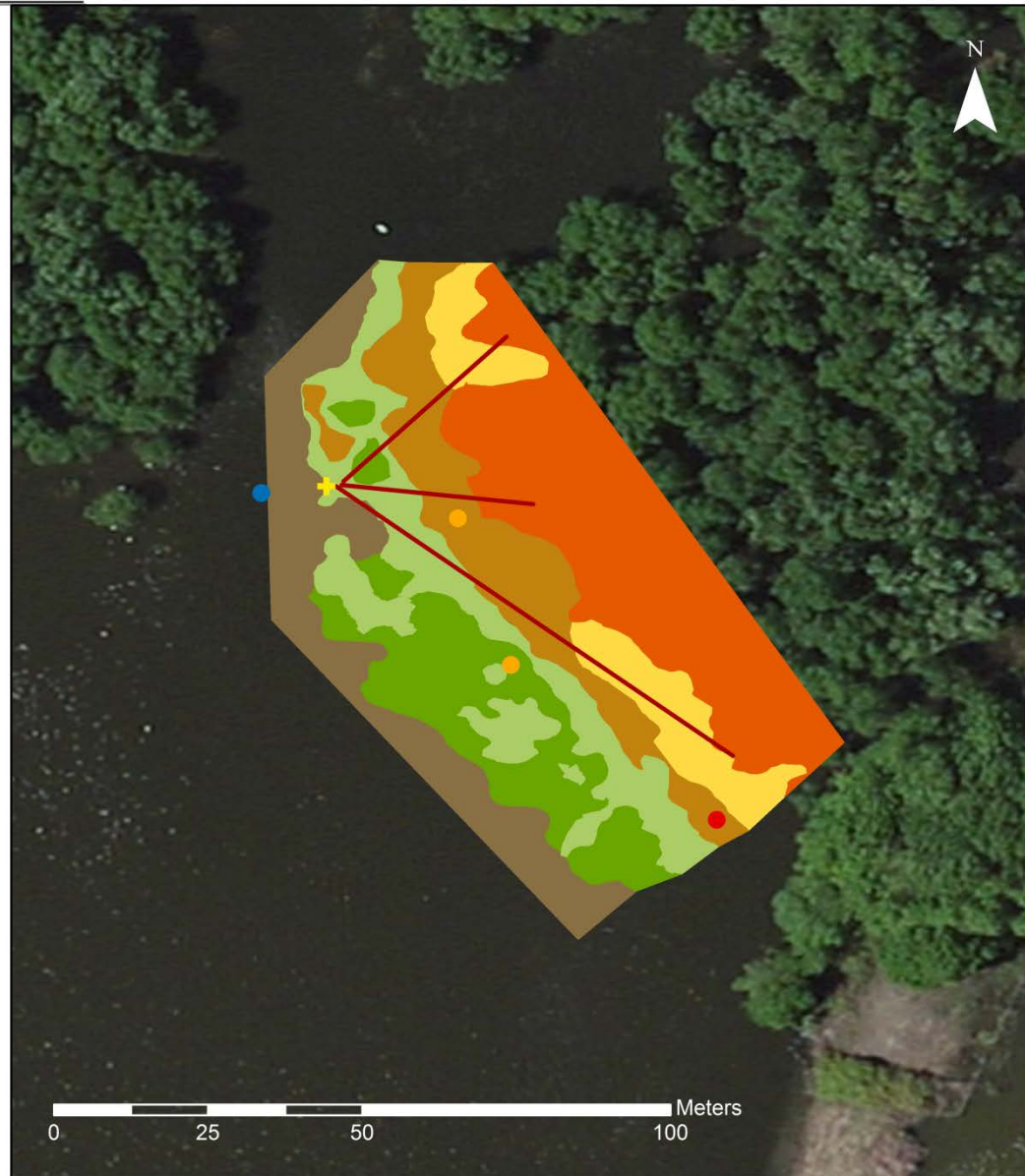
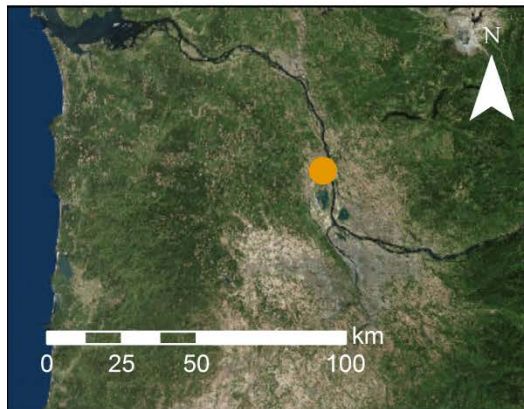
GPS Mapping

Vegetation Communities

-  *Eleocharis palustris*, *S. latifolia*
-  *Phalaris arundinacea*
-  *P. arundinacea*, *S. latifolia*
-  *Sagittaria latifolia*
-  *Salix* spp.
-  Mud

Monitoring Locations









-  Cross section endpoints
-  Depth sensor
-  Photo point
-  Sediment accretion stakes
-  Vegetation/Elevation









Campbell Slough, 2015

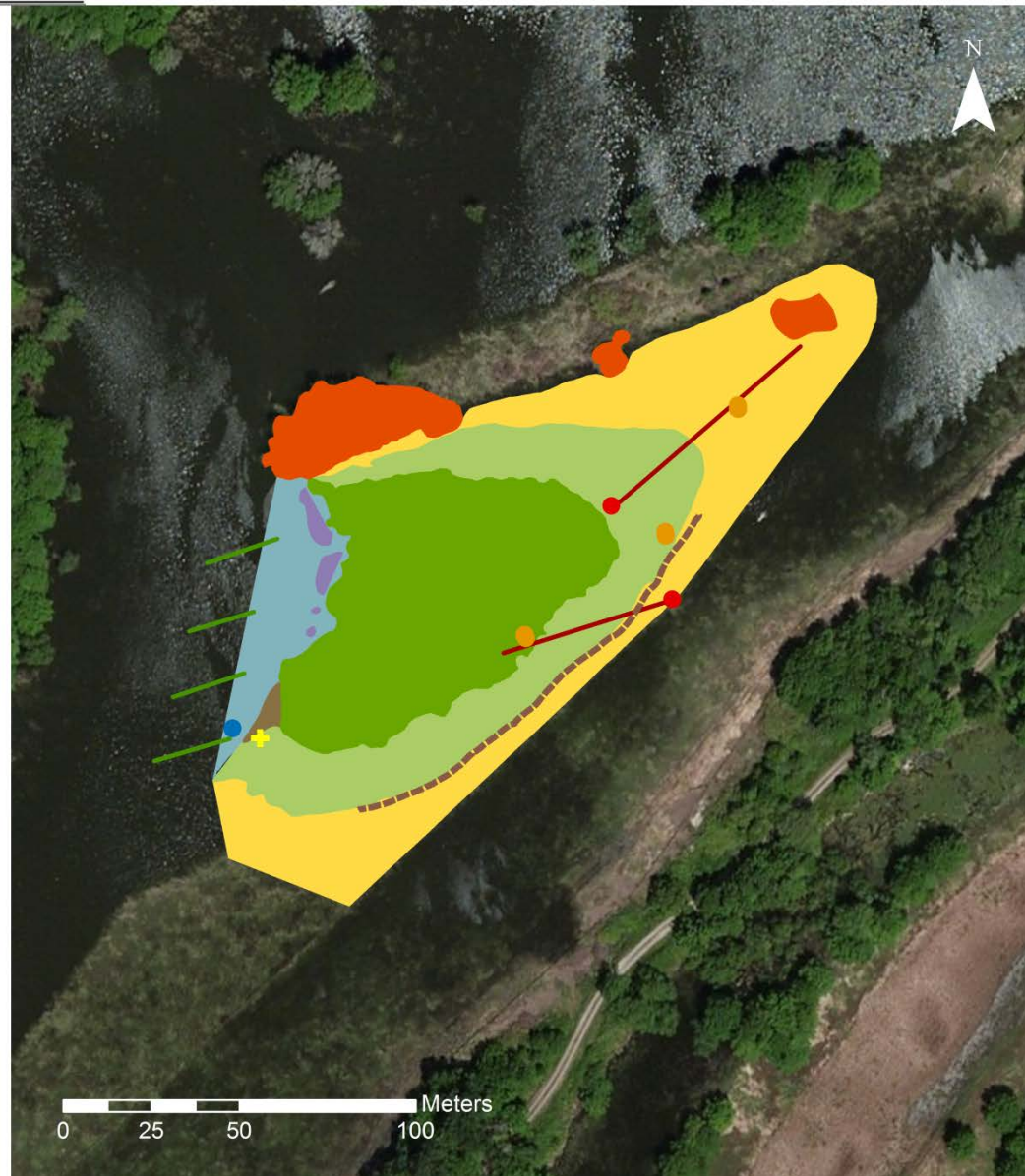
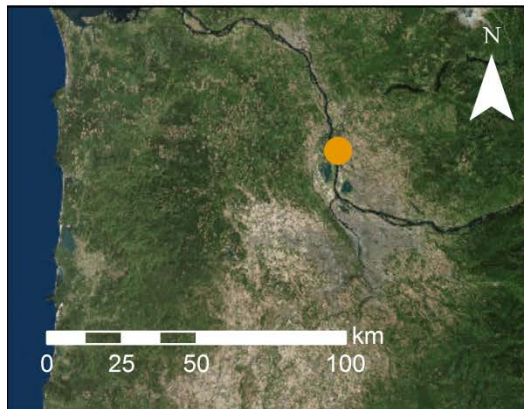
GPS Mapping

Vegetation Communities

-  *E. palustris*, *S. latifolia*
-  *Phalaris arundinacea*
-  *Potamogeton natans*
-  *Sagittaria latifolia*
-  *Salix* spp., *Fraxinus latifolia*
-  Channel
-  Mud
-  cow trample

Monitoring Locations

-  Cross section end point
-  Depth sensor
-  Photo point
-  Sediment accretion stakes
-  SAV/Elevation
-  Vegetation/Elevation








Franz Lake, 2015

GPS Mapping

Vegetation Communities

-  Carex spp.
-  Eleocharis palustris
-  E. palustris, S. latifolia
-  Phalaris arundinacea, Helonium autumnale
-  Polygonum amphibium
-  P. amphibium, Salix spp.
-  P. arundinacea, P. amphibium
-  Sagittaria latifolia
-  Salix spp.
-  Salix spp., P. arundinacea
-  S. latifolia, E. palustris, Carex spp.

Monitoring Locations

-  Cross section endpoints
-  Depth sensor
-  Photo point
-  Sediment accretion stakes
-  Vegetation/Elevation

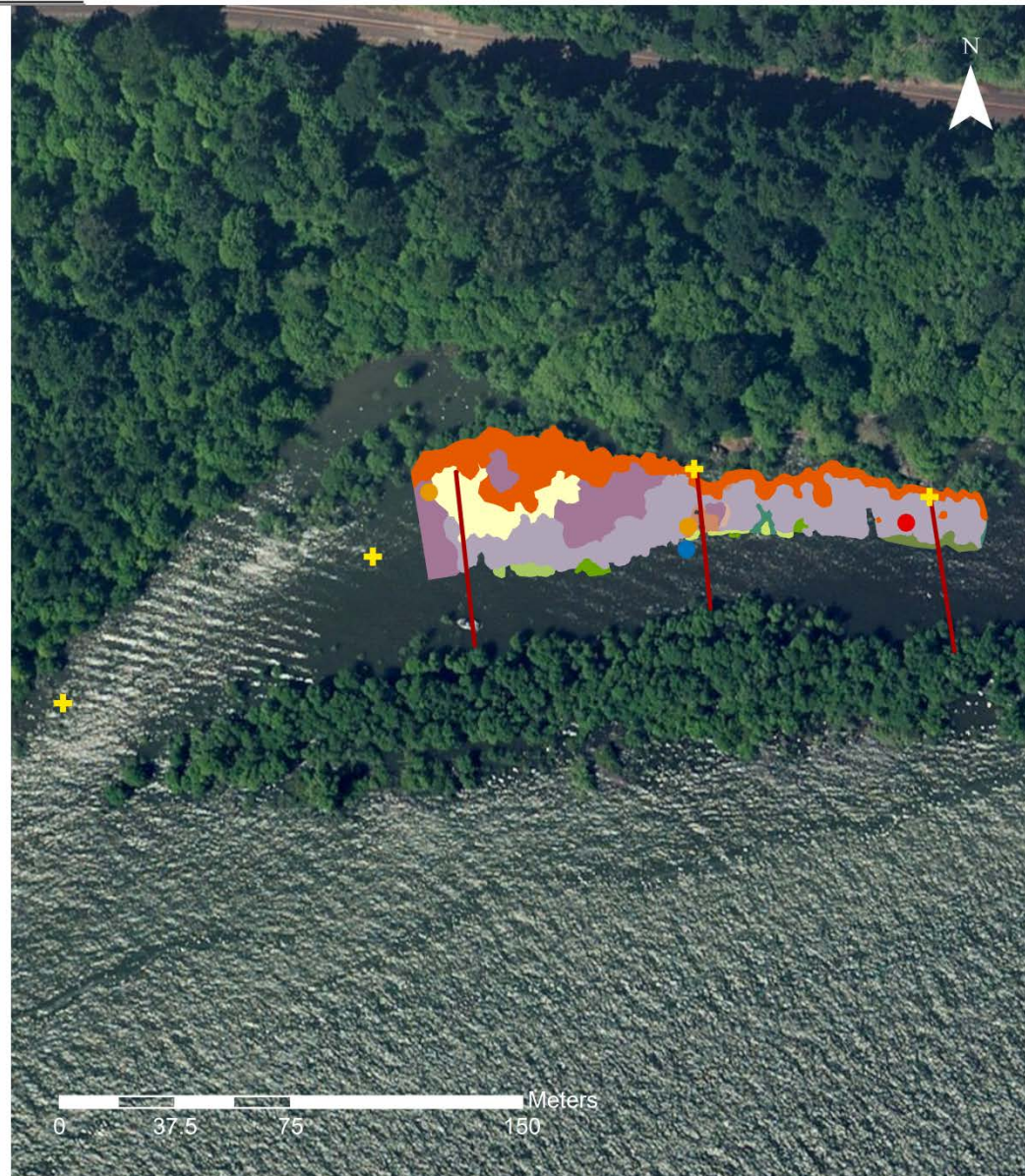
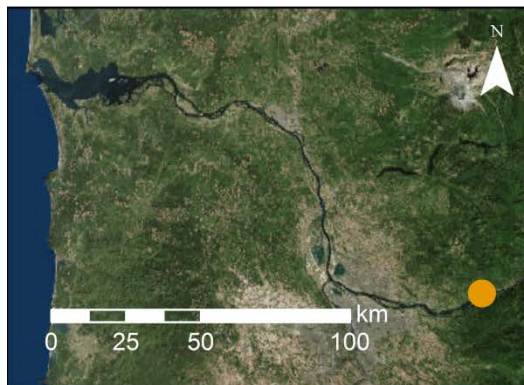


Table A1. Habitat change analysis of vegetation communities at the trend sites; comparison of overlapping areas for the earliest year mapped and the latest year mapped. All area units are square meters. Vegetation communities are ordered from the lowest elevation to the highest elevation at a site; species codes are provided in Appendix D. Sites are ordered in the table starting at the mouth of the Columbia River and moving upstream.

Ilwaco		2011 Vegetation Community							
Area Compared:	13312								
		AGSP							
Area Changed:	6416	Channel, ZAPA	Pan	CALY	CAL Y	TYSP			
No Change:	6895	1558	383	6455	4792	134			
2015 Vegetation Community	Channel	2164	1548						
	Pan	804		241	559	4			
	Bare	127			68	58			
	CALY	3898	10	142	3045	85			
	AGSP, CALY	4048			1188	2860			
	AGSP, DECE, GLSP	1754				1754			
	TYSP	517			356	28	134		
Welch Island		2012 Vegetation Community							
Area Compared:	1126								
		PHAR							
Area Changed:	603	Channel	SALA	CALY, high marsh	PHAR RSAL A	PHAR	PHAR LYSA	LYSA	
No Change:	523	8	15	126	8	838	116	15	
2015 Veg Community	PHAR	812	8	15	126	8	523	116	15
	Un-mapped Vegetation	314					314		

Whites Island

		2009 Vegetation Community						
Area Compared:	1585							
Area Changed:	729	Channel	SALA	ELPA	ELPA, SALA	ELPA, SCAM	CALY	PHAR
No Change:	855	163	252	115	18	82	191	763
2015 Vegetation Community	Mud	15	6	8				
	ALPL, BICE	43	31			12		
	SALA	55		14	31		10	
	SALA, ALPL, BICE	107	86			14		8
	SALA, ELPA, BICE	297		230	36	13		17
	SCAM	34			34			
	SCAM, MIGU	19	7				12	
	SCAM, CALY	39	5					23 11
	ELPA	40	13				26	
	CALY	114						114
	PHAR	823	14		14	5	18	44 727

Cunningham Lake

		2006 Vegetation Community					
Area Compared:	4033						
Area Changed:	1800	SALA	ELPA, SALA	ELPA	PHAR, ELPA	PHAR	SASP
No Change:	2232	1059	1041	44	278	492	1118
2015 Vegetation Community	Mud	587	557	30			
	SALA	634	366	269			
	ELPA, SALA	673	136	537			
	PHAR, SALA	612		205	44	234	107 21
	PHAR	381				44	285 52
	SASP	1145					100 1045

Campbell Slough

		2005 Vegetation Community				
Area Compared:	13476					
Area Changed:	2551	SALA	ELPA, SALA	PHAR	SASP	
No Change:	10925	4719	2905	5636	216	
2015 Vegetation Community	SALA	4434	4133	301		
	ELPA, SALA	3632	586	2276	770	
	PHAR	4955		328	4441	111
	SASP, FRLA	381			276	105
	Cow Trample	74			74	

Franz Lake

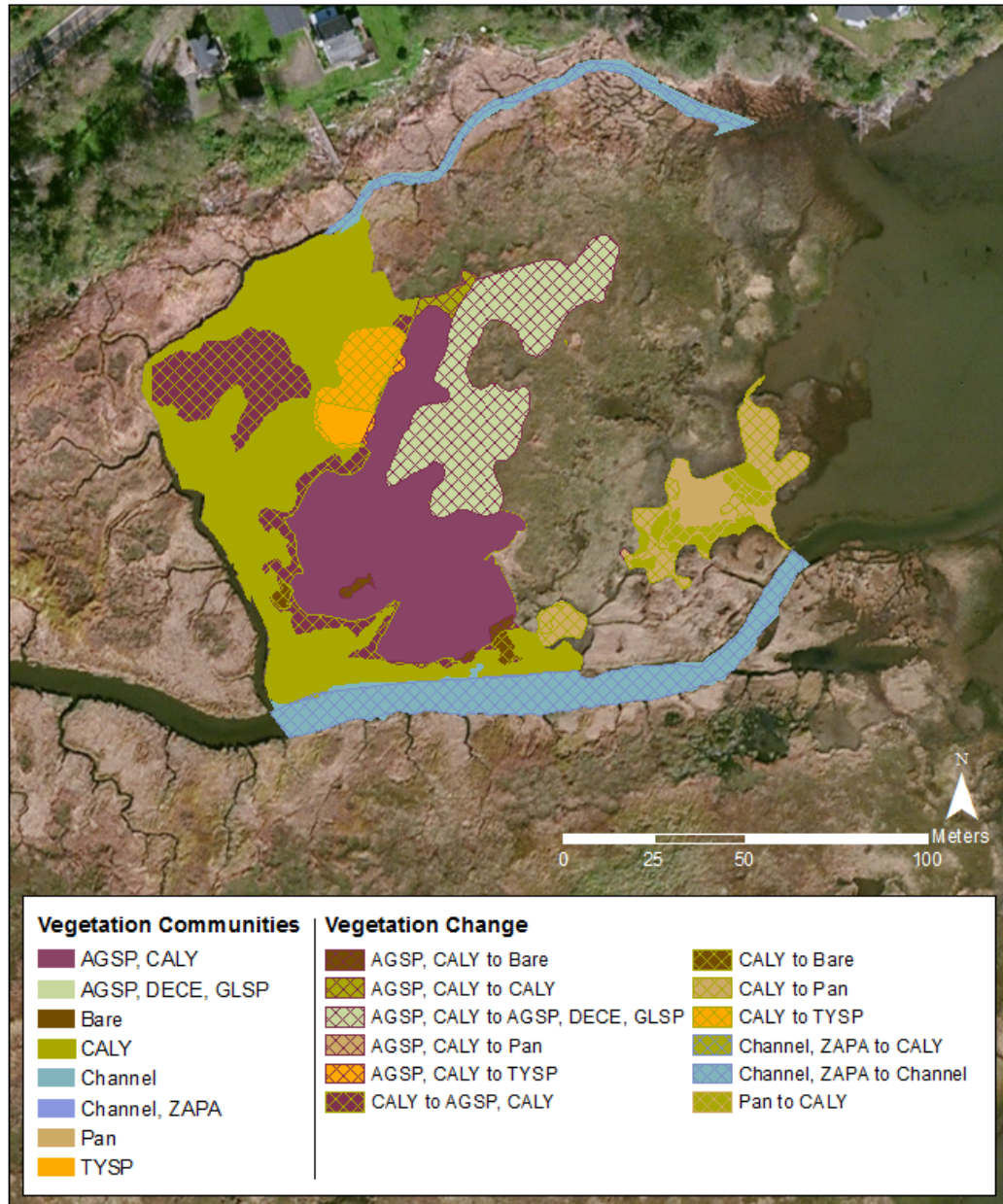
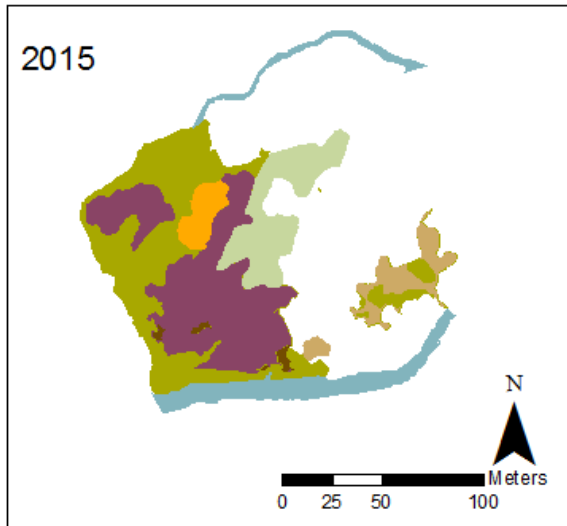
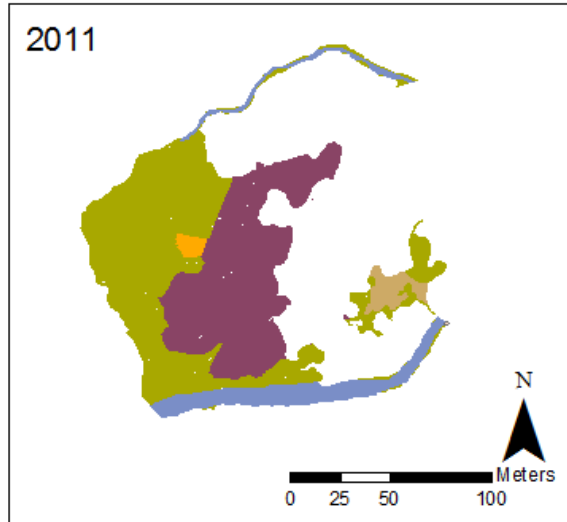
		2008 Vegetation Community					
Area Compared: 1762		Channel, SALA	ELPA	PHAR, POAM	SASP	Rock	
Area Changed: 1430							
No Change: 331		25	372	1047	303	15	
2015 Vegetation Community	SALA	5	5				
	SALA, ELPA, CASP	81	16	65			
	ELPA	35		35			
	CASP	34	9	25			
	POAM	1097		216	848	34	
	POAM, SASP	10			10		
	PHAR, HEAU	27		27			
	PHAR, POAM	28			28		
	SASP	445			161	269	15

Franz Lake		2008 Vegetation Community						
Area Compared:	5720	Channel, SALA	ELPA, SALA	ELP A	PHAR, POAM	SASP	Rock	
Area Changed:	4336							
No Change:	1384	1417	24	488	2177	1579	35	
2012 Vegetation Community	Channel	1182	1081	4	69	28		
	Channel, SALA	147	112		35			
	SALA	37	15	9	4	9		
	ELPA	344	133	5	92	106	8	
	CASP	178	6	6	39	121	6	
	POAM, SALA	7				7		
	POAM	2310	71		249	1645	344	
	SASP, CASP	41					41	
	SASP	1475				260	1180	35

Franz Lake		2012 Vegetation Community												
Area Compared:	5203	Bare Ground	Beaver Activity	Channel	Channel, SALA	SALA	ELPA	CASP	POAM, SALA	POAM	PHAR	SASP, PHAR	SASP, CASP	SASP
Area Changed:	2344													
No change:	2859	9	14	194	50	5	193	192	25	2159	196	279	20	1865
2015 Vegetation Community	SALA	41	9	11	13					8				
	SALA, ELPA, CASP	79		19	27		9			24				
	ELPA	25		7	6		11							
	ELPA, SALA	58		45		5	8							
	CASP	37			4		14			18				
	PHAR, HEAU	49					18	31						
	POAM	2131		8	40		69	93	25	1748	12			137
	POAM, PHAR	867		6	72		47	27		152	103	135		324
	POAM, SASP	10						10						
	SASP	1387					18	31		170	39	8	20	1100
	SASP, PHAR	522								39	43	136		304

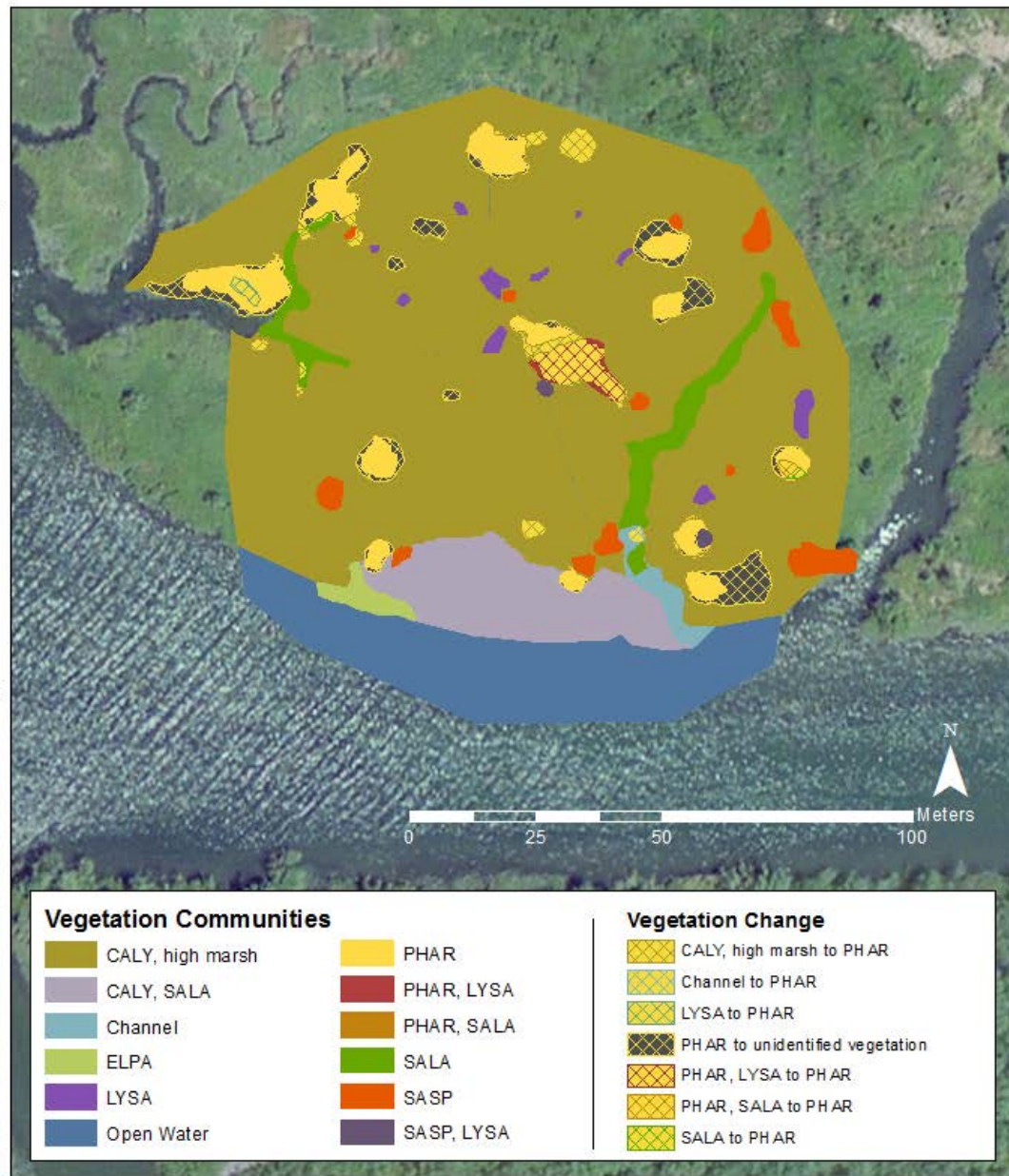
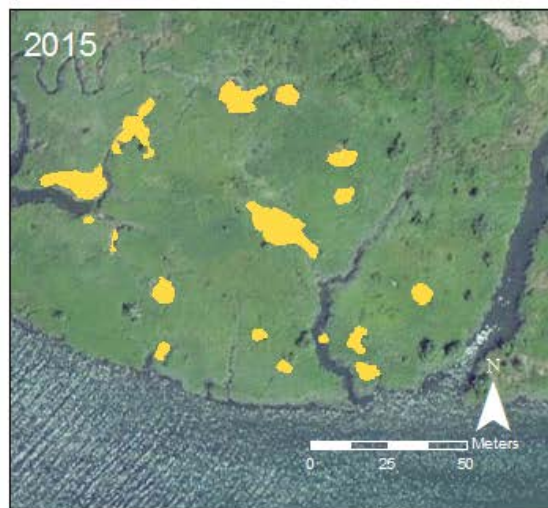
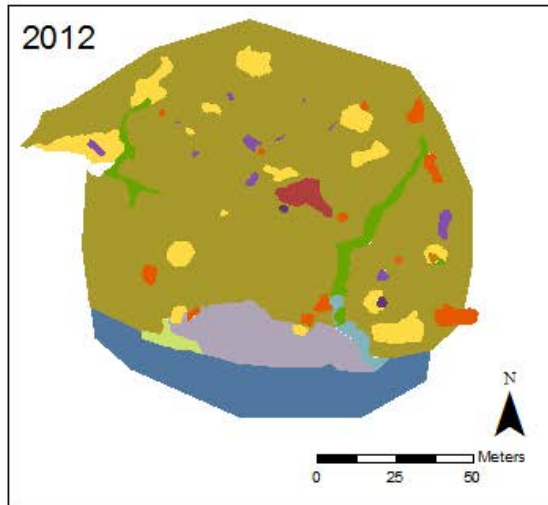
Baker Bay

Vegetation Change 2011 to 2015



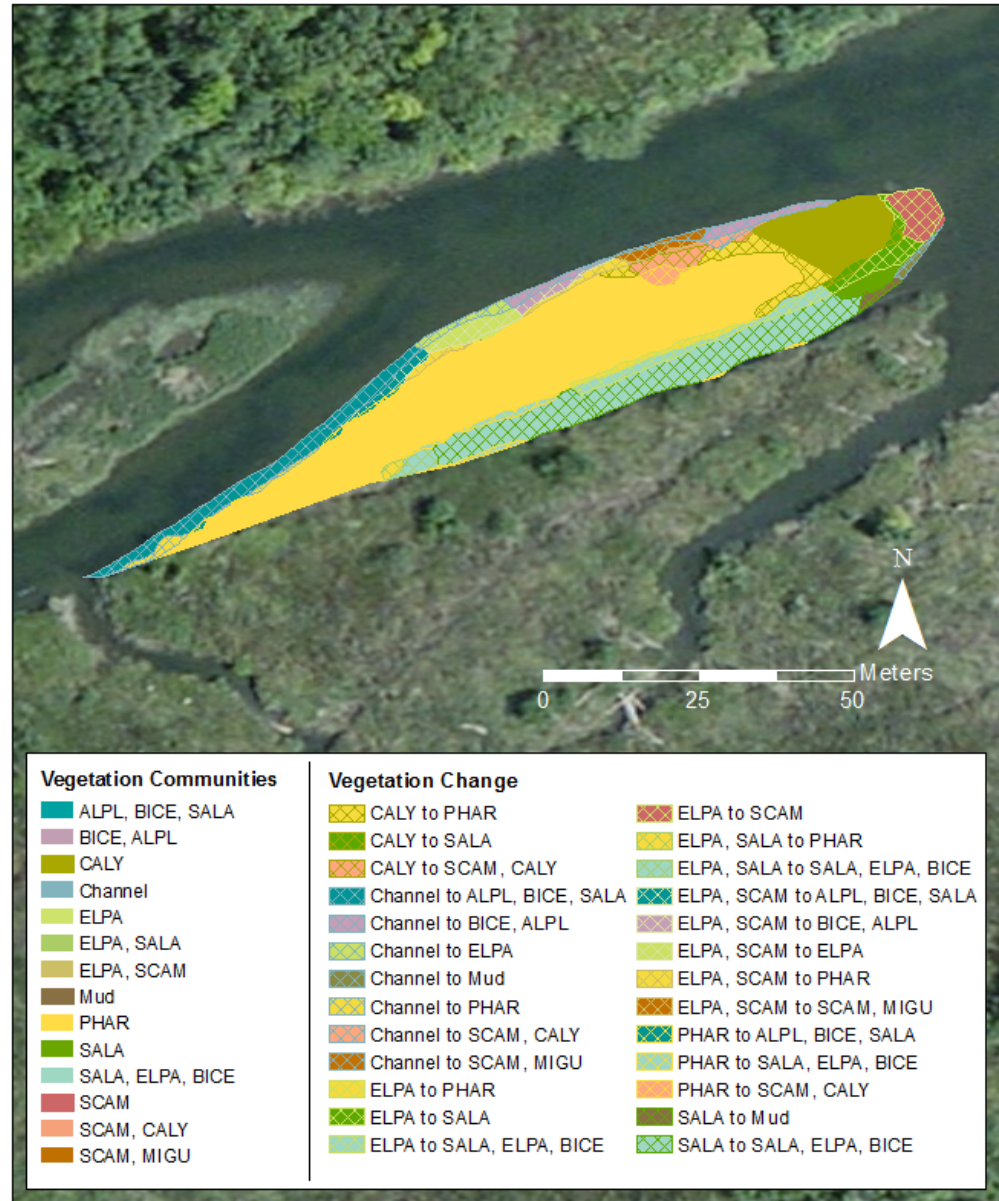
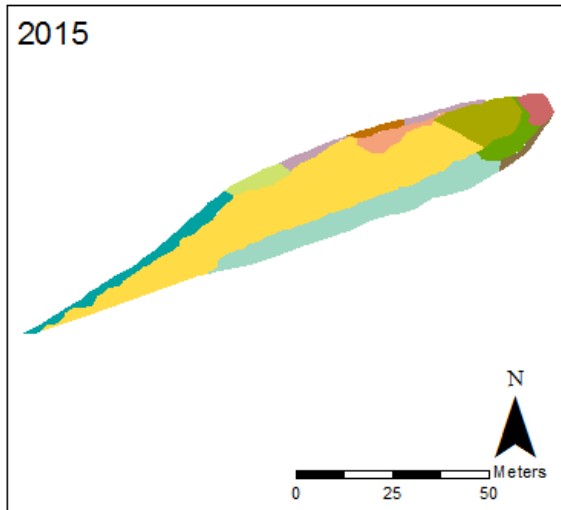
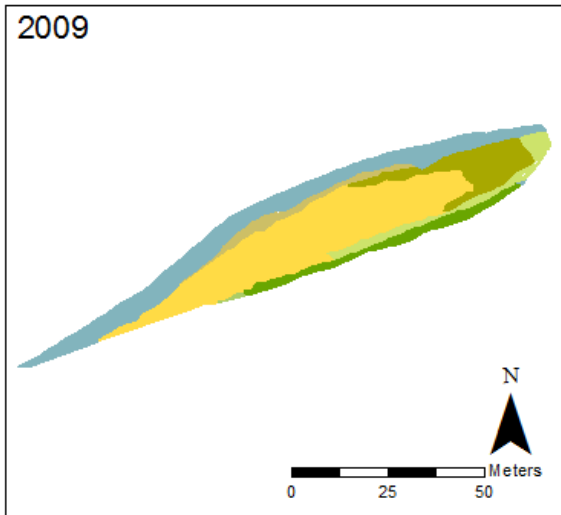
Welch Island

Vegetation Change 2012 to 2015
PHAR Specific



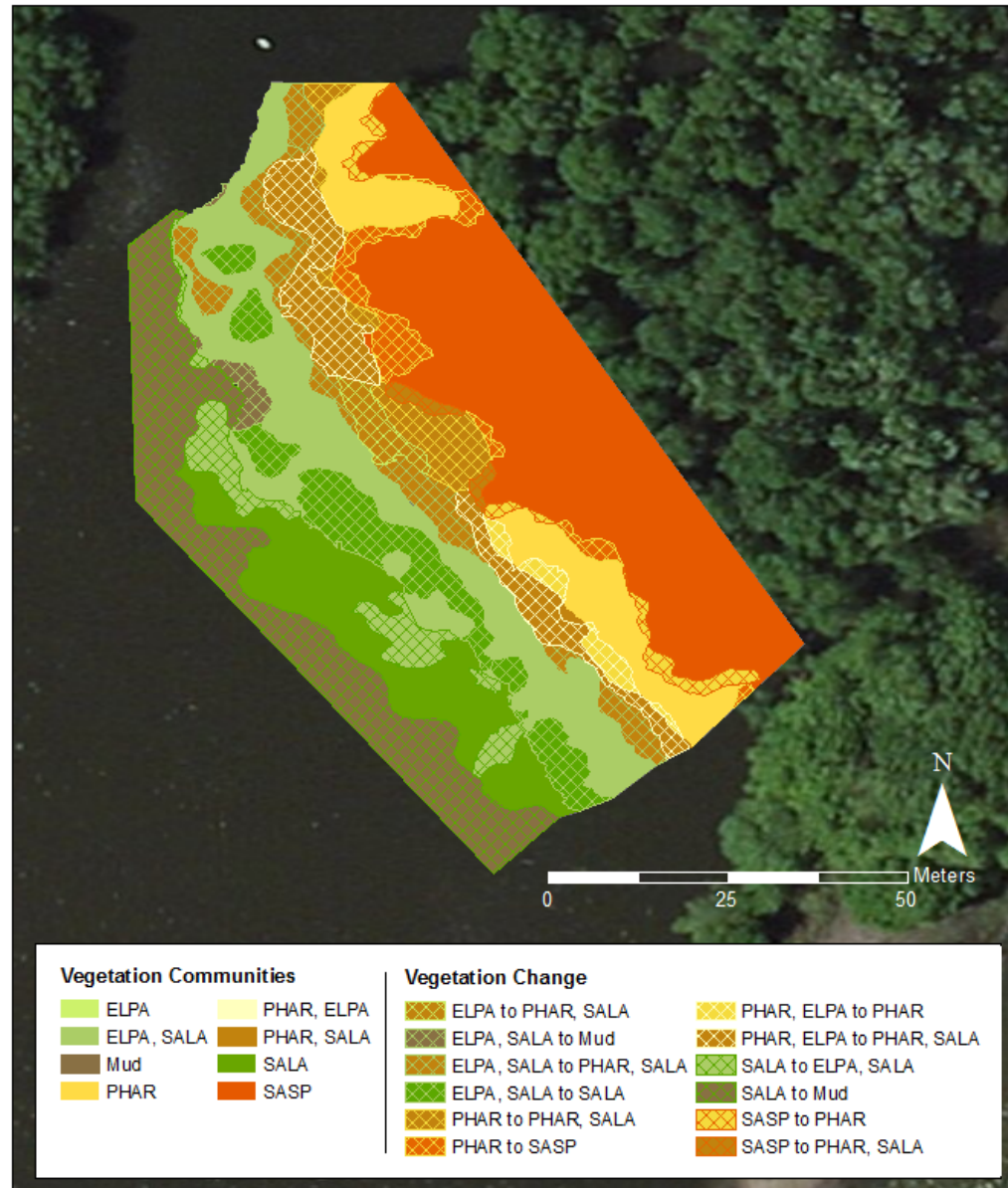
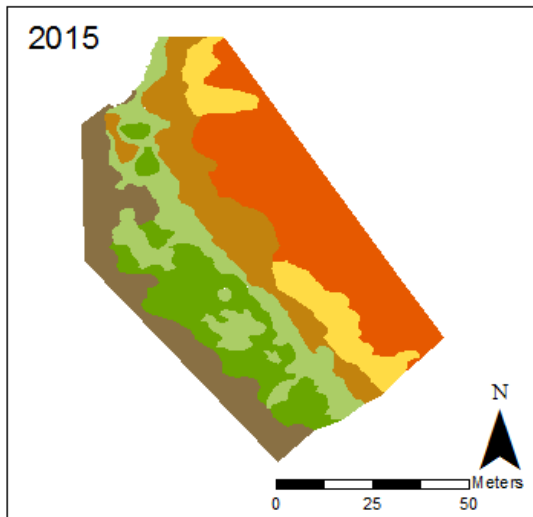
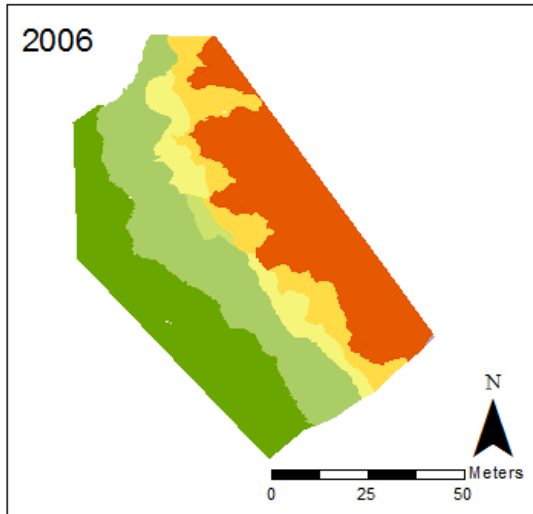
White's Island

Vegetation Change 2009 to 2015



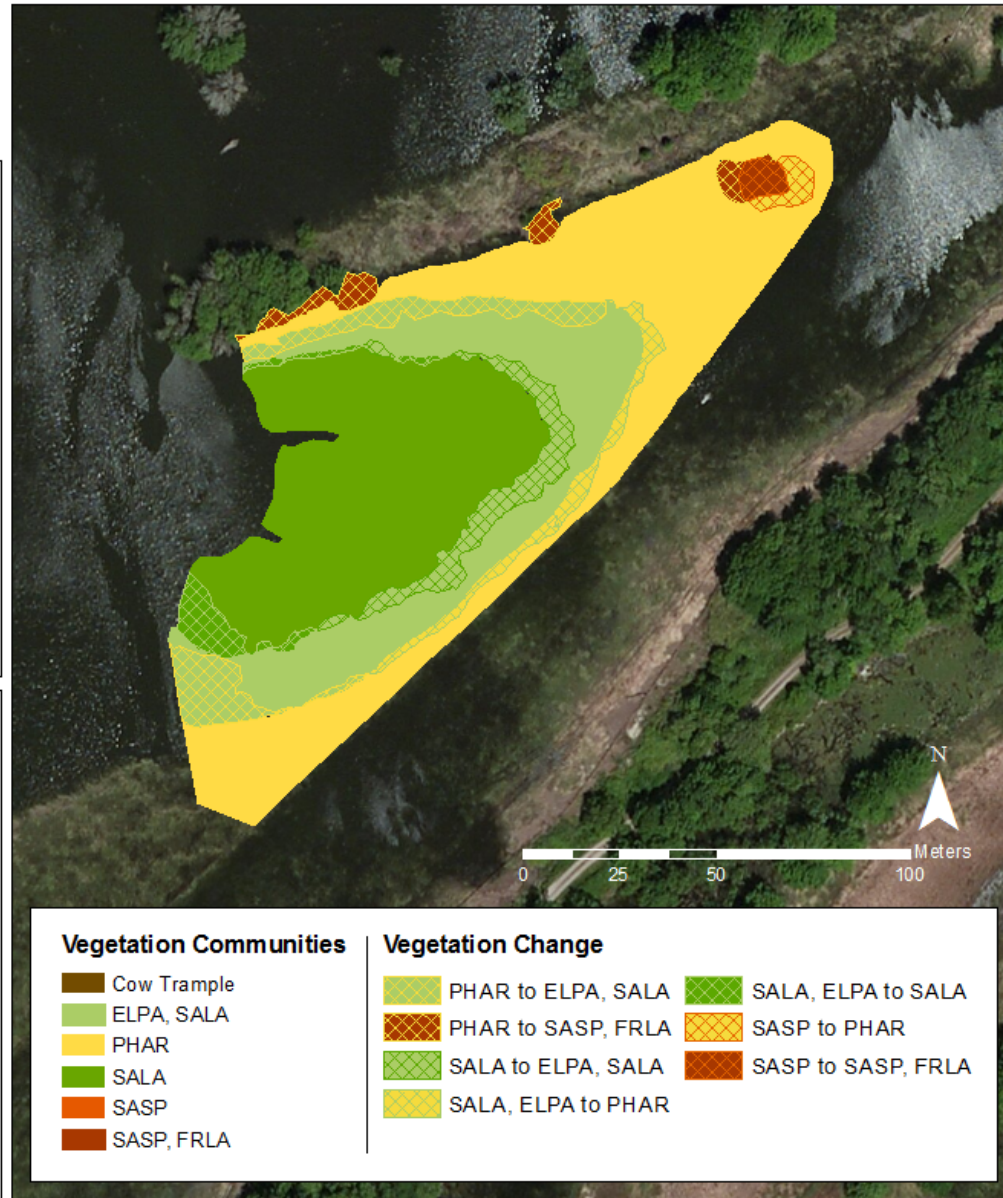
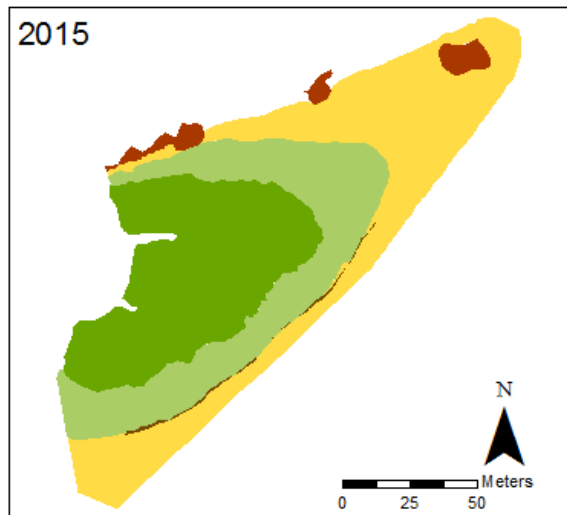
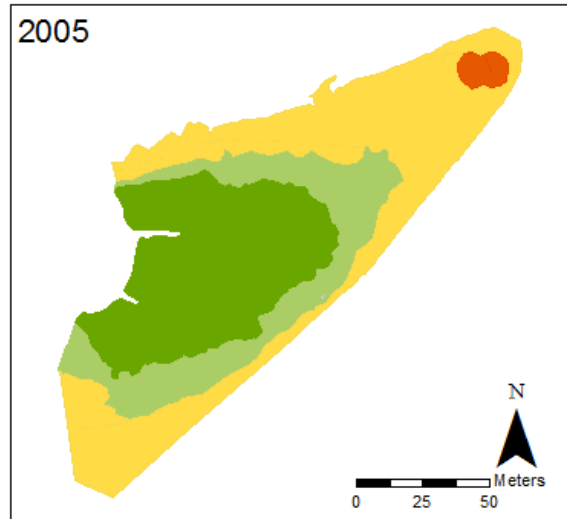
Cunningham Lake

Vegetation Change 2006 to 2015



Campbell Slough

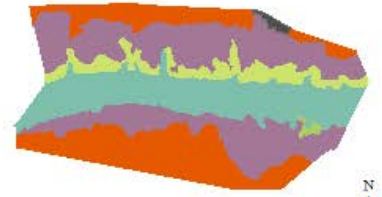
Vegetation Change 2005 to 2015



Franz Lake

Vegetation Change 2008, 2012 & 2015

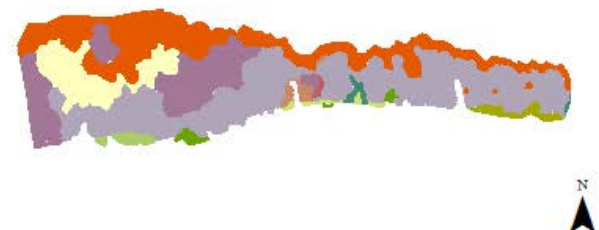
2008



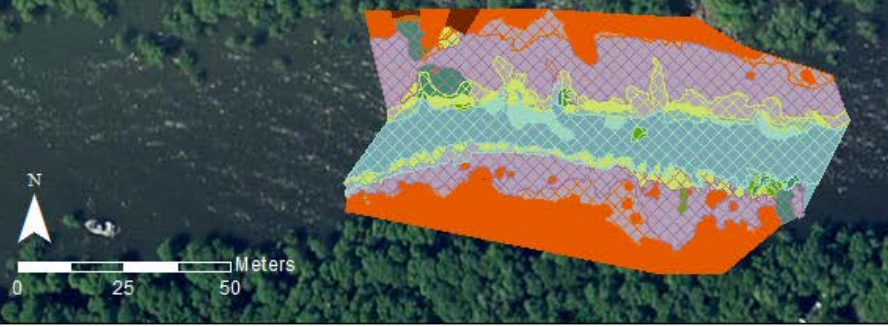
2012



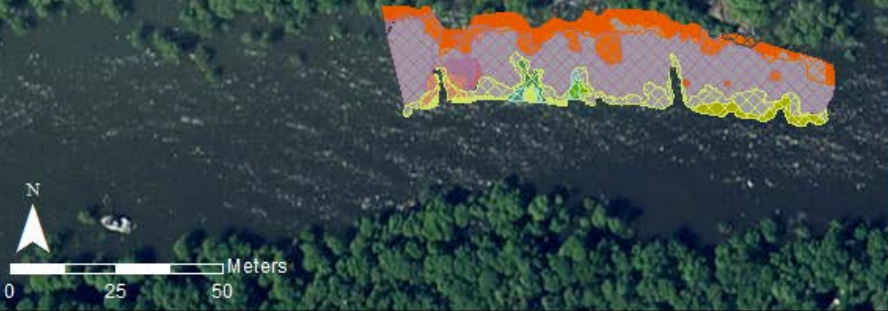
2015



2008 to 2012



2008 to 2015



2012 to 2015



Baker Bay – PP1

Appendix B. Annual photo points from EMP trends sites

Photo points collected in 2017 are still under analysis and unavailable at the time of the writing of this report.

31 July 2011



15 February 2012



4 August 2012



4 February 2013



Baker Bay – PP1

26 July 2013



20 September 2013



3 February 2014



27 June 2014



Baker Bay – PP1

2 August 2015



7 August 2016



Secret River – PP1 [HIGH MARSH]

5 February 2010



2 August 2012



9 August 2013



1 August 2015



Secret River – PP1 [HIGH MARSH]

6 August 2016



Secret River – PP2 [LOW MARSH]

1 December 2011



2 August 2012



15 July 2014



1 August 2015



Secret River – PP2 [LOW MARSH]

6 August 2016



Secret River – PP3 [CHANNEL]

1 December 2011



15 July 2014



Secret River – PP3 [CHANNEL]

1 August 2015



6 August 2016



Welch Island – PP1

1 August 2012



3 February 2013



23 July 2013



Welch Island – PP1

1 August 2014



31 July 2015



5 August 2016



Whites Island – PP1

22 July 2009



13 July 2010



2 August 2011



15 February 2012



Whites Island – PP1

31 July 2012



5 February 2013



22 July 2013



Whites Island – PP1

4 February 2014



31 July 2014



30 July 2015



Whites Island – PP1

4 August 2016



Cunningham Lake – PP1

26 July 2005



18 July 2007



21 July 2008



Cunningham Lake – PPI

25 July 2009



17 May 2010



28 July 2010



Cunningham Lake – PPI

30 July 2011



8 August 2012



29 July 2013



18 July 2014



Cunningham Lake – PP1

28 July 2015



1 August 2016



Campbell Slough – PP1

29 July 2005



15 July 2006



5 September 2006



Campbell Slough – PP1

17 July 2007



26 July 2010



29 July 2011



Campbell Slough – PP1

15 February 2012



21 July 2012



10 August 2012



Campbell Slough – PP1

27 July 2013



18 July 2014



29 July 2015



Campbell Slough – PP1

3 August 2016



Campbell Slough – PP2

25 July 2005



27 July 2009



26 July 2010



29 July 2011



10 Aug 2012



Campbell Slough – PP2

27 July 2013



18 July 2014



29 July 2015



3 August 2016



22 July 2008



28 July 2009



25 August 2011



14 February 2012



21 July 2012



30 August 2012



11 October 2012



6 February 2013



31 July 2013



12 February 2014



7 August 2014



27 July 2015



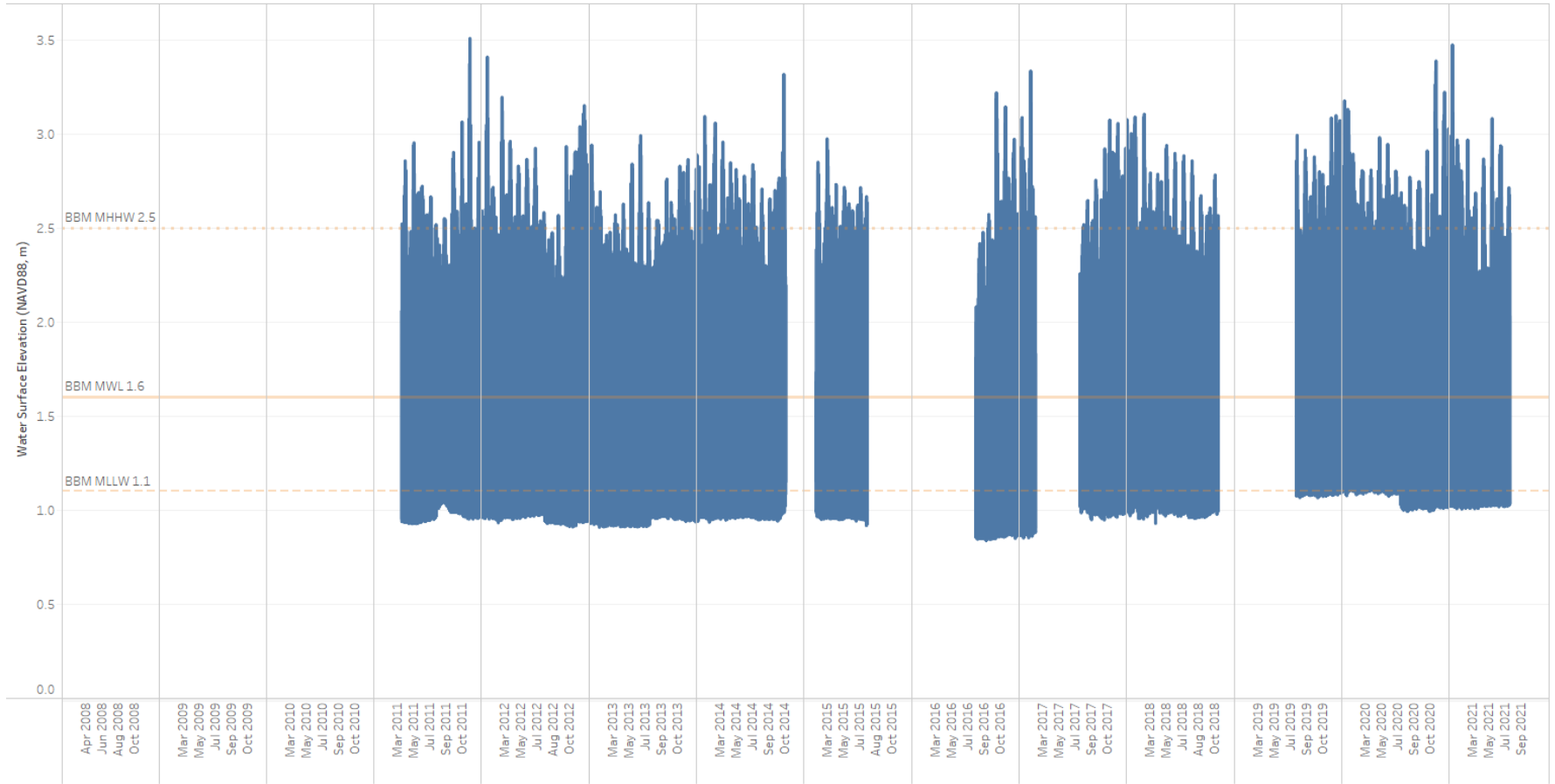
2 August 2016



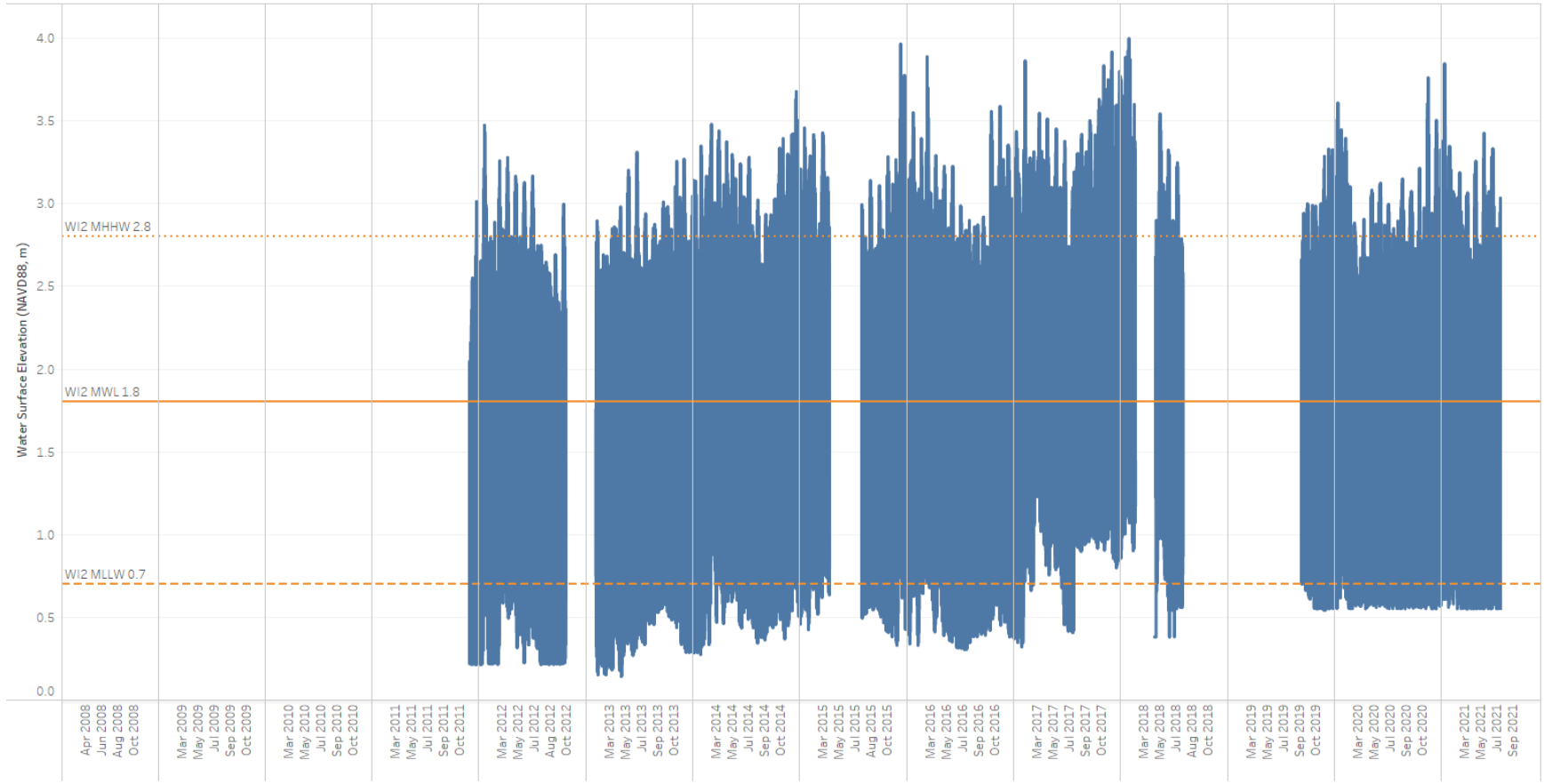
Appendix C. Site Hydrographs

Hydrographs are in order by site location in the River, starting at the mouth. Followed by hydrology summary statistics for each site. *2012 data for Welch Island is of questionable quality due to movement of logger during deployment.

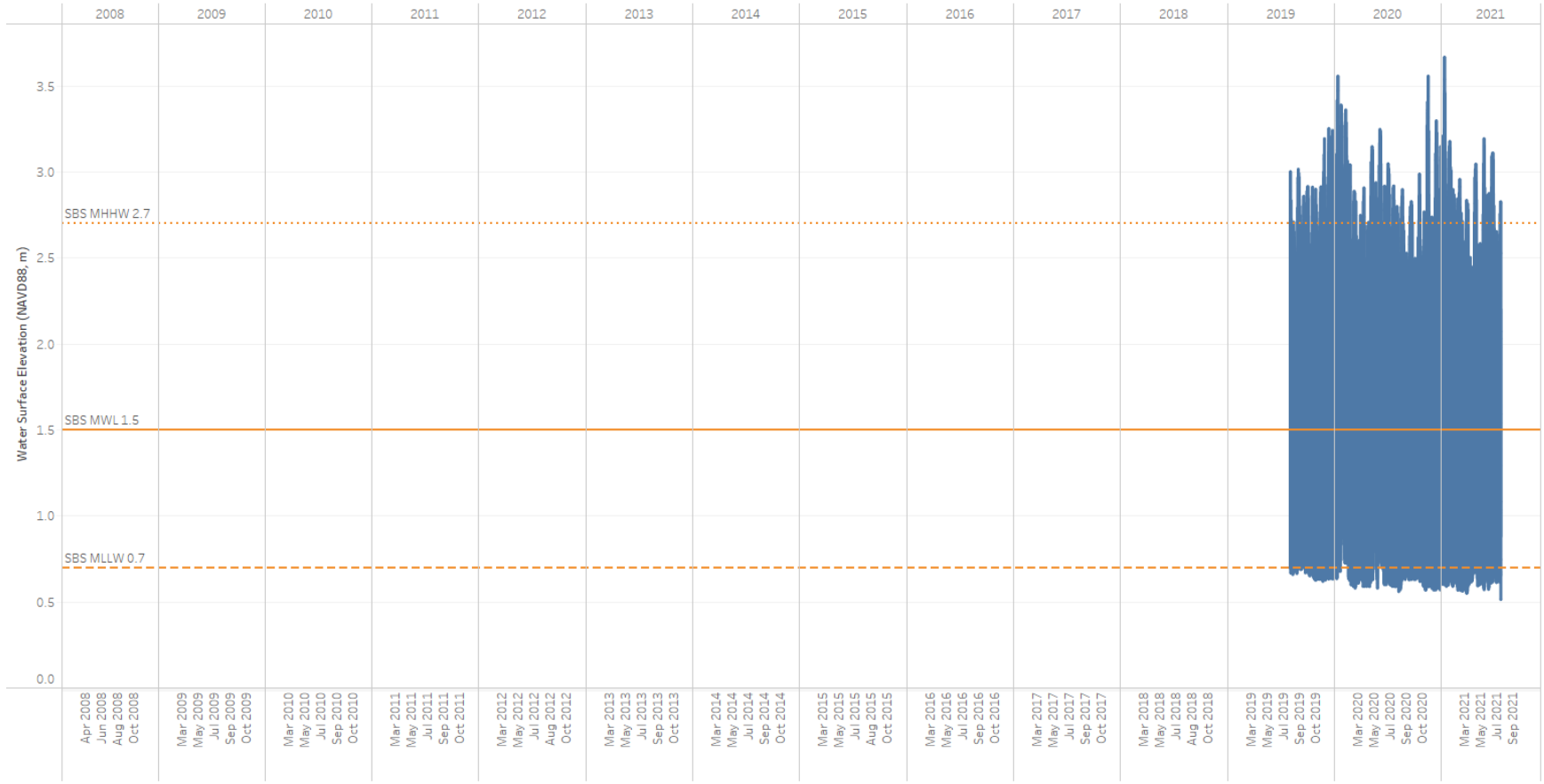
Ilwaco Water Surface Elevation



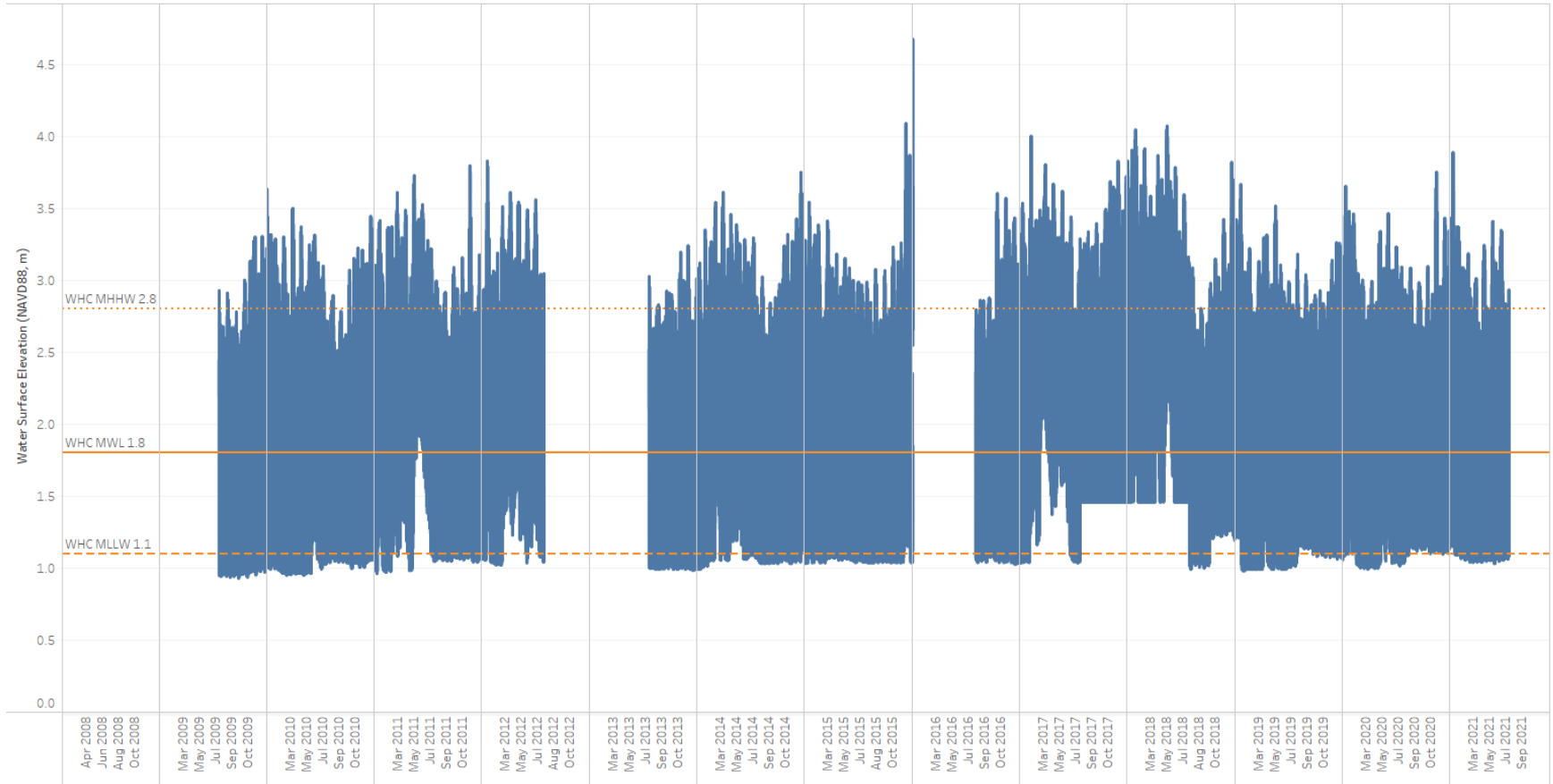
Welch Island Water Surface Elevation



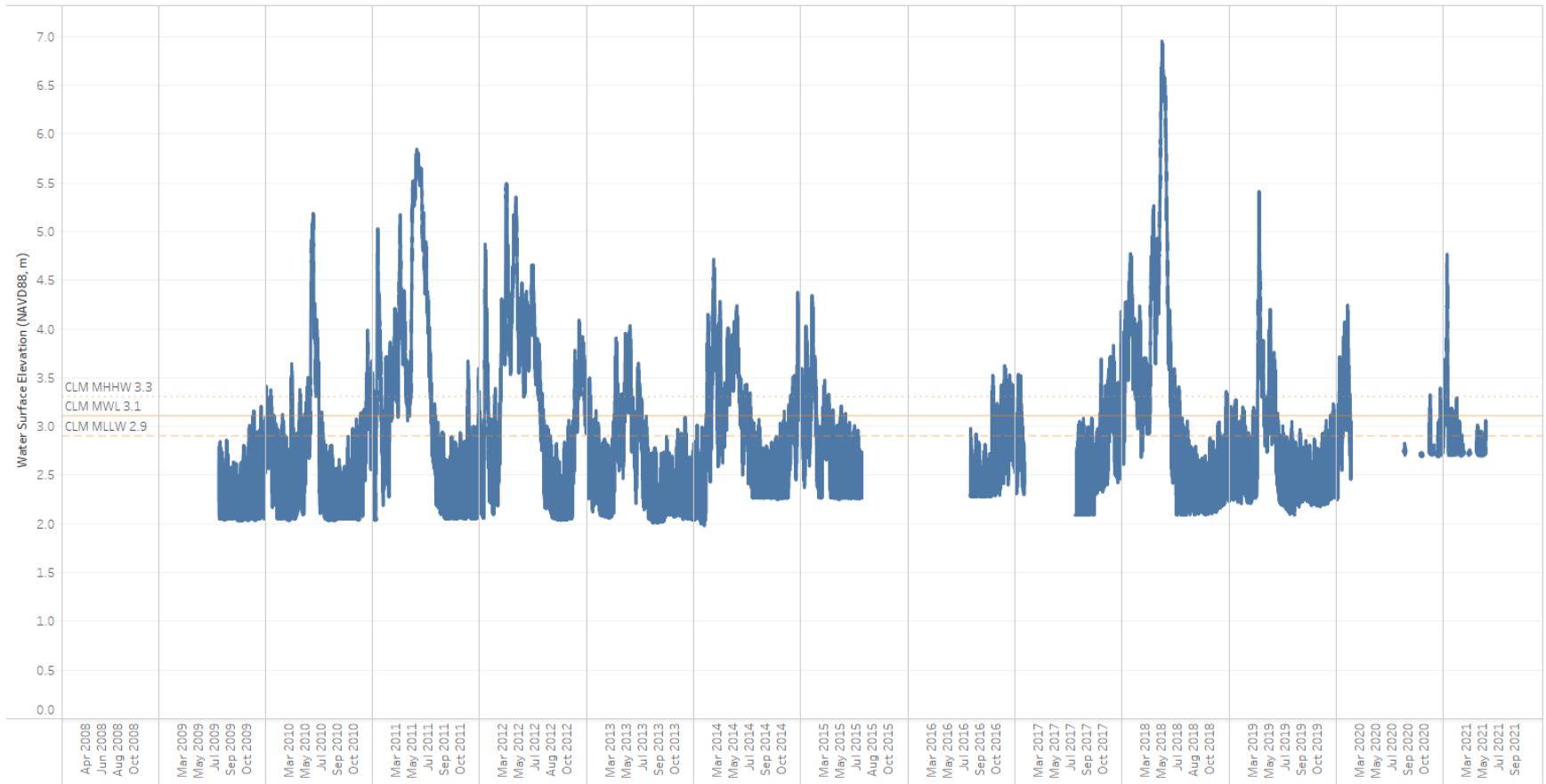
Steamboat



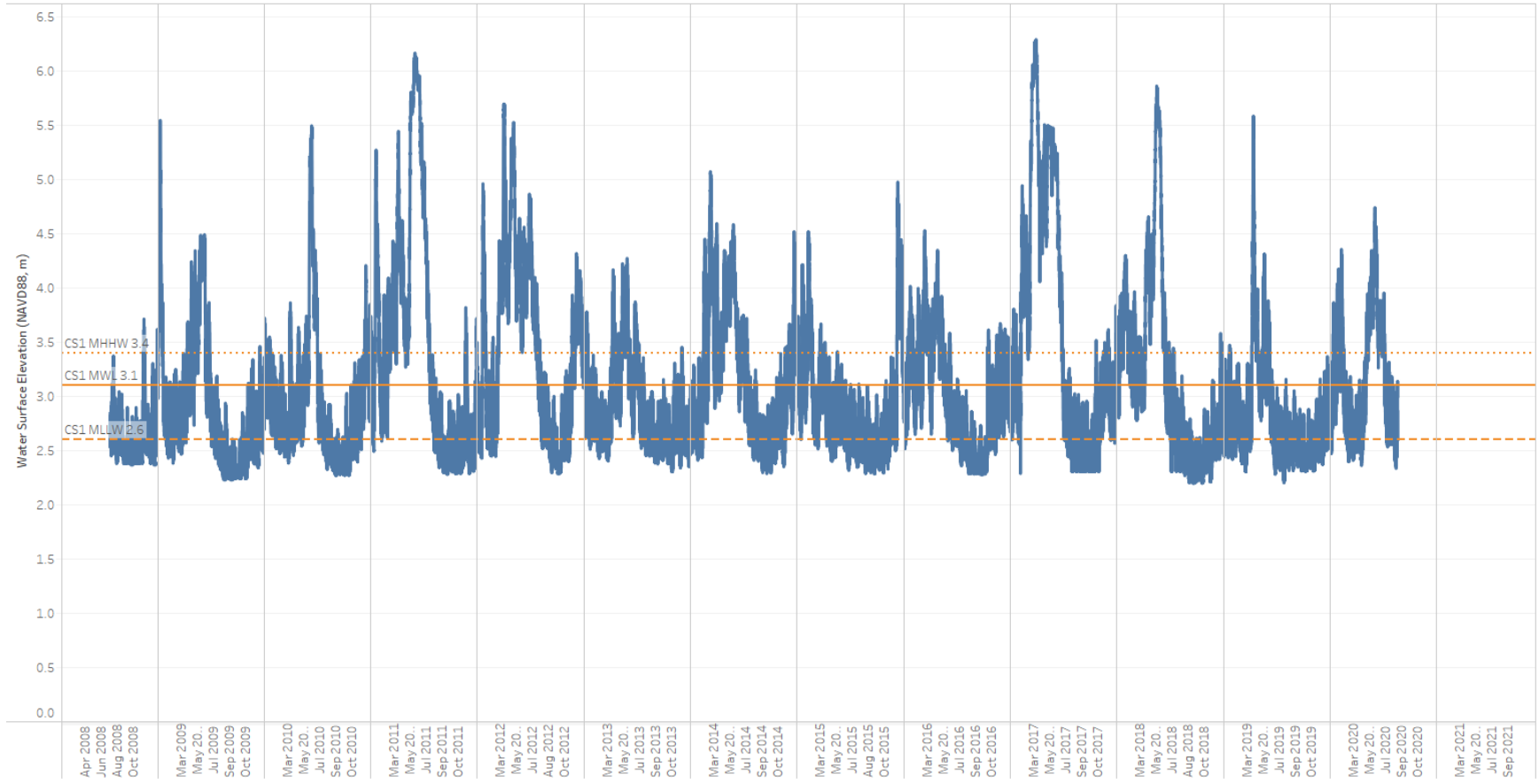
Whites Island Water Surface Elevation



Cunningham Lake Water Surface Elevation



Campbell Slough Water Surface Elevation



Franz Lake Water Surface Elevation

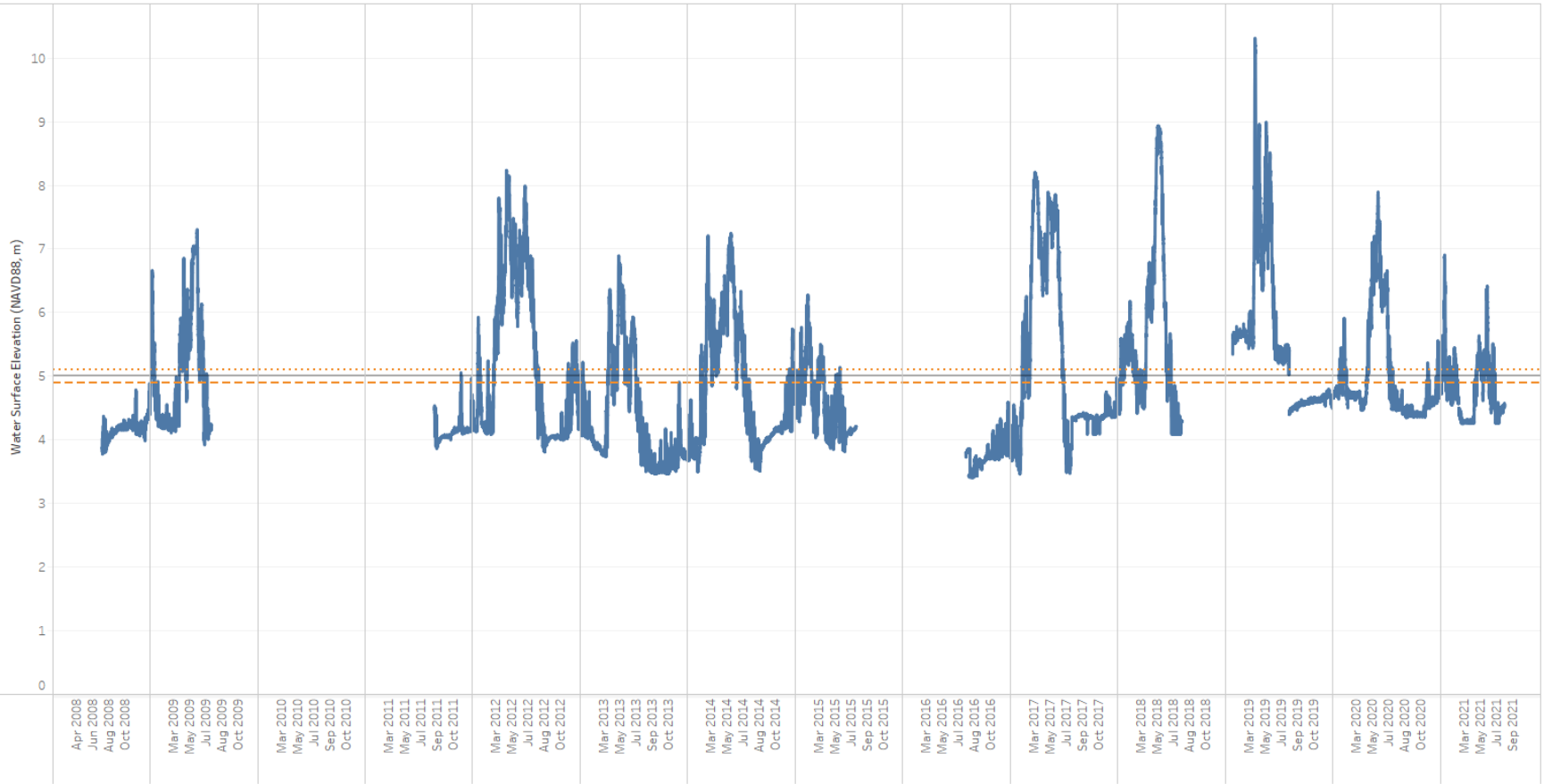


Table C.1. Hydrologic summary statistics for each site and year. See methods section 2.3.2.1 for definitions and calculations.

Years		2021	2020	2019	2018	2017	2016	2015	2014	2013	2012	2011	2010	2009	2008
Whites Island	Duration	Jan-Jul	Jan-Dec	Jan-Dec	Jan-Jul	Jan-Dec	Aug-Dec	Jan-Dec	Jan-Dec	Jul-Dec	Jan-Jul	Jan-Dec	Jan-Dec	July-Dec	
	Days	202	366	365	212	365	153	365	365	163	213	365	365	163	
	MHHW	2.9	2.8	2.8	3.4	3.1	2.8	2.8	2.9	2.6	3.0	2.9	2.8	2.6	
	MLLW	1.1	1.1	1.1	1.6	1.5	1.1	1.1	1.1	1.0	1.3	1.2	1.1	1.0	
	MWL	1.9	1.9	1.8	2.4	2.2	1.9	1.9	1.9	1.7	2.1	1.9	1.8	1.6	
	Annual Range	1.7	1.7	1.7	1.8	1.6	1.7	1.7	1.7	1.6	1.7	1.6	1.7	1.6	
	Annual Max	3.9	3.8	3.7	4.1	4.0	4.7	4.1	3.8	3.2	3.8	3.8	3.6	3.3	
Cunningham Lake	Duration	Jan-May	Jan-Feb, Aug-Dec	Jan-Aug	Jan-Jul	Jan, Aug-Dec	Aug-Dec	Jan-Jul	Jan-Dec	Jan-Dec	Jan-Dec	Jan-Dec	Jan-Dec	Jan-Dec	Aug-Dec
	Days	146	184	223	219	193	152	209	365	365	366	365	365	160	
	MHHW	3.1	3.3	3.1	4.1	3.0	2.9	3.1	3.2	2.9	3.5	3.5	3.0	2.7	
	MLLW	2.8	2.9	2.6	3.6	2.4	2.5	2.6	2.7	2.4	3.1	3.1	2.5	2.1	
	MWL	2.8	2.9	2.8	3.8	2.7	2.7	2.8	2.9	2.6	3.3	3.3	2.7	2.4	
	Annual Range	0.2	0.3	0.5	0.5	0.6	0.4	0.5	0.4	0.5	0.4	0.5	0.5	0.6	
	Annual Max	4.8	4.2	5.4	7.0	4.2	3.6	4.3	4.7	4.0	5.5	5.8	5.2	3.2	
Campbell Slough	Duration	NA	Jan-Aug	Jan-Aug	Jan-Jul	Jan-Dec	Jan-Dec	Jan-Dec	Jan-Dec	Jan-Dec	Jan-Dec	Jan-Dec	Jan-Dec	Jan-Dec	Aug-Dec
	Days	NA	233	225	220	365	362	365	365	365	366	364	365	365	164
	MHHW	NA	3.4	3.2	3.8	3.8	3.2	3.1	3.4	3.1	3.7	3.7	3.1	3.1	2.8
	MLLW	NA	3.0	2.7	3.4	3.4	2.8	2.7	3.0	2.7	3.3	3.3	2.8	2.7	2.5
	MWL	NA	3.1	2.9	3.6	3.6	3.0	2.9	3.2	2.8	3.4	3.5	2.9	2.9	2.6
	Annual Range	NA	0.4	0.4	0.4	0.4	0.4	0.4	0.4	0.4	0.4	0.3	0.4	0.4	0.3
	Annual Max	NA	4.7	5.6	5.9	6.3	4.5	5.0	5.1	4.3	5.7	6.2	5.5	5.6	3.7
Franz Lake	Duration	Jan-Aug	Jan-Dec	Jan-Dec	Jan-Jul	Jan-Dec	Aug-Dec	Jan-Dec	Jan-Dec	Jan-Dec	Jan-Dec	Sep-Dec		Jan-July	Aug-Dec
	Days	217	366	341	218	365	152	208	365	365	366	129		209	163
	MHHW	4.9	5.1	5.6	5.8	5.3	3.9	4.8	4.9	4.5	5.4	4.2		5.2	4.2
	MLLW	4.7	4.9	5.4	5.5	5.1	3.7	4.5	4.7	4.2	5.2	4.1		4.9	4.1
	MWL	4.8	5.0	5.5	5.6	5.2	3.8	4.6	4.8	4.3	5.3	4.1		5.0	4.2
	Annual Range	0.2	0.2	0.3	0.3	0.2	0.2	0.2	0.3	0.3	0.3	0.1		0.3	0.1
	Annual Max	6.9	7.9	10.3	8.9	8.2	4.6	6.3	7.2	6.9	8.2	5.1		7.3	4.9

Appendix D. Vegetation Species Cover

Table D.1. Site marsh elevation range in meters based on the vegetation plot elevation (with $\geq 5\%$ absolute living plant cover), relative to the North American Vertical Datum of 1988 (NAVD88). Mean number of plots, mean elevation, standard deviation (SD), minimum elevation (Min), and maximum elevation (Max).

		Mean (SD)	2021	2020	2019	2018	2017	2016	2015	2014	2013	2012	2011	2010	2009	2008	2007	2006	2005
Ilwaco Slough	Plots (n)	39.64 (0.88)	40	40	40	40	40	39	37	40	40	40	40						
	Mean	1.95 (0.05)	2.03	1.95	1.86	1.94	1.91	1.94	2.00	2.03	1.96	1.96	1.92						
	SD	0.22 (0.04)	0.26	0.16	0.30	0.23	0.23	0.17	0.16	0.24	0.23	0.23	0.23						
	Min	1.06 (0.3)	0.81	1.55	0.70	0.95	0.94	1.44	1.61	0.93	0.94	0.95	0.89						
	Max	2.36 (0.07)	2.45	2.31	2.28	2.31	2.31	2.31	2.38	2.53	2.37	2.36	2.31						
	Range	1.29 (0.32)	1.64	0.76	1.58	1.36	1.38	0.87	0.77	1.60	1.44	1.41	1.42						
Welch Island	Plots (n)	40.6 (0.92)	41	41	43	40	41	40	40	40	40	40							
	Mean	2.05 (0.03)	2.09	2.06	1.98	2.00	2.06	2.06	2.06	2.06	2.06	2.06							
	SD	0.17 (0.01)	0.16	0.16	0.21	0.17	0.16	0.16	0.16	0.16	0.16	0.16							
	Min	1.32 (0.05)	1.34	1.34	1.22	1.22	1.34	1.34	1.34	1.34	1.34	1.34							
	Max	2.2 (0.04)	2.28	2.25	2.14	2.14	2.20	2.20	2.20	2.20	2.20	2.20							
	Range	0.89 (0.03)	0.94	0.91	0.92	0.92	0.86	0.86	0.86	0.86	0.86	0.86							
Whites Island	Plots (n)	41.46 (5.46)	44	43	45	44	42	42	47	43	45	42	42	35	25				
	Mean	2.1 (0.08)	2.14	2.16	2.33	2.09	2.08	2.08	2.03	2.08	2.06	2.10	2.09	2.02	2.01				
	SD	0.39 (0.03)	0.41	0.40	0.45	0.36	0.38	0.38	0.40	0.38	0.38	0.33	0.34	0.38	0.45				
	Min	1.22 (0.05)	1.21	1.36	1.29	1.21	1.20	1.20	1.20	1.20	1.20	1.21	1.16	1.18	1.25				
	Max	2.58 (0.11)	2.64	2.66	2.92	2.63	2.53	2.53	2.53	2.53	2.53	2.52	2.50	2.56	2.49				
	Range	1.36 (0.09)	1.43	1.30	1.63	1.42	1.33	1.33	1.33	1.33	1.33	1.31	1.35	1.39	1.24				

Table D.1. Site marsh elevation range in meters based on the vegetation plot elevation (with ≥5% absolute living plant cover), relative to the North American Vertical Datum of 1988 (NAVD88). Mean number of plots, mean elevation, standard deviation (SD), minimum elevation (Min), and maximum elevation (Max).

		Mean (SD)	2021	2020	2019	2018	2017	2016	2015	2014	2013	2012	2011	2010	2009	2008	2007	2006	2005	
Cunningham Lake	Plots (n)	57.94 (14.61)	69*	69	69	67	68	69	69	36	31	59	59	61	62	62	64	62	20	
	Mean	2.7 (0.07)	2.71*	2.71	2.67	2.69	2.78	2.78	2.76	2.52	2.83	2.67	2.66	2.67	2.68	2.69	2.71	2.70	2.71	
	SD	0.19 (0.05)	0.35*	0.35	0.20	0.19	0.19	0.19	0.19	0.24	0.16	0.17	0.17	0.17	0.17	0.17	0.17	0.17	0.16	0.14
	Min	2.31 (0.1)	2.29*	2.29	2.30	2.29	2.41	2.41	2.40	2.00	2.48	2.28	2.28	2.28	2.28	2.28	2.25	2.31	2.33	2.41
	Max	3.1 (0.43)	4.74*	4.74	3.01	3.07	3.02	3.02	3.02	3.02	2.79	3.05	2.96	2.96	3.01	2.96	3.01	2.95	3.02	2.98
	Range	0.78 (0.44)	2.45*	2.45	0.71	0.77	0.60	0.60	0.62	0.78	0.56	0.68	0.68	0.73	0.68	0.76	0.65	0.68	0.56	
Campbell Slough	Plots (n)	61.06 (17.87)	112	62	62	60	60	61	62	59	61	61	60	62	61	64	62	61	8	
	Mean	2.92 (0.23)	2.01	2.92	2.96	3.01	2.95	2.99	2.98	3.02	3.00	2.98	2.98	2.98	3.10	2.95	2.95	2.97	2.86	
	SD	0.43 (0.18)	1.12	0.38	0.37	0.37	0.32	0.36	0.36	0.36	0.36	0.37	0.37	0.38	0.38	0.42	0.41	0.38	0.57	
	Min	2.34 (0.48)	0.45	2.38	2.50	2.40	2.51	2.51	2.51	2.53	2.53	2.47	2.46	2.45	2.59	2.22	2.41	2.41	2.45	
	Max	3.99 (0.07)	4.02	3.94	3.97	4.01	3.76	4.00	4.00	4.02	4.02	3.96	4.00	4.02	4.17	4.01	4.01	4.00	3.98	
	Range	1.65 (0.49)	3.56	1.56	1.47	1.61	1.25	1.49	1.49	1.48	1.48	1.49	1.53	1.57	1.58	1.78	1.60	1.59	1.53	
Franz Lake	Plots (n)	59.77 (11.24)	71	76	66	64	60	61	67	61	59	62	58		35	37				
	Mean	4.57 (0.07)	4.37	4.53	4.63	4.62	4.60	4.60	4.56	4.62	4.60	4.54	4.64		4.60	4.51				
	SD	0.28 (0.07)	0.47	0.38	0.30	0.29	0.23	0.23	0.27	0.23	0.23	0.33	0.23		0.27	0.21				
	Min	3.84 (0.24)	3.32	3.36	3.97	3.87	3.95	3.95	3.85	4.00	4.04	3.63	4.09		3.90	3.96				
	Max	5.06 (0.08)	5.3	5.05	5.05	5.05	5.01	5.01	5.01	5.05	5.05	5.00	5.07		5.13	5.00				
	Range	1.22 (0.29)	1.98	1.70	1.08	1.19	1.06	1.06	1.15	1.05	1.01	1.36	0.98		1.22	1.04				

*2021 RTK data was unavailable for Cunningham Lake. We utilized the 2020 values for analysis.

Table D.2. Average percent cover of each plant species at trend sites in 2019, only species with >5% cover shown below. Species are sorted by their four-letter code (1st two letters of genus and 1st two letters of species).

Sp Code	Scientific Name	Status	Ilwaco Slough		Welch Island		Whites Island		Cunningham Lake		Campbell Slough		Campbell Slough (New 2021)	Franz Lake	
			2021	2020	2021	2020	2021	2020	2021	2020	2021	2020	2021	2020	2021
AGST	<i>Agrostis stolonifera</i> L.	Non-native	17	12											
AREG	<i>Argentina egedii</i> ssp. <i>Egedii</i>	Native	9	12		5	10								23
BICE	<i>Bidens cernua</i>	Native					9	17							
BOMA7	<i>Bolboschoenus maritimus</i>	Non-native		9											
CAAM	<i>Castilleja ambigua</i>	Native		11											
CAAP	<i>Carex aperta</i>	Native												9	11
CAHE	<i>Callitriche heterophylla</i>	Native				6	7								
CALY	<i>Carex lyngbyei</i>	Native	40	48	28	29	14	13							
CAPA	<i>Caltha palustris</i>	Native			6	8									
CASE	<i>Calystegia sepium</i>	Non-native					7	7							
CASP2	<i>Callitriche</i> sp.	Unknown			14										
COAR	<i>Convolvulus arvensis</i>	Non-native						7							
DECE	<i>Deschampsia cespitosa</i>	Native	7	9											
ELCA	<i>Elodea canadensis</i>	Native			7		37	13	8				12		
ELOV	<i>Eleocharis ovata</i>	Native									12		13	20	
ELPA	<i>Eleocharis palustris</i>	Native			7	6	9	15	24	17	10	9	22	9	
ELPAR	<i>Eleocharis parvula</i>	Native		12											
EQFL	<i>Equisetum fluviatile</i>	Native			6	6		6							
FRLA	<i>Fraxinus latifolia</i>	Native									23	17	38	20	16
GAAP	<i>Galium aparine</i>	Native			14										
GATR2	<i>Galium triflorum</i>	Native				5		7							
GATR3	<i>Galium trifidum</i>	Native			6		5								
GLMA	<i>Glaux maritima</i>	Native	6	8											

Sp Code	Scientific Name	Status	Iiwaco Slough		Welch Island		Whites Island		Cunningham Lake		Campbell Slough		Campbell Slough (New 2021)	Franz Lake	
			2021	2020	2021	2020	2021	2020	2021	2020	2021	2020	2021	2021	2020
HEAU	<i>Helenium autumnale</i>	Native									16	15			
IMCA	<i>Impatiens capensis</i> , <i>Impatiens noli-tangere</i>	Native			10	10	15	15							
IRPS	<i>Iris pseudacorus</i>	Non-native			6	10	9	8	31	25					
ISCE	<i>Isolepis cernua</i>	Native	7	15											
JUAC	<i>Juncus acuminatus</i>	Native		6									16		
JUEF	<i>Juncus effusus</i>	Non-native						9							
JUOX	<i>Juncus oxymeris</i>	Native				6					5				
JUTE	<i>Juncus tenuis</i>	Native									6				
LAPA	<i>Lathyrus palustris</i>	Native				6									
LEOR	<i>Leersia oryzoides</i>	Native						9		7			14		5
LIAQ	<i>Limosella aquatica</i>	Native					6	7							
LIDU	<i>Lindernia dubia</i>	Native									10	9	14		
LIOC	<i>Lilaeopsis occidentalis</i>	Native	9	9											
LOCO	<i>Lotus corniculatus</i>	Non-native			9	8	11	9			17	11			
LUPA	<i>Ludwigia palustris</i>	Native							16		9	13			
LYAM	<i>Lysichiton americanus</i>	Native						13							
LYAM2	<i>Lycopus americanus</i>	Native				7	5								
LYNU	<i>Lysimachia nummularia</i> L.	Non-native									12	15			
LYPO	<i>Lythrum portula</i>	Non-native									6	7			
LYSA	<i>Lythrum salicaria</i>	Non-native			9	8	14								
LYUN	<i>Lycopus uniflorus</i>	Native										9			
MEAR	<i>Mentha arvensis</i>	Native						15			15	6			
MEPU	<i>Mentha pulegium</i>	Non-native									14				
MEXPI	<i>Mentha x piperita</i>	Native					13	11							
MIGU	<i>Mimulus guttatus</i>	Native			6		9	6							

Sp Code	Scientific Name	Status	Iiwaco Slough		Welch Island		Whites Island		Cunningham Lake		Campbell Slough		Campbell Slough (New 2021)	Franz Lake	
			2021	2020	2021	2020	2021	2020	2021	2020	2021	2020	2021	2021	2020
Moss	Moss	Native									6				
MUKE	Murdannia keisak	Non-native				7									
MYLA	Myosotis laxa	Native				14			6						
MYSC	Myosotis scorpioides	Non-native			17	18	12	12							
MYSP	Myosotis laxa, M. scorpioides	Unknown						17							
MYSP3	Myriophyllum spicatum	Non-native					7								
OESA	Oenanthe sarmentosa	Native			8	6	7	6							
PHAR	Phalaris arundinacea	Non-native			14	31	25	30	68	52	44	45	63	30	22
PLMA	Plantago major	Non-native									7				
POAM	Polygonum amphibium	Native					7							34	48
POASP	Poa species	Non-native											10		
POHY	Polygonum hydropiper, P. hydropiperoides	Unknown					7	9		8		8			
PONA	Potamogeton natans	Native							5		7	5	23		
POPE	Polygonum persicaria	Non-native			8	7				10					
ROPA	Rorippa palustris	Native								6					
RUAR	Rubus armeniacus	Non-native									20				
RUCO	Rumex conglomeratus	Non-native				6									
RUCR	Rumex crispus	Non-native						7							
SAFL	Salix fluviatilis	Native												9	19
SALA	Sagittaria latifolia	Native			7	9	10	9	20	14	12		22	30	24
SALU	Salix lucida	Native							25	27				35	33
SASI	Salix sitchensis	Native					18	26							
SCAM	Schoenoplectus americanus	Native	28	19											
SCMA	Schoenoplectus maritimus	Native	7												
SCTA	Schoenoplectus tabernaemontani	Native				16									

Sp Code	Scientific Name	Status	Ilwaco Slough		Welch Island		Whites Island		Cunningham Lake		Campbell Slough		Campbell Slough (New 2021)	Franz Lake	
			2021	2020	2021	2020	2021	2020	2021	2020	2021	2020	2021	2021	2020
SD_CALY	Carex lyngbyei	Native		6											
SD_TYAN	Typha angustifolia	Non-native		10											
SISU	Sium suave	Native				6									
SODU	Solanum dulcamara	Non-native					5	6							
YSU	Symphotrichum subspicatum	Native	22	14											
TRMA	Triglochin maritima	Native	10	15											
TRWO	Trifolium wormskioldii	Native				7									
TYAN	Typha angustifolia	Non-native	10	20	8	5	11	9							
ZAPA	Zannichellia palustris	Native	12	9											

Appendix E. Fish catch summaries, 2008–2021

Appendix Table E-1. Species list of fishes captured during the EMP study, by year, 2008-2021 at the five trend sites, Ilwaco Slough, Welch Island, White Island, Campbell Slough and Franz Lake.

Family	Species	2008	2009	2010	2011	2012	2013	2014	2015	2016	2017	2018	2019	2020	2021
Clupeidae	American shad ⁱ	x	x	x	x	x	x	x	x	x	x	x	x		x
	Pacific herring												x		
Salmonidae	brown trout ⁱ					x									
	Chinook salmon	x	x	x	x	x	x	x	x	x	x	x	x	x	x
	chum salmon	x	x	x	x	x	x		x	x	x	x	x	x	x
	coho salmon	x	x	x	x	x		x	x	x	x	x	x	x	x
	cutthroat trout		x				x	x							
	mountain whitefish					x		x			x				
	sockeye salmon						x	x							
	steelhead (rainbow trout)													x	
	Pink salmon												x		
	unid whitefish					x									
Osmeridae	eulachon						x	x							
	longfin smelt						x								
	Surf smelt													x	x
	unid smelt				x	x	x		x	x		x	x		
Cyprinidae	chiselmouth	x	x	x	x	x	x	x	x	x					
	golden shiner ⁱ				x	x					x	x			x
	northern pikeminnow ^p	x	x	x	x	x	x	x	x	x		x	x		
	peamouth	x	x	x	x	x	x	x	x	x	x	x	x	x	x
	redside shiner									x		x		x	
	speckled dace					x									
	tui chub		x	x	x	x	x	x	x	x					

Family	Species	2008	2009	2010	2011	2012	2013	2014	2015	2016	2017	2018	2019	2020	2021
	Common Carp											x	x	x	x
	unid carp ⁱ	x	x	x	x	x	x	x	x	x					
	unid Cyprinidae ⁱ		x		x							x		x	x
Catostomidae	largescale sucker	x	x	x	x	x	x	x	x	x	x	x	x	x	x
Cobitidae	oriental weatherfish ⁱ			x						x					
Ictaluridae	brown bullhead ⁱ	x	x						x						
	channel catfish	x													
	yellow bullhead	x	x	x	x	x	x	x	x	x					
Fundulidae	banded killifish ⁱ	x	x	x	x	x	x	x	x	x	x	x	x	x	x
Poeciliidae	gambusia ⁱ			x							x	x			
Gasterosteidae	threespine stickleback	x	x	x	x	x	x	x	x	x	x	x	x	x	x
Centrarchidae	bluegill ⁱ		x	x	x	x	x	x	x			x		x	x
	largemouth bass ^{ip}		x							x	x	x	x		x
	pumpkinseed ⁱ	x	x	x	x	x	x	x	x	x		x			
	smallmouth bass ^{ip}	x	x	x	x	x	x	x	x	x					
	Black crappie											x	x		
	unid crappie ⁱ		x	x	x	x	x	x	x	x		x			
	Unidentified centrarchid ⁱ														
	warmouth ^{ip}				x										
Percidae	walleye ^{ip}	x													
	yellow perch ^{ip}	x	x	x	x	x	x	x	x	x	x	x	x		x
Embiotocidae	shiner perch				x	x	x		x	x	x		x		x
Ammodytidae	sandlance				x					x					
Gobiidae	Amur goby ⁱ									x	x	x	x	x	x
	unid goby ⁱ		x						x	x					
Cottidae	mottled sculpin		x												
	Pacific staghorn sculpin				x	x	x	x	x	x	x	x	x	x	x
	Prickly sculpin										x	x	x	x	x

Family	Species	2008	2009	2010	2011	2012	2013	2014	2015	2016	2017	2018	2019	2020	2021
	unid sculpin	x	x	x	x	x	x	x	x	x	x	x	x		x
Pleuronectidae	starry flounder		x	x		x	x	x	x			x	x		x

Appendix Table E-2a. Species list of fishes captured at the five EMP trend sites in 2020.

Family	Species_Name	Ilwaco Slough	Welch Island	Whites Island	Campbell Slough	Franz Lake
Catostomidae	largescale sucker					x
Centrarchidae	bluegill					x
Cottidae	Pacific staghorn sculpin	x				
	Prickly sculpin					x
Cyprinidae	Common carp					x
	peamouth				x	x
	reidside shiner					x
Fundulidae	banded killifish	x	x	x	x	x
Gasterosteidae	threespine stickleback	x	x	x	x	x
Gobiidae	Amur goby					x
Osmeridae	Surf smelt	x				
Salmonidae	Chinook salmon	x	x	x	x	x
	chum salmon	x		x	x	
	coho salmon		x			x
	Rainbow trout (steelhead)					x

Appendix Table E-2b. Species list of fishes captured at the five EMP trend sites in 2021.

Family	Species_Name	Ilwaco Slough	Welch Island	Whites Island	Campbell Slough	Franz Lake
Catostomidae	largescale sucker				x	x
Centrarchidae	bluegill				x	
	largemouth bass				x	
	Unidentified sunfish				x	x
Clupeidae	American shad		x	x	x	x
Cottidae	Pacific staghorn sculpin	x				
	Prickly sculpin		x	x	x	x
	Unidentified sculpin					x
Cyprinidae	Common carp					x
	golden shiner					x
	northern pikeminnow			x	x	x
	peamouth			x	x	
	Unidentified cyprinid				x	
Embiotocidae	shiner perch	x				
Fundulidae	banded killifish	x	x	x	x	x
Gasterosteidae	threespine stickleback	x	x	x	x	x
	Amur goby				x	x
Osmeridae	Surf smelt	x				
Osteichthyes	Unidentified fish					x
Percidae	yellow perch				x	x
Pleuronectidae	starry flounder		x	x	x	

Family	Species_Name	Ilwaco Slough	Welch Island	Whites Island	Campbell Slough	Franz Lake
Salmonidae	Chinook salmon		x	x	x	x
	chum salmon		x	x	x	
	coho salmon				x	

Table E-3. Juvenile coho (unmarked and marked), chum salmon, sockeye salmon, and trout densities (fish per 1000 m²) (SD), by year captured at trends sites 2008 - 2019. Total number of salmonids captured at a site is presented in parentheses under site/species/#.

Site/Species/#	Year											
	2008	2009	2010	2011	2012	2013	2014	2015	2016	2017	2018	2019
Ilwaco Slough												
Coho (unmarked) (1)	ns	ns	ns	0	0.12 (0.67)	0	0	0	0	0	0	0
Coho (marked) (0)	ns	ns	ns	0	0	0	0	0	0	0	0	0
Chum (531)	ns	ns	ns	27.60 (139.62)	0.71 (2.49)	25.01 (108.97)	0	0.24 (1.10)	11.19 (32.39)	11.70 (26.16)	32.11 (54.55)	11.08 (5.51)
Sockeye (0)	ns	ns	ns	0	0	0	0	0	0	0	0	0
Trout sp (0)	ns	ns	ns	0	0	0	0	0	0	0	0	0
Welch Island												
Coho (unmarked) (2)	ns	ns	ns	ns	0.15 (0.78)	0	0	0	0	0	0	0
Coho (marked) (1)	ns	ns	ns	ns	0.11 (0.54)	0	0	0	0	0	0	0
Chum (70)	ns	ns	ns	ns	0.14 (0.71)	0.26 (1.01)	0	0	0.65 (2.68)	2.50 (5.02)	26.87 (36.55)	2.28 (1.40)
Sockeye (1)	ns	ns	ns	ns	0	0	0.12 (0.41)	0	0	0	0	0
Trout sp (1)	ns	ns	ns	ns	0	0.27 (1.05)	0	0	0	0	0	0
Whites Island												
Coho (unmarked) (7)	ns	0	1.12 (2.03)	0	0	0	0	0	0	0.12 (0.46)	0	0.51 (0.50)
Coho (marked) (0)	ns	0	0	0	0	0	0	0	0	0	0	0
Chum (42)	ns	0.14 (0.59)	1.03 (2.55)	0	0.34 (1.23)	0	0	1.55 (5.62)	1.13 (3.80)	0.45 (1.23)	2.93 (7.21)	1.50 (1.81)

Sockeye (7)	ns	0	0	0	0	1.32 (5.77)	0	0	0	0	0	0
Trout sp (0)	ns	0	0	0	0	0	0	0	0	0	0	0

Continued from Table E-3

Site/Species/#	Year												
	2008	2009	2010	2011	2012	2013	2014	2015	2016	2017	2018	2019	
Campbell Slough													
Coho (unmarked) (2)	0	0	0	0	0	0	0	0.18 (0.70)	0	0	0	0	
Coho (marked)	0	0	0	0	0	0	0.18 (0.51)	0	0	0	0	0	
Chum (10)	0.29 (0.99)	0	0.67 (2.24)	0	0	0	0	0.09 (0.35)	0.35 (1.09)	0.13 (0.48)	0.26 (1.11)	0	
Sockeye (1)	0	0	0	0	0	0	0.09 (0.38)	0	0	0	0	0	
Trout sp. (1)	0	0	0	0	0	0	0.78 (0.33)	0	0	0	0	0	
Franz Lake													
Coho (unmarked) (32)	0.56 (1.01)	2.09 (4.85)	ns	4.86 (13.36)	2.29 (7.15)	0	1.17 (2.29)	0.20 (0.87)	0.27 (1.06)	ns	1.53 (2.65)	ns	
Coho (marked) (60)	5.75 (10.72)	7.92 (17.99)	ns	0	0.51 (2.17)	0	0	0	0	ns	0	ns	
Chum (7)	2.11 (5.23)	0.32 (1.09)	ns	0	0	0	0	0	0	ns	0	ns	
Sockeye (2)	0	0	ns	0	0	0	0.55 (1.56)	0	0	ns	0	ns	
Trout sp. (5)	0	0.95 (2.30)	ns	0	1.43 (6.54)	0	0	0	0	ns	0	ns	

Table E-4. Total number of unmarked and marked Chinook salmon captured by year at each site 2008 – 2021, ns = site not sampled.

Site	Years													
	2008	2009	2010	2011	2012	2013	2014	2015	2016	2017	2018	2019	2020	2021
Iiwaco Slough														
Unmarked	ns	ns	ns	1	5	0	0	6	0	4	2	0	34	0
Marked	ns	ns	ns	0	0	0	0	0	0	1	1	0	0	0
Welch Island														
Unmarked	ns	ns	ns	ns	280	154	241	39	121	398	1339	130	30	180
Marked	ns	ns	ns	ns	23	35	20	4	6	13	4	18	1	21
Whites Island														
Unmarked	ns	36	114	54	83	64	134	33	144	111	245	71	334	684
Marked	ns	6	26	7	3	20	7	15	6	1	0	16	1	7
Campbell Slough														
Unmarked	25	15	40	3	46	30	17	36	20	45	13	42	11	27
Marked	26	69	48	31	21	22	18	72	2	61	33	21	0	0
Franz Lake														
Unmarked	11	13	ns	2	0	2	15	40	24	ns	2	ns	10	65
Marked	49	7	ns	0	0	0	0	1	0	ns	1	ns	0	0